NASA CR-66649
REPORT NO. GDC-DCL-68-001
CONTRACT NAS 1-7309

FINAL REPORT

# FEASIBILITY STUDY
# OF A CENTRIFUGE EXPERIMENT FOR THE
# APOLLO APPLICATIONS PROGRAM

VOLUME I

SPACE RESEARCH CENTRIFUGE CONFIGURATION,
INSTALLATION AND FEASIBILITY STUDIES

**GENERAL DYNAMICS**
*Convair Division*

Final Report

FEASIBILITY STUDY OF A CENTRIFUGE EXPERIMENT

FOR THE

APOLLO APPLICATIONS PROGRAM

VOLUME I

SPACE RESEARCH CENTRIFUGE CONFIGURATION,

INSTALLATION AND FEASIBILITY STUDIES

# ACKNOWLEDGMENTS

# CONTENTS

# FIGURES

# TABLES

# ABBREVIATIONS

| | | |
|---|---|---|
| AAP | – | Apollo Applications Program |
| A/P | – | Autopilot |
| ATM | – | Apollo Telescope Mount |
| BSM | – | Basic Subsystems Module |
| CAC | – | Cluster Associated Configuration |
| CB | – | Compression Buckling |
| CC | – | Compression Crippling |
| CM | – | Command Module, or Center of Mass |
| c.g. | – | Center of Gravity |
| CMG | – | Control Moment Gyro |
| CSM | – | Command and Service Module |
| DAP | – | Digital Autopilot |
| dc | – | Direct Current |
| ECG | – | Electrocardiogram |
| ECO | – | Engine Cut-Off |
| ECS | – | Environmental Control System |
| EEG | – | Electroencephalogram |
| EOSS | – | Early Orbital Space Station |
| FARADA | – | Failure Rate Data (Handbook) |
| F.E.A. | – | Failure Mode and Effects Analysis |
| FF | – | Fastener Failure |
| FMFR | – | Failure Mode Frequency Ratio |
| GD/C | – | General Dynamics/Convair |
| hp | – | Horsepower |
| LM | – | Lunar Module |
| M | – | Million |
| MDA | – | Multiple Docking Adaptor |
| MF | – | Material Failure |
| MSC | – | NASA Manned Spacecraft Center (Houston) |
| MY | – | Material Yield |
| MW | – | Material Wear |
| Po | – | Probability of Occurrence |
| RCS | – | Reaction Control System |
| RCVR | – | Receiver |
| rf | – | Radio Frequency |
| rpm | – | Revolutions per Minute |
| RSS | – | Root Sum Squared |
| S-IC | – | First Stage of Saturn V Booster |
| S-II | – | Second Stage of Saturn V Booster |

| | | |
|---|---|---|
| SB | – | Shear Buckling |
| SCO | – | Subcarrier Oscillator |
| S–IVB | – | Saturn V Booster 3rd Stage |
| SMC | – | System Mass Center |
| SRC | – | Space Research Centrifuge |
| SW | – | Switch |
| T. V. | – | Television |
| TLM | – | Telemetry |
| TRAJ | – | Trajectory |
| VHF | – | Very High Frequency |
| WS–LO–C | – | S–IVB work shop low–orbit cluster |
| XMTR | – | Transmitter |

# SYMBOLS

To eliminate multiple interpretation, the symbols used in this report are grouped according to the major section in which they occur.

## CENTRIFUGE OPTIMIZATION AND INSTALLATION CONSIDERATIONS SECTION

Symbols

| | | |
|---|---|---|
| $g$ | – | Load, gravities |
| $g_c$ | – | Gravitational constant, $\dfrac{lbs_m \; ft}{lbs_f \; sec^2}$ |
| $H_c$ | – | CMG momentum requirement. ft-lb-sec. |
| HP. | – | Horsepower |
| $I_{oc}$ | – | Centrifuge moment of inertia, slug-ft$^2$ |
| $K_1$ | – | Arbitrary constant |
| $M_o$ | – | Centrifuge momentum, ft-lb-sec. |
| $r_c$ | – | Maximum radial dimension of centrifuge, ft. |
| $r_m$ | – | Maximum useful centrifuge radius to test subjects center of gravity, ft. |
| $T$ | – | Torque, ft-lbs |
| $t$ | – | time, sec. |
| $V_c$ | – | Volume occupied by the centrifuge, ft$^3$ |
| $V_m$ | – | Centrifuge room or module volume, ft$^3$. |
| $W_a$ | – | Translation arm weight, lbs. |
| $W_c$ | – | Weight of couch, pivot & roll frame, and all power, communication equipment and experiment instrumentation attached to the couch, lbs. |
| $W_{cf}$ | – | Center frame weight, lbs. |
| $W_{ci}$ | – | Communications and illumination systems weight, lbs. |
| $W_{cm}$ | – | Weight of the counter momentum system, lbs. |
| $W_{cw}$ | – | Weight of counter balance, lbs. |
| $W_d$ | – | Rotational drive system weight, lbs. |
| $W_e$ | – | Contingency weight allowance, lbs. |
| $W_{en}$ | – | Non-rotating weight contingency allowance, lbs. |
| $W_h$ | – | Drive hub weight, lbs. |
| $W_p$ | – | Power and distribution system weight, lbs. |
| $W_t$ | – | Total centrifuge parametric weight function, lbs. |
| $W_{ts}$ | – | Test subject weight, lbs. |
| $W_{vd}$ | – | Weight of noise and vibration damping material, lbs. |
| $W_x$ | – | Weight of non-rotating experiment systems and expendables, lbs. |

Symbols

$\eta_s$     -     Centrifuge space utilization efficiency factor, non-dimentional

$\dot{\theta}$     -     Angular velocity, radians/sec

$\ddot{\theta}$     -     Angular acceleration, radians/sec$^2$

$\psi$     -     Cross-coupled acceleration, rad/sec$^2$

$\omega$     -     Head turn rate, rad/sec

## STABILITY AND ATTITUDE CONTROL FEASIBILITY ANALYSIS SECTION

B     -     Perpendicular displacement of the centrifuge CM from the spin axis, ft

$F_s$     -     Force due to static imbalance, lbs

g     -     Load, gravities

H     -     Angular momentum of the centrifuge

$H_G$     -     CMG Momentum, ft-lb-sec

$I_C$     -     Moment of inertia of the centrifuge about the spin axis, slug-ft$^2$

$I_B$     -     Moment of inertia of the balancer about the centrifuge spin axis, slug-ft$^2$

$J_1$     -     Principle moment of inertia about the spacecraft roll axis, slug-ft$^2$

$J_2$     -     Principle moment of inertia about the spacecraft pitch axis, slug-ft$^2$

$J_3$     -     Principle moment of inertia about the spacecraft yaw axis, slug-ft$^2$

K     -     Gain contant

$K_D$     -     Flexural displacement bias

$K_G$     -     CMG gain constant

$K_R$     -     Flexural displacement rate bias

$\ell$     -     Force location relative to spacecraft center of mass

M     -     Net angular momentum of the centrifuge and balance bodies relative to the spacecraft, ft-lb-sec

$M_c$     -     Centrifuge rotational mass, slugs

m     -     Generalized mass of flexural mode

P     -     Coning motion period, sec

R     -     Linear acceleration at the couch, ft/sec$^2$

$R_c$     -     Distance from the system center of mass to the intersection of the centrifuge spin axis and plane, fixed in the spacecraft body, ft

$R_s$     -     Perpendicular distance to the subject area of interest from the centrifuge spin axis

S     -     Centrifuge spin rate, radians/sec, also Laplace operator

SYMBOLS (CONTINUED)

STABILITY AND ATTITUDE CONTROL FEASIBILITY ANALYSIS SECTION, Cont'd

Symbols

$S_A$    -    Distance between the system center of mass and the spacecraft center of mass, ft

$S_B$    -    Distance between the system center of mass and the centrifuge balance center of mass, ft

$\tau_1$    -    time constant of CMG

$S_C$    -    Distance between the system center of mass and the centrifuge center of mass, ft

$T_c$    -    Centrifuge spin-up reaction torque on the spacecraft, ft-lbs

$T_D$    -    Torque on the spacecraft due to dynamic unbalance, ft-lbs

$T_G$    -    CMG Bandpass time constant

$T_S$    -    Torque on the vehicle resulting from static imbalance, ft-lbs

t    -    time, sec

$\alpha$    -    Angle between the centrifuge spin axis and the spacecraft minimum inertia axis, radians

$\dot{\gamma}_B$    -    Angular rate of balancer

$\dot{\gamma}_C$    -    Angular rate of the centrifuge with respect to the spacecraft

$\delta$    -    Angle between centrifuge momentum vector and CMG Momentum vector

$\delta_1$    -    Deflection of mode shape curve at disturbance force location

$\Theta$    -    Pitch deviation of the spacecraft with respect to an inert reference, Radians. Also, total angular deflection at sensor location

$\Theta_1$    -    Slope of mode shape curve at location of control torque

$\Theta_2$    -    Slope of mode shape curve at location of disturbance torque

$\Theta_3$    -    Slope of mode shape curve at attitude sensor location

$\Delta\Theta_{FB}$    -    Perturbation of angular displacement due to flexure

$\Theta_{RB}$    -    Rigid body angular displacement

$\phi$    -    Roll deviation of the spacecraft with respect to an inert reference, Radians

$\psi$    -    Yaw deviation of the spacecraft with respect to an inert reference, Radians

$\omega$    -    Centrifuge angular rate with respect to inert space, radians/sec, also natural frequency of flexural mode

$\omega_A$    -    Angular rate of spacecraft relative to inert space, radians/sec

$\omega_C$    -    Centrifuge angular rate relative to the spacecraft, radians/sec

# SYMBOLS (CONTINUED)

## STABILITY AND ATTITUDE CONTROL FEASIBILITY ANALYSIS SECTION, Cont'd

For notation above symbols

| | | |
|---|---|---|
| $-$ | - | Vector quantity |
| $\doteq$ | - | Total derivitive of vector quantity |
| $\cdot$ | - | 1st derivitive with respect to time |
| $\cdot\cdot$ | - | 2nd derivitive with respect to time |

Subscripts

| | | |
|---|---|---|
| 1 | - | roll axis |
| 2 | - | pitch axis |
| 3 | - | yaw axis |

## ORBITAL CENTRIFUGE DESIGN SECTION

### Symbols

| | | |
|---|---|---|
| A | - | Area, $in^2$ |
| $a_n$ | - | Entry maneuver acceleration normal to the flight path, $ft/sec^2$ |
| $a_R$ | - | Radial component of acceleration, $ft/sec^2$ |
| $a_T$ | - | Tangential component of acceleration, $ft/sec^2$ |
| D | - | Diameter, in. |
| E | - | Modulus of elasticity, $lbs/in^2$ |
| F | - | Force, lbs |
| $F_{CW}$ | - | Force acting on counterweight ball screw |
| $F_{MC}$ | - | Force acting on radius arm, lbs |
| $F_N$ | - | Force parallel to the N axis, lbs |
| $P_P$ | - | Force parallel to the P axis, lbs |
| $F_R$ | - | Radial Force, lbs |
| $F_T$ | - | Tangential force, lbs |
| G, g | - | Load, gravities |

# SYMBOLS (CONTINUED)

## ORBITAL CENTRIFUGE DESIGN, Contd

### Symbols

| | | |
|---|---|---|
| $g_c$ | - | Gravitational constant, 32.2 ft/sec$^2$ |
| HP | - | Horsepower |
| I | - | Section moment of inertia, in$^4$, or Moment of Inertia, slug-ft$^2$ |
| K | - | Required structural stiffness of an individual structural element |
| $K_E$ | - | Equivalent spring constant for the centrifuge structure, lbs/in. |
| $K_n$ | - | Average spring constant of individual segments of structure, lb/in. |
| M | - | Mass, slugs |
| $M_c$ | - | Momentum ft-lb-sec |
| $M_N$ | - | Moment about the N axis, ft-lbs |
| $M_P$ | - | Moment about the P axis, ft-lbs |
| $M_V$ | - | Moment about the V axis, ft-lbs |
| n | - | Load factor, gravities, also an arbitrary number of segments |
| P | - | Load, lbs |
| q | - | Aerodynamic pressure, psf |
| R | - | Radius, ft |
| T | - | Torque, ft-lbs |
| $T_p$ | - | Torque at the pivot, ft-lbs |
| t | - | time, sec, or thickness, in |
| W | - | Weight, lbs |
| $\alpha$ | - | Centrifuge angular acceleration rad/sec$^2$ |
| $\Delta$ | - | Increment of the indicated variable |
| $\delta_E$ | - | Deflection of the couch center of mass under load, in. |
| $\delta_n$ | - | Deflection of individual elements of structure under load as referenced to the couch center of mass, in. |
| $\Theta$ | - | Angle between centrifuge radii to the pivot axis and the test subject/couch center of mass |
| $\phi$ | - | Rate of change of acceleration with respect to time for entry. ft/sec$^3$ |
| $\phi_M$ | - | Maximum rate of change of acceleration with respect to time for entry. ft/sec$^3$ |
| $\omega$ | - | Centrifuge angular velocity, rad/sec |
| $\omega_f$ | - | Final angular velocity, radians/sec |
| $\omega_n$ | - | Natural frequency of the centrifuge structure |
| $\omega_o$ | - | Initial angular velocity, radians/sec |
| $\omega_{op}$ | - | Operating frequency |

# SUMMARY

This study examines the feasibility of employing an orbital, on-board centrifuge to perform a series of physiological experiments with human subjects in space. It has as its objectives:

a. Configuring a baseline orbital centrifuge capable of supporting the specified experiment series.

b. Determining the feasibility of the experiment in terms of cost, safety, reliability, stability, weight and other parameters.

c. Defining a ground-based, engineering development test model of the centrifuge and its corresponding test plan.

d. Determining the effect of cross-coupled angular accelerations on the experiment by performing manned centrifuge tests to evaluate this condition.

## Experiment Requirements

In the initial configuration studies it became immediately apparent that the principal configuration drivers would be the experiments themselves. These were identified as:

| | |
|---|---|
| T-010A | Greyout Thresholds |
| T-010B | Therapeutic |
| T-010C | Angular Acceleration Thresholds |
| T-010D | Tilt Table |
| T-010E | Coupled Angular Velocities |
| T-010F-1 | g-Sensitivity (Y axis, pitch - measured by VOG) |
| T-010F-2 | g-Sensitivity (X axis, roll - measured by eye counter-rolling) |
| T-010G | Re-entry Simulation |
| T-010H | Mass Measurement |

Preliminary design of each experiment was accomplished and is detailed in Volume IV of this report. Each experiment was analyzed for requirements which provide a range of rotational velocity, acceleration, control threshold, dead band time requirements, radius and positioning capability defining the centrifuge mechanism and its systems.

## Parametric Sizing and Installation

A parametric study of the centrifuge configuration was performed to determine optimum radius and other pertinent characteristics. Significant findings are that centrifuge radius does not optimize to a specific value but can be bounded within the range of 7 to 10.5 ft. A review of possible spacecraft installations lead to the selection of the S-IVB Ground Fitted Station (EOSS), an S-IVB Workshop Cluster and a CSM/LM assembled with a special centrifuge module as the most desirable. For compatibility with these three installation situations, an 8.5 foot centrifuge radius is recommended. Other approximate characteristics associated with this size centrifuge are: total experiment weight, 3050 lbs; moment of inertia, 1441 ft-lb-sec$^2$; maximum momentum, 8040 ft-lb-sec; volume requirement, 2200 ft$^3$; volume efficiency, 13.3%; maximum disturbance frequency, 1.08 Hz.

## Stability and Control

An extensive analysis of the stability and control dynamics associated with operation of the centrifuge aboard the selected spacecraft was made. This analysis considered the effect of spacecraft perturbation on the centrifuge experiment, as well as stabilization of the vehicle itself. The order of magnitude of allowable spacecraft motion can be approximated by considering a sinusoidal attitude oscillation yielding an equivalent maximum acceleration and rate. This was found to be: 2.4 degrees at 1.9 rad/sec for high-g experiments; 28.8 arc minutes at 0.66 rad/sec for low-g experiments; and 1.7 arc minutes at 1.0 rad/sec for low angular acceleration experiments. Evaluation of attitude control system performance revealed that CSM type reaction control was too coarse for all except the high-g experiments but that a CMG system such as is provided for the ATM would give sufficient control. The presence of the large momentum of the centrifuge does not change the performance of the attitude control system appreciably. Vehicle stabilization requires that a counter-momentum system be employed to react spin-up and spin-down torques and that an automatic balancing system be included to limit static unbalance forces to a maximum of 10 lbs. Dynamic unbalance need not be compensated for unless further experiment design requires test subject motion out of the plane of centrifuge spin.

Centrifuge static unbalance causes a disturbance torque at centrifuge spin/ frequency. It is desirable that the maximum spin rate be below the installation first mode bending frequency. Those flexural modes caused by small mass appendages (solar panels, etc.) may be excluded if excitation at their structural frequency can be tolerated. In any event, installation and structural dynamics analysis is an important aspect of the centrifuge design.

Comparison of the experiment requirements with the resulting spacecraft control capability indicates that sufficient stability can be achieved

for the three installations studied. In the case of the CSM/LM/SRC configuration, the spent S-IVB booster must remain attached to the spacecraft for adequate control performance.

## Centrifuge Design

The centrifuge design is dictated by the motion and performance requirements of the experiments. These are summarized as:

- Primary Rotation

    a.  Manual and automated control

    b.  Controlled deceleration - integral, fail-safe brake

    c.  Overspeed cut-out

    d.  Hub mounted sealed drive unit.

- Radius Arm Translation

    a.  Powered operation for each position

    b.  Dual, positive, manual locks at each position

    c.  Drive interlock with couch pivot

- Couch Pivot Drive

    a.  Manual and automated control

    b.  Positive position control by manual lock

    c.  Drive interlocks with radius arm position

- Couch Roll Drive

    a.  Automatic operation through function generator

    b.  Dual manual locks at fixed positions

- Couch Translation and Body Adjustments

    a.  Manual positioning only.

In providing these motions, the centrifuge evolves into a highly integrated system of structure, mechanisms, controls and instrumentation. The overall design, however, is found to be straightforward and within the capability of existing technology.

A configuration for the ground based, engineering development prototype of the orbital centrifuge was derived from consideration of the test and development objectives to be met. These require that the ground based prototype be designed with complete structural and systems simalarity to the orbital centrifuge. In addition, a 90 degree repositioning capability for the couch pivot axis appears desirable to allow g-vector alignment during geo-baseline data development.

### Feasibility Studies

Additional studies were performed to develop data concerning feasibility of the centrifuge experiment. The areas investigated included reliability, failure mode and effects, safety, cost, weight, power, life support and environmental control.

In the area of reliability, failure mode and effects analysis, it was determined that man-rated reliability levels are achievable through the use of high reliability components, active parallel redundancy in critical functions and a limited number of spares. Practical solutions were found to all critical failure modes.

Safety review and analysis was conducted with respect to centrifuge design and operation. Safety ground rules were postulated and implemented as the design emerged. While many areas which affect the safety of the experiment were disclosed by this review, no situation appeared which was judged inherently unsafe or which could not be avoided by sensible design and experiment procedure.

Economic feasibility was evaluated and a cost estimate prepared with detailed breakdowns for the two phases of the program covering the ground test unit and the flight unit. Baseline cost was estimated at $2.9M for the ground test unit and $9.1M for the flight unit. For the level of detail available for this estimate, a variance range of -10% to +50% is recommended.

A detailed weight breakdown was made for each of the centrifuge installations studied. Weights chargeable to the centrifuge were 3,158 lbs. for the EOSS installation, 12,972 lbs. for the CAC and 42,719 lbs. for the CSM/LM/SRC version. The payload capability of existing launch vehicles was found to be adequate for each installation option.

Power requirements of the centrifuge and experiments were evaluated and found to be reasonable. A solar cell/battery source was recommended for supplying centrifuge requirements. This consists of a 100 ft$^2$ solar array and 220 lbs. of batteries.

Life support and environmental control requirements were also evaluated and found to introduce no new equipment requirements for the advanced spacecraft studied.

## Conclusions

As a result of this study effort the centrifuge experiment is judged to be a reasonable and desirable future program which will contribute significantly to our knowledge of human physiology in both the space and terrestial environments. All major factors affecting the centrifuge experiment have been evaluated. In no case has a serious challenge to its feasibility arisen.

# INTRODUCTION

This study program is a detailed design and planning activity leading toward orbital application of an on-board centrifuge for the study of human physiology. It is the first phase of an anticipated four-phase program accomplishing the over-all experiment. These phases are identified as:

Phase I:    The present study effort, which configures the orbital centrifuge, establishes its feasibility and defines a ground-based prototype of the machine.

Phase II:   Detail design and fabrication of the ground-based engineering development prototype and appropriate testing using this machine.

Phase III:  Detail design, fabrication, integration and qualification of the flight centrifuge and experiments.

Phase IV:   The orbital experiment flight.

Previous conceptual design studies and test programs have served to outline experiment requirements and narrow the range of investigation of equipment mechanization required to perform these experiments. Using such background, this program provides the realistic detail which clearly establishes the feasibility of the flight equipment configuration and allows an advance of procurement activity for the ground-based test hardware.

## Program Objectives

The objectives of the initial phase of the over-all experiment program are defined as follows:

a.    Establish the feasibility of incorporating the flight version of a manned centrifuge, its systems and its associated equipment in realistic, near-term space vehicles, including the modified LM/CSM combination, the S-IVB Workshop Cluster and ground fitted orbital stations.

b.    Provide a complete conceptual design for the flight experiment centrifuge.

c.    Provide a detailed predesign of a full-scale, ground-based, engineering development test model of the flight centrifuge.
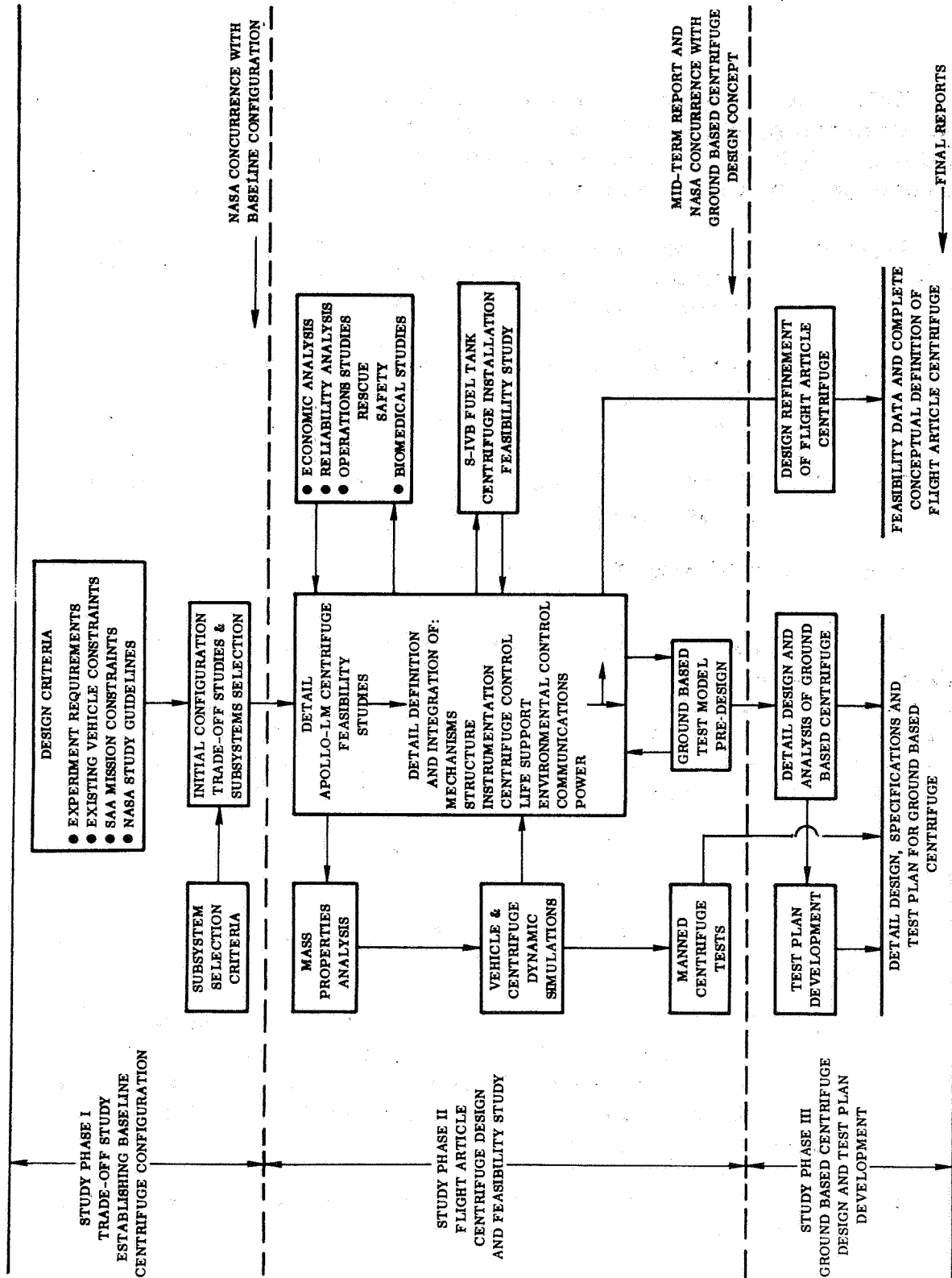
**Figure 1 - CENTRIFUGE FEASIBILITY STUDY PROGRAM TASK FLOW DIAGRAM**

STUDY PHASE I
TRADE-OFF STUDY
ESTABLISHING BASELINE
CENTRIFUGE CONFIGURATION

STUDY PHASE II
FLIGHT ARTICLE
CENTRIFUGE DESIGN
AND FEASIBILITY STUDY

STUDY PHASE III
GROUND BASED CENTRIFUGE
DESIGN AND TEST PLAN
DEVELOPMENT

NASA CONCURRENCE WITH
BASELINE CONFIGURATION

MID-TERM REPORT AND
NASA CONCURRENCE WITH
GROUND BASED CENTRIFUGE
DESIGN CONCEPT

FINAL REPORTS

**DESIGN CRITERIA**
- EXPERIMENT REQUIREMENTS
- EXISTING VEHICLE CONSTRAINTS
- SAA MISSION CONSTRAINTS
- NASA STUDY GUIDELINES

INITIAL CONFIGURATION
TRADE-OFF STUDIES &
SUBSYSTEMS SELECTION

SUBSYSTEM
SELECTION
CRITERIA

- ECONOMIC ANALYSIS
- RELIABILITY ANALYSIS
- OPERATIONS STUDIES
- RESCUE
- SAFETY
- BIOMEDICAL STUDIES

S-IVB FUEL TANK
CENTRIFUGE INSTALLATION
FEASIBILITY STUDY

DETAIL
APOLLO-LM CENTRIFUGE
FEASIBILITY
STUDIES

DETAIL DEFINITION
AND INTEGRATION OF:
MECHANISMS
STRUCTURE
INSTRUMENTATION
CENTRIFUGE CONTROL
LIFE SUPPORT
ENVIRONMENTAL CONTROL
COMMUNICATIONS
POWER

MASS
PROPERTIES
ANALYSIS

VEHICLE &
CENTRIFUGE
DYNAMIC
SIMULATIONS

MANNED
CENTRIFUGE
TESTS

GROUND BASED
TEST MODEL
PRE-DESIGN

DETAIL DESIGN AND
ANALYSIS OF GROUND
BASED CENTRIFUGE

TEST PLAN
DEVELOPMENT

DESIGN REFINEMENT
OF FLIGHT ARTICLE
CENTRIFUGE

DETAIL DESIGN, SPECIFICATIONS AND
TEST PLAN FOR GROUND BASED
CENTRIFUGE

FEASIBILITY DATA AND COMPLETE
CONCEPTUAL DEFINITION OF
FLIGHT ARTICLE CENTRIFUGE

d.    Develop a test plan for the next over-all program phase to be used to verify the centrifuge and experiment design.

These program objectives have been attained by identification and timely completion of all necessary related task areas.

## Study Approach

The major task areas necessary to reach program objectives were analyzed and expanded to provide the program schedule. The sequence and interrelation of these tasks is as shown by Figure 1. Three sequential phases were employed to insure orderly progress through the study. As indicated, an initial trade-off study was employed to reduce the centrifuge and installation configuration to a single, well defined, baseline which is most representative of the future experiment requirement. Experiment requirements and design, as detailed in Volume IV of this report, were most influential in establishing the initial mechanism parameters. Other selection criteria such as stabilization and control dynamics, weight, safety, reliability and cost were also applied as necessary to arrive at an appropriate baseline which was compatible with the most likely installation possibilities.

With selection of the baseline mechanisms and systems, a detailed predesign of the centrifuge was made and its feasibility studied in depth. This was the major assignment of the Phase II study period. In conjunction with the feasibility studies of the flight configuration, predesign of the ground-based centrifuge was accomplished to ensure that compatibility of these concepts was maintained and to allow immediate entry into the detail predesign of the ground-based prototype.

In the third phase of the program, emphasis was directed toward the detailed description of the ground-based engineering development prototype and its test plan. Complimentary activity was concerned with the performance of manned centrifuge tests to determine the threshhold values of cross-coupled angular acceleration effects such as may result from the combined motions of the centrifuge, the spacecraft and the test subject. The cross-coupled acceleration test activity is documented in Volume III of this report.

# CENTRIFUGE OPTIMIZATION & INSTALLATION CONSIDERATIONS

The orbital, on-board, centrifuge is designed primarily as a mechanism for the support of physiological experimentation in space. Its function is to apply centripetal forces to an individual after varying lengths of exposure to weightlessness while he is still in the weightless environment and to measure the results of such exposure. In this respect, it has the same relation to basic physiology as tensile, shear and hardness testers have to materials research or particle accelerators have to nuclear physics. In essence, it is a stress applicator which allows the study of physiological response under controlled conditions which are unique to the orbital situation.

## Radius and Rate

One of the more interesting preliminary questions regarding the centrifuge involves determining the radius and angular velocity requirements of the device. In more specific terms, what optimum combination of these parameters should be employed to provide the required experimental conditions? For this, we must evaluate the demands of the spacecraft installation, the requirements of the experiment and the reactions of the astronaut subject himself. As will be shown, centrifuge radius will not optimize to a specific value, but can be bounded by consideration of these factors. In this regard, the items which are most influential to centrifuge radius are:

- Geometry of available boosters
- Centrifuge inertial properties
- Space utilization efficiency
- Disturbance frequency
- Cross-coupling acceleration

Booster Geometry. - The size of boosters which may launch the centrifuge experiment is most influential in fixing an upper limit to centrifuge radius. This is simply the result of the device having to be "internal" to some spacecraft whose dimentions are generally established by booster characteristics, principally the diameter of the upper stage. The centrifuge radius will be incrementally bounded by housing diameters of 10 ft. , such as provided by Atlas or Titan launched modules, 22 ft. diameters representative of the S-IVB, and 33 ft. module diameters, such as would be possible if the S-IC/S-II combination served as a booster. This gives us a limiting range of 5 to 16.5 ft. for the centrifuge radius.

From an examination of the preliminary designs of the centrifuge, it is apparent that the useful maximum radius of the centrifuge will differ slightly from the maximum radial dimension of the unit. This is due primarily to the roll frame clearance requirements. If we designate $r_c$ as the maximum radial centrifuge dimension and $r_m$ as the maximum useful radius to the test subjects center of gravity, then:

$$r_c \approx r_m + 2.16 \text{ ft.} \tag{1}$$

This relationship is used in the following development to examine the influence of the housing on the centrifuge design.

Centrifuge inertial properties. -    In determining the weight scaling of the centrifuge, consider that weight variation as a function of radius will involve mainly changes in arm weight and counterweight mass for static balance. Some variation in the distance over which the counterweight must travel will also affect overall weight but will be of second order influence. Most components of the centrifuge which affect the counterweight will be independent of radius. For the present design, these constants are identified as:

$$W_{ts} \quad = \quad \text{Test Subject Wt.} \qquad\qquad = 175 \text{ lbs}$$

$$W_c \quad = \quad \begin{cases} \text{Couch Wt.} & = 167 \text{ lbs} \\ \text{Pivot \& Roll Frame Wt.} & = 140 \text{ lbs} \\ \text{Power \& Communications Wt.} & = 150 \text{ lbs} \end{cases}$$

$$\overline{632 \text{ lbs}}$$

This 632 lbs operates at a radius $(r_m)$ of 6.33 ft. in the base line design. Assuming that the maximum position of the counter balance is fixed at 5.33 ft., and including the influence of the translation arm weight, $W_a$, which is related by:

$$W_a \quad = \quad 18\, r_m + 80 \tag{2}$$

Then

$$632\, r_m + \frac{r_m}{2}\, (18\, r_m + 80) = 5.33\, (W_{cw} + 285)$$

The counterweight mass then becomes:

$$W_{cw} = \quad 1.69\, r_m^2 + 126\, r_m - 285 \tag{3}$$

In a similar manner, simple linear weight scaling relations are developed from the base line design for:

$$\text{Centerframe Weight} \quad = W_{cf} = 40\, r_m + 147 \tag{4}$$

$$\text{Drive Hub Weight} \quad = W_h = 4\, r_m + 17.7 \tag{5}$$

A constant contingency allowance, $W_e$, of 125 lbs is carried for the rotating system weight.

For the non-rotating systems, dependance of the counter momentum system, rotational drive system and power system weights on centrifuge momentum makes it necessary to derive inertial and momentum characteristics as a function of $r_m$ at this point.

Centrifuge moment of inertia, $I_{oc}$, may be approximated from the relation:

$$I_{oc} = \frac{W_a}{g_c} \left(\frac{r_m}{2}\right)^2 + \left(\frac{W_c + W_{ts}}{g_c}\right) r_m^2 + \frac{W_{cw}}{g_c} (5.33)^2 + K_1 \qquad (6)$$

Knowing the expressions for $W_a$, $W_c$, $W_{ts}$ and $W_{cw}$ as previously derived, the value of the constant, $K_1$, can be found from the base line values of $I_{oc} = 1441$ slug ft$^2$ at $r_m = 6.33$ ft. In this case, $K_1 = 84$. The parametric expression for centrifuge inertia then becomes:

$$I_{oc} = .1395 \, r_m^3 + 21.762 \, r_m^2 + 111.2 \, r_m - 167.5 \qquad (7)$$

Centrifuge momentum, $M_o$, is related to inertia by the expression

$$M_o = I_{oc} \, \dot{\theta}, \text{ ft-lb-sec} \qquad (8)$$

where

$\dot{\theta}$ is the angular velocity in radians/sec.

Knowing that the g loading at $r_m$ is

$$g = \frac{r_m}{g_c} \left(\dot{\theta}\right)^2 \qquad (9)$$

Equation (9) can be used to find $\dot{\theta}$ by assuming $g = 9.0$ based on the desired mechanical capability of the centrifuge for re-entry simulation. Thus:

$$\dot{\theta} = \sqrt{\frac{g g_c}{r_m}} = \frac{17}{\sqrt{r_m}} \qquad (10)$$

It is significant that equation (10) also represents the maximum disturbance frequency. Substituting equations (7) and (10) in (8), the centrifuge momentum becomes:

$$M_o = 2.375 \, r_m^{2.5} + 370 \, r_m^{1.5} + 1890 \, r_m^{1/2} - 2850 \qquad (11)$$

In calculating the counter momentum system weight, $W_{cm}$, the CMG is the dominant factor. The momentum requirement of each single axis CMG is

$$\Delta H_c = \left(\frac{M_o - 1000}{4}\right)\left(\frac{2}{\sqrt{3}}\right) \tag{12}$$

$$\frac{Torque}{\Delta H_c} = \frac{I_{oc}\ddot{\theta}}{\Delta H_c} = \frac{1441\,(.17)}{\Delta H_c} \approx \frac{1}{20}$$

From Reference 9, the weight of each CMG for a $T/H = \frac{1}{20}$ is 150 lbs. Scaling is quite linear in this range and can be approximated by:

$$W_{cm} = 2\left[.052\,\Delta H_c + 25\right] = .03\,M_o + 20 \tag{13}$$

Substituting equation (11) in (13), the counter momentum system weight becomes:

$$W_{cm} = .07125\,r_m^{2.5} + 11.1\,r_m^{1.5} + 56.7\,r_m^{1/2} - 65.5 \tag{14}$$

For the rotational drive system, the weight, $W_d$ is taken as a function of centrifuge inertia and reduces to:

$$W_d = 12\,r_m^2 - 152\,r_m + 595 \tag{15}$$

Scaling power and distribution system weight, $W_p$, as a function of $r_m$, the predominant relation is:

$$HP = \frac{I_{oc}\,(\dot{\theta})^2}{550t} \tag{16}$$

Using 140 lbs/HP as a function of the base line design and applying a linear scaling law

$$W_p = \frac{140\ I_{oc}\,(17)^2}{550\,(40)\,r_m}$$

$$W_p = .256\,r_m^2 + 40\,r_m - \frac{308}{r_m} + 204.5 \tag{17}$$

As a part of the non-rotating centrifuge weight allocation, a number of additional items must be included. These are:

$$W_x = \text{Experiment Systems and Expendables} = 200\ \text{lbs}$$

$W_{ci}$ = Weight of communications and illumination systems; taken as a function of sweep area and related by:

$$W_{ci} = .494 \, r_m^2 + 21.35 \, r_m + 23 \qquad (18)$$

$W_{vd}$ = Weight of noise and vibration damping provisions = 110 lbs

$W_{en}$ -= Non-rotating weight contingency = 100 lbs

Collecting all of the rotating and non-rotating weight items in a single expression results in a total centrifuge parametric weight function ($W_t$)

$$W_t = W_c + W_a + W_{cw} + W_{cf} + W_h + W_e + W_x$$
$$+ W_{cm} + W_d + W_p + W_{ci} + W_{vd} + W_{en} ,$$
$$= .07125 \, r_m^{2.5} + 16.74 \, r_m^2 + 11.1 \, r_m^{1.5} + 17.35 \, r_m$$
$$+ 56.7 \, r_m^{1/2} + 1709 - \frac{308}{r_m} \qquad (19)$$

Values of $W_t$ are shown plotted over the most likely range of $r_m$ by Figure 2. While a sharp increase in $W_t$ is reflected for increasing centrifuge radius, the actual weights are not so great that large radius centrifuges would be prohibitive even if experiment requirements were strongly in their favor. In fact, considering that the larger radius centrifuges would be associated with much heavier spacecraft, the percentage of the configuration weight devoted to the centrifuge is likely to decrease with increased $r_m$. Some appreciation of this trend can be obtained by including the spacecraft module and other weights with the centrifuge weight.

An approximation of the manner in which the SRC module characteristics change in relation to centrifuge radius is found from the data of Table I. This data is based on a series of point designs using the modular centrifuge housing concept illustrated in Figure 8. Adding the module and other weights to the basic centrifuge weight results in the weight variation shown by Figure 3. In terms of the percentage of total spacecraft weight, the variation from $r_c$ = 5 to 15 feet again illustrates that weight is not an overriding factor in specifying centrifuge radius. Consideration of the centrifuge as a payload may be obtained from boost capability data included in Figure 3. For the 5 foot radius centrifuge, launch of a centrifuge module, LM control station and a CSM type manned entry vehicle is beyond the capability of the TitanIIIC plus transtage. For the CSM, this would also result in a hammer head payload envelope which may have some aerodynamic problems. A more practical launch vehicle would be the Saturn-IB/Centaur which, with adaptor, would have an

8
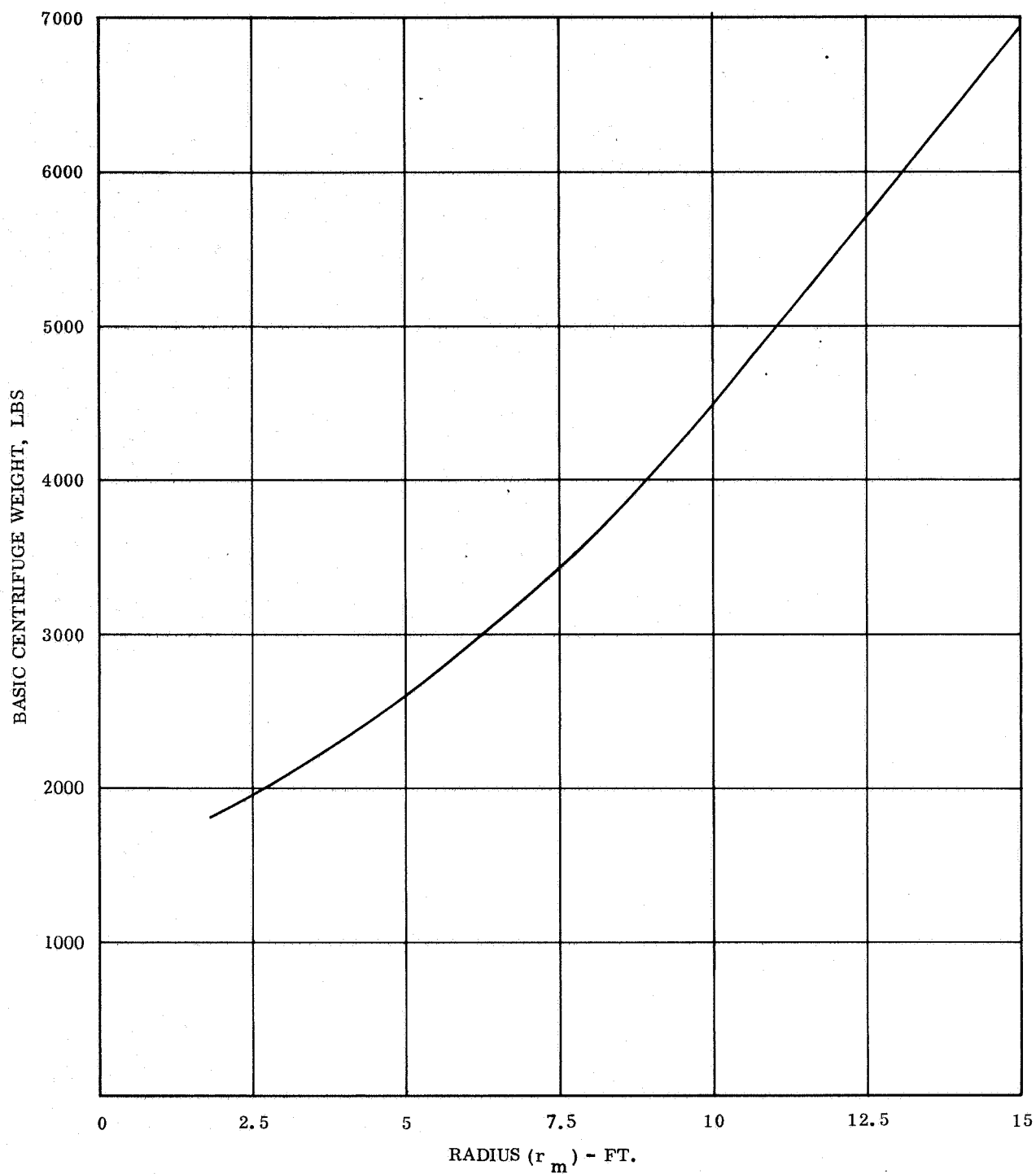
Figure 2.  Basic Centrifuge Weight as a Function of Maximum Radius
of the Test Subject c.g.

Table I.  Centrifuge Module Characteristics as a Function of Diameter

|  | MOL 10 ft. Dia. | SRC 18 ft. Dia. | S-IVB 21. 25 ft. Dia. | S-II 33 ft. Dia. |
|---|---|---|---|---|
| Rotating Mass. , lbs | 1349 | 2021 | 3432 | 4507 |
| Shell (bulkheads + cylinder), lbs | 330 | 945 | 1320 | 3050 |
| Support Structure, lbs | 386 | 543 | 646 | 866 |
| Insulation (. 69lb/ft$^2$), lbs | 216 | 464 | 585 | 1130 |
|  | 932 | 1952 | 2561 | 5046 |
| Meteoriod Shield Thickness, in. | .056 | .072 | .080 | .095 |
| Weight/ft$^2$ x 1. 34 (Normalized) | .78 | 1.04 | 1.16 | 1.36 |
| Surface Area, in$^2$ | 45,200 | 97,600 | 122,600 | 239,500 |
| Surface Area, ft$^2$ | 315 | 675 | 850 | 1,660 |

Table 2. Centrifuge Configuration Weight (lbs) as a Function of Maximum Radius

| ITEM | WEIGHT - lbs | | | |
|---|---|---|---|---|
| | $r_c = 5.00'$ | $r_c = 9.00'$ | $r_c = 10.62'$ | $r_c = 16.50'$ |
| $W_c$ | 457.0 | 457.0 | 457.0 | 457.0 |
| $W_a$ | 131.1 | 203.1 | 232.5 | 338.0 |
| $W_{cw}$ | 86.6 | 656.1 | 904.0 | 1871.0 |
| $W_{cf}$ | 260.8 | 421.0 | 485.5 | 721.0 |
| $W_h$ | 29.0 | 45.1 | 51.5 | 75.1 |
| $W_e$ | 125.0 | 125.0 | 125.0 | 125.0 |
| $W_x$ | 200.0 | 200.0 | 200.0 | 200.0 |
| $W_{cm}$ | 84.0 | 290.0 | 388.0 | 804.0 |
| $W_d$ | 260.7 | 116.0 | 165.0 | 885.0 |
| $W_p$ | 211.0 | 445.0 | 524.0 | 810.0 |
| $W_{ci}$ | 5.0 | 40.0 | 55.8 | 135.0 |
| $W_{vd}$ | 110.0 | 110.0 | 110.0 | 110.0 |
| $W_{en}$ | 100.0 | 100.0 | 100.0 | 100.0 |
| Basic Centrifuge | 2060.2 | 3208.3 | 3796.3 | 6631.1 |
| SRC Module | 932.0 | 1952.0 | 2561.0 | 5046.0 |
| ECS & Interface | 880.0 | 880.0 | 880.0 | 880.0 |
| SRC | 3872.2 | 6040.3 | 7237.3 | 12557.1 |
| LM and Sys. | 5900.0 | 5900.0 | 5900.0 | 5900.0 |
| LM/SRC | 9772.2 | 11940.3 | 13137.3 | 18457.1 |
| Stab. Propellant | 1879.0 | 1879.0 | 1879.0 | 1879.0 |
| Life Support | 3400.0 | 3500.0 | 3600.0 | 4000 |
| De-orbit Propellant | 1300.0 | 1300.0 | 1300.0 | 1300.0 |
| CSM | 23900.0 | 23900.0 | 23900.0 | 23900.0 |
| | 40251.2 | 42519.3 | 43816.3 | 49536.1 |
| Contingency | 200.0 | 200.0 | 200.0 | 200.0 |
| CSM/LM/SRC | 40451.0 | 42719.0 | 44016.0 | 49736.0 |
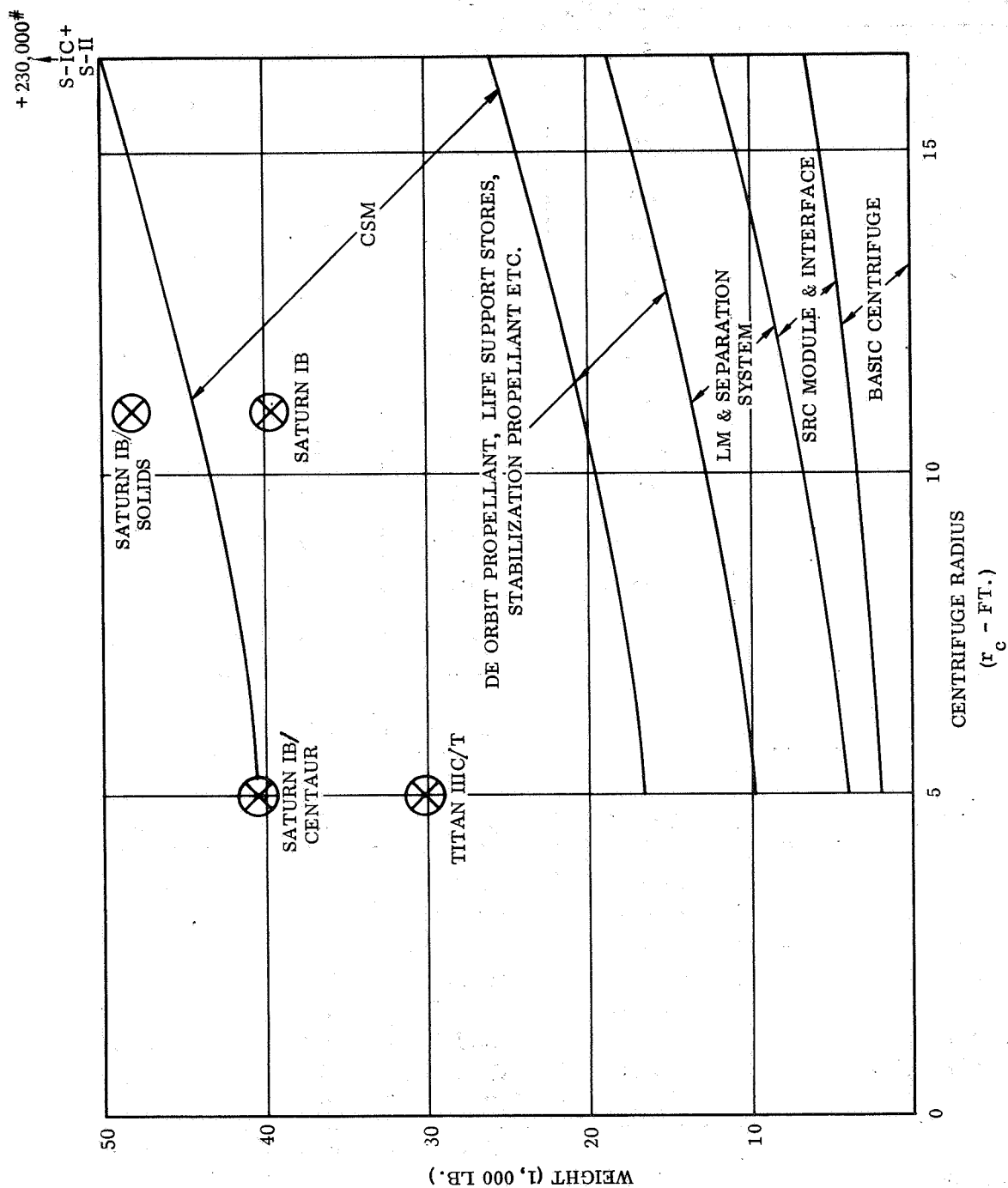
Figure 3. Total Experiment Weight as a Function of Centrifuge Radius and Available Boosters.

CENTRIFUGE RADIUS ($r_c$ – FT.)

WEIGHT (1,000 LB.)

+230,000#
S-IC +
S-II

SATURN IB/
SOLIDS

SATURN IB

CSM

DE ORBIT PROPELLANT, LIFE SUPPORT STORES,
STABILIZATION PROPELLANT ETC.

LM & SEPARATION
SYSTEM

SRC MODULE & INTERFACE

BASIC CENTRIFUGE

SATURN IB/
CENTAUR

TITAN IIIC/T

adequate payload weight capability and envelope. For intermediate sized units up to $r_c = 10.5$ ft, the Saturn-IB is the appropriate booster. At 10.5 ft $r_c$, the full configuration, including CSM, is slightly beyond Saturn-IB capability to a 250 n. mi. orbit and would require some sort of uprating such as the addition of 120 in. solid rockets as a 0 stage. Alternately, two Saturn-IB launches with a split payload would suffice. For centrifuge module and spacecraft configurations between 10.5 and 16.5 ft, launch by an S-IC/SII combination is indicated. Here, the centrifuge spacecraft weight is only a small fraction of the total payload capability.

Centrifuge space utilization. - Many spacecraft configuration studies have shown that space rather than weight is the limiting design parameter. This is particularly the case in the Workshop and EOSS versions of the S-IVB. As orbital stay-times lengthen, increasingly larger allocations are being specified for crew facilities, storage and experiment volume. The efficiency with which the centrifuge employs its required experimental volume is, therefore, an important optimizing criteria. If we designate the centrifuge module volume as $V_m$ and the actual volume occupied by the machine as $V_c$, then we may express space utilization efficiency as:

$$\eta_s = \frac{V_c}{V_m} \tag{20}$$

Considering the centrifuge hub volume central support frame, counterweight enclosure and couch volume as fairly constant over the applicable range of $V_c$, then a simple expression for the volume change with $r_c$ can be derived. This function, which is plotted in Figure 4, is found to be:

$$V_c = 9.88\, r_c + 258.5 \tag{21}$$

If the volume of the centrifuge module is taken to be the sweep volume of the machine with a clearance allowance of 6 inches from the center frame, then $V_m$ is simply:

$$V_m = 8.7\,\pi\,(r_c + .5)^2 \tag{22}$$

This factor is also shown in Figure 4 and represents minimum space requirement of the unit which optimistically may be achieved in installations such as the EOSS. In the modular concepts, the volume requirements will be somewhat greater because the module closures will be pressure bulkheads rather than mearly separators. The optimistic volume utilization factor for the centrifuge is then:

$$\eta_s = \frac{9.88\, r_c + 258.5}{8.7\pi\,(r_c + .5)^2} \tag{23}$$
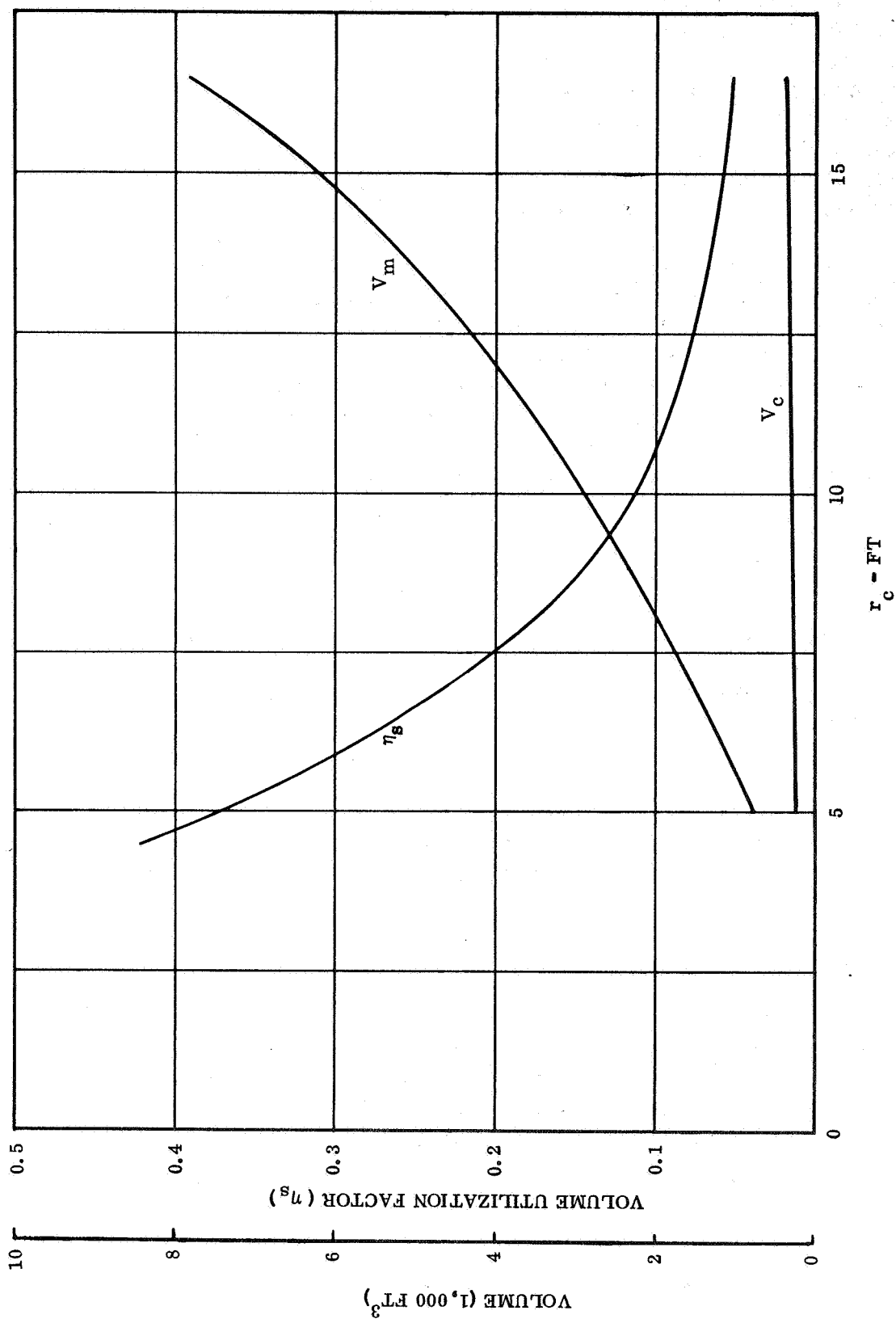
Figure 4.  Centrifuge Volumes and Volume Utilization Efficiency
as a Function of Maximum Radius

This function is plotted in Figure 4. While even small radius machines do not exhibit particularly good space efficiency, the desirability of keeping the centrifuge radius as small as is consistent with experiment requirements is clearly indicated with respect to this parameter.

Drive motor power. - The possibility that large radius centrifuges would require excessive power or impose some undesirable motor development requirements was investigated by developing a parametric expression for motor horsepower in terms of centrifuge radius. A factor of 1.5 was assumed to cover electrical efficiency, bearing loss and aerodynamic effects. Then, for maximum acceleration,

$$ HP = \frac{1.5\,I_{oc}\,(\dot{\theta})^2}{550\,(40)} \tag{24} $$

Knowing expressions for $I_{oc}$ and $\dot{\theta}$ from equations (7) and (10), horsepower becomes:

$$ HP = .01975 \left[ .1395 r_m^2 + 21.762 r_m + 111.2 - \frac{167.5}{r_m} \right] \tag{25} $$

This horsepower relationship is seen ploted in Figure 5. In the 5 to 10 foot $r_c$ range, power is shown to be quite modest. Even for the 15 foot machine, the power requirement of 8 horsepower is not unduly compromizing. While the desirability of minimizing radius is shown for this parameter, it is not a strong factor in configuring the device.

Disturbance frequence. - A detail evaluation of the implications of centrifuge unbalance and frequency effects is given in the stability and attitude control section of the report. One of the most significant factors revealed by this work is the importance of keeping the disturbance frequency of the centrifuge well separated and below the first bending mode frequencies of the spacecraft. As a general rule, fewer dynamic and control problems are likely to occur if the centrifuge disturbance frequencies are kept as low as possible. In as much as disturbance frequency decreases with increased centrifuge radius, this becomes one of the few factors which favor a larger radius machine than is necessary from an experimental standpoint. While this factor is very difficult to treat in general terms because of the elusiveness of spacecraft bending criteria, parametric presentation does reveal some interesting trends. If we use equation (1) in equation (10) and plot the values of $\dot{\theta}$ vs $r_c$ over the range of experiment centrifugal force requirements, a region of probable disturbance may be established. This is shown in Figure 6. Taking bending data points such as are provided by references 7 and 8 and using the observation that the more massive the spacecraft becomes . (larger $r_c$) the lower its natural frequency is likely to be, a region of possible bending frequency occurance can be deduced. Superimposing the bending frequency region on the disturbance frequency region in Figure 6 reveals a high probability of coincidence between these mutually exclusive parameters unless specific steps are taken to avoid it. Further inspection reveals these general trends:
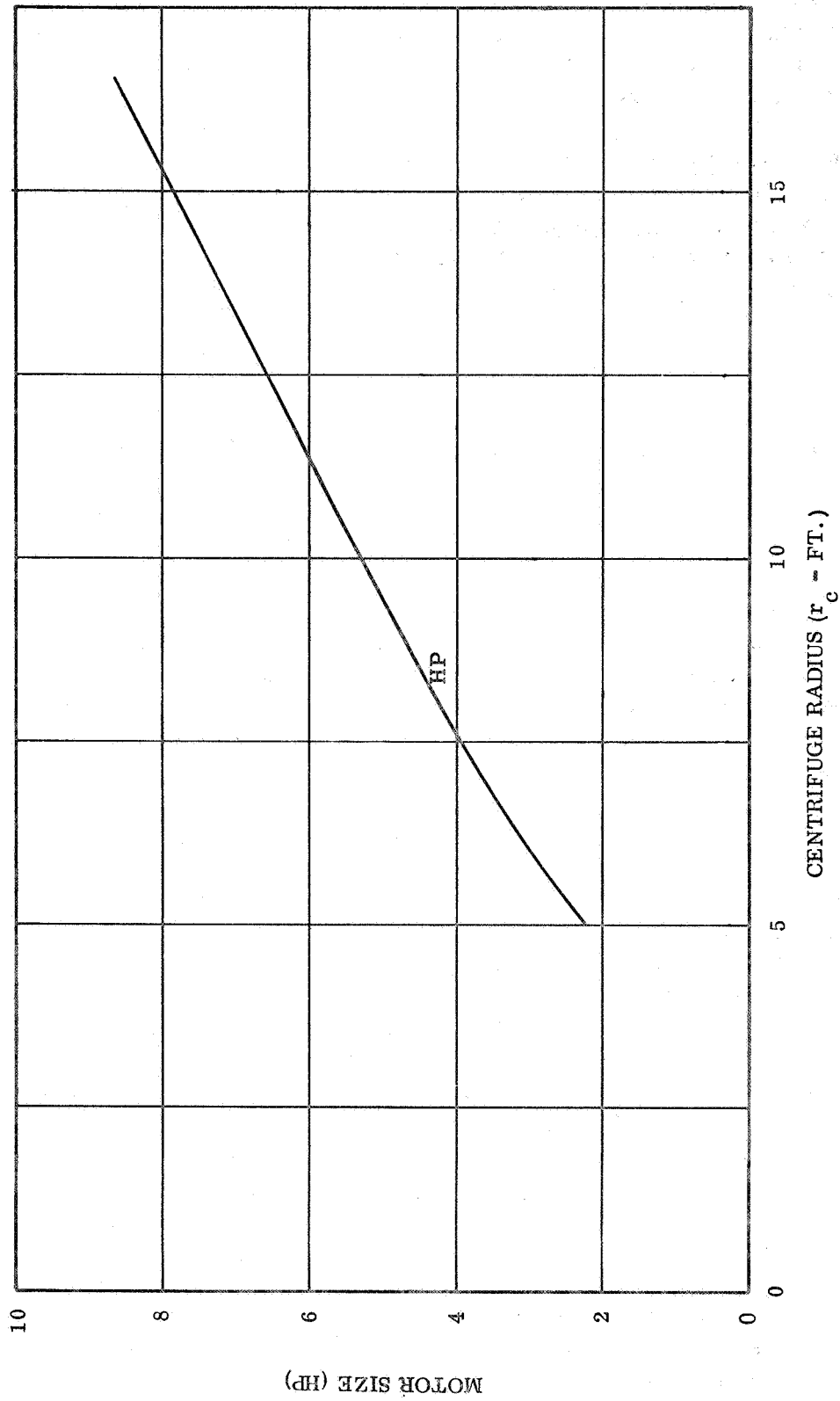
Figure 5. Centrifuge Power Characteristics
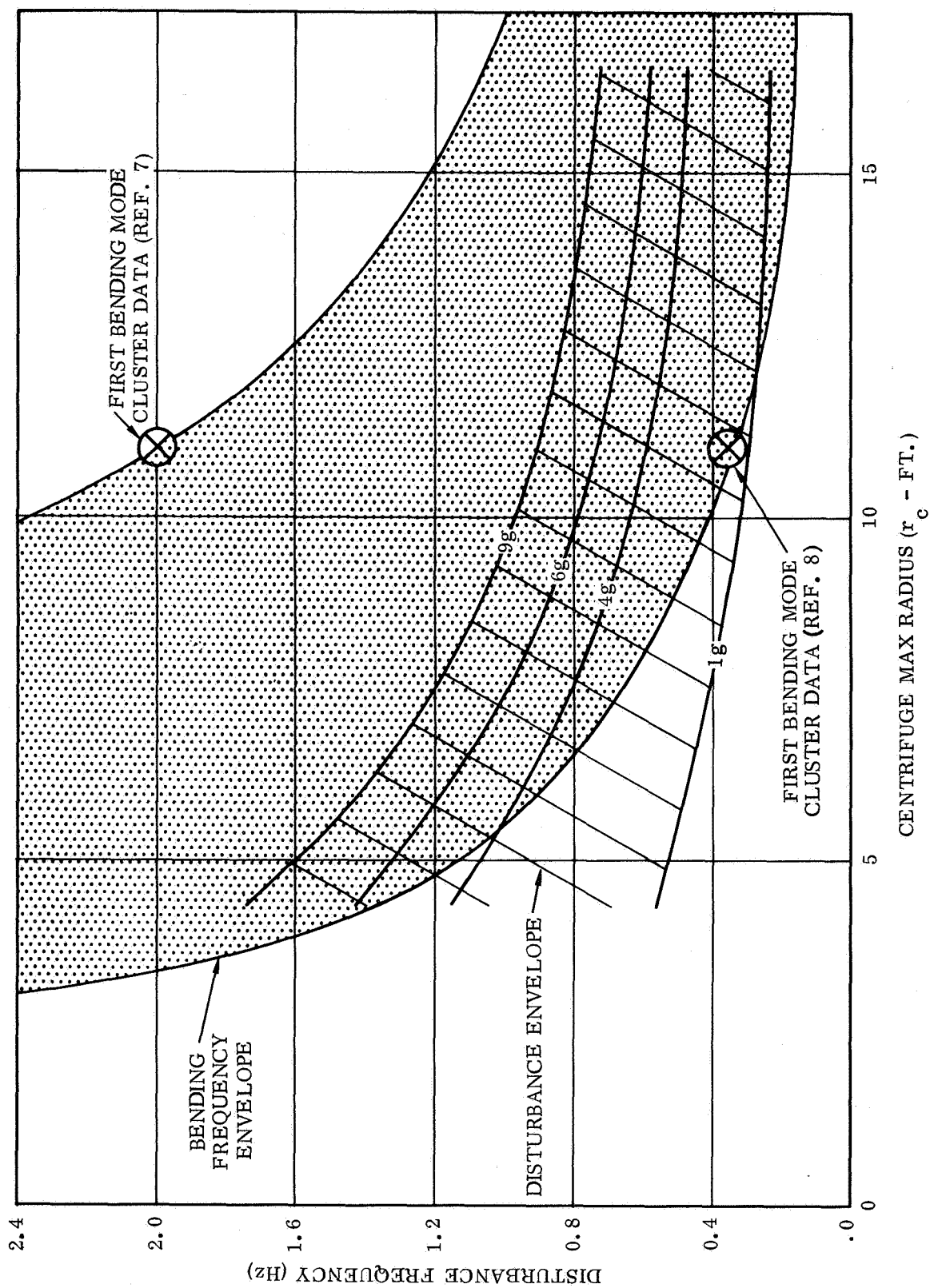
Figure 6 – Disturbance Frequency

a.  Most of the advantages of a larger radius have been gained at an $r_c$ of 10 or 11 ft. and further increase in $r_c$ will probably be counteracted by the tendency to lower bending frequencies.

b.  Reducing disturbance frequency by lowering experimental g capability, for instance, from 9-g to 6-g maximum, is not significant enough to be attractive.

c.  The installation of a small radius centrifuge in a large diameter vehicle does not appear to be practical in the extremes. Up to an $r_c$ of 10-11 ft, the tendency will be to utilize the full diameter of the stage available for installation.

In general, the installation of the centrifuge should be included as an integration factor early in spacecraft configuration studies so that the tendency to low bending frequencies may be counteracted by appropriate design.

Cross-coupled acceleration. - A final aspect in the question of centrifuge radius selection is the reaction of the test subject to short radius operations. The factor in question is mainly the cross-coupled accelerations produced by head turns out of the plane of centrifuge spin. If we designate this cross-coupling as $\Psi$, then

$$\Psi = \dot{\theta} \times \omega \tag{26}$$

where

$\dot{\theta}$ = Centrifuge angular velocity, rad/sec.

$\omega$ = Head turn rate, rad/sec.

To evaluate the significance of this factor, a limit of $\Psi = 100^{\circ}/\text{sec}^2$ may be assumed at which performance degradation and disorientation may occur from the resulting stimulation. This is consistant with the experimental work of References 10 and 11. For the orthogonal case, the limiting condition becomes simply:

$$\omega = \frac{1.745}{\dot{\theta}} \tag{27}$$

Introducing $\dot{\theta}$ from equation (10) results in:

$$\omega = 1.745 \sqrt{\frac{r_c - 2.16}{32.2g}} \tag{28}$$

This relationship is plotted in Figure 7 for various levels of g required by experimentation. It is evident that head turning activities will be limited at high-g with the short radius machine but even at 15 ft. the situation is not improved significantly enough to make this an attractive solution. A better approach is to eliminate head turning at high-g which is the case in the experiment protocols now specified.
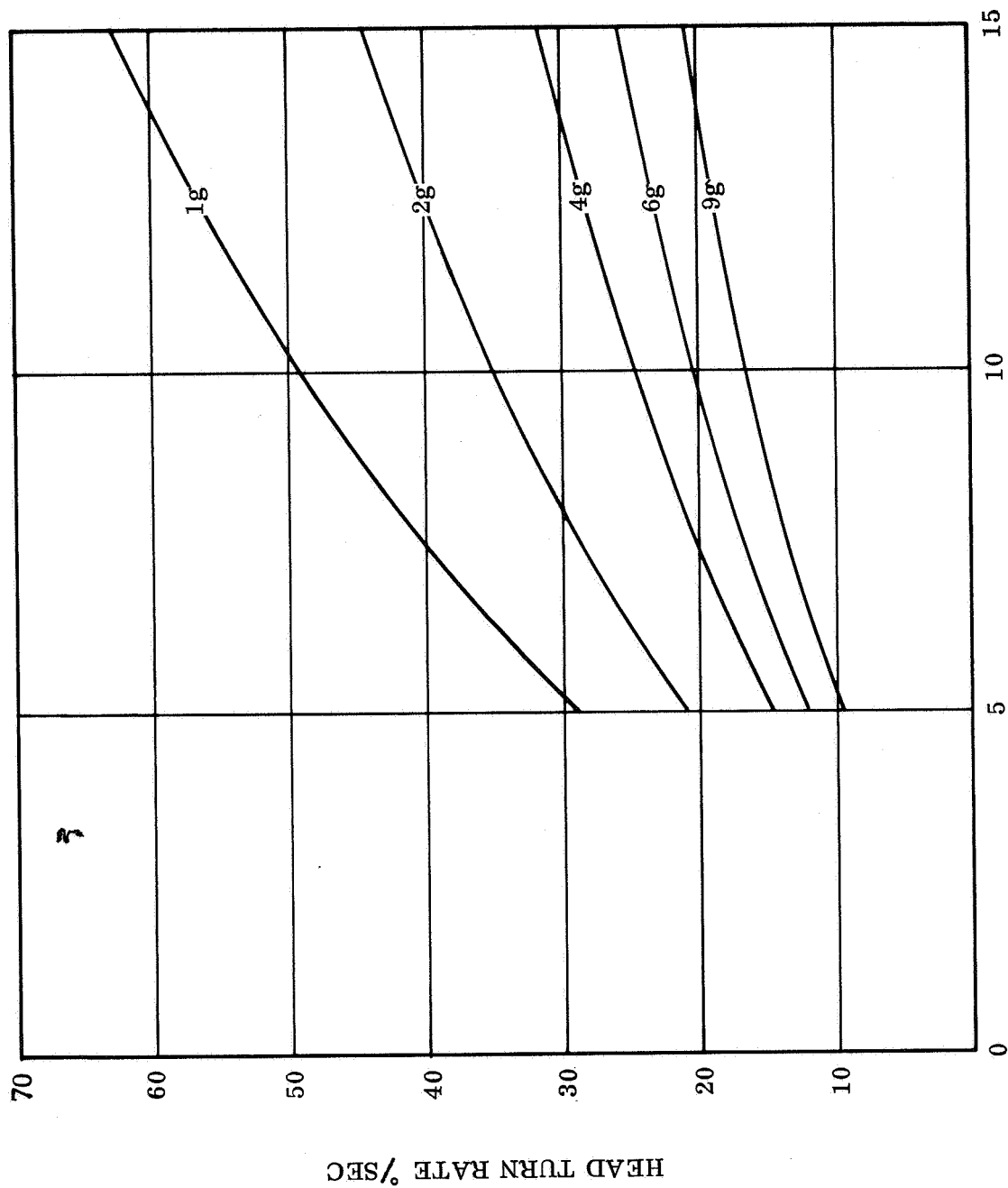
Figure 7. Head Turn Rate as a **Function** of Centrifuge Radius for $100^\circ/\sec^2$ Cross Coupling Acceleration.

Radius selection. - Having observed the behavior of significant parameters as a result of varying centrifuge radius, the question remains, where within the range studied should the centrifuge radius be fixed? Clearly, no firm optimum presents itself but the bandwidth of acceptability can be narrowed to reasonable limits. Considering the lower side of the range of $r_c$ in terms of experiment requirements the 5 ft. radius machine is seen to have an effective arm of only 2.84 ft. This is quite restrictive to subject manipulation and in achieving radial difference for experiments in which radius is a factor. Considerable experimenter resistance has been found to fixing radius at so short a length and this resistance does not diminish until an $r_c$ of 7 or 8 ft. is reached. From the standpoint of weight, volume efficiency and power, the radius should remain at about this minimum. On the other hand, disturbance frequency and cross-coupling effects are relieved by specifying a slightly larger radius, in the range of 10 to 11 ft. In this range, the 22 ft. diameter of the S-IVB stage is the logical candidate and with clearance requirements will fix the upper radial limit of the centrifuge at 10.5 ft. For this study further considerations of installation and launch requirements have resulted in the selection of 8.5 ft radius as the optimum consistent with both modular launch and direct spacecraft incorporation.

## Installation Configuration Trade-Off Studies

In early contract studies, various applications and installations of the centrifuge were reviewed with the object of selecting a single base line configuration to be examined in detail as to its feasibility as an experiment. This approach was taken in order to allow concentration of sufficient effort on the base line. In general, the configurations examined were selected to differentiate between vehicles involving:

 a. Apollo CSM/LM Stationary centrifuge module

 b. Apollo CSM/LM/Rotating centrifuge module

 c. Apollo LM/Stationary centrifuge module/S-IVB workshop cluster

 d. S-IVB workshop/centrifuge installation

 e. S-IVB, EOSS (dry launched)/centrifuge installation

The method used to make this differentiation was a numerical rating scheme based on selected parameters which are most influential in establishing feasibility of the gross configuration. The resulting ratings are summarized in Table 3. As this type of evaluation is highly subjective, no absolute significants should be assigned to the numerical totals. Only relative values are of significance. The rating should be considered only as a method of presenting a balanced opinion based on present knowledge of the factors involved.

Basic module identification. - The basic modules used in the various configurations are identified as follows and grouped as illustrated in Figures 8 through 18:

 A. Extended capability Command and Service Module (CSM)

 B. LM Lab. - AES LM with extended mission capability (45-90 day)

  1. LM Lab. Same as (b) but detachable from centrifuge module

 C. Space Research Centrifuge (SRC) Module - configured for permanent attachment to LM Lab. Access to SRC Module through tunnel from LM side docking hatch. Separate docking hatch located at center of SRC lower bulkhead.

  1. SRC Module configured for permanent attachment to LM Lab. Optional separation from SLA (S-IVB stage). Side docking hatch is provided for CSM docking or emergency/resupply docking.

  2. SRC Module configured for separation from LM Lab after launch. Axially symetric docking hatches provided in both top and bottom bulkhead of SRC.

3. SRC Module configured for separation from LM Lab after launch. Docking hatches for CSM and LM Lab provided at opposite sides of of cylindircal section of SRC as slightly offset to prevent centrifuge arm from simultaneously blocking both openings.

4. SRC Module configured for rotation as an integral unit. SRC is permanently attached to LM Lab at rotation interface. Access to SRC provided by tunnel from LM side hatch to rotating interface. Expandable structure and counter balance may be hardened after deployment or used to provide variable radius.

5. SRC Module configured from S-IVB stage. (Consider both wet or dry launched versions.)

D. S-IVB Spent Stage used as stabilizing mass or housing.

Configuration trade-off factors. - Combinations of the basic modules were selected which emphasize differences in the selected trade-off criteria. These factors and their weighted relationship are:

|  | | | POINT VALUE (Best Configuration) |
|---|---|---|:---:|
| 1. | Orbital Assembly Time | Vehicle Docking Systems Tie-in Checkout | 10 |
| 2. | Dynamic Stability | | 10 |
| 3. | Structural Complexity | Launch Configuration Orbital Configuration | 5 |
| 4. | Relative Reliability - Operational | | 20 |
| 5. | Relative Complexity | Existing Equipment Changes New Systems | 10 |
| 6. | Relative Cost | | 10 |
| 7. | Weight Difference | | 5 |
| 8. | Safety | | 30 |
| | | Maximum Total | 100 |

Baseline installation selection. - Based on the evaluation criteria and weighting values outlined, a clear preference is shown for the dry launched S-IVB (EOSS) as a gross installation base line. While this may be optimum from the standpoint of centrifuge feasibility, consideration must also be given to the validity of this choice in terms of probable future missions and the type of hardware which will be available. Some observations which support the selection of the EOSS base line are:

a.   Centrifuge is identical for EOSS or LM/SRC module installation

b.   EOSS installation allows study of centrifuge interaction with cluster bending frequencies and elastic behavior.

c.   EOSS installation allows study of centrifuge experiment integration with low "g" experiments, ATM operation and other experiment activity proposed for the zero "g" clusters and space stations.

d.   SRC module is a simple uncomplicated state-of-art structure. Depth of detail presently available from the trade-off study is sufficient to provide preliminary data should this approach become a preferred flight installation.

e.   In the event that the S-IVB workshop is the only available configuration in which to use the centrifuge, the study indicates that a cluster associated LM/SRC module will be more economical than a tank installed, $LH_2$ qualified machine. Dynamic problems and experiment integration in such a cluster arrangement will be similar to those evaluated in treating the EOSS as the base line installation.

On the other hand, the cluster associated LM/SRC is also an excellent installation. Justification for this approach is based on the following observations:

a.   The centrifuge is again applicable to both installations.

b.   Cluster LM/SRC installation still allows study of the centrifuge interaction with bending frequencies.

c.   Study based on the cluster LM/SRC installation will result in subsystems definition applicable to the modular concept.

d.   In the event that the EOSS becomes the available configuration, sufficient background will be established to allow installation in the EOSS or docking of the LM/SRC to the EOSS.

In addition to the EOSS and cluster associated installations, the CSM/LM/SRC module approach rates high as a possible orbital configuration particularly in the AB(C1) and AB(C1) D versions.

As a result of these observations, the study effort has been directed toward definition of a base line centrifuge which is common to these three most promising installations.

ORBITAL

ACCESS TUNNEL

CENTRIFUGE SPIN PLANE

RESUPPLY/RESCUE DOCKING

CENTRIFUGE SPIN AXIS

A

B

C

LAUNCH

IU

S-IVB

A

B

C
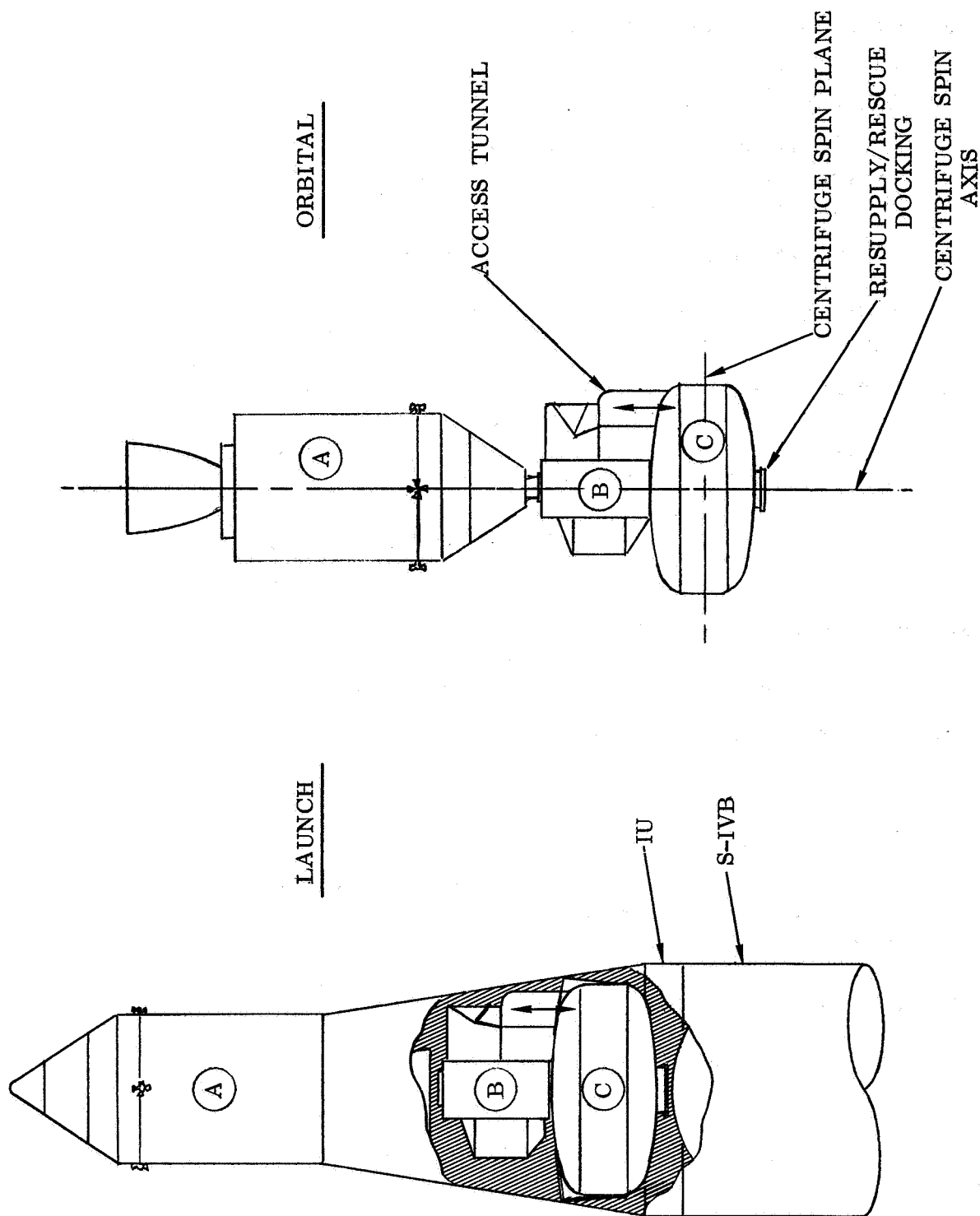
Figure 8. SRC Configurations ABC.
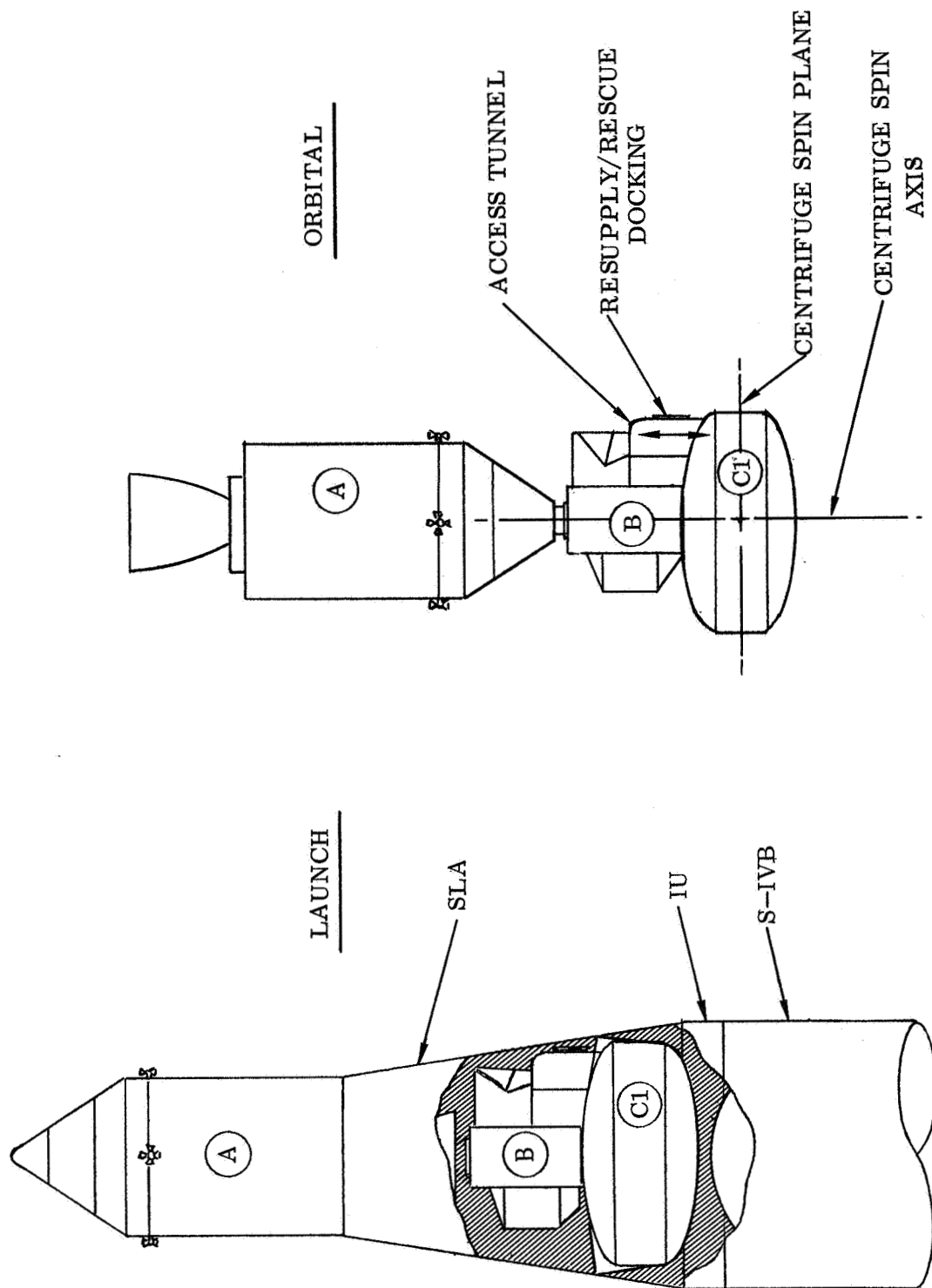
Figure 9. SRC Configuration AB(C1)

ORBITAL

ACCESS TUNNEL

RESUPPLY/RESCUE DOCKING

CENTRIFUGE SPIN PLANE

CENTRIFUGE SPIN AXIS

A

B

C1

LAUNCH

SLA

IU

S-IVB

A

B

C1

ORBITAL CONFIG.

LAUNCH SAME AS AB(C1)

A

ACCESS TUNNEL

RESUPPLY/RESCUE DOCKING

B

C1

CENTRIFUGE SPIN PLANE

D

CENTRIFUGE SPIN AXIS
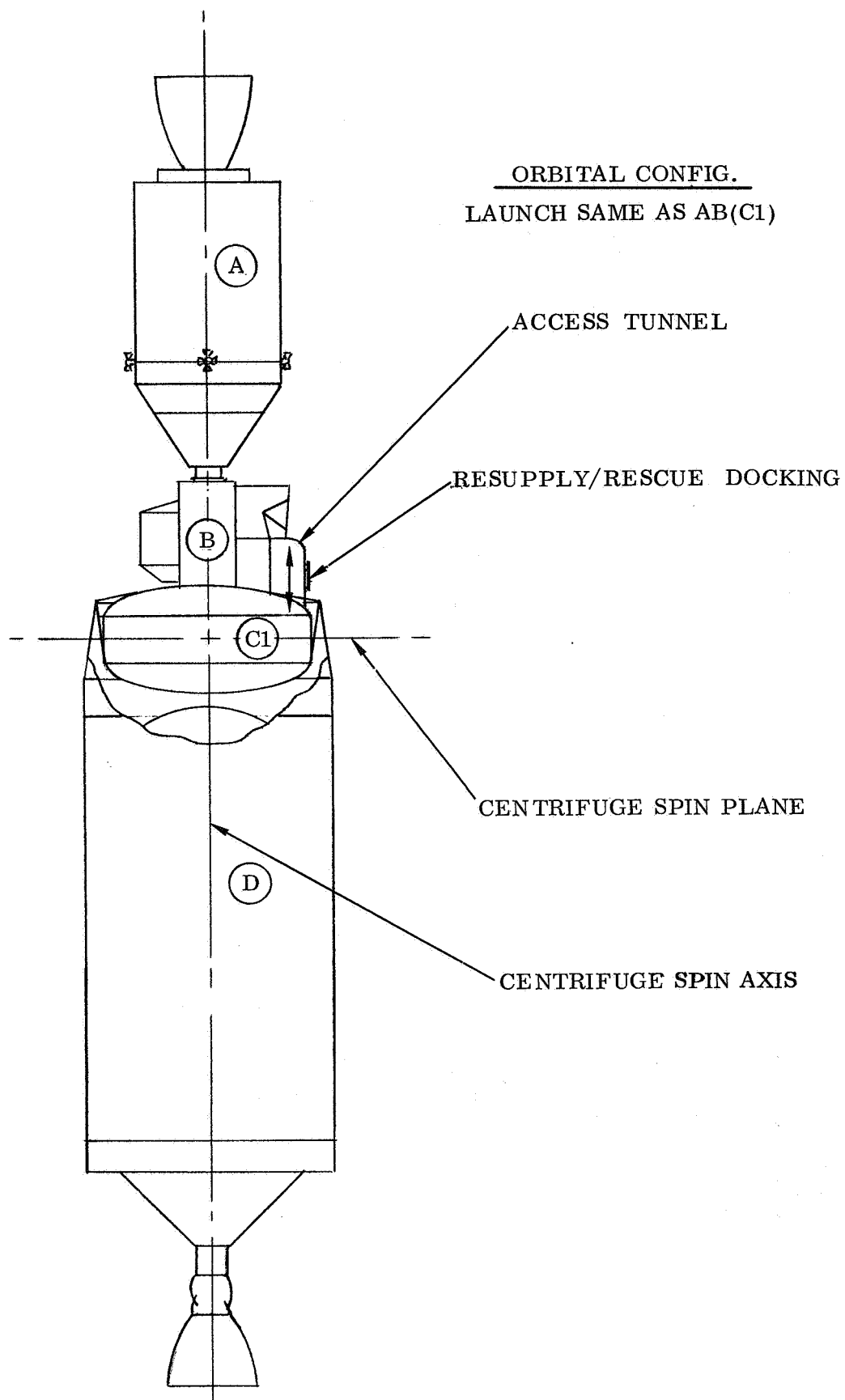
Figure 10. SRC Configuration AB(C1)D.

SPIN AXIS

SPIN PLANE

ORBITAL
LAUNCH SAME AS AB(C1)

Figure 12.   SRC Configuration BA(C1)

ORBITAL
(LAUNCH SAME AS ABC)
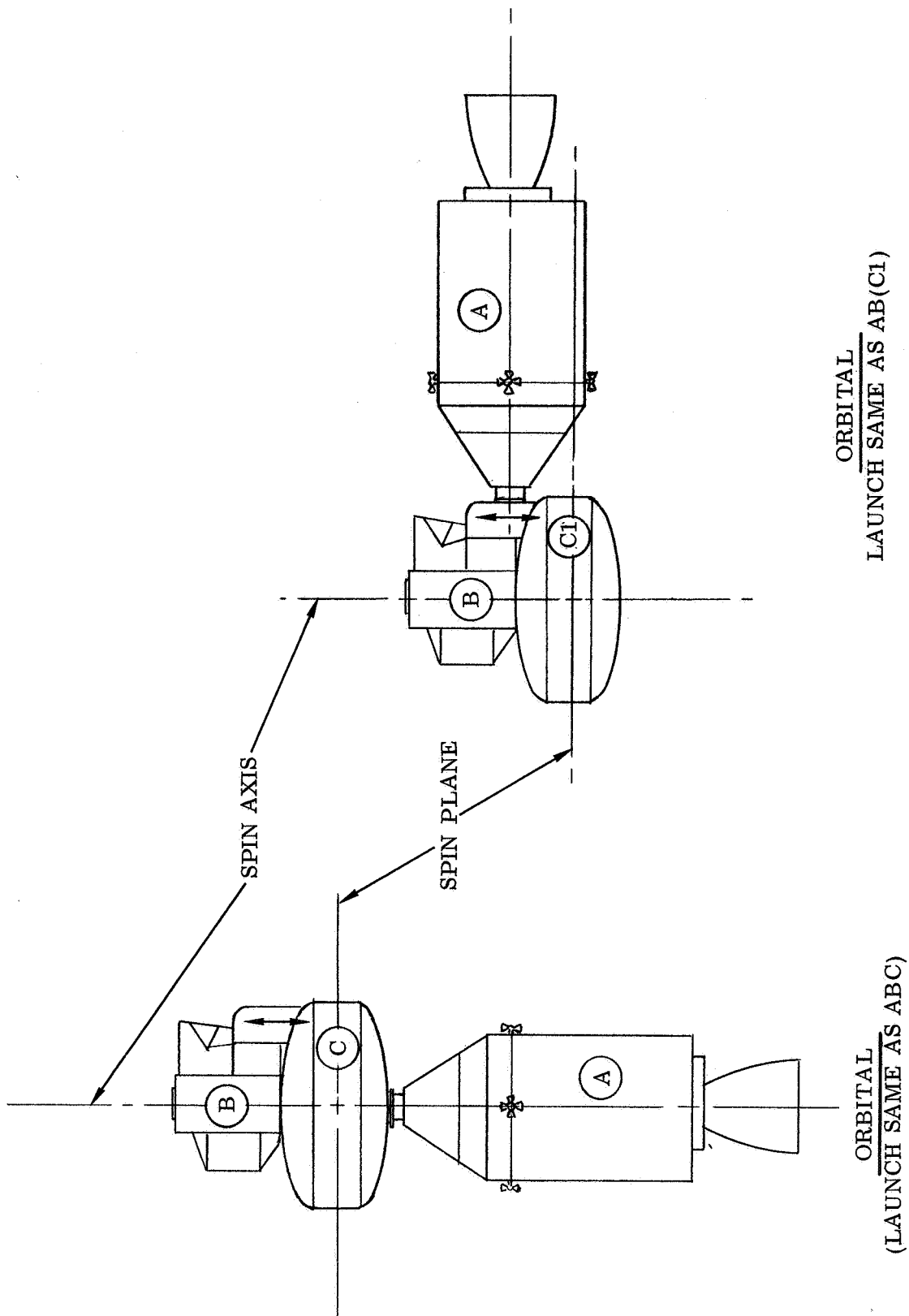
Figure 11.   SRC Configuration, BCA

Figure 14.    SRC Configuration A(C2) (B1)

Figure 13.    SRC Configuration A9C3) (B1)
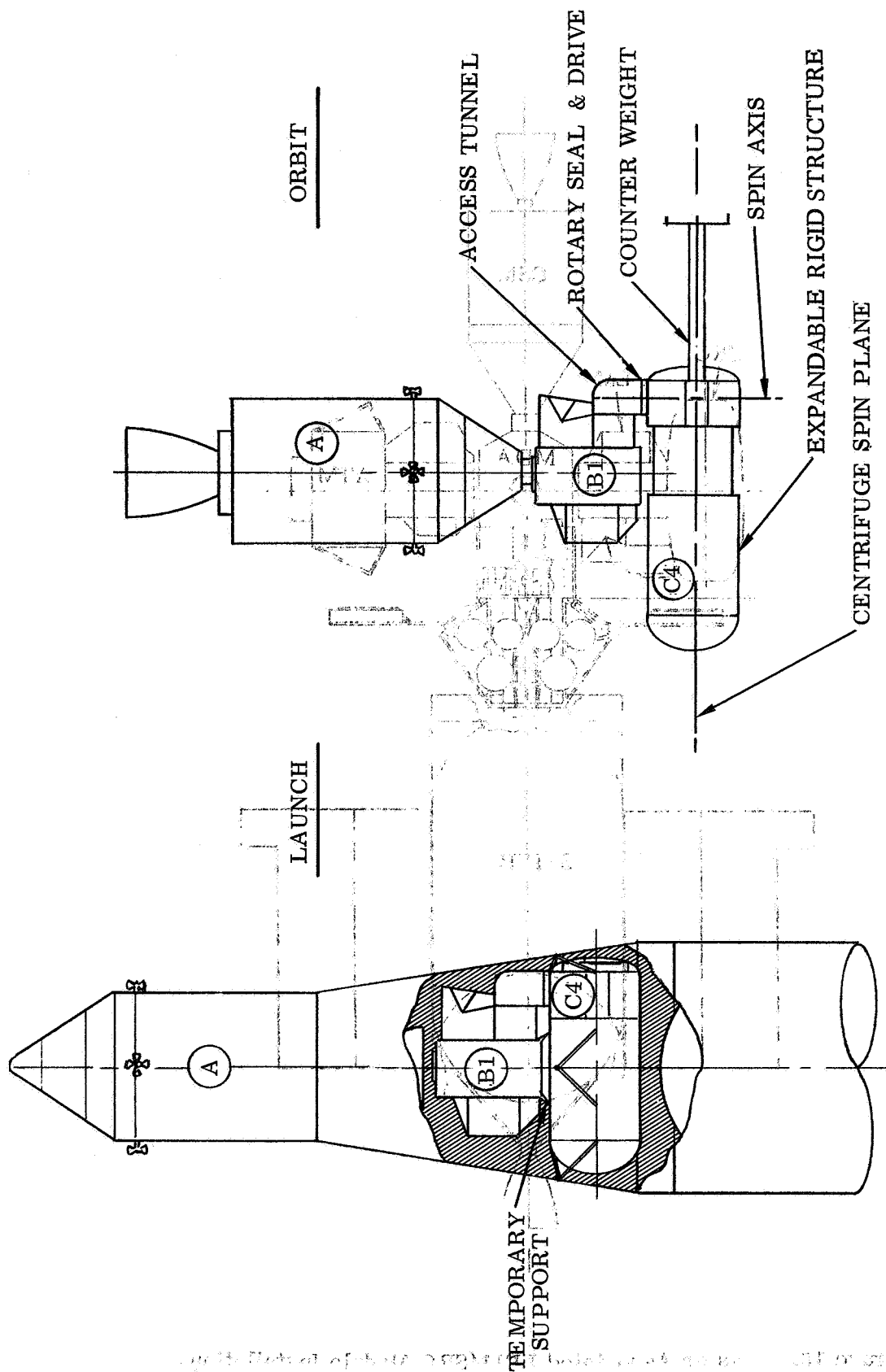
**Figure 15.** SRC Configuration A(B1) (C4)

ORBIT

ACCESS TUNNEL

ROTARY SEAL & DRIVE

COUNTER WEIGHT

SPIN AXIS

EXPANDABLE RIGID STRUCTURE

CENTRIFUGE SPIN PLANE

LAUNCH

TEMPORARY SUPPORT
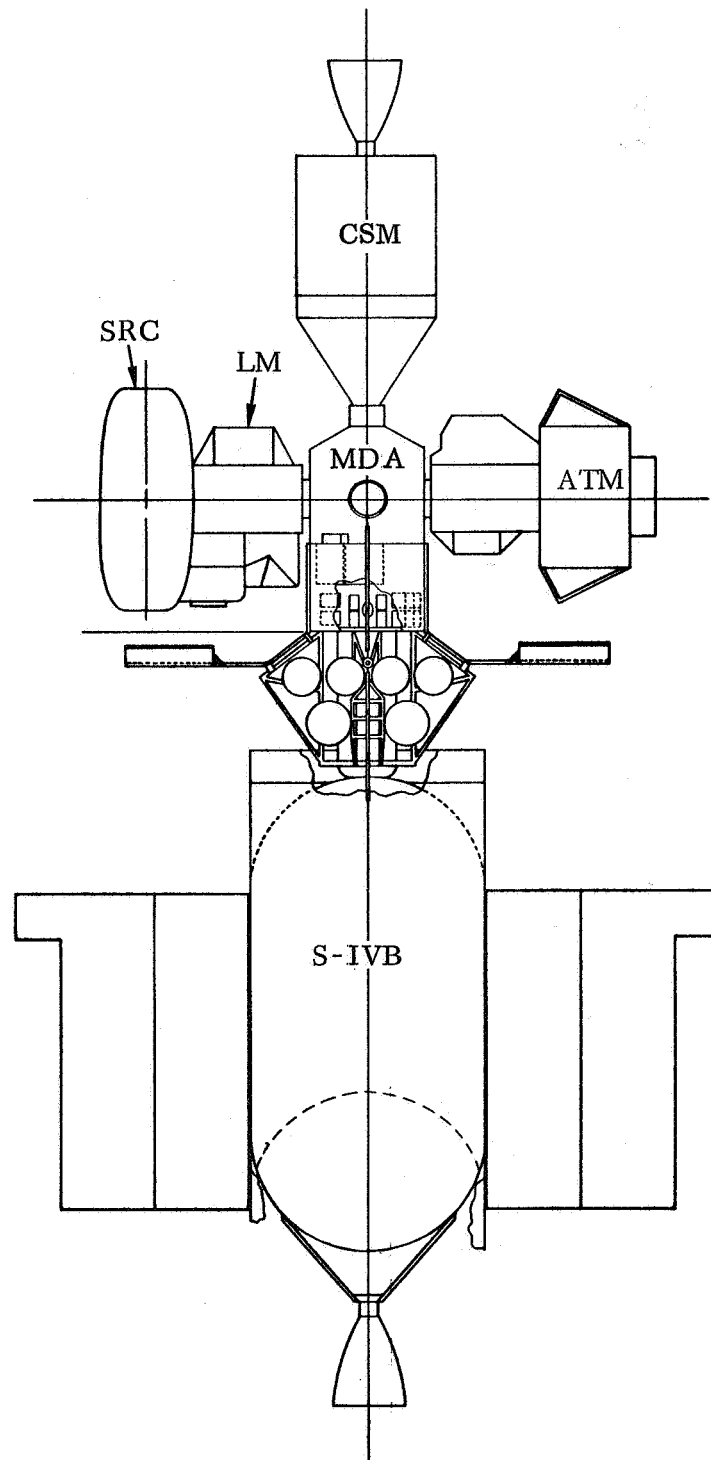
Figure 16.   Cluster Associated LEM/SRC Module Installation.

MAX LENGTH
SATURN 1B FAIRING

MDA TYPE
AIRLOCK MODULE

APPLICABLE CENTRIFUGE
LOCATIONS

LAUNCH NO. 3
SPENT STAGE
NO. 2

CLAM SHELL DOORS
PREPACKED/INSTALLED
EXPERIMENTS

LAUNCH NO. 1
LCSM NO. 1

LAUNCH NO. 2
SPENT STAGE
NO. 1

SOLAR ARRAY
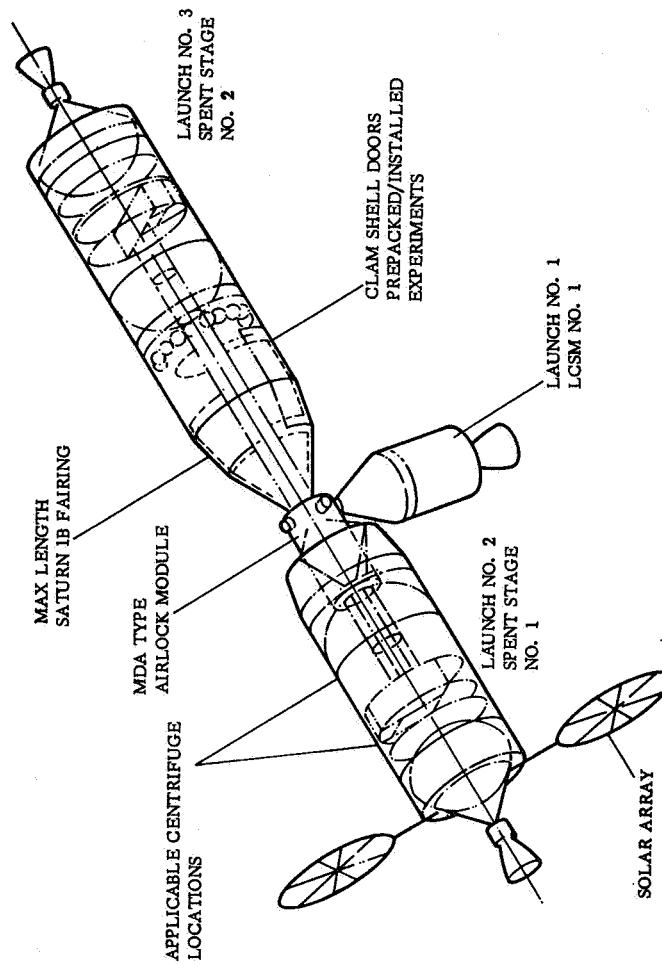
Figure 17. S-IVB Workshop Installation (WS-LO-C Configuration, Douglas).

MDA

CORE MODULE

EXPERIMENT BAYS

SRC

SRC SUPPORT

APOLLO DOCK
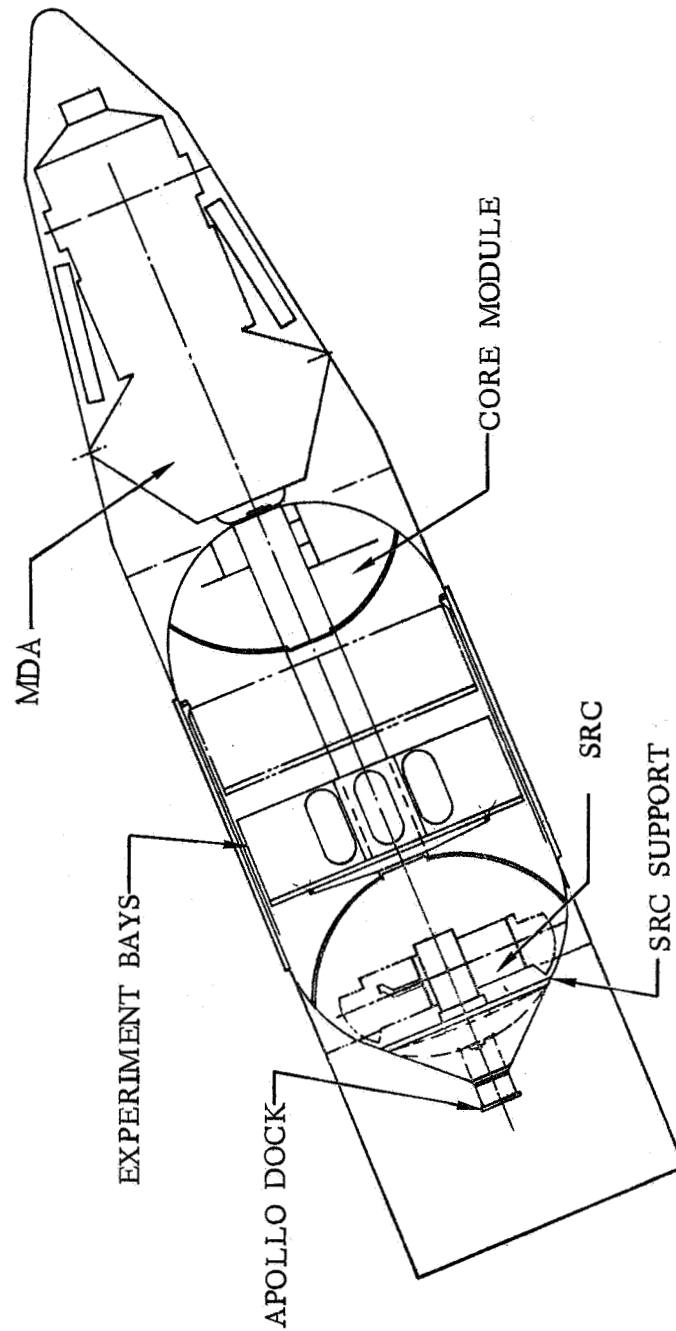
Figure 18. S-IVB – (EOSS) Configuration.

Table 3. – Rating Comparison Chart

| Criteria | | | | | CONFIGURATION | | | | | | |
|---|---|---|---|---|---|---|---|---|---|---|---|
| | ABC | AB(C1) | AB(C1)D | BCA | BA(C1) | A(C3)(B1) | A(C2)(B1) | A(B1)(C4) | LEM/SRC) Cluster | Workshop/ Centrifuge | EOSS/ Centrifuge |
| Orbital Assembly Time | 9 | 9 | 9.5 | 8 | 8 | 5 | 5 | 6 | 7 | 0 | 10 |
| Dynamic Stability | 8 | 8 | 6 | 8 | 6 | 6 | 8 | 6 | 5 | 4 | 6 |
| Structural Complexity | 4 | 4.5 | 5 | 4 | 4.5 | 3 | X | 1 | 4.5 | 5 | 5 |
| Relative Reliability | 14 | 14 | 19 | 14 | 14 | 9 | 9 | 5 | 14 | 7 | 19 |
| Relative Systems Complexity | 5 | 5 | 5 | 5 | 5 | 3.5 | 3.5 | 4 | 5 | 5 | 5 |
| Relative Cost | 5 | 5 | 5 | 5 | 5 | 4 | 4 | 3 | 5 | 5 | 10 |
| Weight Difference | 3 | 3.5 | 4 | 2.5 | 3.5 | 2.5 | 2.5 | 1 | 4.5 | 5 | 0 |
| Safety | 25 | 25 | 26 | 24 | 25 | 23 | 23 | X | 25 | 15 | 30 |
| Total | 73 | 74 | 77.5 | 70.5 | 71 | 56 | 55 + X | 26 + X | 70 | 46 | 85 |

# STABILITY AND ATTITUDE CONTROL
# FEASIBILITY ANALYSIS

## Preliminary Considerations

This portion of the study evaluates the dynamic feasibility of orbiting a specially designed centrifuge to accommodate the performance of particular experiments in a zero-g environment.

Analysis of the specified experiments has configured the centrifuge as shown in Figure 75. In space the centrifuge will be hardmounted to the spacecraft through the primary rotation drive. Ideally, the spacecraft should be an inertially and angularly fixed support for the centrifuge spin axis. That is, it is undesirable that the spacecraft installation inject any extraneous accelerations to the subject due to spacecraft angular motion.

In operation, the spacecraft will move in response to perturbing torque sources from the environment, from the installation (man-motion), and from centrifuge itself (unbalance). The question of feasibility reduces to comparison of realistic experiment requirements with the effects of the perturbing torques. The purpose of many of the experiments is to obtain physiological data associated with man's response to low level linear and angular accelerations induced in a controlled manner by the various couch controls and centrifuge primary spin. Based upon anticipated low level data points established by GD/C-Langley experimenter coordination, the experiment requirements were set one order of magnitude below the lowest level data point anticipated. It should be mentioned that the requirements adopted are thought to be conservative, that is, they are subject to change as a function of experiment design, but it is more probable that the requirements be relaxed rather than become more stringent.

Figure 75 lists the pertinent centrifuge information regarding spin inertia, primary rotation rpm, angular momentum ranges, rotating weight and overall dimensions which immediately characterize the machine as a sizeable rotating mass with a large range of variability in momentum. As the centrifuge is accelerated up to speed, equal countertorque must be exerted on the spacecraft to avoid spacecraft motion. In addition, the mass distribution changes due to couch position, orientation, and subject/equipment variation, etc., must be compensated to the extent that the rotating body center of mass lies on the physical spin axis and also that the principal inertial axis of the centrifuge be maintained in alignment with the spin axis. Observance of these requirements places the centrifuge in balance for the same reason that automobile wheels are periodically balanced, that is, to avoid generating unbalance torques which induce motion of vibratory character at spin frequency.

In Phase I of the centrifuge study many orbital spacecraft installations were evaluated in a gross manner to determine candidate installations to be analyzed in more detail in Phase II. The installations selected are shown in Figures 8, 16 and 18. They are the CSM/LM/SRC, the Cluster Associated Configuration (CAC) and the Early Orbital Space Station (EOSS).

In the CSM/LM/SRC installation, the centrifuge is the only experiment. In the CAC and EOSS configurations, the centrifuge is one of several; for example, the Apollo Telescope Mount (ATM) experiment is mounted to the Multiple Docking Adaptor (MDA) as shown.

In the EOSS configuration, the S-IVB is not used for propulsion into orbit; it is dry launched and houses numerous experiments in locations normally occupied by propellant. For this case, the SRC is located in the most aft position considering that its bulk may interfere with experiments and mobility of personnel elsewhere in the S-IVB. This places the centrifuge a large distance from the ideal location, the mass center. However, if this separation does not cause poor attitude control, it is thought to be the best location from an overall design viewpoint.

The CAC configuration reflects use of the S-IVB in propulsion to orbit. The centrifuge installation in this case is identical in concept to that of the ATM in that it is an attachment to the basic configuration.

For each of three configurations, the gross attitude control requirement of the centrifuge experiments is the same - maintain the spin axis fixed to the degree required. In addition, considering other experiments installed in the EOSS and CAC installation, centrifuge operation should not adversely affect other experimental activity.

Control of the spacecraft is secured by the installation autopilot. The CSM on-off type reaction control system is available in all three configurations. In the EOSS and CAC configurations, Control Moment Gyro (CMG), a momentum transfer type autopilot control, is currently installed in the ATM module. Evaluation of these autopilots' capabilities relative to experiment requirements is pertinent to the control feasibility study.

Installation of the centrifuge changes basic spacecraft dynamics qualities in that incorporation of a rotating body with large momentum causes the familiar torque coupling about axes perpendicular to the momentum vector. Evaluation of this effect in regard to autopilot control capability for the CSM and CMG type is needed.

The centrifuge operates at frequencies of 0 to 65 rpm. In operation some small residual mass unbalance inherently exists and will exert perturbing torques on the spacecraft. The effect of these torques on spacecraft

attitude is readily obtained when the spacecraft is assumed rigid. However, the more involved case, including spacecraft flexibility, should be included in those installation where bending frequencies lie in or near the centrifuge operating band.

All of these preliminary considerations serve to identify the objectives and scope required of the dynamic investigations and are summarized as follows:

1. Determine experiment requirements on spacecraft attitude control.

2. Determine the effect of installation of a large momentum device on basic vehicle dynamics.

3. Establish operating capabilities of the CSM and CMG autopilots.

4. Determine need for centrifuge unbalance control.

5. Determine need for countermomentum control.

6. Evaluate autopilot control capability relative to experiment requirements, including effects of spacecraft flexibility.


Centrifuge Experiment Attitude Control Requirements

Ideally the centrifuge spin axis is held stationary in inert space as the spacecraft orbits. Stated grossly, the requirements are that the spin axis be controlled to low linear or angular accelerations. The degree to which this gross requirement must be achieved is dependent upon the experiment. Those experiments involving threshold measurements in linear and angular acceleration require more stability than those involving operation at the higher g levels. Table 4 separates the experiments into three classes and gives the quantitative requirement for low linear or angular acceleration at the couch.

While the degree of control is naturally specified at the couch to identify experiment requirements, it is desirable to translate the requirements at the couch to spacecraft permissable motion.

Figure 19 illustrates pertinent coordinates from which the linear and angular acceleration at the couch is computed from spacecraft motion.

Table 4 - Experiment Requirements (Couch)

| EXPERIMENT | | REQUIREMENT | |
|---|---|---|---|
| Type | Description | Angular Acc($^\circ/\sec^2$) | Linear Acc (g's) |
| High-g Type | (a) Grayout<br><br>(b) Re-entry Sim.<br><br>(c) Therapeutic Use | — | $\leq 0.02$ g's transverse to radial g field per g generated at the subject area of interest, (ears, heart, etc. ) |
| Low-g Type | (a) Tilt Table<br><br>(b) g Threshold<br><br>(c) Oculogravic Illusion and eye Counterrolling<br><br>(d) Mass Determination | — | $\leq 0.002$g's at the subject area of interest. Where a g level is used, the transverse component only is considered. |
| Low Ang. Accel. | (a) Angular Accel.<br><br>(b) Semi Circular Canal Stimulation | $\leq 0.03$ | — |
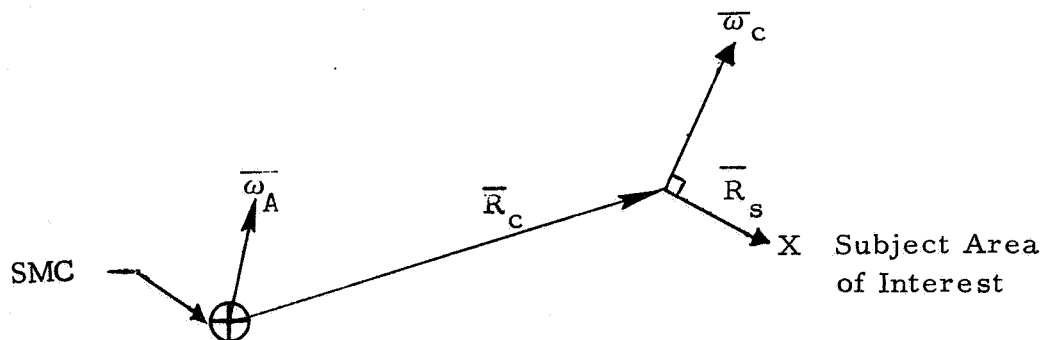


Figure 19- Couch Linear and Angular Acceleration
Computation Coordinates

In Figure 19,

$\bar{\omega}_A$ is the angular rate vector of the spacecraft relative to inert space.

$\bar{\omega}_c$ is the centrifuge angular rate relative to the spacecraft. It is aligned with the centrifuge spin axis and controlled by the centrifuge main drive control system.

$\bar{R}_s$ is the perpendicular distance to the subject area of interest from the centrifuge spin axis.

$\bar{R}_c$ is the distance from the system center of mass (SMC) to the centrifuge, fixed in the spacecraft body.

The linear acceleration at the couch is

$$\overset{..}{\bar{R}} = \overset{..}{\bar{R}}_c + \overset{..}{\bar{R}}_s = \bar{\omega}_A \times (\bar{R}_c + \bar{R}_s) + \bar{\omega}_c \times \bar{R}_s + \left[\bar{\omega}_A \cdot (\bar{R}_c + \bar{R}_s)\right]\bar{\omega}_A$$

$$- \omega_A^2 \cdot \bar{R}_c + (\bar{\omega}_A \cdot \bar{R}_s)\bar{\omega}_c - \left[(\bar{\omega}_A + \bar{\omega}_c) \cdot (\bar{\omega}_A + \bar{\omega}_c)\right]\bar{R}_s \quad (1)$$

The spacecraft angular rate and acceleration is very small in comparison to that of the centrifuge. Also, the locations of the centrifuge relative to the SMC is, for all configurations, located so that $R_c > R_s$ so with some error $R_s$ is neglected in comparison to $R_c$. The result is

$$\overset{..}{\bar{R}} = \underbrace{\dot{\bar{\omega}}_A \times \bar{R}_c}_{} + \underbrace{\dot{\bar{\omega}}_c \times \bar{R}_s}_{} + \underbrace{(\bar{\omega}_A \cdot \bar{R}_s)\bar{\omega}_c - 2(\bar{\omega}_A \cdot \omega_c)\bar{R}_s}_{} - \underbrace{\omega_c^2 \bar{R}_s}_{}$$

| Unwanted linear acceleration due to space-craft angular acceleration | Inherent linear transverse acceleration due to centrifuge rotary acceleration | Unwanted linear acceleration due to space-craft angular rate | Desired Centrifuge acceleration |

---

* The dot above the vector means the total derivative. The dot below means the time derivative of the components in spacecraft body fixed axes.

For purposes of this study the source of unwanted linear acceleration is identified to be due to the spacecraft angular acceleration as controlled by the offset of the centrifuge from the SMC and the cross coupling component as controlled by the angular rate of the spacecraft. The worst case assumed is identified in Figure 20.

$$\ddot{\overline{R}} = \dot{\overline{\omega}}_A \times \overline{R}_c + (\overline{\omega}_A \cdot \overline{R}_s) \overline{\omega}_c$$
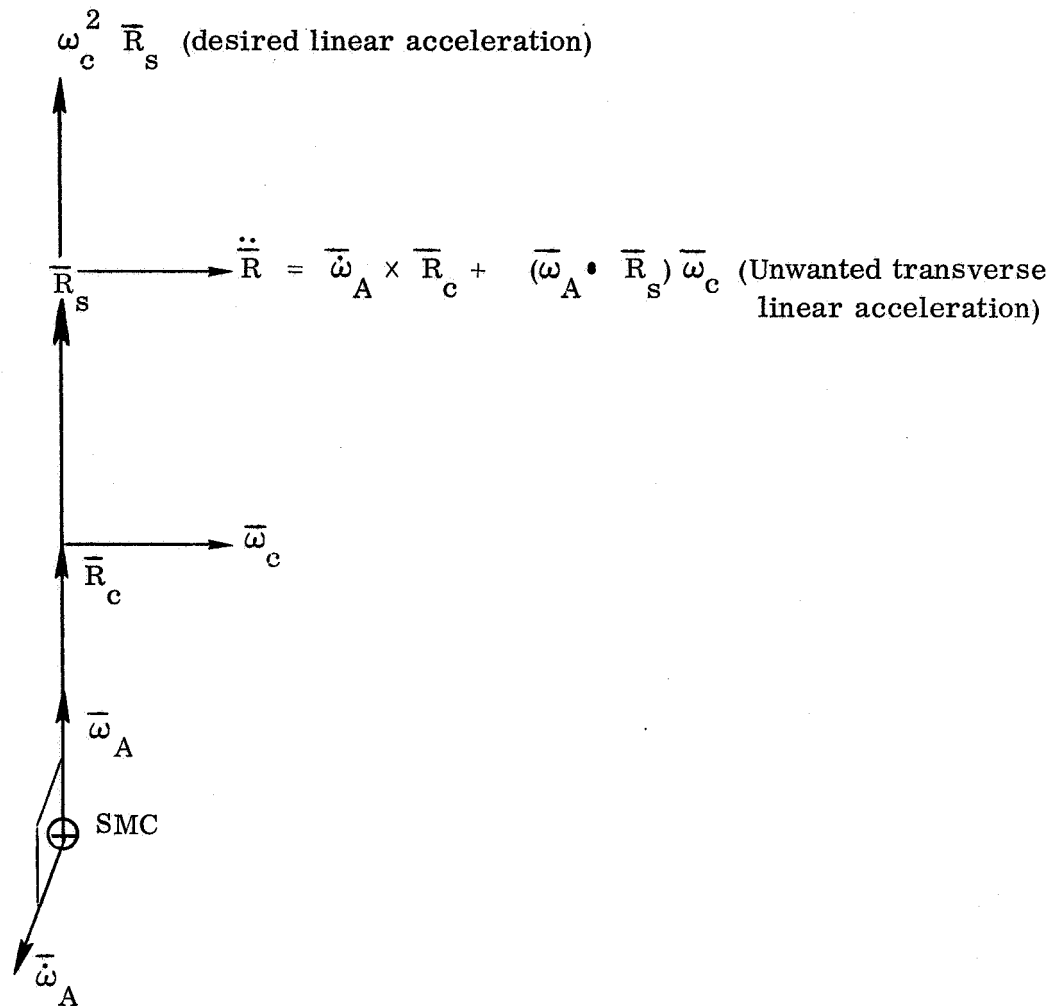


Figure 20- Worst Case Definition of Required Spacecraft Control (Linear Acceleration)

Figure 20 purposely places the Apollo angular rate and acceleration in such a position that an additive unwanted transverse linear acceleration results. Using this model should yield conservative results in regard to specifying limits of permissable spacecraft motion for a particular installation. For the low-g type of experiments, permissable spacecraft motion is given by:

$$\ddot{\overline{R}} = \frac{\dot{\omega}_A R_c + \omega_A R_s \omega_c}{32.2} \leq 0.002$$

For the high-g type experiments, permissable spacecraft motion is given by,

$$\frac{\dot{\omega}_A R_c + \omega_A R_s \omega_c}{\omega_c^2 R_s} \leq 0.02 \tag{4}$$

Consider a similar development for the low angular acceleration requirement. (See Figure 19.) The angular rate with respect to inertia is,

$$\bar{\omega} = \bar{\omega}_A + \bar{\omega}_c, \quad \dot{\bar{\omega}} = \dot{\bar{\omega}}_A + \dot{\bar{\omega}}_c \tag{5}$$

Taking the total derivative yields

$$\dot{\bar{\omega}} = \underbrace{\dot{\bar{\omega}}_A}_{\substack{\text{Unwanted} \\ \text{due to} \\ \text{spacecraft} \\ \text{angular} \\ \text{acceleration}}} + \underbrace{\dot{\bar{\omega}}_c}_{\substack{\text{Centrifuge} \\ \text{induced} \\ \text{angular} \\ \text{acceleration}}} + \underbrace{\bar{\omega}_A \times \bar{\omega}_c}_{\substack{\text{Unwanted} \\ \text{due to} \\ \text{spacecraft} \\ \text{angular} \\ \text{rate}}} \leq 0.03 \text{ deg/sec}^2 \tag{6}$$

To again develop a worst case model, the directions of the Apollo angular rate and acceleration are purposely set to yield a maximum amount of unwanted angular acceleration at the couch. This model is shown in Figure 21. Note that the spacecraft angular rate component transverse to the centrifuge spin axis is the dominant angular rate axis as it was for the linear acceleration worst case model shown in Figure 20. The angular acceleration is important regardless of the direction.
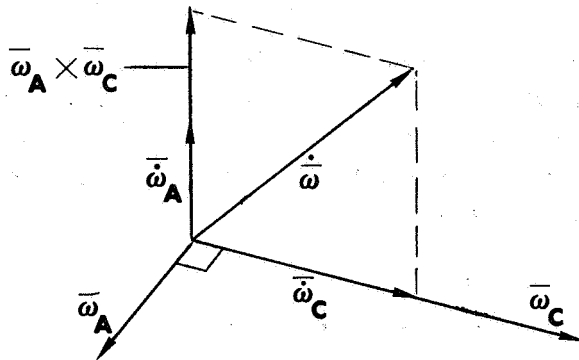


Figure 21 – Angular Acceleration Worst Case Model

Using the model of Figure 21 the requirement on spacecraft motion is,

$$57.3 \, \dot{\omega}_A + \omega_A \, \omega_c \leq (0.03) \, 57.3 \quad \text{(deg-sec units)} \tag{7}$$

Equations (3), (4) and (7) were used to determine experiment require-
ments on spacecraft motion. As indicated these requirements depend upon
centrifuge parameters for a particular experiment and the installation dis-
tance of the centrifuge from the spacecraft center of mass. Table 5 gives
these parameters for each installation and experiment type. In regard to
experiment type, the parameters given reflect the most sensitive experiment
within that class.

Table 5 - Installation and Centrifuge Parameters for Spacecraft
Motion Requirements Analysis

| Configuration | $R_c$(ft) | Experiment Type | | | | |
|---|---|---|---|---|---|---|
| | | High-g | | Low-g | | Low Ang. Acceleration |
| | | $R_s$(ft) | $\omega_c$(rpm) | $R_s$(ft) | $\omega_c$(rpm) | $\omega_c$(rpm) |
| CSM/LM/SRC | 23.4 | 8.33 | 36.1 | 4.17 | 26.5 | 10 |
| EOSS | 41.7 | ↓ | ↓ | ↓ | ↓ | ↓ |
| CAC | 17.4* | | | | | |

When the values from Table 5 are inserted in equations (3), (4), and
(7), the spacecraft requirements given in Table 6 , result. Table 6 shows
both the spacecraft angular acceleration and rate limit assuming one to be
zero and identifies the particular spacecraft axis where the numbers apply.
However, the extraneous acceleration is a function of the instantaneous value
of both. By considering an attitude sinusoid exhibiting the appropriate max-
imum acceleration and rate, some appreciation of the magnitude of the

---

* This distance is the effective value of $R_c$ along the centrifuge spin axis for
the CAC configuration.

Table 6. Experiment Requirements Analysis –
Spacecraft Attitude Control

| Experiment | | | Requirement | | | | | | |
|---|---|---|---|---|---|---|---|---|---|
| | | | Spacecraft (spin axis) Motion | | | | | | |
| | | | CSM/LM/SRC | | CAC | | EOSS | | |
| Type | Description | Couch Motion | Deg./Sec.² | Deg./Sec. | Deg./Sec.² | Deg./Sec | Deg./Sec.² | Deg./Sec. | Attitude Motion |
| High-g Type | Grayout Re-entry Simu. Therapeutic Use | ≤ 0.02g/g | (P, Y, ) 6.32 | (P, Y, ) 4.50 | (P, R, ) 8.5 | (P, R, ) 4.50 | (P, Y, ) 3.54 | (P, Y, ) 4.50 | 2.4 Degrees at 1.9 Rad/Sec. |
| Low-g Type | Tilt Table g-threshold OGI & ECR Mass Determination | ≤ 0.002g | (P, Y) 0.158 | (P, Y, ) 0.32 | (P, R, ) 0.426 | (P, R, ) 0.32 | (P, Y, ) 0.089 | (P, Y, ) 0.32 | 28.8 Arc Min at 0.66 Rad/Sec. |
| Low Ang. Accl. | Angular ACC. SCS | ≤ 0.03 Deg./Sec.² | (P, Y, R) 0.03 | (P, Y, R) 0.029 | (P, Y, R) 0.03 | (P, Y, R) 0.029 | (P, Y, R, ) 0.03 | (P, Y, R, ) 0.029 | 1.7 Arc Min. at 1 Rad./Sec. |

R – Apollo CSM Roll
P – Apollo CSM Pitch
Y – Apollo CSM Yaw

requirement may be obtained. This value is also given in Table 6, using the installation exhibiting the most severe requirement. This installation is identified by underlining the angular acceleration and rate applicable to the installation.

Table 6 is the end item of the requirements analysis. In summary, it tabulates the installation maximum motion allowances which avoid placing excessive unwanted accelerations at the subject area due to spacecraft motion. The installation autopilot is required to provide this degree of control in the presence of perturbing torques from the orbit environment and from the installation.

## Attitude Control Systems Background

The intent of this section is to provide background on the capabilities of the CSM on-off reaction type and the ATM-CMG type autopilots in the three candidate installations. The change in basic spacecraft dynamics caused by installation of the centrifuge is presented first because it shows that the essentials of spacecraft motion can be predicted by single rather than 3-dimensional analysis in regard to autopilot capability. Single axis models of the CSM and CMG autopilots are then described.

<u>Unperturbed Spacecraft Motion Modified by Centrifuge Installation.</u> - In the initial phase of the program, emphasis was on the CSM/LM/SRC installation controlled by the CSM autopilot. A three dimensional digital simulation was prepared to study the control capability of this combination. The detail derivation of equations of motion for this combination is given in Appendix A.

This simulation was used to determine spacecraft motion until analysis indicated that the CSM autopilot would not meet the more demanding experiment requirements. The use of the simulation was then deemphasized in regard to determination of CSM autopilot performance but used to confirm hand calculations of the change in dynamics of the basic vehicle, excluding the A/P. Appendix B makes reasonable simplifying assumptions in regard to calculating the motion of the spacecraft with an on-board centrifuge, developing a set of differential equations which are hand solvable.

The centrifuge installation model used for analysis is defined in Figure 22.
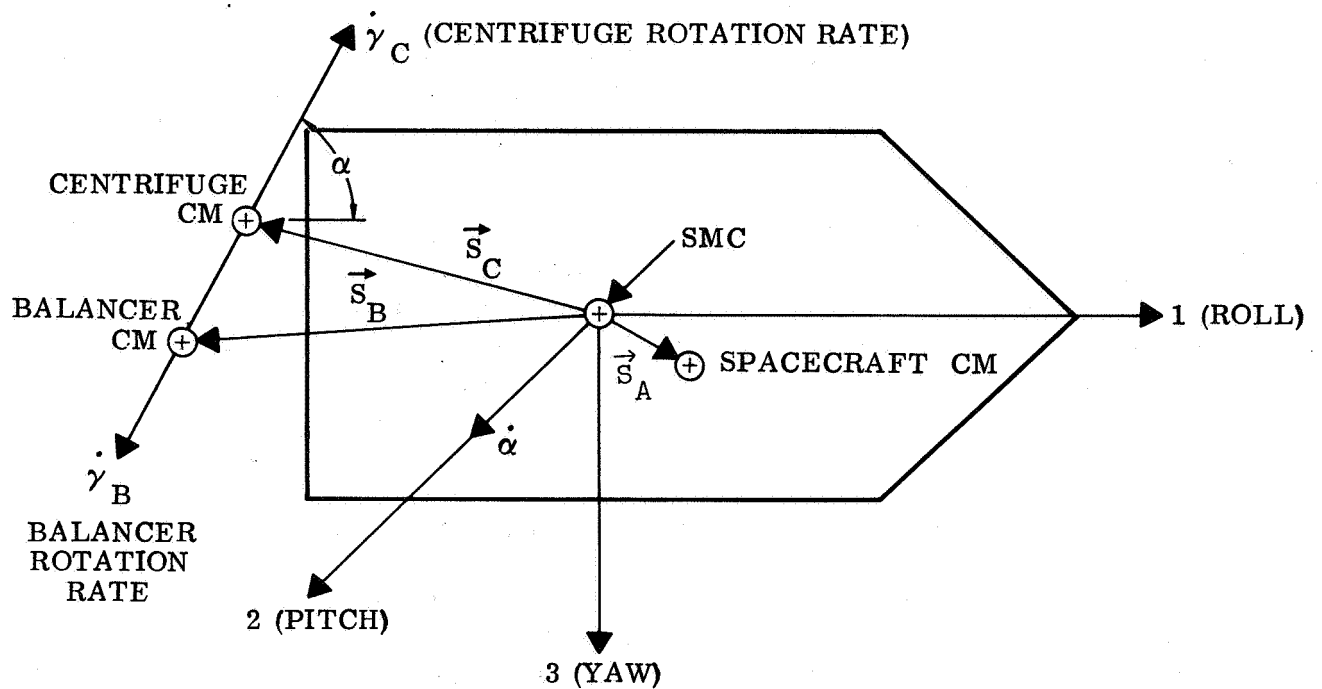
Figure 22 - Centrifuge, Balancer Installation Coordinates

As indicated, the centrifuge and balancer bodies are hardmounted to the spacecraft body at an arbitrary angle $\alpha$ with the long or minimum inertia spacecraft axis. A coordinate frame 1, 2, and 3 is defined fixed to the spacecraft body.
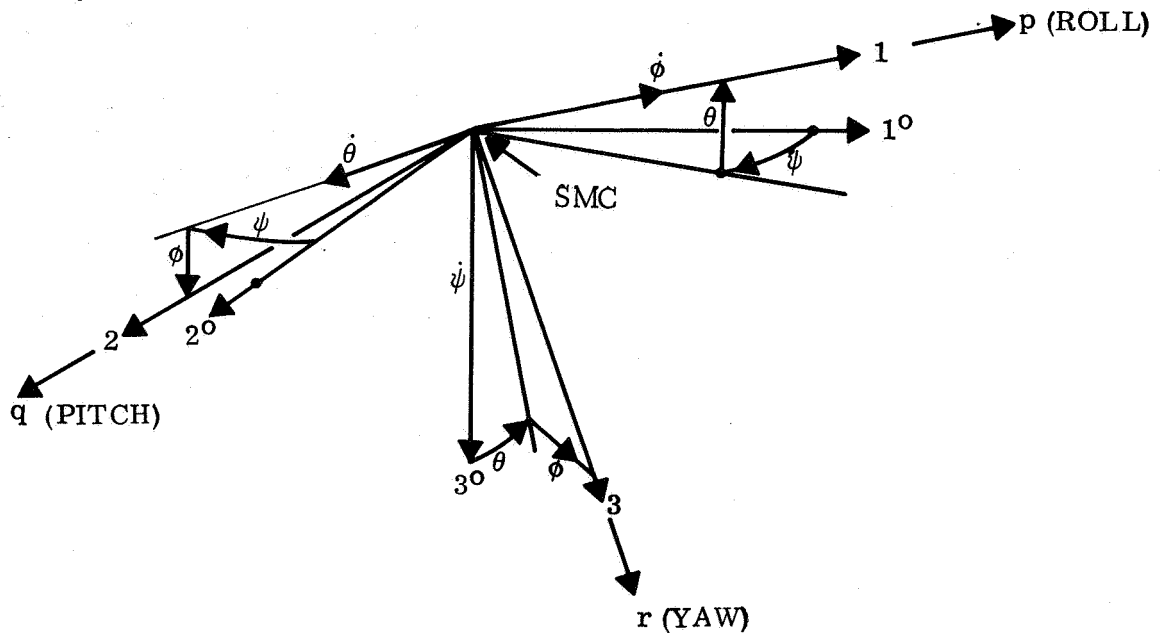


Figure 23 - Vehicle Angular Perturbation Model Coordinate Definition

Figure 23 defines the angular excursions of the spacecraft body from an inert (super 0) frame. These angular excursions are small.

Assume no external torques from the autopilot or environment and no unbalance torques from the centrifuge. Then, the net momentum of the centrifuge-balancer combination is defined to be

$$M = I_C \dot{\gamma}_C - I_B \dot{\gamma}_B \tag{8}$$

where

$I_C$, $I_B$ are the spin moment of inertia of the centrifuge and balancer bodies respectively

$\dot{\gamma}_C$, $\dot{\gamma}_B$ are the angular rates of the centrifuge and balancer bodies respectively.

As will be shown later, the value of M will be maintained constant by suitable additional on-board equipment. This constant value of M is assumed and it is presently desired to obtain the effect of its magnitude and installation angle on the basic installation.

With the assumptions given above, the differential equations of motion reduce to

$$J_1 \ddot{\phi} - M \sin \alpha \, \dot{\theta} = 0 \qquad\qquad J_3 \dot{\psi} - M \cos \alpha \, \dot{\theta} = 0$$
$$J_2 \ddot{\theta} + M \cos \alpha \, \dot{\psi} + M \sin \alpha \, \dot{\phi} = 0 \tag{9}$$

where $\theta$, $\psi$ $\phi$ are the small deviation angles in pitch, yaw and roll of the spacecraft from the inert reference.

$J_1$, $J_2$, $J_3$ are the spacecraft roll, pitch and yaw principal moments of inertia.

M is the net angular momentum of the centrifuge, balancer bodies relative to the CSM.

$\alpha$ is the angle between the centrifuge rotational axis and the CSM roll axis.

Note that the simplified equations (9) are readily understood. The product of inertia and angular acceleration is simply the inertial reaction torque to the stabilizing torque of the centrifuge proportional to the product of the net momentum and transverse angular rate.

The two cases of interest correspond to the installation angle $\alpha$ equal to zero degrees (alignment of the centrifuge spin axis with the spacecraft roll axis) and $\alpha$ equal to 90 degrees (centrifuge spin axis perpendicular to the spacecraft roll axis.) For the two cases of interest the solution of Equation (9) subject to an initial condition in pitch angle and rate are tabulated below.

$\underline{\alpha = 0 \text{ deg.}}$

$$\ddot{\phi} = \dot{\phi} = \phi = 0$$

$$\dot{\theta} = \dot{\theta}_o \cos(Mt/\sqrt{J_2 J_3}) = \dot{\theta}_o \cos(Mt/J)$$

$$\theta = \theta_o + \dot{\theta}_o \sqrt{J_2 J_3}/M \, \text{Sin}(Mt/\sqrt{J_2 J_3}) = \theta_o + \dot{\theta}_o \, J/M \, \text{Sin}(Mt/J)$$

$$\dot{\psi} = \dot{\theta}_o \sqrt{J_2/J_3} \, \text{Sin}(Mt/\sqrt{J_2 J_3}) = \dot{\theta}_o \, \text{Sin}(Mt/J)$$

$$\psi = (\dot{\theta}_o J_2/M) \left[ 1 - \text{Cos}(Mt/\sqrt{J_2 J_3}) \right] = \dot{\theta}_o \, J/M \left[ 1 - \cos(Mt/J) \right] \quad (10)$$

$$\text{where } J = J_2 = J_3$$

For the $\alpha = O$ case (equation 10 set), the simplification resulting from the essentially equal spacecraft yaw and pitch moments of inertia is used.

The spacecraft moments of inertia, pitch axis initial conditions and centrifuge momentum are needed to obtain the motion given by numerical evaluation of Equations (10) and (11). The centrifuge net momentum is 5000 lb-ft-sec. The initial pitch angular rate arbitrarily used is 0.13 degrees/sec. The installation moments of inertia used are given in Table 7.

$$\underline{\alpha \ = \ 90 \ \text{Deg.}}$$

$$\ddot{\psi} \ = \dot{\psi} \ = \psi = \ O$$

$$\dot{\theta} \ = \dot{\theta}_o \ \cos \ (Mt/ \ \sqrt{J_1 J_2})$$

$$\theta \ = \ \theta_o + (\dot{\theta}_o \ \sqrt{J_1 J_2} \ /M \ \text{Sin} \ (Mt/ \ \sqrt{J_1 J_2})$$

$$\dot{\phi} \ = \dot{\theta}_o \ \sqrt{J_2/J_1} \ \text{Sin}(Mt/ \ \sqrt{J_1 J_2} \ )$$

$$\phi \ = \ (\dot{\theta}_o \ J_2/M) \ \left[ 1 - \text{Cos} \ Mt/ \ \sqrt{J_1 J_2} \right] \tag{11}$$

Table 7 - Configuration Moments of Inertia (Slug ft.$^2$ )

| Installation | Axis | |
|---|---|---|
| | ROLL | PITCH/YAW |
| CSM/ LM/ SRC | 24,000 | 170,000 |
| CAC | 385,000 | 3,000,000 |
| EOSS | 330,000 | 3,500,000 |

The smallest configuration, the CSM/ LM/ SRC, is the most sensitive to installation of the centrifuge. Using its inertial parameters, Figure 24 shows the coning motion about the momentum vector for the two installation angles of interest. For the $\alpha$ = O case, it is seen that the crossplot of the pitch and yaw angle move on a circle of radius and period depending on the value of centrifuge net momentum. That is, the roll axis cones in a circular motion with period given by

$$P = \frac{2 \pi J}{M} \tag{12}$$

As the centrifuge net momentum is reduced to zero, the coning motion is in ever larger circles such that when the momentum is zero, it is replaced by a continuous increase in pitch angle with no coupling to yaw. The period of revolution increases from 3.56 minutes to infinity as the centrifuge momentum decreases from 5000 to 0 ft-lb-sec.

The $\alpha$ = 90 degree case is not a candidate installation for the CSM/ LM/ SRC configuration but, for purposes of explanation of the effect of installation angle, the motion for this case is also given on Figure 24. As indicated, the circular coning is replaced by an elliptical coning at a lower period indicating an overall higher inter-axis coupling.

The period of the coning motion at a momentum of 5000 ft-lb-sec. is considered to be the significant parameter in regard to determining the effect of autopilot control on the installation. A tabulation of the period of this motion for all installations is given in Table 8.

Table 8 - Coning Motion Periods (M = 5000 ft-lb-sec)

| CONFIGURATION | $\alpha$ (DEG) | PERIOD (MIN) |
|---------------|----------------|--------------|
| CSM/LM/SRC    | 0              | 3.56         |
| EOSS          | 0              | 73.4         |
| CAC           | 90             | .22.2        |
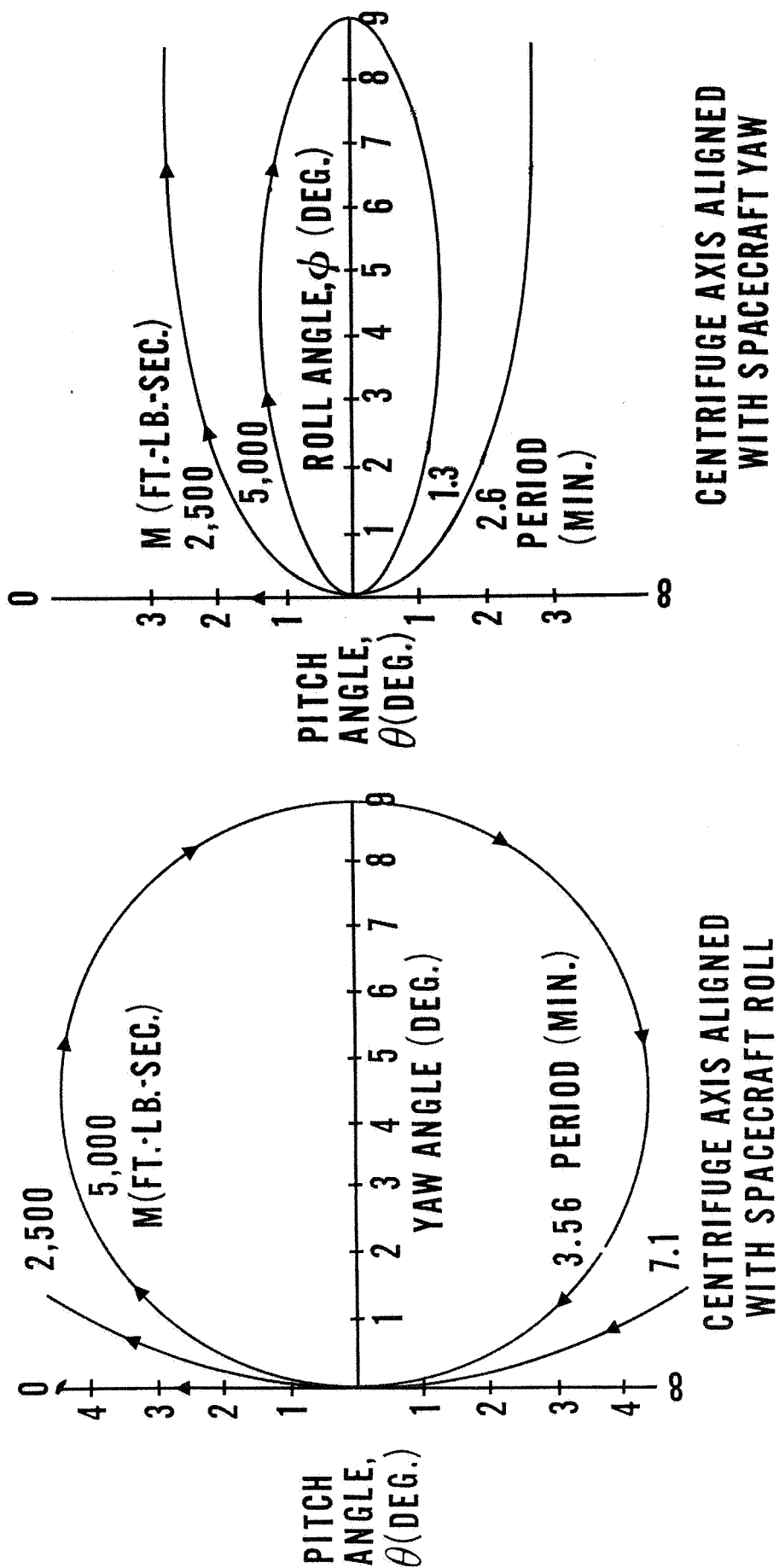
Figure 24. Uncontrolled Spin Axis Coning Motion

The significance of the period stems from the fact that if vehicle inertias increase or the momentum decreases, the effect is the same in regard to extent of inter-axis coupling; that is, the effect is diminished since the period tends toward infinity (corresponding to no cross-coupling). Given a choice, it is best to use an installation angle of zero. Of the three configurations used, only the CAC uses $\alpha$ = 90 degrees. The adverse orientation is compensated by the large vehicle size.

Comparing the coning motion periods to those of CMG control indicates that the centrifuge momentum is not so large that the autopilot will not work very much like it would without the centrifuge present.

The CSM autopilot is non-linear. It will evidence the coning motion within its dead zone (no action area). Outside the dead zone, it should again operate very much as it would without the centrifuge present.

In summary, autopilot control analyses using single axis models will give adequate results. This simplification is used henceforth.


Command and Service Module Autopilot Capability. - A detailed description of the applicable portion of the CSM autopilot is given in Appendix A. This information was derived from references 1 and 2 obtained from cognizant personnel at MSC, Houston, Texas. The essential aspects of its operation are briefly covered below to evaluate its control capability in regard to meeting centrifuge experiment requirements.

Figure 25 illustrates the phase-plane logic used in all three control axes. All three axes are identical and, excluding some minor cross coupling, operate independently so it is only necessary to describe a single axis, for example, the pitch axis.

Assume the pitch rate and displacement is such that the point appears between the positive and negative decision lines, for instance, at point A. Under this circumstance, the autopilot does nothing and the vehicle will maintain the same rate and must move to intersect the decision line at point B. When this occurs, the autopilot commands engine ignition. The engine configuration is such that ignition causes a 1400 lb-ft. pure couple of polarity to reduce the magnitude of the rate. The ignition command remains in force until two conditions are met. One, the minimum "on-time" is 0.014 seconds (minimum impulse). Two, the angular rate is reduced to that designated as the desired rate on Figure 25 or point C. Ideally all vehicle motion would stop at this point, however, there is some small residual rate such that the vehicle rate will probably move slight past C to the point D (not to scale). At this point it enters into what is termed a limit cycle, that is, it traverses the rectangle EFGH.

Figure 25.   Apollo CSM Autopilot Logic

NOTE:   LIMIT CYCLE EFGH NOT TO SCALE

If it is assumed that the initial point is outside the decision line to begin with (at point I), then "engine on" is commanded until the desired rate line is crossed (point J). The motion corresponds to passage through point A. Subsequently, the motion is the same as described before.

The preceding CSM autopilot description assumes no external torques and is introductory to the more complex realisitic situation where external torques due to orbit environment are considered (gravity gradient, interaction of on-board magnetics with the earth magnetic field, etc.). For this study, the environment torque is estimated to be that corresponding to maximum gravitational torque. This torque depends upon the installation and is about 0.25 ft-lbs for the CSM/LM/SRC configuration, and 3.75 ft-lbs for the CAC and EOSS configuration.

For scaling purposes, use 1 ft-lb and the CSM/LM/SRC configuration to illustrate the operation of the CSM autopilot in the orbit environment. The shape of the limit cycle (perturbed limit cycle) is changed as is shown in Figure 26* (Figure 26A is for roll, Figure 26B is for pitch or yaw). As indicated for either axis the motion occurring is identical in form but the quantitative dimensions of the limit cycle change. Note that it is assumed that the start point (the initial angular rate and displacement) is in the final perturbed limit cycle path. Regardless of the initial rate and displacement, the autopilot will cause this final motion to occur.

In the presence of environmental perturbing torques, the time between autopilot minimum impulse firings is inversely proportional to the external torque magnitude. Table 9 lists the angular accelerations, minimum impulse, angular rates and time between firings for each configuration.

Comparison of Table 9 data to the requirement summary of Table 6 indicates that generally the accelerations from the CSM exceed those of the more sensitive experiments but that they do not exceed those allowable for the high-g type. Experiment durations range from a few minutes to several hours. The CSM autopilot will produce firings during the experiment.

In short, the control afforded by the CSM autopilot is not considered adequate for the centrifuge experiments.

---

* Figure 26 is an exploded view of the right hand, zero angular rate area of Figure 25.

ROLL RATE
(DEG/SEC.)

0.05

CONTROL TORQUE (NEG)

t = 10.5 Sec.
B

0.025

5 or 0.5 DEG
ATTITUDE LIMIT

t = 0
A
.2      .15      .1      .5      0

ROLL DEVIATION
(DEG)

C
t = 10.5⁺
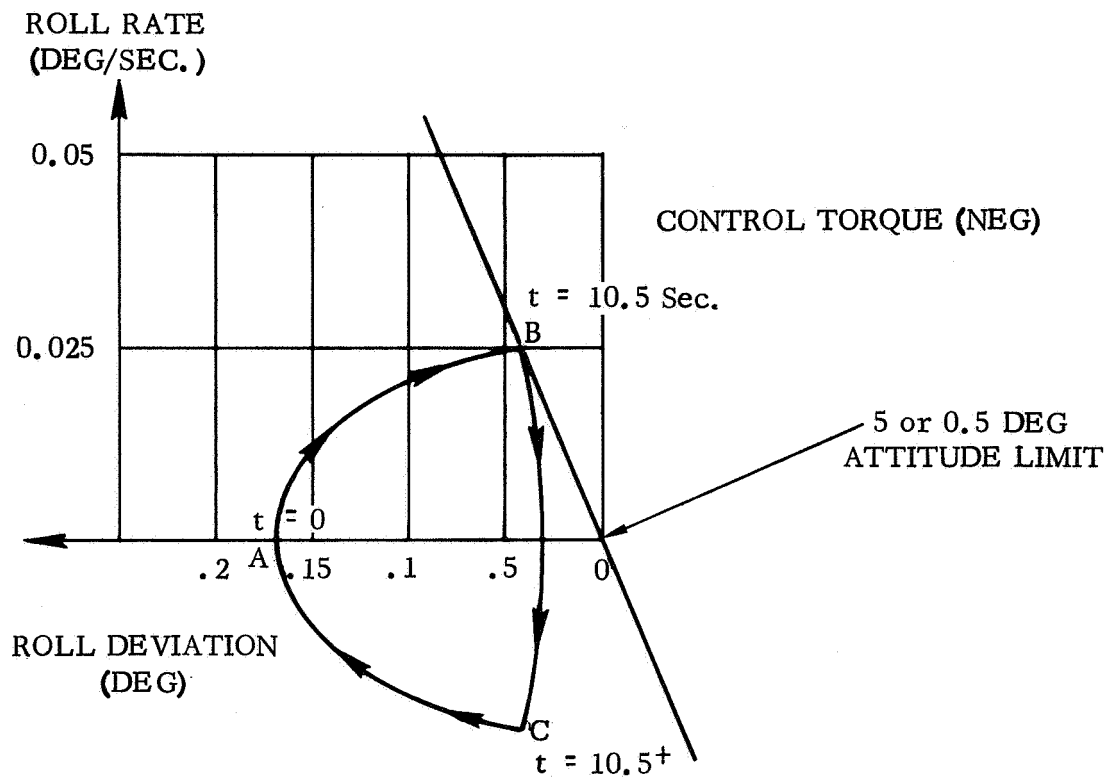
Figure 26A.  Perturbed Limit Cycle (Roll)


PITCH RATE
(DEG/SEC.)

0.0075

0.005

t = 10.5 Sec.
B

0.0025

5 OR 0.5 DEG
ATTITUDE LIMIT

t = 0
A
.03      .02      .01      0

PITCH DEVIATION
(DEG)

C
t = 10.5⁺
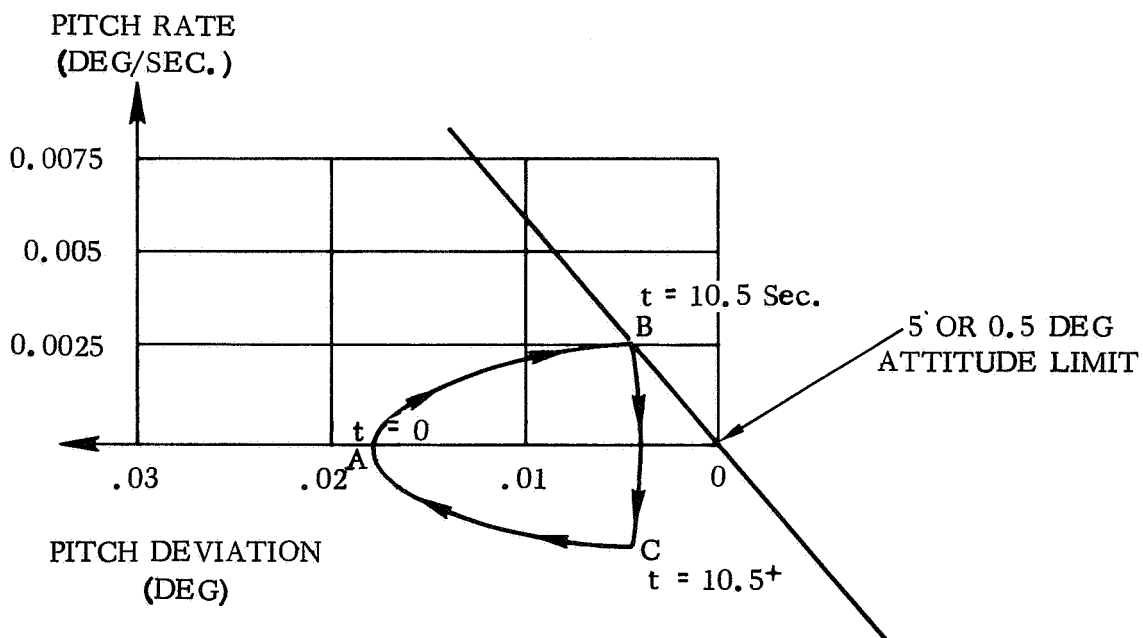
Figure 26B.  Perturbed Limit Cycle (Pitch)

Table 9 - CSM Performance Tabulation

| Characteristics | Installation | | | | | |
|---|---|---|---|---|---|---|
| | CSM/LM/SRC | | CAC | | EOSS | |
| | Roll | Pitch/Yaw | Roll | Pitch/Yaw | Roll | Pitch/Yaw |
| Ang. Accl. (firing) (deg/sec$^2$) | 3.24 | 0.48 | 0.208 | 0.268 | 0.243 | .0222 |
| Ang. Rate (Minimum impulse)(deg/sec) | .0453 | .0067 | .0029 | .00038 | .00034 | .00031 |
| Environment Torque Estimate (ft-lb) | 0.25 | | 3.75 | | 3.75 | |
| Time Between Firings (sec) | 84 | | 5.6 | | 5.6 | |

Current Control Moment Gyro Autopilot Description. - As for the CSM A/P, the CMG type enters into the centrifuge study because of its availability in the EOSS and CAC configurations and its inherent superiority with respect to fineness of control and fuel economy for long duration missions. Control limitations, where they exist, must also be considered.

There are many CMG configurations. The particular configuration used in this study corresponds to the Langley or ATM (Apollo Telescope Mount) version which appears to be the current baseline configuration. It has been publicized in connection with its application to the ATM installed in the CAC or EOSS spacecraft (as identified herein) in References 3 and 4.

Figure 27 summarizes this configuration. As indicated, there are three two-degree-of-freedom CMG's with the outer gimbals hardmounted in alignment with the three primary spacecraft axes. Their size, power, momentum and torque output capability are listed for reference. The three units are currently mounted on the ATM module.

Spacecraft angular displacement and rate errors are sensed in response to external torque. These signals are processed through a vehicle control
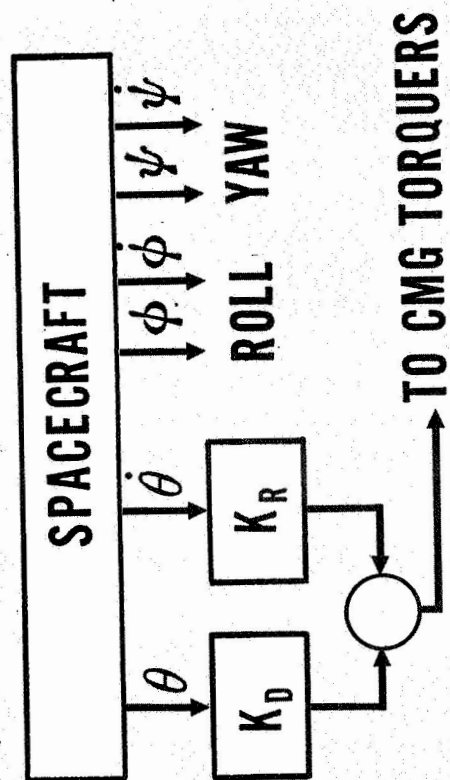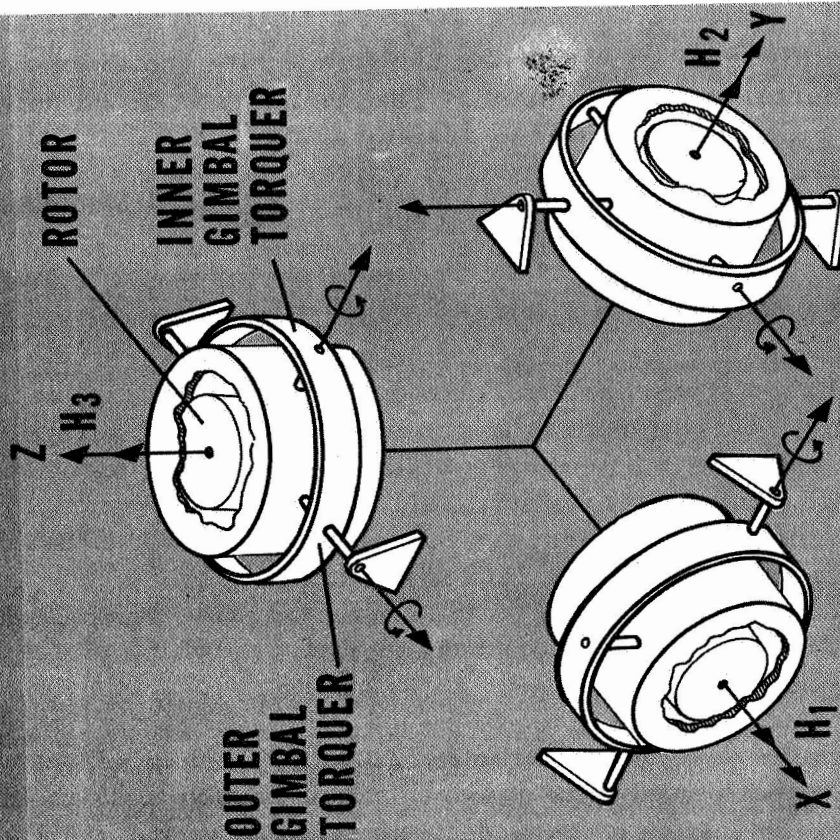
Figure 27. ATM CMG Autopilot Description

law comprising a familiar linear addition of vehicle rate and displacement errors to form a countertorque command. This countertorque command is processed through a CMG control law to develop appropriate inner and outer gimbal torque signals for all three gyros. Complex geometry associated with the dependence of these gimbal torques commands upon the current position of the gyro rotors is involved and is an important area in CMG control system design (Reference 3).

The countertorque is generated by commanding rotor angular rate to produce a rate of change of momentum. However when the accumulated gimbal position change corresponds to alignment of all three gyro rotors in any direction, the system is momentum saturated. Desaturation by means of the CSM autopilot is required to restore the three gyro rotors to some initial orientation after which the process repeats. It is desired that desaturation cycle time be as long as possible (at least a few hours).

The gimbal rates are limited currently to that rate which yields an output torque of 160 ft-lbs/gyro.

The CMG autopilot is a linear autopilot with good threshold characteristics (5000/1 torque output range). Its dynamic range is from 0 to about 40 rad/sec in regard to the transfer characteristic between torque command and generation. Its capability in regard to counteracting the orbit frequency and low magnitude orbit environment torques (i.e. gravitational torque) with essentially zero spacecraft motion is quite adequate.

The centrifuge is capable of generating a change in momentum of about 9500 ft-lb-sec at a maximum rate equivalent to 240 ft-lbs torque. At any time, the maximum momentum change that the CMG autopilot can accommodate with a reasonable (better than 90%) probability that saturation will not occur is 1000 ft-lb-sec. If the CMG autopilot is to be used, a counter-momentum system is required. It could be sized according to the requirement that the net centrifuge-countermomentum system momentum change not exceed 1000 ft-lb-sec and that the countermomentum system be capable of exerting a countertorque on the spacecraft equal to the centrifuge maximum spin up torque currently sized at 240 ft-lbs. Configuring feasible countermomentum systems so that the current CMG autopilot can be used is a pertinent study area.

Centrifuge Counterbalancing & Countermomentum Systems

Centrifuge Perturbing Torque Output. - A centrifuge body center of mass (CM) offset from the spin axis produces a force normal to the spin axis and through the offset CM. This is termed static unbalance. The force

obtains leverage from the distance between the centrifuge rotating body CM and the spacecraft CM causing a torque on the spacecraft. Figure 28 gives pertinent coordinates for evaluation of this torque.
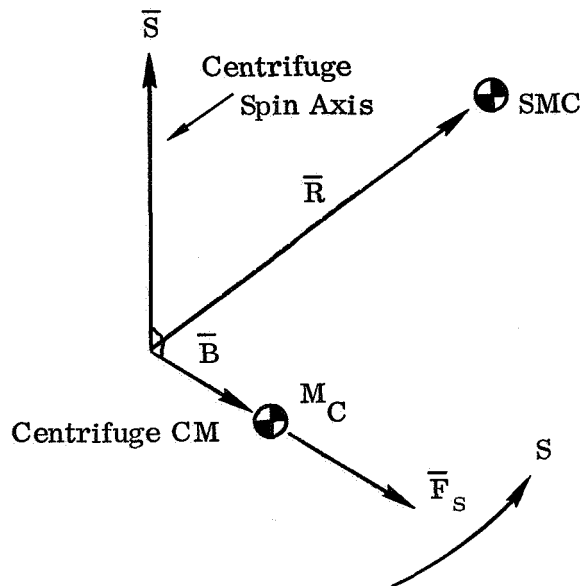


Figure 28 - Static Unbalance Coordinates

The force exerted by the centrifuge on its support is the familiar centripetal force and is

$$\overline{F}_s = M_c \, \overline{B} \, S^2 \qquad\qquad (13)$$

where:

$\overline{F}_s$ is the force vector due to static unbalance

$S$ is the spin rate

$\overline{B}$ is the rotating body CM perpendicular displacement from the spin axis

$M_c$ is the mass of the centrifuge rotating body

The force is fixed in centrifuge rotating body coordinates, is in the spin plane, and passes through the instantaneous position of the rotating body CM. The torque on the vehicle caused by the static unbalance is

$$\overline{T}_s = \overline{F}_s \times \overline{R}_c = M_c \, S^2 \, \overline{B} \times \overline{R}_c \tag{14}$$

where

$\overline{R}_c$ is the distance between the centrifuge installation and the SMC.

An angular misalignment of the centrifuge principal axis with the spin axis produces a pure couple acting along a normal to the spin axis and fixed to the centrifuge rotating body. This is termed dynamic unbalance. The torque on the spacecraft is the same regardless of centrifuge location. To identify moments of inertia, assume axes fixed to the centrifuge rotating body centered at the centrifuge CM with axes 1, 2 and 3. The 1 axis is along the spin vector, the 2 along the couch radius axis. In this rotating frame the momentum is

$$
\begin{bmatrix} H \end{bmatrix} = 
\begin{bmatrix}
I_{11} & -I_{12} & -I_{13} \\
-I_{12} & I_{22} & -I_{23} \\
-I_{13} & -I_{23} & I_{33}
\end{bmatrix}
\begin{bmatrix} S \\ 0 \\ 0 \end{bmatrix} =
\begin{bmatrix} SI_{11} \\ -SI_{12} \\ -SI_{13} \end{bmatrix}
\tag{15}
$$

where $I_{11}$, $I_{12}$, $I_{13}$ are the moments of inertia about the 1, 2 and 3 axes

$I_{12}$, $I_{13}$, $I_{23}$ are the familiar cross products of inertia due to misalignment from principal axes.

The torque in this body fixed rotating frame is,

$$
\overline{T} = \dot{\overline{H}} = \dot{S}
\begin{bmatrix} I_{11} \\ -I_{12} \\ -I_{13} \end{bmatrix}
+ S
\begin{bmatrix} \dot{I}_{11} \\ -\dot{I}_{12} \\ -\dot{I}_{13} \end{bmatrix}
+ S^2
\begin{bmatrix} 0 \\ I_{13} \\ -I_{12} \end{bmatrix}
\tag{16}
$$

$$
\begin{cases}
\dot{S}I_{11} \;+\; S\dot{I}_{11} & \text{Torque along spin axis}\\[2ex]
=\; -\dot{S}I_{12} \;-\; S\dot{I}_{12} \;+\; S^2\,I_{13} & \\[2ex]
\quad -\dot{S}I_{13} \;-\; S\dot{I}_{13} \;-\; S^2\,I_{12} & \text{Dynamic Unbalance Torque}
\end{cases}
\qquad (17)
$$

The first component is the spin-up torque and not dependent upon dynamic unbalance. The torque due to dynamic unbalance is covered by the second and third components which locate the torque direction to be in the spin plane. While the magnitude of this torque is affected by spin acceleration and cross product time derivative, the major effect is reflected in the spin rate squared term. That is, the torque due to dynamic unbalance is very nearly

$$
T_D \;=\; S^2
\begin{bmatrix}
0 \\[1ex]
I_{13} \\[1ex]
-I_{12}
\end{bmatrix}
\qquad (18)
$$

The centrifuge body is hardmounted to the spacecraft. If static and dynamic unbalances exist, a net torque is transmitted to the spacecraft body. This torque causes motion of the spacecraft/centrifuge system of a vibratory character at centrifuge spin frequency because the torque direction is rotating at spin frequency. The expressions given above are used later to numerically evaluate the unbalance inherent in the centrifuge design. The result of this evaluation is to set a requirement for an automatic balancing system comprising unbalance sensing and appropriate motion of counterweights to reduce the unbalance to an acceptable level. This mechanism is termed the centrifuge spin balance system. The perturbing torque on the spacecraft, due to centrifuge unbalance, is the residual output of centrifuge unbalance as controlled by the spin balance system.

The centrifuge spin-up/down torque during centrifuge operation is also a perturbing torque on the spacecraft. A reaction torque and change in momentum is transmitted to the spacecraft in a direction parallel to the centrifuge spin axis. The worst case corresponds to a spin up to 65 rpm at a maximum angular acceleration of 0.17 rad/sec$^2$ with a centrifuge moment of inertia of 1440 slug-ft$^2$. The maximum torque is 240 ft-lbs. The maximum change in momentum is 9500 lb-ft-sec. This amount of momentum cannot be

absorbed by the basic spacecraft control moment gyro autopilot. Inclusion of a system to separately absorb this momentum is required and is termed the centrifuge countermomentum system. The system comprises dual single gimbal control moment gyros (CMG) driven such that an equal, oppositely directed, torque and change in momentum results. The net perturbing torque on the vehicle due to centrifuge angular acceleration is the residual output of this countermomentum system.

In theory the requirement for the spin balance and countermomentum systems would exist only for the orbital version of the centrifuge. Hard supports on the ground based version would assume the unbalance loads with no centrifuge vibration excepting those due to structural deformation under dynamic unbalance loads. However, because of rather large static unbalance inherent in the centrifuge design it is likely that vibration will be large enough to require spin balance in the ground based version. The countermomentum system will not be required since the spin torque maximum is only 240 lb ft. and is easily reacted out with negligible effect on centrifuge spin axis motion.

Herein we are concerned with the orbital version where both the spin balance and countermomentum systems are required. The two systems together are referred to as the counterbalancing system.

Counterbalancing System Requirements - Spin Balance. - The data required to evaluate the amount of unbalance force and torque consists of weight distribution and maximum centrifuge rotational speed, as tabulated in Table 10 for each experiment. This tabulation lists the experiments with the distances that the counterweight was moved from a reference position to obtain a static balance. The reference position selected is the average of the balance position for the high-g experiments or 45 inches from the spin axis. These distances multiplied by the ratio of counter-to-total weight yield the static unbalance which would exist if the counterweight was not moved. These static unbalances are tabulated together with the total force they cause.

Under the assumption that only static balancing was implemented, the moments of inertia, including the cross-products, are also tabulated. These figures allow calculating the indicated amount of dynamic unbalance torque existing should there be no attempt to dynamically balance the centrifuge in addition to the static balance.

The amount of force resulting from static unbalance confirms the need for static balancing previously judged necessary from casual inspection of the centrifuge design. Much of the static unbalance force can be removed by manually setting the counterweight prior to the experiment. If this is done, automatic control requirements could be reduced to trimming the position to account for subject weight variation and couch motion during the

Table 10. Static and Dynamic Unbalance Tabulation *

| Experiment | Moments of Inertia (Slug ft²) | | | | | Counterwgt. Pos. (inches) | | Exp. RPM | Uncomp. Static Unb. (inches) | | Static Unb. Force (lbs) | | Dyn. Unb. Torque (ft-lbs) | |
|---|---|---|---|---|---|---|---|---|---|---|---|---|---|---|
| | $I_1$ | $I_2$ | $I_3$ | $I_{12}$ | $I_{13}$ | 2 Axis | 3 Axis | | 2 Axis | 3 Axis | 2 Axis | 3 Axis | 2 Axis | 3 Axis |
| High "g" Type — Greyout | 594 | 113 | 609 | -3.1 | 0. | -25.9 | 0. | 54.2 | 6.37 | 0. | 1050 | 0. | 0. | 100 |
| Therapeutic | 594 | 113 | 609 | -3.1 | 0. | -25.9 | 0. | 37.6 | 6.37 | 0. | 461 | 0. | 0. | 48 |
| Reentry | 1441 | 132 | 1438 | 3.2 | 0. | -64. | 0. | 65.3 | 6.37 | 0. | 1520 | 0. | 0. | 150 |
| Tilt Table (I) | 517 | 155 | 492 | -1.5 | 0. | -26.3 | 7.6 | 38.3 | 6.25 | 2.54 | 514 | 209 | 0. | 24 |
| (II) | 569 | 147 | 552 | -1.5 | 0. | -28.6 | 6.2 | | 5.48 | 2.07 | 450 | 170 | 0. | 24 |
| Lin. Acc. (IA&B) | 594 | 113 | 609 | -3.1 | 0. | -25.9 | 0. | 31.2 | 6.37 | 0. | 347 | 0. | 0. | 33.2 |
| Sensing (2A&B) | 405 | 202 | 333 | -3.5 | 0. | -12.4 | 13.2 | | 10.85 | 4.41 | 593 | 242 | 0. | 37.4 |
| Low "g" Type — ECR (I) | 885 | 119 | 906 | 13.4 | 0. | -42.2 | 0. | 26.5 | 0.92 | 0. | 36.2 | 0. | 0. | 102 |
| (II) | 804 | 149 | 796 | 11.7 | 4.5 | -38.6 | 8.4 | | 3.14 | 2.8 | 123 | 110 | 35 | 85 |
| OGI (I) | 890 | 119 | 900 | -1.2 | 0. | -42.2 | 1.8 | 26.5 | 0.92 | 0.6 | 43.4 | 28.4 | 0. | 9.25 |
| (II) | 841 | 133 | 837 | -1.2 | 0. | -40. | -7.0 | | 1.67 | 2.34 | 65.8 | 92.0 | 0. | 9.25 |
| Mass (76") | 1441 | 132 | 1438 | 3.2 | 0. | -64. | 0. | 21.6 | 6.37 | 0. | 166 | 0. | 0. | 16.4 |
| Det. (50") | 573 | 132 | 570 | -1.2 | 0. | -30.6 | 0. | 26.5 | 4.82 | 0. | 190 | 0. | 0. | 9.2 |
| Low Ang. Acc. Type — SCS, 0", A | 249 | 119 | 259 | -4.8 | 0. | 1.2 | 1.8 | 10. | 15.4 | 0.6 | 86.0 | 3.35 | 0. | 5. |
| 0", B | 243 | 119 | 264 | 1.8 | 0. | 1.2 | 0. | | 15.4 | 0. | 86.0 | 0. | 0. | 1.9 |
| 49", A | 1351 | 119 | 1361 | 3.4 | 0. | -61.9 | 1.8 | | 5.65 | 0.6 | 31.5 | 3.35 | 0. | 3.7 |
| 49", B | 1346 | 119 | 1367 | 17.9 | 0. | -61.9 | 0. | | 5.65 | 0. | 31.5 | 0. | 0. | 19.5 |

Centrifuge rotating weight is 1,973 lbs. Counterweight weight is 660 lbs; reference position is -44.95 inches.
The 1 axis is along the centrifuge spin axis, the 2 along the couch.

* The angular acceleration experiment is excluded from the above tabulation because centrifuge is not rotated about its primary spin axis.

experiment. Subject weight variation is conservatively estimated to produce about 2.2 inches of static unbalance based upon subject weight variation (including equipment) of 90 lbs. at a radius of 4 feet. In addition, the couch and subject movement during the experiment contribute a maximum of approximately 1 inch within two seconds.

Counteracting this unbalance requires the counterweight to be moved a total of 10.5 inches (equivalent to 3.5 inches of static unbalance) referred to the rough manual position. The dynamic requirement sizing the counterweight motor is based on correcting 1 inch of static unbalance in 2 seconds with an acceleration capability of 5 inches/sec$^2$ maximum. The 2.5 inches of unbalance due to subject weight variation should be accomplished during the longer time spin-up. It is not desirable to size the drive motor to any greater level than necessary so that, in case of a possible malfunction, sufficient time is available to disable the drive motor before unbalance forces become large.

The permissable static unbalance force level after balancing is determined by comparison of its effect on spin motion to the requirements for the three installations currently being considered.

In the CSM/LM/SRC installation, the residual is determined by comparison of the centrifuge induced spin axis motion to the spin axis motion requirement for the most sensitive experiments. The most severe requirement is specified for the angular acceleration experiment and is 0.03 degrees/sec$^2$.

In the EOSS and CAC configurations, the angular acceleration experiment requirement and those of the other experiments are expected to roughly coincide because the motion is of a magnitude which would be caused by inherent man motion in these configurations.

The leverage or distance to the vehicle center of mass multiplied by the force residual produces the residual torque. This torque applied about the minimum moment of inertia axis normal to the centrifuge spin axis produces an angular acceleration level which was set equal to .03 deg/sec$^2$ to determine the permissable force residual for each configuration. Table 11 gives the resulting applicable numerical values.

As indicated by Table 11, the permissible force residual varies between 3.8 and 37.6 lbs depending upon the configuration. The most demanding installation is the smaller CSM/LM/SRC. A hardware study was conducted to determine how well an automatic spin balance system could reduce the residual. This study is covered in detail in Appendix C. The essential results of the study were that a force sensor configuration could be used but friction would limit the sensor actuation point to some value always below 10 lbs. This value is above that desired for the CSM/LM/SRC configuration but is acceptable for the large configurations.

62

Table 11- Permissable Force Residual

| Configuration | Inertia Slug $ft^2$ | Leverage ft. | Force Residual lbs. |
|---|---|---|---|
| CSM / LM/ SRC | $0.169 \times 10^6$ (Pitch & Yaw) | 23.4 | 3.8 |
| EOSS | $3.0 \times 10^6$ (Pitch & Yaw) | 41.7 | 37.6 |
| CAC | $0.385 \times 10^6$ (roll) | 12.6 | 16.0 |

The previous discussion of requirements has centered upon removal of static unbalance because (refer to Table 10) the torques due to dynamic unbalance are small enough such that there is no current requirement for dynamic unbalance correction.

A note of caution is advisable at this point. It is recalled that during the initial phase of this centrifuge study, experiment procedures calling for rotation of the subject out of the spin plane existed. This subject motion did set a requirement for dynamic as well as static balancing. While current experiment design does not require dynamic balancing, changes or additional experiments using motion of the subject out of the spin plane would produce a requirement for dynamic as well as static balancing.

To compensate for static imbalance, movement of a single weight in a plane parallel to the spin plane is satisfactory. However, the counterweight required is physically large. In order to best integrate the mass motion into the centrifuge design it has been split into two weights of half size capable of motion in planes parallel to the spin plane and located on top and bottom of the centrifuge. To satisfy the requirement for static balance the two weights would be moved identically. It should be noted that if a later change in experiments causes large dynamic unbalance torques, differential motion of the upper and lower weights would enable removal of the unbalance torque.

For reference, the control requirements developed in the preceding paragraphs are tabulated in Table 12.

Table 12- Spin Balancing System Requirements

| | |
|---|---|
| Counterweight | 660 lbs. |
| Travel | +1/2 to -64 inches along couch axis. |
| | -7 to 13.2 inches transverse to couch axis. |
| Force residual | 10 lbs. |
| Maximum velocity | 1.5 inch/sec. |
| Maximum acceleration | 15 inches/sec$^2$ |

Counterbalancing System Requirements - Countermomentum. - The countermomentum system requirements are based upon the spin momentum and torque of the centrifuge compared to the CMG autopilot system capability. The primary CMG control system is assumed to be that currently planned for the CAC configuration. Pertinent sizing information is listed in Table 13.

Table 13- CMG Autopilot Reference Data

(Three, 2 gimbal, CMG's)

| Characteristics/CMG | |
|---|---|
| Size | 19 ft$^3$ |
| Weight | 400 lbs |
| Power | 60 watts operating, 170 watts startup |
| Type | 2 gimbal $\pm$ 80 degree inner and $\pm$ 175 degree outer |
| Capacity | 2000 ft-lb-sec |
| Spin Speed | 8000 rpm |
| Activation | 7 hrs. spin up |
| Torque Range | 160 ft-lbs maximum, 160/5000 ft-lbs min. |

Of immediate interest is the maximum momentum capability of somewhat under 6000 ft-lb-sec. and the maximum torque of 480 ft-lbs for the 3 CMG's. These maximums are not always available. They depend upon the orientation of the 3 momentum wheels. Exceeding the remaining momentum capability causes the CSM A/P to fire to unload this momentum thereby causing accelerations in excess of most experiment requirements. Exceeding the torque capability has obvious results.

The criteria selected for sizing the amount of countermomentum to be supplied with centrifuge spin up is based on the following:

a.  The momentum to be absorbed by the CMG's due to centrifuge operation shall not exceed 1000 lb-ft-sec. Allowing that the momentum state of the CMG's along the centrifuge spin axis can be between $\pm$ 6000 ft-lb-sec. yields a better than 90% probability that the CMG's will not saturate while the centrifuge is being operated.

b.  The maximum centrifuge spin up down torque is 240 ft-lbs. The countermomentum system shall be capable of exerting a maximum countertorque of the same magnitude.

The countermomentum system is sized by the requirement for absorption of 8500 lb-ft-sec. at a maximum rate consistent with 240 ft-lbs torque.

Proposed Countermomentum System Configuration. - Figure 29 illustrates the proposed countermomentum system. Two single degree of freedom control moment gyros (CMG) are initially spun up with the centrifuge at rest. The CMG momentum vectors are displaced 30 deg. from the centrifuge spin momentum vector occurring when the centrifuge is in operation. Their net momentum is directed along the centrifuge spin axis and is equal to one-half the maximum required value of 8500 ft-lb-sec. This results in a spin momentum per gyro of 2450 ft-lb-sec. Assuming that the particular experiment requires maximum centrifuge speed, the CMG's are driven at the same rate in opposite directions, as shown in Fig. 29, to final positions again 30 deg. from the spin vector but with their momentum oppositely directed. The net change in momentum due to centrifuge plus countermomentum system would be the difference between the centrifuge and countermomentum system which is, for the sizing assumed, 1000 ft-lb-sec. plus dynamic errors associated with control of the CMG gimbals. The required output torque of the two CMG's, including worst case geometry, is 246 lb-ft/gyro and is based upon the torque output along the centrifuge axis being capable of counteracting the centrifuge spin-up torque maximum of 240 ft-lbs. The two CMG's are shown geared together to provide the opposite direction gimbal motion. However, the CMG units are physically large and it may be
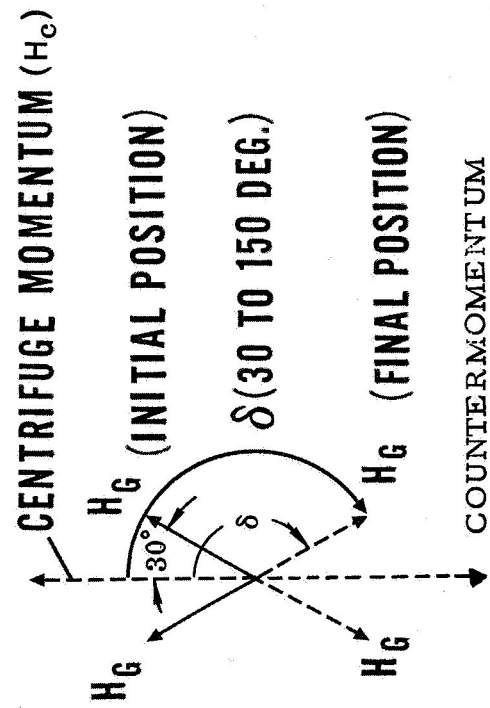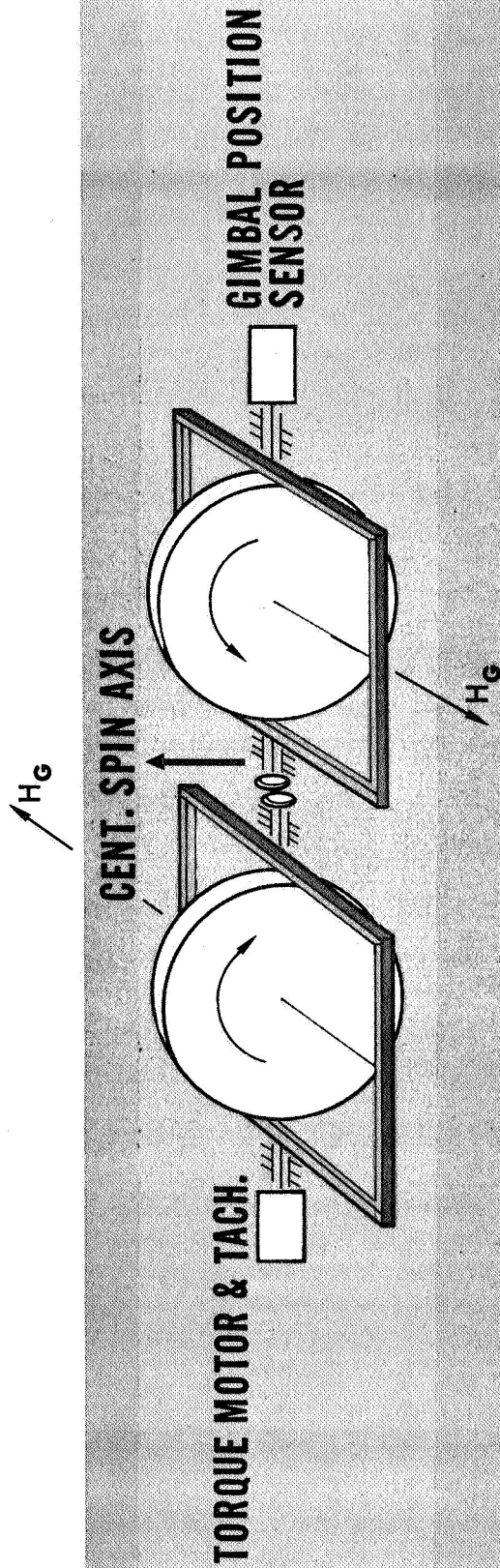
Figure 29. Proposed Countermomentum System

desirable to separate the two units. If this is done, the required gimbal motion can be provided by separate torquers on each unit. One unit torque would receive the gimbal position command based upon centrifuge speed or motor torque while the other would be commanded to follow using individual gimbal position sensor outputs. Sizing information for the CMG units comprising the countermomentum system is given in Table 14.

Table 14- CMG Countermomentum System Sizing Data*

(2 Single Degree of Freedom CMG's, $\pm 60^{\circ}$)

| | |
|---|---|
| Total $\Delta$ H requirement | 8500 lb-ft-sec. |
| Spin Momentum/gyro | 2450 lb-ft-sec. |
| Output torque/gyro | 246 lb-ft |
| Spin motor power/gyro | 56 watts |
| Size (outside diameter)/gyro | 32 inches |
| Weight/gyro | 200 lbs |
| Total Weight | 400 lbs |
| *Sizing data estimated by GD/C based upon average of vendor inputs | |

The control diagram for the CMG countermomentum system is shown by Figure 30. Sensing of angular momentum is derived from either centrifuge spin rate or the time integral of a spin torque sensor. If angular rate is used, it is suggested that counterweight position (along the couch axis) be used to generate a measure of the centrifuge spin inertia. Figure 31 is a plot of spin axis inertia values against counterweight position along the couch axis. It is taken from Table 10.

As indicated there is good correlation between spin inertia and counterweight position. Inserting this information into a multiplier on angular rate should give an adequate measure of centrifuge momentum.

As indicated in Figure 30, centrifuge momentum is compared with the change in momentum of the CMG's. The difference in momentum is the error signal used to establish a balance. Excluding dynamic errors, the balance implies no torque or momentum transmitted to the spacecraft. The stability of the closed loop is dependent upon details of CMG design. The ATM system design is understood to have a bandpass of approximately 40 rad/sec. With this bandpass no unusual problems are anticipated in providing outer loop bandpass, with adequate damping, to 1 cps or better. This
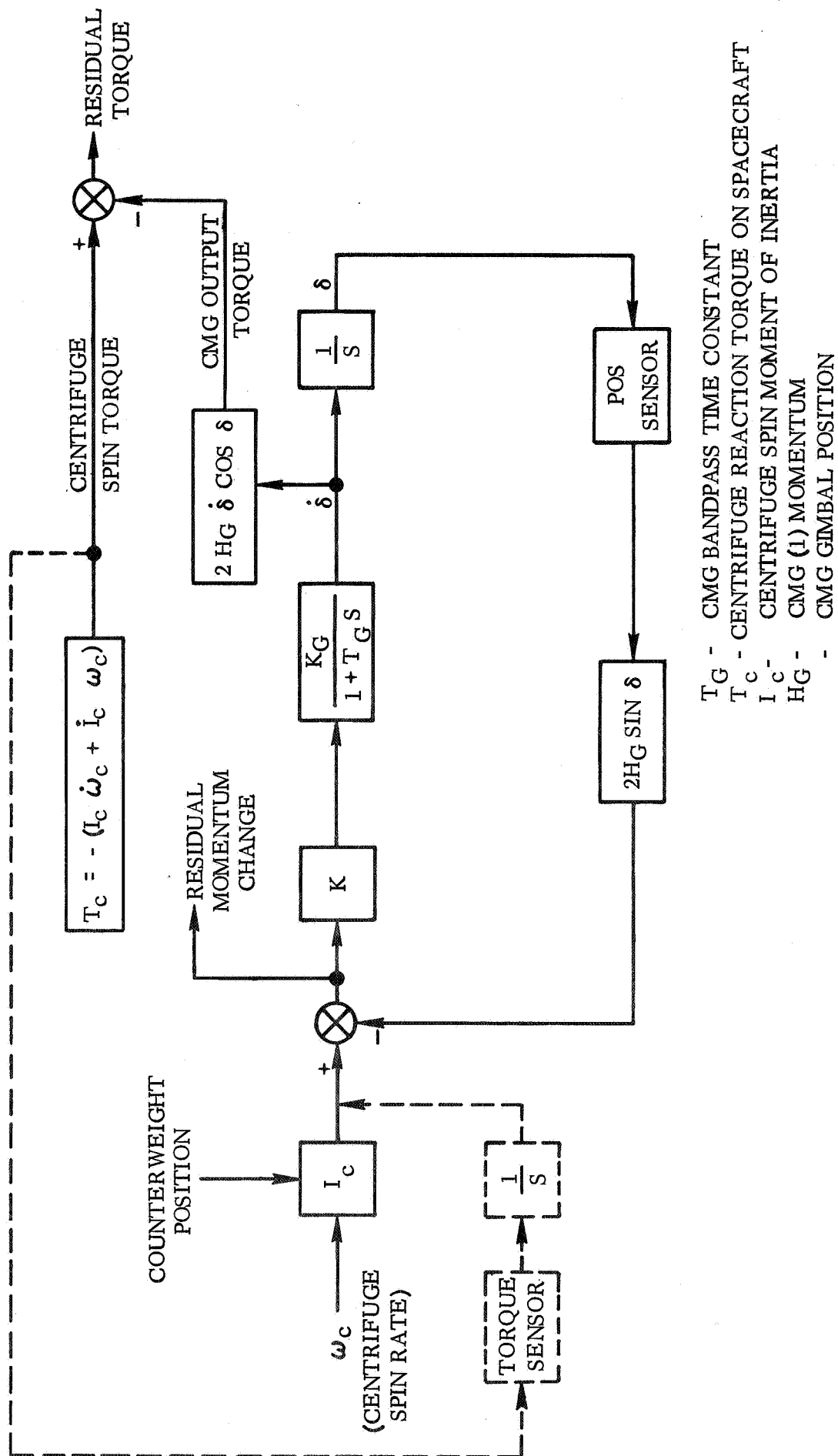
Figure 30.   Centrifuge Countermomentum System Control Diagram

$T_G$ -   CMG BANDPASS TIME CONSTANT
$T_c$ -   CENTRIFUGE REACTION TORQUE ON SPACECRAFT
$I_c$ -   CENTRIFUGE SPIN MOMENT OF INERTIA
$H_G$ -   CMG (1) MOMENTUM
   -   CMG GIMBAL POSITION

overall bandpass would be adequate to follow angular rate changes limited to .17 rad/sec$^2$ with little dynamic error.
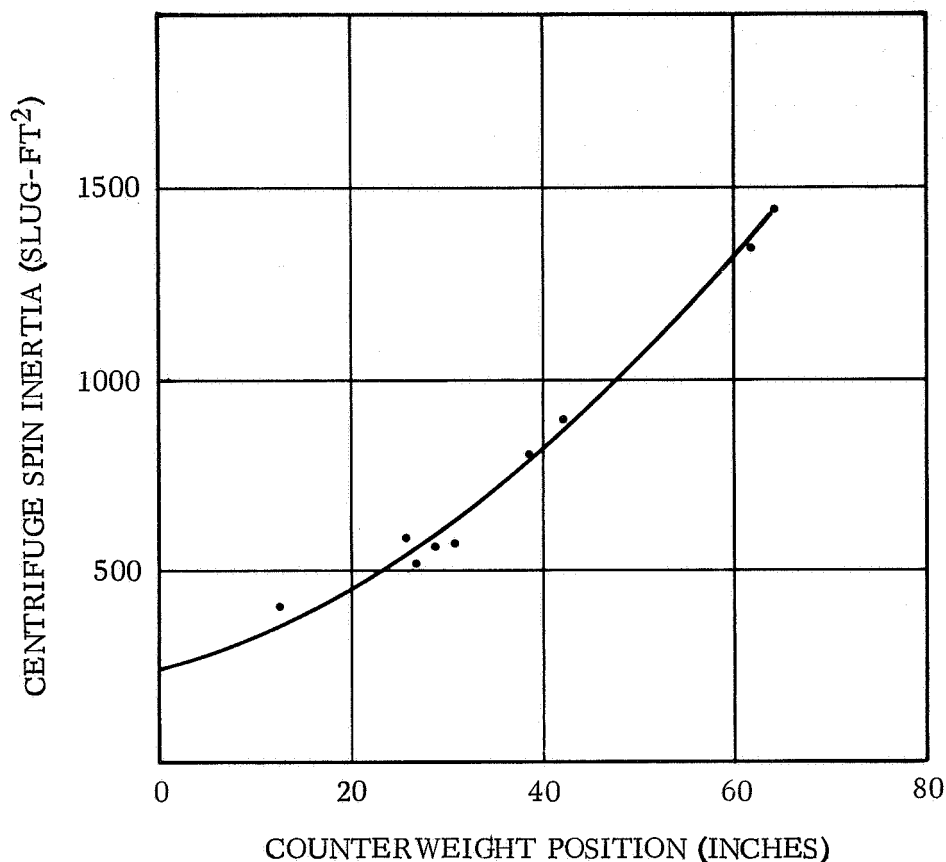


Figure 31. Counterweight Position Measure of Spin Inertia

Countermomentum System Alternates. - There are some alternate countermomentum system configurations worthy of brief description. They were considered because they potentially improve momentum matching performance and reduce electrical power requirements considerably over that of the proposed system but exhibit about the same weight and size. They were rejected because they do not interface with the present design as well as that proposed.

Figure 32 shows the concept in one such system.
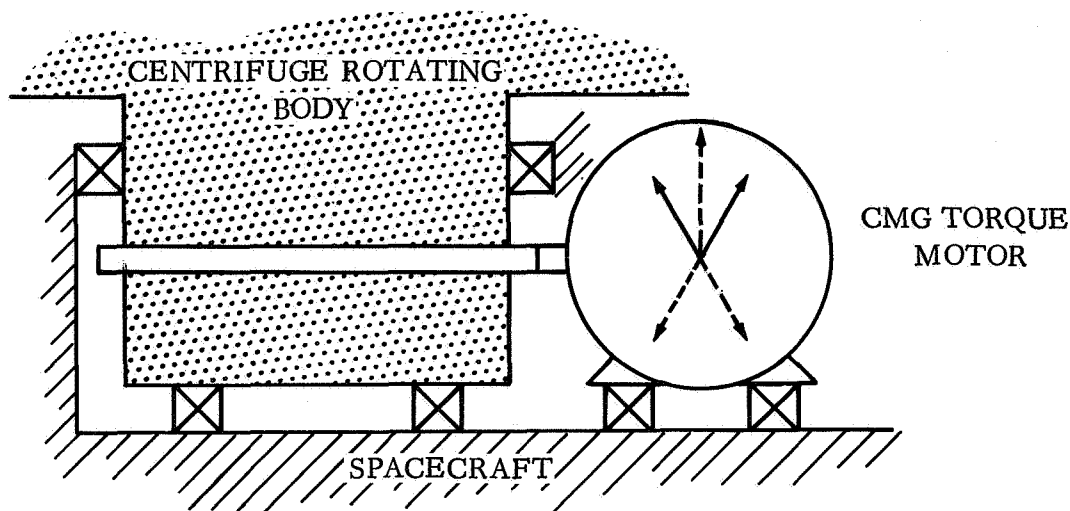
Figure 32. Alternate Countermomentum Configuration

Two single degree of freedom CMG's are paired as shown previously in Figure 29. The same change in momentum procedure described for the proposed configuration is used to impart the primary spin torque. However, the twin CMG assembly must rotate at centrifuge speed eliminating the possibility of routine electrical interwiring from the spacecraft to the CMG. In addition the CMG's must supply the bearing friction and centrifuge windage torques. These torques may be small but are continuous and somewhat difficult to predict. The bulk of the CMG's is also a problem in that their direct connection to the centrifuge poses a design interface problem. The advantages are the negligible reaction torque on the vehicle, and deletion of the spin motor. Electrical power is reduced to that required to maintain the CMG spin rate and torque operation.

A similar system (not shown) hardmounts the CMG's to the rotating centrifuge body. Operation is identical but larger CMG units are needed due to the increased momentum requirements derived from the increased rotating weight. Electrical power would, in this case, be taken from the supply integral with the centrifuge rotating body.

Proposed Spin Balance System Control Configuration

As mentioned previously in the requirements discussion, static balancing is required. The control system comprises the use of force sensors to measure the existing unbalance, motors to drive the two counterweights and threshold logic to activate the motors when the unbalance force exceeds 10 lbs. The force sensing study is described in detail in Appendix C.

70

The resultant proposed sensor configuration uses six force sensors arranged in a plane. These sensors are interconnected, as shown in Figure 33, to provide force signals along the couch axis ($F_{S2}$) and lateral axis ($F_{S3}$). The configuration inherently provides spin torque which would possibly be used by the countermomentum system in the manner previously discussed.



$T_C$ - CENTRIFUGE SPIN TORQUE

$F_S$ - STATIC UNBLANCE FORCE
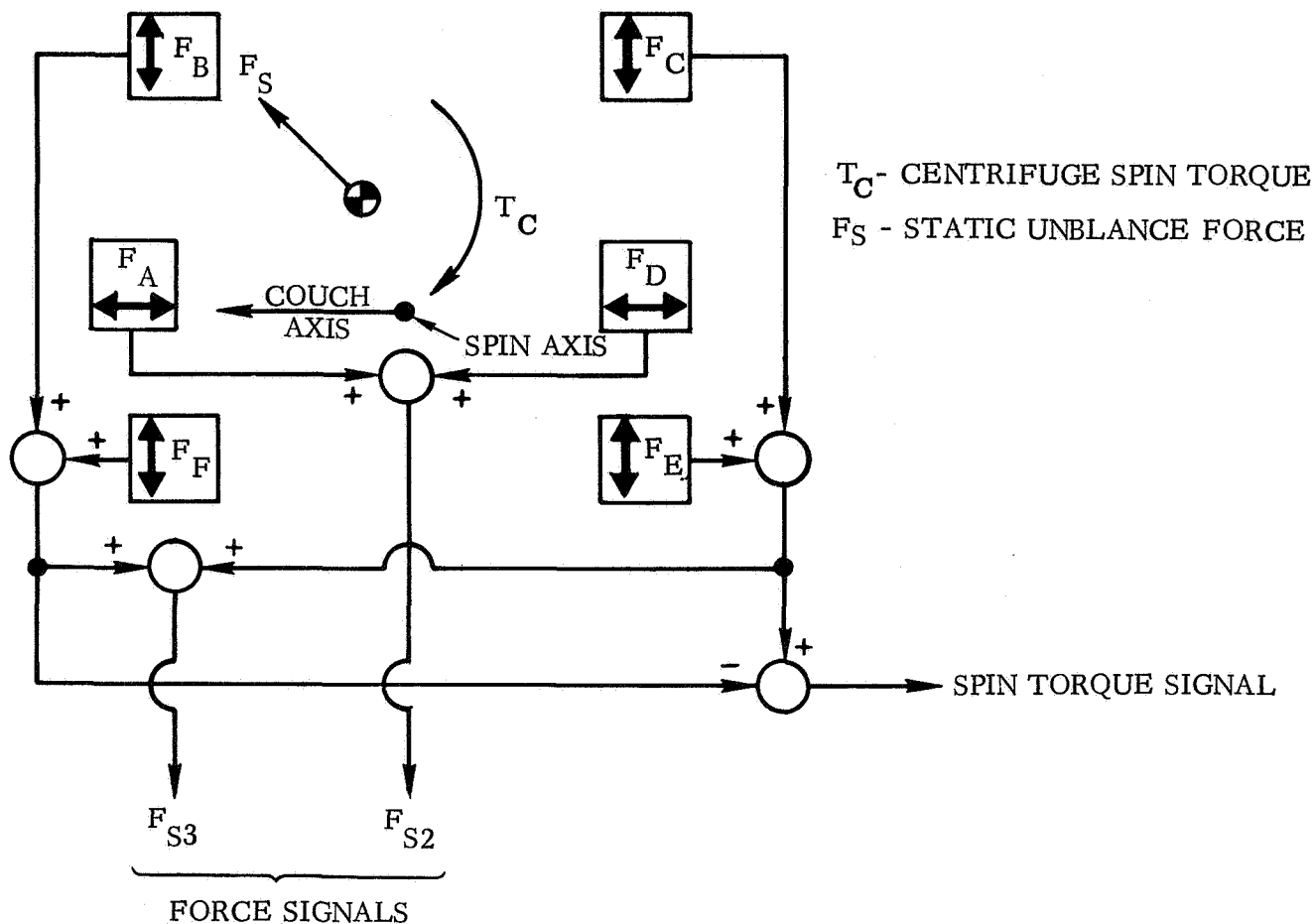
Figure 33. Proposed Centrifuge Unbalance Force Sensor Configuration

Figure 34 illustrates the counterweight drive configuration. As indicated, two weights are used and driven by a single motor along the centrifuge radial direction. Lateral motion is provided by a motor on each weight.
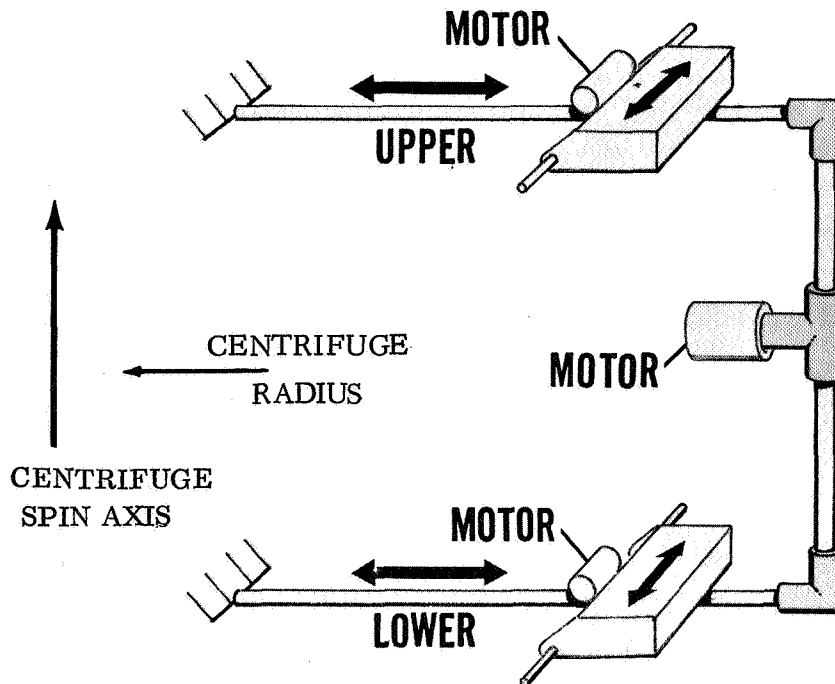
Figure 34. Counterweight Drive Configuration

The control configuration which seems satisfactory is illustrated in Figure 35. Both the couch axis and lateral force sensor signals are passed through deadzones corresponding to $\pm10$ lbs force. Upon exceeding this threshold the drive motor is energized to move at a fixed maximum rate of 1.5 inches/sec. until the force signal drops below 10 lbs. The centrifuge operator is required to make an initial setting of counterweights by inserting a "run" signal to the couch axis drive motor prior to the centrifuge operation.

A single motor is used to drive both the upper and lower counterweights along the couch axis. Two separate motors are used to move the upper and lower counterweights in the lateral direction. The upper and lower weights move together. This is done electrically by causing one weight to track the other based upon the outputs of lateral position sensors. As illustrated in Figure 35, the upper weight was arbitrarily used as the reference weight and the lower weight tracks through a linear control.

The on-off nature of the control system, while usually easier to implement compared to proportional control systems, can exhibit a hunting instability depending on deadzone size and motor start-stop characteristics. The worst case corresponds to maximum centrifuge speed with the counterweight being moved toward the center of the deadzone at the maximum speed of 1.5 inches/sec. The time constant of 0.1 sec. on the counterweight drive

motor corresponds to a maximum acceleration-deceleration capability of $15$ inches/sec$^2$. With these characteristics the motor will enter the $\pm 10$ lb deadzone, a distance of 0.15 inches. The minimum total width of the deadzone corresponds to operation at maximum centrifuge speed and is 0.254 inches. The drive motor should then be capable of stopping the counterweight within the deadzone with no hunting.
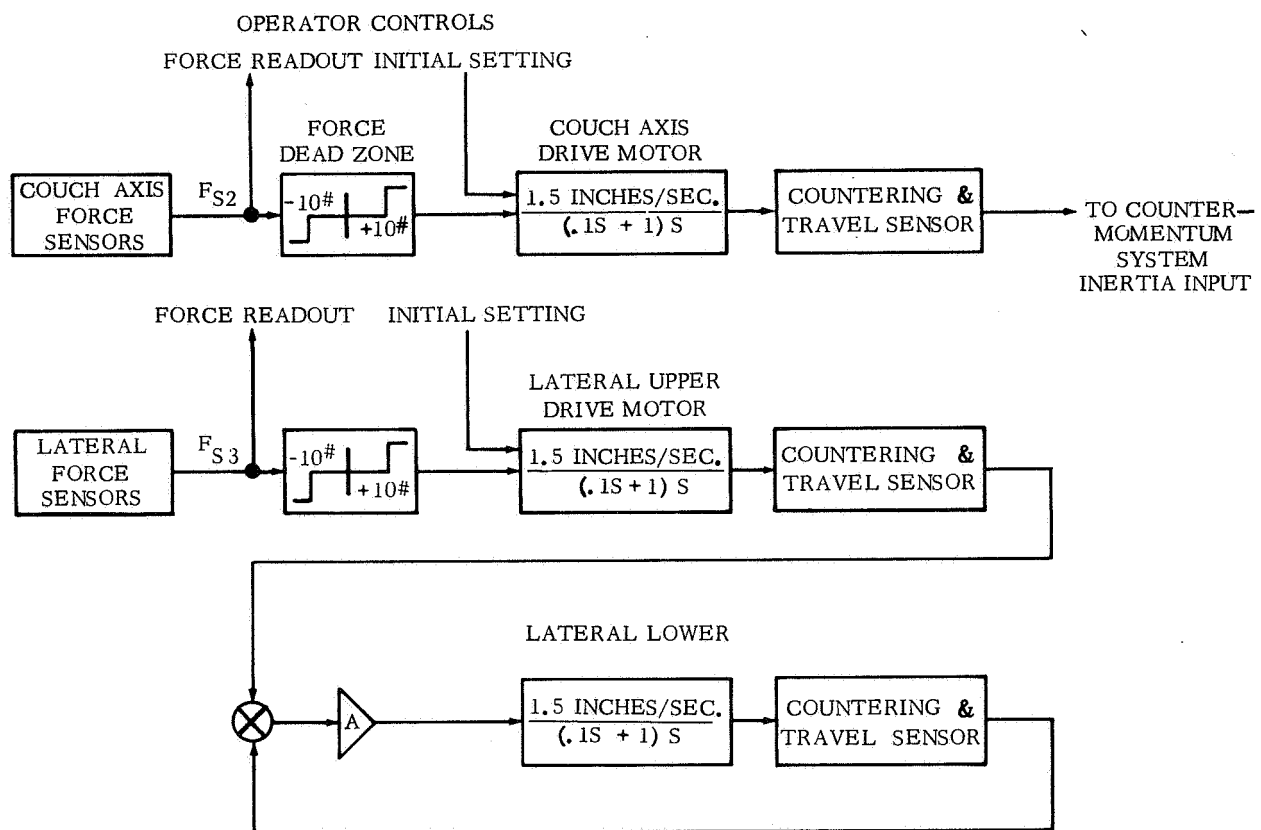


Figure 35 - Spin Balance Control Block Diagram

The lower weight drive motor does not use a deadzone type control because the allowable deadzone may be too small to avoid hunting. Assume that the upper weight is at its correct lateral position. About 40 lbs of static unbalance force is caused per inch of difference between upper and lower weight lateral position. In order to prevent unnecessary hunting between the upper and lower weight control loops, the deadzone in lower weight control travel should be no more than about .05 inches (equivalent to 2 lbs unbalance force). Comparing the .05 inches to the overtravel obtained previously of 0.15 inches indicates that a linear amplifier rather than deadzone logic is desired.

## Spacecraft Perturbing Torques

After incorporation of the countermomentum and spin balance system, the centrifuge produces residual perturbing torques which cause spacecraft motion. The major centrifuge perturbing torque is caused by the residual 10 lb static unbalance force with leverage gained by the location of the centrifuge relative to the spacecraft center of mass. The previously given equations (13) and (14) evaluated the force and torque respectively. As would be shown by expansion of equation (14), the torque on each of the spacecraft axes is sinusoidal at spin frequency due to the rotation of the force vector with the centrifuge body. The maximum value of this sinusoidal torque and the spacecraft axes about which it appears (using conventional CSM axes designation) is given in Table 15. The frequency range varies from 0.75 rad/sec to the centrifuge maximum rotation rate of 6.5 rad/sec. Below centrifuge spin rate of 0.75 rad/sec the unbalance force level of 10 lbs cannot be generated by the expected maximum amount of centrifuge unbalance.

Other than the perturbing torque induced by the centrifuge, the most significant disturbance will be that due to man motion. The amount of torque perturbation from this source was estimated and is also given in Table 15. The RSS total of the centrifuge and man-motion torques is considered to represent the major part of spacecraft torque disturbances causing significant spacecraft motion. Comparison of the spacecraft motion induced by both centrifuge unbalance and man-motion torques with experiment requirements is the end item of the attitude control feasibility study.

The man-motion torques were based upon examination of data supplied in Reference 5. From the data it was felt that a 4 lb force (sinusoidal maximum) at 1.5 to 6 rad/sec. was a reasonable estimate per crew member for normal motion aboard a spacecraft. A distribution of crew members for each of the centrifuge installations was assumed and the resultant torque was calculated based upon root sum squaring the torques from each crew member. It is emphasized that the resultant total is an estimate only.

Table 15- Perturbing Torque Summary

| Configuration | Perturbing Torques (lb-ft) | | |
|---|---|---|---|
| | Centrifuge | Man Motion | RSS Total |
| **CSM/LM/SRC** | | | |
| Pitch & Yaw | 230 | 140 | 270 |
| Roll | -- | 45 | 45 |
| **EOSS** | | | |
| Pitch & Yaw | 460 | 330 | 565 |
| Roll | -- | 75 | 75 |
| **CAC** | | | |
| Pitch | 200 | 230 | 305 |
| Yaw | -- | 230 | 230 |
| Roll | 200 | 200 | 280 |

It is pertinent to make some comparisons. Spacecraft motion resulting from man-motion induced torques is currently identified to be the major limitation in fine-pointing (Reference 4). Comparison of the magnitudes of torques from the centrifuge and man motion given in Table 15 would then imply that the centrifuge torque is a significant source of perturbation torque.

Further, the torque output capability of the ATM CMG on a per spacecraft axis is estimated to be 1.5 times the maximum available from a single gyro or 240 ft-lbs. It is noted that this torque output is exceeded in all configurations.

CMG Autopilot Control Capability

Preliminary to conducting an analysis of the CMG autopilot capability to counter the effect of the perturbing torques on the spacecraft, information in regard to spacecraft flexural characteristics were studied to determine whether inclusion of flexure was required.

Effect of Spacecraft Flexibility. - Reference 6 indicated that the significant lower frequency modes for the Apollo vehicle were contributed by the CSM/LM docking tunnel interface. The spring constant at this joint was calculated from the given lowest value bending frequency. This spring constant was used to establish a model for the CSM/LM/SRC installation comprising two rigid bodies, the CSM and the LM/SRC modules, connected by a torsion spring. The resultant first bending and torsion frequencies calculated were 3.5 and 3.7 cps respectively.

The EOSS and CAC configurations were assumed to be sufficiently similar to the SIVB workshop with cluster configuration such that flexural data supplied in Reference 7 would be applicable. The first bending and torsion frequencies noted were 2.0 and 2.3 cps respectively.

Reference 8 also applies to the EOSS and CAC configurations and is an updating of information supplied in Reference 7. It was received by GDC at a time too late to be incorporated into the centrifuge study. Review of this data indicates that the present MDA-LM/ATM docking joint causes flexural frequencies of 0.373 cps (solar panels undeployed) to 0.495 cps (solar panels deployed). Numerous lower frequency solar panel flexure frequencies are also to be noted. The panels having relatively low mass are not expected to seriously affect the attitude results given in this study but the lower frequency bending at the MDA joint is. A considerable increase in motion, due to excitation at this frequency from the perturbing torque sources, relative to rigid body analysis would be expected.

Figure 36 illustrates and defines a control system block diagram including flexure. As indicated, the many parameters associated with sensor, disturbance force and torque locations, together with spacecraft flexural characteristics, yield a complex situation.

The initial intent was to increase the A/P transfer gains so that control could be secured in the range of 0.5 to 1.0 cps, but it was found that attainment of such a control band was quite dependent upon flexural model specifics and CMG torque authority for the magnitude of disturbance torques encountered. Eventually it was decided to set the A/P gains low enough so that these dependencies were removed.

Figure 37 is a frequency response plot of spacecraft attitude acceleration, rate and displacement to torque disturbance. As indicated, the closed loop break or corner frequency of autopilot control was set at about 0.3 cps by using the gains indicated. The familiar effect of vehicle flexibility in causing rather sharp peaking is also shown for the various configurations. The frequency band of the centrifuge unbalance torque terminates at the maximum centrifuge spin rate of 1.08 cps. Major man-motion torques (not shown) are thought to lie in about the same band but do not terminate
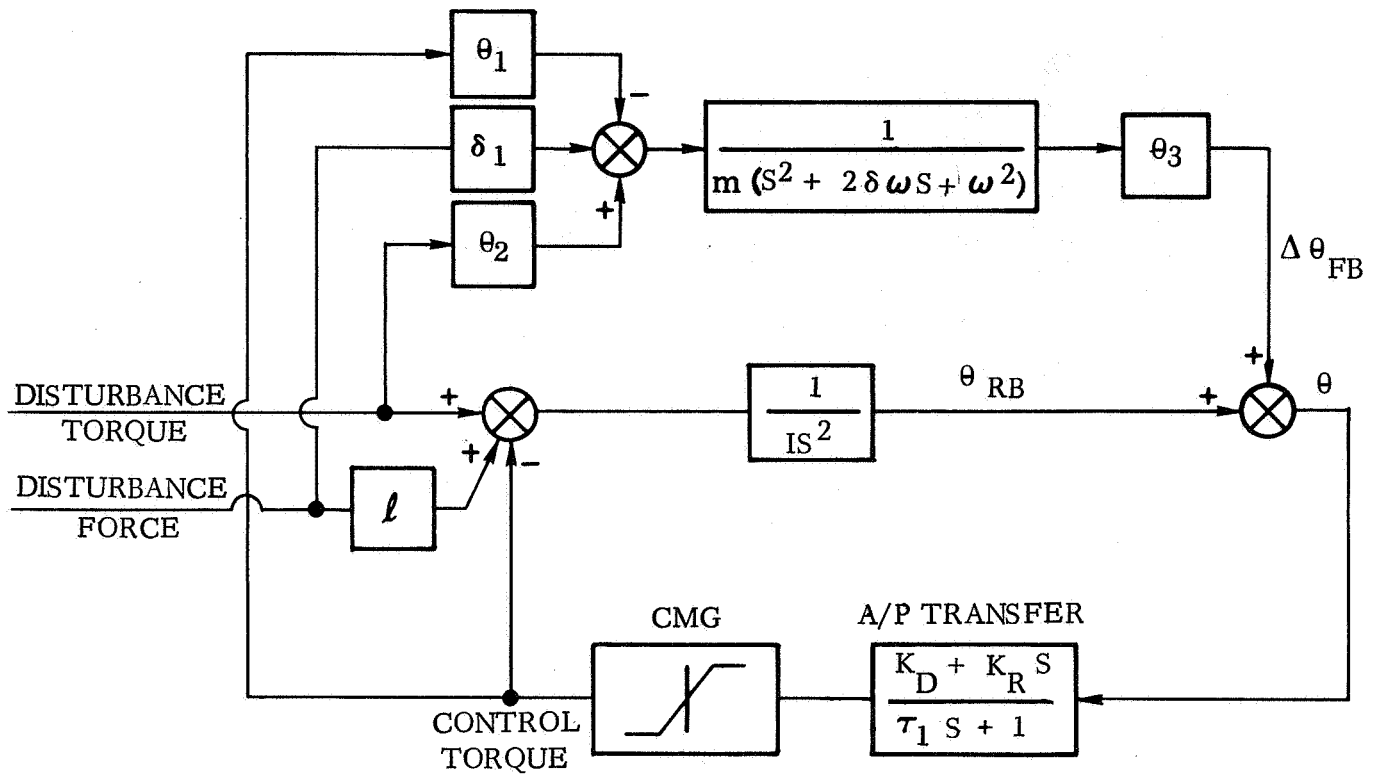
where

$\theta_{RB}$    –    rigid body angular displacement

$\Delta\theta_{FB}$    –    perturbation of angular displacement due to flexure

$\theta$    –    total angular deflection at sensor location

$I$    –    moment of inertia of vehicle

$m$    –    generalized mass of mode considered

$\delta$    –    damping ratio of flexural mode

$\omega$    –    natural freq. of flexural mode

$K_D, K_R$    –    displacement and rate bias respectively

$\tau_1$    –    time constant characteristic of CMG

$\theta_1, \theta_2$    –    slope of mode shape curve at location of control torque and disturbance torque respectively

$\theta_3$    –    slope of mode shape curve at attitude sensor location.

$\ell$    –    force location relative to center of mass

$\delta_1$    –    deflection of mode shape curve at disturbance force location

Figure 36. CMG-Controlled Flexural Body Model
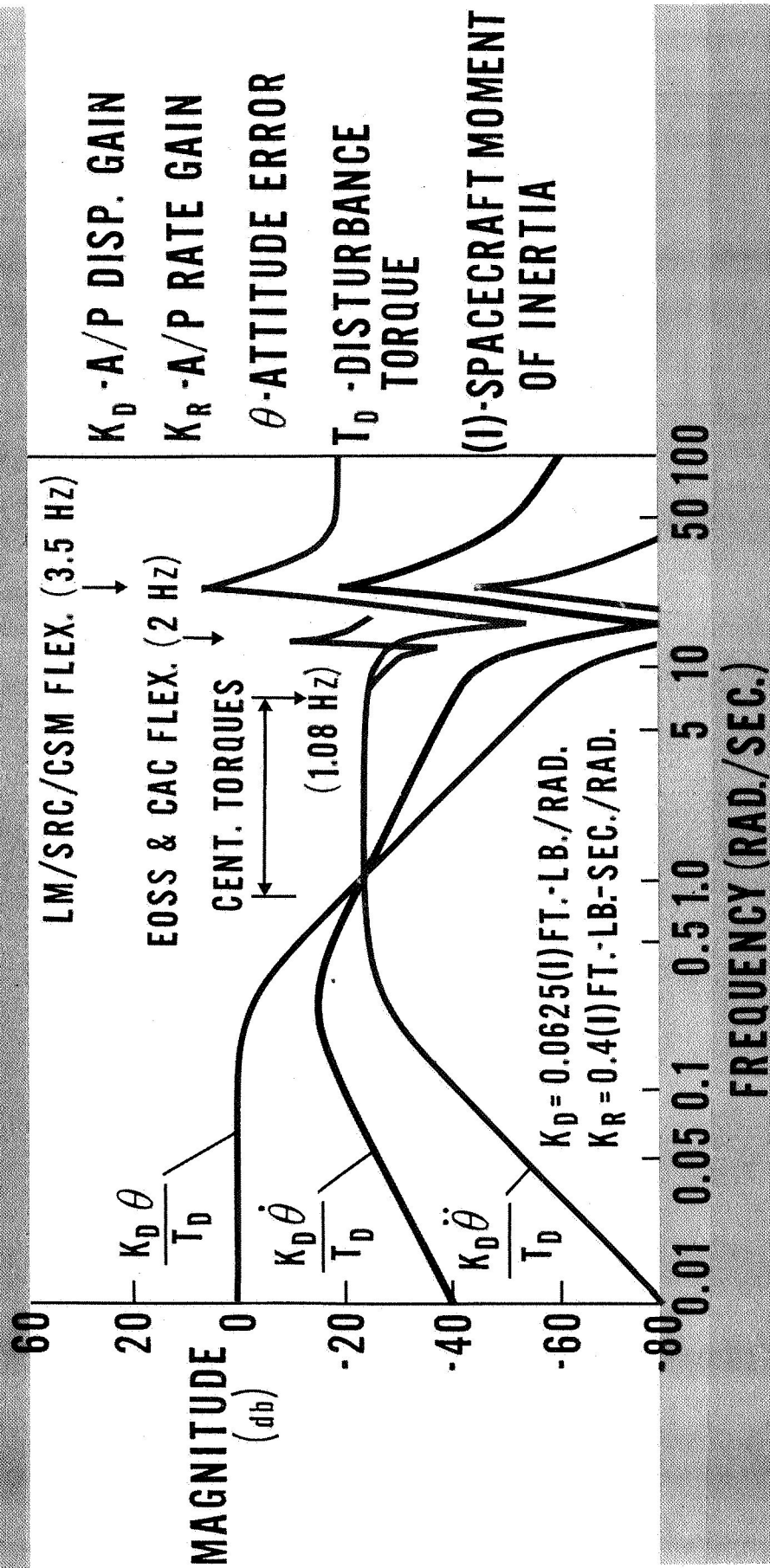
Figure 37. CMG-Control System Frequency Response - (Including Flexure).

sharply at a frequency of 1 cps as does the centrifuge. Rather, the torque magnitude is thought to decrease with frequency thereafter in an unknown manner.

The autopilot gains used to calculate the frequency response reflect the use of low values to avoid coupling at the bending frequency. As indicated by the flat portion of the acceleration frequency response at centrifuge and man-motion torque disturbance frequencies, the response is the same as simply applying the torque to the rigid body with no autopilot control at these frequencies. This information permits easy calculation of the effect of these torques upon vehicle motion.

It is highly significant to note the adverse effect of increasing centrifuge operating frequency such that it encompasses the bending natural frequency. The reverse situation, the spacecraft bending frequency decreasing within the centrifuge band, would also yield identical results.

Spacecraft Attitude Control Results (Rigid Body). - Centrifuge experiment dynamic feasibility is determined by comparison of the experiment attitude requirements with the results of CMG and CSM RCS autopilot studies. Only the requirements for the low-g and low-ang-acc. types (see Table 6), are included because the high-g type requirements are not demanding in comparison. Log-log plots of angular acceleration versus angular rate have been developed for each configuration.

Figure 38 applies to the CAC configuration. A locus of acceptable simultaneous maximum vehicle angular rate and acceleration is shown for the experiment classes indicated. The on-off operation of the CMS autopilot against the environment is indicated by plotting the constant "on" acceleration caused between rate limits bounded by the minimum impulse lower value and autopilot design actuation point upper value. Comparison with the requirements indicates that the CSM autopilot is not adequate for the centrifuge experiment with the exception of the high-g type.

The linear nature of the CMG autopilot replaces the short bursts of control torque with continuous counteracting torque of equal magnitude. The net result is essentially no attitude motion due to the environment.

The perturbing torques in roll, pitch and yaw due to centrifuge unbalance and man-motion (see Table 15) yield the locus of maximum simultaneous angular rate and acceleration shown. The acceleration is directly the perturbing torque divided by the spacecraft moment of inertia. The angular rate magnitude increases as the frequency of the perturbing torque is decreased. The value used a lower limit of 1.0 rad/sec. As the resultant unwanted extraneous motion is well below that required, the configuration is acceptable.
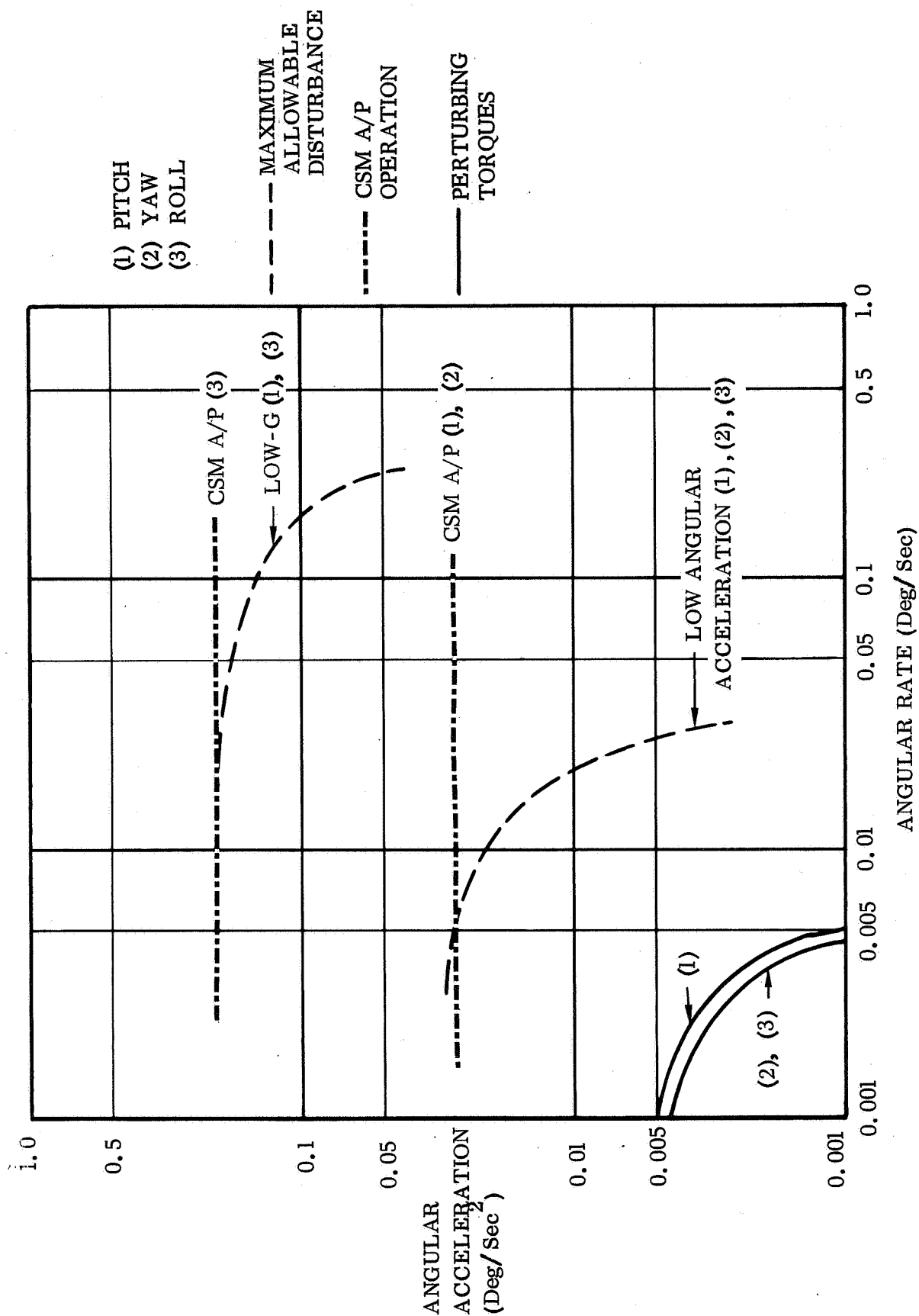
Fig. 38 Attitude Control Study Results (CAC)

Figure 39 applies to the EOSS configuration. There is a difference in numerical results but the conclusion of acceptability of the CMG control and non-acceptability of the CSM autopilot is the same as that for the CAC configuration.

Figure 40 applies to the CSM/LM/SRC configuration. In this configuration, the same conclusion again applies in regard to CSM autopilot operation against the environment. However, CMG control only improves the attitude control to the extent that low-g experiment requirements are met. The low-ang-acc requirements are not met by about a factor of 3. To meet the requirements for these experiments, the CMG autopilot gains could be raised to yield about a 3 rad/sec closed loop bandpass. This increase in gain may be shown to be possible in later development study including body flexibility and non-linear effects of CMG torque output limitations. Such a study should include the centrifuge unbalance and man-motion torques as the dominant attitude error sources.

An alternative solution would be to retain the expended S-IVB injection stage as part of the orbiting configuration rather than separating from it. In this case, the location of the centrifuge is closer to the system center of mass than in the EOSS or CAC configurations while exhibiting about the same amount of inertia. If this is done, the resultant configuration, from the attitude control performance viewpoint, becomes the best of the three considered.

Dynamics Feasibility Summary

Dynamic problems peculiar to the centrifuge orbital installation have been examined in the preceding material. It is found that the orbital installation of the centrifuge is feasible for all three installation if the centrifuge operating frequency and vehicle structural bending frequencies are sufficiently separated. It is remarked that this analysis used a first mode bending frequency of 2 cps for the CAC and EOSS configurations, as indicated by Reference 7. If actual bending frequencies are substantially lower than this value, as predicted by Reference 8, then structural modification to increase stiffness in areas such as the docking joints may be expected. In any event, quantitative analysis using actual bending data for the particular vehicle installation specified is recommended as a necessary part of any future centrifuge integration study.

The larger installation (EOSS and CAC) are more suitable for centrifuge installation because they provide a CMG autopilot and have greater mass. The CMG autopilot is necessary to meet the more demanding experiment requirements. The larger size minimizes cross coupling induced by centrifuge momentum.
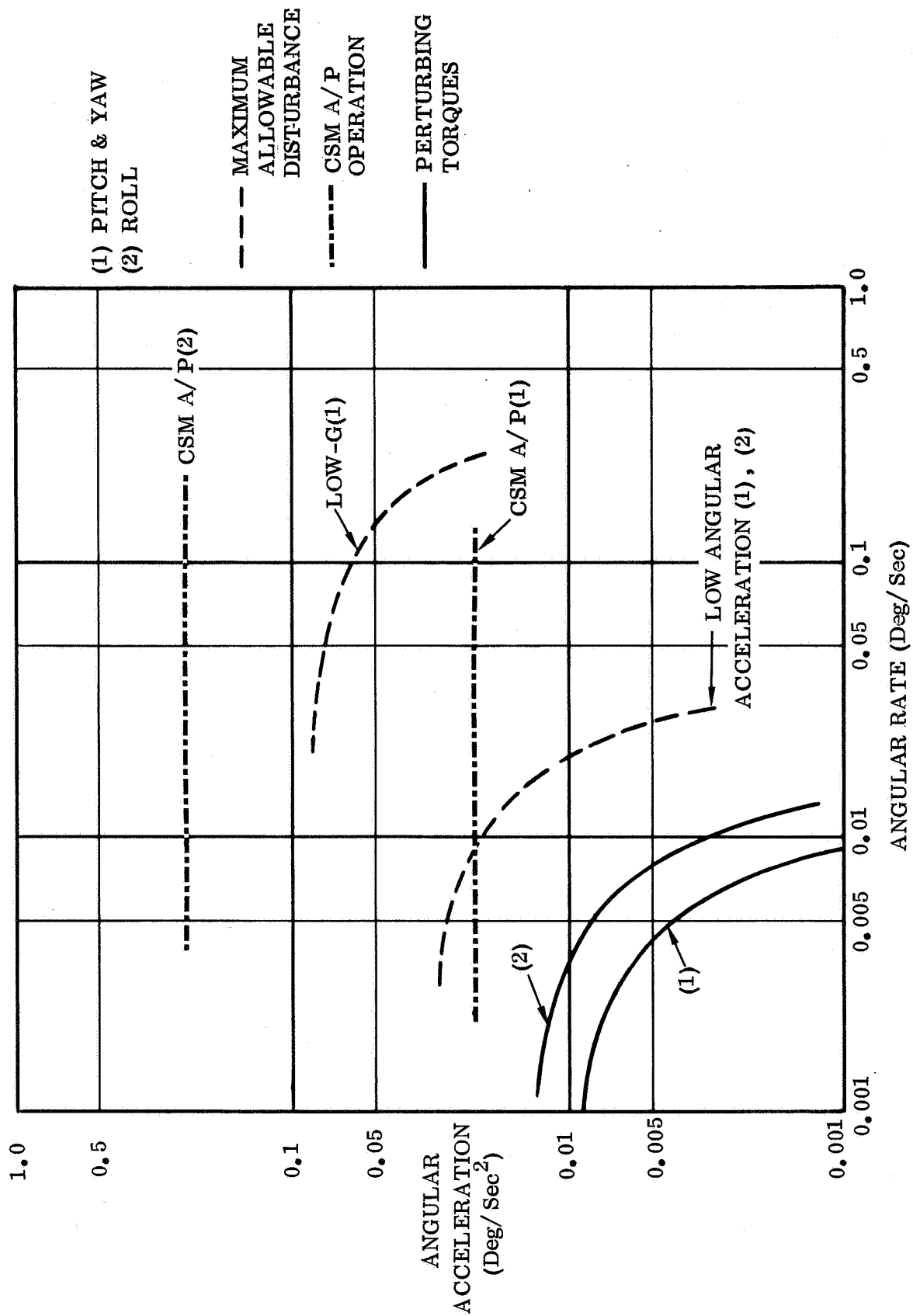
Figure 39. Attitude Control Study Results (EOSS)
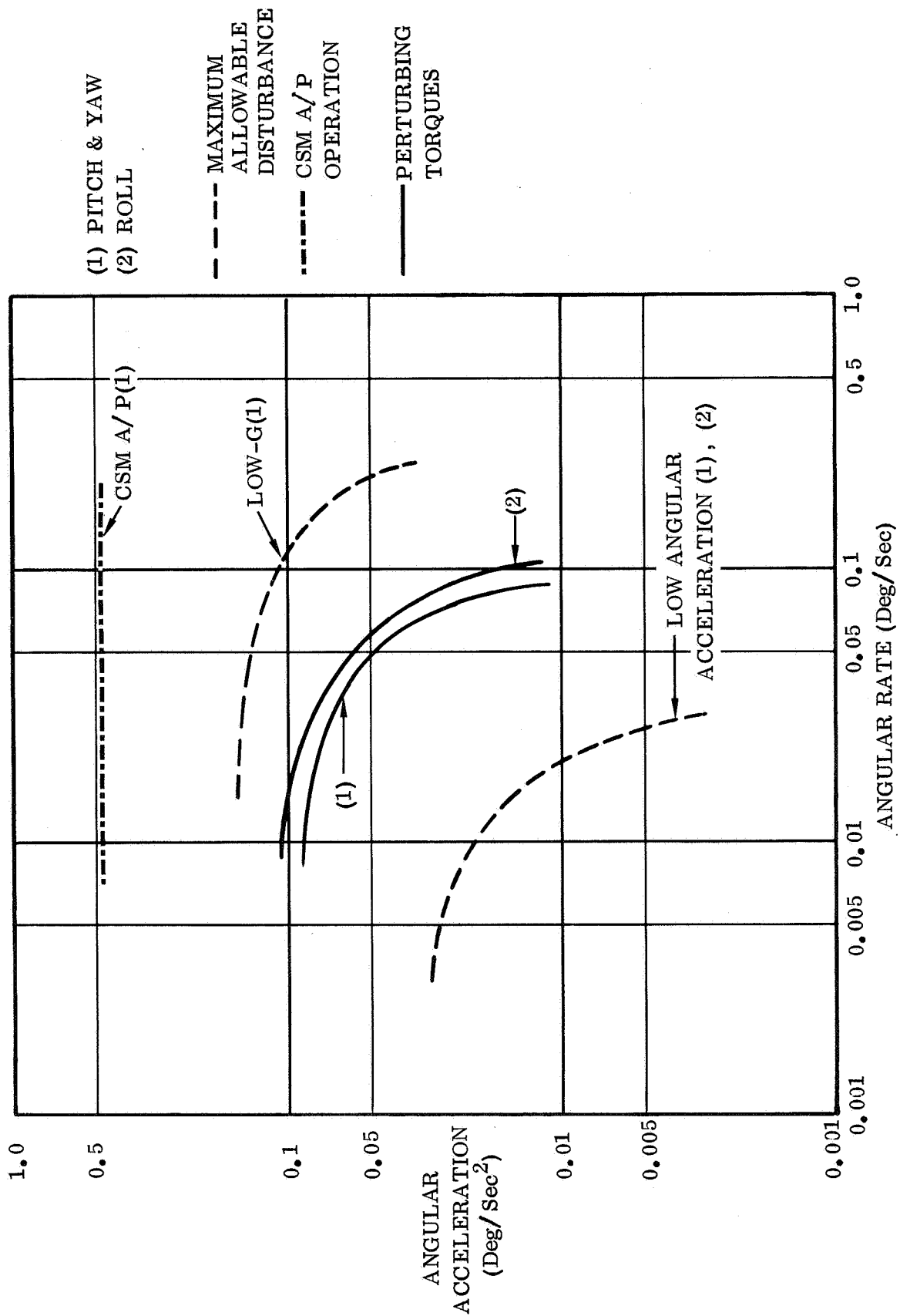
Figure 40. Attitude Control Study Results (CSM/LM/SRC)

The smaller configuration is the least attractive on an overall basis. Addition of a CMG autopilot is required. With the CMG autopilot at conservative gain levels adopted for this study (0.3 rad/sec closed loop band pass), the more sensitive experiment requirements are still not accommodated. Increasing the autopilot band pass to about 3 rad/sec (stability permitting) is indicated. However, alternatively retaining rather than separating the S-IVB launch vehicle makes this installation better than the others.

A countermomentum system is required to maintain the change in momentum caused by centrifuge spin up within the CMG autopilot saturation limits. A pair of single degree of freedom CMG's added and controlled appropriately is considered the optimum way to implement the countermementum system.

An automatic dynamic balancing system involving sensing centrifuge unbalance and appropriately moving counterweights to eliminate the unbalance is recommended. This system is incorporated in the basic centrifuge design.

# ORBITAL CENTRIFUGE DESIGN

## Structural Design and Analysis

This section summarizes all significant data derived during the "in-depth" preliminary design of the centrifuge structural sub-system. Specific activities of the structural design and analysis effort throughout the three program phases were as follows.

Phase I. - Phase I of the study was begun by preliminary definition of the ground rules, criteria, and constraints governing development of the structural sub-system. This activity included analysis of the preliminary experiment definitions to determine subject orientation, degree-of-freedom requirements, motion envelopes, and g-levels for all tests. In addition, initial estimates of maximum operating speeds, spin-up and de-spin rates, and rough mass properties were established. A table of approximate operational loads, for each test, was derived from this data.

During the same time interval a first attempt at generating candidate subsystem concepts was in progress. The primary emphasis was on preparing simplified structural schematics, compatible with the degree-of-freedom requirements which could be used to evolve realistic and efficient load paths. These led to identification of the primary sub-system elements. Subsequent conceptual studies directed at individual elements as well as at the integrated assembly produced a number of competitive candidates. These candidate concepts were refined and brief stress, deflection and weight studies were performed to provide firmer quantitative definition.

This phase of effort concluded with a numerical trade-off analysis of each set of competitive candidates which resulted in definition of the elements of the baseline structural sub-system.

Phase II. - Phase II activity was devoted almost exclusively to providing detail definition of the baseline orbital configuration. This effort was supported by a thorough updating of the ground rules, criteria, and constraints to reflect the additional intelligence assembled in all areas of study as a result of the first phase of work. Particular emphasis was placed on translating improved experiment definitions into more accurate geometrical constraints and load criteria. Estimates of the stiffness properties required of the system to avoid structural resonance during all phases of operation were also established.

Continuation of the refinement process resulted in some revision of the baseline concept as total system requirements were integrated. Extensive stress and deflection analysis paralleled this design evolution which concluded with the preparation of assembly drawings of the primary system elements.

Additional activity in this phase was focused on investigation of the inter-face feasibility of the optimized baseline assembly in both its orbital and ground test modes.

Phase III. - Effort in the final phase of the study was centered in detailing of the primary structural elements by revision of the Phase II drawings, and report preparation.

## Ground Rules, Criteria, and Constraints

Both the mandatory and derived ground rules, criteria and constraints applicable to the structural task are established in the following paragraphs. For the most part, these were finalized prior to or early in the Phase II effort.

Contract Requirements. - Two specific ground rules applicable to the development of the structural subsystem are contained in the contract state-ment of work. The first of these requires a machine capable of producing and withstanding a normal acceleration of 9.0 g - units. The second requires the capability to simulate a typical Apollo earth entry g-profile for re-entry sim-ulation tests.

Experiments. - The baseline experiments, to which the centrifuge structure is configured, are those shown in Figure 41. These were established prior to the Phase I design review and have, in some instances, been revised since that time. In the case of the tilt-table experiment, an increase of mini-mum radius to approximately 3.0 ft. was required to avoid severely compromis-ing the structural concept. This in no way limited the capability to perform the experiment. (The 2.0 ft. minimum radius was a Phase I value which was esti-mated before determination of the baseline radius arm concept, and therefore subject to change. )

Geometrical Constraints. - Configuration and geometry of the structural assembly are governed by a number of requirements, for the most part related to test experiment motion envelopes. As definition of the baseline series of experiments evolved it became possible to establish the degrees of freedom required of the machine for each test. Furthermore, the sequence of positions occupied by the subject during each test forms a corresponding swept-volume envelope. These envelopes establish the clearance envelope for the subject and couch. However, since the couch design progressed simultaneously with the design of the other system elements and its dimensions were not known in advance, it was not possible to establish a fixed clearance envelope. Instead, nominal clearance dimensions between elements in relative motion were estab-lished, and design efforts were coordinated to assure conformance. A 12.0 in. radius sphere is maintained around the center of the subject's head. A minimum of 1.0 in. is maintained elsewhere in all areas remote from the line-to-line motion interfaces.
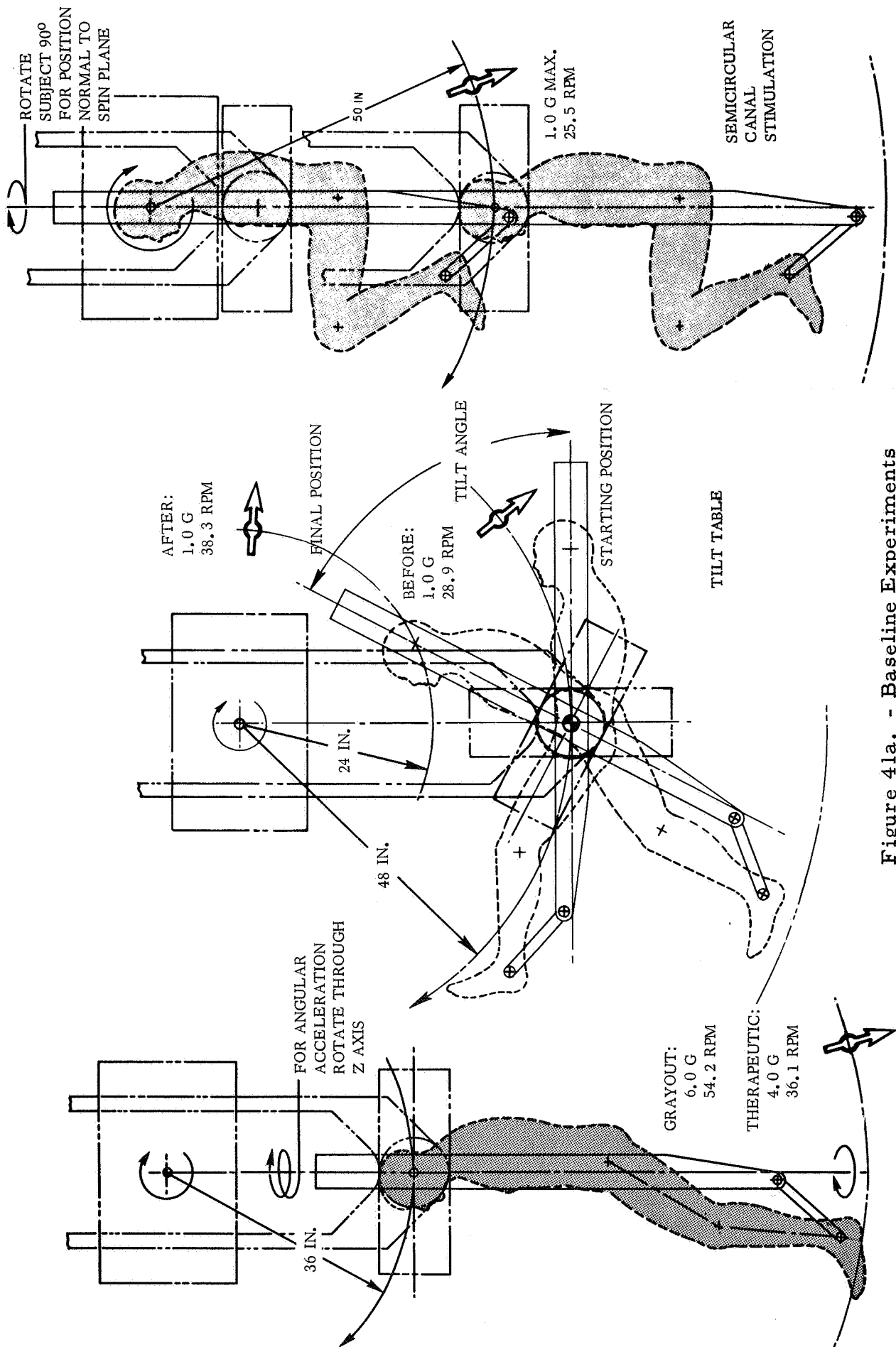
Figure 41a. – Baseline Experiments

ROTATE SUBJECT 90° FOR POSITION NORMAL TO SPIN PLANE

50 IN

1.0 G MAX.
25.5 RPM

SEMICIRCULAR CANAL STIMULATION

AFTER:
1.0 G
38.3 RPM

FINAL POSITION

BEFORE:
1.0 G
28.9 RPM

TILT ANGLE

STARTING POSITION

TILT TABLE

24 IN.

48 IN.

FOR ANGULAR ACCELERATION ROTATE THROUGH Z AXIS

GRAYOUT:
6.0 G
54.2 RPM

THERAPEUTIC:
4.0 G
36.1 RPM

36 IN.

FOR EYE COUNTER ROLLING ROTATE SUBJECT 90° TO NORMAL POSITION

1.0 G
26.5 RPM

50 IN.

OCCULOGRAVIC ILLUSION (SHOWN) AND EYE COUNTER-ROLLING

45°
30°
15°
0°

1.0 G
31.2 RPM

36 IN.

SENSITIVITY TO ACCELERATION

0° to 1°
15° to 16°
30° to 31°
45° to 46°
90°

Figure 41b. - Baseline Experiments

Figure 41c. - Baseline Experiments

In addition to test consideration, the configuration is controlled by two other factors. First, the inside diameter of the roll frame must be sufficient to permit safe and comfortable ingress to and egress from the couch by the test subject. The adopted sizing criteria requires the rigid body sit-up of a 95th percentile man about his hip pivot, with the couch in the maximum extended position and a maximum interference of approximately 1.0 inch with the roll frame. The reasons for permitting some interference are two-fold: the 95th percentile man exceeds the maximum nominal subject size and a rigid-body sit-up doesn't allow for moderate back flexure of head ducking or tilting, any of which would more than make up for the interference. The foregoing is illustrated in Figure 42.
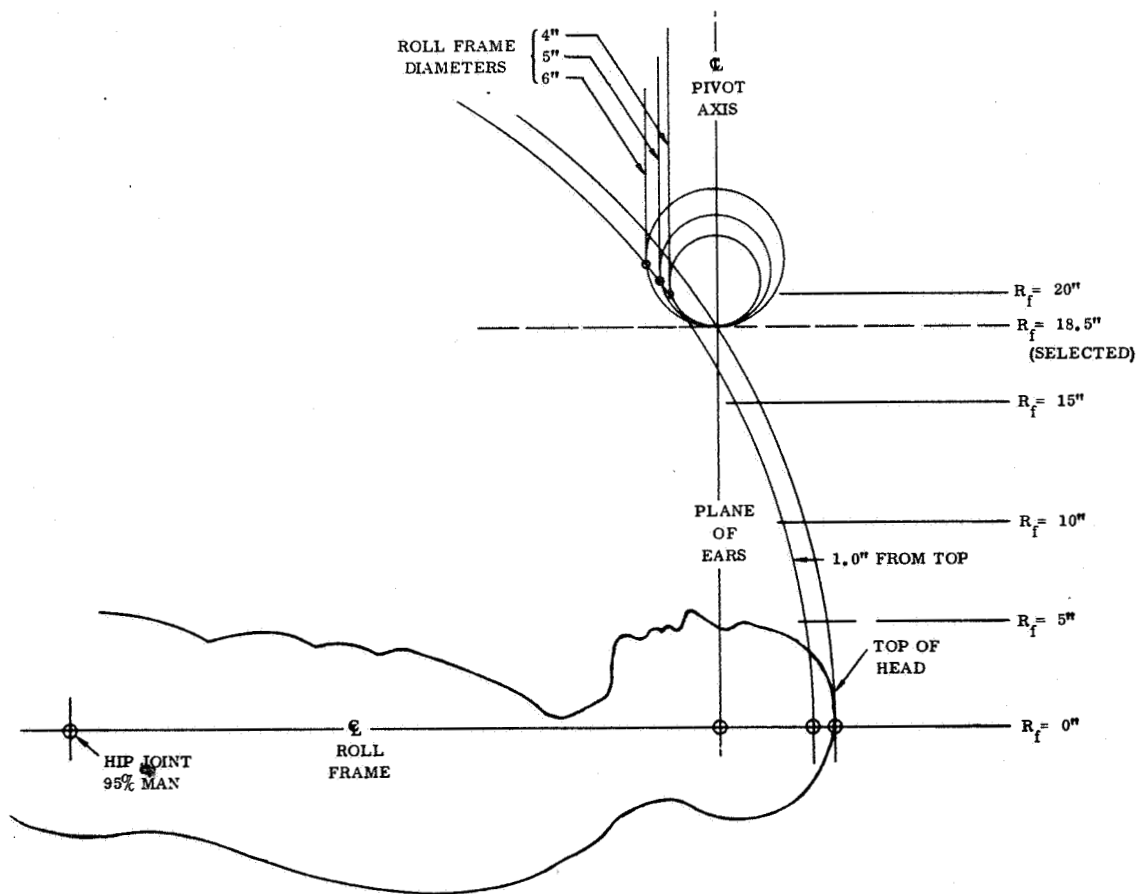


Figure 42. Test Subject Clearance Envelope

Secondly, sufficient height must be provided in the main rotational frame to permit the counterweight assemblies to traverse radially inward to the spin axis.

Loads. - The centrifuge structure must be capable of withstanding a variety of loading conditions during its lifetime. These can be grouped into three environmental categories: ground handling and test; launch and boost to orbit; and orbital operation. Loads experienced in the fabrication, assembly and handling environment were expected to be less severe than the others although inadvertent damage is most likely at this time. It was anticipated that the ground and orbital operational environment would produce the largest radial load factors whereas, the launch/boost environment would produce the largest vertical load factors. Typical load factors for the launch and boost environment of a Saturn V vehicle payload are shown in Table 16.

Table 16. Limit Load Factors-Saturn V Payload

| CONDITION | $n_{AXIAL}$ | $n_{LATERAL}$ |
|---|---|---|
| S-1C Stage ECO | -4.86 | 0.10 |
| Max q | -2.07 | 0.30 |
| Lift Off | -1.00 | 0.65 |
| Rebound | 1.70 | 0.10 |
| S-II Stage Engine Hard Over | -2.15 | 0.40 |

A ground rule was established, however, that the structure would be designed primarily to withstand only its operational loading environment. In the event that the launch/boost environment produced excessive loads at any point in the assembly, it was assumed that sufficient removable bracing would be provided to carry such loads. The rationale justifying this approach follows:

a.  Added material would most likely be located eccentric to the spin axis, increasing the rotary inertia of the system.

b.  Any material added to the radius arm or elements translating with it would require a corresponding counterweight increase, causing, in effect, a double penalty to weight and rotary inertia.

c.  Stiffness requirements were expected to result in a structure stronger in many areas than strictly necessary for operational loads.

d.  The configuration of the centrifuge is somewhat dependent on the configuration of its orbital container, which is not yet selected.

The following section, then, will be confined to developing the operational loads for the experiments previously defined. The coordinate system adopted for defining operational loads is presented in Figure 43. As shown, load components are first established at the center of mass of the subject and couch, then transformed into a coordinate system centered at the pivot axis intersection with the spin plane.
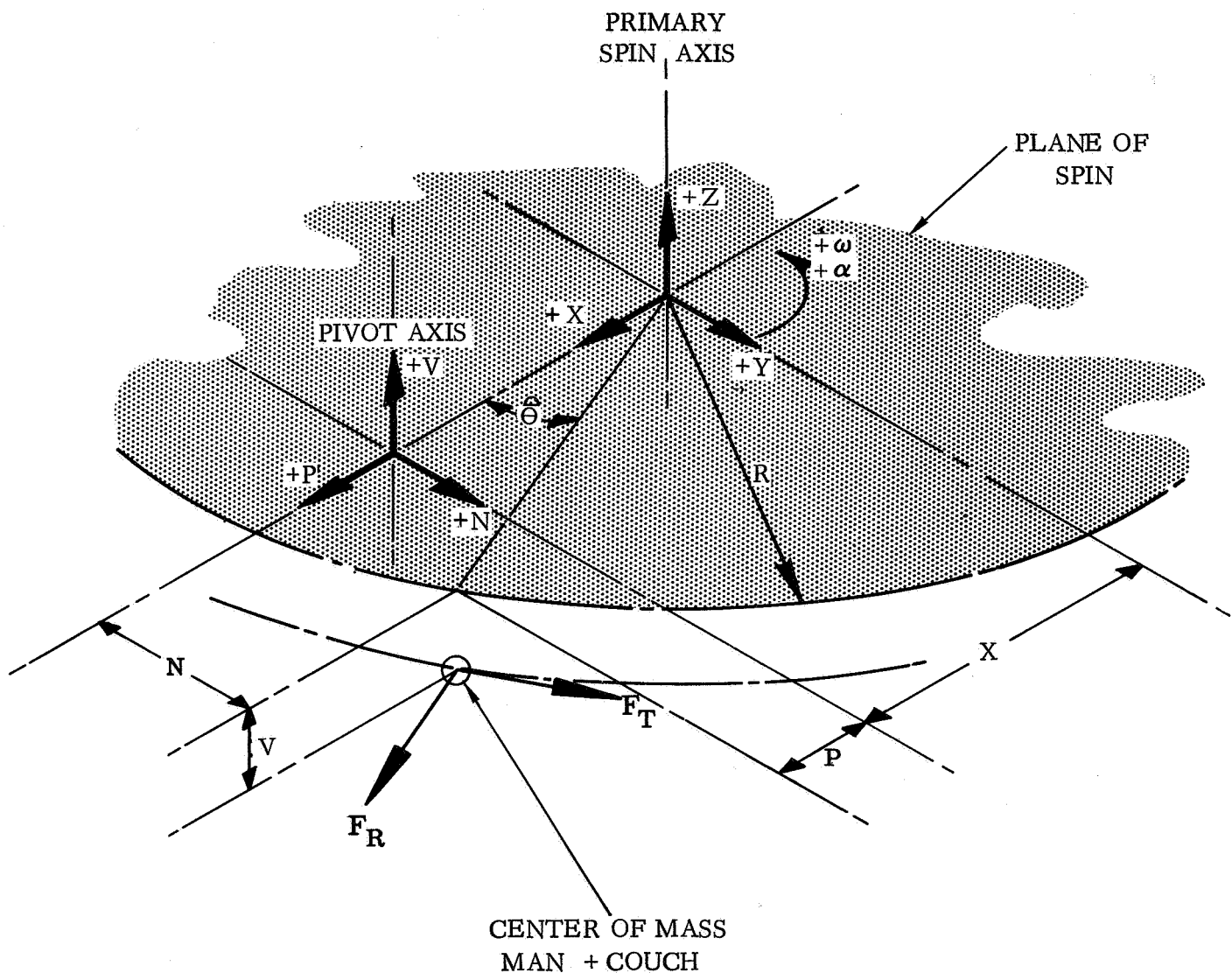


Figure 43.  Coordinate System for Loads

The following relationships are derived directly from Figure 43.

$$F = \left[ (X + P)^2 + N^2 \right]^{1/2} \tag{1}$$

$$\theta = TAN^{-1} \frac{N}{X + P} \tag{2}$$

$$F_P = F_R \cos \theta - F_T \sin \theta = \text{Force parallel to P axis} \tag{3}$$

$$F_N = F_R \, SIN \, \theta + F_T \cos \theta = \text{Force parallel to N Axis} \tag{4}$$

$$M_V = -F_P \, N + F_N P = \text{Moment about V axis} \tag{5}$$

$$M_N = F_P \, V = \text{Moment about N axis} \tag{6}$$

$$M_P = -F_N \, V = \text{Moment about P axis} \tag{7}$$

Three types of loading occur in centrifuge operation: spin-up, steady state, and de-spin. Expressions for the resulting load components are derived in the following sections.

Spin up loads. - The maximum angular acceleration is associated with the Apollo re-entry simulation experiment. Figure 44 shows the radial acceleration vs. time profile for this experiment. The maximum value of $\alpha$ is obtained by graphically determining the maximum slope, $\phi M$, of Figure 44 and using this value in the following derivation.

$$\phi_M = \frac{(3.68 \text{ in}) \left( \frac{240 \text{ ft.} / \text{sec.}^2}{4.215 \text{ in.}} \right)}{(1.39 \text{ in} - .91 \text{ in.}) \left( \frac{80 \text{ sec}}{1.39 \text{ in.}} \right)}$$

$$= \frac{(3.68)(240)(1.39) \text{ft.}}{(.48)(80)(4.215) \text{sec}^3} = 7.59 \text{ ft.} / \text{sec.}^3$$
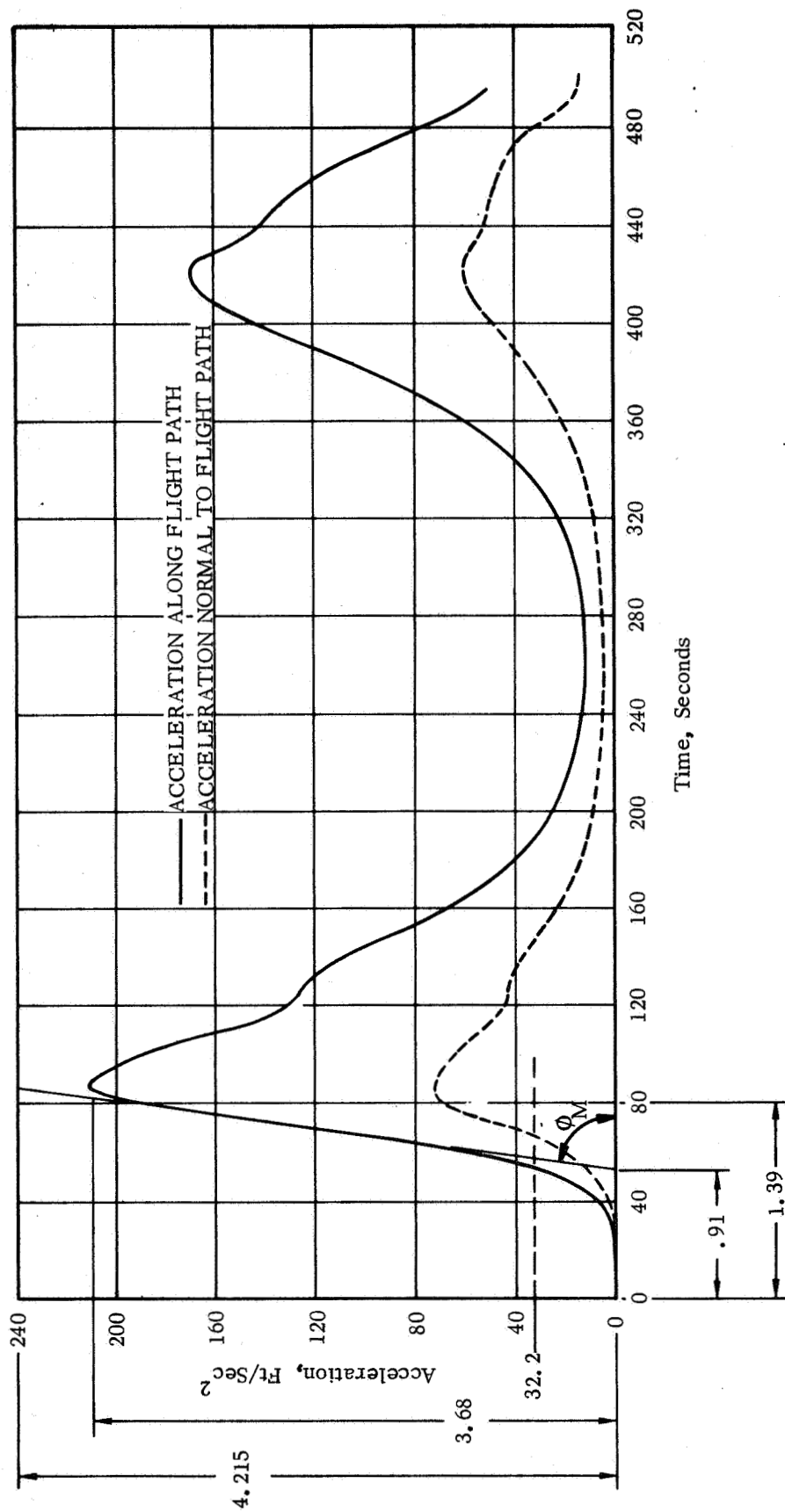
Figure 44 – Total Load Factor Versus Time from Re-entry

but

$$\phi = \frac{d}{dt}\,(a_n) = \frac{d}{dt}\,(R\,\omega^2) = 2R\,\omega\,\frac{d\omega}{dt}$$

$$\phi = 2R\,\omega\,\alpha$$

then

$$\alpha_{max} = \phi_M \Big/ 2R\,\omega_{min}$$

Assume $a_n = 1.0\,g = 32.2\,\text{ft./sec.}^2$ at the foot of the $\phi_m$ region. (This is slightly conservative).

then

$$\omega_{min} = (a_n/R)^{1/2}$$

For the re-entry test, the man and couch will be located at maximum radius. This distance is 76.0 in. = 6.33 ft.

then :

$$\omega_{min} = \left(\frac{32.2}{6.33}\right)^{1/2} = (5.09)^{1/2} = 2.25\ \text{rad/sec.}$$

Furthermore:

$$-F_T = Ma_T = MR\,\alpha$$

then

$$-F_{T_{max}} = MR\,\alpha_{max} = \frac{WR\,\phi_M}{2g_c\,R\,\omega_{min}} = \frac{(W)\,(7.59\ \text{ft./sec.}^3)}{(2)\,(32.2\ \frac{\text{ft.}}{\text{sec}^2})\,(2.25\ \text{rad/sec.})}$$

$$F_T = -.0524\,W \tag{8}$$

De-spin loads. - Assuming, in the worst case, that the subject requires immediate medical attention, then an emergency stop might be required. A tolerable structural criterion for emergency stop is a full stop, at a constant deceleration rate, from the highest speed experiment in 1.0 sec. It is recognized that the selected stopping interval may be many times as long, however the 1.0 sec. criterion can be met structurally and provides a reasonable margin of safety against overloading due to jamming of the

drive mechanism or other unlikely, though potential failures. An expression for the peak tangential load due to emergency stop is derived below:

For a constant deceleration,

$$\alpha = \frac{\Delta \omega}{\Delta t} = \frac{\omega_f - \omega_o}{\Delta t}$$

$$\omega_o = 65.3 \text{ rev/min} = 6.84 \text{ rad/sec.}$$

$$\omega_f = 0$$

$$\Delta t = 1.0$$

$$\alpha = \frac{0 - 6.84}{1.0} = -6.84 \text{ rad/sec.}^2$$

$$-F_T = Ma_T = -\frac{W}{g_c} R \alpha = -(W\#)(R \text{ in.}) \frac{6.84 \text{ rad/sec.}^2}{(12 \text{ in./ft.})(32.2 \text{ ft./sec.}^2)}$$

$$F_T = .0177 \, WR \tag{9}$$

(where R is given in inches)

From the foregoing, it can be seen that the de-spin case provides greater tangential loads than the spin-up case for all tests since $R \geqq 2.25$ ft.

Steady state loads. - In the steady state mode of operation the angular velocity, $\omega$, is constant and the angular acceleration, $\alpha$, is zero. Under these circumstances the tangential component of load vanishes and only a radial force field remains. A derivation of the general value of the radial componet of load is given:

$$F_R = M a_R = \frac{W}{g_c} R \omega^2$$

$$F_R = \frac{WR\omega^2}{(12)(32.2)} = \frac{WR \, \omega^2}{387} \tag{10}$$

(where R is in inches)

Computation of loads. - Values of the majority of the parameters in equations (1) through (10) were derived directly from the definition of experiments. Values for the weight of the subject and couch and for the maximum linear offset of the subject/ couch C. G. from the couch centerline were required. These values were estimated at 400 lb. and 2.0 in. respectively. Noting that equations (3) and (4) include components of both $F_R$ and $F_T$ it is likely that the worst load condition will occur at the instant an emergency stop is initiated when $F_T$ and $F_R$ are both essentially at their full values.

With this information a tabular solution for the resultant loads for each experiment was developed as shown below.

**Equation**     **Columns Required**

**(1)**

① ② ③ ④ ⑤ ⑥ ⑦ ⑧

X   P   ①+②   ③$^2$   N   ⑤$^2$   ④+⑥   $\sqrt{⑦}$ = R

---

**(2)**

⑨ ⑩

⑤/③   $\text{TAN}^{-1}$ ⑨ = θ

---

**(10)**

⑪ ⑫ ⑬

ω   $\omega^2$   $\left[\dfrac{400}{387}\right]$ R $\omega^2$ = 1.035 x⑧x⑫ = $F_R$

---

**(9)**

.0177 WR = (.0177)(400) R = 7.08 x⑧ = $F_T$

---

**(3), (4)**

⑮ ⑯ ⑰ ⑱

sin⑩   cos⑩   ⑬x⑯   ⑭ x⑮

⑲ ⑳ ㉑ ㉒

⑬x⑮   ⑭x⑯   ⑰ - ⑱ = $F_p$   ⑲x⑳ = $F_N$

---

**(5)**

㉓ ㉔ ㉕

㉑x⑤   ㉒x②   ㉔ - ㉓ = $M_V$

---

**(6)**

㉖ ㉗

V   ㉑x㉖ = $M_N$

---

**(7)**

㉘

-㉒ x ㉖ = $M_p$

Columns 29 and 30 are used to indicate whether the subject is facing parallel or normal to the spin plane, respectively.

The complete load computation is shown in Table 17. Maximum values for each load component are enclosed in heavy borders.

## Stress Criteria

Stress analysis of all sub-system elements utilized conventional factors of safety:

$$\text{Ultimate/Limit} = 1.5$$
$$\text{Yield/Limit} = 1.0$$

Material selections were made with due consideration of mechanical properties, fracture toughness, availability, fabricability, and cost. Allowables were taken from MIL-HNBK-5A, "Metallic materials and elements for aerospace vehicle structures."

Dynamics criteria. - Due to the inherent dynamic nature of the total system, the need to provide adequate separation between the natural frequency of the structural assembly and the operating frequencies for all experiments was recognized. This is necessary to prevent resonant conditions. Although the system possesses distributed mass as well as a number of essentially concentrated mass points, it might be idealized as a lumped mass multi-degree-of-freedom system. The analysis of such a system can become quite complex, however, as it depends on both the number of degree of dynamic freedom and the accurate determination of all masses and stiffnesses. In order to conserve time, therefore, it was decided to adopt the further-simplified model of a single-degree system consisting of a massless beam (radius arm) with a mass point at the nominal center-of-mass of the subject and couch. To compensate for the obvious oversimplification of this model, a conservative frequency separation ratio ($\omega_{natural}/\omega_{operating}$) of 5.0 was adopted as a ground rule for all dynamic analysis.

Figure 45 illustrates the idealization of the actual sub-system, in plan view, as a series of springs, $K_n$, subsequently collected into a single equivalent spring, $K_E$, supporting mass M. Figure 46 illustrates the corresponding deflections of the two equivalent representations of the system. The subscripts on stiffnesses and deflections are: (1) support structure; (2) main rotational frame; (3) radius arm; (4) pivot segments; (5) roll frame; (6) couch. Using Figures 45 and 46 an expression for determining the system equivalent stiffness, $K_E$, can be derived.

$$\delta_E = \sum_{n=1}^{6} \left[ \delta_n \right] = \delta_1 + \delta_2 + - - - - + \delta_6$$

Noting that, due to the series configuration, all springs are loaded by the same force, F, and assuming all springs to be linear:

# Table 17. Load Summary

| Test | X ① | P ② | ①+② ③ | ③² ④ | N ⑤ | ⑤² ⑥ | ④+⑥ ⑦ | R √⑦ ⑧ | ⑤/③ ⑨ | Tan⁻¹ ⑩ | ω ⑪ | ω² ⑫ | 1.035×⑫ FR ⑬ | 7.08×⑧ FT ⑭ | sin ⑮ |
|---|---|---|---|---|---|---|---|---|---|---|---|---|---|---|---|
| Grayout | 36 | 27 | 63 | 3970 | 0 | 0 | 3970 | 63.0 | 0 | 0 | 5.67 | 32.1 | 2090 | 446 | 0 |
| Angular Accel. | 36 | 27 | 63 | 3970 | 0 | 0 | 3970 | 63.0 | 0 | 0 | -- | -- | -- | -- | 0 |
| Therapeutic | 36 | 27 | 63 | 3970 | 0 | 0 | 3970 | 63.0 | 0 | 0 | 3.78 | 14.3 | 934 | 446 | 0 |
| Tilt-Table (I) | 48 | -.2 | 47.8 | 2280 | -15.2 | 231 | 2511 | 50.1 | -.318 | -17.63° | 2.84 | 8.05 | 417 | 355 | -.303 |
| Tilt-Table (II) | 48 | 10.7 | 58.7 | 3445 | -10.20 | 104 | 3549 | 59.0 | -.1738 | -9.85° | 3.28 | 10.73 | 663 | 422 | -.1710 |
| Semi-circ. Canal (IA) | 27 | 0 | 27 | 729 | ±.2 | 4 | 733 | 27.1 | ±.0742 | ±4.25° | 2.67 | 7.1 | 199 | 192 | ±.0792 |
| Semi-circ. Canal (IB) | 27 | 0 | 27 | 729 | 0 | 0 | 729 | 27.0 | 0 | 0 | 2.67 | 7.1 | 198 | 191 | 0 |
| Semi-circ. Canal(IIA) | 76 | 0 | 76 | 5780 | -.2 | 4 | 5784 | 76.1 | -.0263 | -1.50° | 2.67 | 7.1 | 559 | 539 | -.0263 |
| Semi-circ. Canal(IIB) | 76 | 0 | 76 | 5780 | 0 | 0 | 5780 | 76.0 | 0 | 0 | 2.67 | 7.1 | 558 | 538 | 0 |
| G Sensitivity (IA) | 36 | 27 | 63 | 3970 | -.2 | 4 | 3974 | 63.1 | -.0318 | -1.82° | 3.27 | 10.7 | 700 | 447 | -.0318 |
| G Sensitivity (IB) | 36 | 27 | 63 | 3970 | 0 | 0 | 3970 | 63.0 | 0 | 0 | 3.27 | 10.7 | 698 | 446 | 0 |
| G Sensitivity (IIA) | 36 | 2 | 38 | 1444 | 27 | 729 | 2173 | 46.6 | .712 | 35.5° | 3.27 | 10.7 | 517 | 330 | .580 |
| G Sensitivity (IIB) | 36 | 0 | 36 | 1296 | 27 | 729 | 2025 | 45.0 | .750 | 36.9 | 3.27 | 10.7 | 499 | 319 | .600 |
| OGI Parallel, Radial | 50 | 27 | 77 | 5939 | ±2 | 4 | 5943 | 77.1 | ±.0260 | ±1.49° | 2.78 | 7.7 | 615 | 546 | ±.0260 |
| OGI Parallel, 45° | 50 | 17.7 | 67.7 | 4580 | 20.5 | 420 | 5000 | 70.7 | .303 | 16.9° | 2.78 | 7.7 | 564 | 501 | .291 |
| OGI Normal, Radial | 50 | 27 | 77 | 5939 | 0 | 0 | 5939 | 77.0 | 0 | 0 | 2.78 | 7.7 | 614 | 545 | 0 |
| OGI Normal, 45° | 50 | 19.1 | 69.1 | 4770 | 19.1 | 365 | 5135 | 71.6 | .277 | 15.5° | 2.78 | 7.7 | 571 | 507 | .267 |
| Counterroll No Roll | 50 | 27 | 77 | 5939 | 0 | 0 | 5939 | 77.0 | 0 | 0 | 2.78 | 7.7 | 614 | 545 | 0 |
| Counterroll 45° | 50 | 27 | 77 | 5934 | 1.4 | 2 | 5941 | 77.0 | .0182 | 1.1° | 2.78 | 7.7 | 614 | 545 | .0182 |
| Reentry | 76 | 2 | 78 | 6084 | 0 | 0 | 6084 | 78.0 | 0 | 0 | 6.83 | 46.6 | 3760 | 553 | 0 |
| Mass Meas. Interim R | 50 | 2 | 52 | 2704 | 0 | 0 | 2704 | 52.0 | 0 | 0 | 2.78 | 7.7 | 414 | 368 | 0 |
| Mass Meas. Max. R | 76 | 2 | 78 | 6084 | 0 | 0 | 6084 | 78.0 | 0 | 0 | 2.26 | 5.1 | 412 | 553 | 0 |

Table 17. (Cont'd)

| Test | cos ⑩ ⑯ | ⑬×⑯ ⑰ | ⑭×⑯ ⑱ | ⑬×⑮ ⑲ | ⑭×⑮ ⑳ | F_P ⑰-⑲ ㉑ | F_N ⑱+⑳ ㉒ | ㉑×⑤ ㉓ | ②×㉒ ㉔ | M_v ㉔-㉓ ㉕ | v ㉖ | M_N ㉗×㉖ | M_P -㉓×㉖ ㉘ | = ㉙ | ⊥ ㉚ |
|---|---|---|---|---|---|---|---|---|---|---|---|---|---|---|---|
| Grayout | 1.000 | 2090 | 0 | 0 | 446 | 2090 | 446 | 0 | 12040 | 12040 | ±2 | ±4180 | -892 | | x |
| Angular Accel. | 1.000 | -- | 0 | 0 | -- | -- | -- | 0 | -- | -- | ±2 | -- | -- | | x |
| Therapeutic | 1.000 | 934 | 0 | 0 | 446 | 934 | 446 | 0 | 12040 | 12040 | ±2 | ±1868 | -892 | | x |
| Tilt-Table (I) | .953 | 397 | -108 | -126 | 339 | 505 | 213 | -7670 | -43 | 7627 | 0 | 0 | 0 | x | |
| Tilt-Table (II) | .985 | 653 | -72 | -113 | 416 | 725 | 303 | -7400 | 3240 | 10640 | 0 | 0 | 0 | x | |
| Semi-circ. Canal (IA) | -.997 | 198 | ±14 | ±15 | 191 | 184/212 | 206/176 | 368/-424 | 0 | -368/424 | 0 | 0 | 0 | | |
| Semi-circ. Canal (IB) | 1.000 | 198 | 0 | 0 | 191 | 198 | 191 | 0 | 0 | 0 | ±2 | ±396 | 382 | x | x |
| Semi-circ. Canal (IIA) | ~1.000 | 559 | -14 | -15 | 539 | 573 | 524 | -1146 | 0 | 1146 | 0 | 0 | 0 | x | x |
| Semi-circ. Canal (IIB) | 1.00v | 558 | 0 | 0 | 538 | 558 | 538 | 0 | 0 | 0 | ±2 | ±1116 | ∓1076 | x | x |
| G Sensitivity (IA) | ~1.000 | 700 | -14 | -22 | 447 | 714 | 425 | -1428 | 11480 | 12908 | 0 | 0 | 0 | x | x |
| G Sensitivity (IB) | 1.000 | 698 | 0 | 0 | 446 | 698 | 446 | 0 | 12040 | 12040 | ±2 | ±458 | ∓1136 | x | x |
| G Sensitivity (IIA) | .814 | 421 | 192 | 300 | 268 | 229 | 568 | 6190 | 1136 | -5054 | 0 | 0 | 0 | x | x |
| G Sensitivity (IIB) | .800 | 399 | 191 | 299 | 255 | 208 | 554 | 5620 | 0 | -5620 | ±2 | ±416 | ∓1108 | x | x |
| OGI Parallel, Radial | 1.000 | 615 | ±14 | ±16 | 546 | 601/629 | 562/530 | 1024/-1030 | 15170/14300 | 14046/15330 | 0 | 0 | 0 | x | |
| OGI Parallel, 45° | .957 | 539 | 146 | 164 | 480 | 393 | 644 | 8050 | 11390 | 3340 | 0 | 0 | 0 | x | |
| OGI Normal, Radial | 1.000 | 614 | 0 | 0 | 545 | 614 | 545 | 0 | 14720 | 14720 | ±2 | ±1228 | ∓1090 | x | x |
| OGI Normal, 45° | .964 | 551 | 136 | 153 | 489 | 415 | 642 | 7930 | 12270 | 4340 | ∓2 | ±830 | ∓1284 | | x |
| Counterroll No Roll | 1.000 | 614 | 0 | 0 | 545 | 614 | 545 | 0 | 14720 | 14720 | ±2 | ±1228 | ∓1090 | | x |
| Counterroll 45° | ~1.000 | 614 | 10 | 11 | 545 | 604 | 556 | 780 | 15020 | 14240 | ±1.4 | ±844 | ∓779 | x | x |
| Reentry | 1.000 | 3760 | 0 | 0 | 553 | 3760 | 553 | 0 | 1106 | 1106 | 0 | 0 | 0 | x | |
| Mass Meas. Interim R | 1.000 | 414 | 0 | 0 | 368 | 414 | 368 | 0 | 736 | 736 | 0 | 0 | 0 | x | x |
| Mass Meas. Max. R | 1.000 | 412 | 0 | 0 | 553 | 412 | 553 | 0 | 1106 | 1106 | 0 | 0 | 0 | x | x |
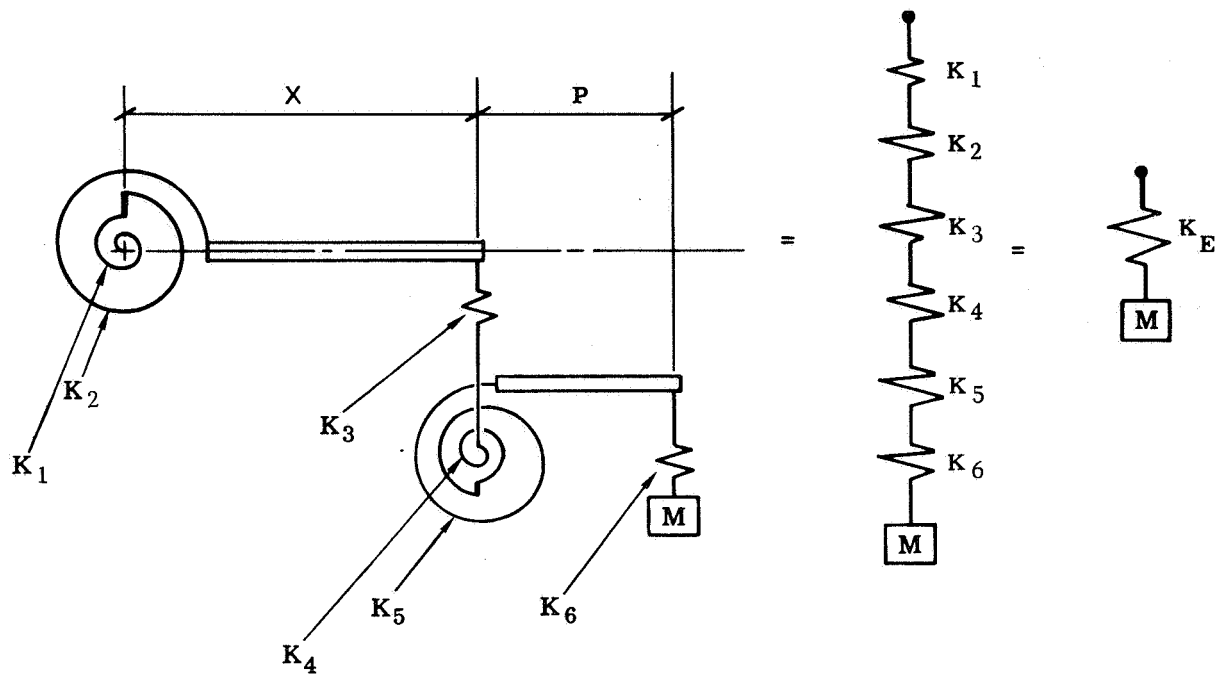
Figure 45. Idealized Spring/Mass System
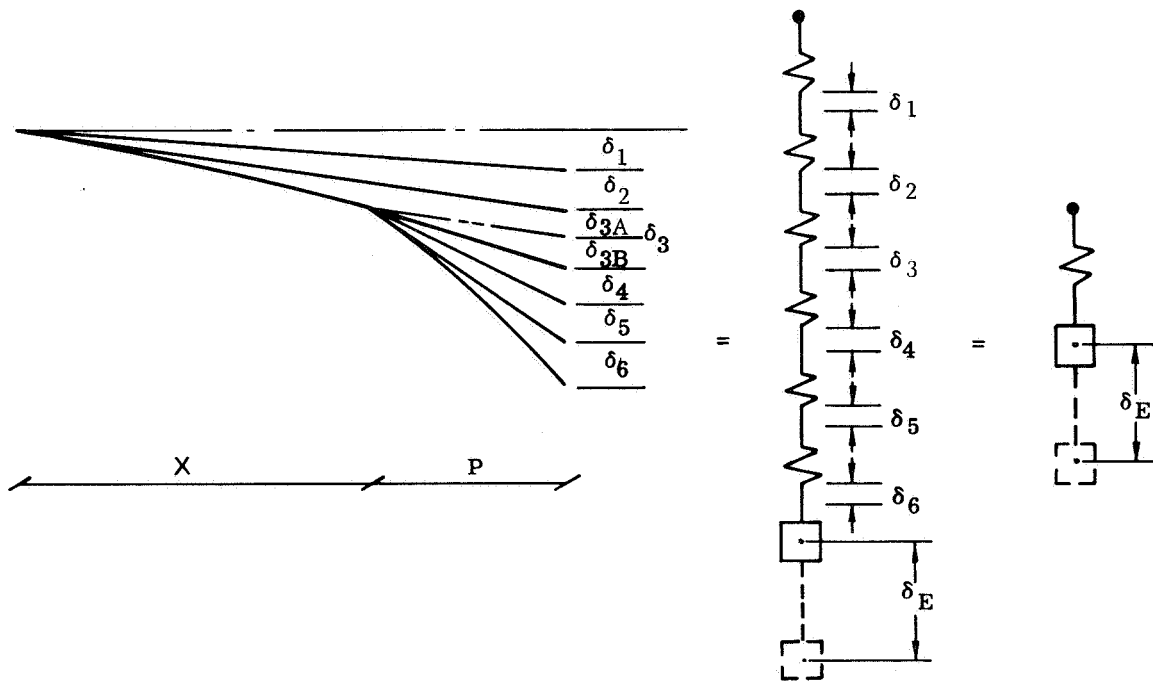


Figure 46. Deflection Summary

$$K_n = F/\delta_n \quad \text{or} \quad \delta_n = F/K_n$$

Substituting this relationship into the deflection equation and cancelling the common term, F, from both sides:

$$\frac{1}{K_E} = \frac{1}{K_1} + \frac{1}{K_2} + \frac{1}{K_3} + \frac{1}{K_4} + \frac{1}{K_5} + \frac{1}{K_6} = \frac{n}{K_n}$$

For early analysis it was assumed that all spring constraints were equal:

$$K_1 = K_2 = K_3 = K_4 = K_5 = K_6 = K$$

This assumption permits a straight forward determination of the natural frequency of the system, which is given by:

$$\omega_n = \sqrt{\frac{K_E}{M}} = \sqrt{\frac{K}{n} \frac{g_c}{W}}$$

But, from the section on loads, W = 400 lbs. and, from our assumed frequency ratio, $\omega_n = (5.0) \omega_{op}$. The required stiffness, K, can be found by manipulation of the above equation:

$$K = \frac{\omega_n^2 \, W}{g} = (25.0 \, \omega_{op}^2) \, (n) \left[ \frac{400}{32.2} \right]$$

$$K = 311 \, n \, \omega_{op}^2$$

(Where $\omega_{op}$ is given in column ⑪ of Table 17.

Note that the quantity (n) is carried through the derivation rather than substituting the total number of springs (six). The reason for this is that in the specific configuration of the centrifuge for certain tests some springs undergo no deflection.

Based upon the preceding development, Table 18 was compiled as a means of determining the most severe stiffness requirements for each spring element.

From Table 18 it was found that the grayout experiment determined $K_1$, $K_2$, $K_4$, $K_5$, and $K_6$ whereas $K_3$ was set by the re-entry simulation experiment, since the arm length, "X", is much greater in this case than for grayout.

Table 18.  Stiffness Requirements

| Spring → / Test ↓ | $K_1$ | $K_2$ | (**) $K_3$ | $K_4$ | $K_5$ | (*) $K_6$ | $\omega_{op}^2$ | n | $K = 311\, \omega_{op}^2\, n$ |
|---|---|---|---|---|---|---|---|---|---|
| Grayout | x | x | 36 | x | x | 27 | 32.1 | 6 | 60,000 |
| Ang. Accel. | x | x | 36 | x | x | 27 | -- | 6 | -- |
| Therapeutic | x | x | 36 | x | x | 27 | 14.3 | .6 | 26,700 |
| Tilt-Table I | x | x | 48 | x | -- | 15.2 | 8.05 | 5 | 12,500 |
| "    "    II | x | x | 48 | x | -- | 15.2 | 10.73 | 5 | 16,700 |
| Semi-Circ.  IA | x | x | 27 | x | -- | 0 | 7.1 | 4 | 8,860 |
| IB | x | x | 27 | x | x | 0 | 7.1 | 5 | 11,040 |
| IIA | x | x | 76 | x | -- | 0 | 7.1 | 4 | 8,860 |
| IIB | x | x | 76 | x | x | 0 | 7.1 | 5 | 11,040 |
| G-Sensitivity IA | x | x | 36 | x | -- | 27 | 10.7 | 5 | 16,650 |
| IB | x | x | 36 | x | x | 27 | 10.7 | 6 | 19,980 |
| IIA | x | x | 36 | x | -- | 27 | 10.7 | 5 | 16,650 |
| IIB | x | x | 36 | x | x | 27 | 10.7 | 6 | 19,980 |
| OG I ‖/Radial | x | x | 50 | x | -- | 27 | 7.7 | 5 | 11,980 |
| ‖/45° | x | x | 50 | x | -- | 27 | 7.7 | 5 | 11,980 |
| ⊥/Radial | x | x | 50 | x | x | 27 | 7.7 | 6 | 14,350 |
| ⊥/45° | x | x | 50 | x | x | 27 | 7.7 | 6 | 14,350 |
| Counterroll 0° | x | x | 50 | x | x | 27 | 7.7 | 6 | 14,350 |
| 45° | x | x | 50 | x | x | 27 | 7.7 | 6 | 14,350 |
| Reentry | x | x | 76 | x | -- | 0 | 46.6 | 4 | 58,000 |
| Mass Meas. - Mid R | x | x | 50 | x | -- | 0 | 7.7 | 4 | 9,580 |
| Mass Meas.- Max. R. | x | x | 76 | x | -- | 0 | 5.1 | 4 | 6,350 |

"x" (or a number in the column) indicates that the spring segment is active during a particular experiment.

*Quantity given in $K_6$ column is distance in inches along couch ₵ from pivot axis to nominal center-of-mass of subject and couch.

**Quantity given in the $K_3$ column is the arm length in inches

## Interface Constraints

A factor which strongly influences the detail design of individual structural elements is the nature of this mechanism at each interface. In the mechanism trade-off studies concluding the Phase I effort, baseline mechanisms were selected for all motion interfaces. The structural sub-system is constrained to incorporate the selected mechanism concepts, which are presented in Table 19.

Table 19. Baseline Motion Mechanisms

| MOTION | MECHANISM |
|--------|-----------|
| ● Couch translation | ● Teflon slides or ball bushings, manual positiong. |
| ● Couch roll | ● Aluminum oxide balls with segmented race and powered roller drive. |
| ● Couch Pivot | ● Teflon journals with powered miter gear drive. |
| ● Radius variation | ● Ball-bushings or teflon slides, powered ball screw actuated. |
| ● Primary rotation | ● Axial drum with two bearing planes, main drive concept not yet selected. |

Trade-off criteria, - The trade-off studies concluding the Phase I effort were performed in accordance with the weighting factors shown in Table 20.

Table 20. Baseline Structure Trade-off Factors and Point Scale

| | | |
|---|---|---|
| Safety | | 30 |
| Fail-safe | 10 | |
| Physical Smoothness | 5 | |
| Dynamic Smoothness | 5 | |
| Accessibility of Subject | 10 | |
| Reliability | | 15 |
| Complexity | 10 | |
| Maintenance | 5 | |
| Physical Characteristics | | 45 |
| Weight | 20 | |
| Strength/Stiffness | 10 | |
| Compatibility with Mechanisms/Systems | 15 | |
| Cost | | 10 |
| Time/$ for Material/Fabrication | 10 | |
| | | |
| Maximum Total | | 100 |

Explanation of the individual categories is given below:

a. Fail-safe: In a structural context this factor includes the effects of continuous vs. discrete attachments, redundant load paths, etc.

b. Physical smoothness: This factor evaluates the relative hazard created by sharp corners and edges, protruding flanges, and confining structural features.

c. Dynamic smoothness: Qualitative evaluation of the tendency toward cross-coupled motions and random excitations is provided by this factor.

d. Accessibility of subject: This factor rates both the ease of access to the subject by a rescue crew and the ease of self release by the subject.

e. Complexity: The number of components in the assembly and the number of attachments is appraised by this factor.

f. Maintenance: This factor rates the need for periodic inspections and the special care requirements of close tolerance surfaces subject to wear or damage during handling and operation.

g. Weight and strength/stiffness: Together these two factors measure the conformance with the basic structural criteria while considering the trend toward stiffness-critical rather than strength-critical design.

h. Compatibility with mechanisms/systems: Access to elements of other sub-systems and the implied addition of weight or complexity to elements of any sub-system are evaluated by this factor.

i. Cost: This factor appraises material costs, implied lead time on materials or assemblies, and both cost and time requirements of manufacturing operations.

## Description of the Structure

As mentioned earlier, the initial design effort was directed toward evolution of candidate concepts for comparison in subsequent tradeoff studies and eventual selection of a baseline structural sub-system. The following sections trace this activity to illustrate the process by which the present baseline configuration evolved. The composite assembly is discussed first since it was necessary to establish an acceptable integrated configuration concept within which the individual elements could be defined and later detailed. Each of the primary structural elements are then discussed individually. In these sections the detail design drawings are also explained in depth to point out specific features of the elements.

Configuration Evolution. - The present baseline structural sub-assembly configuration evolved primarily from consideration of the experiment definitions, the geometrical constraints, and the obvious need to establish an efficient load path from the subject/couch area to the fixed support structure in order to minimize structural weight.

The first configuration to be developed was a space-truss assembly which was presented in the Convair contract proposal and is shown in Figure 47. After the study
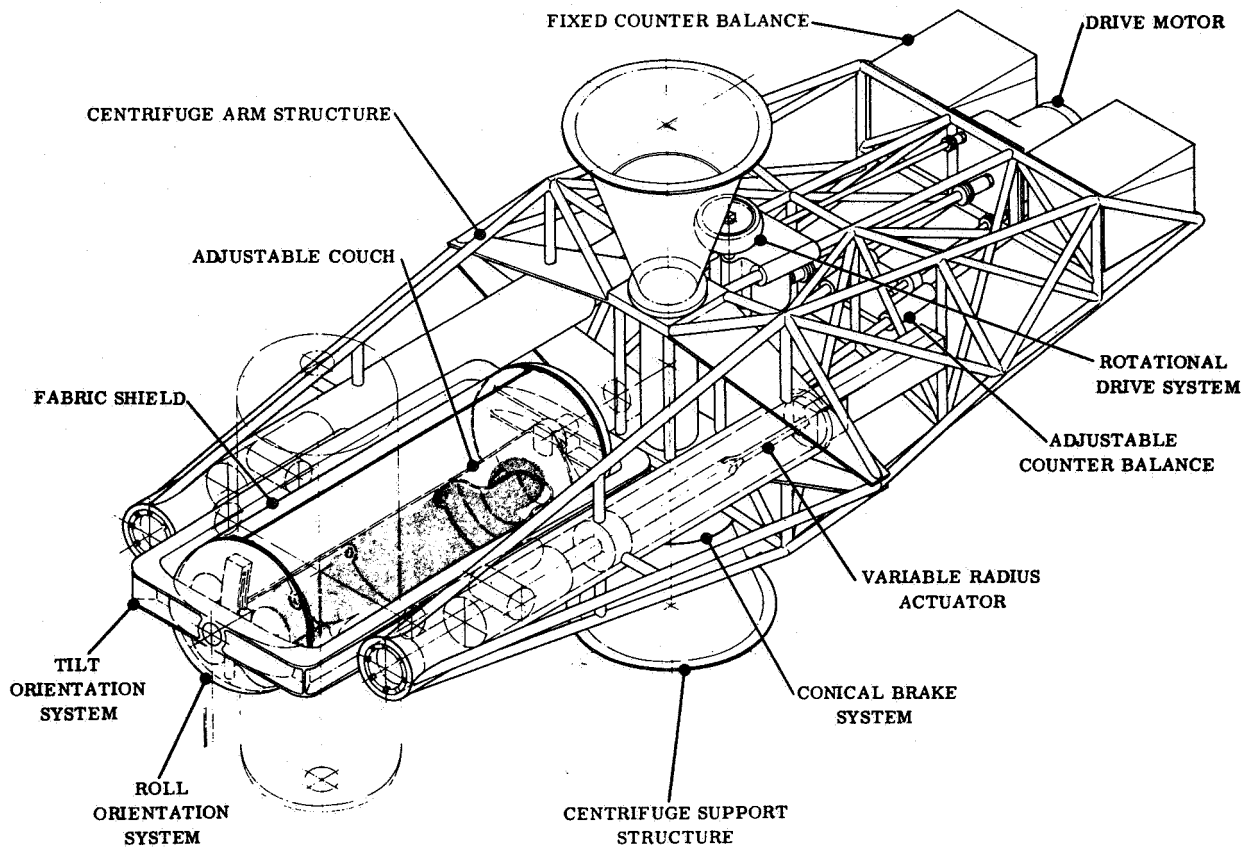


Figure 47. Proposal Baseline Vehicle Configuration

was in progress it became apparent that this original system failed to satisfy certain then-defined experiment criteria and also provided a roundabout load path in the couch support area. Tilt capability normal to the plane of spin had been provided whereas in-plane tilt was not required. Also, due to the presence of the continuous axle, it was not possible to position the subject with his head on the axis of spin. It was conceivable, though, that with extensive modification it might have been possible to rotate the entire assembly (between the hubs) through an angle of 90° to provide the in-plane tilt, and to bridge the couch capsule envelope to permit its inward translation to the spin axis. Upon scrutiny of the basic structural model, however, other questions arose which resulted in a study to optimize the structural load path from the subject/couch center of mass to the drive hub support structure.

Load Path Optimization. - Each of the required degrees-of-freedom of the subject was analyzed in order to generate potential methods of accomplishment. Integrating these into structural schematics provided a means of identifying the most direct load paths. The analysis began at the couch and proceeded inward, finally to the the interface with the support structure.

Couch Roll. - The requirement to roll the subject and couch continuously about a longitudinal axis is established by the angular acceleration test. Also, pre-test positioning requires    90° rotation in this axis as some experiments are conducted with the subject facing parallel to the spin plane and others facing normal.

To provide the required freedom, two basic structural concepts were identified: The axial shaft and the circumferential ring. Figure 48 presents the two candidate alternates of each case.

SHAFT                                    RING



RS-1 END SUPPORTS                    RR-1   SINGLE

RS-2  CANTILEVER                      RR-2  DOUBLE

Figure 48.  Couch Roll Concepts

Couch pivot. - Pivot of the subject/couch about an axis normal to the longitudinal axis is required by the tilt table experiment and the pre-test positioning requirements of various other experiments. It was further determined that the pivot elements should be incorporated "downstream" (mechanically) from the roll provisions and couch since the centerline of the roll system must always coincide with the couch longitudinal axis to achieve all the positioning requirements. This established the requirement that the pivot system should interface with the roll system rather than with the couch.

Combined roll/pivot concepts utilizing the preceding roll alternates are shown in Figure 49. The pivot frames of concepts P-1 and P-2 were rectangular planar



P-1: RS-1 + FRAME

P-3: RR-1 + RP-1, -2, OR -3

P-2: RS-2 + FRAME

P-4: RR-2 + RP-1, -2, OR -3

RP-1: Continuous
Inner and Outer Frames

RP-2: ARL Segment
Pivots with Continuous
Roll Frame

RP-3: Continuous
Pivot Frame
With ARC Segment
Roll Elements
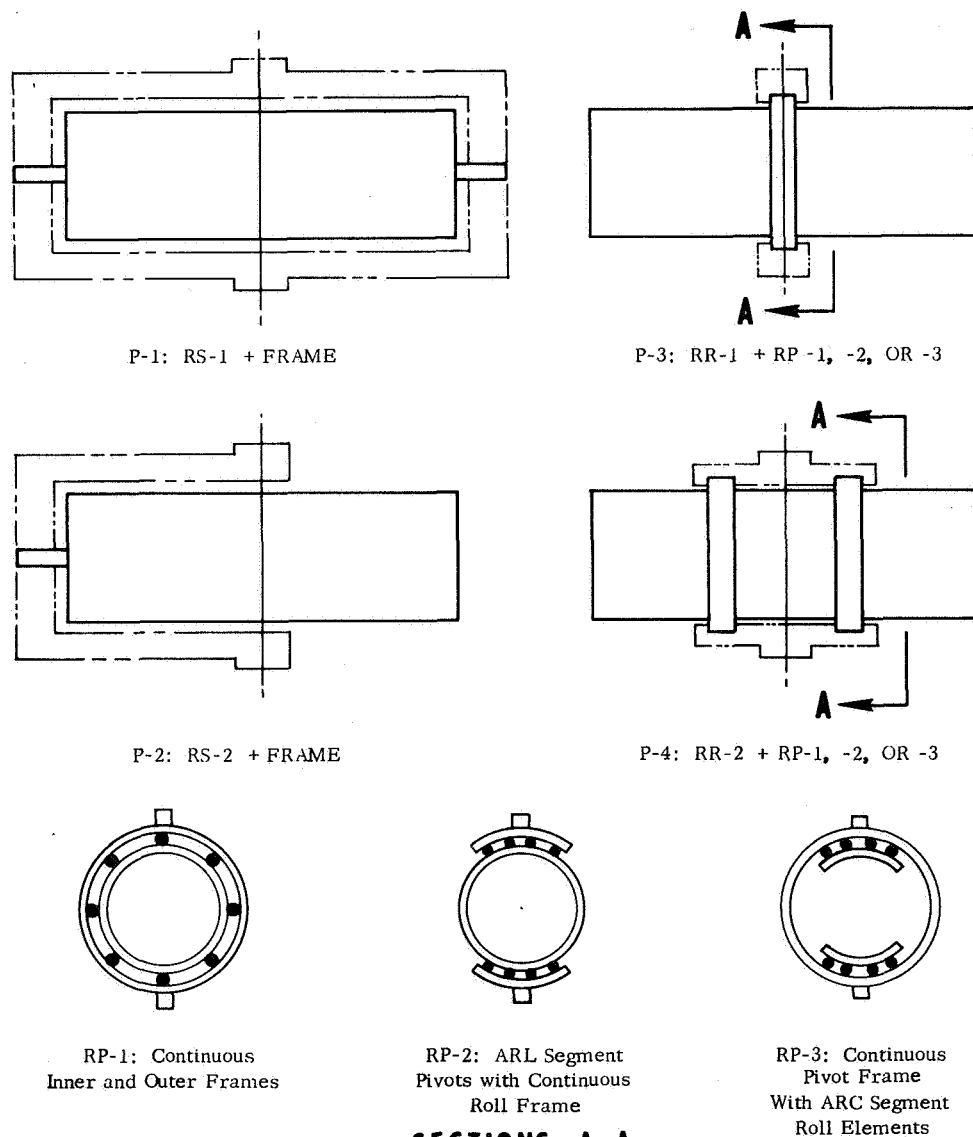
SECTIONS A-A

Figure 49. Combined Roll/Pivot Concepts

structures. For concepts P-3 and P-4 three alternate arrangements are presented in Sections A-A. The first, RP-1, consists of a complete pivot ring(s) concentric with a complete roll ring(s); the second RP-2, consists of a complete roll ring(s) contained by a pair(s) of arc-segment pivot elements; and the third, RP-3, is comprised of arc-segment roll elements contained within a continuous pivot ring(s).

The following qualitative comparisons can be drawn between the various concepts:

a.  P-1 requires a full-perimeter frame whereas P-2 requires only a half-perimeter frame, implying considerable weight penalty in P-1.

b.  P-4 requires a three-dimensional space frame to connect the two ring planes whereas no interconnect structure is required for the planar P-3 concept, implying a weight penalty in P-4.

c.  P-4 interconnect framing is probably lighter and stiffer than the P-2 frame but the rings are heavier than the shaft implying more or less equal weight configurations.

d.  RP-1 provides maximum structural redundancy but also suggests a weight penalty due to parallel load paths, and increased structural depth to provide torsional capability in both elements.

e.  RP-2 permits a smaller diameter ring than RP-3 with the same general mechanical interface implying a minor weight penalty for RP-3.

f.  RP-3 must be driven from the couch side of the interface implying the need for a separate power source (batteries) on the couch whereas both RP-1 and RP-2 can be driven from the pivot side of the roll/pivot interface, permitting use of the same power source used for pivot, radius variation and other functions.

g.  In RP-1, if the rings are of approximately equal stiffness an indeterminate elastic foundation situation exists in which load transfer is accomplished by relatively inefficient differential bending. Also, if either ring is significantly stiffer than the other, the majority of load stays in it and the parallel material in the adjacent ring becomes relatively useless.

Couch translation relative to pivot axis. - The complete spectrum of experiments sets the requirement to pivot the subject about various body points. For example, the "sensitivity to linear acceleration" and "oculographic illusion" experiments specifically require pivot through the head whereas torsional loads about the pivot axis during the "re-entry simulation" experiment become extremely high unless the pivot axis is essentially coincident with the subject/couch center of mass. The "tilt table" experiment requires yet another pivot location, likely between these two.

It is necessary, then, that longitudinal translation of the couch relative to the pivot be provided. Considering again the combined roll/pivot configurations of Figure 49, it became apparent that the axial shaft concepts, P-1 and P-2, would be severely compromised to provide this motion. Since it highly desirable that the subject/couch center of mass lie approximately on the roll centerline, the couch cannot slide on an axle fixed to the frame without providing a long couch overhang(s) plus full-travel frame clearance to avoid skewing the subject. Therefore, an axle fixed to the couch would be required. But this still implies extension of the frame "jaw" length for concept P-1 by an amount equal to the maximum length of travel. It also implies a similar extension of the shaft length for both concepts P-1 and P-2. Not only do frame and shaft weights increase due to these geometrical considerations but many operating loads increase as well, implying still further weight penalty to provide the necessary strength and stiffness.

Variable Radius.- The extremes of the variable radius requirement are established by the semi-circular canal stimulation experiment, which requires the subjects head on the axis of spin, and the re-entry simulation experiment, in which it is highly desirable to place the subject at maximum radius to avoid unnecessarily high angular velocities.

Essentially two concepts are available for providing variable radius capability, the fixed arm and the translating arm. Figure 50 shows two alternates of each concept.

Concepts VF-1 anf VF-2 consist of a structural radius arm, rigidly fixed in relation to the spin axis. The couch/roll/pivot assembly translates along the arm as a unit, in essence providing a variable radius from spin axis to pivot axis. On the other hand, in concepts VT-1 and VT-2 the position of the pivot axis is fixed in relation to the arm, which, in turn translates relative to the spin axis.

Appraisal of the four alternates fails to establish a clear winner but does bring to light some faults not readily apparent from the simplified sketches of Figure 50.

a.   VF-1 and VT-1 are both excellent in providing access to the test subject whereas VT-2 offers some impairment (which can be minimized by selected couch positioning) and VF-2 greatly restricts access, particularly when the subject is in at the spin axis.

b.   VT-1 and VT-2 provide minimum complexity at the arm/pivot interface whereas VF-1 and VF-2 concentrate three mechanisms in a small geometrical envelope implying a sophisticated, highly complex interface situation at a discrete point(s) in the load path.

c.   VF-1 and VT-1 appear preferable, at first glance, in terms of weight. This is an illusion, however, since the centrifugal forces at the subject/ couch center of mass are eccentric to the arm neutral axis by approximately 30 inches which results in a constant arm bending moment on the order of 110,000 inch-lbs for the re-entry simulation experiment! Furthermore, a torsional/bending vibration coupling can result from disturbances in the

FIXED ARM                                    TRANSLATING ARM

VF-1: SINGLE BEAM                            VT-1: SINGLE BEAM

VF-2: DOUBLE BEAM                            VT-2: DOUBLE BEAM
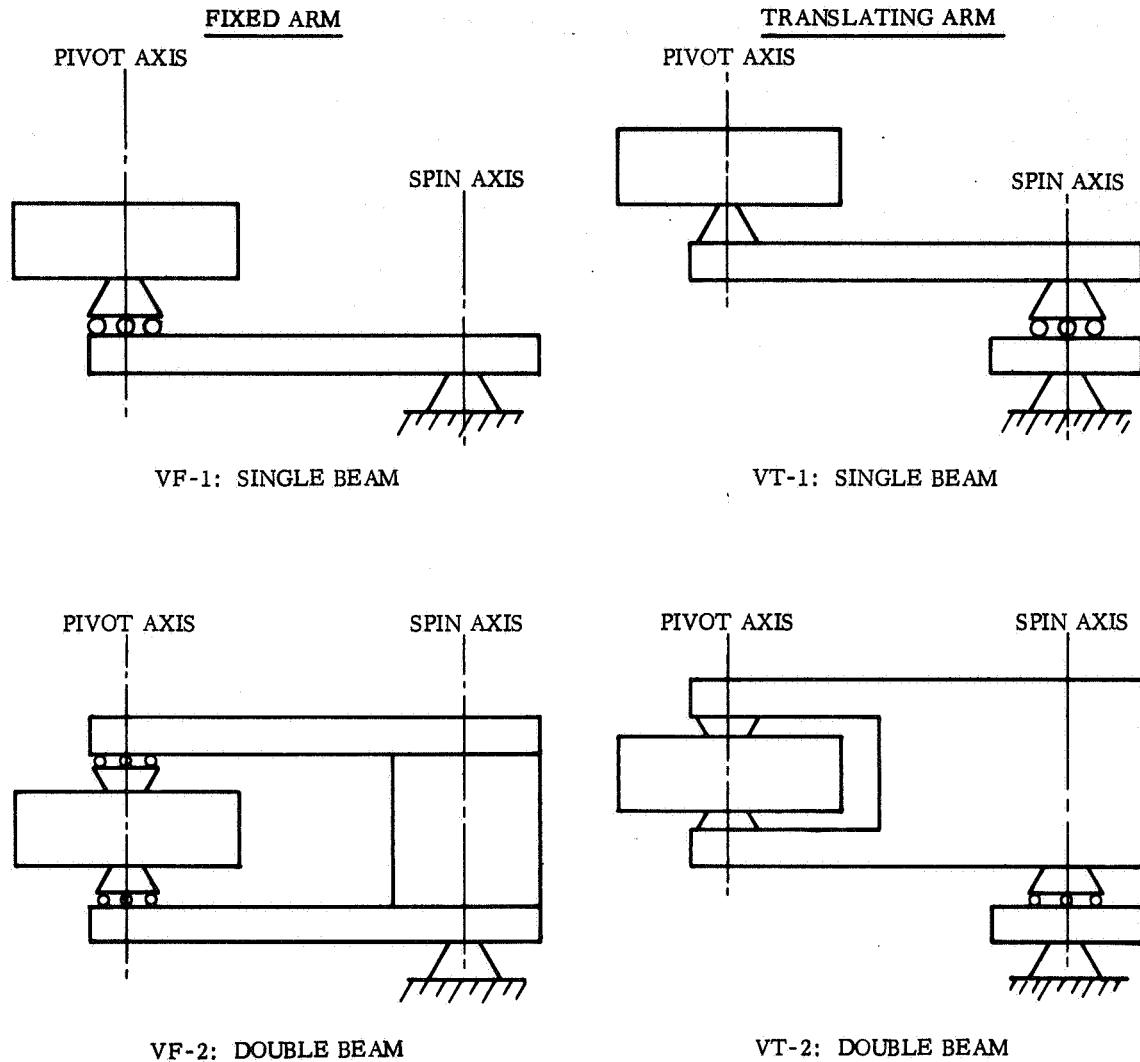
Figure 50. Variable Radius Concepts

spin plane tangent to the path of rotation due the lack of symmetry about
the spin plane, implying the need of a significant stiffness increase. On
the other hand, VF-2 and VT-2 provide support symmetry to both minimize
dynamic coupling and load eccentricity at the arm/pivot interface.

d.  VT-2 requires more movable counterweight (not necessarily more total
    counterweight) than VF-2 to compensate for its greater eccentric mass.
    However a continuous cavity must be maintained betweenthe beams of
    VF-2 to permit the full inward translation of the couch/roll/pivot assembly
    whereas in VT-2 the arms can be interconnected at the couch clearance

envelope plane innermost with respect to the pivot axis. This implies less span at shallow depth for the beams of VT-2 hence a somewhat lighter assembly.

Primary rotation. - Three basic support concepts are available for primary rotation of the centrifuge: the cantilever hub, the twin hub, and the peripheral track. The cantilever hub concept has already been shown in conjunction with the candidate variable radius systems in the previous section. (Ref. Figure 50) The twin hub concept is most probably adaptable only to arm concepts VF-2 and VT-2, and the peripheral support concept is suitable only with arm concepts VF-1 and VF-2. These latter four assemblies are shown in Figure 51.

TWIN HUB                                PERIPHERAL TRACK

PV-1: TRANSLATING ARM                   PV-3: SINGLE BEAM

PV-2: FIXED ARM                         PV-4: DOUBLE BEAM
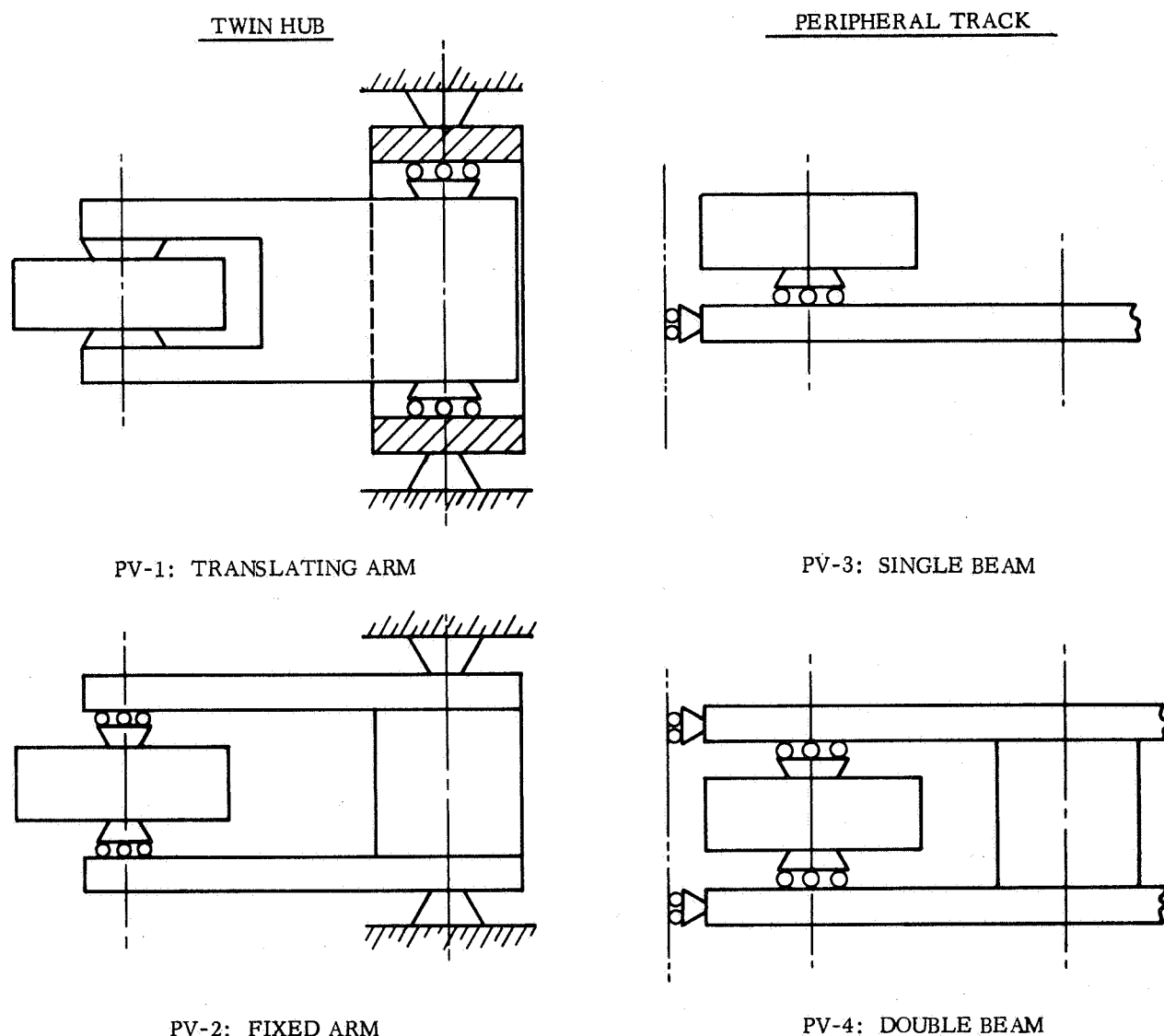
Figure 51. Support Concepts for Primary Rotation

Several significant conclusions were drawn from comparison of the alternate concepts.

a.  Concepts PV-3 and PV-4 are the most sophisticated, consisting primarily of a beam(s) spanning the enclosure, with no center structure and its associated weight increment. High tolerance control on the peripheral track assembly is essential for several reasons. Roundness must be rigidly maintained to prevent oscillation of the spin axis. This requirement further implies the need of high in-plane track stiffness to prevent a travelling load depression under the rollers, which, if permitted, would produce spin axis oscillation in spite of roundness control. This requirement implies a weight penalty in the enclosing structure. Stringent track flatness control is also required to avoid a "washboard" vibratory sensation at high angular velocities. Damping devices might minimize this problem, however, at a small weight penalty. Access to the subject is excellent in PV-3, though quite restricted in PV-4. Load eccentricity is minimized in PV-4 whereas PV-3 has sizeable eccentric moments but these are introduced near a support in the most severe case. End slopes might be a factor in forcing greater stiffness in the PV-3 beam to prevent uplift of rollers from the track. PV-3 and PV-4 are the most highly "enclosure - dependent" configurations.

b.  Concepts PV-1 and PV-2 offer complete symmetry of loading. This situation permits simple-support hub joints, a factor which should result in a weight saving in the support structure since essentially no moment would be transmitted at the interface. A further advantage in the twin-hub concepts lies in the ability to provide a center tension tie between the end bulkheads of its pressurized container thereby further reducing container weight of a small penalty for thrust bearing provisions. These concepts must also be closely integrated with the enclosure.

c.  The cantilever hub concepts, VF-1 and -2, and VT-1 and -2, are similar to existing ground-based centrifuges in their use of a single pedestal for support. This reduces the hub and bearing weight relative to the twin-hub concepts. The primary centrifugal forces are no longer symmetrically reacted though this presents no problem so long as the counterbalance system is functioning properly and holding static unbalance forces to the levels specified in the Stability and Control section.

Counterweight support. - The preceding paragraphs have been concerned with providing a load path from the subject/couch to the support structure. Since the center of mass of the subject/couch is inherently eccentric to the spin axis, the resulting centrifugal forces must be counterbalanced in order to prevent the application of large cyclic forces and moments to the support. In order to provide balance capability for the full experiment regime, a variable capability must be provided for the counterweight. This implies the need of a structure to support and guide the counterweight. The configuration of this structure is not sensitive to the primary

rotational concept, but is intimately influenced by the couch/subject variable radius concept as shown schematically in Figure 52.

CF-1: FIXED ARM, SINGLE BEAM

CT-1: TRANSLATING ARM, SINGLE BEAM

CF-2: FIXED ARM   DOUBLE BEAM

CT-2: TRANSLATING ARM, DOUBLE BEAM
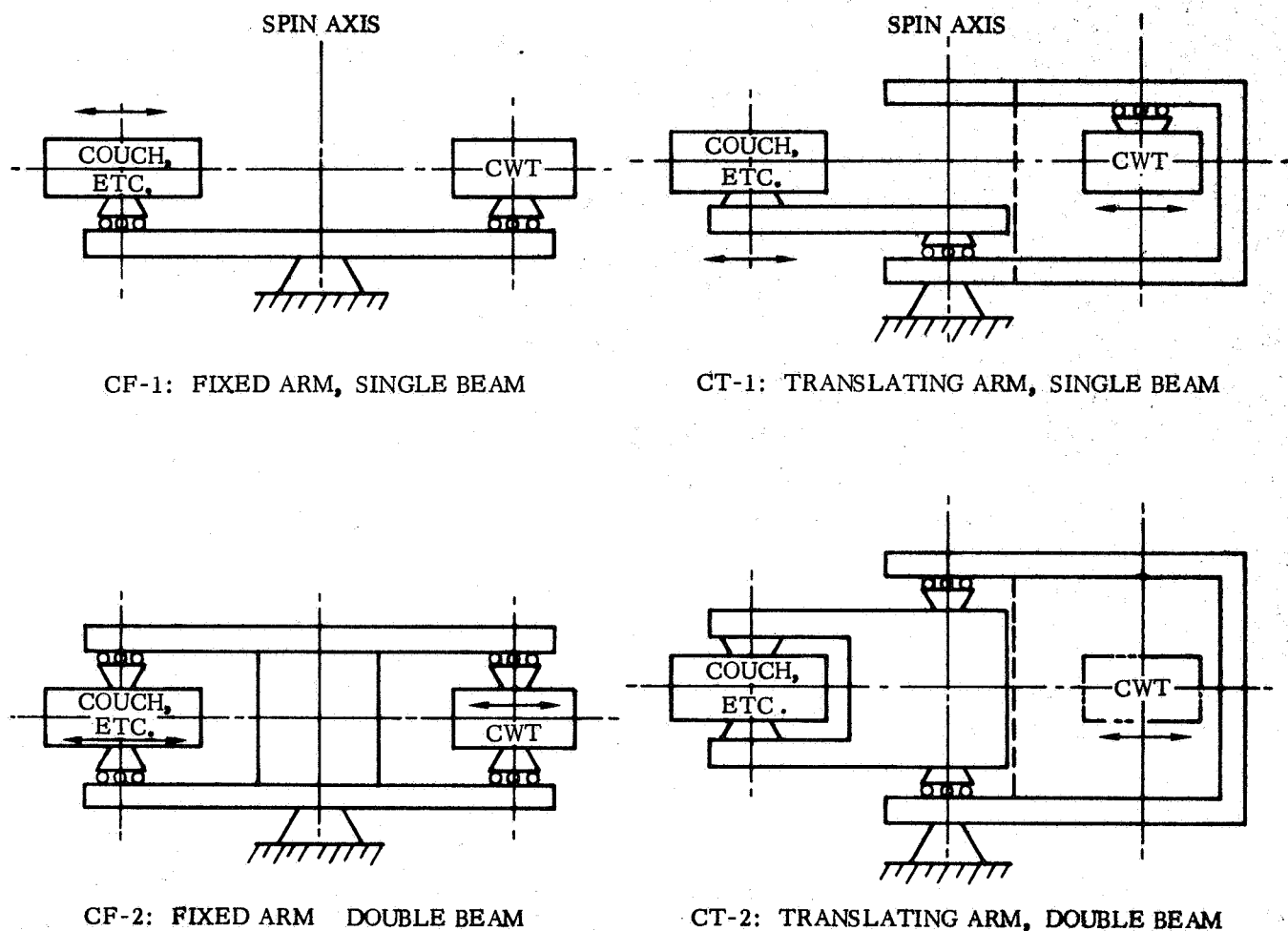
Figure 52.  Counterweight Support Concepts

A cursory appraisal of Figure 52 would seem to indicate a weight saving in the counterweight support structure for concepts CF-1 and CF-2. This is most likely true in comparing CF-1 with CT-1, where in CT-1 a structure is required which permits free arm translation yet places the counterweight mass center in the spin plane. Initial counterbalance studies, however, established the desirability of multiple movable counterweights in order to provide maximum capability to compensate for all types of force imbalance. Dividing the counterweight into top and bottom and/or a pair of side weights to satisfy balance criteria penalizes CF-1 by requiring additional structure but affects CT-1 much less significantly.

Comparing CF-2 and CT-2, then, the fact that the counterweight must not violate the arm translation envelope of CT-2 is only a minimum handicap since the envelope merely sets the minimum span between weight pairs. The penalty to CF-2 is greater, particularly if side weights are required.

A further factor narrowing the difference between the fixed arm and the translating arm concepts is the fact that even should a single counterweight element be permissible, a conflict of interest for space near the spin axis could result in the semicircular canal stimulation experiment, when the subjects head is on the spin axis and the couch frame would undoubtedly extend several inches beyond.

Integrated systems. - As the concepts of the preceding paragraphs were developed and evaluated, a series of integrated system concepts evolved. The main line of evolution is presented in Figures 53, 54, and 55 showing, respectively, the ground-based estimating model used in the additional task proposal (Report No. GDC-PIN-67-495), a Phase I orbital concept, and the final baseline centrifuge in its present configuration. As the figures illustrate, some early concept selections survived to the final configuration.

In the light of preceding discussions roll/pivot concept P-3 was a natural selection (Ref. Figure 49). The earliest configuration used twin integrally stiffened cylindrical barrels (Concept RP-1, Figure 49 to accomplish the roll/pivot function. The need for greater torsional stiffness and the desirability of minimum enclosure of the subject resulted in the toroid-plus-ring configuration (still concept RP-1) in the Phase I concept. The baseline trade-off study resulted in selection of concept RP-2 by a wide margin over RP-1, however, the primary reason for this was the need for good torsional properties at reasonable weight. A number of element cross-section combinations were also evaluated in the trade-off. The favored configuration, shown schematically in Figure 56, was the "box/c-clamp". This concept provides both ample torsional area in the roll frame and good bending properties in the pivot segment in a minimum envelope depth.

From the "variable radius" paragraph the basis for early adoption of the double beam concepts is clear. (single-beam concept VF-1 (Ref. Figure 50) was evaluated in the baseline trade-offs, however, but was not competitive, primarily due to low ratings in fail-safety and weight). The translating arm concept (VT-2) appears in all three assembly figures. In the baseline structure trade-offs it was a close second

COUCH PIVOT GEAR ASSY.

PIVOT & ROTATIONAL DRIVE SYS.
ARM TRANSLATION SYS.
TRANSLATION & COUNTER-
BALANCE DRIVE ASSY
COUNTER-BALANCE

TRANSLATION SYS.
SUPPORT FRAME

ARM ASSY.

ARM SUPPORT FRAME

COUCH ROLLER ASSY.

INSTRUMENTATION

COUCH FRAME
& RESTRAINT ASSY.

COUCH SUPPORT FRAME
ASSY.

DRIVE HUB ASSY.

DRIVE SYS.

VIEW A-A
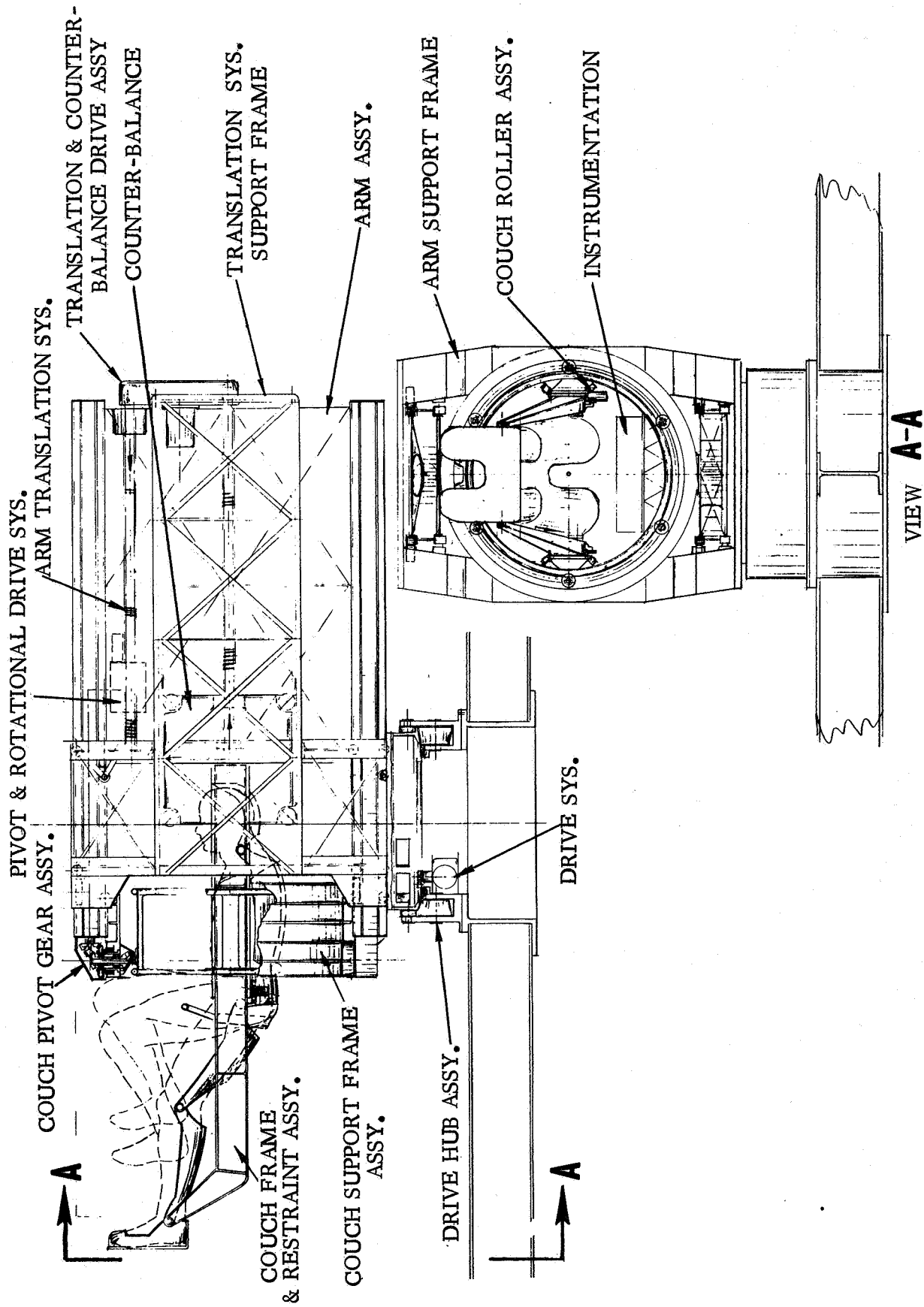
Figure 53. Ground Based Estimating Model

DRIVE HUB

RADIUS ARM

COUCH FRAME

A

B

G

D

E

F

C

FRAME
STRUCTURE

HEAD SHIELD

PIVOT & ROLL
FRAME

COUCH
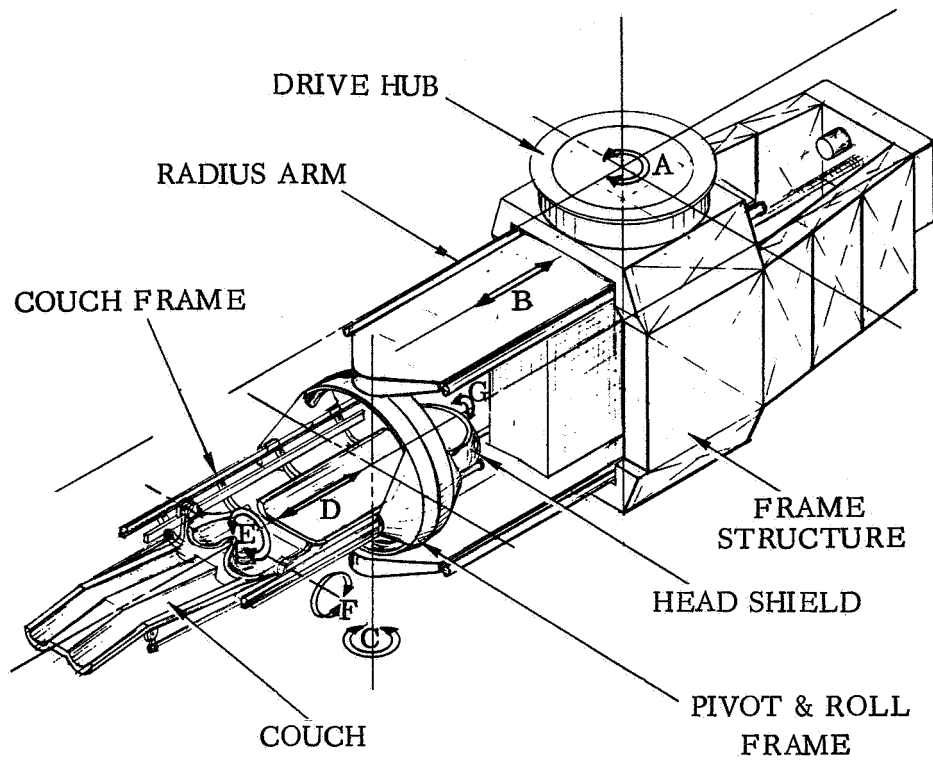
Figure 54. Phase I Orbital Concept



1

3

2

6

5
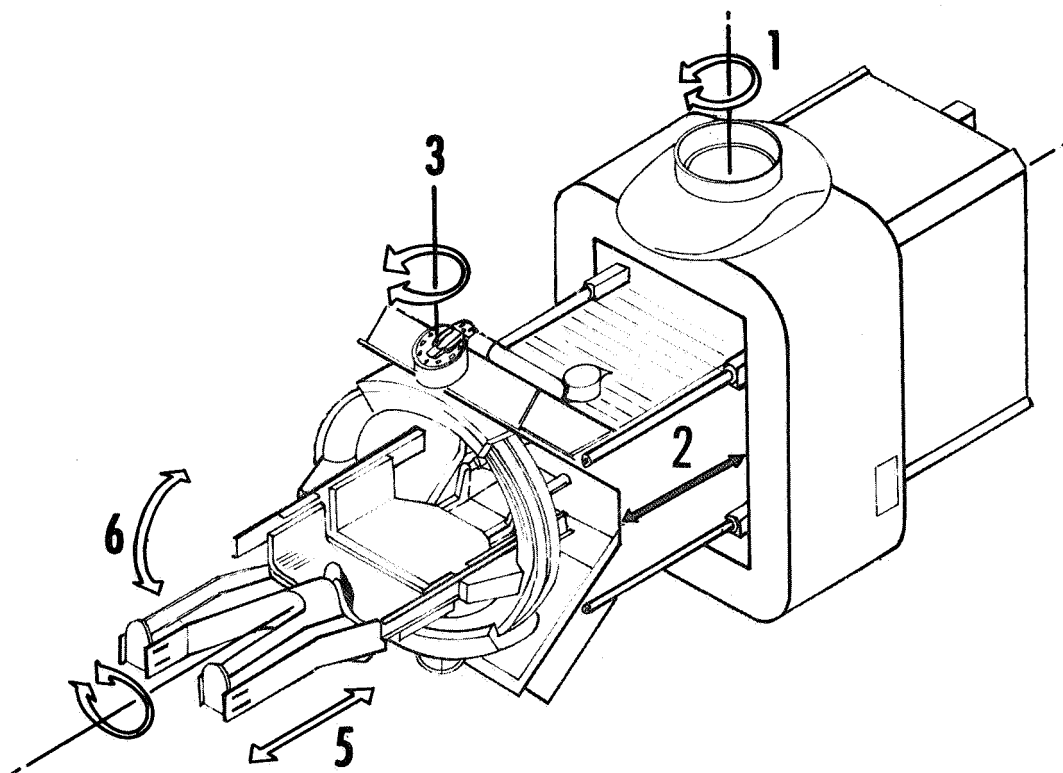
Figure 55. Baseline Centrifuge
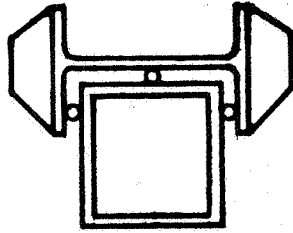
Figure 56. Box/C-Clamp Roll/Pivot Cross-Section Concept

to the fixed arm concept (VF-2) but was nevertheless retained and ultimately adopted due to the problem of interface complexity in VF-2. In the final configuration the double-beam support has been modified to a jaw assembly terminating a single large box beam. The primary reason for this is to minimize beam height, provide consistent strength and stiffness requirements, and to provide volume for the top and bottom corner weight elements eventually required.

All assembly concepts utilized a cantilevered hub. This was done primarily to render the design relatively insensitive to the enclosure configuration in order to avoid identifying with a specific module or vehicle. Note, however, that the double-arm concepts are inherently compatible with the twin-hub concept requiring only minor structural modification.

Changes in counterweight orientation requirements are evident in the three assemblies, the two early ones using a lateral pair whereas the final baseline uses a vertical pair with lateral as well as axial translation capability. The earlier counter-weight support structures were open truss rectangular frames whereas the final configuration is a closed box. The box structure provides much greater stiffness in both the vertical and lateral directions. The flat outer surface also minimizes the probable tendency toward audible wind whistles in the open configurations, at a small penalty in aerodynamic drag. To minimize the amount of inert counterweight, the drive system components for both arm and counterweight translation are positioned at the extreme outer end of this counter weight support structure.

## Couch

Structural assembly and details of the couch are shown in Figures 57, 58, 59 and 60. (Convair Drawings SRC-SD-507, -508, -509 and -510).

The primary structural elements are a pair of channel side beams tied together by two built-up transverse frames, a head restraint assembly, a pelvic saddle assembly, and a leg support assembly.

The couch is both guided in manual pre-test translation and supported structurally by the side rails. The integral guide/support concept was favored in the trade-off study, due primarily to weight, dynamic smoothness, and fail safety.

The transverse frame assemblies are hung between the side rails and transfer all loads to them. These loads consist mainly of subject and equipment inertia. The subject is supported by contoured, padded shell segments in four areas: head trunk, pelvis and legs.

Head support is provided by a helmet mounted on a tube-frame which is in turn supported by beams cantilevered from the upper-body transverse frame. This arrangement, though lengthy in terms of load path, permits all head motions required by the experiments. A shell segment on the upper-body transverse frame supports the subject



Figure 57. Couch Structural Arrangement
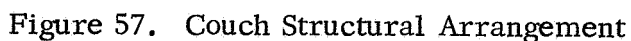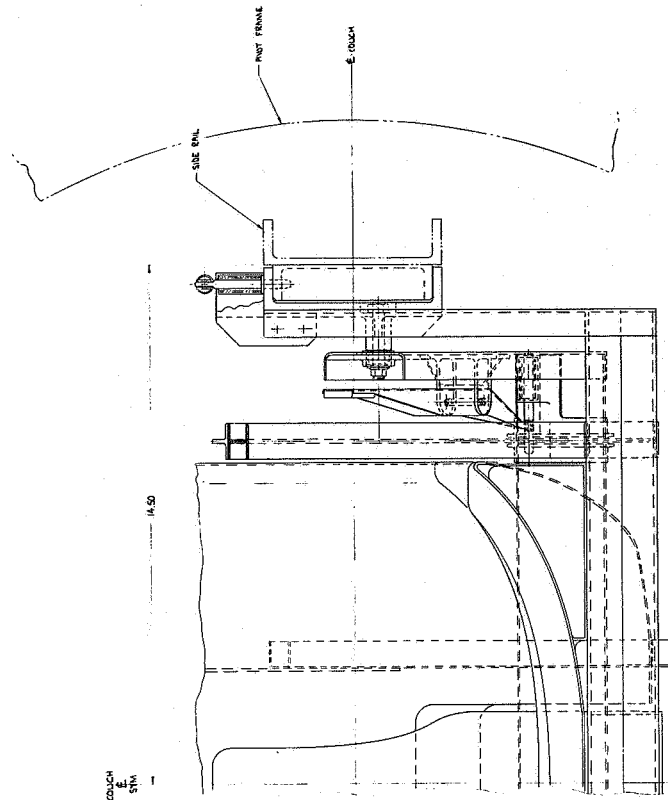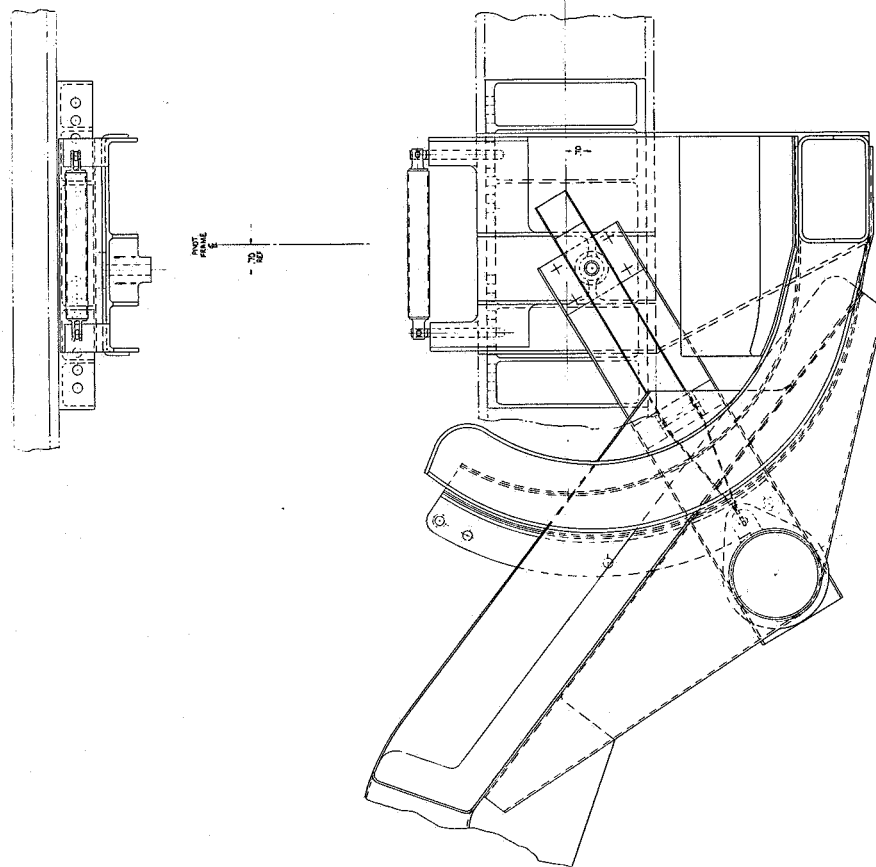
Figure 58. Couch Saddle and Adjustment

FAFLON - FBJI6TF22B20 (2)
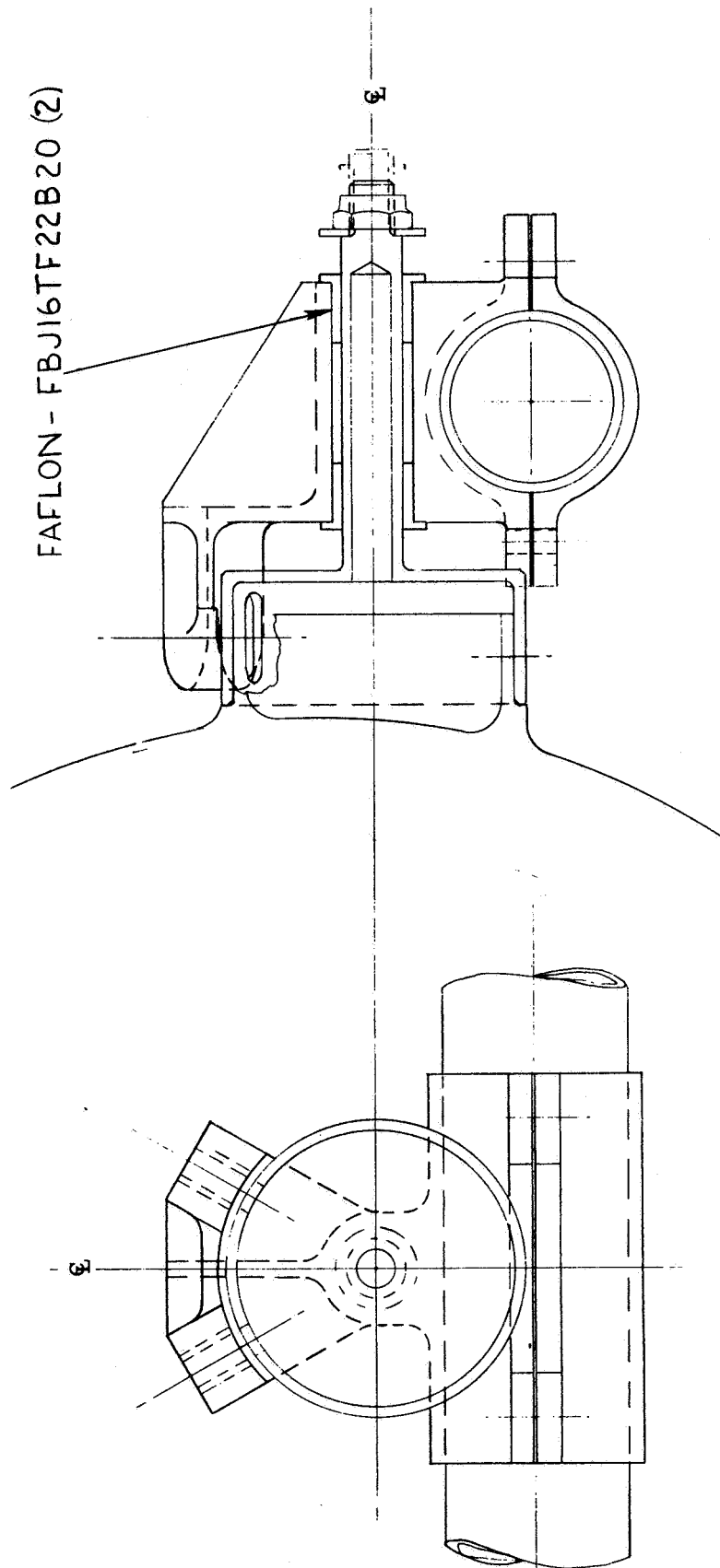
Figure 59. Centrifuge Couch Headrest Pivot
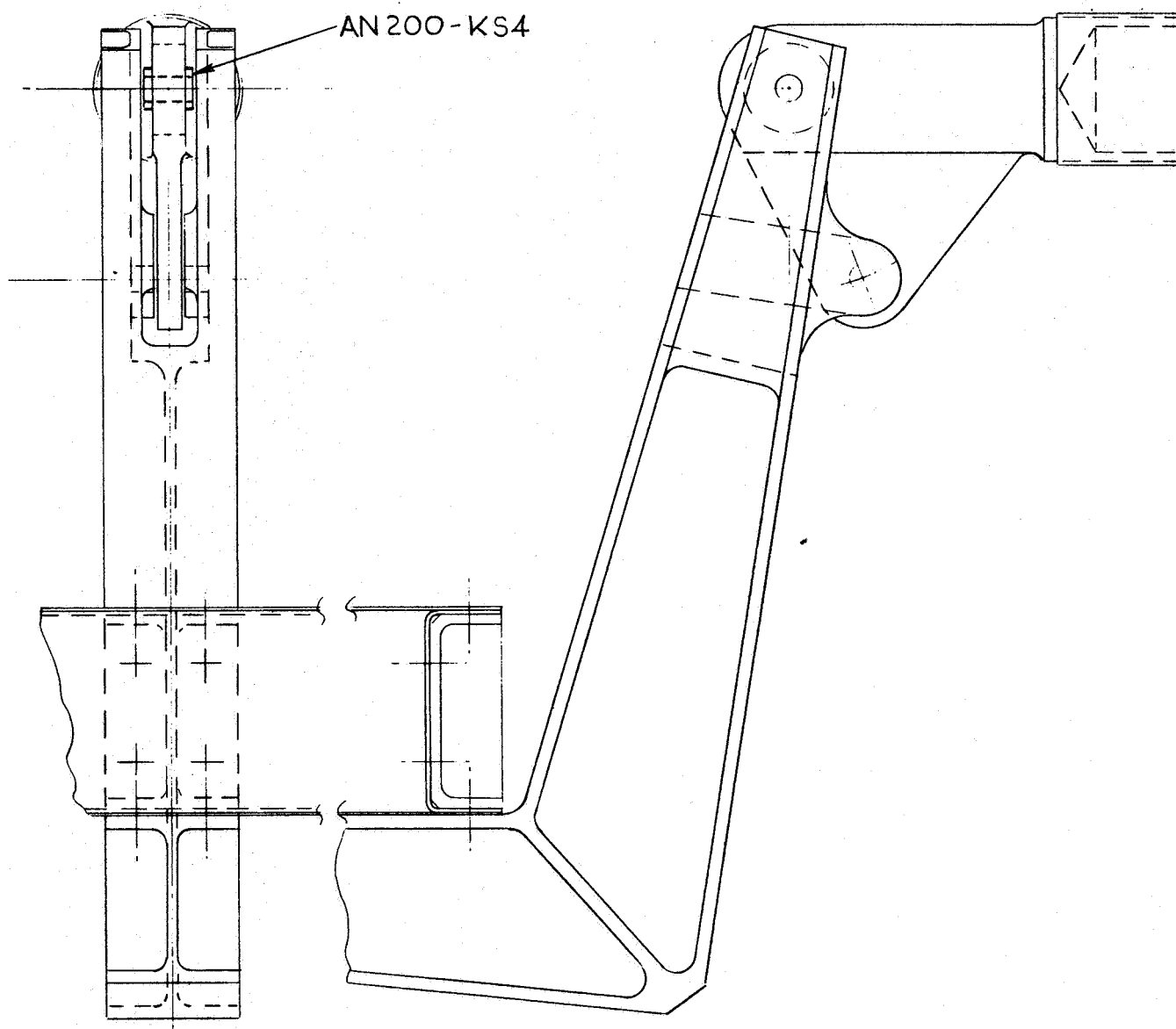
Figure 60. Centrifuge Couch Headrest Frame Pivot and Lock

from the waist to the top of the shoulders.

The lower-body transverse frame provides support for both the pelvic saddle and the leg support frame. It consists of a complete transverse torque tube which furnishes the primary reaction to all loads along the longitudinal axis of the subject, and to lower body loads both normal and transverse to the longitudinal axis.

The pelvic saddle is supported directly by the torque tube whereas the leg support frames attach to both the couch side rails and a flange on the saddle.

The couch assembly provides two adjustment features to accomodate variations in subject size. The hip pivot axis, located at the points of leg frame attachment to the side rails can be varied a maximum of three inches: The foot sole plate in the leg support frame can be set at various points within a six inch travel. These features provide the capability to accommodate subjects in the percentile range of 25 to 75.

Further manual adjustment provisions to satisfy subject positioning requirements for the experiments are also included. Axial translation over a maximum travel range of 27 inches with specific stopping points and positive locks is provided. Rotation about the hip pivot to inclinations of $25^{\circ}$, $53^{\circ}$, and $81^{\circ}$ is also permitted.

Support for the couch is provided by two cantilever beams integral with the roll frame (discussed in the next section). The support geometry and load reaction system is shown in Figure 61.
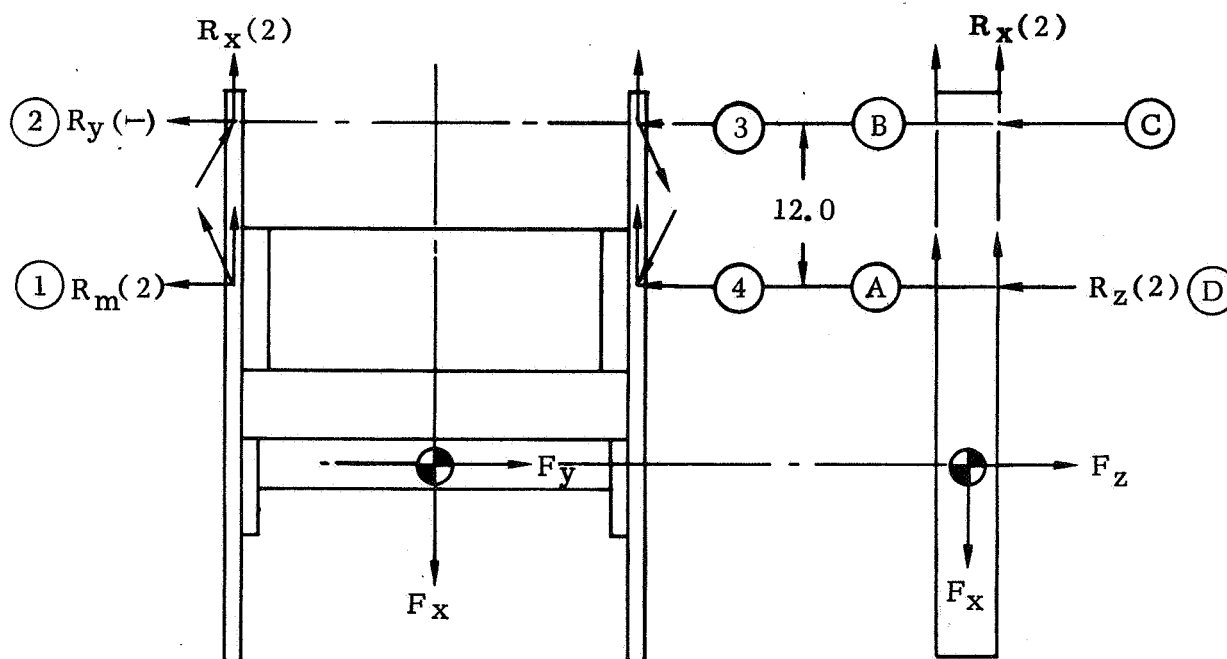


Figure 61. Couch Reaction System

Of the experiments performed with the subject facing normal to the spin plane "grayout" and "oculogravic illusion" produce the highest couch loads. The resulting values are shown in Table 21 (Note that in this case $F_x$ and $F_y$ represent $F_p$ and $F_n$, respectively, from Table 17.

Table 21. Maximum Couch Reactions - Subject Facing Normal

| TEST | LOADS (LBS.)* | | | | | | | |
|------|------|------|------|------|------|------|------|------|
| | $R_{x1}$ | $R_{x2}$ | $R_{x3}$ | $R_{x4}$ | $R_{y1}$ | $R_{y2}$ | $R_{y3}$ | $R_{y4}$ |
| G. O. | 334 | 334 | 188 | 188 | 88 | 24 | 24 | 88 |
| O. G. I. | 166 | 166 | -12 | -12 | 106 | 26 | 26 | 106 |

\* R means the sum of the R-term and the component of the $R_m$ term in the appropriate coordinate direction.

With the subject facing tangent to the spin plane the re-entry simulation and oculogravic illusion experiments produce the highest couch loads. The resulting values are shown in Table 22. (Note that for re-entry $F_x$ and $F_y$ represent $-F_n$ and $F_p$, respectively, in Table 17. Whereas for oculogravic illusion $F_x$ and $F_y$ represent $F_p$ and $F_n$ respectively).

Table 22. Maximum Couch Reactions - Subject Facing Parallel

| TEST | LOADS (LBS.) | | | | | | | |
|------|------|------|------|------|------|------|------|------|
| | $R_{xa}$ | $R_{xb}$ | $R_{xc}$ | $R_{xd}$ | $R_{za}$ | $R_{zb}$ | $R_{zc}$ | $R_{zd}$ |
| R. E. S. | -385 | -385 | -247 | 247 | -475 | 0 | 1415 | 940 |
| G. O. | 266 | 266 | -116 | -116 | 0 | -287 | 141 | 428 |

For determining couch stiffness in the spin plane two planes of loading must be considered: couch rail plane in the spin plane and normal to the spin plane. In the former case, couch stiffness is required to be 60,000 lb/in per Table 18. This stiffness is affected by two deformation modes: deflection of the total couch assembly as a beam and local deflection of the side rails remote from points of lateral support.

The cap area requirement for the side rails, considering the entire couch as a beam is quite small (.05 in.$^2$) indicating very high inherent stiffness in that deformation mode. Assuming, then that all flexibility occurs in the local deformation mode, a required moment of inertia of .09 in.$^4$ was established for each side rail. Since the final couch design and the prior assumed local deflection model are not identical, additional stiffening at the cantilevered couch rail ends is required but has not been evaluated since it is a relatively minor detail.

Stiffness in the opposite plane was expected to be dependent on either the re-entry simulation experiment (K = 58,000 lb./in. and load 6.0 inches off reaction pattern center) or the acceleration sensitivity experiment (K = 16,650 lb./in. and load 21.0 inches off center). Moment of inertia requirements for the two cases were determined and the acceleration sensitivity case was found to govern (I = 2.57 in.$^4$ vs. .21 in.$^4$). A 5.0 inch section provides this stiffness and was therefore established as the baseline couch rail beam depth. Total weight of the couch primary structure and subject support provisions is approximately 49.9 lbs. in aluminum alloy with fiberglass countoured shells.

## Roll Frame

The structural assembly of the roll frame is shown in Figure 62 (Convair Drawing SRC-SD-514).

The primary structural elements are a toroidal circular frame and a pair of cantilevered box beams for support of the couch. The toroid cross-section is essentially circular and is composed of three elements: two identical arc segments and a crown. Each element is fabricated as a complete annulus prior to butt-welding together to form the toroidal ring. The circular cross-section was selected primarily to provide maximum physical smoothness in the structure nearest the head of the subject. (Ref Figure 42) This results in an efficient structural section but implies added cost in the forming of the doubly-curved arc segment annuli. A square cross-section, though cheaper to build, would provide some hazard to the subject during ingress and egress.

It is expected that the arc segments might be spin, bulge, or explosive formed from sheet stock whereas the crown would be machined from a forged ring billet. The crown ring provides the interface with the pivot segments, the canted sides and the center raised stub acting as roller tracks. A driven ring gear of the roll drive mechanism is inserted between the twin center roller tracks. All three track surfaces are turned and ground after all welding of the toroid assembly to assure precision control of interface geometry. Stiffening webs are incorporated at 5° intervals around the track ring perimeter to reinforce the flared tracks for the high local roller loads they experience. Protective cover strips would be bounded to the outer surface of the track ring (except on the roller contact surface) to eliminate the hazard of finger damage during roll mode operation in checkout, test, or experimentation.
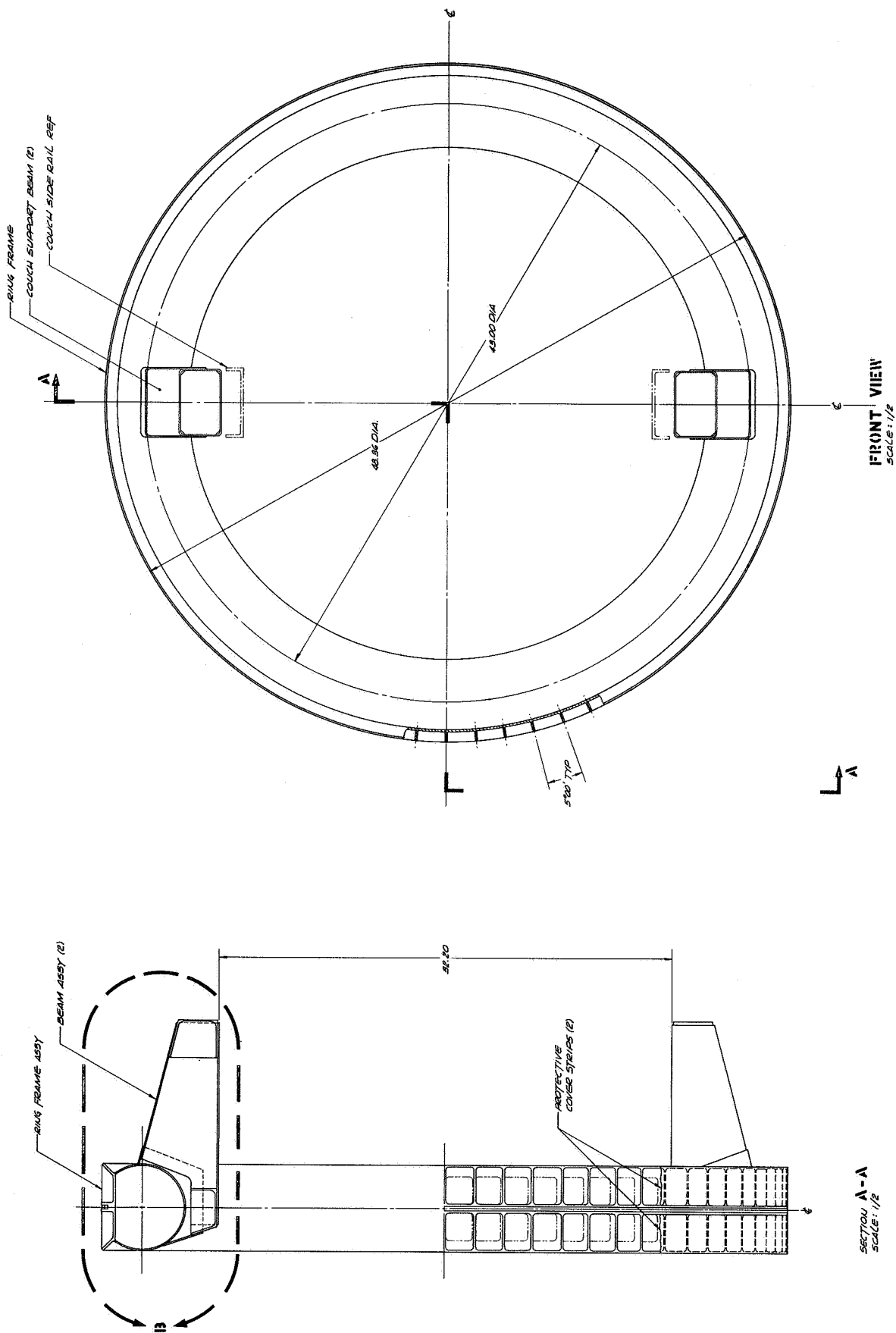
Figure 62a. Roll Frame Assembly

Figure 62b. Roll Frame Assembly

The couch support cantilevers are attached to the toroid by bent-up plate frames welded to it. The beams are identical closed boxes of rectangular cross section, formed from bent-up and butt welded plate material. Machined load distribution fittings are incorporated into the beams to receive couch loads and distribute them to the boxes.

Though not shown in Figure 62, it is now proposed that periodically spaced internal stiffeners be incorporated in the toroid cross-sectional plane to prevent the tendency toward ellipticity which a toroidal structure exhibits under combined bending and torsional loading.

In determining the stiffness of the roll frame, it was first recognized that it acts a spring only for those experiments in which the subject faces normal to the spin plane. (For the parallel - facing orientation the couch support beams react into the toroid at the pivot axis, midway between the ends of the pivot segments. The load is essentially transferred directly to the pivot segments and then directly into the radius arm.) Stiffness analysis of the roll frame and cantilevers was a complex problem because of the several simultaneous modes of deflection under the action of typical couch support loads. The structural model adopted for stiffness analysis is shown in Figure 63. In the model the frame is idealized as a pair of 180° arc with segments with analytically identical load systems. All loads are assumed to be
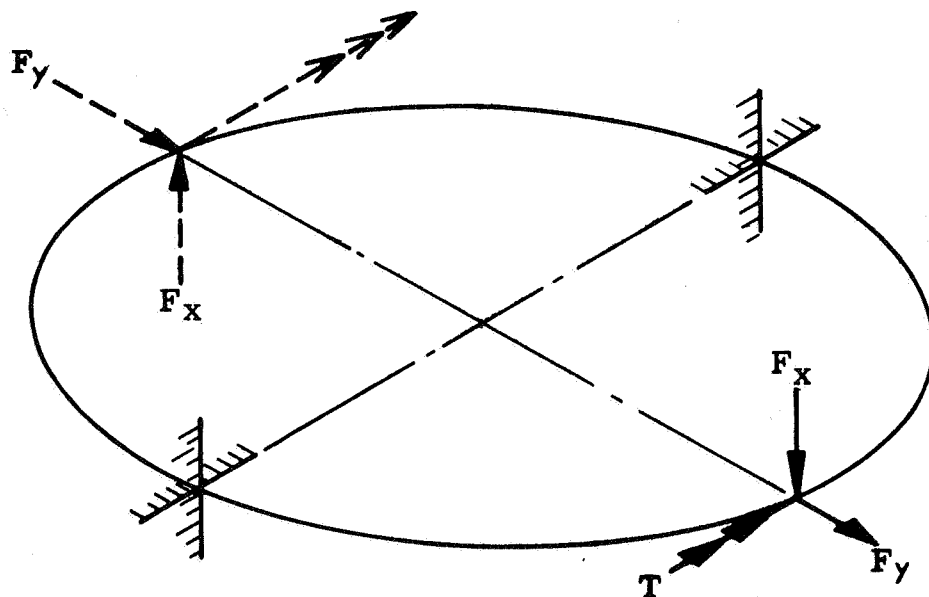


Figure 63. Roll Frame Structural Model

applied at the mid-point of the arch. End conditions were assumed to consists of slope fixity (due to the moment resistance provided by the pivot segments) and roll fixity (due to the self reaction of the loads which produce torque at the supports). The effect of pivot segment support several inches each side of the ends is conservatively neglected. General deflection expressions were obtained by considering the

response of the frame to each load separately (including bending of the cantilevers). Summing these resulted in the following equation yielding roll frame stiffness under the action of loads in the spin plane:

$$\frac{1}{K_S} = \frac{1}{(EI)_R} \left[ .0845R^3 - 0.73\ R^2 + 147.2R \right] + \frac{1}{(EI)_C} \qquad (341\text{-}25r)$$

where

$(EI)_R$ and $(EI)_C$ are the flexural rigidities of the toroid and cantilevers, respectively and R and r the centroidal and cross-sectional radii of the roll frame.

Using this equation, an optimization study was undertaken to minimize the weight of the frame, consistent with the stiffness criteria. In the course of this study it became apparent that the initial assumption of equal stiffness for all structural elements was unrealistic. Furthermore, a significant potential relief to the roll frame spring constant requirements was seen in altering the orientation of the subject for the gray-out experiment. Consultation with the life sciences group resulted in agreement that the subject could be oriented to facing tangent to the spin plane for this experiment. This alteration in no way compromises the experiment, yet does render the roll frame inactive as a spring and thereby reduces its required stiffness to that of the acceleration sensitivity test (19,980 lb./in.). By taking advantage of increased radius arm and couch stiffnesses in conjunction with this test, a tentative optimum roll frame stiffness of 5,500 lb/in. was derived. This value, though subject to total system stiffness optimizations recommended for the hardware design effort, was adopted, and the design of Figure 62 is nominally based upon it. Resulting roll frame total weight is approximately 43.5 lbs. in aluminum alloy.

## Pivot Segments

Structural details of the pivot segment are presented in Figure 64 (Convair Drawing SRC-SD-405).

Two nearly identical segments are required in the centrifuge assembly. The only feature distinguishing the two pieces is the roll drive system mounting provision required on only one segment. They are essentially one-piece, 60° arc segments, each permitting attachment of five sets of three rollers and incorporating a 10.00 in. diameter flange for attachment to the pivot drive mechanism. The roller sets are mounted at 15° intervals along the arc. The cross-section varies with location, as shown in Figure 64, though the top and bottom plates, which primarily resist bending stresses, are essentially constant. The only inner-surface interruptions are rectangular sockets in which the center rollers (and, at one location only, the roll drive pinion also) are mounted. On the outer surface access slots are provided on
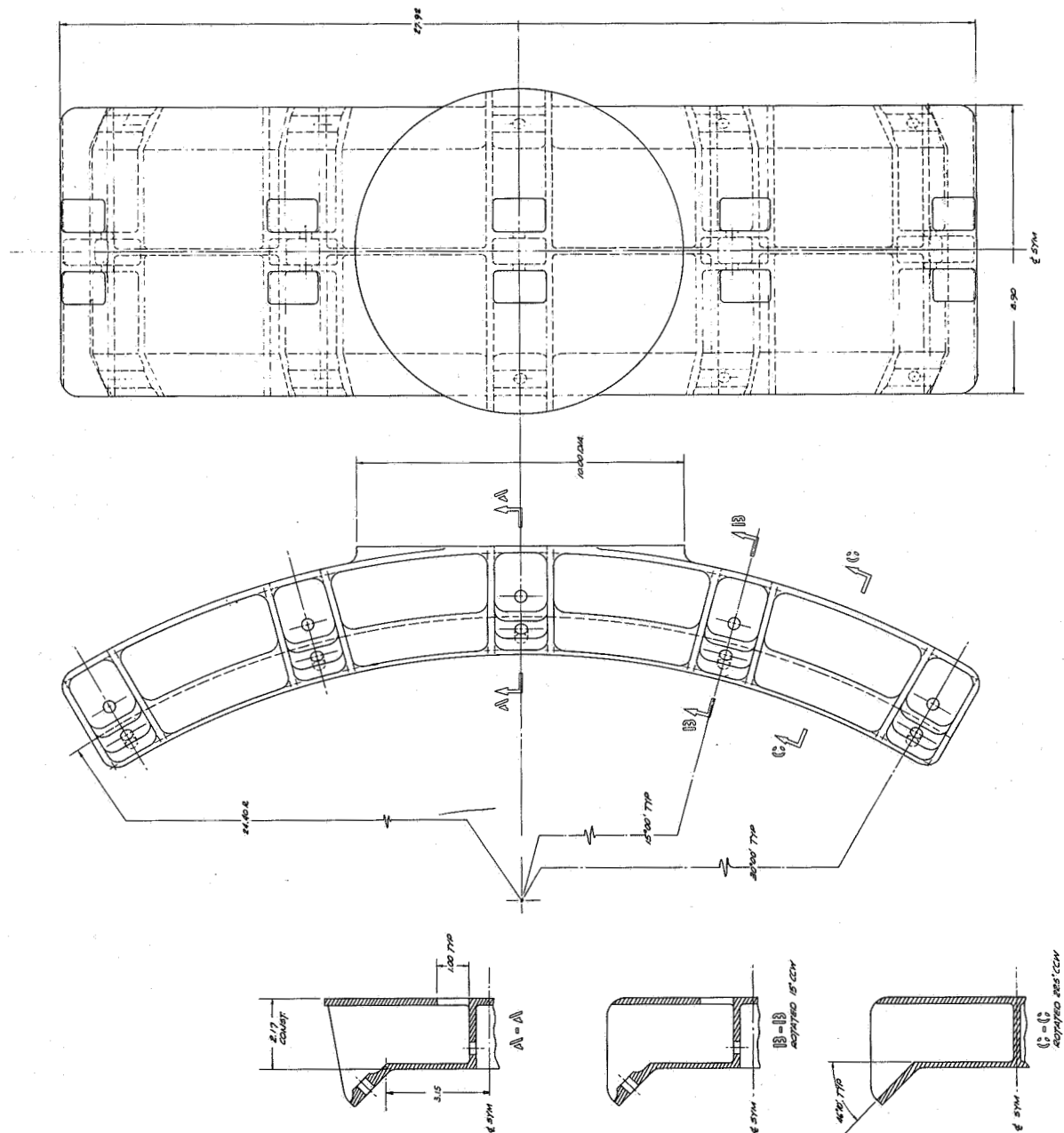
Figure 64.  SRC Pivot Segment

each side of the roller sockets to aid in installing and adjusting the rollers. Transverse stiffening webs, spanning the full segment width, are incorporated on each side of each roller mounting plane. These provide stabilization for the cap plates and help distribute both shear and bending stresses from the reactions at the outer rollers. The exterior corners of each segment are rounded, insofar as possible, to minimize the injury hazard.

The pivot segments act as dynamic springs for all tests, but load application is more severe for experiments with the subject facing normal to the spin plane. For determing the stiffness under the action of loads in the spin plane the structural model of Figure 65 was used. Determination of the load intensity, for a given experiment,
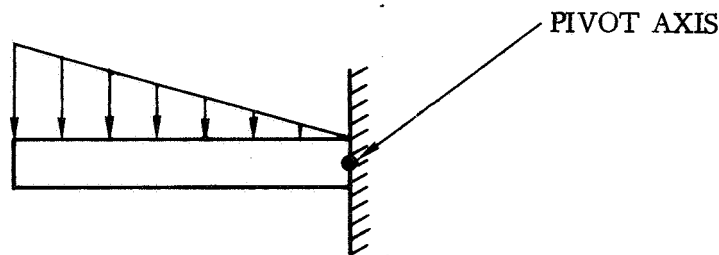


Figure 65. Pivot Segment Structural Model - Lateral Direction

was based on distributing any in-plane moment equally between the four pivot segment cantilevers (two active beams per segment). From the geometry of the pivot arc and the subject/couch center of mass relationship to the pivot axis, an expression for required pivot stiffness in the grayout experiment was derived:

$$K_4 = EI/652 \qquad lb./in.$$

This resulted in a moment of inertia requirement of 3.91 in.$^4$ in the lateral direction The area requirements to provide this capability are quite small, as illustrated by considering the two caps as a single plate 8.9 inches high:

$$I = th^3/12 = 3.91$$

$$t = \frac{(12)(3.91)}{(8.9)^3} = 0.33 \text{ in.}$$

Since bending in the other direction will require much greater cap thickness, it is seen that a benefit in lateral stiffness of the segments is inherent. This permits selective relaxation of the stiffness requirements of other elements of the structure.

Bending stresses under the action of grayout experiment loads are below 10,000 psi at the nominal moment of inertia, hence will be very low in the final design.

For establishing the stiffness requirements in the "vertical" direction the structural idealization of Figure 66 was used.
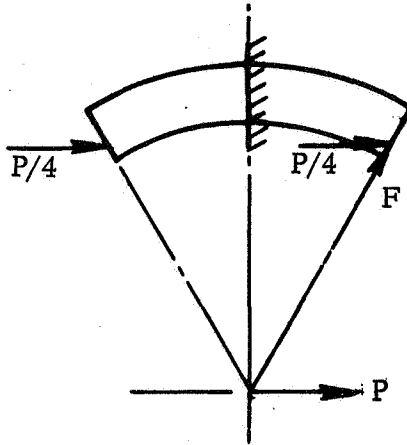


Figure 66. Pivot Segment Structural Model - Vertical Direction

The maximum load in this direction is produced by the re-entry simulation experiment and is assumed to be equally divided between the four pivot cantilevers and to be concentrated at the outermost roller planes. The approximate bending load is derived below (Ref. Figure 66).

$$P = 3760 \text{ lbs.}$$

$$F = \frac{P}{4} \left[ \frac{1}{\sin 30^\circ} \right] = \frac{2P}{4} = \frac{P}{2} = 1880 \text{ lbs.}$$

Assuming the use of a moderate strength aluminum alloy, a required section modulus, $I/c$, of .853 in.$^3$ was established. The present design, selected from a variety of cross-section candidates, provides more than twice this capability ($I/c = 1.966$ in.$^3$) primarily because material thicknesses were initially estimated from preceding, less deep, configurations. It was decided not to optimize the sectional properties further, at this time, for two reasons. First, refined local stress analysis under the concentrated loads remains to be accomplished in the hardware design phase, and may very well require local retention of the comparatively heavy sections now shown. Secondly, and most importantly, the benefit to in-plane stiffness, at a relatively small weight penalty, might also be preferable depending upon later total system stiffness optimization studies.

Segment weights in the existing configuration are 13.0 lbs. each whereas in a refined configuration tailored strictly to the preceding section modulus requirements a weight of approximately 7.0 lbs. per segment is reasonsable.

Radius Arm

Details and assembly of the radius arm structure are shown in Figure 67 (Convair Drawing SRC-SD-402).

The arm is essentially a 35.6 in. by 40.0 in. box beam with an integral forward "jaw" structure for support of the pivot/roll/couch elements, a pair of removable transverse bulkheads, and two internal beam assemblies for local loads and equipment support.

The basic box is formed by four corrugation-stiffened semi-sandwich skin panel assemblies which join four integral beam-cap/guide-rail assemblies. Aluminum corner angles are used to connect intersecting box panels while radial translation capability, compatible with the ball-bushing concept selected in the mechanism trade-offs, is accomplished by hollow circular steel guide rails. The guide rails are rigidly attached to their respective corner angles by special T-head bolts inserted through slots in the rails. It is desirable to develop the guide rails as active elements of the beam cap, but this could not be accomplished through the primary fasteners because the slots preclude shear transfer across the interface. By inserting shear pins in match reamed holes in an alternating bolt-pin-bolt . . . pattern, the desired continuity is achieved.

The corrugation stiffening concept was selected in the baseline trade-off study. It is low in weight, high in stiffness, and simple to produce from a single set of dies. Trapezoidal corrugations were favored due to the fastening requirement with the face sheet. The means of attachment has not been selected although continuous roll-spot welding appears favorable, and adhesive bonding is also attractive. The most compelling factor in favor of the corrugation stiffening concept is its unique ability to provide a constant foundation under the ball-bushing reaction points independent of arm radial position. This feature was especially preferable at the time of the baseline concept selection when active arm translation during centrifuge rotation was an operational requirement. Since that time the experiments have been modified to delete this requirement. It was still desirable, nevertheless, to retain this attribute for a number of reasons:

a. If deleted, it would be natural to provide local stiffening at those arm points falling under the support fittings, but this doesn't permit changes in specific experiment radii in the future without structural modification;

b. Soft spots under the guide rails are incompatible with the rigid support required by the guide rails to prevent flexing and possible cracking of the high hardness, brittle surface treatment;

Figure 67a. Radius Arm Structural Assembly

ARM TRANSLATION NUT REF

TOP SKIN PANEL

CORNER ANGLE

AFT SKIN PANEL

AUXILIARY STIFFENER

TRANSLATION NUT
ATTACH FITTING

INCLINED BEAM ASSY (2)

8.90

SECTION C-C
SCALE: 1/1

⊄ SYM

ARM TRANSLATION NUT REF

TOP SKIN PANEL

TRANSLATION NUT ATTACH FITTING

INCLINED BEAMS

AUXILIARY STIFFENER

SECTION D-D
SCALE: 1/1
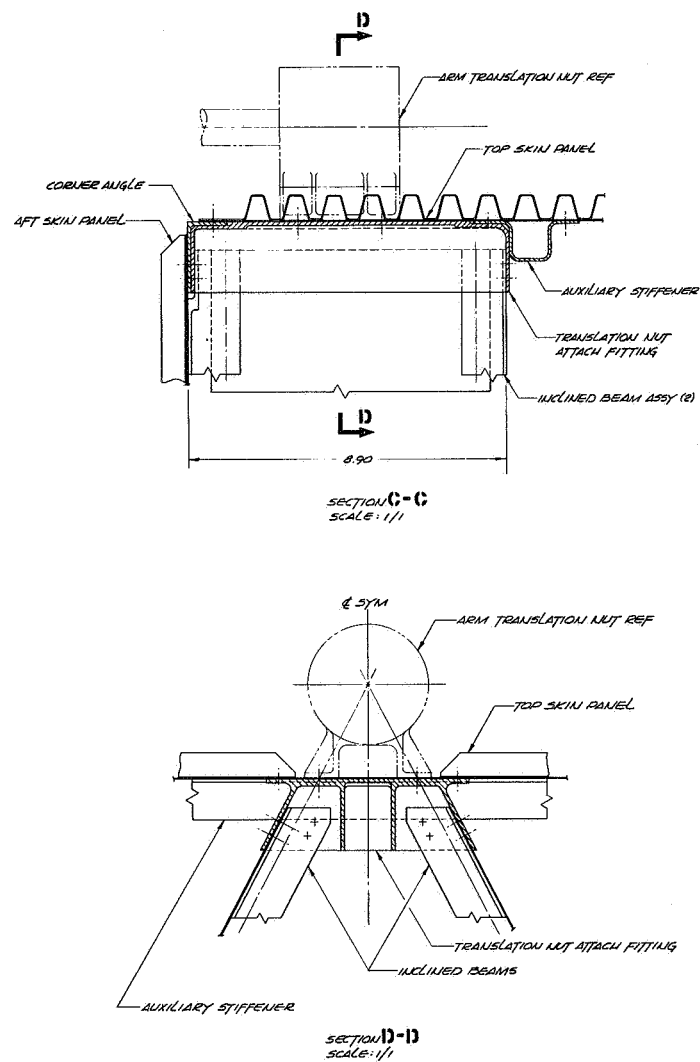
Figure 67b.  Radius Arm Structural Assembly

c.      If "in-test" translation is later re-instated the structure is compatible without modification.

The detail skin and corrugation design is based upon reacting, without buckling or yielding, the lateral forces which occur at the supports in an emergency stop from a 9.0 g test with the arm at maximum radius. The 553 lb. load at approximately 78.0 in. radius results in a distributed load of 96 lb./in. under each ball-bushing fitting. Selecting a 75° corrugation with an efficiency of .65 or greater as initial criteria, a skin/corrugation combination was developed. Skin and corrugation gages of approximately .012 and .021, respectively, resulted (assuming aluminum alloy). Skin gage requirements to preclude shear buckling were found to be on the order of .005 in., indicating excellent margin in the selected configuration.

The same skin/corrugation panel assembly optimized for the arm box was adopted, as well, for the end bulkheads and jaw assembly transverse webs. This was based primarily on reducing fabrication costs since use of a single set of dies for forming all corrugations minimizes die costs. Further saving would be possible by selecting a corrugation section for which dies already exist. Convair has a number of trapezoidal corrugation dies but they have not yet been inventoried for possible use in this application.

The jaw structure is a space framework spliced to the box skin panels and supporting the forward portion of the guide rails. It is composed of machined or built-up elements. Centrifugal loads are carried in bending on the transverse end beams and thence by direct tension and bending down the converging sides of the jaw where they are sheared directly into the guide rails. The vertical side panels carry the moment in the root of the jaw. The transverse beams are not loaded in a principal plane of bending but are constrained to deflect in a radial direction only by the roll/pivot assembly which ties them together. Loads applied parallel to the transverse beams are essentially carried in shear by the skin panels on the outer jaw surfaces, which provide excellent lateral sway stiffening for the otherwise open rectangular frames. The transverse beams and inclined jaws are of zee cross-section with 2 in. flanges and 9 in. maximum depth.

The jaw geometry is the key to the configuration of this remaining chain of structure supporting it. It is configured to permit unrestricted rotation of the roll/pivot assembly. The subject/couch motion envelope, however, sets the side panel root position and the width and height of the throat. The radius arm box dimensions derive directly from the jaw throat geometry while the main rotational frame and drive/counterweight frame are configured to the arm box envelope.

The removable transverse bulkheads in the arm box are composed of corrugation stiffened sheets with continuous edge frame angles. The edge angles attach to similar angle frames integral with the arm box, permitting removal of the bulkheads for unconstrained access to equipment mounted within.

Near the center of the box is a cruciform beam assembly whose primary function is to support the pivot drive system on the box centerline. Its dimensions are established primarily by the size of the drive motor and gearbox which are mounted at the intersection of the beams by sliding in from the aft end and bolting in place. The aft flanges of both beams are discontinued near the intersection to permit the mechanism installation but the forward flanges are carried through to form the "X" and to provide continuity for support of the assembly before the mechanism is installed. Attachment at the four corners of the box is accomplished by machined fittings nesting in the cap angles. In addition to supporting the pivot drive system, the cruciform assembly is also utilized for mounting of miscellaneous equipment.

At the aft end of the arm is an A-frame beam assembly whose primary function is to support the arm translation nut. This beam system also provides an auxiliary flange on the top skin panel, which forms a transverse beam on the aft top surface. This beam reacts the horizontal component of load applied to the ball nut whereas the A-frame reacts the moment. A torque box was also considered for the moment reaction function but, though comparable in weight, it was less efficient in terms of auxiliary equipment mounting capability. A machined fitting, occupying a cut-out in the top skin panel, is provided for support of the translation nut. The A-frame beam caps and the auxiliary transverse beam flange pick up this fitting as does the top transverse corner angle of the aft bulkhead attach frame. The opposite ends of the A-frame inclined beams are attached to the lower beam cap angles by machined fittings. This reaction system is designed to sustain the total centrifugal load resulting from 9.06-g operation with the couch at maximum radius. This provides a safety back-up capability for failure of the translation system manual position locks.

The stiffness of the radius arm box is inherently greater than that required by the equal element stiffness assumption. This is illustrated by using the arm structure model of Figure 68 below and developing an expression for stiffness in terms of cap area.
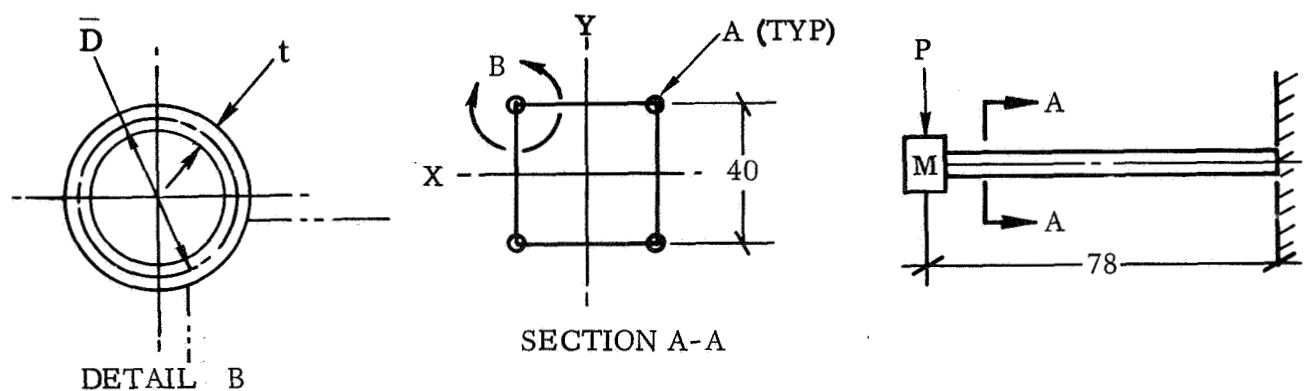


Figure 68. Arm Structure Model

For a cantilever beam

$$K = \frac{P}{\delta} = \frac{3EI}{L^3}$$

For a 4-cap box

$$I = 4A \left[\frac{d^2}{2}\right] = (4A)(20)^2 = 1600A$$

For a hollow steel guide rail (neglecting the additional area in the aluminum corner angle)

$$A = \pi \bar{D} t; \quad E = 30 \times 10^6$$

then

$$K = \frac{(3)(30 \times 10^6)(1600)(\pi \bar{D}t)}{78^3} = (9.53 \times 10^5)(\bar{D}t)$$

Assuming a 1.0 O.D. rail with a minimum permissible wall thickness of .12:

$$\bar{D} = 1.0 - .12 = .88$$

$$K = (9.53 \times 10^5)(.88)(.12) = 100,700 \text{ lb/in.}$$

This approaches twice the required stiffness (58000 lb/in) without considering the additional stiffness provided by the corner angles!

Aluminum was investigated as a candidate rail material but, although high suface hardness is achievable by hard anodizing or electroless nickel deposition, the depth of hardening is limited by surface cracking considerations and substrate crushing becomes a potential problem.

Main Rotational Frame and Drive Counterweight Support Frame

The structural assembly and pertinent details of both the main rotational frame and the drive/counterweight frame are shown in Figure 69 (Convair Drawing SRC-SD-403, Sheets 1 and 2).

The main rotational frame is essentially a continuous rectangular rigid frame whose constant local cross-section is a closed single cell 10 in. by 30 in. rectangular
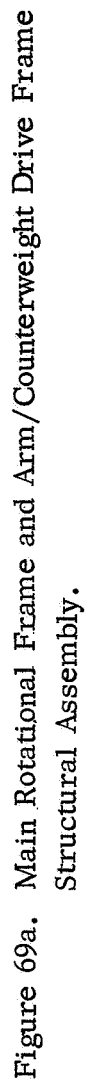
Figure 69a. Main Rotational Frame and Arm/Counterweight Drive Frame Structural Assembly.

Figure 69b. Main Rotational Frame and Arm/Counterweight Drive Frame Structural Assembly

CORNER ASSEMBLY (4)
OUTER SKIN
FRAME (4)
PARTITIONING SKIN (2)
ANGLE (2)

OUTER SKIN PANEL ASSY REF

INNER SKIN PANEL ASSY REF

BEAM CAP/GUIDE RAIL ASSY REF

SECTION D-D

30.0 REF

SPLICE STRIP REF
OUTER SKIN REF
ANGLE REF
PARTITIONING SKIN REF
FRAME REF

END FRAME REF

BEAM CAP/GUIDE RAIL ASSY REF

SECTION F-F
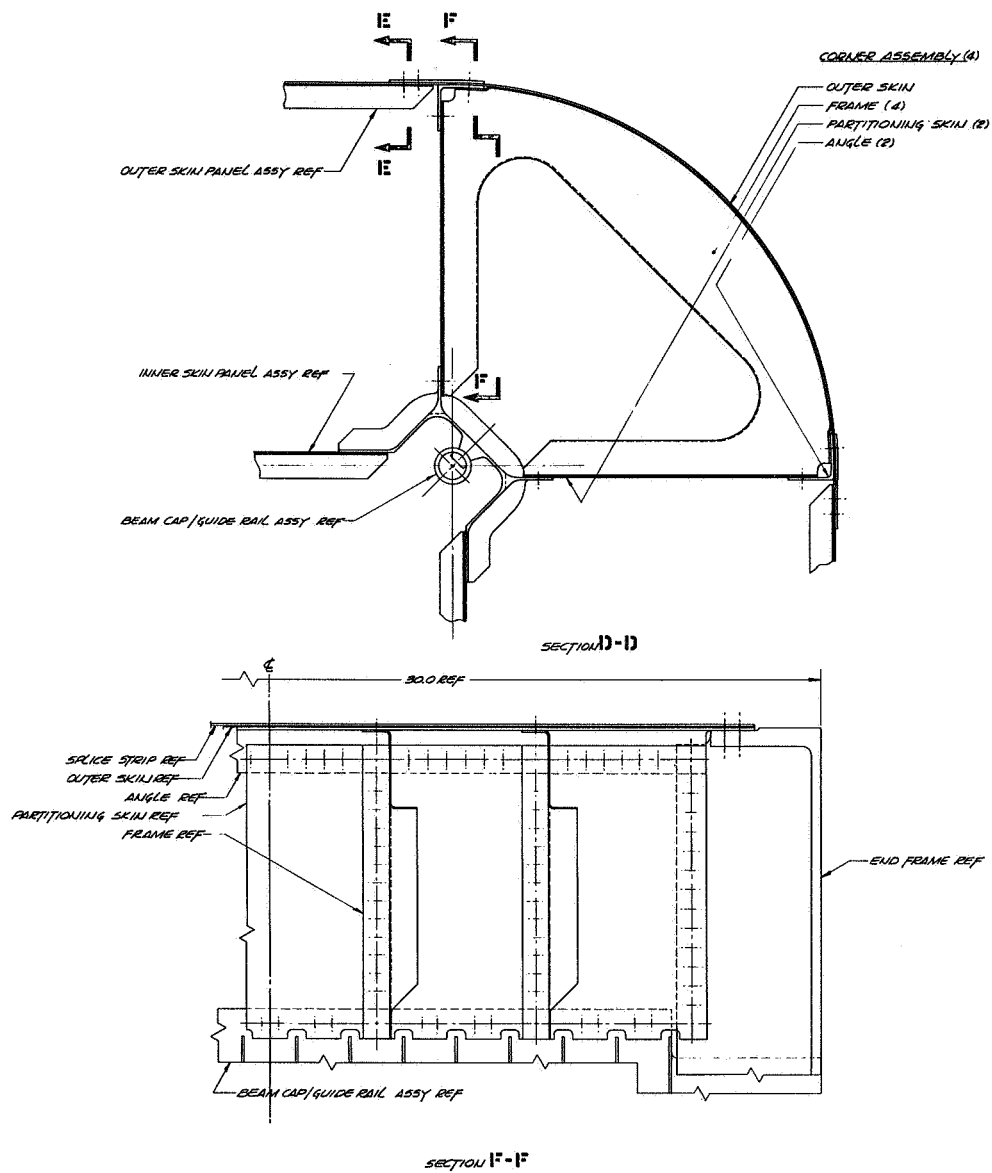
Figure 69c. Main Rotational Frame and Arm/Counterweight Drive Frame Structural Assembly.

END FRAME

10.00 TYP

BEAM CAP/GUIDE RAIL ASSY REF

INNER SKIN PANEL ASSY REF

SECTION M - M

SIDE PANEL REF
REMOVABLE COVER REF

END COVER
SKIN REF

OUTER SKIN PANEL ASSY (TYP)
SKIN
CORRUGATIONS
SPLICE STRIP

END FRAME REF

SECTION E - E

SECTION J - J
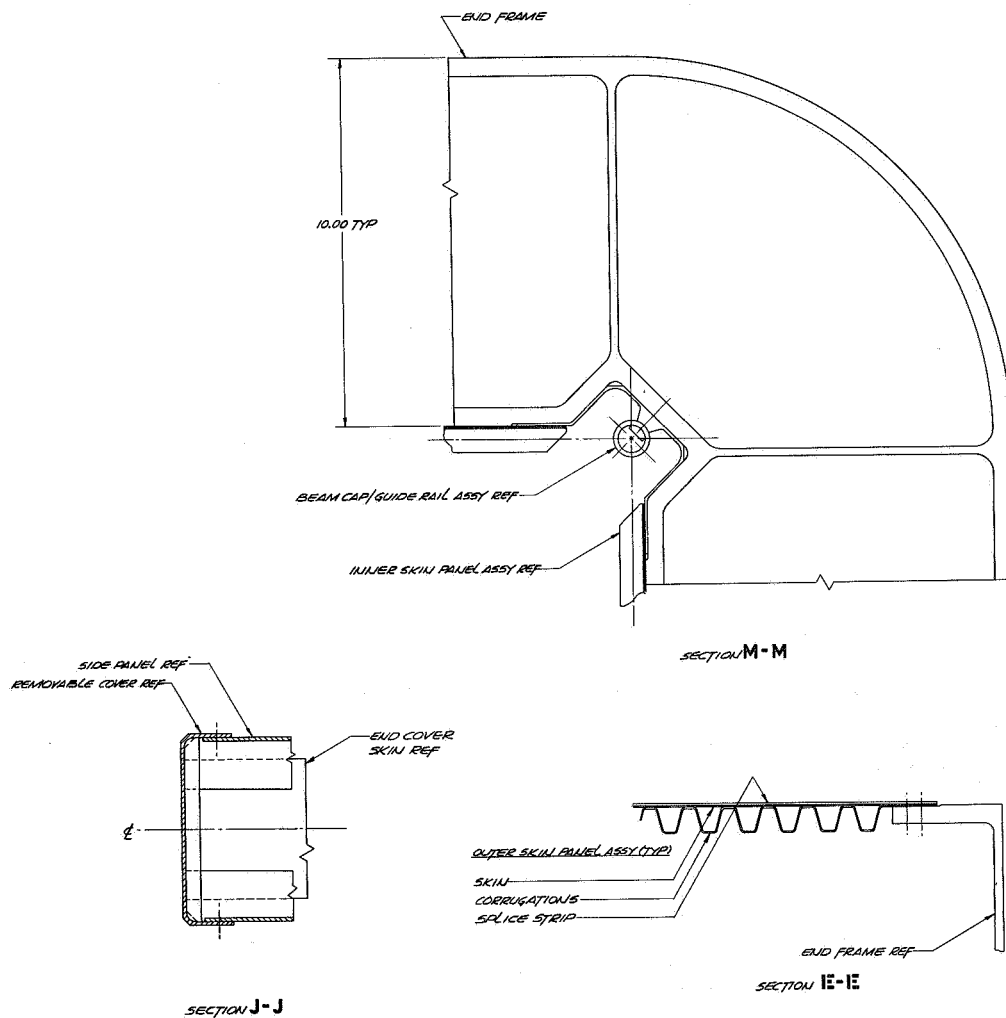
Figure 69d.  Main Rotational Frame and Arm/Counterweight Drive
Structural Assembly.

DRIVE SUPPORT BEAM ASSY

SIDE PANEL (2)
END COVER SKIN (2)
REMOVABLE COVER

6.00

DRIVE BEAM ATTACH FITTING
AUXILIARY PANEL STIFFENER

UPPER SKIN PANEL ASSY REF
CORNER ANGLE
END SKIN PANEL ASSY REF

COUNTERWEIGHT DRIVE
SUB-SYSTEM REF

END SKIN PANEL ASSY

SPLICE STRIP
CORRUGATIONS
SKIN

DRIVE SUPPORT BEAM REF

SECTION K-K

SECTION G-G

5.00
REF

DRIVE SUPPORT BEAM ASSY REF
DRIVE BEAM ATTACH FITTING REF

UPPER SKIN
PANEL ASSY REF

CORNER ANGLE REF

END SKIN PANEL REF

COUNTERWEIGHT DRIVE
SUBSYSTEM REF

SECTION H-H

Figure 69e.  Main Rotational Frame and Arm/Counterweight Drive
Structural Assembly.

END BEARING SUPPORT BEAM ASSY
CAP ANGLE ~ CONTINUOUS
SKIN
CAP ANGLE (2)

INNER SKIN PANEL ASSY REF

INNER LONGERON (2)

END FRAME REF

10.00 REF

OUTER LONGERON (2)

OUTER SKIN PANEL ASSY REF

DETAIL L
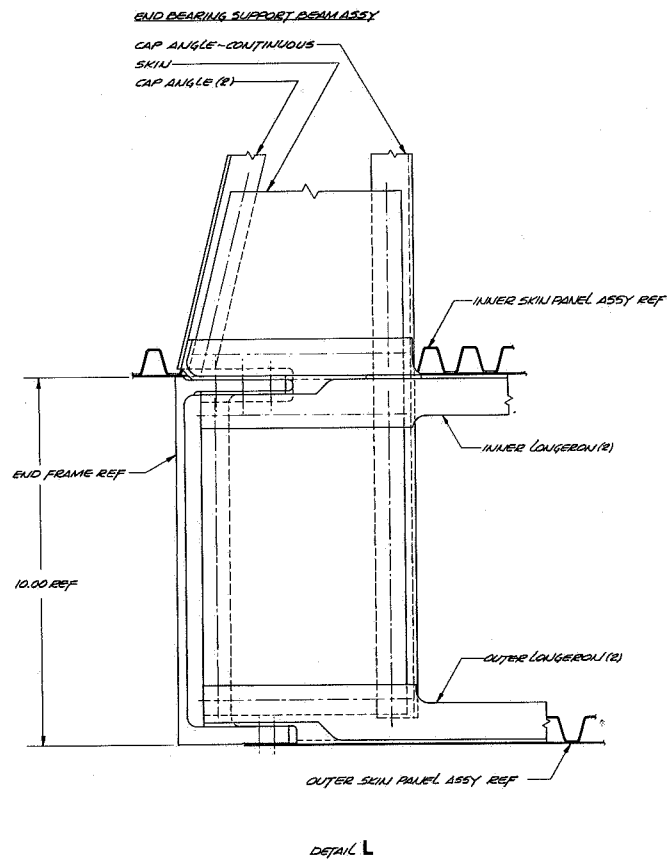
Figure 69f. Main Rotational Frame and Arm/Counterweight Drive Structural Assembly.

box. Its primary components are a pair of identical end channels, corrugation stiffened skin panel assemblies connecting the flanges of the end channels on both the inner and outer flat sides of the frame, four longitudinal corner assemblies, a transverse beam, and four ball bushing retainer fittings. The four beam cap/guide rail assemblies from the drive/counterweight frame also tie the end channels together, extending the full width of the main frame cross-section.

In the baseline trade-off studies, a channel-shaped local cross section was provided for the main frame. Subsequent deflection analysis, however, indicated insufficient in-plane stiffness of the end channels and low torsional rigidity. The present configuration provides greatly improved torsional properties by simply closing the fourth side of the cross section. Furthermore, by orienting all skin stiffening elements in the direction of the frame perimeter, a much increased moment of inertia, due to the additional effective area, is achieved for resisting moments due to loads in the frontal plane of the frame. The structure has not been subsequently analyzed for its deflection characteristics, however, so quantitative stiffness data is not available. (This topic is discussed further in the "conclusions/recommendations" section of this report). As a result, the material gages illustrated for the end channels are arbitrary. They are felt to be very conservatively heavy, but have been retained due to the lack of specific stiffness data. For the present it is expected that they would be machined from aluminum alloy forgings or from welded plate assemblies.

The skin panels are identical in gage and stiffener configuration to those used in the radius arm box. All outer skin panel assemblies are removable to provide access to equipment mounted within the frame. The corrugated sheet faces inward on all outer skin panels so that a smooth outer surface will be maintained. This orientation also eliminates the possibility of audible "organ pipe" effects in the hollow corrugations.

The corner assemblies are built up from sheet metal components and act with the beam cap/guide rail extensions to provide stiffening in the corners of the frame. Flanges are provided on the beam cap elements to permit continuous attachment of the corner assemblies between the end channels. Four z-section frames are used to provide the equivalent skin-panel moment of inertia and to feed skin panel running loads around the corners. As in the outer skin panels, exterior surface smoothness is maintained in the corners by cylindrical-segment skins. Edge angles are also incorporated to provide attachment for the removable outer skin panels.

The transverse beam supports the end bearing for the radius arm drive shaft. It is a dual-tapered fixed ended shear beam which extends through the full depth of the main frame cross-section to achieve moment resisting support. End moments are sheared into the inner and outer skin panels by longerons running the full width of the cross-section.

The ball bushing retaining fittings are machined elements which are attached to both flange and web of the end channels and cantilever inward to pick up the radius arm guide rails. Each contains two 1 in. I. D. ball bushings.

Four types of primary loading are applied to the main rotational frame. The radius arm is supported by the ball bushing fittings, which shear concentrated reactions into the end channel webs. The drive/counterweight frame is supported by virtue of the continuation of both its skin panels and beam caps directly into the main frame assembly. Driving and stopping torques and load imbalances are transmitted to the cross-bridge sensor assembly interface by the end channels and a pair of beams spanning between them. Shear and moment transfer is accomplished by twelve discrete attachments. Preloads and some radius arm inertia forces are applied to the transverse beam. These are reacted by torsion in the plane of the local main frame cross-section.

The drive/counterweight support frame is essentially a four cornered hollow box, providing a continuation of the main rotational frame inner surfaces, and closed at the outboard end by a transverse bulkhead. All side panels and the end bulkhead are corrugation stiffened, with the corrugated sheets on the inside to provide a smooth exterior and avoid wind whistles. The panels are of the same shape and gage as those used elsewhere in the structure. The stiffening concept was selected for the same reason as on the radius arm: The counterweights can assume any position along the full length of the structure and it is preferable to provide a continuous foundation under them. In addition to axial loading of the panels by the counterweights, a dynamic pressure due to relative wind velocity is also applied to them. The selected panel concept provides the capability to support the maximum pressure and axial loads simultaneously without buckling.

The beam cap/guide rail assemblies are much more complex than those of the radius arm. The present concept resulted from the decision to translate the counter-weights inside the supporting structure on ball bushings. In order to eliminate eccentricities in loading the skin panels, since high panel weight results, the guide rail centerlines must lie along the line of intersection of the skin panel neutral surfaces. Furthermore, an envelope must be maintained over a $300^{\circ}$ arc around the guide rail to provide clearance for the ball bushings. This situation forces kinks into the beam cap corner angle member. These kinks experience bending loads ranging from zero at the skin panel neutral axis plane to a maximum at the peak of the kink. To carry these loads, closely spaced stiffening fins were required. Although this concept results in complicated machining requirements, it produces a much lighter member than a simple thickening of the basic cross-sectional thickness of the member. A light weight cover skin is installed over the fins to provide smoothness and elminate wind noise. The guide rails are the same as those used on the radius arm, as is the bolt-pin-bolt attachment concept.

The outboard closing bulkhead is formed by two removable skin panel assemblies and a drive system support beam assembly. The beam consists of two mirror-image, machined side panels which incorporate integral flanges and stiffening provisions for attachment of the drive system components. Fixed outer cover skins are provided at each end and a removable cover panel along the length of the beam provides closure and and additional stiffness but permits ready access to all drive system components. The beam assembly not only provides sufficient rigidity to assure accurate installation and and adjustment of the mechanisms, but is further designed to carry the same 9.0 g,

78 in. radius centrifugal load as the radius arm translation nut support system. The beam is purposely provided with simple supports at each end to prevent local twist and skin buckling in the supporting structure. This is accomplished by using transverse bolts in the neutral plane of the corresponding skin panels. Machined beam attachment fittings are provided to transmit the beam end reactions into the skin panels. Transverse auxiliary panel stiffeners are provided to form a beam cap for transmitting the fitting shear load laterally to the beam cap/guide rail assemblies. The corner angles of the aft bulkhead attach frame act as the other flanges of these beams.

## Conclusions and Recommendations

The first, and foremost, conclusion to be drawn from the structural summary is that it is definitely feasible to analyze design, and fabricate a structural system which is compatible with all the requirements of a space research centrifuge. The baseline design has been shown to be compatible with the full spectrum of candidate experiments. Although in two experiments (tilt table and grayout) revisions to the original geometric parameters were required, these in no way compromised the experiments. Also it has been shown that the structural sub-system is compatible with the specific contractual requirements of 9.0 g and Apollo re-entry profile simulation, and in fact, provides capability greatly in excess of that required for the latter (can withstand 1.0 second stop from 65.3 RPM). Furthermore the total structural sub-system provides sufficient stiffness to preclude structural resonance in any operating mode. This conclusion is justified by the design of the system to an extremely conservative frequency separation ratio as a safety factor against simplification of the system model. Finally, a sub-system has been conceived which is fully compatible with the baseline mechanism concepts at all interfaces.

The most important recommendation which results from the study effort is in the field of structural dynamics. In the course of the study it became apparent that the key to final weight optimization of the structural sub-system was the determination of optimum stiffness distribution throughout. This can best be achieved by establishing a lumped-mass multi-degree-of-fredom model, which closely approximates the actual physical system, and performing weight sensitivity studies by variation of the weight/stiffness parameters. This assumes the accuracy of inputs, in particular the element stiffnesses, implying the need for detailed and realistic deflection analyses. Computer programs capable of performing the dynamic analysis are in use at Convair. The task then becomes one of deflection analysis, preparation of a structural weight optimization program which can use the dynamic programs as subroutines, and time for programming, output evaluation, and iteration. It is strongly recommended that this effort be undertaken in support of any further structural sub-system design on the space research centrifuge.

## Systems and Mechanisms Analysis Summary

<u>Phase I</u> - Initial efforts in the mechanisms and systems portion of the feasibility study were directed toward translating the defined experiment objectives into terms of basic motion requirements. The experiments, upon which this initial analysis was made, are defined in detail in Volume IV of this report, and are only identified in this section in terms of their affect on the baseline definition of the centrifuge motion requirements.

The follow-on activities during Phase I of the study were oriented toward the integration of the mechanism requirements of the centrifuge with a structural system which would meet the man-motion envelope requirements and still provide the necessary structural stiffness to insure system stability.

A final evaluation of the possible mechanical systems, which would meet the experiment requirements, was conducted at the close of Phase I. This evaluation was conducted on the basis of a numerical trade-off analysis which provided a means of correlating the elements affecting hardware development and establishing the feasibility of the baseline approach.

It was concluded at the end of Phase I that there were no major state of the art development areas which would compromise the development of a space research centrifuge.

<u>Phase II</u> - During the Phase II study period the primary effort was to establish a more detailed definition of the configuration and sub-system requirements for an orbital centrifuge system. Based on the optimum approaches, established during the Phase I trade-off studies, a baseline configuration was developed.

It became evident during this phase of the study that some development or technology improvements would be required in the areas of dry running bearings and gear systems and variable speed drive motors. Some development work in these areas is already being pursued by the industry; however, performance to the centrifuge standards will have to be demonstrated.

A more definitive structural configuration was developed in this phase of the study and the integration of all the required mechanical systems was evaluated to determine the feasibility factors of fabrication, installation, and baseline operation.

Phase III - Based on the orbital centrifuge configuration defined during phase II, a sub-system level of specification requirements was established during the Phase III study effort. These specifications establish a preliminary design for the ground-based engineering prototype of the space research centrifuge.

The level of definition established during Phase III is based on the presently proposed experimental program development plan (ref. SRC-MS-112), and is representative of a baseline configuration only. Final definition of the detailed sub-system requirements will necessarily be established during the detailed design phase of the program and will be subjugated to the experiment requirements as defined at that time.

The intent of the Phase III engineering definition, coupled with the test requirements documents, is to provide a realistic bid package from which definitive cost estimates can be established.
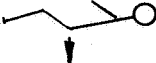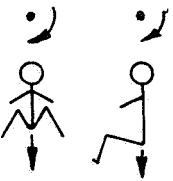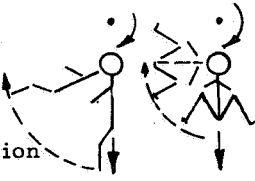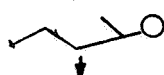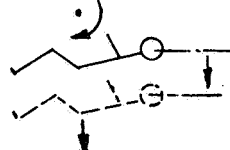
The conclusions which can be drawn from the preceding studies, with respect to the mechanical systems involved, are as follows:

1. There are no major state of the art development areas indicated at this time, based on presently defined experiment requirements.

2. The lead times for highly specialized equipments, i.e., dry bearings and variable speed drive motors, will probably dictate the final schedule for the space research centrifuge.

3. Early definition of the final experimental program is imperative in order to avert unnecessary and costly complication of the motion mechanisms.

Phase I - Analysis

Initial Experiment Definition. - In the contract statement of work a series of suggested experiments was defined as the baseline for establishing the extent of flexibility required for an orbital space research centrifuge. These baseline experiments were reviewed and further defined by the GD/C Life Sciences Department to establish the initial baseline experimental requirements shown in Table 23.

Table 23. Baseline (Phase I) Experiments

| Experiment | Subject Orientation | "g" Level Requirement | Location Of "g" Force | Motions Required |
|---|---|---|---|---|
| Grayout | | 6 g | Feet | Primary Rotation |
| Therapeutic | | 4 g | Feet | Primary Rotation |
| Angular Acceleration | | N.A. | —— | Z-Axis Rotation |
| Tilt Table | | 1 g | Heart | Primary Rotation + Pivotal Tilt Equivalent to 70% Earth Tilt. |
| Semicircular Canal Stimulation | | 1 g | Ears | Variable Radius in-Plane;Roll- 90° |
| Sensitivity to Linear Acceleration | | .002 g to .1 g | Ears | Primary Rotation + Pivotal Tilt in 15° Increments thru - 90° |
| Oculogravic Illusion | | 1 g | Ears | Primary Rotation + Pivotal Tilt in 15° Increments thru - 45° |
| Eye Counter Rolling | | 1 g | Ears | Primary Rotation + Pivotal Tilt in 15° Incrementals thru - 45° |
| Re-Entry Simulation | | 9. g Max. | C.G. | Primary Rotation |
| Mass Determination | | 1 g | C.G. | Primary Rotation + Radius Variation |
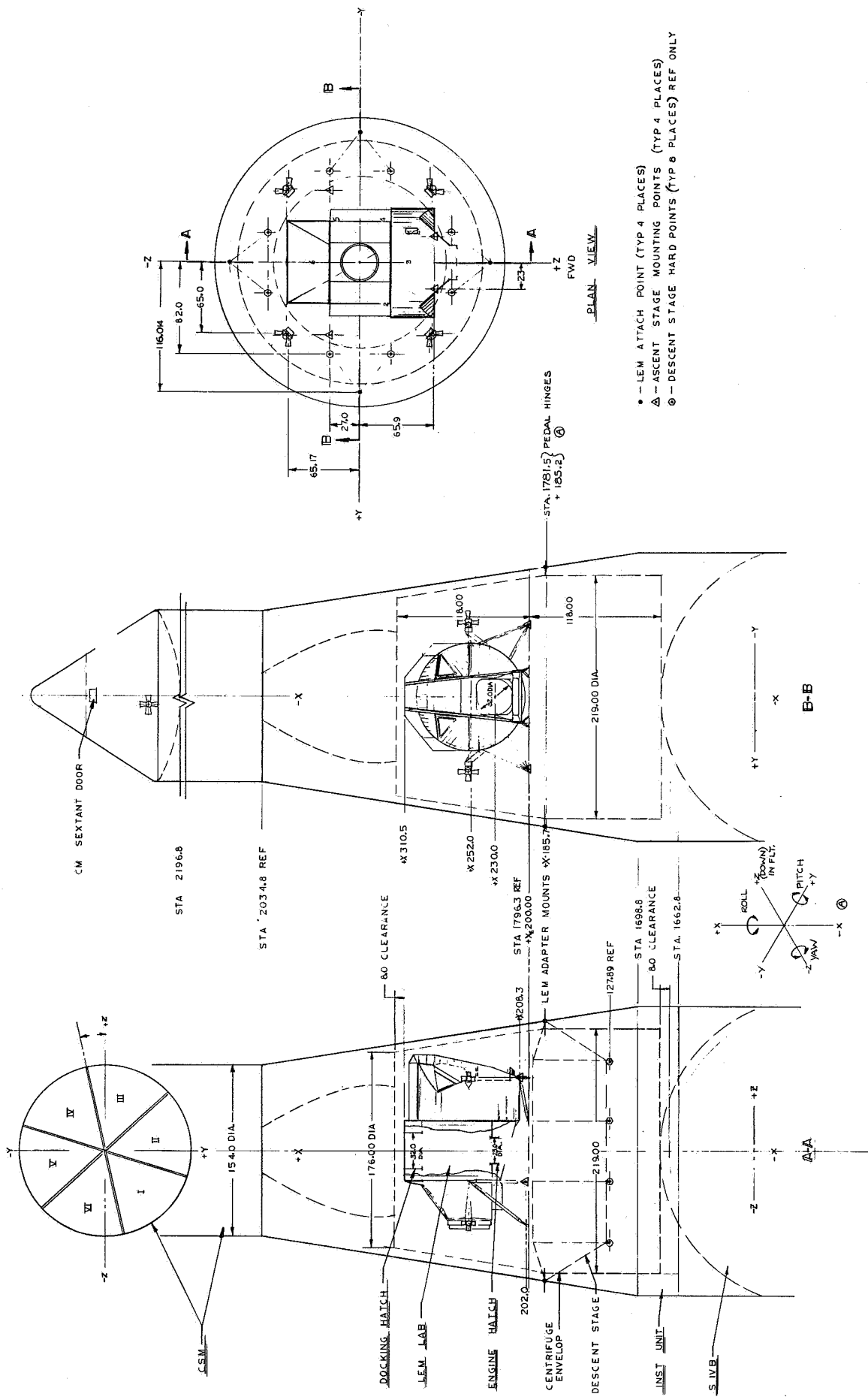
Figure 70. Baseline Envelope-Space Research Centrifuge

Space Capsule Evaluation. - During the initial study phase several orbital configurations were established as tradeoff candidates. It became apparent at this time that the envelope size which will be available during the proposed experiment time period would be restrictive. This is especially true if the experiment mission is confined to a single launch.

Evaluation of the tradeoff configurations established a basic envelope volume which appeared to be compatible with all of the proposed candidates. Figure 70 illustrates the baseline centrifuge envelope established during this phase of the study.

Centrifuge Motions. - Analysis of the baseline experiment requirements, along with the physical constraints imposed by present day boosters, was at this point in the study integrated into an evaluation of the centrifuge motion requirements. Figure 71 presents the initial centrifuge configuration developed during this phase of the study and identifies the baseline motion considerations.



BASIC MOTIONS

A - PRIMARY ROTATION
B - RADIUS ARM TRANSLATION
C - RADIUS ARM PIVOT
D - COUCH TRANSLATION
E - COUCH ROLL
F - LEG POSITIONER
G - HIP ADJUSTMENT
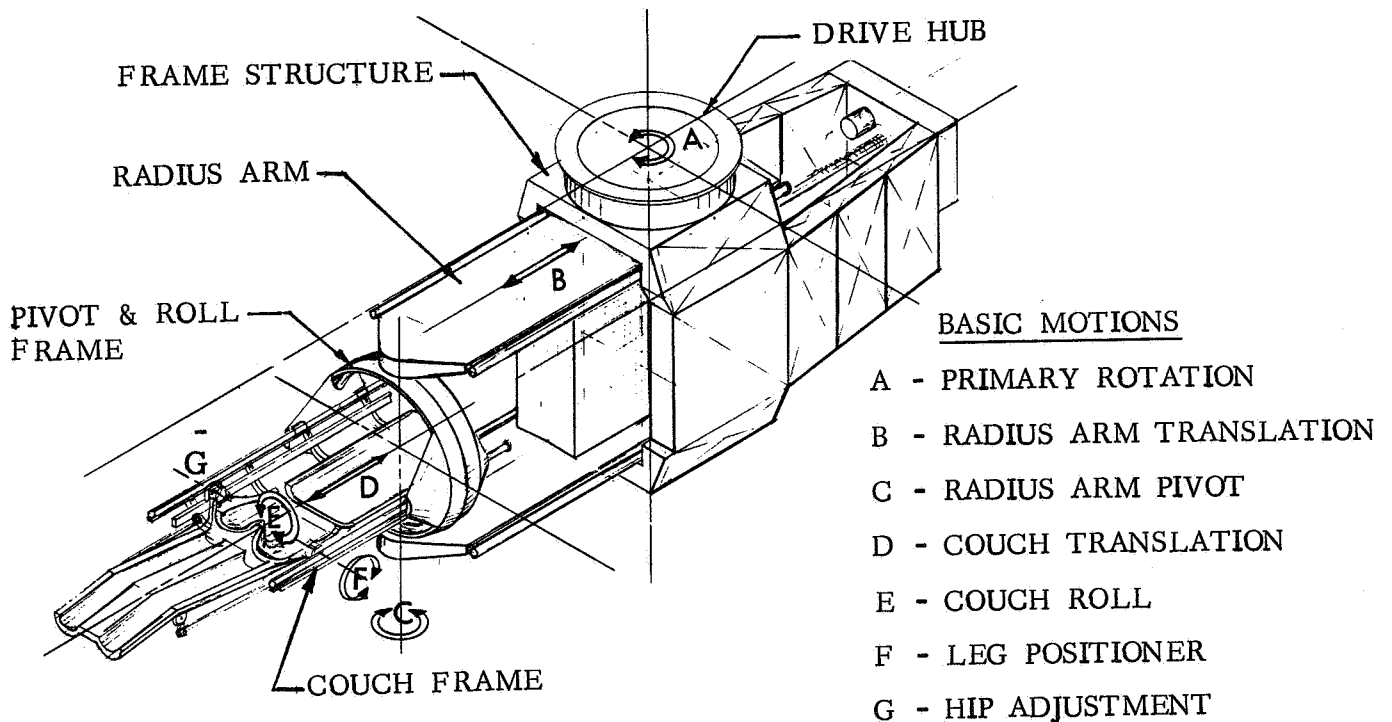
Figure 71.  Initial Centrifuge Concept

Primary rotation: From Figure 70 it can be seen that the diametral constraint within the proposed centrifuge module is approximately 18 feet. Since the spin axis of the centrifuge will necessarily have to fall at the center of this diameter, it was determined that the maximum clearance radius for a rotating body within the space module would be 9 feet. Additionally, it was determined during the initial anthropometric evaluation and preliminary structural analysis that the structure required to support a man load of 9 g would require a minimum spherical envelope about the subject's center of mass of 4 ft. in diameter. From these initial geometrical considerations the maximum baseline centrifuge radius was fixed at 76 inches.

108 in. - 24 in. - 8 in. (safety margin) = 76 inches.

Once the maximum centrifuge radius was established, it was possible to determine the maximum rotational rate required of the centrifuge.

$$rpm = \sqrt{\frac{"g"\ level}{2.84 \times 10^{-5} \times radius}}$$

Max "g" = 9 (from contract work statement)
Radius = 76 inches

$$rpm = \sqrt{\frac{9\ g}{2.84 \times 10^{-5} \times 76}} = 64.3$$

$$\omega = \frac{64.3 \times 6.28}{60} = 6.72\ rad/sec$$

Also defined in the contract work statement was a requirement that the centrifuge be capable of duplicating the Apollo re-entry g environment. By evaluating the re-entry profile, which was graphically presented in the work statement, it was determined that the maximum rate of acceleration required to duplicate the Apollo re-entry g environment would be .171 rad/sec$^2$. With this data, and the preliminary mass properties estimates, it was established that the primary rotational drive would require between 4 and 5 h.p.

From Table 23 it can be seen that the minimum rotational rates, required for experiments in linear acceleration sensitivity, are extremely small. It was therefore established early in Phase I that centrifuge primary drive system should have the following characteristics.

1. 5 h.p. rating

2. Variable speed control range between 0 and 70 rpm.

3. Maximum acceleration capability of .171 rad/sec$^2$.

4. Explosion proof (sealed unit).

5. A braking system capable of decelerating the centrifuge from the maximum speed to a full stop within 30 sec.

Variable radius arm: One of the unique features of the proposed centrifuge is the required capability, per the contract work statement, to place the test subject's ears at a point coincident with the spin axis. This requirement is related to the semicircular canal stimulation experiments which also established the requirement of being able to vary the test subject's radius while the centrifuge is rotating. This, in turn, established the requirement for a powered, remotely-controlled translation drive system.

Analysis of the geometry required to provide this degree of adjustment, coupled with the physical volume occupied by a suitable structure, dictated that the variable radius feature would have to be accomplished in two stages. It was further determined that in all of the other experiment configurations it would be possible to preset the radius prior to rotating the centrifuge. Taking this approach would permit the use of manually operated locking devices, for the preset conditions, which could be designed to provide an alternate load path during the high g experiments, and thereby reduce the structural requirements of the drive system.

The centrifuge couch system must be adaptable to varying man sizes and center of gravity locations. It was determined that by creating a secondary reference axis at the couch end of the radius arm, a geometry could be developed which would provide the necessary man/c.g. adjustment and also accommodate the requirement of being able to place the subject's head on the centrifuge primary spin axis.
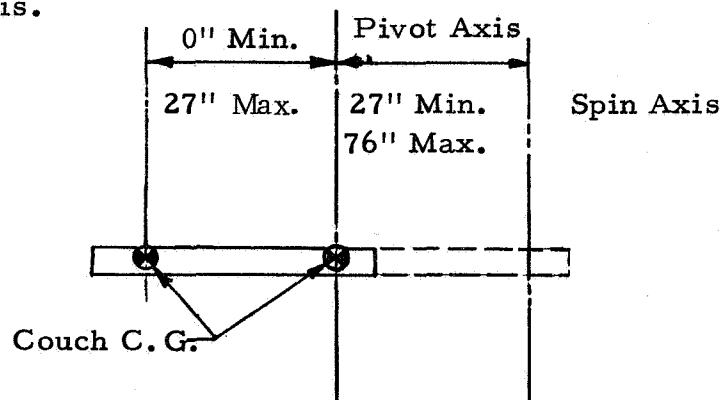


Figure 72. Variable Radius Arm and Couch Translations

With the geometry shown in Figure 72, a cursory structural analysis was made to establish the feasibility of this approach. At the conclusion of this portion of the study effort the following baseline parameters were established with respect to the variable radius capability of the centrifuge.

1.  Using the pivot axis as a reference the radius arm stroke could be variable between 27 inches and 76 inches.

2.  The radius arm should be restrained by a manual locking device during all experiments where a single radius can be maintained during the experiment. This is particularly significant during the high-g level of experimentation.

3.  The couch system should provide the adjustment capability to enable placement of either the test subject's head, or his body c.g. coincident with the pivot axis. This will also allow placement of the subject's head on the primary spin axis.

4.  The radius arm translation drive system should be designed to react only the loads, plus a suitable safety factor, which are imposed during experiments involving arm translation concurrent with centrifuge rotation.

Couch pivot:   The contract-defined experiments establish a broad range of test subject body orientations with respect to centrifuge axes in addition to the variable radius capability. Figure 73 provides a graphic illustration of the pitch and roll motions required to meet the experiment objectives.

Since the pivotal motion capability is required concurrently with centrifuge rotation, it becomes necessary to provide a remotely operable system. Also during the initial study phase it became evident that the physical space around the test subject's head would be at a premium. The experiment instrumentation which would have to be attached in this area, and the installation of a drive unit in close proximity to these measuring devices could cause interferences. Also, the need of unimpaired access to the test subject's head area for first aid assistance was of considerable concern.

As in the case of the radius arm, it was found that the concurrent operation (pivot and primary rotation) requirement was only applicable to the experiments involving rotational rates of 1 g or less. It would therefore be possible to provide a suitable system of manual locks to react the greater loads imposed during high g level experimentation. Also, because of the high torque loads which can be generated during an emergency stop, (ref. Structural Analysis Section), it would be desirable to provide symmetrical load paths into the radius arm. This could be accomplished by providing

restraints at both ends of the pivot axis. For the low g experiments, how-
ever, it was concluded that the generated torque loads would have to be
reacted through the drive system components. Also, since the inertial
loads about the pivot axis are small, due to the low accelerations required,
it was determined that the torque loads generated during centrifuge spin-
down and stop probably will be the governing design factor.
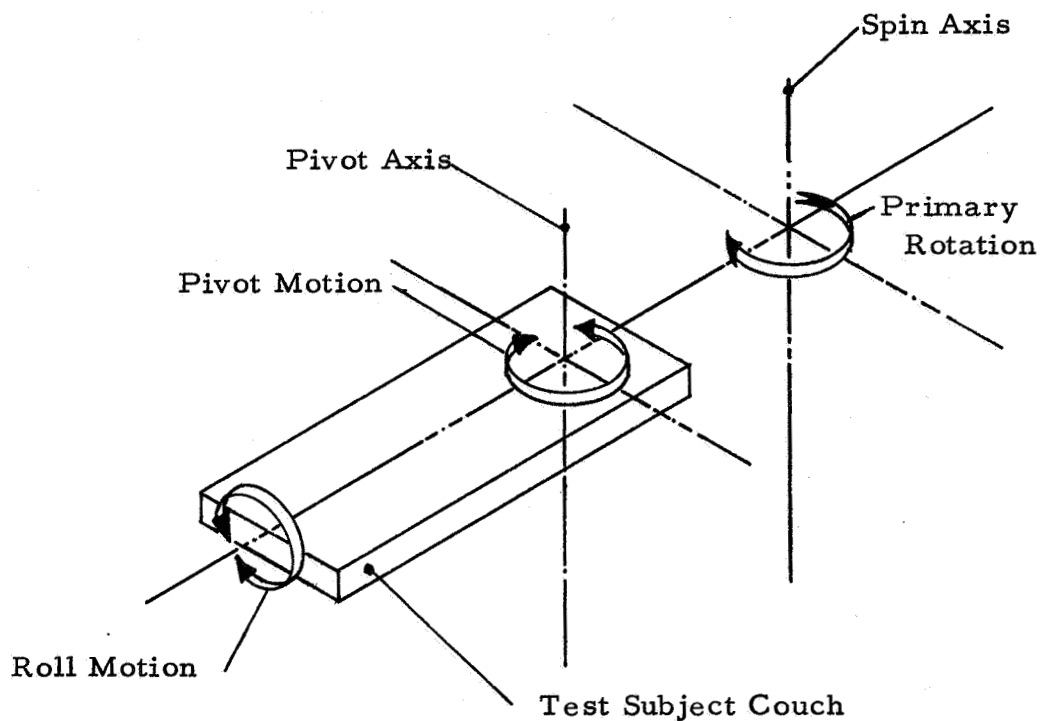


Couch Pitch and Roll Motions

Figure 73

From these considerations the following baseline parameters were assigned to the couch pivot system during the Phase I study period.

1. The pivot system should enable $\pm 100°$ rotation about the pivot axis in the plane of spin.

2. The system should provide a symmetrical load path to the radius arm structure.

3. A system of manual locks should be provided to transmit directly the torque loads during high g tests into the radius arm structure and by-pass the pivot drive system.

4. The pivot drive system should be interlocked with the radius arm translation system to prevent over extension of the test subject's couch.

5. The high speed elements of the pivot drive system should be located as remotely as possible from the test subject's head area.

Couch roll: One of the proposed experiments to be conducted on the space research centrifuge will evaluate man's threshold levels of sensitivity to angular acceleration. This experimentation requires that the test subject be rotated about his long body axis (Z-axis), with precise variations in rpm being controlled through a computer. The roll motion capability is not required during centrifuge rotation. It was therefore reasoned that this degree of freedom could be designed to support only the inertia loads of the man and couch rotating about the Z-axis. During all other modes of operation the roll capability could be mechanically locked to provide a direct load path to primary structure. The locking system would, however, have to provide for pre-set, fixed orientations of $0°$, $45°$ and $90°$.

The roll drive will have to respond to a series of random commands from the computer control to accelerate or decelerate as a function of the test subject's response.

The baseline approach to the roll mechanism was influenced considerably by the couch support structural development tradeoffs. (Ref. Structural Design Analysis) With the toroidal ring, which surrounds the couch assembly, being driven by a drive unit mounted on the pivot segment, the inherent mechanical advantages can readily be seen. Based on these considerations, the Phase I definition of the roll drive system was as follows.

1. The system should provide for continuous rotation of the test subject's couch about its long body, Z-axis at variable speeds from 0 to 20 rpm.

2. The test subject's couch should be provided with a rotational adjustment capability to enable fixed angular orientations about the Z-axis.

3. The roll drive system should be designed to react only the operating loads imposed during Z-axis rotation. A suitable locking system should be provided to rigidly fix the roll frame to the pivot segments and provide a direct load path to the prime structure during the rotational experiments.

Couch mechanisms: In addition to the motion capabilities discussed thus far, there are the position adjustments and body articulation motions which must be considered in the couch design. Evaluation of the defined experimentation establishes two basic types of motions which must be provided in the couch system.

1. Body Adjustments. - The physical body size of potential test subjects can vary widely. It was therefore established during Phase I that, for the purpose of this study, the orbital centrifuge would be able to accommodate a range of test subject between the 25th and 75th percentile. This established a need for 3.2 inches of adjustment in the over-all couch length. Since a majority of the experiment instrumentation is related to the subject's head area, it was concluded that the test subject's head should be fixed with respect to the couch frame. The variations in body sizes could be compensated for by adjusting the lower couch section about the hip hinge point. Installation of the various instrumentation packages could then be standardized to accommodate all test subjects.

Table 2 4

Test Subject Sizes

| Percentile | Weight | Height | Body C.G. |
|---|---|---|---|
| 25% | 148.7 lbs. | 67.5 in. | 37.3 in. |
| 35% | 154.2 lbs. | 68.2 in. | 37.7 in. |
| 45% | 159.4 lbs. | 68.9 in. | 38.1 in. |
| 55% | 164.5 lbs. | 69.4 in. | 38.4 in. |
| 65% | 170.4 lbs. | 70.1 in. | 38.8 in. |
| 75% | 176.6 lbs. | 70.7 in. | 39.1 in. |

Initial experiment evaluation indicated that knee articulation would be required as one of the couch motion capabilities. Further analysis, however, established that by articulating the leg about the hip hinge point all of the experiment objectives could be met.

The test subjects shall have free movement of their hands and arms except that provision should be made to insure hand and arm containment during high g experimentation.

Provision would also have to be made for an adjustment at the foot restraint system. This adjustment shall be in excess of the body size requirement since for some of the experiments it is desirable to take the body loads through the couch saddle rather than the feet.

2. Experiment Motions. - The second type of couch motion can be defined as those motions which are experiment oriented. Head motions must necessarily be integrated with a restraint system which will permit either pitch or yaw movement with respect to the long body axis. The restraint locking system should rigidly hold any pre-set position in either pitch or yaw and still allow free movement in the unlocked plane. With respect to the presently defined experiments, all couch motions can be man powered. It is necessary, however, to provide an accurate means of monitoring and recording the head motions during an experiment.

Numerical Tradeoff Studies. - At the conclusion of the Phase I effort a series of numerical tradeoff analyses was conducted to develop a realistic design approach to the various hardware elements of the space research centrifuge. These tradeoffs were also concerned with identifying potential problem areas with respect to hardware development.

Ground rules: During the initial definition effort the following ground rules were developed to insure continuity during the tradeoff studies. These guidelines were established on the basis of both the contract requirements and the considerations established during the initial study phase.

1. All mechanical systems shall be compatible with a 15 psia pure oxygen atmosphere.

2. All materials which are exposed to the atmosphere within the centrifuge module shall be non-flamable.

3. All elements of the various mechanical systems shall be compatible with an 0-g environment (i.e., no loose pieces, friction devices, etc.).

4.  All mechanical systems shall be capable of operation in a 0-g, 1-psia atmosphere without injecting contamination of any sort into the atmosphere.

5.  All adjustment devices which require manipulation under 0-g conditions shall be designed for one hand operation without the use of tools.

6.  All mechanisms shall be driven by electro-mechanical means to eliminate the possibility of fluid contamination.

7.  All degrees of freedom which are not required during a particular experiment shall be provided with a mechanical lock to prevent inadvertent operation.

8.  All locking devices shall be designed to react the maximum loads which can be transmitted through its elements, and shall provide an alternate load path around the operating mechanisms.

9.  All systems shall be powered by rechargeable 28 VDC batteries. There shall be no slip-rings or other arcing devices used.

10. All mechanical tradeoff evaluations shall be based on the numerical ratings shown in Table 25.

Table 25

Mechanism Trade-off Factors

| Item | Max. Value |
|---|---|
| Safety (SA) | 30 |
| Failsafe | |
| Fire Resistance | |
| Contamination | |
| Accessability | |
| Reliability (RE) | 30 |
| Complexity | |
| Strength | |
| Dynamic Smoothness (DS) | 15 |
| Weight (W) | 10 |
| Maintenance & Checkout (MC) | 10 |
| Availability & Cost (AC) | 5 |
| Max. Total | 100 |

Mechanisms considered: The initial effort during the trade-off evaluation
was to establish a number of mechanical approaches which could feasibly support
the basic motion requirements. Of the mechanisms considered, those illustrated
in Figure 74 seemed to be the best candidates.

Figure 74. Trade-off Summaries
Mechanisms Considered

Support Systems

- Track &
  Rollers

- Ball
  Bushings

- Teflon
  Slides

- Air
  Bearings

Transmission Systems

- Ball
  Screws

- Rack &
  Pinion

- Roller
  Drives

- Harmonic
  Drives
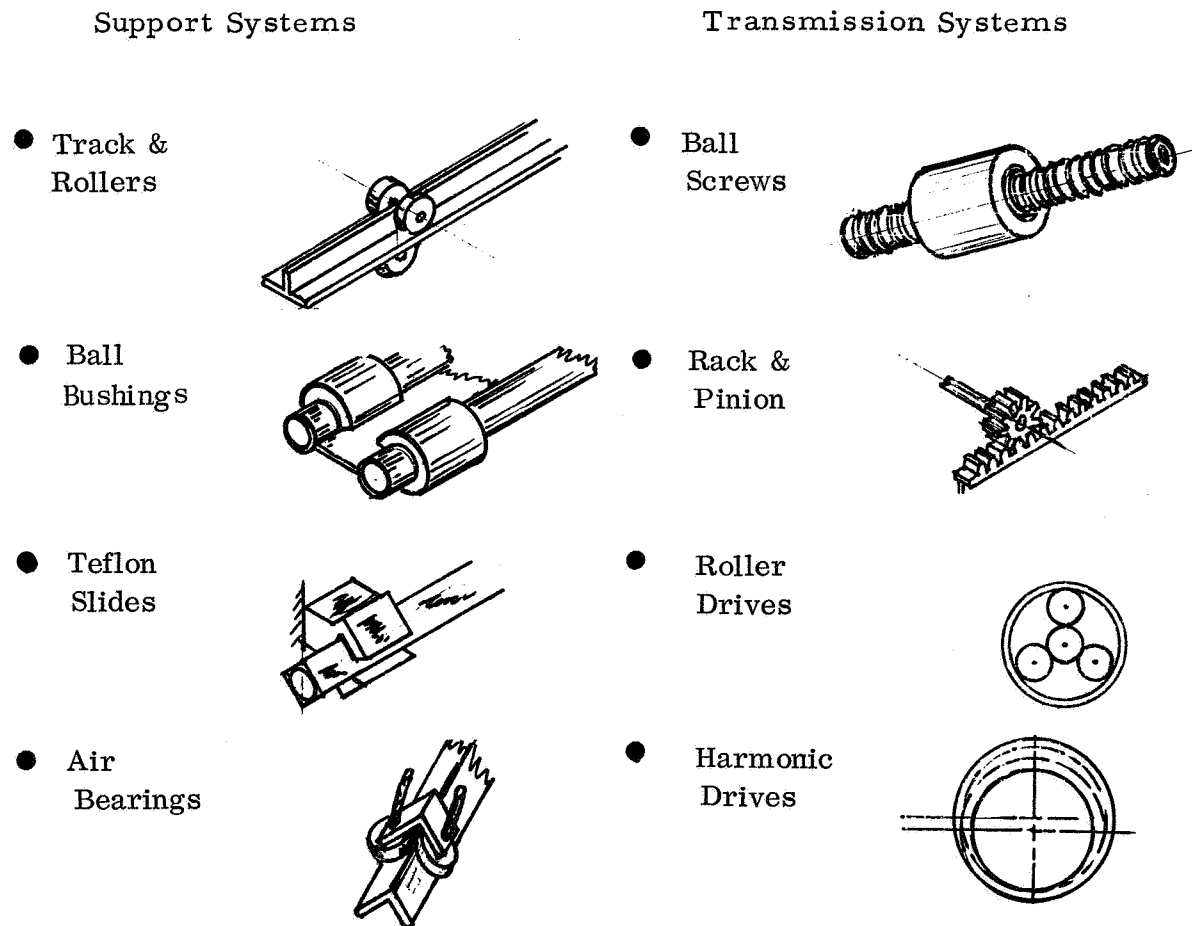
Trade-off summaries: Tables 26 through 29 present the numerical summations for each of the trade-off studies.

## Table 26

### Trade-off Summary Primary Rotational System

| Item | Factors (Ref. Table 25) | | | | | | | Remarks |
|---|---|---|---|---|---|---|---|---|
| | SA | RE | DS | W | M/C | A/C | Total | |
| 1. Support Systems | | | | | | | | |
| A. Radial Track & Roller Syst. | 27 | 20 | 15 | 8 | 6 | 5 | 81 | 1. Too Many Parts<br>2. Poor Reliability |
| B. Slewing Ring- Single Large Dim. Bearing | 27 | 25 | 15 | 6 | 10 | 2 | 85 | 1. Special Development<br>2. Heavy |
| C. Axial-2 Bearing System* | 28 | 27 | 13 | 10 | 10 | 3 | <u>91</u> | 1. Dry Running<br>2. Lightest Weight<br>3. Special Development |
| 2. Transmission Systems | | | | | | | | |
| A. Gear Driven | 25 | 28 | 11 | 7 | 8 | 5 | 84 | 1. Precision (No Backlash) |
| B. Harmonic Drive* | 25 | 28 | 12 | 9 | 8 | 3 | <u>85</u> | 1. Compact-Light Weight |
| C. Roller & Traction Drives | 20 | 28 | 15 | 8 | 10 | 3 | 84 | 1. Questionable for Main Drive Torques. |
| 3. Motors | | | | | | | | |
| A. Brushless D.C. | 25 | 25 | 15 | 9 | 10 | 2 | 86 | 1. Not Developed for 5 H.P. |
| B. Frequency Control A.C. Motors* | 25 | 28 | 15 | 7 | 8 | 5 | <u>88</u> | 2. Hardware Exists – Needs Wt. Optimizing. |

*Approaches Selected for Baseline Configuration.

Table 27

Trade-off Summary Translation Systems

| | Factors (Ref. Table 25) | | | | | | | Remarks |
|---|---|---|---|---|---|---|---|---|
| | SA | RE | DS | W | M/C | A/C | Total | |
| 1. Radius Arm & Counter-Weight Support Systems | | | | | | | | |
| A. Track & Rollers | 25 | 20 | 14 | 7 | 7 | 5 | 78 | 1. Tolerance & Adjustment Problems. |
| B. Ball Bushings* | 28 | 28 | 15 | 8 | 10 | 5 | 94 | 1. Wt. Penalty-Load in Both Directions |
| C. Air Bearings | 20 | 25 | 14 | 6 | 5 | 3 | 73 | 1. Contamination |
| D. Teflon Slides | 29 | 27 | 14 | 10 | 10 | 4 | 94 | 1. Adjustment & Tolerances could be Prob. |
| 2. Transmission Systems. (Radius Arm & C/W) | | | | | | | | |
| A. Ball Screws* | 22 | 28 | 14 | 10 | 8 | 5 | 87 | 1. Precision Quality |
| B. Rack & Pinion | 22 | 28 | 13 | 7 | 8 | 4 | 82 | 1. Noise & Backlash would be Problem. |
| C. Rohlix Smooth Shaft Actuators | 15 | 15 | 14 | 6 | 9 | 3 | 72 | 1. Friction System Undesirable. |
| 3. Couch Support | | | | | | | | |
| A. Ball Bushings | 28 | 26 | 14 | 9 | 8 | 5 | 90 | 1. Wt. Penalty-Direction of Loads. |
| B. Roller Systems | 27 | 24 | 11 | 7 | 7 | 5 | 81 | 1. Difficult Adjustment. |
| C. Teflon Slides* | 29 | 29 | 15 | 10 | 10 | 4 | 97 | 1. For Manual Operation-simplest. |

*Approaches Selected for Baseline Configuration.

Table 28

Trade-off Summary Couch Pivot

| | Factors (Ref. Table 25) | | | | | | | Remarks |
|---|---|---|---|---|---|---|---|---|
| | SA | RE | DS | W | M/C | A/C | Total | |
| 1. Pivot Support | | | | | | | | |
|   A. Teflon Bushings* | 28 | 30 | 15 | 10 | 10 | 5 | 98 | 1. Slow Speeds Make Teflon Attractive. |
|   B. Ball Bearings | 27 | 27 | 11 | 8 | 8 | 4 | 85 | 2. Weight & Noise could be Problems. |
|   C. Rollers Bearings | 28 | 27 | 11 | 6 | 8 | 4 | 84 | 3. Same as above. |
| 2. Pivot Drive | | | | | | | | |
|   A. Miter Gearing & Torque Shafting to Drive in Radius Arm.* | 28 | 28 | 13 | 9 | 8 | 5 | 91 | 1. Positive Acting - must be Free of any Backlash. |
|   B. Ball Screw Actuators & Linkage. | 26 | 27 | 10 | | 9 | 5 | 86 | 1. Tolerances would be Difficult - Could be Lighter. |

*Approaches Selected for Baseline Configuration

Table 29

Trade-off Summary Couch Roll

| | Factors (Ref. Table 25) | | | | | | | Remarks |
|---|---|---|---|---|---|---|---|---|
| | SA | RE | DS | W | M/C | A/C | Total | |
| 1. Couch Roll Support. | | | | | | | | |
|   A. Radial Track & Rollers* | 28 | 26 | 10 | 7 | 7 | 5 | 83 | 1. Noise could be Prob. - Weight |
|   B. Teflon Segmented Slides | 26 | 26 | 12 | 10 | 9 | 3 | 86 | 2. Development & Adjustment Difficult |
| 2. Roll Drive | | | | | | | | |
|   A. Ring Gear & Pinion* | 28 | 26 | 11 | 9 | 8 | 5 | 87 | 1. Noise could be a Problem. |
|   B. Roller (Friction Drive) | 28 | 26 | 15 | 8 | 10 | 2 | 87 | 2. Special Development |

*Approaches Selected for Baseline Configuration.

Phase II Analysis

Objectives - The Phase II study effort was directed toward establishing a
realistic orbital centrifuge configuration based on the trade-off evaluations con-
ducted during Phase I. Of primary concern was the integration of the motion
mechanisms with a structural system which would meet the couch clearance re-
quirements and still provide the required structural stiffness. An effort was made
to re-evaluate the initial weight and mass distribution estimates. With this data,
plus a more detailed experiment definition, Ref.-Volume IV of this report, it was
possible to develope the various mechanism detail requirements. Fig. 75 illus-
trates the baseline configuration developed during this period.
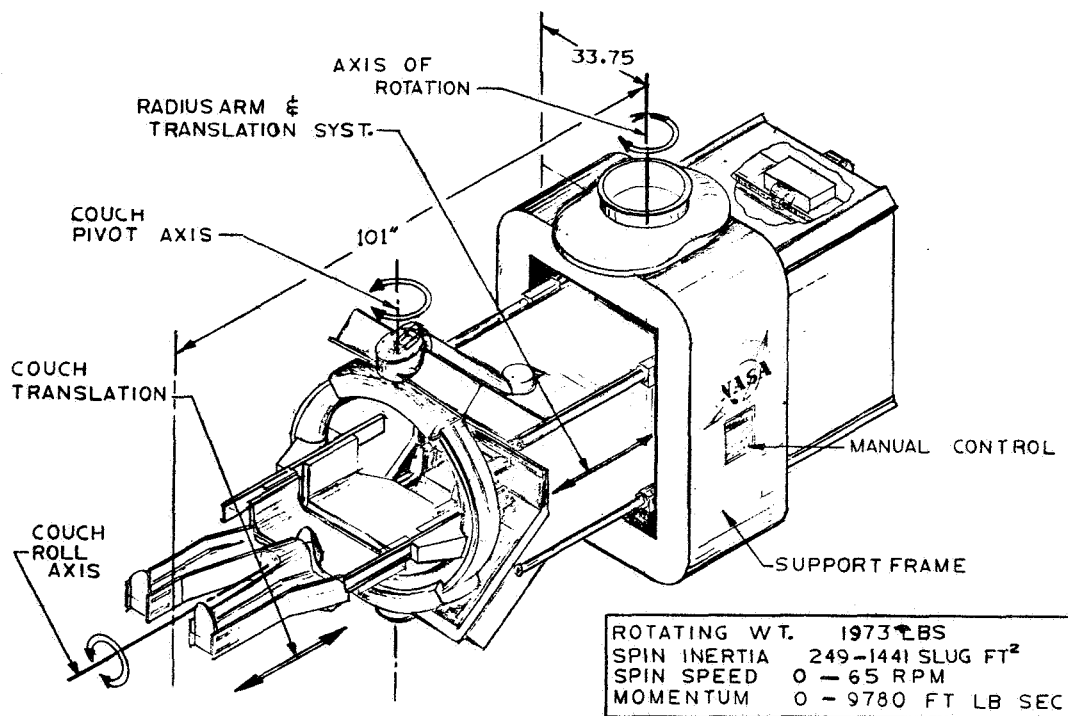


Figure 75. Space Research Centrifuge Baseline Configuration

Centrifuge parameters by experiment – Initially, during the Phase II study, a detailed evaluation was made of the individual experiments to determine the operating parameters of the centrifuge. Figures 76 through 84 summarize these parameters.
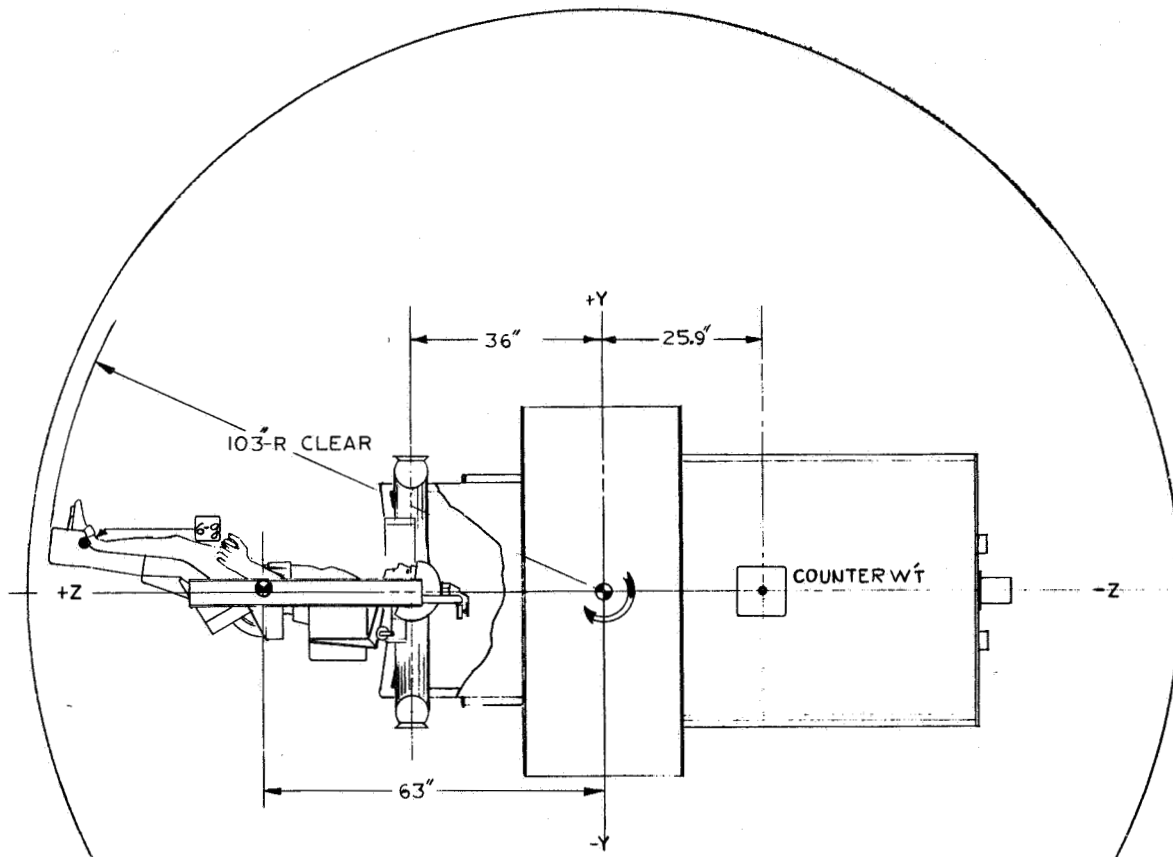


Figure 76. T-010A, Grayout Sensitivity Thresholds.

T-010A experiment parameters – (balanced system):

Primary rotation

$$\text{rpm}_{(max)} \quad \sqrt{\frac{6g}{2.84 \times 10^{-5} \times 96 \text{ inches}}} = 46.8 \text{ rpm} = 4.9 \text{ rad/sec} = \omega$$

$$\text{Acceleration } (\alpha) = \frac{\omega}{t} \quad \frac{4.9}{60 \text{ sec}} = .08 \text{ rad/sec}^2$$

Centrifugal force acting or radius arm

(Man & couch weight = 367 lbs.)

$$F_{MC} = 2.84 \times 10^{-5} \times W \times R \times \omega^2$$

$$= 2.84 \times 10^{-5} \times 367 \text{ lbs.} \times 63 \text{ in.} \times 46.8^2$$

$$= 1442 \text{ lbs.}$$

Moment of Inertia (I) = 594 slug ft$^2$

Momentum (M$_c$) I$\omega$ = 2915 ft.- lb.- sec.

Torque (T) = I$\alpha$ = 47.5 ft.-lbs.

Centrifugal force acting on count erweight ball screw.  (Each counterweight = 330 lbs. - 2 req.)

$$F_{cw} = 2.84 \times 10^{-5} \times 330 \times 25.9 \times 46.8^2$$

$$F_{cw} = 532 \text{ lbs.}$$
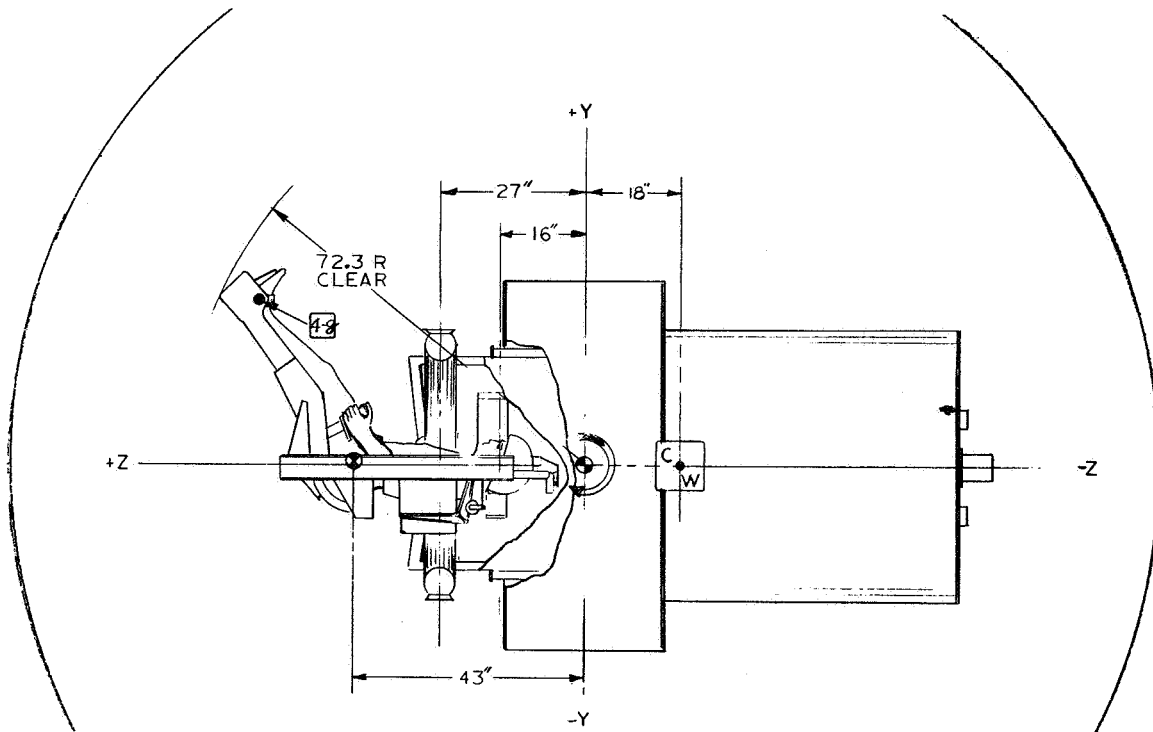


Figure 77.  T-010B Therapeutic.

T-010B - Experiment parameters:

Primary Rotation

$$\text{rpm}_{(max)} = 53 \text{ rpm} = 5.5 \text{ rad/sec}$$

$$\text{Acceleration} = \frac{5.5}{40 \text{ sec}} = .139 \text{ rad/sec}^2$$

Centrifugal Force $(F_{Mc}) = 1260$ lbs.

Centrifugal Force $(F_{cw}) = 474$ lbs.

Moment of Inertia $(I) = 594$ slug ft.$^2$

Momentum $(M_c) = 3270$ ft.-lb.-sec.

Torque $(T) = 82.8$ ft.-lbs.
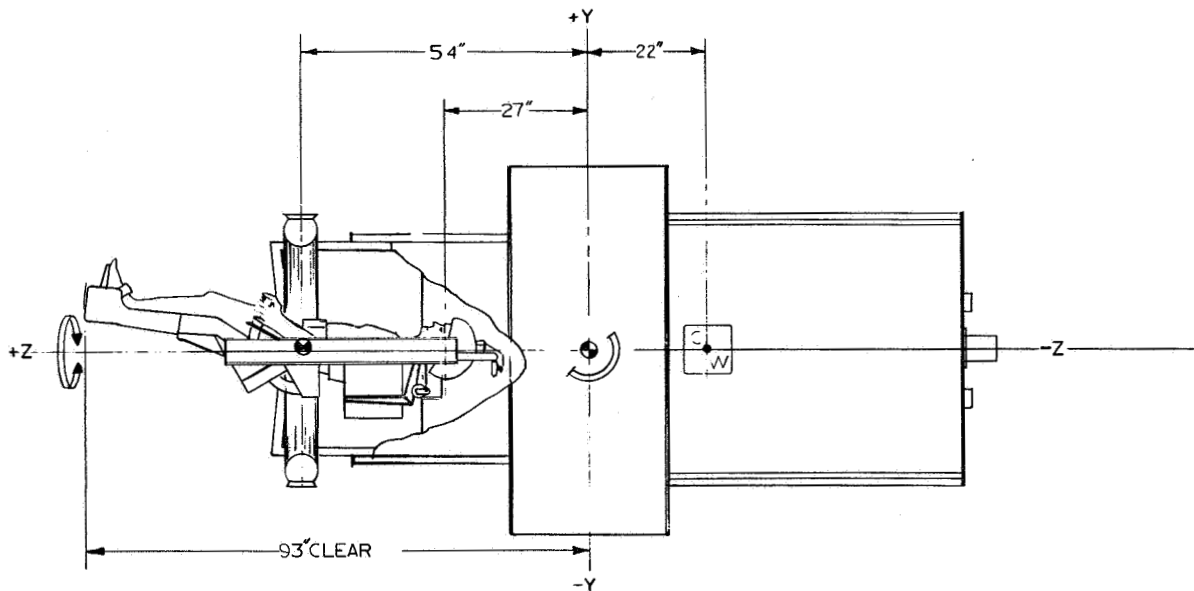


Figure 78.  T-010C, Angular Acceleration Threshold

T-010C - Experiment parameters:

rpm = 0 - (Primary rotation locked)

Note: Since the only motion during this experiment is about the couch "Z" axis all of the primary rotating parameters will be "0". The Z axis - roll parameters, assuming a 6 inch max. C.G. eccentricity, will be.

rpm(roll) = 0 to 6 rpm

Accelerations = .1° to 1.0°/sec$^2$ in 10 sec bursts.

$$I_{(Z-axis)} = 2.85 \text{ slug ft}^2$$

$$T_{(Z-axis)_{(max.)}} = .05 \text{ ft.-lbs.}$$
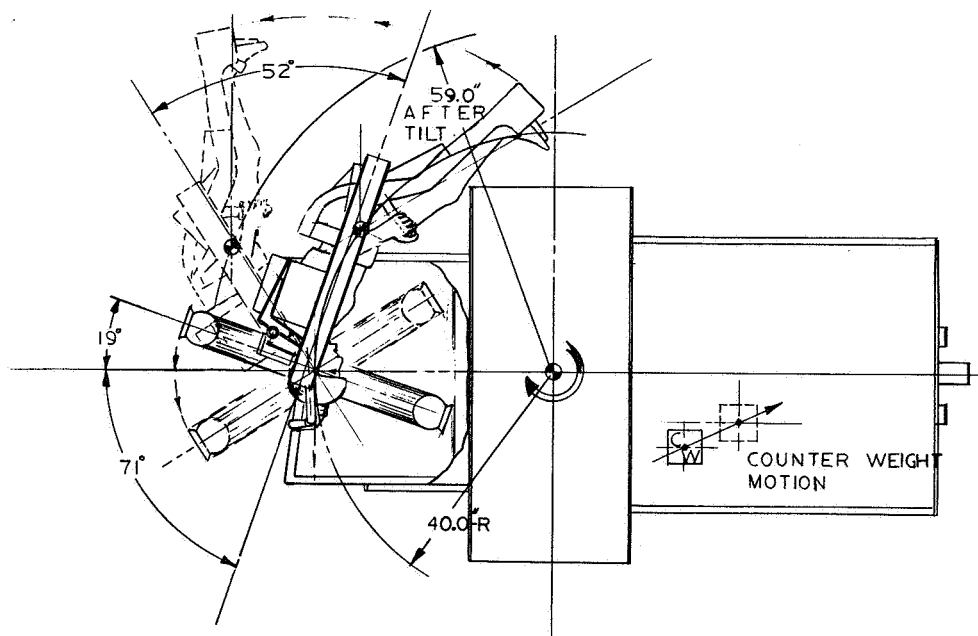


Figure 79. T-010D, Tolerance to Tilt Simulation

T-010D Experiment parameters:

Primary rotation = 29.6 rpm = 3.1 rad/sec = $\omega$

Acceleration ($\alpha$) = .171 rad/sec$^2$

Centrifugal Force ($F_{Mc}$) = 538 lbs.
Max after tilt

Moment of Inertia (I) = 585 slug ft$^2$
(after tilt)

Momentum (Mc) = 1758 ft.-lb.-sec.

Torque (T) = 100 ft.-lbs.

Pivot Drive

Torques about pivot axis

Before tilt = 9,900 in-lbs.

After tilt = 8,795 in-lbs.

Rotational speed = 1.5°/sec = .026 rad/sec = $\omega$

Acceleration = .0174 rad/sec$^2$

Moment of inertia = 57.8 slug-ft$^2$
(about pivot axis)
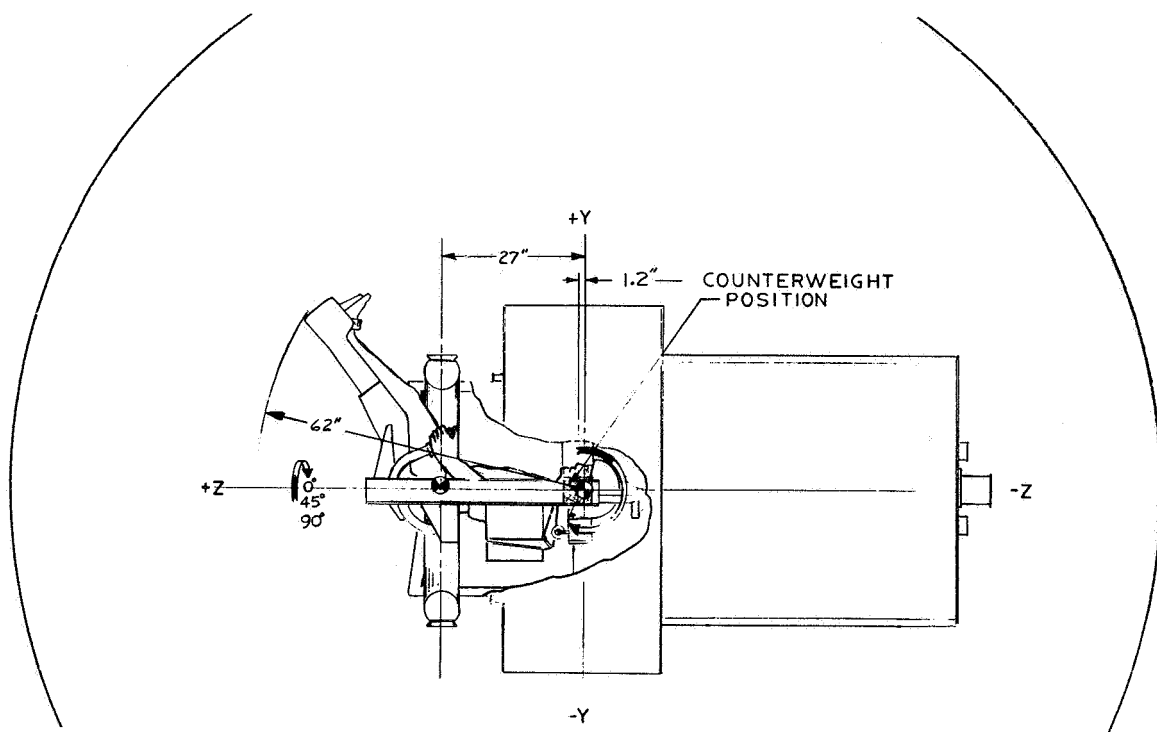
Figure 80. T-010E, Coupled Angular Velocities (Part I)
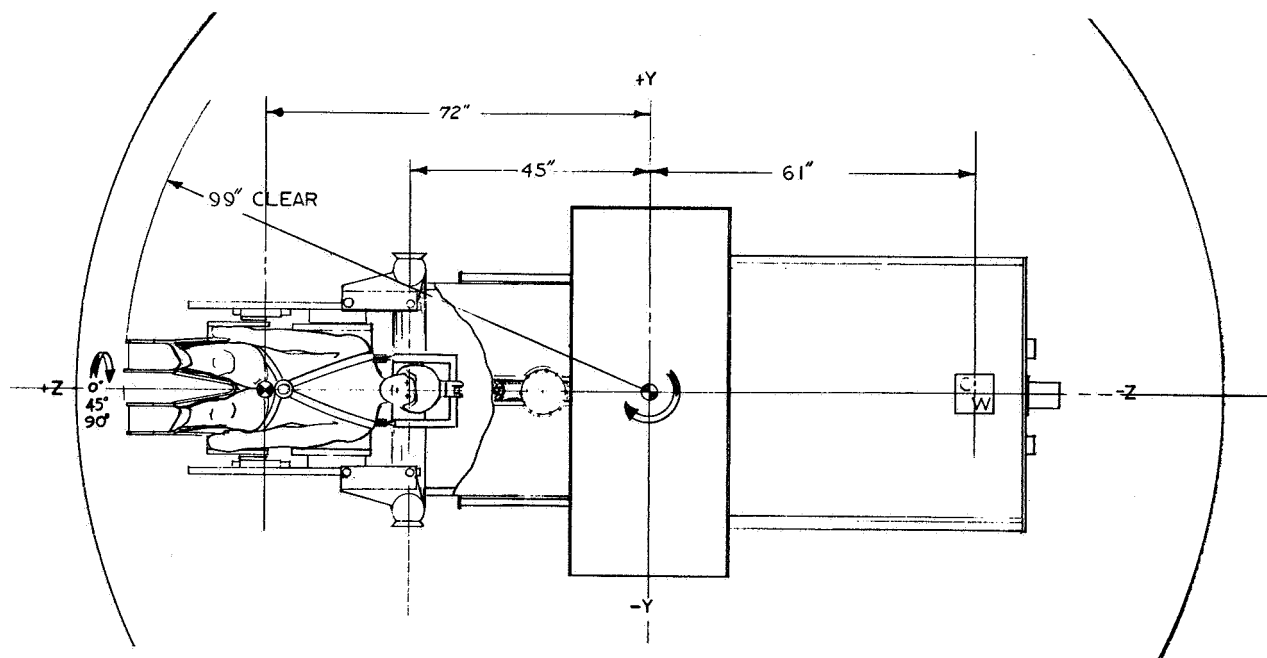


Figure 81. T-010E, Coupled Angular Velocities (Part II)

T-010E (Part 1) experiment parameters: (Test subject's head is on spin axis.)

Primary rotation –

4 rpm = .4185 rad/sec

10 rpm = 1.05 rad/sec,

Accelerations = .035 rad/sec$^2$ (max)

Centrifugal forces on radius arm

@ 4 rpm - $F_{Mc}$ = 4.5 lbs.

@ 10 rpm - $F_{Mc}$ = 27 lbs.

Moment of Inertia (I) = 249 slug ft$^2$

Momentum @ 4 rpm - $M_c$ = 104 ft.-lb.-sec.

@ 10 rpm - $M_c$ = 262 ft.-lb.-sec.

Torque (T) = 8.72 ft.-lbs.

T-010E (Part 2) experiment parameters primary rotation – Same as Part 1

Primary rotation – same as Part 1

Accelerations – same

Centrifugal forces on radius arm

@ 4 rpm - $F_{Mc}$ = 7.5 lbs.

@ 10 rpm - $F_{Mc}$ = 47 lbs.

Moment of Inertia (I) = 1351

Momentum @ 4 rpm $M_c$ = 323 ft.-lb.-sec.

@ 10 rpm $M_c$ = 1420 ft.-lb.-sec.

Torque (T) = 47.3 ft. lbs.
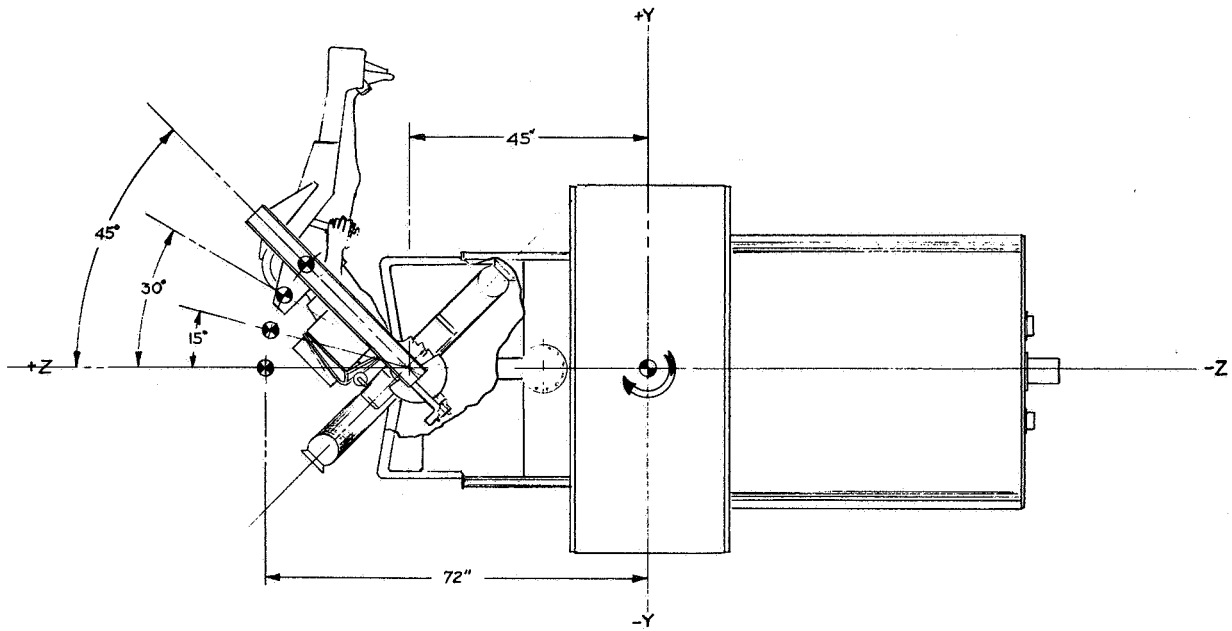
Figure 82. T-010F, Otolith "g" Sensitivity (Part I)
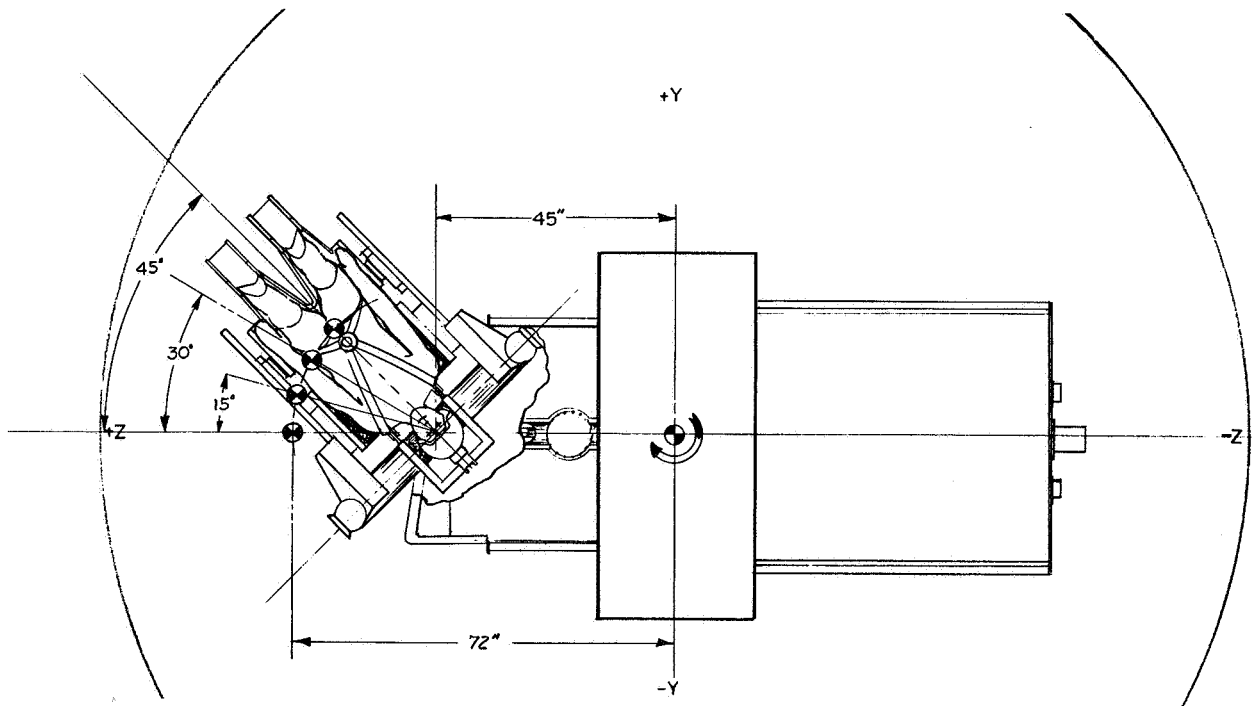


Figure 83. T-010F, Otolith "g" Sensitivity (Part II)

T-010F (Part 1) experiment parameters: each position requires that three g levels be simulated, 0.25g, 0.5g, and 1.0g.

Primary rotations

$0.25g = 14.0 \text{ rpm} = 1.46 \text{ rad/sec} = \omega_1$

$0.5g = 19.8 \text{ rpm} = 2.08 \text{ rad/sec} = \omega_2$

$1.0g = 28.0 \text{ rpm} = 2.93 \text{ rad/sec} = \omega_3$

Acceleration $= .171 \text{ rad/sec}^2$ max.

Centrifugal force (max) $F_{Mc} = 588 \text{ lbs.}$

Moment of Inertia (I) $= 1351$

Momentum (max) $M_c = 396 \text{ ft. lb. sec.}$

Torque (max) (T) $= 231 \text{ ft. lbs.}$
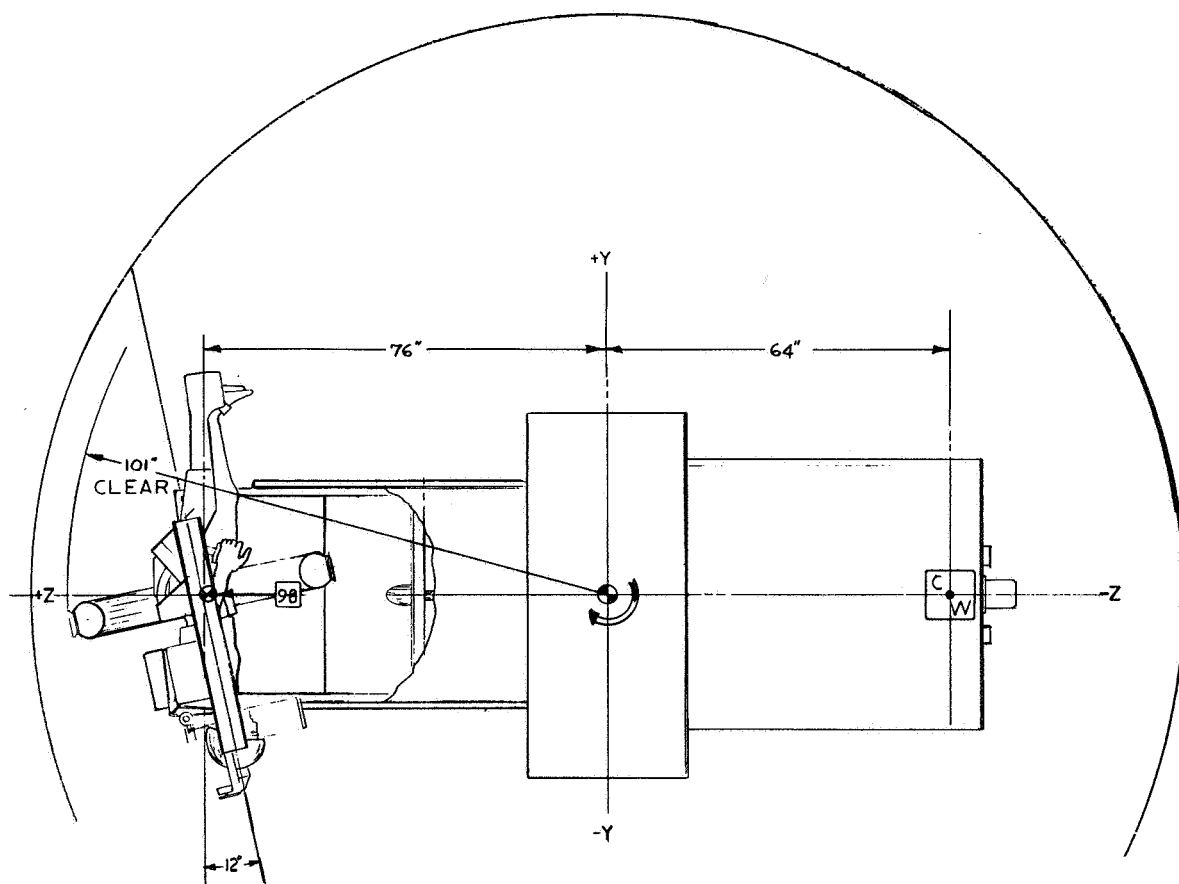


Figure 84. T-010G, Re-entry Simulation

T-010G - Experiment parameters: the presently defined re-entry experiment requires that only a 4.4g environment be simulated. Commensurate with the contract requirements, however, the centrifuge should be able to develope a 9g force field. Both sets of parameters were therefore considered.

Primary rotations

$$4.4g = 45 \text{ rpm} = 4.7 \text{ rad/sec} = \omega_1$$

$$9.0g = 64.5 \text{ rpm} = 6.75 \text{ rad/sec} = \omega_2$$

Accelerations

Defined experiment

.1-g/sec onset, $\alpha_1 = .108 \text{ rad/sec}^2$

9g - Apollo re-entry, $\alpha_2 = .171 \text{ rad/sec}^2$

Centrifugal forces $F_{M_{c_1}} = 1425 \text{ lbs.}$

$$F_{M_{c_2}} = 3295 \text{ lbs.}$$

Moment of Inertia $(I) = 1440 \text{ slug ft}^2$

Torques $T_1 = 155 \text{ ft. lbs.}$

$$T_2 = 246 \text{ ft. lbs.}$$

Momentums. $M_{c_1} = 6760 \text{ ft. lb. sec.}$

$$M_{c_2} = 9715 \text{ ft. lb. sec.}$$

Sub-system analysis. Having established a baseline of experiment parameters, the next step, in the study effort, was to define the sub-system requirements. Special effort was made during this definition phase to maintain the maximum degree of flexibility possible. This was done to insure support of the still developing experiment definition and analysis effort. It should be noted that once the final experimental program has been established, the centrifuge systems should be re-evaluated to develope the maximum degree of weight optimization commensurate with the final experiment requirements

Primary drive sub-system: from the experiment parameters and the Phase I trade-off study the following parameters were developed.

1. Horse Power:

$I$ = 1440 slug ft$^2$

$\alpha$ = .171 rad/sec$^2$

$T_{(max)}$ = 246 ft. lbs.

$\omega$ = 6.75 rad/sec

$HP = \dfrac{T \times rpm}{5250}$ (100% EFF.)

$HP = \underline{3.02}$

2.  Speed Reductions. - The operating range of the centrifuge = 4 - 64.5 rpm. Using the variable frequency motor control system, with a 3-Phase AC motor (Hoover Electric Co. - deep submersible motor development) a variable speed range from 35 to 3500 RPM can be obtained. Using this as a design point, it was determined that the overall input/output ratio of the system would be:

Ratio = 3380:65 = 52:1

3.  Drive Transmission. - The geometric development of the drive hub assembly provided a natural interface between the drive motor and the centrifuge main rotational frame. The cylindrical hub design enables the integration of an internal ring gear as part of the rotating structure and will permit the drive motor and transmission assembly to be mounted on the non-rotating structure and thereby simplify the electrical interface. Also, it was found that the physical dimensions of the drive hub sould allow a 4:1 reduction between the driven ring gear and the driving pinion. The main drive transmission could then be simplified since it need only provide a 13:1 speed reduction. This approach also simplified the data transmission link by permitting the rotary capacitor to be mounted on the centrifuge spin axis.

The motor and transmission assembly should be integrated into a single package with an integral mechanical holding brake which is applied as a function of electrical power loss. The brake should also have an override circuit which would enable brake release direct from the 28V - battery source.

Normal acceleration and deceleration of the centrifuge will be controlled through a ramp generator which provides a varying signal which is compared with a tachometer output; to produce the resultant drive commands.

4.  GearingLubrication. - An operating environment at between 5 and 15 P.S.I.A. atmospheric pressure is anticipated for the centrifuge. Out-gassing of lubricants which are contained in sealed units is, therefore, not considered to be a problem. Sealed units will however, have to be pressure compensated to prevent potential external leakage should the capsule pressure be lost.

Exposed Gearing, i.e. - Primary drive gear and pinion, should be designed using materials which will be self lubricating. It was felt that dry operation of these slower speed elements of the drive, could be tolerated by using hard anodized aluminum for the driven ring gear and a laminated teflon & fiberglass pinion. Final material selection would of course have to be verified by test.

5.  Efficiencies. - Based on the vender data available, the following efficiencies could be expected.

| | |
|---|---|
| Drive motor and transmission | 80% |
| Gear system | 95% |

$$\text{Eff. factor} = \frac{1}{.8 \text{ x } .95} = 1.33$$

Therefore:

Actual hp for the primary drive = 1.33 x 3 = 4 hp.

Translation Drive Sub-System. - The variable radius arm was originally invisioned to have two modes of operation.

1.  Manual Positioning. - Wherein a predetermined setting would be made and a system of manual locks could be engaged such that the drive components could be unloaded during the high "g" experiments.

2.  The Automatic Mode. - Which would enable variations in the test subjects radius while the centrifuge was rotating. This capability was to be limited to the low "g" level experiments, i.e. The T-010E experiments, involving rotational speeds of 10 rpm.

It was determined that the translation drive should be sized to react only the loads, imposed by the automatic mode of operation, and the radius arm structure plus the support system and the manual locking system would react the high "g" loads. On the basis of this rationale, the following design parameters were developed.

1.  Sub-System Approach. - During the trade-off evaluations it was determined that the translation motion could best be provided by a ball screw actuator driven by a fractional HP electric motor. The support system would be designed to react all transverse loads and the actuation system would react only the radial loads.

2.  Operational Requirements. - The maximum radial load on the drive system is imposed during 10 rpm rotations with the test subject and couch C.G. located at 72 inches from the axis of rotation. Two load conditions will exist.

A. Centrifugal Load

Couch/man/radius arm combined wt. = 689 lbs. Effective displacement of load C.G. from spin axis = 62.6 in.

Radial Load = $2.84 \times 10^{-5} \times 689 \times 62.6 \times 10^{2}$

$$L_1 = 122 \text{ lbs.}$$

B. Inertial load as a result of translation during rotation

$$L_2 = \frac{Wa}{g} \quad \begin{array}{l} W = \text{weight} \\ a = 5 \text{ in/sec}^2 \end{array}$$

$$L_2 = \frac{689 \times 5}{32.16} = 107 \text{lbs.}$$

C. The combined load – which must be reacted by a single ball screw actuator is therefore

$$122 + 107 = 229 \text{ lbs.}$$

D. Assuming a lead of .25 in. the ball screw torque would be:

$$T = \frac{\text{Lead} \times \text{Load}}{2\pi}$$

$$T = \frac{.25 \times 229}{6.28} = 11.6 \text{ in. lbs.}$$

E. Ball screw speed: nominal speed for an average radius arm velocity of 1 in./sec. would be:

$$V = 4 \times 1 \times 60 = 240 \text{ rpm}$$

F. Horse Power – @ 100% efficiency.

$$HP = \frac{T \times \text{rpm}}{63025}$$

$$HP = \frac{11.6 \times 240}{63025} = .024 \text{ hp}$$

3.  Runaway system:  . Since the nominal operating requirements were so small, a more severe operational condition was considered wherein the system was allowed to rotate at the maximum design speed of 65 rpm.

    A.  Radial Load  $L = 2.84 \times 10^{-5} \times 689 \times 62.6 \times 65^2$

          $L = 5165$ lbs.

    B.  Combined load on single ball screw

       $5165 + 107 = 5272$ lbs.

    C.  Torque on ball screw

$$T = \frac{.25 \times 5272}{6.28} = 210 \text{ in. lbs.}$$

    D.  $HP = \dfrac{210 \times 240}{63025} = .913$

4.  This approach was felt to be excessively conservative in light of the defined experiment parameters.  It was therefore decided to size the translation drive on a basis of providing an operational capability factor of three times the then defined experiment requirement.  This would provide a reasonable flexibility without excessive penalty.

    A.  Radial load 30 rpm  = 1102 lbs.

    B.  Combined load  = 1102 + 107 = 1209 lbs.

    C.  Torque  = 48 in. lbs.

    D.  HP = .183

5.  Efficiency factor

| | |
|---|---|
| Motor       – 80% | |
| Transmission   – 90% | $\dfrac{1}{.8 \times .9 \times .95 \times .95} = 1.54$ |
| Gear box      – 95% | |
| Ball screw & nut – 95% | |

6.  Hp for drive  = .183 x 1.54  = .282
    (.25 would be adequate for intermediate duty)

7. Gear reduction required - (assuming the use of presently developed hardware)

$$\frac{11,040 \text{ rpm motor speed}}{240 \text{ rpm ball screw}} = 46:1$$

Pivot Drive Subsystem. — Three of the baseline experiments require that the centrifuge couch be rotated about the pivot axis while the centrifute is rotating. During these experiments, (ref - T-010D, T-010E and T-010F) the test subject's head is located on the pivot axis and his body is rotated about it. This configuration creates torsional moments about the pivot axis during centrifuge rotation. In addition to the steady state, torsional loads the pivot drive must also be capable of accelerating, or decelerating the test subject about the pivot axis while the centrifuge is rotating.

The pivot system must also provide the capability of positioning a test subject such that his long body "Z" axis is perpendicular to the radius arm and his c.g. is coincident with the pivot axis. In this configuration, (ref. T-010G experiment) the pivot system would not be heavily loaded since the test subject's mass would be closely aligned with the radius arm center line. Also the pivot system manual lock could be engaged and would react any eccentric loads directly into the radius arm.

The most severe operating condition, to which the pivot system must respond, would be during the T-010F series of experiments.

1. Experiment Requirement. — 10°/sec pivot, in the direction of rotation, with the centrifuge rotating at 28 rpm. Pivot commands would be in 15° increments.

2. Centrifugal Force — The most severe pivotal torque would be the 45° couch offset position, ref. Figures - 82 and 83. This would place the test subject and couch c.g. at 69 inches from the spin axis.

Therefore:

$$F_{MC} = 2.84 \times 10^{-5} \times 69" \times 367 \text{ lbs.} \times 28^2$$

$$F_{MC} = 563 \text{ lbs.}$$

3. Torque @ Pivot. — With the couch in this position, the effective moment arm about the pivot axis would be:

$$27 \text{ in.} \quad x \sin 29° \ 23' = 13.25 \text{ inches}$$

Then:

$$T_p = 13.25 \times 563 = 7450 \text{ in. lbs.}$$

4. The inertial torques induced during rotation about pivot axis are small since the acceleration is low, i.e. .465 rad/sec$^2$

$$T_I = I\alpha \text{ where } I = 57.8$$

$$T_I = 57.8 \times .465 = 26.9 \text{ in. lbs.}$$

5. Combined torisional load on the pivot drive (operating):

$$27 + 7450 = 7477 \text{ in. lbs.}$$

From the structural loads summary,(ref. Table 17 structural analysis section), it can be seen that the emergency stop condition could impose loads as high as 15,330 in. lbs. Since the pivot manual locks would not be engaged during these experiments, the system should be designed to, structurally, react these higher stopping loads. By reacting the load through both the upper and lower pivot segments it was determined that this approach would be feasible provided that the pivot drive was not energized concurrently with an emergency stop. The drive system holding brake would then react this load through the gear train.

An evaluation was then made to determine the mechanical horse-power requirements necessary to meet operating conditions.

Operating Torque = 7477 in. lbs.

Pivot Speed (max) = 10°/sec = 1.67 rpm

$$HP = \frac{7477 \times 1.67}{63025} = .197 \ (100\% \text{ efficient})$$

A preliminary design was created to determine the geometric relationships with the centrifuge structure, and to estimate the drive ratios required. A primary emphasis was placed on keeping the high speed elements of the drive subsystem as remote from the couch area as possible , (see Volume II, SRC-SD-604). An overall gear reduction of 6500:1 was estimated as being required based on the available drive motors suitable for this application. A multi-stage harmonic drive was therefore considered to be the best approach to meet this requirement.

An estimate of system efficiencies was then conducted to establish an efficiency factor for the system.

| | |
|---|---|
| Pivot gear boxes (2) | - 95% |
| Transition Gear boxes (2) | - 95% |
| Distribution boxes (1) | - 95% |
| Torque shafting | - 90% |
| Drive transmission | - 95% |
| Motor | - 90% |

Efficiency factor:

$$\frac{1}{.95 \times .95 \times .95 \times .9 \times .95 \times .9} = 1.52$$

Actual hp required $= 1.52 \times .197$

$$HP = .3$$

Roll Drive Subsystem — The roll capability of the centrifuge is required to provide the necessary positioning of the test subject and to support the angular acceleration threshold experiments, ref. Figure - 78. The centrifuge main rotation system is always fixed during the roll experiments. It can readily be seen, therefore, that since the test subjects c.g. is placed on the center line of the roll frame, the system would be completely balanced in a "0" g environment. The demands on a drive system would be extremely small since the only torques imposed would be the inertial torques resulting from the small eccentric variations in c.g. location. If we assume a maximum c.g. displacement from the roll frame "Z" axis of 6 inches.

Then $\quad I = \dfrac{W \times .25}{g_c} = 2.85 \text{ slug ft}^2$

The accelerations desired during the angular acceleration experiments have been developed by prior testing at Ames Research Center, ref. Vol. IV of this report. These accelerations range from $.011°/\text{sec}^2$ to $10°/\text{sec}^2$.

$$T = I\alpha = 2.85 \times .01745 = .048 \text{ ft. lbs.}$$

$$HP = \frac{.048 \times 20(\text{rpm})(\text{max})}{5252} = .0001825$$

Using the inherent reduction available through the roll frame geometry a preliminary design was developed. Because the power requirements are so extremely low it was determined that a compact power unit using a brushless d.c., fractional hp motor, could be mounted on the pivot segment and react the roll drive loads directly into the centrifuge radius arm. The overall reduction required for this system would be:

$$\frac{\text{Motor Speed} = 3000 \text{ rpm}}{\text{Max Roll Speed} = 20 \text{ rpm}} = 150{:}1$$

An initial reduction of 24.25:1 can be attained between the roll frame ring gear and the drive unit output pinion.

Counterweight Subsystem. — An analysis of the counterbalance design approach, for the Space Research Centrifuge, is given in Appendix C of this report.

During this phase of the study a preliminary design for the counterbalance system was created to establish the geometric interfaces. It was determined that the system should consist of two counterweights, mounted above and below the radius arm, which would be electrically driven to synchronously translate, along the main rotating frame, and move transversely to the frame.

The counterweights are driven by a system of ball screw actuators, driven by fractional hp a-c drive motors, to provide the necessary responses defined in the "stability and attitude control feasibility analysis" portion of this report.

## Phase III Activity

During this phase of the study a depth predesign of a "Ground based, space research centrifuge prototype," was developed. The results of this effort are presented in Volume II of this report.

Control and Communications

Control General. — The study and conceptual design of the controls for the Space Research Centrifuge engineering prototype was subdivided into a number of subsystems to simplify the approach. They are the primary drive control, the translation drive control, the counterweight drive control, the pivot drive control, the roll drive control and the perturbation control. The perturbation control is used only in the ground based version of the centrifuge, it will not be used in the flight article. It is used to control actuators attached to the centrifuge support structure. The actuators are used to simulate the dynamic environment that the centrifuge flight article is expected to encounter.

An analysis of the operations to be performed in setting up for an experiment showed that a manual control station mounted on the centrifuge was needed in addition to the operator's console. The operator must be able to position various parts of the centrifuge while working in the immediate area. The most practical solution was to provide a manual control station with the necessary controls. Table 30 identifies the control functions provided at the manual control console and the operator's console. The perturbation controls are located on the ground systems performance console.

Primary Drive Control. — The primary drive control subsystem logic is typical of the control subsystems. It must provide a 100 to 1 range of rotational speeds as well as variable onset rates which are required for the various experiments proposed. As shown in Figure 85, Primary Drive Controls, there are two modes of operation, manual and automatic. The manual mode is used to move the centrifuge arm for setting up the experiments and for experiments requiring a fixed rate of rotation. The automatic mode was provided to perform preprogrammed onset rates and rotational rates in accordance with the experiment requirements. The primary drive logic has been designed to permit abort by the test subject, the operator or out-of-tolerance sensors. The logic is fail-safe, therefore, in the absence of power the brake on the drive motor is engaged. A time constant is built into the logic to prevent braking at an excessive rate. Using the ground rule that the electrical and electronic equipment shall be capable of operating in an explosive atmosphere reduced the suitable types of motors to the brushless dc type and the squirrel cage induction type. The squirrel cage induction motor was chosen for

Table 30

Location of controls

| DRIVE SUBSYSTEM | MANUAL CONSOLE | OPERATOR'S CONSOLE |
|---|:---:|:---:|
| PRIMARY DRIVE | | |
| Manual/Auto | | X |
| +Run/Stop/-Run | | X |
| Speed Change | | X |
| TRANSLATION DRIVE | | |
| In/Stop/Out | X | |
| Slow/Fast | X | |
| COUNTERWEIGHT | | |
| Manual/Auto | | X |
| Out/Stop/In | | X |
| Left/Stop/Right | | X |
| PIVOT DRIVE | | |
| +Deg/Stop/-Deg | X | X |
| Slow/Fast | | X |
| ROLL DRIVE | | |
| Manual/Auto | | X |
| +Deg/Stop/-Deg | X | X |
| Slow/Fast | | X |
| EXPERIMENT EQUIPMENT | | |
| On/Off | | X |
| Bright/Dim | | X |

the primary drive principally because variable speed integral hp induction motors are within the current state-of-the-art, while brushless dc motors have been designed only up to 1/2 hp.

A variable frequency/variable voltage 3 phase inverter is required to power the 3 phase induction motor. The input to the inverters is a function of the summed outputs of the ramp generator and the tachometer connected to the motor shaft. The ramp generator output is programmed for the desired onset rate at the beginning of the experiment.

The primary drive is interlocked with the translation arm to prevent operation of the primary drive when the translation arm is not in one of the five mechanically locked positions. It is also interlocked with the roll drive logic to prevent operation of the primary drive when the roll drive is being operated.

Translation Drive Control. . — The radius arm length is positioned by a 1/3 hp two speed reversible motor. An In/Stop/Out control and a Slow/Fast control on the manual console are used to operate the motor. Mechanical locks hold the radius arm in one of five positions. The translation arm drive control is interlocked with the pivot frame position. The translation drive cannot be operated to extend the arm beyond the 45 inch position when the pivot frame is not in the "0° " position.

The operator's console is provided with indicator lights to show when the mechanical locks are engaged and the translation arm position. Figure 86, Translation Arm Controls, shows the functional operation of the subsystem.

Counterweight Control System — A functional schematic of this subsystem is shown in Figure 87, Counterweight Control System. Controls are provided on the operator's console to position the counterweights manually or automatically. In the automatic mode, the summed output of four sensors, mounted on the centrifuge main frame, are fed to the logic unit which controls the counterweight translation and transverse drive motors. The manual mode control is provided to permit initial positioning of the counterweights before the start of an experiment. During an experiment the counterweight control will normally be in the automatic mode. This subsystem is not interlocked with any other control systems. The operator's panel is provided with readouts of the net force unbalance and the counterweight positions.

Couch Pivot Controls. — The couch pivot control subsystem provides for positioning the couch manually from the operator's console and the manual control console or automatically at the operator's console. Automatic operation is accomplished by setting the desired pivot frame position on the input registers. When the input and the position registers are balanced the drive will stop. Figure 88, Couch Pivot Controls, shows the functional operation of the subsystem. Light indications on the operator's console show when the pivot frame is in a locked position. The

pivot drive logic is interlocked with the translation arm position to prevent operation of the pivot drive when the translation arm is extended beyond the 45 inch position.

Roll Drive Control. — Controls are provided at both the manual console and the operator's console. Additionally, at the operator's console, a Slow/Fast control and a Manual/Auto control are provided. The control functions of the subsystem are shown in Figure 89, Couch Roll Drive Controls. In the automatic mode, a pre-programmed tape will control the roll onset rate as determined by the subject's response to the experiment. The roll drive is interlocked with the primary drive circuit to prevent operation of the primary drive when the roll drive circuit is activated.

Readouts are provided on the operator's console to monitor the roll acceleration and velocity rates.

A 28 volt dc brushless motor was selected for the roll drive because of the variable speed and low torque requirements.

Perturbation Control. — The perturbation control, as mentioned previously, is used to control the actuators attached to the support frame of the ground based centrifuge. The actuators induce motion in the centrifuge in simulation of the dynamic environment expected to be encountered by the flight article. The control circuit is designed as shown in Figure 90, Perturbation Control, Electrical, to provide X-X, Y-Y or circular motion in the X-Y plane. This may be done at a single frequency or with a high frequency excitation superimposed on low frequency signal. The amplitude of both frequencies may be adjusted. Resolvers were selected as signal generators because of the quadrature phase relationship that must be maintained over the wide range of low frequencies employed.

Experiment Equipment Control. — Ancillary equipments used in conjunction with different experiments will require control from the operator's console. A "black box" approach was used in arriving at the control requirements, since these equipments are not presently defined. Controls provided at the operator's console permit the concurrent operation of two black boxes, varying one parameter on each and providing one stepping function for each. An electrical interface is provided at the couch for connecting to the ancillary equipments.

Communications, General. — The communications system provides four main functions; two-way voice communications between the operator and the test subject, closed circuit TV monitoring of the test subject, data transmission of the instrumentation to the biomedical panel, the operator's panel and recorders, and transmission of the commands from the couch, the manual control console and the operator's console to the centrifuge control systems. This is shown in Figure 91, Communication Block Diagram. Signal transmission across the rotary and translatory mechanisms was studied relative to the experiment requirements and the constraint that the electrical and electronic equipment shall be compatible with an explosive atmosphere. The rotational limits of the pivot mechanism, ±100 degrees, and the ±38 inch motion of the translation arm make hard wiring feasible across these mechanisms.

With the exception of the angular acceleration experiment, the roll frame rotation is limited to 90 degrees. However, during the angular acceleration experiment the roll frame is rotated through many revolutions. It was decided that a pair of omni-antennas shall be used for the communication link during the angular acceleration experiment and that hard wiring shall be used across the rotary mechanism for all the other experiments. This compromise benefits from the advantages of hard wiring for the majority of the experiments and provides a simple means of communications changeover for the angular acceleration experiment.

Since the main pivot of the centrifuge rotates continuously it is not feasible to hard wire across it. A trade-off analysis was made of the use of rotary capacitors vs the use of antennas. The results of the study show rotary capacitors to be most feasible for this application. The hub design accommodates the installation of three rotary capacitors to be used for the transmission of information between the stationary and rotating portions of the centrifuge. A rotary capacitor will have to be developed for the centrifuge. Commercially available capacitors were not designed for the number of cycles of operation required in this application. The problem is one of providing bearings rated at 5000 hours of operation, the rating on the bearing for the main pivot.

The TLM component parts, SCO's, multiplexers, transmitters, receivers, etc. for this application are commercially available in miniaturized form.

Two-way Voice Communications. — Voice communications between the couch and the operator's panel will be provided for all experiments. The test subject will be provided with headphones and a lip or throat microphone. A microphone and speaker will be installed at the operator's console. Because the transmission is via either a rotary capacitor or an antenna, r f transceivers will be required. For safety purposes, a tone generator and detector will be provided for transmission in each direction. The absence of a tone at either end will raise an alarm at the operator's console.

<u>Closed Circuit TV</u>. — A TV camera and its associated controls will be mounted behind the test subject's head and pointed at a mirror in front of the subject's face. Small portable videon cameras operating from 28 volts dc suitable for use in the ground prototype are commercially available. Miniature cameras, fully qualified for the space environment are availalable at considerably more cost. From an evaluation of the TV monitors available several suitable monitors were found that will operate from 28 volts dc, have good picture quality and are compact. A VHF rf modulator is included in the camera control module to provide the modulated rf carrier needed for transmission through the rotary capacitor at the primary drive.

<u>Data Transmission</u>. — The biomedical data, subject's experiment data and voice communications will be time and frequency multiplexed on one RF link. This is due to the fact that these data must be transmitted during all experiments and therefore must be transmitted via the omni-antennas during the angular acceleration experiment when the roll frame wiring is disconnected from the pivot frame. Multiplexing the data with this commonality simplifies the switchover to the angular acceleration experiment.

The centrifuge parameters and the up link and down link commands will be multiplexed and transmitted through one rotary capacitor. The TLM components required for this link are commercially available.
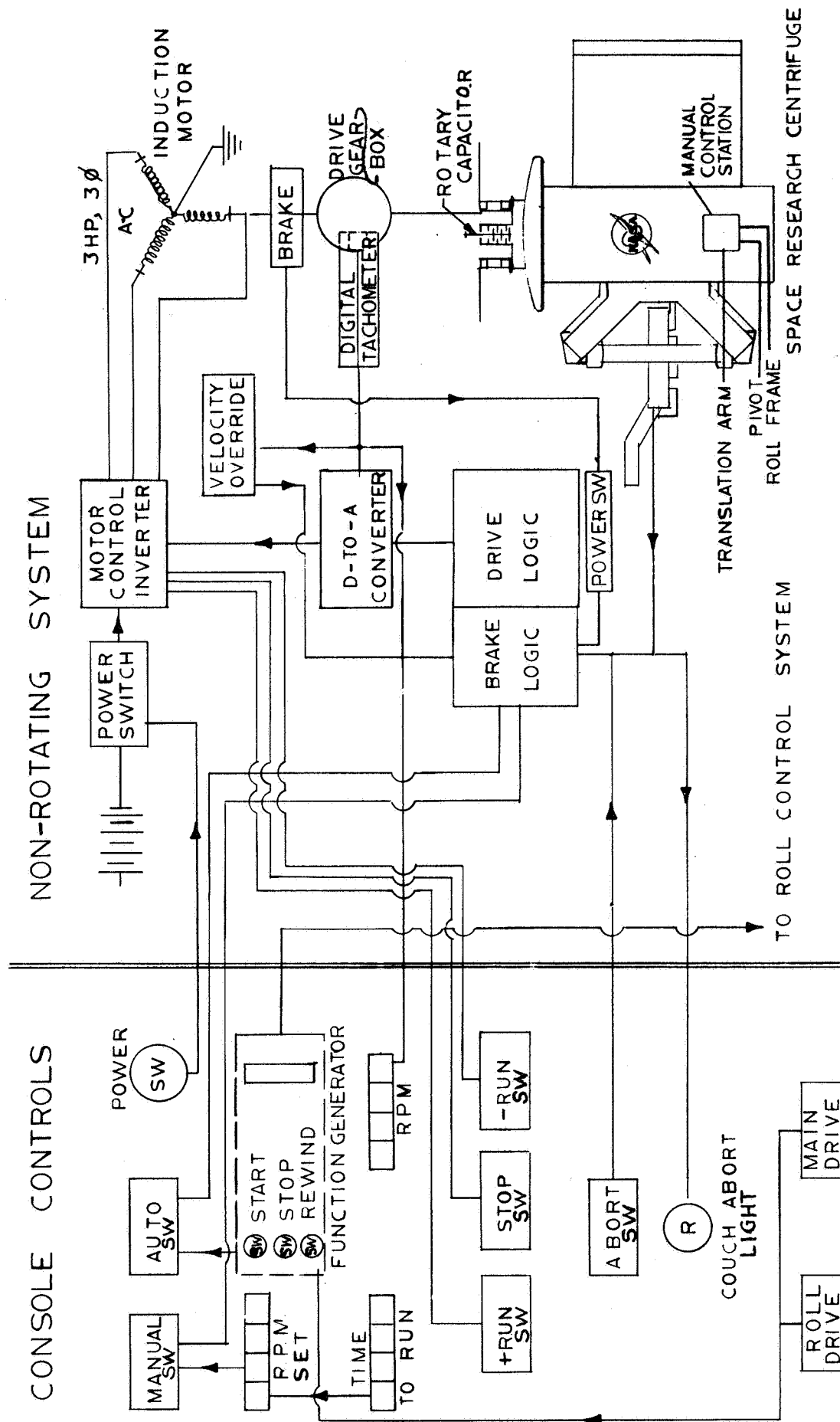
Figure 85. Primary Drive Controls
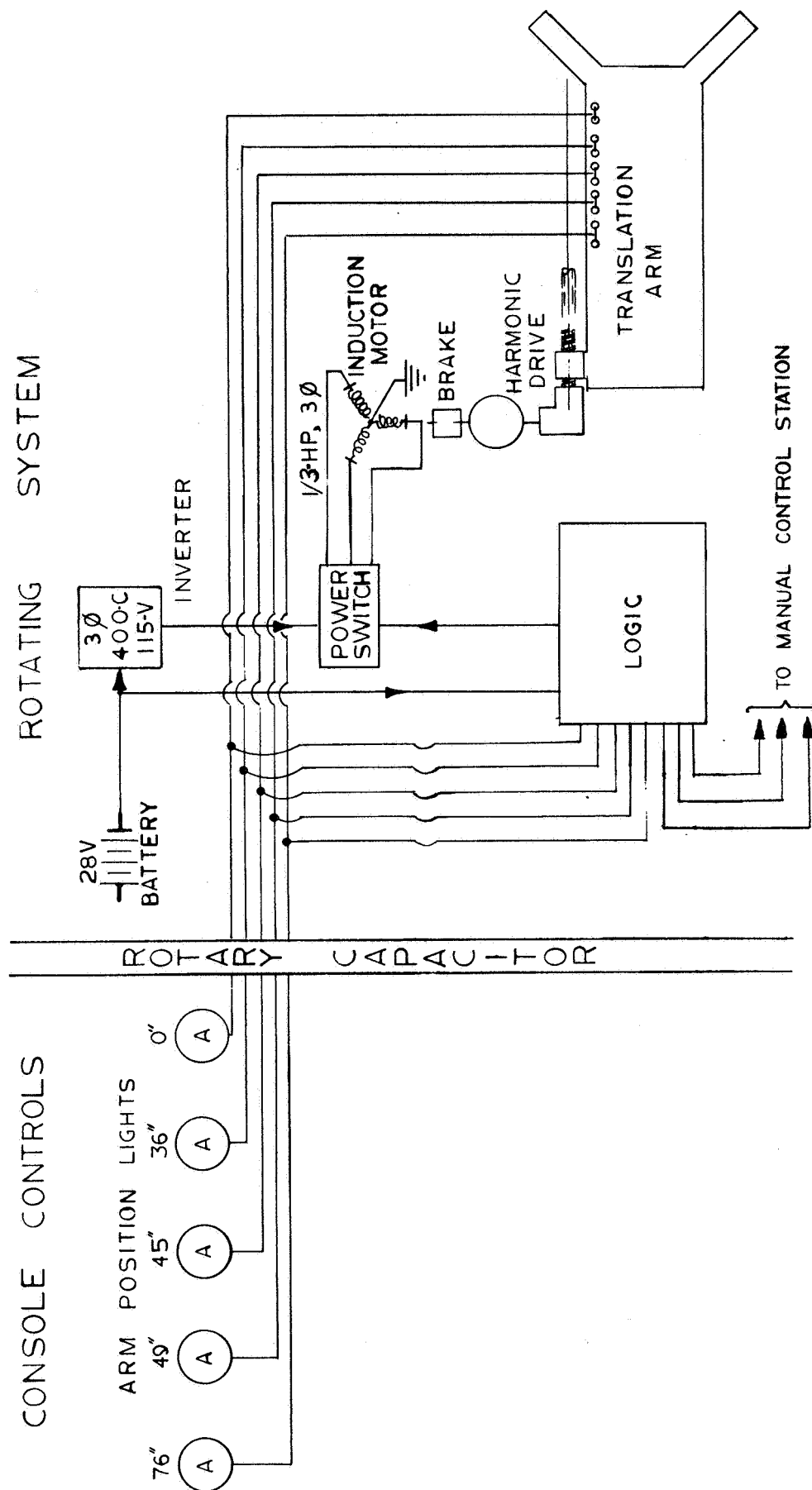
Figure 86.  Translation Arm Controls
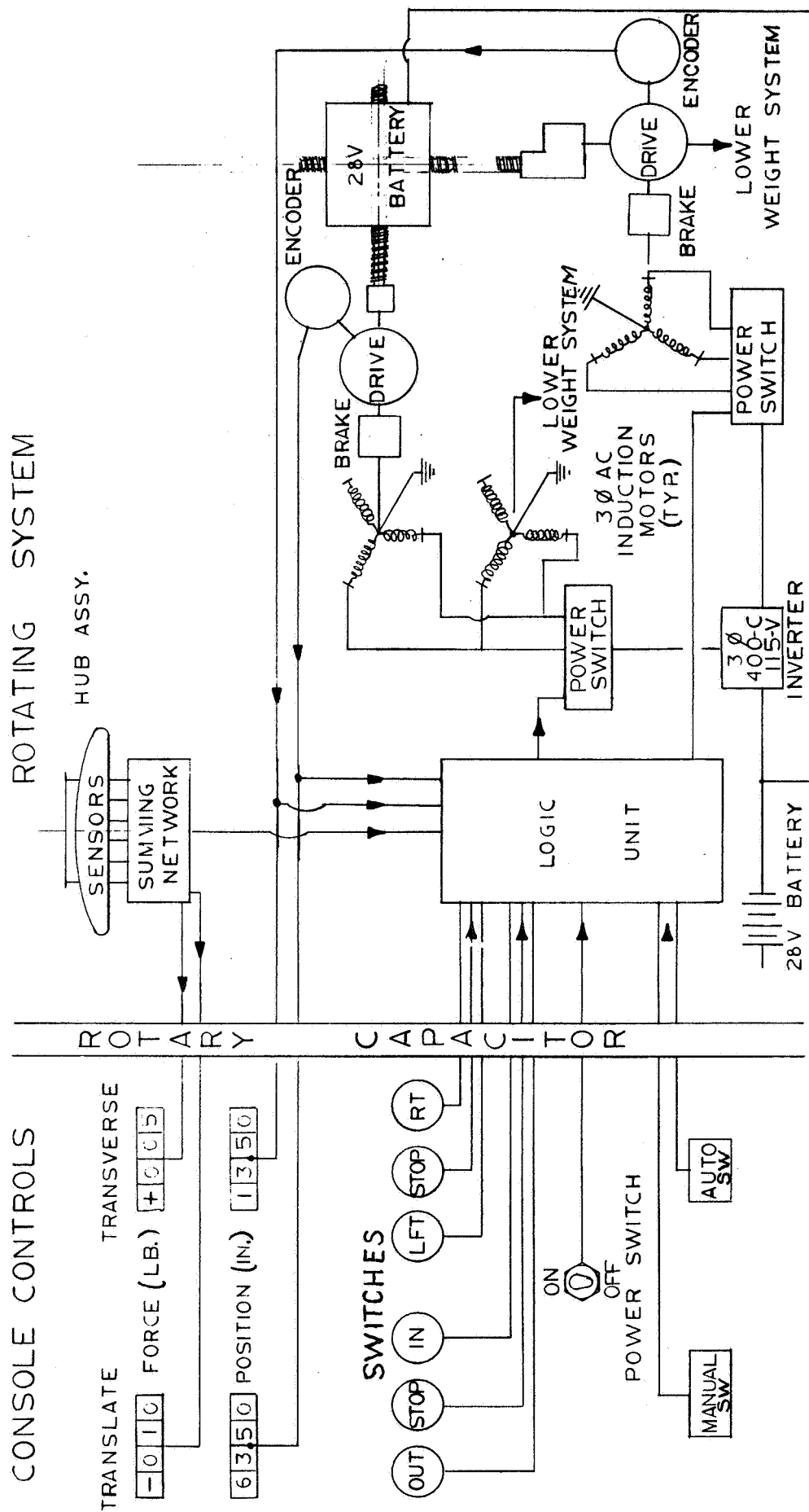
Figure 87. Counterweight Control System
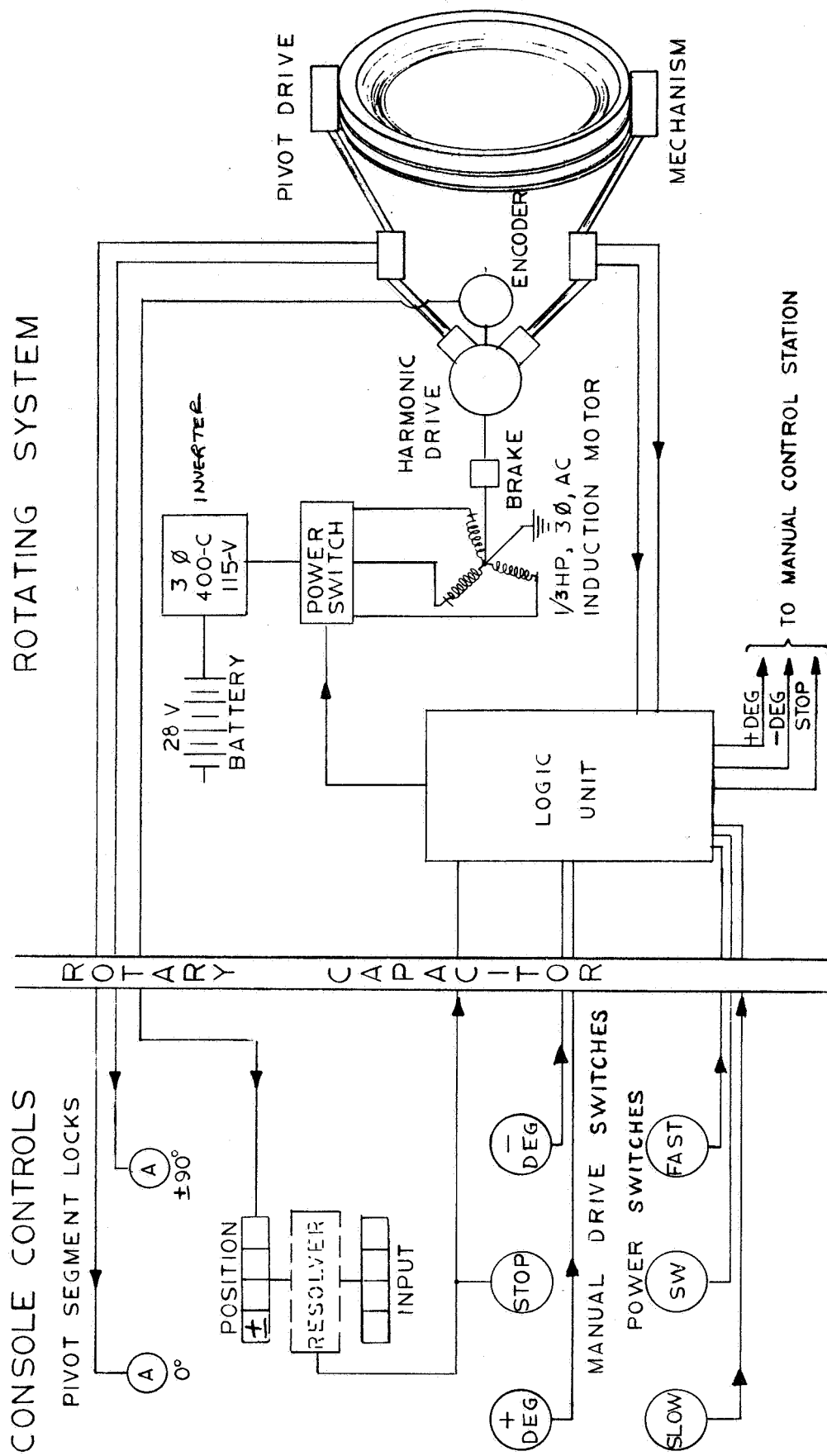
Figure 88. Couch Pivot Controls
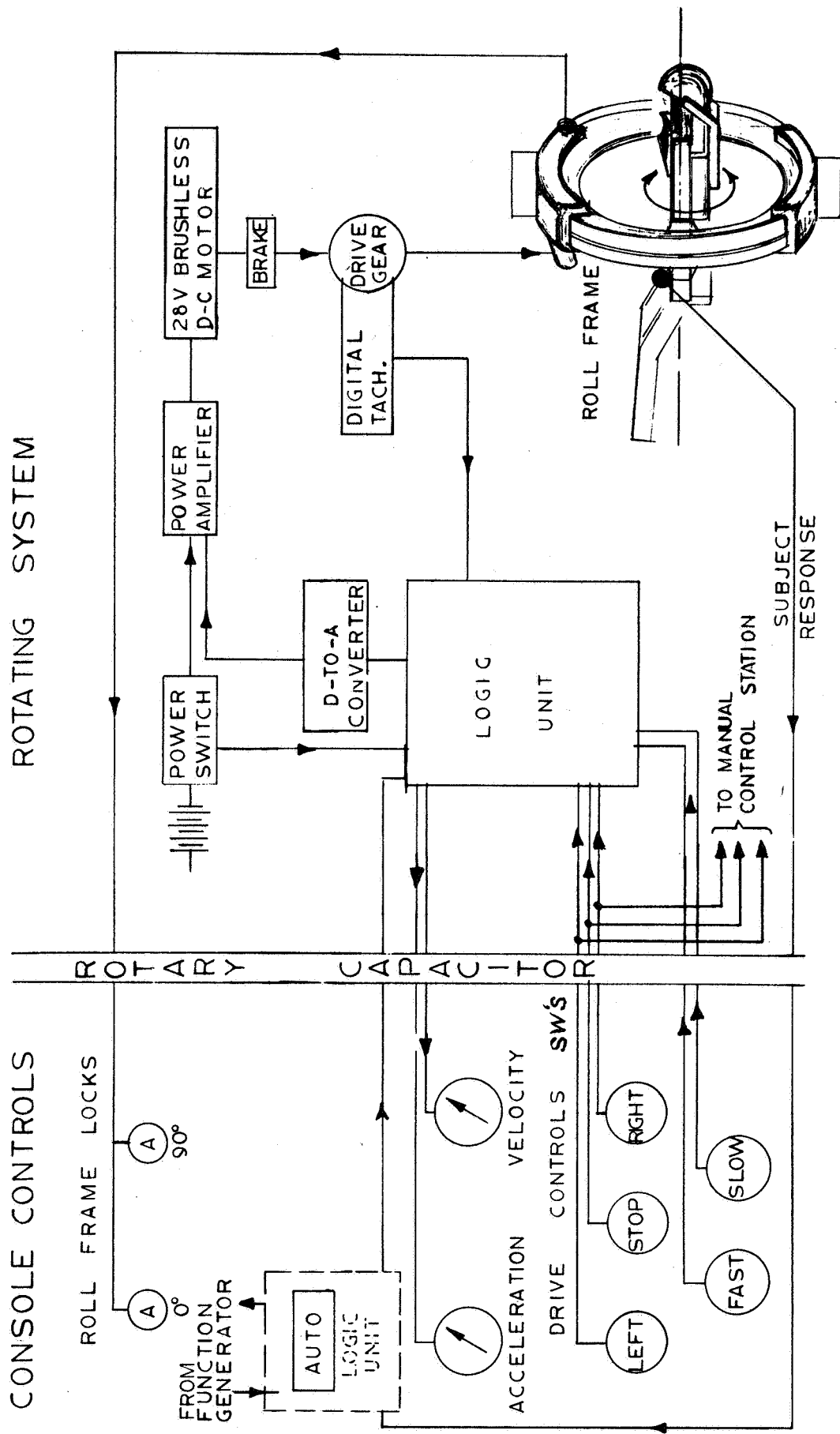
Figure 89. Couch Roll Drive Controls
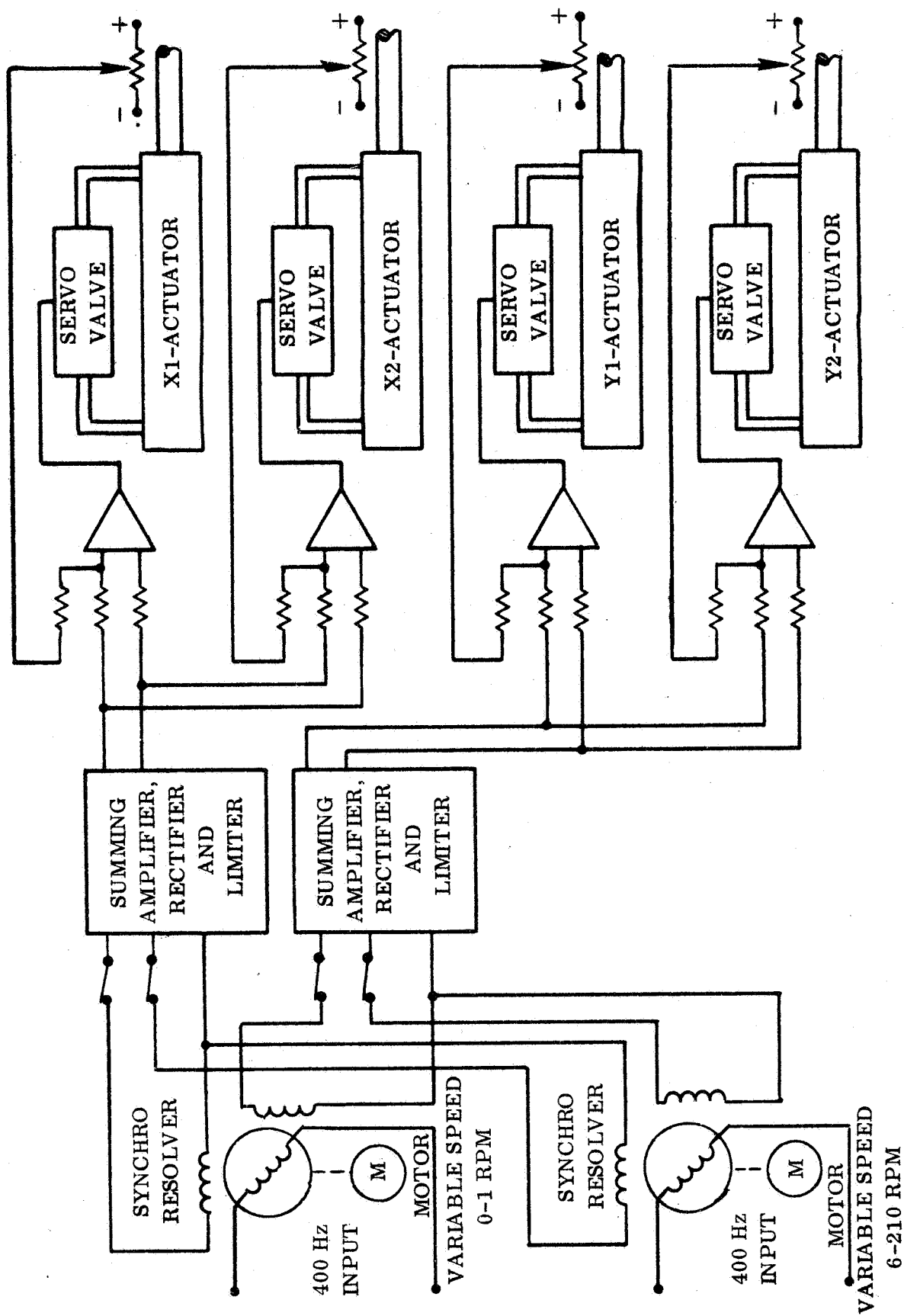
Figure 90.  Perturbation Controls
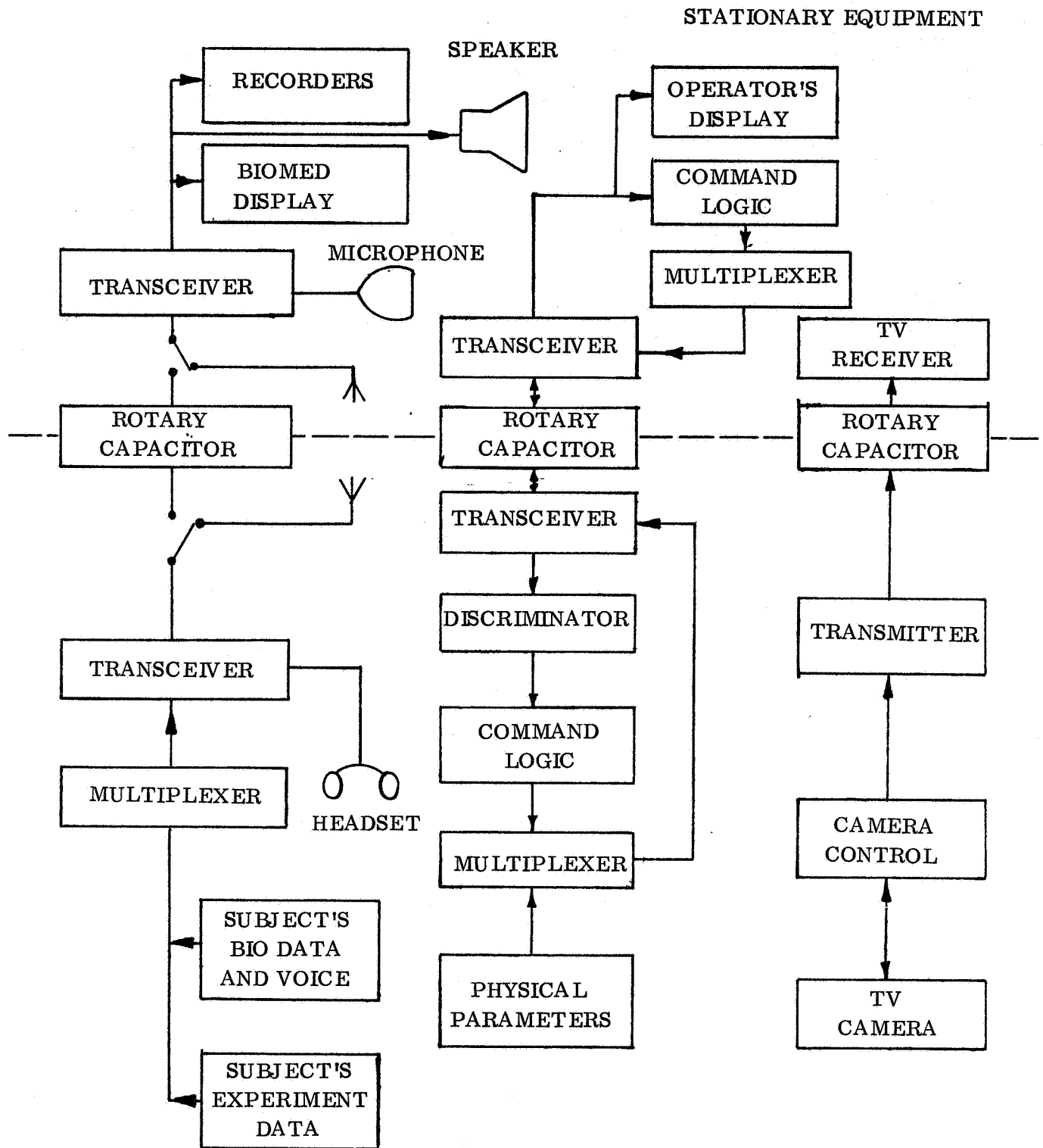
Figure 91. Communication Block Diagram

FEASIBILITY STUDIES

### Reliability, Failure Mode and Effects Analysis

Reliability analysis was conducted through the functional approach, determining what functions are performed or required as a part of the experiments to be performed. For this system, the functions include, first, the various modes of motion, rotation, translation, roll and pivot. In addition, other functions such as structural integrity, communication, dynamic stability or balance as required for satisfactory operation were identified. Finally, these must be supported by provisions for power. Each function is performed or assured by an assembly or combination of hardware. A prediction of reliability was made for each named subsystem and by consideration of the failure modes of the hardware, the effect of various failures was identified on the functions. The failure rates of the hardware resulting in function failure were then allocated to the function distribution providing an estimate of the probability of successfully completing the mission.

Functional allocation. Table 31 provides a list of functions necessary to operate the centrifuge. For each function, a combination of the subsystems essential to the performance is named.

Reliability prediction. A reliability prediction for each subsystem is given in Tables 34 through 46. Data sources are tabulated on the backup sheets accompanying each system reliability block diagram.

Failure analysis. The intent of failure analysis was to investigate, in limited depth, the action and interaction of the various system elements to determine the over-all effect of system failures on mission (experiment) accomplishment and crew safety. The analysis is effective in:

1.  Determining the gross effect of certain failures on the over-all mission (experiment) and the crew safety.

2.  Identifying those areas where emphasis in a development program should be placed to improve the reliability of hardware.

3.  Identifying, classifying and determining the number of and consequence of failures such as:

    A.  Minor - Mission (experiment) can be completed and crew is safe. (Classification Symbol "M")

B. Abort - Mission (experiment) cannot be completed, but crew is safe. (Classification Symbol "A")

C. Catastrophic - Mission (experiment) cannot be completed, crew is trapped and possible injury might result. (Classification Symbol "C")

4. Developing recommendations for crew action to cope with the failures.

5. Developing recommendations for modifications to the systems.

For each function tabulated in Table 31, the equipment failure that would have an effect on the function is tabulated and the fraction of total functions attributable to that equipment is estimated. The primary effect, recommended crew action and suggestions for improvement are recorded in Table 47.

Subsystem failure distributions. The functional reliabilities are computed by summing the probabilities of occurrence ($P_o$) from the reliability predictions across the functional matrix, Table 48. These probabilities of occurrence are then distributed across the failure modes to provide a measure for evaluation of the importance of each component failure mode.

Recommendations. Baseline reliability estimates reflect the functional reliability of each system without any attempt to improve or optimize the reliability of the total device. These estimates indicate that control, instrumentation and communications will require the most emphasis with regard to selection of high reliability components and intensive qualification effort.

In order to assess the effect of introducing spares for certain critical components and providing a limited amount of active parallel redundancy, a reliability re-estimate was made in the most sensitive areas. These items and their disposition are shown by Table 33. The resulting improvement in over-all reliability to .903075 indicates that these techniques will be adequately effective in raising predicted reliability to appropriate man-rated levels. Spares and active parallel redundancy as well as a vigorous qualification program are firmly recommended for the flight centrifuge development.

Table 31. - Centrifuge Functions and Essential Subsystem Requirements

| SYSTEM FUNCTION | ESSENTIAL SUBSYSTEMS REQUIRED |
|---|---|
| Primary Rotation (PR) | Primary Drive System |
| | Power System (External Source) |
| | Rotational Control Systems |
| Radius Arm Translation (RAT) | Arm Assembly Drive System |
| | Arm Translation Control |
| | Battery System (On Board) |
| | Counterbalance Drive System |
| Couch Roll (CR) | Couch Roll Drive System |
| | Battery System (On Board) |
| | Coach Roll Control |
| Couch Pivot (CP) | Couch Pivot Drive Assembly |
| | Battery System (On Board) |
| | Couch Pivot Control |
| Structural Integrity (SI) | Structure |
| Power (P) | Battery System (On Board) |
| | (Undefined External Source) |
| Communication (C) | Communication |
| | Couch Instrumentation |
| | Battery System (On Board) |
| Dynamic Balance (DB) | Dynamic Balancing Control |
| | Counterbalancing Drive System |
| | Battery System (On Board) |

## Table 32. - Space Centrifuge Reliability Summary

| SYSTEMS AND SUBSYSTEMS | | FAILURES EXPECTED PER 1000 FLIGHTS | PREDICTED RELIABILITY |
|---|---|---|---|
| 1.0 | STRUCTURE | 3.1694 | 0.996836 |
| 1.1 | Drive Hub Assembly | 0.0250 | 0.999975 |
| 1.2 | Frame Assembly | 0.0100 | 0.999990 |
| 1.3 | Arm Assembly | 0.0100 | 0.999990 |
| 1.4 | Control Console and Display | 0.0050 | 0.999995 |
| 1.5 | Couch Assembly | 3.1194 | 0.996885 |
| | | | |
| 2.0 | DRIVE SYSTEMS | 29.1121 | 0.971308 |
| 2.1 | Primary Drive | 3.4977 | 0.996508 |
| 2.2 | Arm Assembly Drive | 1.2973 | 0.998704 |
| 2.3 | Counterbalance Drive | 20.2991 | 0.979906 |
| 2.4 | Couch Pivot Drive | 1.6984 | 0.998303 |
| 2.5 | Couch Roll Drive | 2.3196 | 0.997683 |
| | | | |
| 3.0 | POWER SYSTEM | 12.3937 | 0.987683 |
| 3.1 | Battery System (Arm) | 12.3937 | 0.987683 |
| | | | |
| 4.0 | CONTROL SYSTEMS | 95.9550 | 0.908505 |
| 4.1 | Rotation Control, Main Drive | 22.2076 | 0.978038 |
| 4.2 | Arm Translation | 3.5812 | 0.996425 |
| 4.3 | Couch Pivot | 4.1837 | 0.995825 |
| 4.4 | Couch Roll | 15.8021 | 0.984322 |
| 4.5 | Dynamic Balancer & CMG's | 50.1804 | 0.951056 |
| | | | |
| 5.0 | COUCH INSTRUMENTATION | 55.2254 | 0.946270 |
| | | | |
| 6.0 | COMMUNICATIONS | 197.1193 | 0.821093 |
| 6.1 | Intercommunications | 191.8811 | 0.825405 |
| 6.2 | Television | 2.5944 | 0.997409 |
| 6.3 | Medical Displays | 1.2787 | 0.998722 |
| 6.4 | Rotary Capacitors | 1.3651 | 0.998636 |
| | | | |
| | CENTRIFUGE ASSEMBLY | 392.9749 | 0.675046 |

Table 33. - Effect of Spares and Redundancy on Basic Systems Reliability

| Item* | Disposition | Basic Reliability | Revised Reliability |
|---|---|---|---|
| 2.2 | | .998703 | .9996495 |
| 2.2.1 | Spare | | |
| 2.2.4 | " | | |
| 2.3 | | .979905 | .991293 |
| 2.3.1 | Spare | | |
| 2.3.4 | " | | |
| 2.3.16 | " | | |
| 2.3.19 | " | | |
| 2.4 | | .998303 | .999383 |
| 2.4.1 | Spare | | |
| 2.4.4 | " | | |
| 2.5 | | | |
| 2.5.1 | Spare | .997683 | .999829 |
| 3.1 | | | |
| 3.1.1 | Spare | .987682 | .9983764 |
| 3.1.4 | " | | |
| 4.1 | | .978038 | .9927818 |
| 4.1.2 | Redundancy | | |
| 4.1.7 | " | | |
| 4.1.8 | " | | |
| 4.1.11 | Spare | | |
| 4.4 | | .984322 | .993109 |
| 4.4.2 | Redundancy | | |
| 4.4.10 | Delete | | |
| 4.4.18 | Redundancy | | |
| 4.5 | | .951055 | .958793 |
| 4.5.2 | Redundancy | | |
| 4.5.5 | " | | |
| 5.0 | | .946270 | .998838 |
| 5.0.1 | Spare | | |
| ↓ | ↓ | | |
| 5.0.11 | Spare | | |
| 5.0.13 | " | | |
| 5.0.18 | " | | |
| 5.0.19 | " | | |

Table 33 (cont'd. )

| Item | Disposition | Basic Reliability | Revised Reliability |
|------|-------------|-------------------|---------------------|
| 6. 0 | | .821093 | .981602 |
| 6. 1. 1 | Spare | | |
| 6. 1. 2 | Redundancy | | |
| 6. 1. 5 | " | | |
| 6. 1. 6 | Spare | | |

*Reference Tables 38, 40, 42, 44, 46 for item identification.

Table 34. - Space Centrifuge Reliability Model
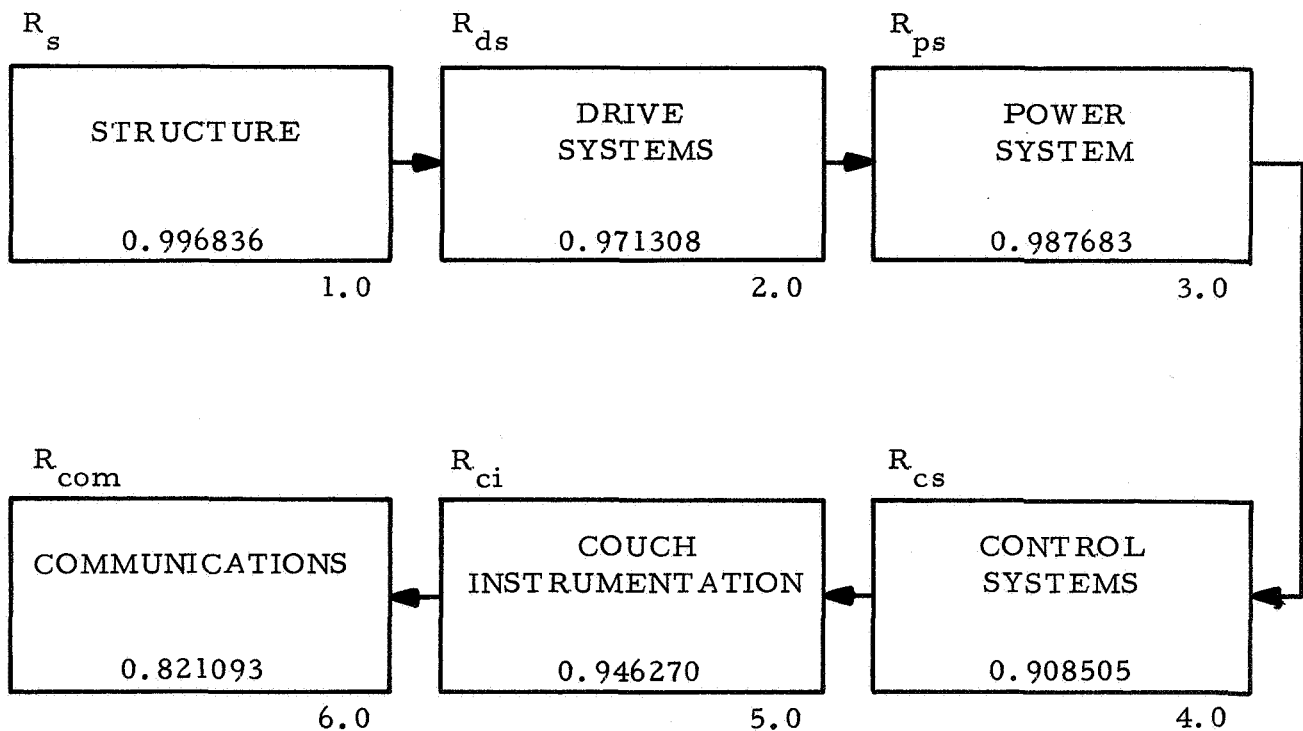


$$R_{sc} = R_s \times R_{ds} \times R_{ps} \times R_{cs} \times R_{ci} \times R_{com} = 0.6750$$

Table 35. - Structure Reliability Model

$$R_s$$

```
+-----------------------+
|      STRUCTURE        |
|                       |
|      0.996836         |
+-----------------------+
                     1.0
```

SYSTEM

```
+-------------------+      +-------------------+      +-------------------+
|      DRIVE        |      |      FRAME        |      |       ARM         |
|       HUB         | -->  |    ASSEMBLY       | -->  |    ASSEMBLY       |
|    ASSEMBLY       |      |                   |      |                   |
+-------------------+      +-------------------+      +-------------------+
               1.1                        1.2                       1.3
```

Assumed Reliability = 0.99995

```
+-------------------+      +-------------------+
|      COUCH        |      |     CONTROL       |
|    ASSEMBLY       |      |     CONSOLE       |
|                   | <--  |       &           |
|  λ = 20.2         |      |     DISPLAY       |
|  R = 0.996885     |      |                   |
+-------------------+      +-------------------+
               1.5                        1.4
```

SUBSYSTEMS

$$R_s = R_{1.1} \times R_{1.2} \times R_{1.3} \times R_{1.4} \times R_{1.5} = 0.996836$$
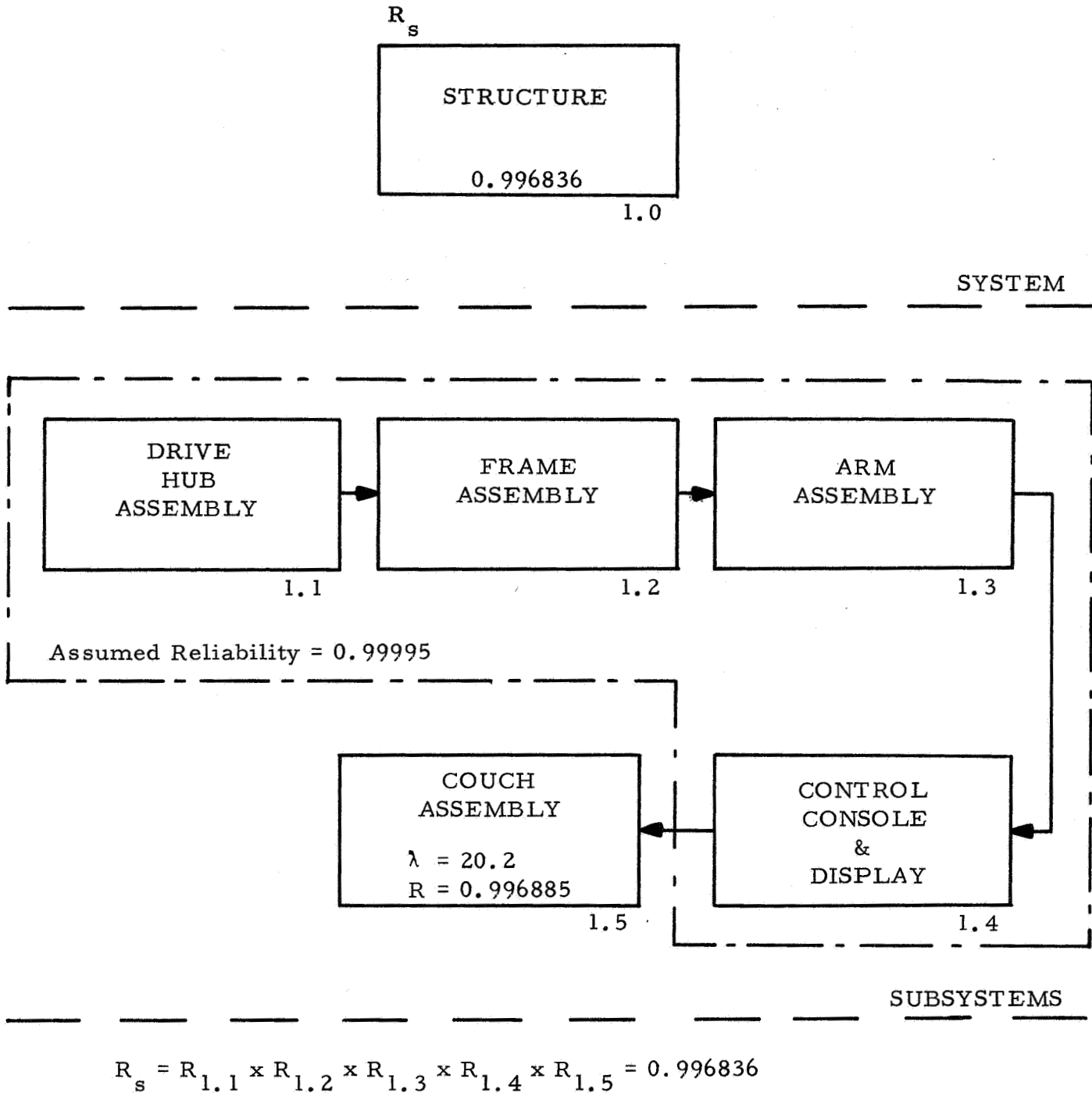
Table 36. – Structural Reliability

| | | OPERATIONAL PERIOD | | | | | | DORMANT PERIOD | | | SUMMARY | |
|---|---|---|---|---|---|---|---|---|---|---|---|---|
| Number | Name | No.of Comp. Req'd $n$ | Fail. Rate (Oper) $\lambda \times 10^{-6}$ | No. Times Rate (Oper) $n\lambda \times 10^{-6}$ | Comp. Oper. Time Hours $t_o$ | Expected No.of Fail. (Operational) $n\lambda t_o$ | Data Sources | No. Times Rate (Dorm) $n\lambda' \times 10^{-6}$ | Comp. Dormant Time – Hours $t'$ | Expected No.of Fail. (Dormant) $n\lambda' t'$ | $\Sigma n\lambda t$ | Reliab. |
| 1.0 | STRUCTURE | | | | | | | | | | | |
| 1.1 | DRIVE HUB ASSEMBLY | | | | | | Estimate | | | | 0.000,050,0 | 0.99995 |
| 1.2 | Frame Assembly | | | | | | " | | | | | |
| 1.3 | Arm Assembly | | | | | | " | | | | | |
| 1.4 | Control Console & Display | | | | | | " | | | | | |
| 1.5 | Couch Assembly | 1 | 20.2 | 20.20 | 153.5 | 0.003,100,7 | FARADA | 0.02020 | 926.5 | 0.000,018,7 | 0.003,119,4 | 0.996885 |
| | | | | | | | | | | | $\Sigma$ 0.003,169,4 | .996836 |

Table 37. - Drive Systems Reliability Model

$$R_{ds}$$

```
┌─────────────────────────┐
│        DRIVE            │
│       SYSTEMS           │
│                         │
│       0.971308          │
└─────────────────────────┘
                      2.0
```

SYSTEM

```
┌──────────────────┐    ┌──────────────────┐    ┌──────────────────┐
│    PRIMARY       │    │      ARM         │    │  COUNTERBALANCE  │
│    DRIVE         │───▶│   ASSEMBLY       │───▶│     DRIVE        │
│    SYSTEMS       │    │    DRIVE         │    │     SYSTEM       │
│                  │    │    SYSTEM        │    │                  │
│   0.996508       │    │   0.998704       │    │    .979906       │
└──────────────────┘    └──────────────────┘    └──────────────────┘
              2.1                       2.2                      2.3
```

```
┌──────────────────┐    ┌──────────────────┐
│   COUCH ROLL     │    │   COUCH PIVOT    │
│    DRIVE         │◀───│     DRIVE        │
│    SYSTEM        │    │     SYSTEM       │
│                  │    │                  │
│   0.997683       │    │   0.998303       │
└──────────────────┘    └──────────────────┘
              2.5                       2.4
```

SUBSYSTEMS

$$R_{ds} = R_{2.1} \times R_{2.2} \times R_{2.3} \times R_{2.4} \times R_{2.5} = 0.971308$$

## Table 38. - Drive Systems Reliability

| Number | Name | No.of Comp. Req'd n | Fail. Rate (Oper) λx10⁻⁶ | No. Times Rate (Oper) nλx10⁻⁶ | Comp. Oper. Time-Hours $t_o$ | Expected No. of Fail. (Operational) $n\lambda t_o$ | Data Sources | No. Times Rate' (Dorm) $n\lambda'$x10⁻⁶ | Comp. Dormant Time - Hours $t'$ | Expected No.of Fail. (Dormant) $n\lambda't'$ | $\Sigma n\lambda t$ | Reliab. |
|---|---|---|---|---|---|---|---|---|---|---|---|---|
| 2.0 | DRIVE SYSTEMS | | | | | | | | | | | |
| 2.1 | PRIMARY DRIVE SYSTEM | | | | | | | | | | | |
| 2.1.1 | Drive motor | 1 | 36.0 | 36.0 | 75 | | MILHDBK 217A | | 1005 | | | |
| 2.1.2 | Gear Box | 1 | .9 | | | | FARADA | | | | | |
| 2.1.3 | Pinion Gear | 1 | .12 | 46.02 | 75 | 0.003,451.5 | FARADA | .04602 | 1005 | 0.000,046.2 | 0.003,497,7 | 0.9965084 |
| 2.1.4 | Brakes | 1 | 9.0 | | | | FARADA (MODIFIED) | | | | | |
| 2.2 | ARM ASSY. DRIVE SYS. | | | | | | | | | | | |
| 2.2.1 | Drive Motor | 1 | 36.0 | 36.0 | 20 | | MILHDBK 217A | | 1060 | | | |
| 2.2.2 | Harmonic Drive | 1 | 2.46 | 2.46 | | | FARADA (MODIFIED) | | | | | |
| 2.2.3 | Primary Gear Box | 1 | .90 | .90 | | | FARADA | | | | | |
| 2.2.4 | Disc Brakes | 1 | 9.0 | 9.0 | | | FARADA (MODIFIED) | | | | | |
| 2.2.5 | Miter Gear Box | 1 | .64 | .64 | | | FARADA | .0616 | | 0.000,065.2 | | |
| 2.2.6 | Ball Screw Assy. | 1 | .40 | .40 | | | FARADA | | | | | |
| 2.2.7 | Ball nut Assy. | 1 | .88 | .88 | | | FARADA | | | | | |
| 2.2.8 | Bearing | 1 | .5 | .5 | | | FARADA | | | | | |
| 2.2.9 | Rail Ball Bushings | 16 | .05 | 8.0 | | | FARADA | | | | | |
| 2.2.10 | Arm Latch Assy. | 1 | 2.82 | 2.82 | 20 | 0.001,232 | FARADA | | 1060 | | 0.001,297,3 | 0.9987035 |
| 2.3 | COUNTER WEIGHT DRIVE SYS. | | | | | | | | | | | |
| 2.3.1 | Translation Drive Motor | 1 | 36.00 | 36.00 | 129.75 | | MILHDBK 217A | | 950.25 | | | |
| 2.3.2 | Harmonic Drive | 1 | 2.46 | 2.46 | | | FARADA (MODIFIED) | | | | | |
| 2.3.3 | Gear Box | 1 | 1.11 | 1.11 | | | FARADA | | | | | |
| 2.3.4 | Disc Brake System | 1 | 9.00 | 9.00 | | | FARADA (MODIFIED) | | | | | |
| 2.3.5 | Torque Tube Assy. | 2 | .35 | 0.70 | | | FARADA | | | | | |
| 2.3.6 | Miter Gear Box | 2 | .64 | 1.28 | | | FARADA | | | | | |
| 2.3.7 | Translation Ball Screw | 2 | .40 | 0.80 | | | FARADA | | | | | |
| 2.3.8 | Bearing Assy. | 2 | .50 | 1.00 | | | FARADA | | | | | |
| 2.3.9 | Translation Ball Nut | 2 | .88 | 1.76 | | | FARADA | .155,31 | | .000,147,6 | | |
| 2.3.10 | Translation Tracks | 2 | .18 | 0.36 | | | FARADA | | | | | |
| 2.3.15 | Track Ball Bushings | 2 | .05 | .10 | | | FARADA | | | | | |
| 2.3.16 | Horiz. C.W. Drive Motor | 2 | 36.00 | 72.00 | | 0.020,151.5 | MILHDBK 217A | | | | | |
| 2.3.17 | Horiz. Harmonic Drive | 2 | 2.46 | 4.92 | | | FARADA (MODIFIED) | | | | | |
| 2.3.18 | Gear Box | 2 | .90 | 1.80 | | | FARADA | | | | | |
| 2.3.19 | Disc Brakes | 2 | 9.00 | 18.00 | | | FARADA (MODIFIED) | | | | | |
| 2.3.20 | Horiz. Ball Screw Assy. | 2 | .90 | 1.80 | | | FARADA | | | | | |
| 2.3.21 | Horiz. Ball Nut Assy. | 2 | .88 | 1.76 | | | FARADA | | | | | |
| 2.3.22 | Torque Tube, Horiz. | 2 | .18 | .36 | | | FARADA | | | | | |
| 2.3.23 | Horiz. Ball Bushings | 2 | .05 | .10 | 129.75 | | FARADA | | 950.25 | | 0.020,299,1 | 0.979,905,7 |

9

## Table 38. - Drive Systems Reliability (Cont'd)

| | | | OPERATIONAL PERIOD | | | | | DORMANT PERIOD | | | SUMMARY | |
|---|---|---|---|---|---|---|---|---|---|---|---|---|
| Number | Name | No.of Comp. Req'd $n$ | Fail. Rate (Oper) $\lambda \times 10^{-6}$ | No. Times Rate (Oper) $n\lambda \times 10^{-6}$ | Comp. Oper. Time - Hours $t_o$ | Expected No. of Fail. (Operational) $n\lambda t_o$ | Data Sources | No. Times Rate' (Dorm) $n\lambda' \times 10^{-6}$ | Comp. Dormant Time - Hours $t'$ | Expected No.of Fail. (Dormant) $n\lambda't'$ | $\Sigma n\lambda t$ (Init) | Reliab. |
| 2.4 | COUCH PIVOT DRIVE SYSTEM | | | | | | | | | | | |
| 2.4.1 | Drive Motor | 1 | 36.00 | 36.00 | 23.0 | | MILHDBK 217A | | 1057 | | | |
| 2.4.2 | Harmonic Drive | 1 | 2.46 | 2.46 | | | FARADA(MODIFIED) | | | | | |
| 2.4.3 | Gear Box | 1 | 1.11 | 1.11 | | | FARADA | | | | | |
| 2.4.4 | Disc Brakes | 1 | 9.00 | 9.00 | | 0.001,619,9 | FARADA(MODIFIED) | 0.07043 | | .000,078,5 | | |
| 2.4.5 | Torque Shafting Assy. | 2 | 2.37 | 4.74 | | | FARADA | | | | | |
| 2.4.6 | Bevel Gear | 2 | .24 | .48 | | | FARADA | | | | | |
| 2.4.7 | Pivot Bearing | 2 | .50 | 1.00 | | | FARADA | | 1057 | | | |
| 2.4.8 | Pivot Manual Override | 2 | 2.82 | 5.64 | 23.0 | | FARADA | | | | .001,698,4 | 0.9983030 |
| 2.5 | COUCH ROLL DRIVE SYSTEM | | | | | | | | | | | |
| 2.5.1 | Drive Motor | 1 | 36.00 | 36.00 | 58.0 | | MILHDBK 217A | | 1022 | | | |
| 2.5.2 | Spur Gear | 1 | 2.18 | 2.18 | | 0.002,279,4 | FARADA | 0.0393 | | .000,040,2 | | |
| 2.5.3 | Roll Ring Gear | 1 | .12 | .12 | | | FARADA | | 1022 | | | |
| 2.5.4 | Roller Assembly | 2 | .5 | 1.0 | 58.0 | | FARADA | | | | .002,319,6 | 0.9976830 |
| | | | | | | | | | | | $\Sigma$ 0.029,112,1 | 0.971,307,8 |

Table 39. - Power System Reliability Model

$$R_{ps}$$

```
        ┌──────────────────────┐
        │      POWER            │
        │      SYSTEM           │
        │                       │
        │      0.987683         │
        │                  3.0  │
        └──────────────────────┘
```

SYSTEM
— · — · — · — · — · — · — · — · — · —

```
┌──────────────────────┐           ┌ ─ ─ ─ ─ ─ ─ ─ ─ ─ ─ ┐
│      BATTERY          │           │  (UNDEFINED          │
│      SYSTEM           │           │   EXTERNAL           │
│     (ON-BOARD)        │───────────│   POWER              │
│                       │           │   SUPPLY)            │
│      0.987683         │           │                      │
│                  3.1  │           │                 3.2  │
└──────────────────────┘           └ ─ ─ ─ ─ ─ ─ ─ ─ ─ ─ ┘
```

SUBSYSTEMS
— · — · — · — · — · — · — · — · — · —

$$R_{ps} = 0.987683$$
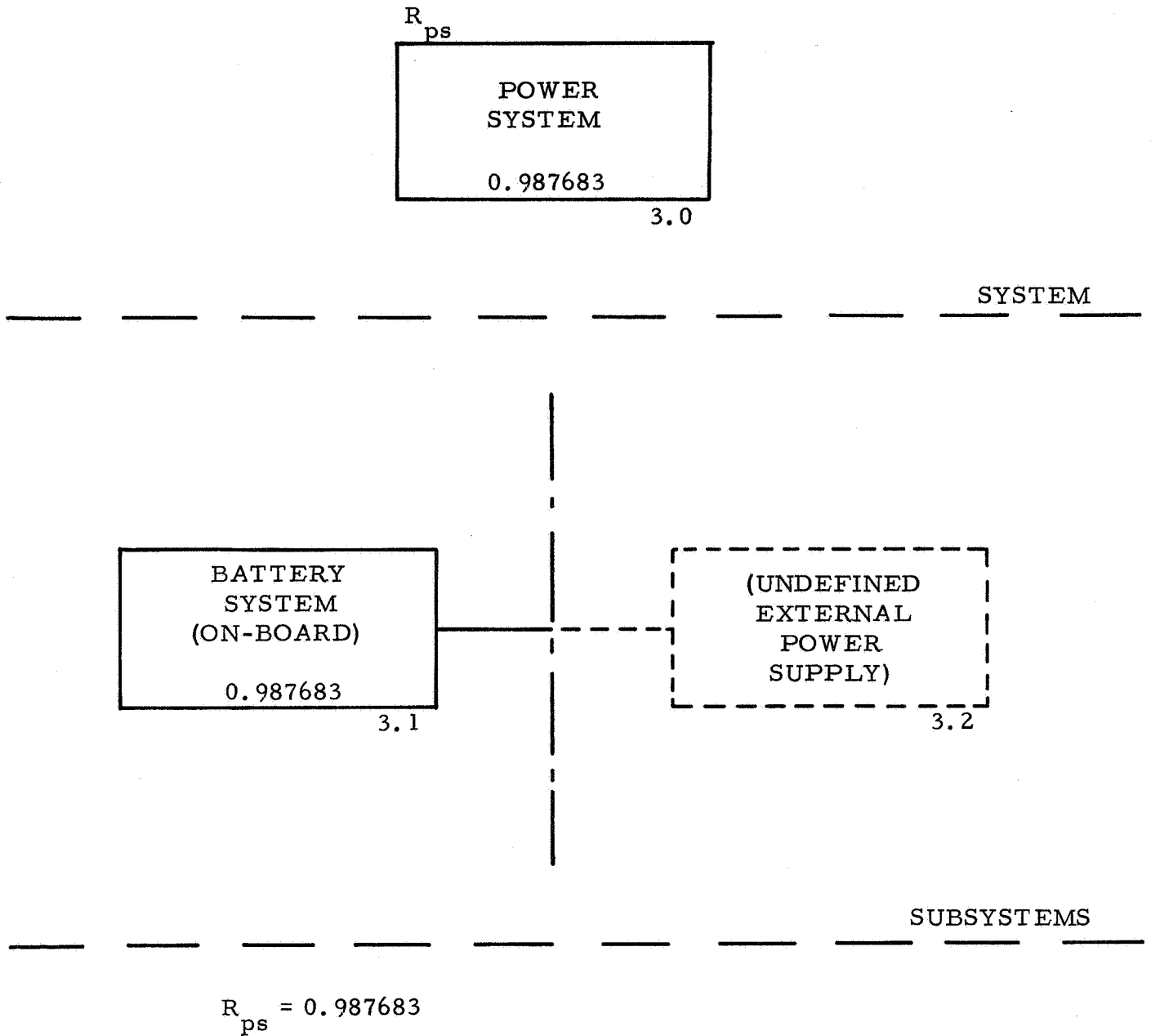
## Table 40. – Power Systems Reliability

| Number | Name | OPERATIONAL PERIOD | | | | | | DORMANT PERIOD | | | SUMMARY | |
|---|---|---|---|---|---|---|---|---|---|---|---|---|
| | | No.of Comp. Req'd $n$ | Fail. Rate (Oper) $\lambda \times 10^{-6}$ | No. Times Rate (Oper) $n\lambda \times 10^{-6}$ | Comp. Oper. Time-Hours $t_o$ | Expected No. of Fail. (Operational) $n\lambda t_o$ | Data Sources | No. Times Rate' (Dorm) $n\lambda' \times 10^{-6}$ | Comp. Dormant Time – Hours $t'$ | Expected No.of Fail. (Dormant) $n\lambda' t'$ | $\Sigma n\lambda t$ | Reliab. |
| *3.0 | POWER SYSTEM | | | | | | | | | | | |
| 3.1 | BATTERY SYSTEM | | | | | | | | | | | |
| 3.1.1 | Battery Cells | 80 | 0.1484 | 11.87 | 600 | 0.007,122,0 | ESTIMATE (BSM) | 0.01187 | 480 | 0.000,005,7 | | |
| 3.1.2 | Switch, Power Control | 1 | 2.0 | 2.0 | 153.5 | | FARADA | | | | | |
| 3.1.3 | Voltage Regulator | 1 | 8.1 | 8.1 | 153.5 | 0.005,234,4 | FARADA | 0.03410 | 926.5 | 0.000,031,6 | | |
| 3.1.4 | Power Inverter | 1 | 24.0 | 24.0 | 153.5 | | ESTIMATE (BSM) | | | | | |
| | | | | | | | | | | | 0.012,393,7 | 0.9876826 |

* Interface

Table 41. - Control Systems Reliability Model

$R_{cs}$

```
┌─────────────────────┐
│      CONTROL        │
│      SYSTEMS        │
│                     │
│     0.908505        │
└─────────────────────┘
```

— — — — — — — — — — — — — — — — SYSTEM

```
┌──────────────────┐    ┌──────────────────┐    ┌──────────────────┐
│    ROTATION      │    │      ARM         │    │     COUCH        │
│    CONTROL,      │───▶│   TRANSLATION    │───▶│     PIVOT        │
│   MAIN DRIVE     │    │    CONTROL       │    │    CONTROL       │
│    0.978038      │    │    0.996425      │    │    0.995825      │
└──────────────────┘    └──────────────────┘    └──────────────────┘
              4.1                     4.2                     4.3

       ┌──────────────────┐    ┌──────────────────┐
       │    DYNAMIC       │    │      COUCH        │
       │    BALANCER      │◀───│      ROLL         │
       │ CONTROL & CMG'S  │    │     CONTROL       │
       │    0.951056      │    │    0.984322       │
       └──────────────────┘    └──────────────────┘
                     4.5                     4.4
```

— — — — — — — — — — — — — — — — SUBSYSTEM
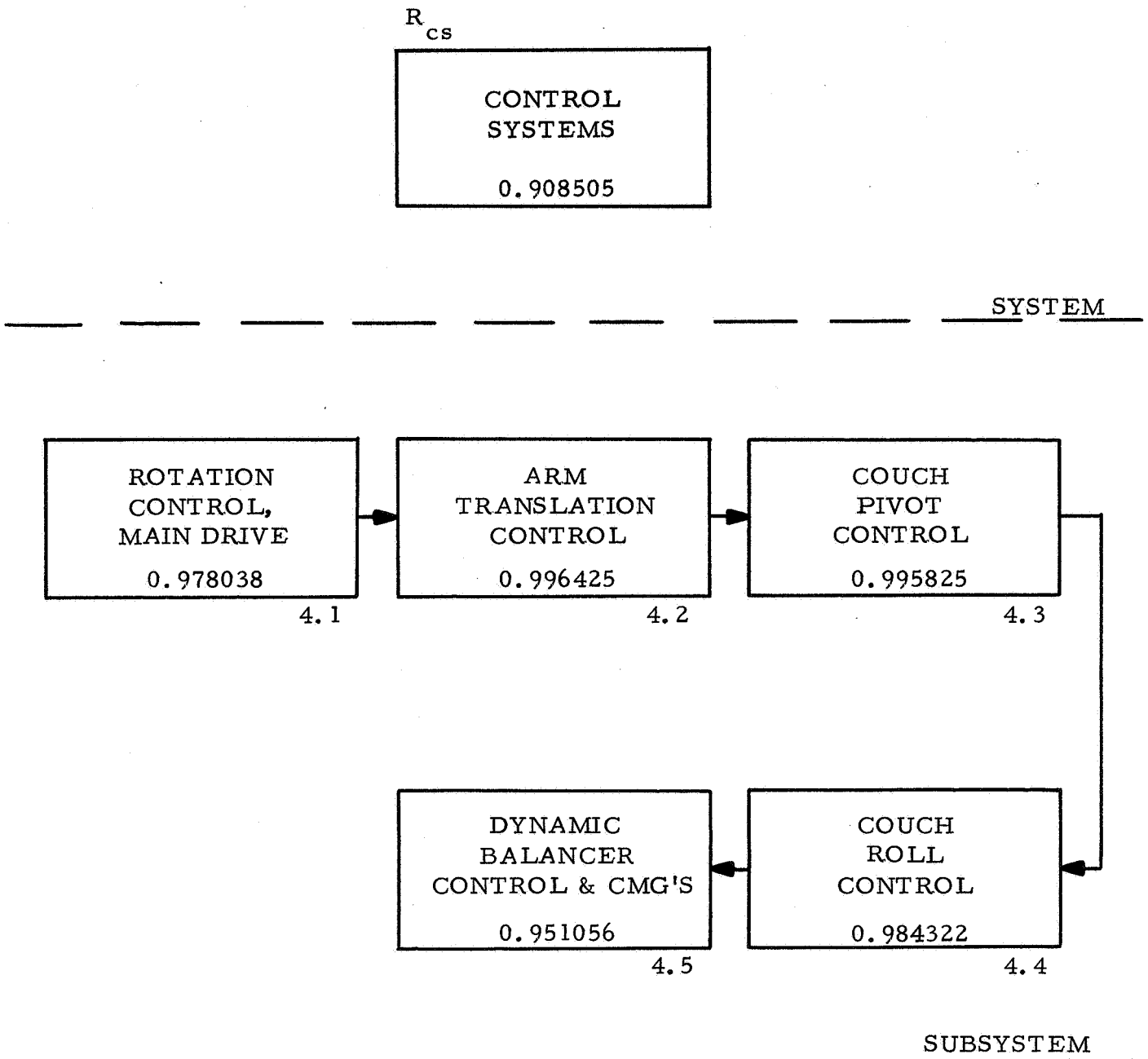
$$R_{cs} = R_{4.1} \times R_{4.2} \times R_{4.3} \times R_{4.4} \times R_{4.5} = 0.908505$$

## Table 42. – Control Systems Reliability

| | | | | | OPERATIONAL PERIOD | | | DORMANT PERIOD | | | SUMMARY | |
|---|---|---|---|---|---|---|---|---|---|---|---|---|
| Number | Name | No.of Comp. Req'd $n$ | Fail. Rate (Oper) $\lambda \times 10^{-6}$ | No. Times Rate (Oper) $n\lambda \times 10^{-6}$ | Comp. Oper. Time Hours $t_o$ | Expected No. of Fail. (Operational) $n\lambda t_o$ | Data Sources | No. Times Rate' (Dorm) $n'\lambda' \times 10^{-6}$ | Comp. Dormant Time – Hours $t'$ | Expected No.of Fail. (Dormant) $n\lambda' t'$ | $\Sigma n\lambda t$ | Reliab. |
| 4.0 | CONTROL SYSTEMS | | | | | | | | | | | |
| 4.1 | MAIN DRIVE ROTATION CONTR. | | | | | | | | | | | |
| 4.1.1 | Function Generator | 1 | 100.00 | 100.00 | 14.00 | 0.001,400,0 | APOLLO | .100 | 1066.00 | 0.000,106,0 | | |
| 4.1.2 | RPM Setting Register | 1 | 16.20 | 16.20 | 129.75 | | MILHDBK 217A/FARADA | | 950.25 | | | |
| 4.1.3 | Digital to Analog Converter | 1 | 8.78 | 8.78 | | | FARADA | | | | | |
| 4.1.4 | Auto/Manual Selector | 1 | 3.00 | 3.00 | | | FARADA | | | | | |
| 4.1.5 | Timer (Synchro.) | 1 | 1.50 | 1.50 | | | FARADA | | | | | |
| 4.1.6 | RPM Comparison Register | 1 | 5.00 | 5.00 | | | MILHDBK 217A/FARADA | | | | | |
| 4.1.7 | Digital Tach. & Readout | 1 | 25.00 | 25.00 | | | ESTIMATE | | | | | |
| 4.1.8 | SCR Motor Control | 1 | 24.00 | 24.00 | | | ESTIMATE (BSM) | | | | | |
| 4.1.9 | Time to Run Register | 1 | 6.71 | 6.71 | | 0.020,551,1 | FARADA | .15839 | | 0.000,150,5 | | |
| 4.1.10 | Running Time Readout | 1 | 4.20 | 4.20 | | | FARADA | | | | | |
| 4.1.11 | G-Profile Display | 1 | 50.00 | 50.00 | | | MILHDBK 217A | | | | | |
| 4.1.12 | Power Switch & Indicator | 1 | 3.00 | 3.00 | | | FARADA | | | | | |
| 4.1.13 | Motor Power Switch & Ind. | 1 | 3.00 | 3.00 | | | FARADA | | | | | |
| 4.1.14 | Brake Switch & Ind. Light | 1 | 3.0 | 3.0 | | | FARADA | | | | | |
| 4.1.15 | Interlock Lights, Hold or Go | 2 | 1.0 | 2.0 | | | FARADA | | | | | |
| 4.1.16 | Current Overload Light | 1 | 1.0 | 1.0 | | | FARADA | | | | | |
| 5.1.17 | Abort Indicator & Bell | 1 | 2.0 | 2.0 | 129.75 | | FARADA | | 950.25 | | 0.022,207,6 | 0.9780380 |
| 4.2 | ARM TRANSLATION CONTROL | | | | | | | | | | | |
| 4.2.1 | Limit Indicator, Arm Posit. | 2 | 1.0 | 2.00 | 129.75 | | FARADA | | | | | |
| 4.2.2 | Digital Readout, Arm Posit. | 1 | 4.2 | 4.20 | | | FARADA | | | | | |
| 4.2.3 | Motor Switches & Logic | 1 | 5.2 | 5.20 | | | FARADA | | | | | |
| 4.2.4 | Limit Switch | 3 | 1.0 | 3.00 | | 0.003,555,2 | FARADA | .0274 | 950.25 | 0.000,026,0 | | |
| 4.2.5 | Power Switch & Ind. Light | 1 | 2.0 | 2.00 | | | FARADA | | | | | |
| 4.2.6 | Indicator, Current Overload | 1 | 1.0 | 1.00 | | | FARADA | | | | | |
| 4.2.7 | Revolution Counter, Shaft | 1 | 10.0 | 10.00 | 129.75 | | FARADA (MODIFIED) | | 950.25 | | 0.003,581,2 | 0.9964253 |
| 4.3 | COUCH PIVOT CONTROL | | | | | | | | | | | |
| 4.3.1 | Indicator, Position | 1 | 4.2 | 4.20 | 129.75 | | FARADA | | | | | |
| 4.3.2 | Register & Position Selector | 1 | 6.2 | 6.20 | | | FARADA | | | | | |
| 4.3.3 | Logic Box | 1 | 5.01 | 5.01 | | | MILHDBK 217A | | | | | |
| 4.3.4 | Motor Controller | 1 | 9.6 | 9.60 | | | FARADA | | | | | |
| 4.3.5 | Limit Switches | 2 | 1.0 | 2.00 | | 0.004,153,3 | FARADA | 0.03201 | 950.25 | .000,030,4 | | |
| 4.3.6 | Encoder, Couch Attitude | 1 | 2.0 | 2.00 | | | FARADA (MODIFIED) | | | | | |
| 4.3.7 | Power Switch | 1 | 2.0 | 2.00 | | | FARADA | | | | | |
| 4.3.8 | Indicator, Current Overload | 1 | 1.0 | 1.00 | 129.75 | | FARADA | | 950.25 | | 0.004,183,7 | 0.9958251 |

Table 42. - Control Systems Reliability (Cont'd)

| Number | Name | OPERATIONAL PERIOD | | | | | Data Sources | DORMANT PERIOD | | | SUMMARY | |
|---|---|---|---|---|---|---|---|---|---|---|---|---|
| | | No.of Comp. Req'd $n$ | Fail. Rate (Oper) $\lambda \times 10^{-6}$ | No. Times Rate (Oper) $n\lambda \times 10^{-6}$ | Comp. Oper. Time Hours $t_0$ | Expected No. of Fail. (Operational) $n\lambda t_0$ | | No. Times Rate' (Dorm) $n\lambda' \times 10^{-6}$ | Comp. Dormant Time - Hours $t'$ | Expected No.of Fail. (Dormant) $n\lambda't'$ | $\Sigma n\lambda t$ | Reliab. |
| 4.4 | COUCH ROLL CONTROL | | | | | | | | | | | |
| 4.4.1 | Switch, Main Power | 1 | 1.0 | 1.00 | 129.75 | | FARADA | | 950.25 | | | |
| 4.4.2 | Logic Box, Arm | 1 | 40.4 | 40.40 | | | MILHDBK 217A | | | | | |
| 4.4.3 | Indicator, Current Overload | 1 | 1.0 | 1.00 | | | FARADA | | | | | |
| 4.4.4 | Switches, Motor Control | 6 | 1.0 | 6.00 | | 0.008,355,9 | FARADA | 0.06440 | | 0.000,061,2 | | |
| 4.4.5 | Switch, Manual Mode | 1 | 1.0 | 1.00 | | | FARADA | | | | | |
| 4.4.6 | Selector, Manual Position | 1 | 5.0 | 5.00 | | | FARADA | | | | | |
| 4.4.7 | Relay Assy., Motor Control | 1 | 10.0 | 10.00 | 129.75 | | FARADA | | 950.25 | | | |
| 4.4.8 | Switch, Automatic Mode | 1 | 1.0 | 1.00 | 65.16 | | FARADA | | 1014.84 | | | |
| 4.4.9 | Remote Control, Function Gen. | 1 | 3.0 | 3.00 | | | FARADA | | | | | |
| 4.4.10 | Indicator, Angular Posit. | 1 | 15.0 | 15.00 | | | VENDOR/ESTIMATE | | | | | |
| 4.4.11 | Indicator, Angular Velocity | 1 | 15.0 | 15.00 | | | VENDOR/ESTIMATE | | | | | |
| 4.4.12 | Indicator, Angular Accel. | 1 | 15.0 | 15.00 | | | VENDOR/ESTIMATE | | | | | |
| 4.4.13 | Indicator, Test No. | 1 | 4.2 | 4.20 | | 0.007,271,8 | FARADA | 0.11160 | | 0.000,113,2 | | |
| 4.4.14 | Indicator, Rotation Direc. | 2 | 1.0 | 2.00 | | | FARADA | | | | | |
| 4.4.15 | Indicator, Astronaut Test | 4 | 1.0 | 4.00 | | | FARADA | | | | | |
| 4.4.16 | Encoder, Position | 1 | 2.0 | 2.00 | | | FARADA (MODIFIED) | | | | | |
| 4.4.17 | Tachometer, Digital | 1 | 10.0 | 10.00 | | | FARADA (MODIFIED) | | | | | |
| 4.4.18 | Logic Box | 1 | 40.4 | 40.40 | 65.16 | | MILHDBK 217A | | 1014.84 | | 0.015,802,1 | 0.9843225 |
| 4.5 | DYNAMIC BALANCER CONTROLS | | | | | | | | | | | |
| 4.5.1 | Force Transducers | 6 | 12.0 | 72. | 75 | 0.005,400,0 | FARADA | .07200 | 1005 | .000,072,4 | | |
| 4.5.2 | Carrier Demodulator | 6 | 4.4 | 26.4 | 129.75 | | FARADA | | 950.25 | | | |
| 4.5.3 | Summing Networks | 4 | 2.0 | 8.00 | | | ESTIMATE | | | | | |
| 4.5.4 | Switches (SCR) Power | 3 | .35 | 1.05 | | | MILHDBK 217A | | | | | |
| 4.5.5 | Logic Boxes | 2 | 14.14 | 28.28 | | 0.011,616,5 | FARADA | | | | | |
| 4.5.6 | Switch, Main Power | 1 | 1.0 | 1.00 | | | FARADA | .08953 | | .000,085,1 | | |
| 4.5.7 | Mode Selector, Auto/Man. | 1 | 2.0 | 2.00 | | | FARADA | | | | | |
| 4.5.8 | Switches, CW Along Arm | 1 | 3.0 | 3.00 | | | FARADA | | | | | |
| 4.5.9 | Switches, CW Across Arm | 1 | 3.0 | 3.00 | | | FARADA | | | | | |
| 4.5.10 | Position Indicators, CW | 2 | 4.2 | 8.40 | | | FARADA | | | | | |
| 4.5.11 | Readouts, Force | 2 | 4.2 | 8.40 | 129.75 | | FARADA | | 950.25 | | | |
| 4.5.12 | Switch, CMG Power | 1 | 1.0 | 1.00 | | | FARADA | | 0 | | | |
| 4.5.13 | Switch, CMG Mode | 1 | 2.0 | 2.00 | | | FARADA | | 0 | | | |
| 4.5.14 | Lights, CMG RPM Indicator | 2 | 1.0 | 2.00 | | | FARADA | 0.0 | 0 | 0.0 | | |
| 4.5.15 | Readout, CMG Angular Pos. | 1 | 4.2 | 4.20 | | 0.031,536,0 | FARADA | | 0 | | | |
| 4.5.16 | Control Moment Gyro | 2 | 10.00 | 20.00 | 1080 | | FARADA | | | | | |
| 4.5.17 | Torque Motor and Gear | 1 | 3.0 | 3.00 | 129.75 | | FARADA | | 950.25 | | | |
| 4.5.18 | Computer | 1 | 1.04 | 1.04 | | | MILHDBK 217A | .01125 | | 0.000,010,7 | | |
| 4.5.19 | Resolver & Scaling Attenuat. | 1 | 6.20 | 6.20 | | 0.001,459,7 | FARADA (MODIFIED) | | | | | |
| 4.5.20 | Amplifier, Power | 1 | 1.01 | 1.01 | 129.75 | | MILHDBK 217A | | 950.25 | | .050,180,4 | .9510557 |

$$\Sigma = .095,955,0 \quad .9085054$$

15

Table 43. - Couch Instrumentation Reliability Model

$$R_{ci}$$

```
┌─────────────────────────┐
│                         │
│         COUCH           │
│    INSTRUMENTATION      │
│                         │
│        0.946270         │
│                         │
└─────────────────────────┘
                      5.0
```
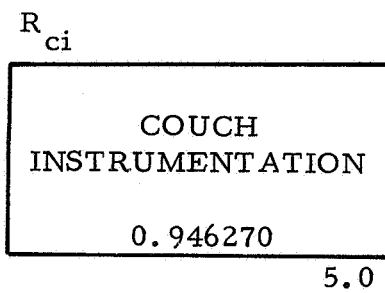
— — — — — — — — — — — — — — SYSTEM

$$R_{ci} = 0.946270$$

## Table 44. - Couch Instrumentation. Reliability

| | | | OPERATIONAL PERIOD | | | | | DORMANT PERIOD | | | SUMMARY | |
|---|---|---|---|---|---|---|---|---|---|---|---|---|
| Number | Name | No.of Comp. Req'd $n$ | Fail. Rate (Oper) $\lambda\times10^{-6}$ | No. Times Rate (Oper) $n\lambda\times10^{-6}$ | Comp. Oper. Time Hours $t_0$ | Expected No. of Fail. (Operational) $n\lambda t_0$ | Data Sources | No. Times Rate' (Dorm) $n\lambda'\times10^{-6}$ | Comp. Dormant Time – Hours $t'$ | Expected No.of Fail. (Dormant) $n\lambda't'$ | $\Sigma n\lambda t$ | Reliab. |
| 5.0 | COUCH INSTRUMENTATION | | | | | | | | | | | |
| 5.0.1 | Electrocardiogram +SC | 1 | 30.0 | 30.00 | 153.5 | | ESTIMATE | | 926.5 | | | |
| 5.0.2 | Body Temperature +SC | 1 | 30.0 | 30.00 | | | ESTIMATE | | | | | |
| 5.0.3 | Oral Temperature +SC | 1 | 30.0 | 30.00 | | | ESTIMATE | | | | | |
| 5.0.4 | Phonocardiogram +SC | 1 | 30.0 | 30.00 | | | ESTIMATE | | | | | |
| 5.0.5 | Pneumograph +SC | 1 | 30.0 | 30.00 | | | ESTIMATE | .31456 | | 0.000,291,4 | | |
| 5.0.6 | Electroculogram, Vert. +SC | 1 | 30.0 | 30.00 | | 0.048,285,0 | ESTIMATE | | | | | |
| 5.0.7 | Electroculogram, Horiz. +SC | 1 | 30.0 | 30.00 | | | ESTIMATE | | | | | |
| 5.0.8 | Ear Oximeter | 1 | 30.0 | 30.00 | | | ESTIMATE | | | | | |
| 5.0.9 | Blood Pressure, Bulb,etc.+SC | 1 | 30.0 | 30.00 | | | ESTIMATE | | | | | |
| 5.0.10 | Blood Pressure, Korothow | 1 | 30.0 | 30.00 | | | ESTIMATE | | | | | |
| 5.0.11 | Communications, MIC.& Headset1 | 1 | 11.76 | 11.76 | 153.5 | | FARADA | | 926.5 | | | |
| 5.0.12 | Accelerometer | 1 | 2.8 | 2.80 | | | FARADA | | | | | |
| 5.0.13 | Plethysmograph +SC | 1 | 30.0 | 30.00 | 88.33 | 0.002,649,9 | ESTIMATE | .03000 | 991.67 | 0.000,029,8 | | |
| 5.0.14 | Perception Response Equip. | 1 | 10.0 | 10.00 | 65.16 | 0.000,651,6 | ESTIMATE | .01000 | 1014.84 | 0.000,010,1 | | |
| 5.0.15 | Parameter Light Set | 1 | 3.13 | 3.13 | 6.20 | 0.000,019,4 | FARADA | .00313 | 1073.80 | 0.000,003,4 | | |
| 5.0.16 | EVLH | 1 | 10.00 | 10.00 | 1.16 | 0.000,011,6 | ESTIMATE | .01000 | 1078.84 | 0.000,010,8 | | |
| 5.0.17 | NVDI | 1 | 10.00 | 10.00 | 1.16 | 0.000,011,6 | ESTIMATE | .01000 | 1078.84 | 0.000,010,8 | | |
| 5.0.18 | Counter Rolling Camera | 1 | 25.00 | 25.00 | 49.16 | 0.001,229,0 | FARADA (MODIFIED) | .02500 | 1030.84 | 0.000,025,8 | | |
| 5.0.19 | V&H Nystagmogram | 1 | 30.00 | 30.00 | 65.16 | 0.001,954,8 | ESTIMATE | .03000 | 1014.84 | 0.000,030,4 | 0.055,225,4 | 0.946,270,2 |

## Table 45. - Communications Reliability Model

$$R_{com}$$

```
┌─────────────────────────┐
│     COMMUNICATIONS      │
│                         │
│        0.821093         │
│                    6.0  │
└─────────────────────────┘
```

SYSTEM
─ ─ ─ ─ ─ ─ ─ ─ ─ ─ ─ ─ ─ ─ ─ ─ ─ ─ ─ ─ ─ ─ ─

```
┌──────────────┐    ┌──────────────┐    ┌──────────────┐
│   INTER-     │ →  │  TELEVISION  │ →  │   MEDICAL    │
│COMMUNICATIONS│    │              │    │   DISPLAYS   │
│              │    │              │    │              │
│  0.825405    │    │  0.997409    │    │  0.998722    │
│         6.1  │    │         6.2  │    │         6.3  │
└──────────────┘    └──────────────┘    └──────────────┘

┌ ─ ─ ─ ─ ─ ─ ┐    ┌ ─ ─ ─ ─ ─ ─ ┐    ┌──────────────┐
│  TELEMETRY  │    │    DATA     │    │    ROTARY    │
│   SYSTEM    │    │  RECORDER   │    │  CAPACITORS  │
│             │    │     &       │    │              │
│             │    │  PLAYBACK   │    │  0.998636    │
│        6.6  │    │        6.5  │    │         6.4  │
└ ─ ─ ─ ─ ─ ─ ┘    └ ─ ─ ─ ─ ─ ─ ┘    └──────────────┘
```

SUBSYSTEM
─ ─ ─ ─ ─ ─ ─ ─ ─ ─ ─ ─ ─ ─ ─ ─ ─ ─ ─ ─ ─ ─ ─
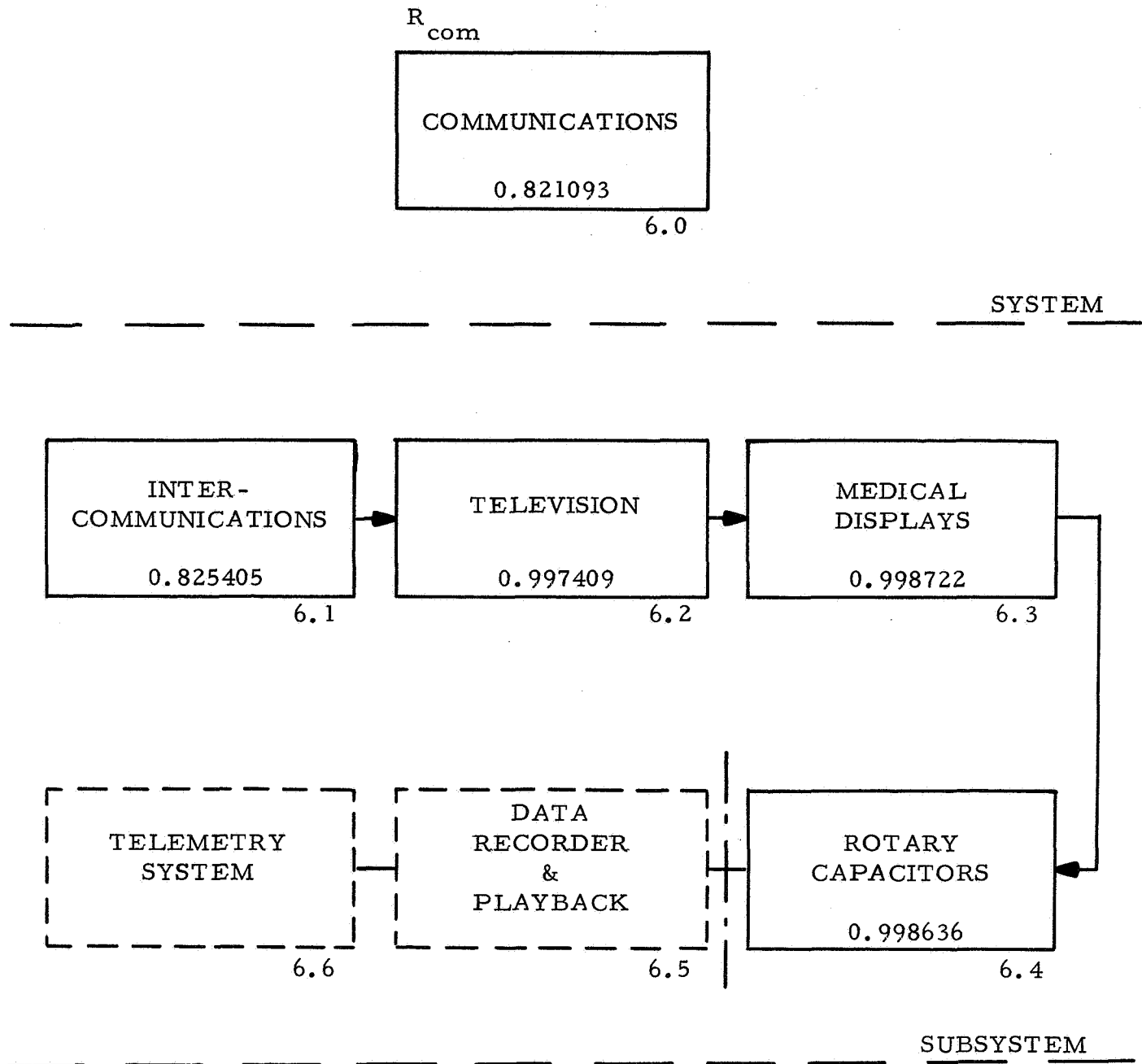
$$R_{com} = R_{6.1} \times R_{6.2} \times R_{6.3} \times R_{6.4} = 0.821093$$

## Table 46. – Communication Reliability

| | | | | OPERATIONAL PERIOD | | | | DORMANT PERIOD | | | SUMMARY | |
|---|---|---|---|---|---|---|---|---|---|---|---|---|
| Number | Name | No.of Comp. Req'd $n$ | Fail. Rate (Oper) $\lambda$x10^-6 | No. Times Rate (Oper) $n\lambda$x10^-6 | Comp. Oper. Time Hours $t_o$ | Expected No. of Fail. (Operational) $n\lambda t_o$ | Data Sources | No. Times Rate' (Dorm) $n\lambda'$x10^-6 | Comp. Dormant Time – Hours $t'$ | Expected No.of Fail. (Dormant) $n\lambda't'$ | $\Sigma n t$ | Reliab. |
| 6.0 | COMMUNICATIONS | | | | | | | | | | | |
| 6.1 | INNERCOMMUNICATION | | | | | | | | | | | |
| 6.1.1 | Subcarrier Oscillators | 10 | 6.96 | 69.60 | 153.5 | | VENDOR, CONIC APOLLO | | | | | |
| 6.1.2 | Time Multiplexer | 1 | 320. | 320.00 | | | FARADA | 1.24217 | 926.5 | 0.001,150,9 | | |
| 6.1.3 | Audio Amplifier | 2 | 12.0 | 24.00 | | | VENDOR, CONIC | | | | | |
| 6.1.4 | Mixer Amplifier | 1 | 4.70 | 4.70 | | 0.190,673,0 | VENDOR, EMR | | | | | |
| 6.1.5 | Discriminators | 8 | 66.7 | 533.60 | | | ESTIMATE | | | | | |
| 6.1.6 | Signal Conditioners | 4 | 69.6 | 278.40 | | | FARADA | | | | | |
| 6.1.7 | Speaker | 1 | 1.07 | 1.07 | 153.5 | | FARADA | | | | | |
| 6.1.8 | Microphone | 1 | 10.8 | 10.80 | | 0.000,050,4 | VENDOR (MODIFIED) | .0063 | 926.5 | 0.000,006,8 | | |
| 6.1.9 | Low Power FM Transmitter | 1 | 3.6 | 3.6 | 8.0 | | VENDOR (MODIFIED) | | 1072.0 | | | |
| 6.1.10 | Low Power FM Receiver | 1 | 2.7 | 2.7 | 8.0 | | | | 1072.0 | | | |
| 6.2 | TELEVISION | | | | | | | | | | | |
| 6.2.1 | Camera & Transmitter | 1 | 8.4 | 8.4 | 153.5 | 0.002,578,8 | FARADA (MODIFIED) | 0.1068 | 926.5 | 0.000,015,6 | | |
| 6.2.2 | Receiver | 1 | 8.4 | 8.4 | 153.5 | | FARADA (MODIFIED) | | 926.5 | | | |
| 6.3 | MEDICAL DISPLAYS | | | | | | | | | | | |
| 6.3.1 | Indicator, Heart Rate | 2 | 1.38 | 2.76 | 153.5 | | FARADA | | 926.5 | | | |
| 6.3.2 | Indicator, Respiration | 2 | 1.38 | 2.76 | 153.5 | 0.001,271,0 | FARADA | .00828 | 926.5 | 0.000,007,7 | | |
| 6.3.3 | Indicator, Blood Press. | 1 | 1.38 | 1.38 | 153.5 | | FARADA | | 926.5 | | | |
| 6.3.4 | Indicator, Rotation Dir. | 1 | 1.38 | 1.38 | 153.5 | | FARADA | | 926.5 | | | |
| 6.4 | ROTARY CAPACITORS | 4 | 2.21 | 8.84 | 153.5 | 0.001,356,9 | FARADA | .00884 | 926.5 | 0.000,008,2 | | |
| | | | | | | | | | | | 0.197,119,3 | 0.8210927 |

Table 47. - Failure Modes Analysis

FUNCTION: PRIMARY ROTATION Po = .0257053

| FAILURE MODE | TRAJECTORY PHASE | FMFR | FAILURE EFFECT | RECOMMENDED CREW ACTION | REACTION TIME | CLASS | Po/1000 FLIGHTS | CENTRIFUGE MODIFICATION OR REMARKS |
|---|---|---|---|---|---|---|---|---|
| Motor failure | Orbit | 15% | Unable to drive centrifuge | Abort mission. If centrifuge turning, apply mechanical brake. | 5 min. | A | 3.85579 | |
| Motor control failure | Orbit | 35% | Unable to control speed | Abort mission. If centrifuge turning, apply mechanical brake. | 5 min. | A | 8.99686 | Possibly repairable by astronaut crew. |
| Brake failure | Orbit | 5% | Minor. Unable to mechanically slow down centrifuge. | Set manual control to .5 RPM and then switch off power to motor after obtaining .5 RPM speed. | 5 min. | M | 1.28527 | Repairable by astronaut crew. |
| Function generator failure | Orbit | 15% | Minor. Reentry simulation not possible. | Switch to manual control. | 5 min. | M | 3.85579 | |
| Digital tachometer failure | Orbit | 10% | No knowledge of RPM. | Abort mission. Apply mechanical brake. | | A | 2.57053 | Replaceable by astronaut crew. |
| Astronaut abort interlock failure | Orbit | 10% | Astronaut on couch; unable to select abort (except by voice.). | Abort mission. Stop centrifuge and investigate cause of failure. | 5 min. | A | 2.57053 | Probably repairable. |
| Manual control failure | Orbit | 10% | Minor; 1/2 of experiments not feasible. | Operate with automatic control. | 5 min. | M | 2.57053 | Carry tapes for automatic control of all experiments (repair manual control). |

## Table 47. – Failure Modes Analysis (Cont'd)

FUNCTION: RADIUS ARM TRANSLATION    Po = .0099013

| FAILURE MODE | TRAJECTORY PHASE | FMFR | FAILURE EFFECT | RECOMMENDED CREW ACTION | REACTION TIME | CLASS | Po/1000 FLIGHTS | CENTRIFUGE MODIFICATION OR REMARKS |
|---|---|---|---|---|---|---|---|---|
| (1) Bearing and/or gear box failure during semi-circular canal experiment:<br><br>Arm Free | Orbit | 10% | Arm extends to full stroke – subject & couch impacts wall of module | Abort – aid subject; trouble-shoot damage. If arm can be moved, place in safe position & use manual locks. Continue other experiments. | 1 Sec | C | .99013 | Redundant manual locks are engaged in all other experiments. |
| Arm freezes | Orbit | 25% | Experiment abort. Mission may be aborted. | Trouble shoot. Free arm and use manual locks if possible. | 30 Sec | A or C | 2.47532 | Gear box failures of this type would not be violent due to slow potential speeds. |
| (2) Motor failure: No Spark | Orbit | 25% | Experiment aborted. | Lock arm & proceed with other experiments. | 30 Sec | A | 2.47532 | |
| Electrical fire. | Orbit | 5% | Catastrophic | Abort – extinguish fire. Isolate chamber. | 5–10 Sec | C | .49506 | |
| (3) Control system failure, tolerance | Orbit | 30% | Data not valid | Adjust and/or calibrate. | Hours | M | 2.97039 | |
| (4) Control system failure, Runaway system erratic operation. | Orbit | 5% | Same as (1) above. | Same as (1) above. | 1 Sec. | A or C | .49506 | |

## Table 47. - Failure Modes Analysis (Cont'd)

FUNCTION: COUCH ROLL    $P_o$ = .0196100

| FAILURE MODE | TRAJ. PHASE | FMFR | FAILURE EFFECT | RECOMMENDED CREW ACTION | REACTION TIME | CLASS | Po/1000 FLIGHTS | CENTRIFUGE MODIFICATION OR REMARKS |
|---|---|---|---|---|---|---|---|---|
| Bearing Failure | Orbit | 30% | Couch roll aborted; crew safe. | Lock couch roll syst. - Continue with other experiments. | Before Running SRC | A | 5.88300 | The higher "G" level experiments may have to be aborted depending on the nature of bearing failure. |
| Manual Lock Fails During Test | " | 5% | Couch free to roll; possible illness or discomfort to test subject. | Abort experiment; provide aid to test subject; if required examine lock & secure couch roll. | 30 Sec. to abort. | A | .98050 | |
| Gear Failure | " | 5% | Couch roll abort. | Lock couch syst.; continue other experiments. | Before Running SRC | A | .98050 | |
| Motor Failure (No spark) | " | 25% | Same as above. | Same as above. | " | A | 4.90250 | |
| Motor Elec. Failure (fire) | | 5% | Catastrophic; crew in oxygen rich atmosphere. | Abort experiment; extinguish fire if possible; get out of chamber; if possible seal hatches between modules. | 5-10 sec. | C | .98050 | Non-metallic, flamable materials will be avoided to the maximum extent possible; motors are sealed units. |
| Control System Failure - (Minor tolerance) | " | 25% | Experiment data not valid. | Adjust and/or calibrate controls; rerun experiment. | Hours. | M | 4.90250 | |
| Control System Failure - Run Away - Erratic Operation | " | 5% | Subject could become sick; experiment data not valid. | Abort experiment; aid subject; trouble shoot syst. fix or lock out and continue other experiments. | 30 Sec. | A | .98050 | |

Table 47. - Failure Modes Analysis (Cont'd)

FUNCTION: COUCH PIVOT    $P_o$ = .0064723

| FAILURE MODE | TRAJ. PHASE | FMFR | FAILURE EFFECT | RECOMMENDED CREW ACTION | REACTION TIME | CLASS | Po/1000 FLIGHTS | CENTRIFUGE MODIFICATION OR REMARKS |
|---|---|---|---|---|---|---|---|---|
| Bearing Failure | Orbit | 30% | Experiments using pivot drive would have to be aborted; the crew would be safe. | Abort test - place pivot frame in manual lock position & proceed with other experiments. | Before Running | A | 1.94169 | Manual lock system bypasses all bearings. |
| Gear Failures | " | 5% | Same as above | Same as above | " | A | .32361 | |
| Manual Lock Failure | " | 5% | Possible injury to test subject & major equipment damage. | Abort test; aid test subject evaluate damage. | 5-10 secs. | C | .32361 | A catastrophic failure could only occur during experiments where the arm is extended. Two locks are provided - one on each side of pivot. |
| Motor Failure (no spark) | " | 25% | Experiments using pivot drive would be aborted. | Use manual locks & continue with other tests. | 5-10 secs. | A | 1.61807 | |
| Motor &/or Elec. Fire | " | 5% | Catastrophic - crew in danger. | Abort experiment; extinguish fire; evacuate chamber. | 5-10 secs. | C | .32361 | Non Metallic, flamable materials will be avoided to the maximum extent possible. |
| Control System Failure (Minor) Tolerances - | " | 25% | Experiment data not valid. | Adjust &/or calibrate re-run tests. | | A | 1.61807 | |
| Erractic Operation Runaway System | " | 5% | Abort tests using pivot drive. | Use manual locks & continue with other tests. | 15 secs. | A | .32361 | Motions would be very slow due to large gear reductions. |

Table 47. - Failure Modes Analysis (Cont'd)

## FUNCTION: STRUCTURAL INTEGRITY

Structural failure modes fall into relatively few categories, groups of which are applicable to each structural element.

The primary failure modes as listed below are shown on the F.E.A. Summary Sheets.

| Mode | Code | Remarks |
|---|---|---|
| Fastener Fracture | FF | Includes weld failures and excessive loosening of joints. |
| Material Fracture | MF | Includes cracking. |
| Material Yield | MY | Includes crushing, brinelling, etc. |
| Material Wear | MW | Same as above |
| Compression Buckling | CB | Applicable to beam flanges and skin stiffeners. |
| Compression Crippling | CC | Same as above. |
| Shear Buckling | SB | Applicable to skin panels. |

## Table 47. – Failure Modes Analysis (Cont'd)

FUNCTION: STRUCTURAL INTEGRITY    Po = .0031694

| COMPONENT | FAILURE MODE | FAILURE DISTRIB Assy.% | Mode % | FMFR 10% | FAILURE EFFECT | RECOMMENDED CREW ACTION | RE-ACTION TIME | CLASS | P0/1000 FLIGHTS | CENTRIFUGE MODIFICATION OR REMARKS |
|---|---|---|---|---|---|---|---|---|---|---|
| ● Main rotation box Main drive attachment Fittings – FF | FF | 30 | 50 | 1.5 | Min: Vibration / Max: Separation or rotating mass. | slow centrifuge to a stop. / Station emergency proced. | Secs. / None | A / C | .04754 | Multiple redundancy required. |
| | MY | | 35 | 1.05 | Vibration / Geometrical misalignment. | Stop centrifuge, perform unmanned slow speed test to eval. | Secs. | A | .03328 | High margins of safety required. |
| | MF | | 15 | .45 | Separation or rotating mass | Station emergency proced. | None | C | .01426 | Same as above. |
| End Frames – FF | FF | 10 | 45 | .45 | Min: Same as above / Max: Same as above | same / Same | Secs. / None | A / C | .01426 | Multiple redundancy required. |
| | MY | | 35 | .35 | Vibration; geom. misalign; translation mech. bind. | Stop centrifuge, perform unmanned slow speed eval. test. | Secs. | A | .01109 | High margins required. |
| | MF | | 10 | .1 | Separation of rotating mass. | Station emergency proced. | None | C | .00317 | Same as above. |
| | CB,CC | | 10 | .1 | Reduced frame strength | Stop centrifuge | None | M or A | .00317 | |
| Skin Panels –FF | FF | 20 | 20 | .4 | Higher local loads on adjacent fasteners; loose parts. | Stop centrifuge | Secs/ None | M or A | .01268 | Evaluate cause & extent of failure – abort if due to normal load condition. |
| | CB | | 35 | .7 | Panel deformity, possible interference. | Stop centrifuge | None | M or A | .02219 | Evaluate cause; if due to normal load condition, abort to avoid repeat. |
| | CC | | 15 | .3 | Permanent panel deformity. reduced panel strength. | Stop centrifuge | None | A | .00951 | |
| | SB | | 30 | .6 | Temporary deformity. | Stop centrifuge | None | M or A | .01902 | Probably OK if only occurs during emerg. Stop mode if no permanent deformity. |
| Beam Assy-Arm Drive Screw end brg. support | FF | 15 | 30 | .45 | Loose parts, loss of drive screw preload. | Stop centrifuge | Secs/ None | A | .01426 | Multiple redundancy required. |
| | MY | | 15 | .22 | Loss of drive screw preload. | Stop centrifuge | None | A | .00697 | High margins required. |
| | MF | | 5 | .08 | Loose parts, loss of drive screw preload. | Stop centrifuge | Secs/ None | A | .00254 | " |
| | CB | | 30 | .45 | Temporary deformity possible, interference with arm/cwt. | Stop centrifuge | None | M or A | .01426 | Evaluate cause; if due to normal load condition, abort to avoid repeat. |
| | CC | | 20 | .30 | Permanent deformity; reduced load carrying capability. | Stop centrifuge | None | A | .00951 | |
| Misc. Fittings – FF | FF | 25 | 50 | 1.25 | Loose parts; loss of cwt drive screw preload; increased arm support loads. | Stop centrifuge | Secs/ None | A | .03962 | Multiple redundancy required. |
| | MY | | 35 | .88 | Geom. misalign, possible trans. mech. binding. | Stop centrifuge; perform slow speed unmanned eval. test. | None | M or A | .02789 | Good margins required. |
| | MF | | 15 | .37 | Loose parts; loss of cwt drive screw preload; higher loads elsewhere. | Stop centrifuge | Secs/ None | A or C | .01173 | Multiple failure could possibly result in loss of arm support capability. |

Table 47. - Failure Modes Analysis (Cont'd)

FUNCTION: STRUCTURAL INTEGRITY (Cont'd)

| COMPONENT | FAILURE MODE | FAILURE DISTRIB Assy. % | Mode % | FMFR | FAILURE EFFECT | RECOMMENDED CREW ACTION | REACTION TIME | CLASS | Po/1000 FLIGHTS | CENTRIFUGE MODIFICATION OR REMARKS |
|---|---|---|---|---|---|---|---|---|---|---|
| **Drive Frame Assy.** | | | | 20% | | | | | | |
| Cwt guide rails - MW | | 40 | 50 | 4.0 | Binding of mech; looseness in mech; loss of hardness in rail. | Stop centrifuge | Hours/days | A | .12678 | Good margin on operational life required. |
| | MY | | 35 | 2.8 | Binding of mech. | Stop centrifuge | None | A | .08874 | Good stress margins required. |
| | MF | | 15 | 1.2 | Separation of cwt from guide rail. | Emergency stop. | Seconds/None | C | .03803 | " |
| Beam Cap Assys. - FF | | 15 | 25 | .75 | Increased load on adjacent fasteners; possible overload. | Stop centrifuge | Seconds/None | M or A | .02377 | Mult. redundancy required. |
| | MY | | 25 | .75 | Binding of mech. | Stop centrifuge | None | A | .02377 | High margins required. |
| | MF | | 10 | .30 | Possible subsequent guide rail failure. | Stop centrifuge | Seconds/None | A or C | .00951 | " |
| | CB | | 15 | .45 | Temporary deformity binding of mech. | Stop centrifuge | None | M or A | .01426 | Eval. cause: if due to normal load condition, abort to avoid repeat. |
| | CC | | 25 | .75 | Permanent deformity; binding of mech. | Stop centrifuge | None | A | .02377 | |
| Skin panels - FF | | 30 | 15 | .90 | Increased local loads on adjacent fasteners; loose parts. | Stop centrifuge | Seconds/None | M or A | .02852 | Evaluate cause and extent. |
| | CB | | 40 | 2.4 | Temporary panel deformity; possible interference. | Stop centrifuge | None | M or A | .07607 | " |
| | CC | | 30 | 1.8 | Permanent panel deformity reduced strength. | Stop centrifuge | None | A | .05705 | |
| | SB | | 15 | .9 | Temporary deformity. | Stop centrifuge | None | M or A | .02852 | Eval. cause: probably OK if no deformity & only occurs during emergency stop. |
| Drive assy. attach. - FF | | 15 | 100 | 3.0 | Loose parts; loss of radial cwt suppt/possible loss of cwt. | Stop centrifuge | Seconds/None | A or C | .09508 | Mult. redundancy required. |
| **Counterweights** **Trans. nut support** | | | | 5% | | | | | | |
| Beams - FF | | 100 | 30 | 1.5 | Loss of cwt suppt/possible loss of cwt. | Stop centrifuge | Seconds to None | A or C | .04754 | Mult. redundancy required. |
| | MY | | 15 | .75 | Misalignment of drive nut; possible mech. bind. | Stop centrifuge | None | A | .02377 | High Margins required. |
| | MF | | 5 | .25 | Loss of cwt suppt; possible loss of cwt. | Stop centrifuge | Seconds/None | A or C | .00792 | " |
| | CB | | 30 | 1.5 | Temporary deformity; possible interference. | Stop centrifuge | None | M or A | .04754 | Eval. cause. |
| | CC | | 20 | 1.0 | Permanent deformity; reduced strength. | Stop centrifuge | None | A | .03169 | |

Table 47. - Failure Modes Analysis (Cont'd)

FUNCTION: STRUCTURAL INTEGRITY (Cont'd)

| COMPONENT | FAILURE MODE | FAILURE DISTRIB Assy.% | Mode % | FMFR 25% | FAILURE EFFECT | RECOMMENDED CREW ACTION | REACTION TIME | CLASS | Po/1000 FLIGHTS | CENTRIFUGE MODIFICATION OR REMARKS |
|---|---|---|---|---|---|---|---|---|---|---|
| ● Translation Arm Guide Rails - | MW | 30 | 50 | 3.75 | Binding or looseness in mech. loss of surface hardness. | Stop Centrifuge. | Hours/Days | A | .11885 | Good margin in operational life required. |
| | MY | | 35 | 2.62 | Binding of mech. | " | None | A | .08304 | Good stress margins required. |
| | MF | | 15 | 1.12 | Separation of arm from main rotation box. | " | Seconds/None | C | .03550 | " |
| Beam cap assys - | FF | 15 | 45 | 1.69 | Increased load on adjacent fasteners. | " | Seconds/None | M or A | .05356 | Mult. redundancy required. |
| | MY | | 25 | .94 | Binding of mech. | " | None | A | .02979 | Good stress margins required. |
| | MF | | 10 | .37 | Possible subsequent guide rail failure. | " | Seconds/None | A or C | .01173 | " |
| | CB | | 10 | .38 | Temporary deformity - Binding of mech. | " | None | M or A | .01204 | Eval. cause. |
| | CC | | 10 | .38 | Permanent deformity - binding of mech. | " | None | A | .01204 | |
| Skin Panels - | FF | 25 | 15 | .94 | Increased local loads on adjacent fasteners. | " | Seconds/None | M or A | .02979 | Eval. cause and extent. |
| | CB | | 40 | 2.50 | Temp. panel deformity; possible interference. | " | None | M or A | .07924 | Eval. cause. |
| | CC | | 30 | 1.88 | Permanent panel deformity. | " | None | A | .05958 | |
| | SB | | 15 | .94 | Reduced strength. Temp. panel deformity. | " | None | M or A | .02979 | OK if no permanent deformity & occurs during emergency. stop only. |
| Fwd Pivot Gear Box Support Frames - | FF | 20 | 35 | 1.75 | Vibration, increased loads on adjacent fasteners; possible sep'n. of pivots. | " | Seconds/None | A or C | .05546 | Mult. redundancy required. |
| | MY | | 25 | 1.25 | Possible misalignment. | " | None | A | .03962 | Good stress margins required. |
| | MF | | 10 | .5 | Sep'n of pivot assys. | Station emergency procedure. | Seconds/None | C | .01585 | " |
| | CB | | 10 | .5 | Temporary deformity. | Stop Centrifuge. | None | M or A | .01555 | Eval. cause. |
| | CC | | 20 | 1.0 | Permanent deformity; reduced strength. | " | None | A | | |
| Lateral Bulkhds. - | FF | 5 | 30 | .38 | Reduced stiffness of box higher loads on other fastnrs. | " | Seconds/None | M or A | .01204 | Eval. cause and extent. |
| | SB | | 70 | .88 | Temporary deformity. | " | None | M or A | .02789 | OK if no permanent deformity & occurs during emer. stop only. |
| Trans Nut Support Beam Assy - | FF | 5 | 40 | .50 | Loss of arm trans. control; possible loss of arm restraint. | " | Seconds/None | A or C | .01585 | Mult. redundancy required. |
| | MY | | 25 | .30 | Misalignment of trans. mech. | " | None | A | .00951 | Good stress margins required. |
| | MF | | 10 | .12 | Loss of arm restraint. | " | Seconds/None | A or C | .00380 | " |

Table 47. – Failure Modes Analysis (Cont'd)

FUNCTION: STRUCTURAL INTEGRITY (cont'd)

| COMPONENT | FAILURE MODE | FAILURE DISTRIB | FMFR | FAILURE EFFECT | RECOMMENDED CREW ACTION | REACTION TIME | CLASS | Po/1000 FLIGHTS | CENTRIFUGE MODIFICATIONS OR REMARKS |
|---|---|---|---|---|---|---|---|---|---|
| Beam Assy – | CB | 15 | .19 | Temp. deformity. | Stop Centrifuge | None | M or A | .00602 | Eval. cause. |
|  | CC | 10 | .12 | Permanent deformity; reduced strength. | " | None | A | .00380 | " |
| ● Pivot Segments |  | 5% |  |  |  |  |  |  |  |
|  | FF | 100 30 | 1.5 | Loss of roller support. | " | Seconds/ | A | .04754 | Good margin required in roller attach design. |
|  | MY | 50 | 2.5 | Vibration/looseness in roll mech; aggravated wear. | " | None | A | .07924 | Good stress margins required. |
|  | MF | 20 | 1.0 | Loss of roller support; possible loss of roll frame. | " | Seconds/ None | A or C | .03169 | " |
| ● Roll Frame Basic Box – |  | 15% |  |  |  |  |  |  |  |
|  | FF | 20 30 | .9 | Possible collapse of roll frame. | " | Seconds/ None | A or C | .02852 |  |
|  | MY | 50 | 1.5 | Binding of roll mech. | " | None | A | .04754 |  |
|  | MF | 20 | .6 | Possible collapse of frame and/ or loss of couch restraint. | " | Seconds/ None | A or C | .01902 |  |
| Roller Track | FF | 45 30 | 2.03 | Higher loads on adjacent fastnrs; possible loss of roller supt. | " | Seconds/ None | A or C | .06434 |  |
|  | MY | 30 | 2.03 | Vibration/looseness in roll mech; aggravated wear/noise. | " | None | A | .06434 |  |
|  | MF | 10 | .68 | Possible loss of roll frame. | " | Seconds/ | C | .02155 |  |
|  | MW | 30 | 2.03 | Vibration, looseness, noise. | " | Hours/ Days | A | .06434 |  |
| Couch Support Beams | FF | 35 50 | 2.62 | Higher loads on adjacent fastnrs; possible loss of couch. | " | Seconds/ None | A or C | .08304 |  |
|  | MY | 35 | 1.83 | Binding in couch trans. mech. | " | None | A | .05800 |  |
|  | MF | 15 | .78 | Possible loss of couch. | " | Seconds/ None | C | .02472 |  |
| ● Drive Hub Hub Attach Ring Reaction Lugs – |  | 20% |  |  |  |  |  |  |  |
|  | MF | 10 10 | .2 | Loss of counter balance control; possible progressive separation vibration. | " | Seconds/ None | A or C | .00614 | Possible early indication from vibration & monitor of sensors. High stress margins required. |
|  | MW | 80 | 1.6 | Wear at stops. eventual over-load of counterbalance sensor. | Invest. cause. | Minutes | M | .05971 | Large wear surfaces req'd low stress level. Actual cause would be from over-limit drive torques or crew inadvertently creating excessive dynamic unbalance conditions (beyond design point). |

Table 47. – Failure Modes Analysis (Cont'd)

FUNCTION: STRUCTURAL INTEGRITY (cont'd)

| COMPONENT | FAILURE MODE | FAILURE DISTRIB | FMFR | FAILURE EFFECT | RECOMMENDED CREW ACTION | REACTION TIME | CLASS | Po/1000 FLIGHTS | CENTRIFUGE MODIFICATION OR REMARKS |
|---|---|---|---|---|---|---|---|---|---|
| Fasteners to Main Box-FF | FF | 20 / 10 | .2 | Excessive vibration at high RPM; possible separation at high RPM. | Stop Centrifuge | Seconds | M,A orC | .00634 | High RPM tests curtailed. High stress margins req'd. multiple load paths. |
| **Sensor Spider Frame** | | | | | | | | | |
| Ribs | CB & MF | 20 / 20 | .8 | Erratic counter balance control binding. | " | Seconds | * | .02536 | High RPM tests curtailed; high stress margins & rigidity req'd. |
| | MY | 50 | 2.0 | Erratic counter balance cont. | " | Seconds | M or A | .06339 | C'balance system affected; curtail high RPM tests; high rigidity required. |
| Skin | SB | 15 | .6 | Erratic c'balance control. | " | Seconds | M or A | .01902 | High RPM tests curtailed; high stress levels required. |
| Sensor Bracket | MF | 15 | .6 | False counterbalance control, especially evident at high RPM. | " | Seconds | M or A | .01902 | Disable sensor circuitry. Make best fit balance & conduct low speed exp. High stress level required. |
| **Bearings** | | | | | | | | | |
| Inner Race Housing | MF | 35 / 10 | .7 | Possible collapse at hub. | " | Seconds/ None | C | .02219 | High stress margins required. |
| Outer Race Housing | MF | 10 | .7 | Possible collapse at hub. | " | Seconds/ None | C | .02219 | " |
| Bearings | MW | 80 | 5.6 | Excessive vibration; may produce erratic counterbalance control. | " | Seconds | M or A | .17749 | Limit exp. to low RPM; condition will be progressively worse. Special bearing design required. |
| **Drive Ring Gear** | | | | | | | | | |
| Gear | MW | 25 / 90 | 4.5 | Progressive condition, Increase in noise level, vibration. | " | Seconds | M to A to C | .14262 | Failure would be final result; adequate indications evident to limit exp. RPMS. Spl. gear design. |
| Fasteners | FF & MW | 10 | .5 | Most likely coupled with above. Same effect. | " | Seconds | " | .01585 | Adequate stress margin required. |
| **Drive Motor Support** | | | | | | | | | |
| Support | MF | 10 / 50 | 1.0 | Excessive noise. Centrifuge would not drive. | Do not start; if centrifuge in motion, stop. | Seconds | A | .03169 | Adequate stress margin req'd. Alt means to stop centrifuge req'd. (not in region of motor). |
| Fasteners | FF | 50 | 1.0 | Loss of motor drive. | Stop centrifuge. | Seconds | A | .03169 | Adequate stress margins required. |

Table 47. - Failure Modes Analysis (Cont'd)

FUNCTION: POWER (BATTERY SYSTEM ON BOARD) Po = .0039388

| FAILURE MODE | TRAJECTORY PHASE | FMPR | FAILURE EFFECT | RECOMMENDED CREW ACTION | REACTION TIME | CLASS | Po/1000 FLIGHTS | CENTRIFUGE MODIFICATION OR REMARKS |
|---|---|---|---|---|---|---|---|---|
| Batteries on arm, failure | Orbit | 25% | Communication system, instrumentation system and couch controls (including drives) inoperative. | Abort mission, stop centrifuge. Install spare battery. | 2 hrs. | A | .98470 | Spare battery should be carried. |
| Power control switch | Orbit | 12% | Loss of all electrical power on arm. | Abort mission. Stop centrifuge. Replace switch. | 2 hrs. | A | .47266 | |
| Power inverter | Orbit | 50% | Loss of AC power. | Abort mission. Stop centrifuge. Repair if possible. | 10 hrs. | A | 1.96940 | Power invertor required only if AC motors selected for couch drives. |
| Voltage regulator | Orbit | 13% | Minor, may disturb instrumentation to biomed experiments. | Repair or replace. | 2 hrs. | M | .51204 | May be required for biomedical instrumentation not determined at this time. |

Table 47. - Failure Modes Analysis (Cont'd)

FUNCTION: COMMUNICATION    Po = .2562835

| FAILURE MODE | TRAJ. PHASE | FMFR | FAILURE EFFECT | RECOMMENDED CREW ACTION | REACTION TIME | CLASS | Po/1000 FLIGHTS | CENTRIFUGE MODIFICATION OR REMARKS |
|---|---|---|---|---|---|---|---|---|
| Biomed monitor (1) | Orbit | 14% | Loss of physiological data. | Stop experiment, replace. | | A | 35.87969 | Spare |
| Audio pickup (1) | | 1% | Loss of oral contact. | Stop experiment, replace. | | A | 2.56284 | Spare |
| SCO (8) | | 1% | Loss of data. | Stop experiment, replace. | | A | 2.56284 | Spare |
| XMTR (1) (Z Axis) | | 7% | No Z axis data | Stop Z axis experiment, replace. | | A | 17.93985 | Spare |
| RCVR (1) (Z Axis) | | 7% | No Z axis data | Stop Z axis experiment, replace. | | A | 17.93985 | |
| Multiplexer (1) | | 8% | Loss of some phys. data. | Continue routine. | | A | 20.50268 | |
| Mixer Amp (2) | | 1% | No data voice or physiological. | Stop Experiment, replace. | | A | 2.56284 | Spare |
| Rotary Capacitors | | 1% | No data | Stop experiment. | | A | 2.56284 | Spare - Make all alike, then multiplex. |
| Discriminators (5) | | 4% | No data that channel | Stop experiment. | | A | 10.25134 | Spare - Reassign channel - Drop least imp. |
| Sig Cond. - Heart, Resp. Bld Pres. | | 8% | Loss of data | Stop experiment. | | A | 20.50268 | Spare - Redundant paths. |
| Displays (5) - Analog | | 7% | Loss of data. | Stop experiment. | | A | 17.93985 | Reassign instr. (switching cap.) |
| TV Camera | | 7% | Loss of visual contact. | Stop experiment. | | A | 17.93985 | Use EVA unit |
| RF XMTR | | 1% | Loss of visual contact. | Stop experiment. | | A | 2.56284 | Spare or repair. |
| TV Monitor | | 7% | Loss of visual contact. | Stop experiment. | | A | 17.93985 | |
| RF RCUR. | Orbit | 1% | Loss of visual contact. | Stop experiment. | | A | 2.56284 | |
| Couch Biomedical Instrumentation | " | 25% | Loss of Biomedical Information. | Stop experiment, replace. | | A | 64.07087 | Spares. |

Table 47. – Failure Modes Analysis (Cont'd)

FUNCTION: DYNAMIC BALANCE (STABILITY CONTROL)   Po = .0678943

| FAILURE MODE | TRAJECTORY PHASE | FMFR | FAILURE EFFECT | RECOMMENDED CREW ACTION | REACTION TIME | CLASS | Po/1000 FLIGHTS | CENTRIFUGE MODIFICATION OR REMARKS |
|---|---|---|---|---|---|---|---|---|
| (1) Force sensor inoperative electrically. | Orbit | 80% | None or improper signal to translation drive motors. Dynamic perturbations of spacecraft. Effects other experiments. | Cease experiment. (1) Test, locate & replace defective sensor or - (2) Conduct experiments by best positioning of counterweights & limit scope of experiments. | Inf. | M | 54.31544 | Existing design adds sets of sensors to obtain signal. It may be possible to have an alternate mode which permits functioning of system with one sensor of set at zero output. This is a control logic problem needing more study. |
| (2) Structural failure of sensor restraint (cable, bracket, etc.) | Orbit | 20% | Same as (1) | Same as (1) | Inf. | M | 13.57886 | Same as (1). The floating structural flange will go to its structural stop. As with (1) above this condition produces worst effects at higher RPMs. The difference between (1) and (2) lies in the low RPM range where an error signal would always be generated in mode (2) even at zero RPM. If replacement cannot be accomplished sensor system should be de-activated & use best manual positioning technique. |

Table 48. – Subsystem Failure Distribution

FUNCTIONS

| SUBSYSTEMS | PRIMARY ROTATION 76 Hrs | RADIUS ARM TRANS- LATION 20 Hrs | COUCH ROLL 58 Hrs | COUCH PIVOT 23 Hrs | STRUCTURAL INTEGRITY 1080 Hrs | POWER 153.5 Hrs | COMMUNI- CATION 153.5 Hrs | DYNAMIC BALANCE 75 Hrs | Po/1000 SYSTEM/ FLIGHT |
|---|---|---|---|---|---|---|---|---|---|
| STRUCTURE | | | | | | | | | |
| Drive Hub Assembly | – | – | – | – | 0.0250 | – | – | – | 0.0250 |
| Frame Assembly | – | – | – | – | 0.0100 | – | – | – | 0.0100 |
| Arm Assembly | – | – | – | – | 0.0100 | – | – | – | 0.0100 |
| Control Console & Display Assembly Structure | – | – | – | – | 0.0050 | – | – | – | 0.0050 |
| Couch Assembly | – | – | – | – | 3.1194 | – | – | – | 3.1194 |
| DRIVE SYSTEMS | | | | | | | | | |
| Primary Drive System | 3.4977 | – | – | – | | | | – | 3.4977 |
| Arm Assembly Drive System | – | 1.2973 | – | – | | | | – | 1.2973 |
| Counter-balance Drive System | – | 4.5096 | – | – | | | | 15.7895 | 20.2991 |
| Couch Pivot Drive System | – | – | – | 1.6984 | | | | – | 1.6984 |
| Couch Roll Drive System | – | – | 2.3196 | – | | | | – | 2.3196 |
| POWER SYSTEMS | | | | | | | | | |
| Battery Systems (On Board) | – | 0.5132 | 1.4883 | 0.5902 | | 3.9388 | 3.9388 | 1.9244 | 12.3937 |
| External Power Supply | Interface | – | – | – | | Interface | Interface | – | Interface |
| CONTROL SYSTEMS | | | | | | | | | |
| Rotation Control, Main Drive | 22.2076 | – | – | – | – | – | – | – | 22.2076 |
| Arm Translation Control | – | 3.5812 | – | – | – | – | – | – | 3.5812 |
| Couch Pivot Control | – | – | – | 4.1837 | – | – | – | – | 4.1837 |
| Couch Roll Control | – | – | 15.8021 | – | – | – | – | – | 15.8021 |
| Dynamic Balance | – | – | – | – | – | – | – | 50.1804 | 50.1804 |
| COUCH INSTRUMENTATION | – | – | – | – | – | – | 55.2254 | – | 55.2254 |
| COMMUNICATIONS | | | | | | | | | |
| Inter-communication | – | – | – | – | – | – | 191.8811 | – | 191.8811 |
| Television | – | – | – | – | – | – | 2.5944 | – | 2.5944 |
| Medical Displays | – | – | – | – | – | – | 1.2787 | – | 1.2787 |
| Rotary Capacitors | – | – | – | – | – | – | 1.3651 | – | 1.3651 |
| Po/1000 FUNCTION/FLIGHT | 25.7053 | 9.9013 | 19.6100 | 6.4723 | 3.1694 | 3.9388 | 256.2835 | 67.8943 | 392.9741 |

## Safety Evaluation

Safety evaluation for the internal centrifuge compartment and mechanism must first begin with those factors which are inherent in all parts of the space vehicle. These include such things as hull penetration and depressurization, fire, radiation, atmosphere toxicity, etc. Special problems related to this man, machine monitor complex add additional problems concerned with safety and rescue. These relate to design concepts and must be recognized early in the design effort to minimize later changes. The formulation of safety procedures and development of rescue techniques is rather limited at this time to more general rather than specific terms, because of a lack of overall integration and final design configuration. Indeed, it may be that only by final experimentation with man interfacing with the equipment will it be possible to determine where or what is dangerous and what to do about it. At this point, design critique from the standpoint of safety and rescue is the most important contribution. While many areas which effect the safety of the experiment have been disclosed by this review, no situation has appeared which is judged inherently unsafe or which cannot be avoided by sensible design and experiment procedure.

Approach - Safety feasibility has been treated in this study by specifying ground rules and recommended practices for centrifuge design and operation, and then comparing these requirements with the emerging design to assure that the requirements can be met. Because potentially hazardous space mechanisms cannot be completely man-rated on earth and the extent of multiple, complex stress factors is unknown, a best estimate of the worst conditions anticipated has been assumed as the basis for safety criteria. This has been tempered with the observation that there is as much danger in being too restrictive in controlling the experimental design from the safety and rescue aspects as there is in allowing some fault to go unnoticed at this early stage of development.

Medical Emergencies - In general, medical emergencies or direct trauma to the subject will undoubtedly pose the worst condition with which the monitor must cope. In such cases, abort controls are essential in as much as conditions are anticipated which will not allow adequate communication between the subject and the monitor. Physiological abort criteria would include the following:

Unconsciousness - This would be apparent to the monitor by observation of the subject, loss of communication, change or loss of EEG pattern, and marked change or loss of ECG pattern. Arm restraint system is indicated to prevent the arms from extending and becoming vulnerable to trauma during unconscious state. Rapid deceleration is indicated to counteract the condition. It should not be necessary to remove the subject to another portion of the spacecraft unless some unusual situation occurs.

Nausea and Vomiting - If this is coupled with unconsciousness, it would probably be the worst case emergency. Any vomitus receptacle probably represents a compromise and will be inadequate if the subject is unconscious. Further work should be accomplished in this area. The best approach is undoubtedly to avoid this combined emergency by careful experiment design.

Alterations of Vital Signs - In biosystems, greater concern is generated by rate of change rather than by change in amplitude alone. Therefore, any sudden change in pulse, respiration, or temperature should abort the run. The time of change concerned would be a matter of a few seconds. Physiological limits for setting alarm functions are tentatively listed as follows:

a. Respiration Rate          5 - 25 breaths per minute

b. Heart Rate                50 - 180 beats per minute

c. Blood Pressure            Systolic 180 max. - 80 min.   Diastolic 50 min.

Injury - Obviously any injury sustained, except for minor bumps and abrasions, whether bleeding or not, should be cause for abort. In instances where the subject is examined after minor injury and found satisfactory the test can proceed.

Probably other problems will arise providing additional criteria for aborting the experimental run.

Should some unusual event occur necessitating experiment abort and placing the subject in jeopardy, a rescue procedure should be in effect and ready to implement. Again, not knowing specific details of installation, finite directions are not possible. In general, the monitor must get to the distressed subject as quickly as possible and apply resuscitative measures to restore physiological function. A maximum of 30 seconds is suggested for this purpose. Once the monitor reaches the subject, he should have at the subject site or carry with him the following:

1. Medication for pain - synthetic preparations in ready to inject capsules.

2. Adrenalin or adrenalin-like medication for restoring blood pressure.

3. Bandages.

4. Anti-nausea medication.

In addition, a provision should be made for suction clearing of the nasopharynx and an airway provided for aritifical respiration.

The monitor should also be able to call for help. This necessitates placement of communications equipment in the centrifuge for the monitor's use.

It would appear that with the complexity of the device that the subject will normally require help to enter and leave the centrifuge. Foot and hand tethers for both subject and monitor should be available for this purpose.

In order to prevent cross-coupling effects, it is advisable to spin-down before changing position for the higher-g experiments. For this purpose, it is reasonable to place positioning controls on the centrifuge. This will provide direct visualization of the subject during positioning and will eliminate an accidental position change at high rpm.

Pain - The onset of pain in abdomen, thorax or head may indicate bleeding or major disturbance of internal structures. Along with this, any overt evidence of bleeding such as from mouth, nose, or ears should cause abort.

Fear - Panic - Last, but not least, are psychological parameters noted here. Change in psychological state will profoundly alter the physiology, and will result in poor data.

### Mechanical & Operational Problems

A major objective of safety evaluation must be the prevention of mechanical failure and assessment of the consequences of such failure. Most important are the failure modes that would result in structural damage to the machine with attendant harm to the test subject. Reviewing the results of the failure mode and effects analysis, cases of catastrophic failure mainly involve centrifuge structure and locks and can be eliminated by the use of high design margins and backup systems. Instances of experiment abort are concentrated mainly in communications, balance control and primary rotation systems and can be reduced to a low probability of occurence by the use of spares, active parallel redundancy and high reliability components.

Impact with any object, loss of equipment during rotation, or control manipulation that would overstress the subject or mechanism or place the test subject in a compromising position must be carefully avoided. This suggests that a thorough check list should be devised and then adhered to for each experimental run. It is early in the program to devise such a check list, but some things can now be considered, such as the following:

1. Subject secured properly in device.

2. All release mechanisms secured.

3. Proper experimental devices in place.

4. Subject briefed and ready for experiment.

5. Monitor in position and tether secured.

6. Power ON.

7. Communications intact.

8. Biomonitoring system functioning.

9. Programmer set and running.

10. Control set sequencing.

11. Begin experimental run.

12. Stop experimental run.

13. Secure control systems.

14. Power OFF.

15. Egress of subject from experimental area.

Obviously the check list will be expanded to include items such as communications intact; check voice link; check T. V. link; etc.

In addition to these considerations other areas which represent a compromise to safety are:

1) Fire Hazard: Particular care must be taken to avoid the possibility and consequences of fire in connection with the centrifuge. As a ground rule, combustible materials must be avoided in the specification of centrifuge equipment. The two most prevalent locations where combustible items may appear are on the couch for padding and contouring and in the motion systems in the form of lubricants. For padding, contouring and covering sharp edges in the couch area, Apollo developed technology in using beta cloth and other noncombustible material must be relied upon. Lubricants as a combustible can be avoided by specification of dry bearings for all exposed systems and complete sealing and explosion proofing of the element where lubrication is required.

With respect to possible ignition sources, particularly the electrical systems, slip rings or commutators can be avoided by the use of rotary capacitors for signal transmission and induction or brushless d-c motors for motion system power. Teflon-insulated conductors must be recessed within the mechanism and not exposed to possible abrasion or breakage by crew activities. All portions of the system must be grounded to prevent buildup of static charge.

Hand-operated fire extinguishing equipment dispensing water or aqueous gel are recommended for location in the centrifuge area. Automatic fire suppression system application should be considered for potential trouble areas, as may arise with detail installation of the machine.

2) <u>Loss of Pressure</u> - This would appear to be difficult to cope with. Emergency suiting of some sort should be considered in the centrifuge area, and emergency air provided at the couch. In case of hull penetration, emergency procedures will be similar to those for other areas of the spacecraft.

3) <u>Power Failure</u> - Provisions should be made to assure that in case of power failure, the mechanism quickly comes to a stop without release of any function.

4) <u>Drive Mechanism Failure</u> - This should result in automatic abort.

5) <u>Communication Failure</u> - Loss of either T. V. or voice should be an abort condition.

6) <u>Abnormal Function of Controls</u> - Any abnormal functioning of controls, particularly the yaw, pitch, and roll controls, should be cause for experiment abort.

<u>Biomonitoring</u> - The requirement for adequate biomonitoring capability is important because of borderline physiological stresses that will be imposed and the poor knowledge that is current on the effects of this stress. More complete description of the experimental equipment and needs is discussed elsewhere, but a listing of the tests and how they will be used is appropriate here.

Routine biomonitoring functions may be reduced even further by the time of the experiment but in any event do not impose a design constraint for the centrifuge experiment. However, the various experiments planned do require instrumentation onboard and some method of direct visualization. Some of the instruments and tests required are noted in Table 49.

The monitor readout requires only vital signs, temperature, respiration rate, cardiac rate, and blood pressure. The remaining information can be recorded and developed or stored. Vital Sign readout is necessary in order to ascertain the subject status. This latter is aided by direct visualization and communication.

## Table 49. Biomonitoring Requirements

### Routine Measurements

1. Electrocardiogram

2. Temperature (thermister probes)

3. Respiratory Data (impedance pneumogram)

4. Phonocardiogram

5. Blood Pressure

6. Electroencephalogram

### Centrifuge Experiment Will Require

1. Subject Positioning Recording

2. Electro-oculogram

3. Plethysmogram

4. Tilt Table Drive and Position Recording

5. Venous Compliance

6. Electromyogram

7. Ear Oximitry

8. Cardiac Output (if available)

Summary of Recommendations – The following recommendations are made in summary:

1. Make sure positioning controls have positive locking function.

2. Provide fire control.

3. Eliminate sharp corners or pad them. Eliminate protruding obstructions.

4. Make certain no control travel can be over extended.

5. Provide manual override provision on all essential controls.

6. Design control panels to eliminate unnecessary control buttons and indicators.

7.  Place all important readout and controls on central board.

8.  Avoid extraneous indicators on T. V. screen.

9.  Use audio warning signals with panel warning signals.

10. Place monitor in position close to subject with careful evaluation of the tradeoff factors involved.

11. Provide foot and hand holds for monitor in centrifuge.

12. Make provisions for resuscitation kit.

13. Provide vomitus receptacle and minimize its possibility of occurence, especially in conjunction with unconsciousness.

14. Provide for arm restraints to protect subject if periods of unconsciousness occur.

15. Group functions on main control board.

16. Avoid mixing biomed and engineering data.

17. Use clear identification of function and readout data on control panels.

18. Provide communication for the monitor while in the centrifuge chamber.

19. Provide communication malfunction indicator.

20. Place position controls on centrifuge and eliminate automatic positioning controls as much as possible.

21. Provide abort control for both subject and monitor.

22. Limit X-axis requirement to 9-g (re-entry) Z and Y loading should not exceed 3-g.  Preferential deceleration after greyout is in the Z-axis direction.

23. Quick release restraint system should be provided for both subject and monitor.

24. Complete check list should be followed for each run.

25. All systems must be grounded to eliminate hazard from shock.

Economic Analysis

A program cost estimate was made for the Centrifuge Experiment, with detailed breakdowns for the two phases of the program covering the ground test unit and the flight unit. A summary of the program cost estimate is presented in Table 50. The principal emphasis in this cost analysis is in the areas where the most detailed design definition was available, principally the centrifuge itself. The flight centrifuge module shell housing and LM lab integration details were treated only in a cursory manner.

Approach - Costs were estimated for the program in two distinct phases, a ground test unit program and a flight unit program. The flight unit program includes both a flight article and a qualification test article. In addition, a breakout for the unit hardware cost of the flight configuration unit was made and total program funding requirements by calendar year were also developed.

The cost estimate presented herein includes all research, development, design, analysis, test, and all development hardware and facilities necessary for a ground unit centrifuge facility and a flight unit program consisting of a single flight unit and one qualification unit. Also included are costs for special test equipment and centrifuge support equipment.

The cost estimates were prepared on the basis of the program schedule presented in Figure 92. This schedule is nominally paced, but it includes a fairly short customer review period at the end of the present study with the ground unit program go-ahead assumed in mid 1968. The go-ahead for the flight unit program is assumed to follow immediately the completion of the ground unit program.

The system and subsystem design and development requirements for both the ground unit and flight unit programs were analyzed to determine general task requirements at the major subsystem level. Manpower requirements were estimated for these tasks and for the over-all system integration task. The development and test plan and a list of major components were analyzed to determine program hardware requirements. Costs were estimated for purchased items based on vendor and subcontractor quotes (of a budgetary or planning nature) and known component costs (which were adjusted where necessary for this application). For manufactured items, material and labor costs for fabrication and subassembly, tooling, quality control, integration and assembly, and checkout were estimated. Factory overhead, material burden, and G&A overhead are included in the detail cost estimates.

Spares were estimated as percentages of the total unit cost because of the lack of detailed definition in this area. In general, the allowances for spares should vary with the type of hardware under consideration. For this

study an allowance of 50% for electrical/electronic systems and 25% for mechanical systems were used.

The major ground rules used in estimating the cost of this experiment program are listed below:

1. The costs developed in this study represent total costs to the government for the Centrifuge system development and fabrication, with the exceptions noted below. These costs are expressed in 1967 dollars.

2. The costs cover the total development program including a ground test unit, qualification unit, one flight unit, spare hardware, and all associated test articles and specimens, facilities, and experiment support equipment (GSE).

3. Cost estimates include the space structure and support hardware and experiment system integration only. Costs for the launch vehicle, Apollo CSM/LM Lab, over-all launch support, over-all launch operations, over-all AAP payload integration, or subsequent flights for rendezvous and/or experiment refurbishment are excluded.

4. Other costs that were excluded in this analysis are:

   a. NASA in-house costs.
   b. Astronaut biomedical sensor instrumentation and other experimental instrumentation and special equipment used for the conduct of the biomedical tests, which are assumed GFE.
   c. Modification to the CSM/LM lab stability and control system, electrical power system, and environmental control and life support system.

5. Present manufacturing and test facilities are assumed adequate and available for the conduct of this program with the exception of the new facilities specified in the cost estimate.

6. Fully developed, flight qualified hardware subsystem elements will be utilized wherever possible.

7. The development program is assumed to be an austere program carried out at a nominally paced schedule with labor costs based on a single shift operation.

8. The emphasis in this cost analysis was on the centrifuge mechanism itself. Less detailed investigation was made of the LM

interface structure, the module can, and other Apollo CSM/LM systems.

Results - The ground test unit consists of a manned centrifuge together with an air bearing support structure, an associated control system, and a facility to house these equipments. The ground unit program costs are shown in Table 51.

The ground test unit is functionally similar to the flight unit using the same materials, design configuration, and equipment wherever possible. Therefore, this ground unit is not a simple test rig but must be similar in function and operation to the flight unit in dynamic operation. This requirement implies near flight weight mass duplication. This unit serves as a prototype feasibility demonstration article and later as a unit for biomedical research and possibly for astronaut training during the flight unit program. (The cost of the follow-on physiological test program is not included in this estimate). Much of the development of components to near-flight configuration must be accomplished in this phase of the program. The principal difference between the ground test unit and the flight unit is that the various subsystem and components for the ground test unit will not be space flight qualified (thus avoiding the associated test program and stringent quality control and reliability requirements).

Test operations include all testing activities including components testing, subsystem testing, and centrifuge system tests through the feasibility or prototype demonstration prior to the initiation of the physiological test program. Approximately one ship-set of hardware is included to cover the component test hardware required for development of the near flight configuration components.

Special test equipment includes the airbearing support structure for the centrifuge and the associated instrumentation and recording equipment necessary for operation of the centrifuge as a test bed and later as a biomedical research tool.

The tooling for the ground test unit is less sophisticated (and less expensive) than that required for the flight unit because of lower tolerance requirements.

It is presently estimated that the only new facilities required will be those required to support the ground test unit. It is assumed that this unit will be housed inside an existing building. The facility includes concrete pads for the centrifuge air bearing assembly, the centrifuge room and control booth, and utilities.

A breakdown of the flight unit program cost estimate is shown in Table 52. The flight unit program includes a qualification test unit, a flight unit, a centrifuge support for qualification testing, a module shell

mockup for swimming pool zero g testing, and software associated with the flight test. In general, the flight unit will be similar to the ground test unit, but it will be flight weight and qualified for manned spaceflight.

The basic structures for both the centrifuge and the module shell and centrifuge support are assumed to be conventional airframe construction and materials (aluminum and steel). The majority of the drive and control components are expected to be procured rather than fabricated. Estimates were not made for modifications to the stability and control, electrical power, or environmental control/life support system modifications required for integration with the Apollo CSM or LM Lab. For the stability and control system costs, allowances were made for two 2000 ft.-lb. control moment gyros and their associated controls. These gyros are used to counteract spacecraft distrubances caused by centrifuge operation.

The electrical power system includes the batteries, battery charger, and power conditioning components necessary for operation of the centrifuge. Also included are 100 square feet of solar cell panels to be used to recharge the centrifuge batteries. It is further assumed that there are no unusual requirements attendant to the installation and integration of these panels into the LM Lab/Centrifuge system.

The communications, TV, and data systems are in general off-the-shelf, space qualified components. Should further definition indicate that new and special components are required, additional costs would be incurred.

The environmental control and life support equipment was assumed to consist of an atmosphere leakage makeup system, atmosphere circulation system, and a heat rejection circuit and radiator.

The biomedical system cost includes the astronaut couch and restraint system and the biomedical display system at the centrifuge control console in the LM Lab.

The qualification unit is identical to the flight unit and is used for qualifying the centrifuge for flight. It appears that testing in a reduced-pressure environment will be required and it is assumed that facilities (e.g. large vacuum chamber) are available to carry out these tests-either at NASA or at other industry locations. It is further assumed that the qualification unit will be refurbished to flight configuration to serve as a backup unit. An allowance of 33% of the hardware cost was included for this task. The module/centrifuge mockup is a full scale representation of the physical dimensions of the module shell and centrifuge that is suitable for use in a swimming pool "Zero g" buoyancy environment for investigation of human factors.

The tooling required for the qualification and flight units is more

expensive than the relatively "soft" tooling required for the ground test unit because of the more stringent tolerance and quality control requirements. In addition, tooling for the module shell is also required.

The ground support equipment includes both mechanical and electrical/electronic equipment. The principal items of mechanical hardware include handling gear and shipping containers. The electrical/electronic equipment includes checkout equipment at the factory and the launch site. This estimate includes design, development, and hardware fabrication.

The mission support category includes mission planning, training, launch operations, and flight analysis. The training cost covers indoctrination of NASA personnel (including astronauts) in the technical and operational aspects of the centrifuge unit. Launch operations covers launch site preparation, installation of GSE, and launch activities that are directly associated with the centrifuge. The flight analysis includes data processing and analysis of the flight test.

Table 53 presents another summary of program cost in terms of fiscal year funding requirements.

Uncertainties - The cost estimates presented in this report are believed to be representative of the present definition of the centrifuge experiment program. It should be emphasized that the cost factors used in the study are sensitive to the design definition and its relationship to the current state-of-the-art. For example, some of the items in the areas of communications, telemetry, and environmental control are assumed to be essentially off-the-shelf equipment. If this proves not to be the case because of design requirements, additional funding will obviously be required. Some centrifuge associated items such as the control moment gyros, solar cell panels, module shell, and GSE were not defined in detail. Therefore, an allowance was included for the cost of these items. Since they account for a large portion of the hardware cost, a more detailed analysis could cause significant changes to the total program cost. Further, unforseen development problems in the areas of greatest risk-principally the area of special bearings and brushless DC motors-would also have detrimental effects on costs. Therefore, these estimates should be regarded as area estimates for planning purposes.

Conclusions

1.    Costs for the Centrifuge Experiment for Apollo Applications are estimated at about $12M for the total program, including vehicle support and facilities.

2.    The ground test unit program cost is estimated at $2.9M.

3.     The flight unit program cost is estimated at $9.1M.

4.     The cost estimate for the centrifuge program is based on extensive use of off-the-shelf equipment and components. Any departure from this approach is likely to have a significant impact on program costs.

5.     Only the centrifuge itself has been analyzed in detail; therefore, the other areas of program cost (which are important contributors to total program cost) remain relatively uncertain at this time.
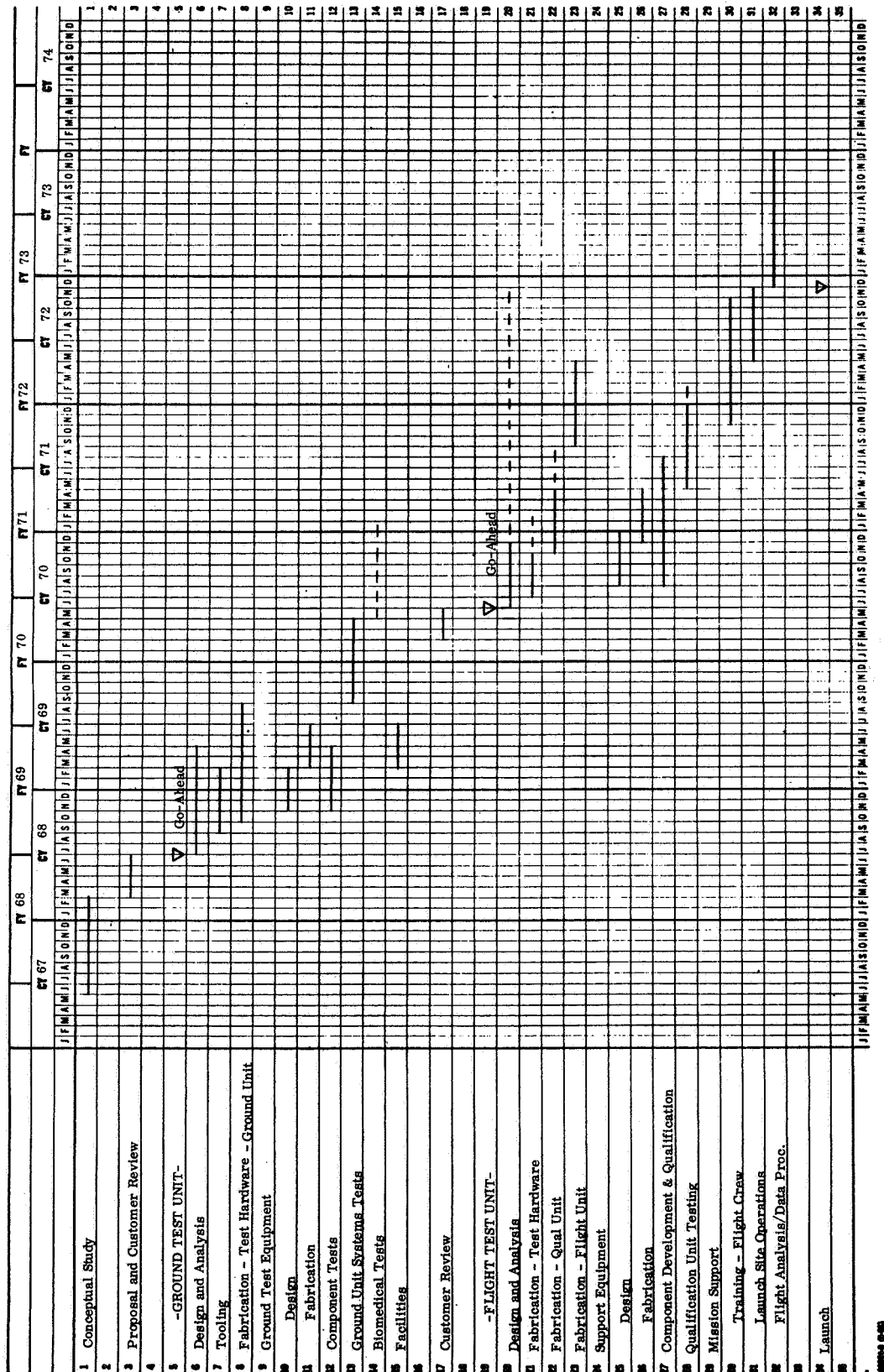
Figure 92. - Program Schedule

1 Conceptual Study
2
3 Proposal and Customer Review
4
5 -GROUND TEST UNIT-
6 Design and Analysis
7 Tooling
8 Fabrication – Test Hardware – Ground Unit
9 Ground Test Equipment
10 Design
11 Fabrication
12 Component Tests
13 Ground Unit Systems Tests
14 Biomedical Tests
15 Facilities
16
17 Customer Review
18
19 -FLIGHT TEST UNIT-
20 Design and Analysis
21 Fabrication – Test Hardware
22 Fabrication – Qual Unit
23 Fabrication – Flight Unit
24 Support Equipment
25 Design
26 Fabrication
27 Component Development & Qualification
28 Qualification Unit Testing
29 Mission Support
30 Training – Flight Crew
31 Launch Site Operations
32 Flight Analysis/Data Proc.
33
34 Launch
35

Go-Ahead

Go-Ahead

FY 67  FY 68  FY 68  FY 69  FY 69  FY 70  FY 70  FY 71  FY 71  FY 72  FY 72  FY 73  FY 73  FY  FY 74

Table 50

Centrifuge Program Cost Summary

(Thousands of Dollars)

| | | |
|---|---:|---:|
| Ground Unit Program | | 2,942 |
|     Program Management | 120 | |
|     Engineering Design and Devel. | 914 | |
|     Hardware | 1,350 | |
|     Tooling | 90 | |
|     Test and Evaluation | 405 | |
|     Special Test Equipment | 53 | |
|     Facilities | 10 | |
| Flight Unit Program | | 9,099 |
|     Program Management and Documentation | 497 | |
|     Engineering Design and Devel. | 2,038 | |
|     Hardware | 4,809 | |
|     Tooling | 235 | |
|     Test and Evaluation | 600 | |
|     GSE | 160 | |
|     Mission Support | 760 | |
| Total Program | | 12,041 |

## Table 51

## Ground Unit Program Cost

## (Thousands of Dollars)

| | | |
|---|---|---|
| Program Management | | 120 |
| Design Analysis | | 112 |
| Engineering Design | | |
|     Systems Engineering/Integration | 262 | |
|     Centrifuge | 315 | |
|     Biomedical/Communications | 195 | |
|     Support Structure | 30 | |
| | | 802 |
| Test Operations | | 405 |
| Special Test Equipment | | 53 |
| Facilities | | 10 |
| Tooling | | 90 |
| Component Test Hardware | | 580 |
| Ground Test Unit Hardware | | |
|     Structure | 100 | |
|     Drive & Control | 405 | |
|     Electric Power | 45 | |
|     Communications | 50 | |
|     Biomedical | 45 | |
|     Integration and Assembly | 125 | |
| | | 770 |
| TOTAL | | 2,942 |

## Table 52
## Flight Unit Program Cost
## (Thousands of Dollars)

| | | | |
|---|---|---:|---:|
| Program Management | | | 225 |
| Documentation Data | | | 272 |
| Design Analysis | | | 224 |
| Engineering Design | | | |
| | Systems Engineering/Integration | 525 | |
| | Centrifuge | 630 | |
| | Biomedical/Communications | 390 | |
| | Module Shell/Support | 269 | |
| | | | 1,814 |
| Test Operations | | | |
| | Component Development & Qualification | 300 | |
| | Qualification Unit Testing | 300 | |
| | | | 600 |
| Production Support | | | 20 |
| Tooling | | | |
| | Planning | 76 | |
| | Fabrication | 107 | |
| | Material | 10 | |
| | Sustaining | 42 | |
| | | | 235 |
| Component Test Hardware | | | 580 |
| Qualification Article Hardware | | | |
| | Fabrication | 1,160 | |
| | Refurbish to Backup | 350 | |
| | | | 1,510 |
| Module Shell Mockup | | | 40 |

| Flight Article Hardware | | Labor | Material | |
|---|---|---:|---:|---:|
| Centrifuge | | | | |
| | Structure | 150 | 25 | |
| | Drive & Control | 215 | 190 | |
| | Electric Power | 25 | 70 | |
| | Communications | 50 | 60 | |
| | Environmental Control/LSS | 10 | 80 | |
| | Biomedical | 30 | 15 | |
| | Integration & Assembly | 175 | – | |
| | Checkout | 65 | – | |
| | | 720 | 440 | 1,160 |

| | |
|---|---:|
| Control Moment Gyros | 560 |
| Solar Cell Panels | 245 |
| Module Shell/Support | 244 |
| Spares | 450 |

Table 52 (Continued)

| | | |
|---|---:|---:|
| Ground Support Equipment | | 160 |
| Mission Support | | |
|     Mission Planning | 176 | |
|     Training | 136 | |
|     Launch Operations | 240 | |
|     Flight Analysis | 208 | |
| | | 760 |
| TOTAL | | 9,099 |

Table 53

Funding Requirements by Fiscal Year
(Thousands of Dollars)

| | FY 1969 | FY 1970 | FY 1971 | FY 1972 | FY 1973 | Total |
|---|---|---|---|---|---|---|
| Ground Test Unit Program | 2,100 | 842 | | | | 2,942 |
| Flight Unit Program | | | 3,680 | 4,150 | 1.269 | 9,099 |
| TOTAL | | | | | | 12,041 |

Mass Properties

Spacecraft mass properties. During the course of the study, estimates of the weight, center of gravity and inertial properties of the three selected in-orbit spacecraft configurations were made. These were the SRC/LM/CSM, the CAC and the EOSS configurations previously identified and are illustrated by Figures 93, 94, and 95. These weight estimates were made in support of the dynamic and stability requirement studies and to allow evaluation of the feasibility of launching the orbital experiment with existing boosters.

Centrifuge mass properties. The weight distribution determined for the rotating portion of the centrifuge is shown in Table 54. At the present stage in design, no attempt at weight reduction through the use of exotic materials or unusual fabrication practices has been made. The results of the mass properties analysis for the various experiment configurations are tabulated in Table 55. The center of gravity shown in the first column is that obtained after the counterbalance of 660 pounds has been moved in the Y-Z plane. The location of the counterbalance is shown in the last column. The counterbalance weight of 660 includes 80 pounds of batteries that are assumed to be movable with the counterweight of 580 pounds. For the Oculogravic illusion and Eye Counter Rolling experiments, position I refers to that position where the axis of the spine of the subject is in the direction of the Z axis.

The reference axes used for the mass properties analysis summarized in Table 55 are as follows:

X Axis - Spin axis with base of drive hub = 0 and positive direction is up from hub.

Y Axis - Parallel to minor axis of centrifuge arm with 0 at spin axis and positive direction to right of subject when in grayout position.

Z Axis - Parallel to major axis of centrifuge arm with 0 at spin axis and positive direction toward feet of subject when in grayout position.
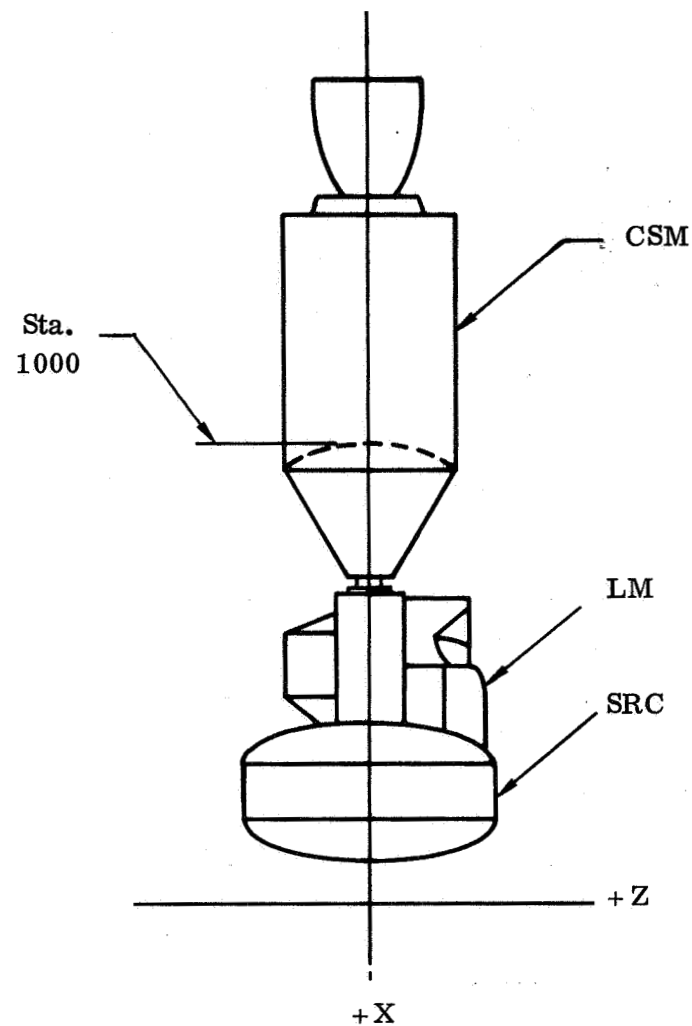
| Weight (lbs) | C. G. (ins.) | | | Moment of Inertia (slug ft$^2$) | | |
|---|---|---|---|---|---|---|
| | $\overline{X}$ | $\overline{Y}$ | $\overline{Z}$ | $I_{xx}$ | $I_{yy}$ | $I_{zz}$ |
| 37,800 | 1019 | 0 | 3 | 24,200 | 170,000 | 168,500 |

Figure 93. CSM/LM/SRC Configuration.
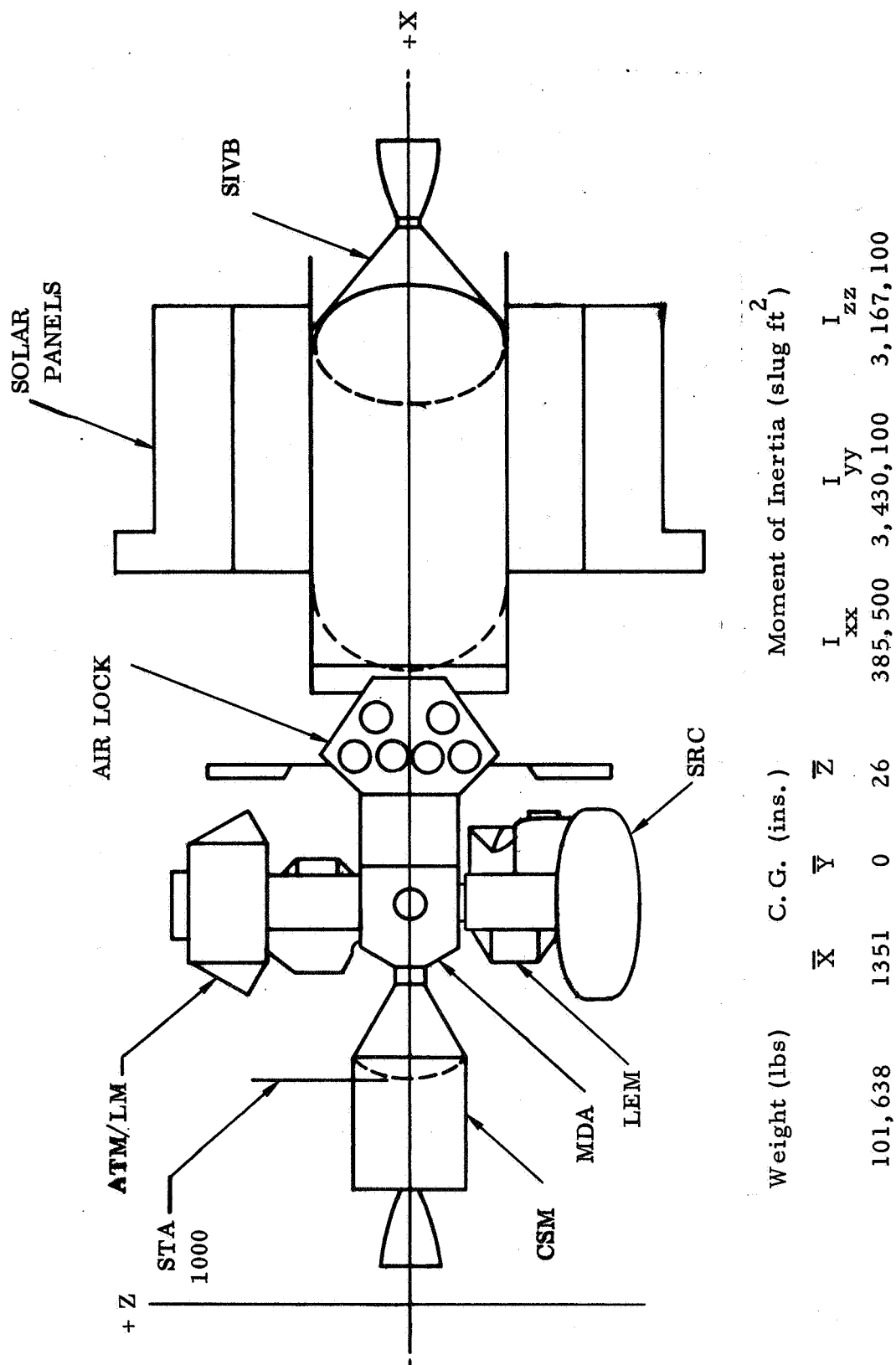
Figure 94. The cluster associated configuration (CAC).

SIVB

SOLAR PANELS

AIR LOCK

SRC

ATM/LM

STA 1000

CSM

MDA

LEM

+X

+Z

| Weight (lbs) | C.G. (ins.) | | | Moment of Inertia (slug ft$^2$) | | |
|---|---|---|---|---|---|---|
| | $\overline{X}$ | $\overline{Y}$ | $\overline{Z}$ | $I_{xx}$ | $I_{yy}$ | $I_{zz}$ |
| 101,638 | 1351 | 0 | 26 | 385,500 | 3,430,100 | 3,167,100 |
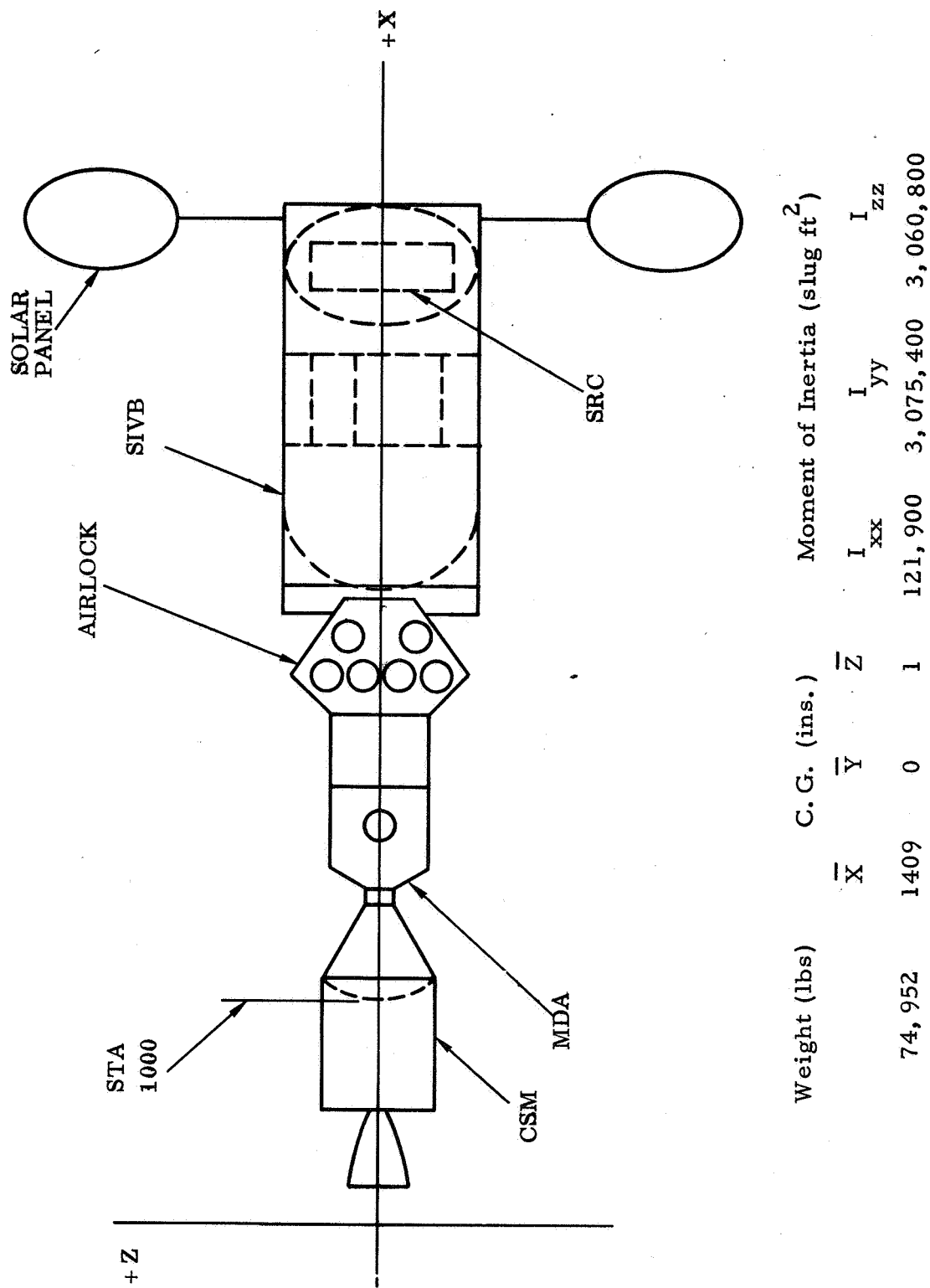
Figure 95. The earth orbital space station configuration (EOSS)

| Weight (lbs) | C. G. (ins.) | | | Moment of Inertia (slug ft$^2$) | | |
|---|---|---|---|---|---|---|
| | $\bar{X}$ | $\bar{Y}$ | $\bar{Z}$ | $I_{xx}$ | $I_{yy}$ | $I_{zz}$ |
| 74,952 | 1409 | 0 | 1 | 121,900 | 3,075,400 | 3,060,800 |

## Table 54. Centrifuge Weights (Rotating Portion)

| | | | |
|---|---|---|---|
| Translation Arm/Pivot and Roll Frame | | | 484 |
| Structure | | 194 | |
| Upper beam | 72 | | |
| Lower beam | 72 | | |
| Center section | 50 | | |
| Power and Communication | | 150 | |
| End fittings | | 40 | |
| Pivot and roll frame | | 60 | |
| Pivot and roll drive | | 40 | |
| | | | |
| Support Frame | | | 400 |
| Structure | | 250 | |
| Batteries | | 80 | |
| Translation and Counterbalance Drive | | 70 | |
| Translation screw | 20 | | |
| Counterbalance screw | 20 | | |
| Motor, gears and control | 20 | | |
| Bearings, etc. | 10 | | |
| | | | |
| Drive Hub | | | 42 |
| Structure | | 17 | |
| Bearings | | 7 | |
| Drive Gear | | 8 | |
| Capacitors | | 10 | |
| | | | |
| Counterweight | | | 580 |
| | | | |
| Couch System | | | 167 |
| Structure | | 54 | |
| Cushioning, harnesses, etc. | | 23 | |
| Power and distribution | | 20 | |
| Inst./comm., etc. | | 20 | |
| Waste collection | | 50 | |
| | | | |
| Man and Gear | | | 200 |
| | | | |
| Contingency | | | 100 |
| | | | |
| Total | | | 1973 |

Does not include counter momentum system or balance system other than gross counterweight allocation.

Table 55.   Rotating Portion of Centrifuge Mass Properties Summary
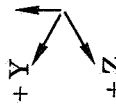
| Experiment | Center of Gravity (ins.) | | | Moment of Inertia (slug ft2) | | | Product of Inertia (slug ft2) | | | Counterbalance C.G. (ins.) | | |
|---|---|---|---|---|---|---|---|---|---|---|---|---|
| | $\bar{X}$ | $\bar{Y}$ | $\bar{Z}$ | $I_{xx}$ | $I_{yy}$ | $I_{zz}$ | $I_{xy}$ | $I_{xz}$ | $I_{yz}$ | $\bar{X}$ | $\bar{Y}$ | $\bar{Z}$ |
| Grayout | 36.9 | 0 | 0 | 594 | 609 | 113 | 0 | -3.1 | 0 | 37.0 | 0 | -25.9 |
| Therapeutic | 36.9 | 0 | 0 | 594 | 609 | 113 | 0 | -3.1 | 0 | 37.0 | 0 | -25.9 |
| Angular Acceleration | 36.9 | 0 | 0 | 594 | 609 | 113 | 0 | -3.1 | 0 | 37.0 | 0 | -25.9 |
| Tilt Table | | | | | | | | | | | | |
| Position I | 37.0 | 0 | 0 | 517 | 492 | 155 | 0 | -1.5 | 72.2 | 37.0 | -7.6 | -26.3 |
| Position II | 37.0 | 0 | 0 | 569 | 552 | 147 | 0 | -1.5 | 68.7 | 37.0 | -6.2 | -28.6 |
| Semicircular Canal Stimulation | | | | | | | | | | | | |
| Position A R = 0 | 37.0 | 0 | 0 | 249 | 259 | 119 | 0 | -4.8 | 7.9 | 37.0 | -1.8 | 1.2 |
| Position A R = 49" | 37.0 | 0 | 0 | 1351 | 1361 | 119 | 0 | 3.4 | 36.2 | 37.0 | -1.8 | -61.9 |
| Position B R = 0 | 37.4 | 0 | 0 | 243 | 264 | 119 | 0 | 1.8 | 0 | 37.0 | 0 | 1.2 |
| Position B R = 49" | 37.4 | 0 | 0 | 1346 | 1367 | 119 | 0 | 17.9 | 0 | 37.0 | 0 | -61.9 |
| Sensitivity to Linear Acceleration | | | | | | | | | | | | |
| Position IA | 36.9 | 0 | 0 | 594 | 609 | 113 | 0 | -3.1 | 0 | 37.0 | 0 | -25.9 |
| Position IIA | 37.0 | 0 | 0 | 405 | 333 | 202 | 0 | -3.5 | 88.8 | 37.0 | -13.2 | -12.4 |
| Position IB | 36.9 | 0 | 0 | 594 | 609 | 113 | 0 | -3.1 | 0 | 37.0 | 0 | -25.9 |
| Position IIB | 37.0 | 0 | 0 | 405 | 333 | 202 | 0 | -3.5 | 88.8 | 37.0 | -13.2 | -12.4 |
| Oculogravic Illusion | | | | | | | | | | | | |
| Position I | 37.0 | 0 | 0 | 890 | 900 | 119 | 0 | -1.2 | 31.2 | 37.0 | -1.8 | -42.2 |
| Position II | 37.0 | 0 | 0 | 841 | 837 | 133 | 0 | -1.2 | -106.7 | 37.0 | 7.0 | -40.0 |
| Eye Counter Rolling | | | | | | | | | | | | |
| Position I | 37.4 | 0 | 0 | 885 | 906 | 119 | 0 | 13.4 | 0 | 37.0 | 0 | -42.2 |
| Position II | 37.4 | 0 | 0 | 804 | 796 | 149 | -4.5 | 11.7 | -125.4 | 37.0 | 8.4 | -38.6 |

Coordinate axes: +X, +Y, +Z

Table 55 (contd.)

| Experiment | Center of Gravity (ins.) | | | Moment of Inertia (slug ft²) | | | Product of Inertia (slug ft²) | | | Counterbalance C.G. (ins.) | | |
|---|---|---|---|---|---|---|---|---|---|---|---|---|
| | $\bar{X}$ | $\bar{Y}$ | $\bar{Z}$ | $I_{xx}$ | $I_{yy}$ | $I_{zz}$ | $I_{xy}$ | $I_{xz}$ | $I_{yz}$ | $\bar{X}$ | $\bar{Y}$ | $\bar{Z}$ |
| Reentry Simulation | 37.0 | 0 | 0 | 1441 | 1438 | 132 | 0 | 3.2 | -2.1 | 37.0 | 0 | -64.0 |
| Mass Determination | | | | | | | | | | | | |
| R = 50" | 37.0 | 0 | 0 | 573 | 570 | 132 | 0 | -1.2 | -1.6 | 37.0 | 0 | -30.6 |
| R = 76" | 37.0 | 0 | 0 | 1441 | 1438 | 132 | 0 | 3.2 | -2.1 | 37.0 | 0 | -64.0 |

Weight feasibility summary. A breakdown of major system and component weights for the Apollo/LM/SRC, CAC, and EOSS applications of the centrifuge is shown in Table 56. In all installations, the basic centrifuge weight remains the same and is represented by the 3158 lbs. chargeable to the centrifuge experiment in the EOSS configuration. For the Apollo/LM/SRC, the total payload weight requires boost capability of an uprated Saturn IB (strap-on solids) or the mission may be flown with two standard Saturn IB launches - one for the CSM and a second for the LM/SRC. Alternatively, the configuration could be launched as a portion of a Saturn V payload. The cluster associated LM/SRC launch is well within the capability of a Saturn IB booster.

Table 56. Weight Feasibility

| | Apollo-LM/ SRC Module | Cluster LM/SRC | EOSS |
|---|---|---|---|
| CSM | 23,900 | | |
| SLA-LM Ascent Stage-separation Sys. | 5,900 | 5,900 | |
| Nose Fairing Penalty | | 337 | |
| De-Orbit Propellant | 1,300 | | |
| Mission Life Support | 3,450 | | |
| Centrifuge ECS & Subsystem Interface | 880 | 880 | |
| Vehicle Stabilization Propellant | 1,879 | 500 | |
| Centrifuge Module | 1,952 | 1,952 | |
| Experiment Sys. & Expendables | 200 | 200 | 200 |
| CMG (Countermomentum) | 400 | 400 | 400 |
| Centrifuge Couch | 167 | 167 | 167 |
| Translation Arm/Pivot & Roll Frame | 484 | 484 | 484 |
| Support Frame-Drive Hub-CW | 1,022 | 1,022 | 1,022 |
| Rotational Drive System | 115 | 115 | 115 |
| Power Distribution | 420 | 420 | 420 |
| Communications & Illumination | 40 | 40 | 40 |
| Noise & Vibration Damping | 110 | 110 | 110 |
| Contingency | 500 | 400 | 200 |
| TOTAL | 42,719 | 12,972 | 3,158 |

## Power Requirements

Evaluation of the power requirements of the centrifuge was made on an individual experiment basis to determine if any prohibitive demands or unusual technological approach would be necessary. No problems were encountered either in power demand or in equipment requirement. A listing of the main power requirements is as follows:

| | |
|---|---|
| Medical instrumentation | 300 watts |
| Mechanical drive control and instrumentation | 300 watts |
| ECS, lights, fans, and control | 200 watts |
| Attitude control and miscellaneous | 50 watts |
| Mechanical drive | |
| Fractional hp translation drive | 200 watts |
| Main drive maximum | 4500 watts |

One hundred watts of the medical instrumentation and the 200 watts for the fractional hp motors must be driven by batteries located on the centrifuge arm. The remaining instrumentation wattage (200 + 300) will be generated at the control panel. The electrical designers feel that the equipment need only be on for 15 minutes prior to the experiments for warmup and checkout. However, the actual times will be evolved from experiment time studies. The current main drive motor is ac with an inverter-converter controller requiring a 28 volt dc battery. The controller efficiencies are quoted at 80% at maximum rating and 60% at lower power setting. D. C. power appears satisfactory for the centrifuge experiments.

Pertinent power data for the proposed experiments are listed in Table 57. The power profile curves listed in Table 57 are shown on Figure 97. The effects of combining the sensitivity threshold experiment with the oculogravic illusion experiment can be noted by comparing the number of runs per day for those two experiments with the combined experiment of Table 57. By combing these two experiments into one, the total electrical energy required is reduced by 12 Kwh and the total experiments times from 418 hours to 389 hours.

As noted on Table 57, the experiments requiring the most electrical energy is the semicircular canal experiment. The grey-out and re-entry simulation experiments require the maximum power. In addition to the electrical energy required for the experiments, coolant pumps must be operated between experiments to remove heat generated by the battery charging operations and to provide a chilled supply of coolant for the next experiment.

The power profile curves on Figure 97 point out the significant energy requirement for the controls and instrumentation. The main drive energy requirement for each experiment is a small part of the total. Therefore, to minimize the electrical energy requirements, it is necessary to evaluate the electrical circuits for the control and instrumentation and to ascertain the astronauts time line for each experiment.

A trade-off study was performed to determine the minimum combined weight of solar arrays and batteries which would satisfy the requirements of the experiment series. The results of this study are shown by Figure 96. With no power being contributed by solar arrays, the minimum battery weight becomes 464 lbs. This is dictated by the 2435 w.h. requirement of the semicircular canal experiment as shown by table 57. If all peak experiment power is supplied by solar arrays, the Grayout and Re-entry simulation experiments size the array with their 5.30 kw peak requirement. (See Figure 97, Profile curves III and VI.) Minimum combined weights are obtained with 100 ft$^2$ of panel mounted arrays (sun oriented) producing 1060 watts and batteries weighing 220 lbs. Since experiment I requires more than two orbits, the solar array power generated during the two orbits can not provide electrical energy used on the centrifuge arm. Therefore the storage batteries, 70 lbs., on the arm must provide the electrical energy for the entire experiment.

A review was made of the experiment's current schedules, power required, the optimized solar array areas and battery sizes to determine the number of orbits required for battery charging between experiments. For the worst case, experiment IV, one orbit was required to recharge the batteries. Hence, for the 38th, 39th, 40th, and 42nd days where there are 4 experiment IV's schedules along with various other experiments there is theoretically sufficient time for the experiments and battery recharging allowing one orbit between experiments for battery charging.

Cooling Circuit - An elemental schematic of the coolant loop is shown on Figure 98 to illustrate the basic concept for maintaining thermal balance in the centrifuge. It is assumed that the coolant will be water-glycol mixture and that the heat from the control panel will be removed in a cold plate heat exchanger. The heat from instrumentation on the centrifuge arm and the astronauts along with part of the braking load will be dissipated into the cabin atmosphere to be removed by the cabin air heat exchanger. Twenty-five pounds of chilled coolant will be available prior to each experiment to remove the initial surge of heat during the centrifuge braking cycle.

The coolant pump, 30 watts, must remain in operation for one orbit after each experiment to remove heat generated by the braking operation, battery charging and to supply a tank of chilled coolant. The total electrical energy required for all of the experiments and the coolant power is 145 Kwh. If the sensitivity threshold and oculogravic illusion experiments are combined into one and conducted during only one run per day, (experiment VIIB of Table 57), the total energy requirements would be 132 Kwh.

SOLAR ARRAY AREA FT$^2$

TOTAL WEIGHT (BATTERYS + ARRAY), LBS

PADDLE MOUNTED

PANEL MOUNTED

BODY MOUNTED
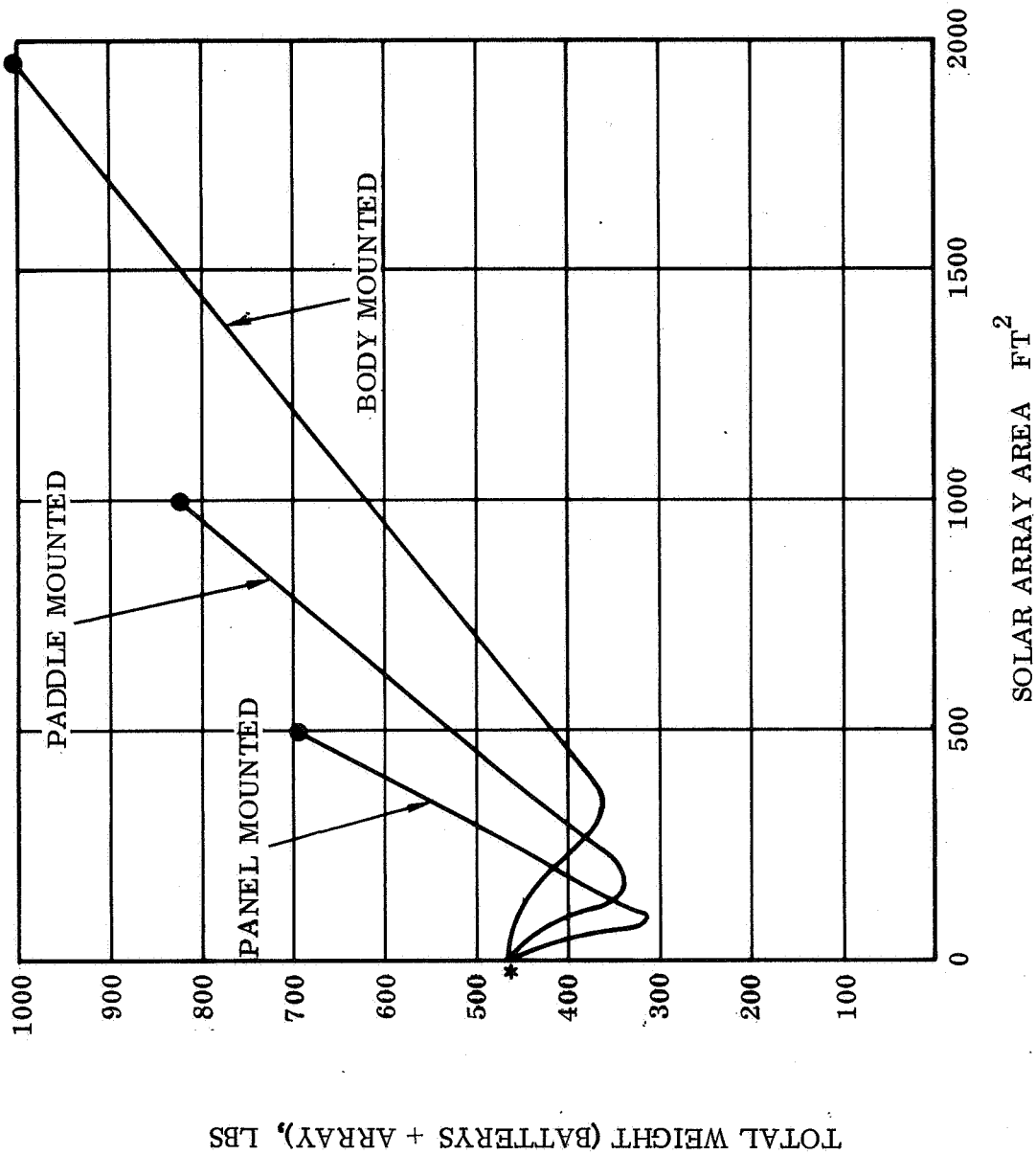
* All power during experiment from batteries
● All peak power during experiment from solar array.

Figure 96. Power Systems Weights
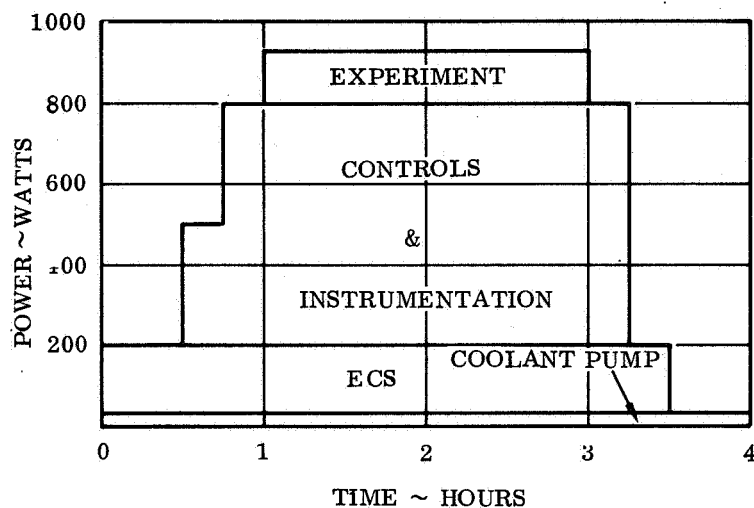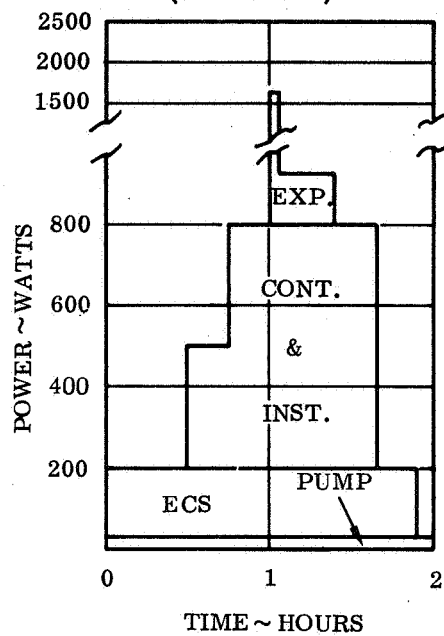
Figure 97. Typical Experiment Power Profile Curves.

PROFILE CURVE V
(Mass Measurement)

PROFILE CURVE VI
(Grayout)
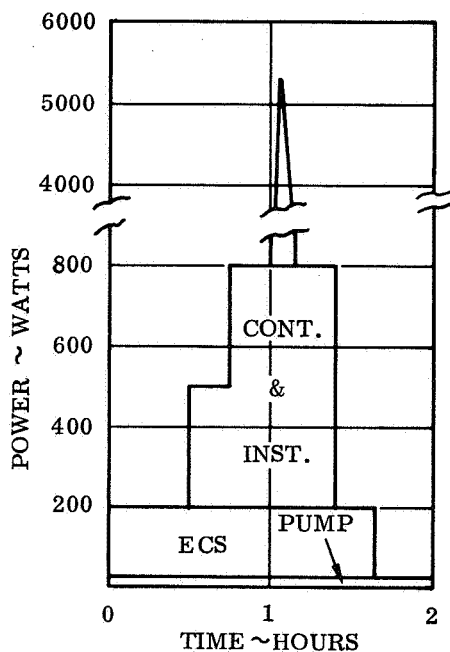
PROFILE CURVE VII
(Sensitivity Threshold or OGI)
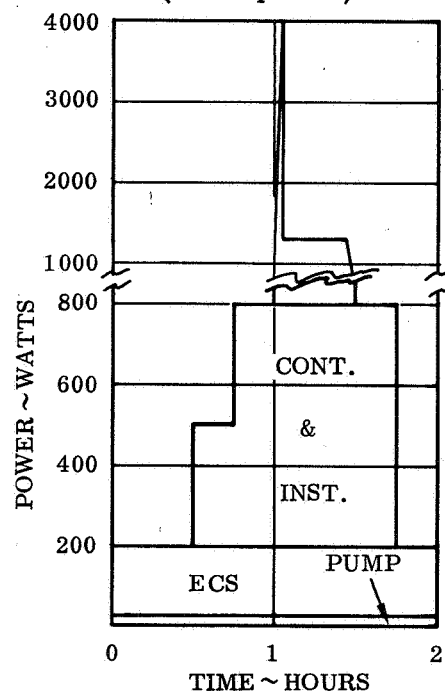
PROFILE CURVE VIIB
(Combined Sensitivity and OGI)
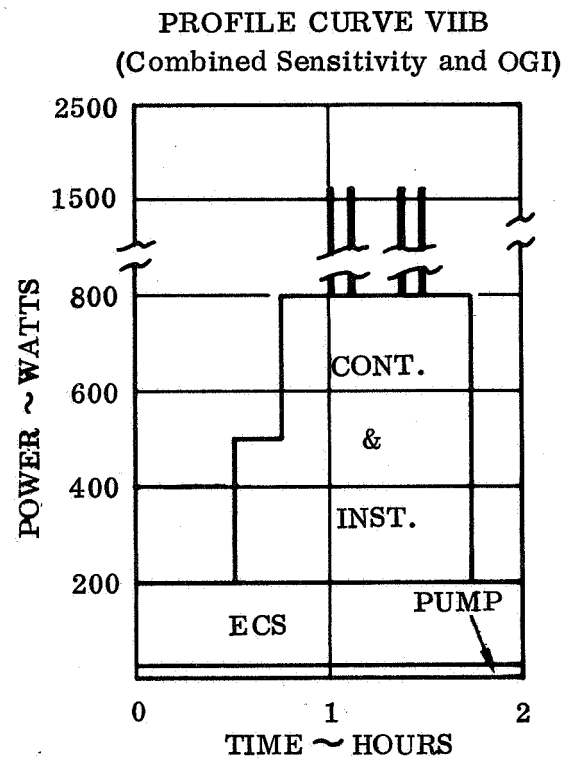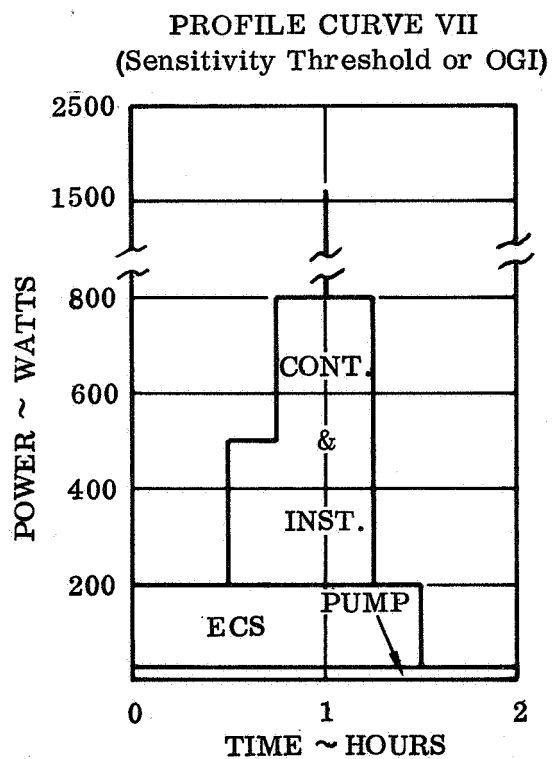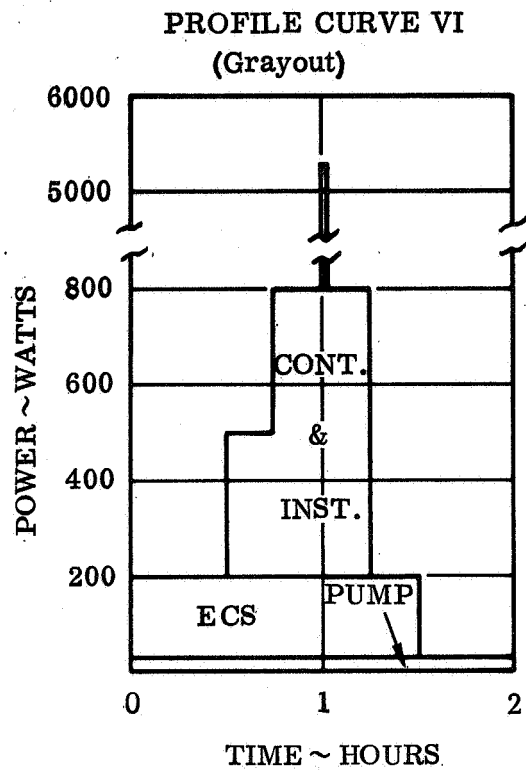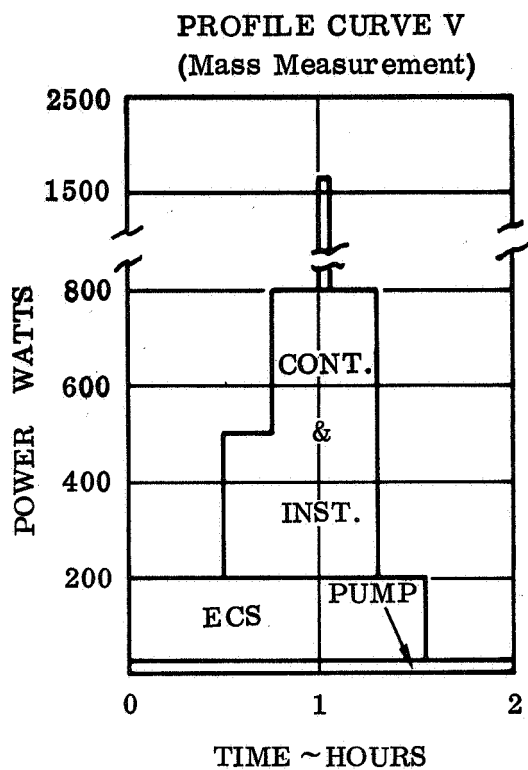
Figure 97. Typical Experiment Power Profile Curves. (cont'd)
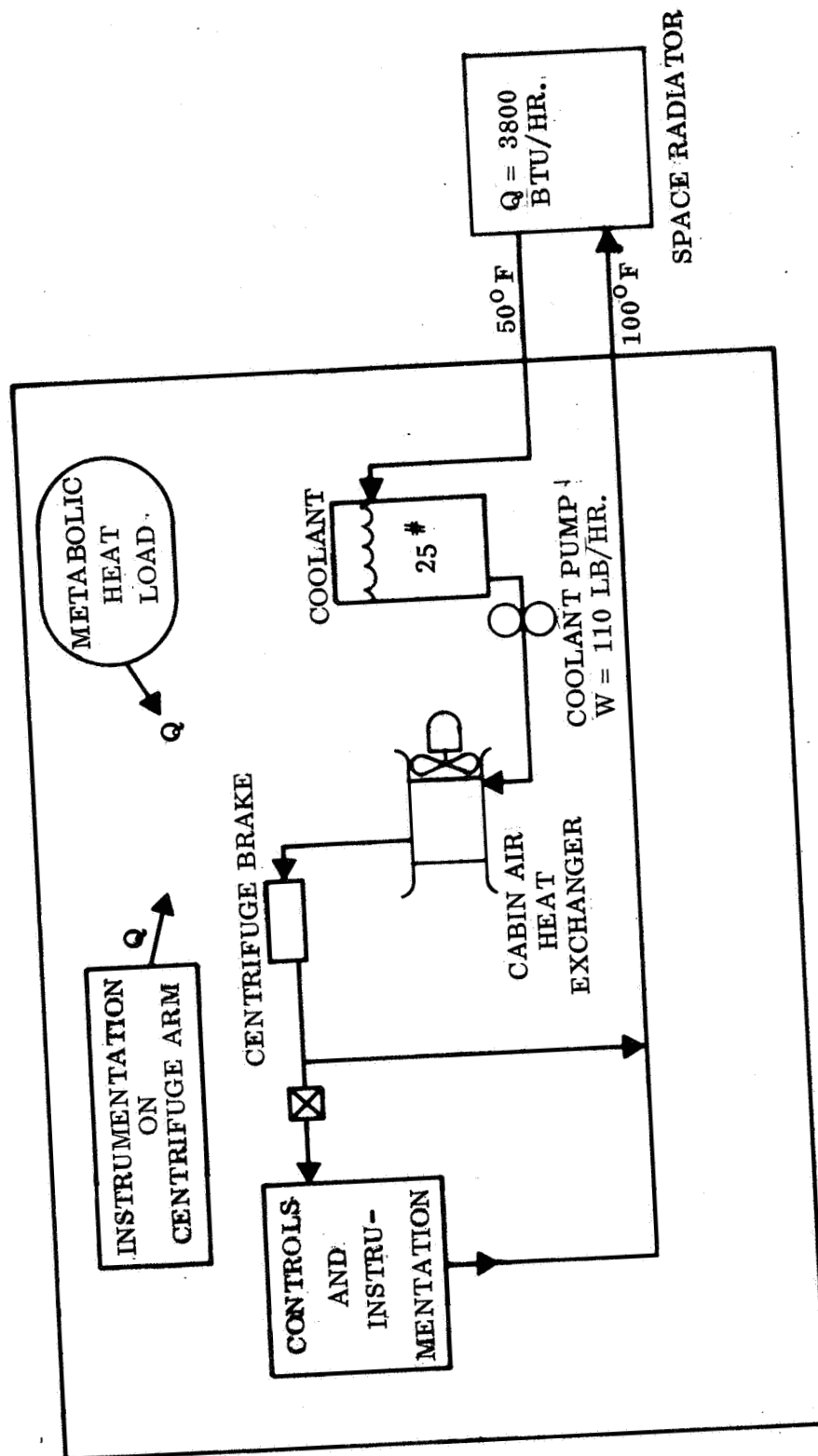
Figure 98. Centrifuge Thermal Control Loop.

Table 57. Power Summary for Centrifuge Experiments

| Experiment | No. of Runs | Runs/ Day | Critical Time | Max. Power | Electric Energy per Experiment | Total Electric Energy | Power Profile Curve |
|---|---|---|---|---|---|---|---|
| Gray-Out | 12 | 2 | 35 sec. | 5.30 kw | 725 w.h. | 8.7 kwh | VI |
| Sensitivity Threshold | 14 | 2 | 1 min. | 1.66 kw | 710 w.h. | 9.9 kwh | VII |
| Oculogravic Illusion | 14 | 2 | 1 min. | 1.66 kw | 710 w.h. | 9.9 kwh | VII |
| Semicircular Canal | 12 | 1 | 2 hrs. | 0.93 kw | 2435 w.h. | 29.2 kwh | I |
| Tilt Table | 12 | 2 | 25 min. | 1.66 kw | 1065 w.h. | 12.8 kwh | II |
| Mass Measure | 12 | 2 | 3 min. | 1.66 kw | 755 w.h. | 0.9 kwh | V |
| Reentry Simulation | 6 | 1 | 9 min. | 5.30 kw | 1020 w.h. | 6.1 kwh | III |
| Therapeutic | 40 | 4 | 30 min. | 4.20 kw | 1375 w.h. | 55.0 kwh | IV |
| Combined Sensitivity and Oculogravic | 7 | 1 | 34 min | 1.66 kw | 1115 w.h. | 7.8 kwh | VIIB |

## Life Support and Environmental Control

The environmental control subsystem required to support the centrifuge experiment will vary with the configuration selected. The AAP philosophy proposed by NASA stipulates maximum utilization of Apollo hardware with minimum alteration of current systems. Determination of current ECS capabilities and available qualified equipment requires analysis of the possible centrifuge configurations and review of Apollo Command and Service Module and planned AAP Mission capabilities.

a.   CSM/LM/SRC - The Apollo Command and Service Module (CSM), as adapted to the AAP, is capable of supporting a 45 day, 3 man mission. In on-orbit configuration with the Command Module (CM) docked to an integral Laboratory Module LM) and centrifuge, the CM will provide water, waste management, power, humidity and contaminant control, atmospheric and metabolic stores and food for the entire spacecraft. The CM has thermal control capabilities which support its own equipment only, during launch, orbit and entry.

The LM, planned for AAP as a mated laboratory for experiment packages, has limited capability for environmental control. The LM-AAP radiator does provide adequate heat rejection for LM equipment, cabin temperature control and a pressure suit circuit at a 2-man level. It has no added capacity comensurate with anticipated centrifuge loads, now estimated at about 4000 Btu/hr.

Though the CM, under many conditions, has some added capacity for heat rejection, the flexibility required of the CM for launch, on-orbit and emergency orientations does not permit plumbing connections to the LM or centrifuge. This obviates the possibility of heat load transfer from the LM and centrifuge except by atmospheric transfer. Limited atmospheric transfer feasible does permit humidity and contaminant control, with some inherent sensible cooling but the LM/SRC must reject a majority of its own heat load.

The LM/SRC has two feasible means of heat rejection available in this configuration. First the LM fluid heat transfer circuit can be expanded into the mated centrifuge to provide one circuit of sufficient capacity to collect all loads. Heat can be rejected by a new radiator of full LM/SRC capacity or the planned LM radiator plus evaporative water cooling utilizing excess fuel cell water plus stored expendables. Secondly, the centrifuge alone may be provided its own independent heat rejection circuit. Again a radiator or evaporative coolant would serve as a heat rejector.

b. CAC (Apollo Mission C Cluster Configuration) - This cluster design is planned by NASA specifically toward LM-mated experiment module docking. Atmospheric control and food, water and waste management are handled within the basic cluster (see Figure 99). Thermal control is the responsibility of each module. The cluster with CSM, has a capability for a one-year mission with 90-day resupply. The LM/Centrifuge environmental control requirements do not change from those indicated for the other configurations. The means of heat rejection are limited by three factors. These are: 1) potential radiator shadowing (reducing capacity when docked), 2) the cluster power is produced by solar arrays which provide no excess evaporative coolant, and 3) there will be a prohibition against evaporative cooling when the Mission C cluster includes the Apollo Telescope Mount (ATM) experiment which has stringent requirements for an optical environment.

c. EOSS Configuration. This configuration offers the advantages of long mission capability and considerable volume for the storage of expendables and experiment equipment. This large volume, in addition to having existing life support, temperature control capability and crew quarters, should have sufficient, appropriately located external surfaces to accommodate additional space radiators.

Equipment Availability - Based on the ECS requirements for the LM/SRC, and capabilities of the CSM, EOSS, and Mission C cluster, Table 58 has been formulated It contains a list of major equipment which could be applicable to meeting environmental control requirements. This equipment could be incorporated into current systems and/or utilized to fabricate new thermal control circuits. All are or should be qualified, under current plans, by the 1971-73 time period.

All components listed are, where possible, described in terms of AAP identification number, capacity, power requirements, weight, size, volume and other pertinent comment. Included are Gemini, Apollo, LEM and AAP qualified equipment. In addition to major components tabulated, a large number of valves, controls, regulators, fittings and other equipment are or will be production articles by 1971.

The heat load data accumulated thus far and the qualified equipment catalogued will be used as feasible centrifuge designs emerge and ECS requirements lend themselves to preliminary ECS design. At this phase in the study no new development articles are anticipated to fulfill environmental control and life support systems requirements.

Table 58. Available System Components

| COMPONENTS | PROGRAM USE | CAPACITY | POWER WATTS | WEIGHT POUNDS | VOLUME CUBIC FEET | DIMENSIONS | REMARKS |
|---|---|---|---|---|---|---|---|
| Heat Exchangers<br>Liquid-to-gas | Apollo<br>LEM | 1130 Btu/hr.<br>2770 Btu/hr. | ---<br>--- | 9.2<br>14.8 | ---<br>1.0 | <br>16.9 x 10.9 x 9.5" | |
| Heat Exchanger Electrical Heating Element | Apollo | 938 But/hr. | 275 | 0.4 | --- | 1.5" dia. x 7.5" | Use as required to meet load. |
| Heat Exchanger Fans | LEM<br>Apollo | 242 cfm<br>91 cfm | 31<br>19 | 3.0<br>1.4 | ---<br>--- | 6.5 x 6" dia. | Two per heat exchanger<br>147 lb/hr. @ 5 psia |
| Porous Plate Sublimator (Evaporative Cooler) | LEM | 9200 Btu/hr @ 90 F | --- | 16.0 | 0.39 | 8 x 12 x 7" | Capacity is function of inlet coolant temperature |
| Water Boiler | Apollo | 7600 Btu/hr. | --- | 12.0 | --- | --- | 3000 hr. life |
| Radiator | Apollo | ~50Btu/hr-ft$^2$ | --- | 1.5 lb/ ft$^2$ | --- | --- | Redundant design |
| Pump Package | LEM | 220 lb/hr. | 60<br>(2 pumps) | 7.5 | 0.28 | 8.5 x 8.5 x 7" | Water, Glycol or Freon 21 Capability |
| Freon 21 Pump Package | Apollo | 660 lb/hr. | 72 | --- | --- | --- | Water or Glycol Capability |
| Suit Circuit Packages | Gemini<br>Apollo | 2 suits<br>3 suits | ---<br>38 | 175.0<br>130.0 | ---<br>--- | --- | 28 day LiOH capability<br>Emergency suit use – 87W, Humidity control –38W<br>4 days LiOH |
| Oxygen Tank – Descent | LEM | 23 lb. GOX | --- | 58.0 | --- | --- | --- |
| Liquid Intercooler | AAP | 1800 Btu/hr. | --- | 10.0 | --- | --- | Liquid-to-liquid |
| Water Tank – Ascent Cooling | LEM | 26 lb. | --- | --- | --- | --- | --- |
| Modular Interchange Fan | Apollo | 180 cfm | 17 | 4.0 | 0.5 | --- | 292 lb/hr. @ 5 psia |
| Interchange Fan Ducts | Apollo | --- | --- | 2.0 | --- | --- | --- |
| Catalytic Burner | AAP | --- | 45 | 25.0 | --- | --- | --- |
| Oxygen Tank – Super. Crit. | AAP | 655 lb. useful | 150 | 237.0 | 10.0 | 32" dia. | Intermittent Power |
| Oxygen Tank – Super. Crit. | AAP | 1200 lb. useful | 150 | 300.0 | 20.0 | 41.5" dia. | Intermittent Power |
| Nitrogen Tank – Super. Crit. | AAP | 126 lb. useful | 150 | 72.0 | 7.4 | 29" dia. | Intermittent Power |
| Molecular Sieve | AAP | 3 man | 120 | 161.0 | --- | --- | Water–Save design |
| Molecular Sieve | MOL | 2 man | 50 | 90.0 | --- | --- | Water discharge |
| Cryogenic Heat Exchanger | Apollo | ~5000 Btu/Hr. | --- | --- | --- | --- | --- |
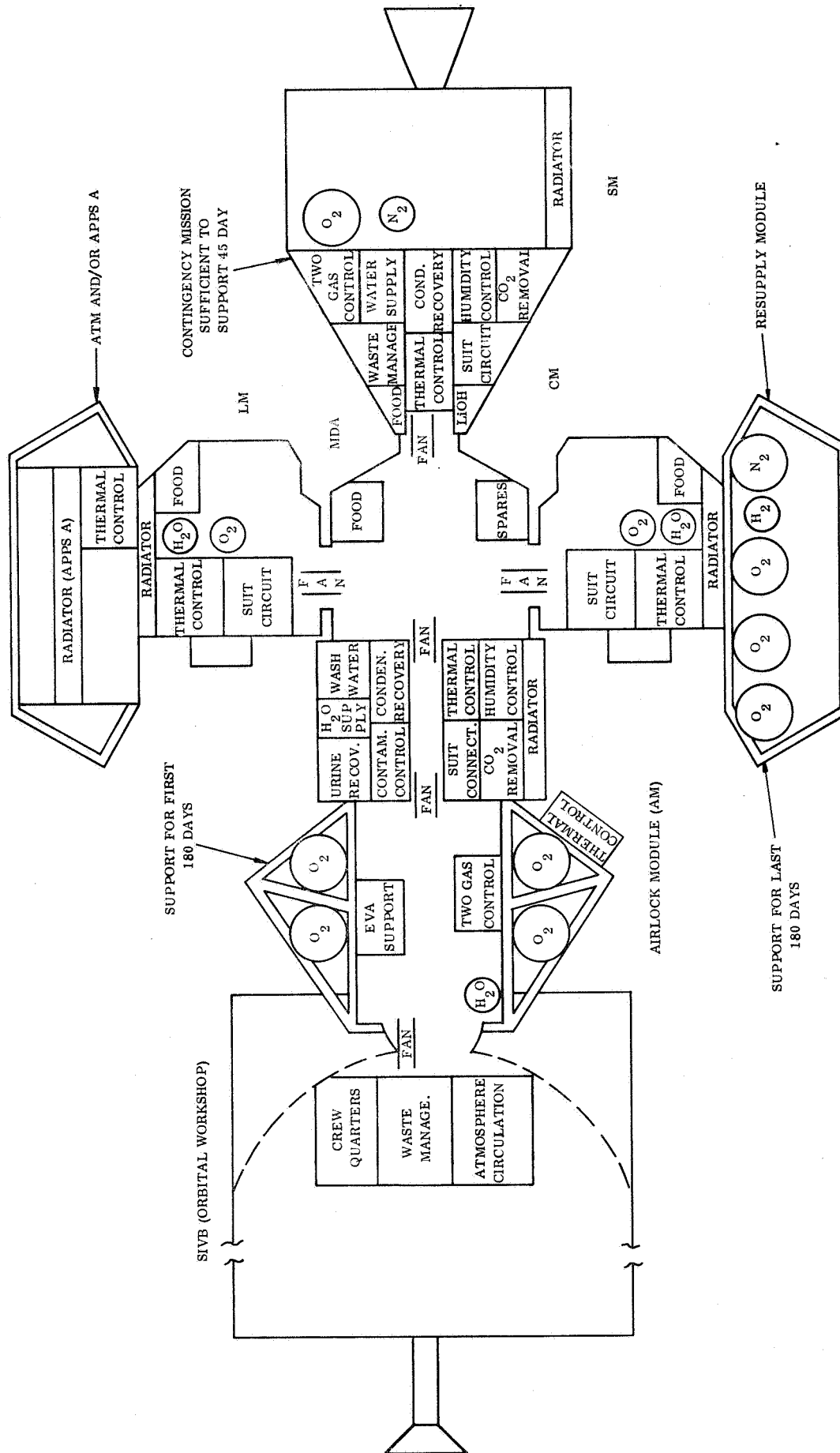
Figure 99.  Environmental Control System – AAP Mission C Concept

## Technology Feasibility

The technology required for the development of the centrifuge has been reviewed to determine if any departure from existing state-of-the-art may be expected. While no technological barriers to centrifuge development have been uncovered, two areas where advanced development is required have been identified. These areas involve bearing design and motor development.

Bearing Design - Centrifuge bearing requirements have been identified as the most significant design areas where development or technology improvement is required. While development work in new bearing concepts applicable to the centrifuge is being pursued by many major bearing suppliers, performance to centrifuge requirements has not been demonstrated. This is the result of the unusual characteristics desired, which include low weight, dry operation, zero noise (couch roll bearings), moderate life, light load capability, and low contaminant generation. A bearing development program is recommended which consists of evaluation of the selected primary approaches to determine which is most suitable. Suggested initial approaches include the application of hollow steel balls on an aluminum race; aluminum oxide balls operating on an anodized aluminum race with a teflon retainer; and teflon or teflon coated roller operating against an aluminum race. If the primary configurations are found to be unacceptable, more conventional backup approaches may be introduced at the expense of greater mechanical complexity, but with good expectation of success because of their greater background of applications technology. Bearings in this category include conventional bearings with sealed dry lubricant incorporated; gas bearings; or conventional grease-lubricated bearings with special sealing provisions.

Motor Development - Analysis of the centrifuge motion requirements shows that three characteristic motor performance patterns are involved: (1) the couch roll motion requires a low-speed, low-power motor with a large speed control range and proportional operation; (2) arm translation, couch pivot and counterweight drives are characterized by low power, quick response, on-off operation; and (3) the main drive requires relatively high power levels and wide-range, proportional speed control. In all cases, spark-free (brushless), lightweight, highly reliable units are desired.

For the couch roll application, requirements appear to be met by units similar to the Sperry Farragut, fractional-hp, brushless d-c motor presently qualified for use on the LM. Only minor alterations, such as mounting provisions, would be necessary. The main drive with its 3 to 4-hp peak power requirement is beyond the present scaling capability of the brushless d-c approach. For this application, an a-c motor used with an inverter and a voltage/frequency control is recommended. Technology

and background for this equipment exists from development of drive units for under-water research vessels such as "Deep Quest." Development requirements for the centrifuge application are seen as repackaging and redesign for low weight and high reliability. For the arm translation, couch pivot and counterweight system, either the brushless d-c or the inverted a-c approach is feasible.

# REFERENCES

1. Crisp, R.; and Keene, D.: Apollo Command and Service Module Reaction Control by the Digital Autopilot. MIT Report E-1964, May 1966.

2. Anon.: Apollo Guidance, Navigation and Control, Guidance System Operations Plan. MIT Report R1547, AS-278, Vol. 1, CM GNCS Operations, October 1966.

3. O'Connor, B. J.; and Morine, L. A.: A Description of the CMG and Its Application to Space Vehicle Control. AIAA Paper No. 67-589, August 1967.

4. Chubb, W. B.; Schultz, D. N.; and Seltzer, S. M.: Attitude Control and Precision Pointing for the Apollo Telescope Mount. AIAA Paper No. 67-534, August 1967.

5. Tewell, J. R.; and Murrish, C. H.: Engineering Study and Experiment Definition for an Apollo Applications Program Experiment on Vehicle Disturbances Due to Crew Activity. NASA CR-66277, March 1967.

6. Anon.: CSM/LM Mode Data for Full Weight Condition. TRW Letter 67.3302.0-45, July 12, 1967.

7. Anon.: Vibration Analysis of the S-IVB Workshop With Cluster in the AAP-3/4 Configuration. Brown Engineering Co. Report T.D. C1-SLS-3-009, Contract NAS 8-20073, May 5, 1967.

8. Anon.: Free-Free Modes and Frequencies for OWS-AM-MDA-C/SM-LM/ATM Cluster Configuration with ATM Solar Panels Both Undeployed and Deployed. Lockheed Missiles and Space Co., Huntsville Research and Engineering Center, TM 54/50-80, LMSC/HREC A784679, September 19, 1967.

9. Davis, L. P.: Optimization of Control Moment Gyro Design. Sperry Phoenix Co. Publication No. LJ-1252-0765, May 1967.

10. Newsom, B. D.; and Brady, J. F.: A Comparison of Performances Involving Head Rotations About Y and Z Cranial Axes in a Revolving Space Station Simulator. Aerospace Medicine, Vol. 37, No. 11, November 1966.

11. Stone, R. W.; and Letko, W.: Some Observations on the Stimulation of the Vestibular System of Man in a Rotating Environment. NASA SP-77, Langley Research Center, January 1966.

12. Anon.: Failure Rate Data Handbook (FARADA), U. S. Naval Fleet Missile Systems Analysis and Evaluation Group, Corona, California. SP-63-470 and Revisions, 1 June 1962.

13. Anon.: Military Standardization Handbook - Reliability Stress and Failure Rate Data for Electronic Equipment. DOD MIL-HDBK-217A, 1 December 1965.

# APPENDIX A
## DERIVATION OF EQUATIONS OF MOTION FOR APOLLO CSM
## WITH ONBOARD CENTRIFUGE AND BALANCER

### Coordinate Definition

Figure A1 defines parameters pertinent to the centrifuge installation on the Apollo vehicle.
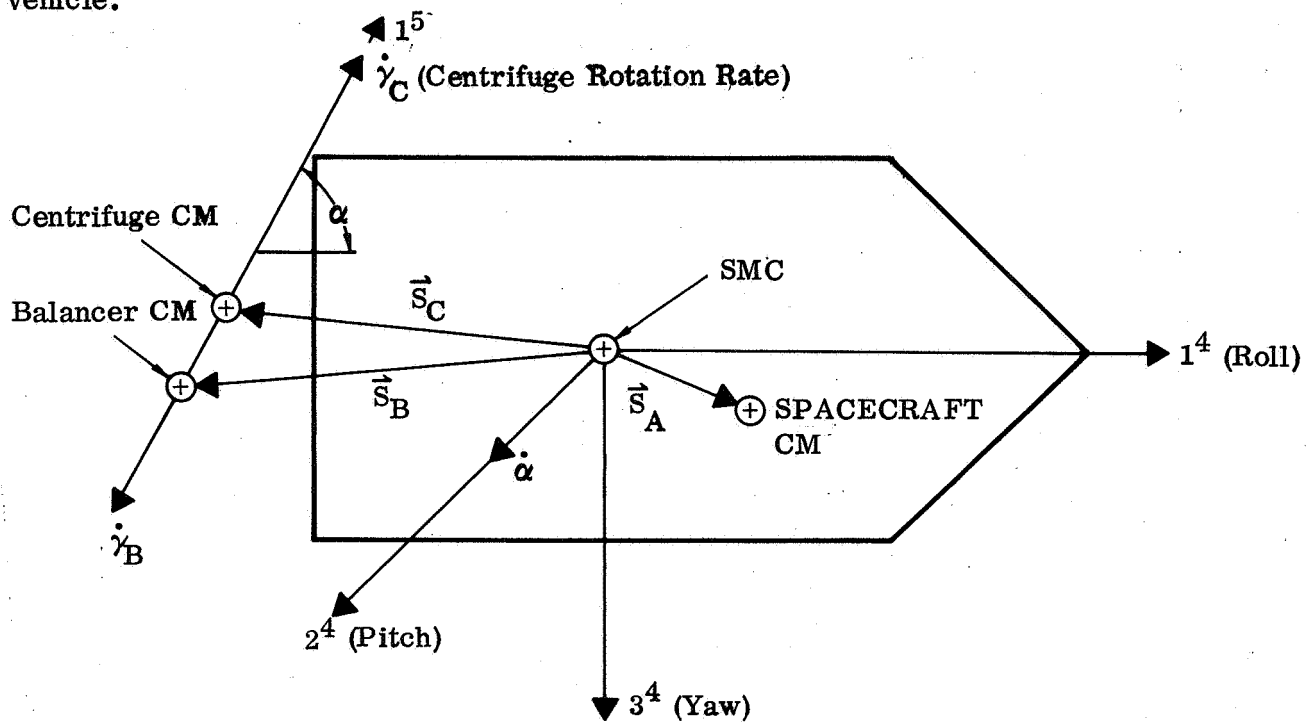


Figure A1. Centrifuge, balancer installation coordinate definitions.

The three bodies comprise the centrifuge, the balancer (if needed) and the Apollo vehicle. Axes, 1, 2 and 3 (super 4) are aligned to convenient Apollo reference axes, not necessarily the principal axes, but centered at the system center of mass (SMC).

The vector quantities $S_A$, $S_C$, $S_B$ are the distances from the SMC to the Apollo, Centrifuge & Balancer bodies center of mass (CM) respectively. Note that these distances from the SMC to the particular body CM are considered fixed in Apollo body coordinates because it has been assumed (for present purposes) that the Balancer, Centrifuge CM's are exactly on the centrifuge rotation axis.

The angle $\alpha$ is the rotation angle, about the Apollo pitch axis, between the centrifuge spin (major principal axis) and the Apollo roll axis. The centrifuge spin angle is $\gamma_C$ whereas the balancer counterspin angle is $\gamma_B$. Frame super 5 is centered at the centrifuge CM and aligned with the centrifuge principal axes. The angles $\gamma_C$ and $\gamma_B$ are defined relative to the Apollo vehicle and are generated by the centrifuge motor.

Figure A2 defines the attitude perturbation of the 3 body system from a desired attitude.
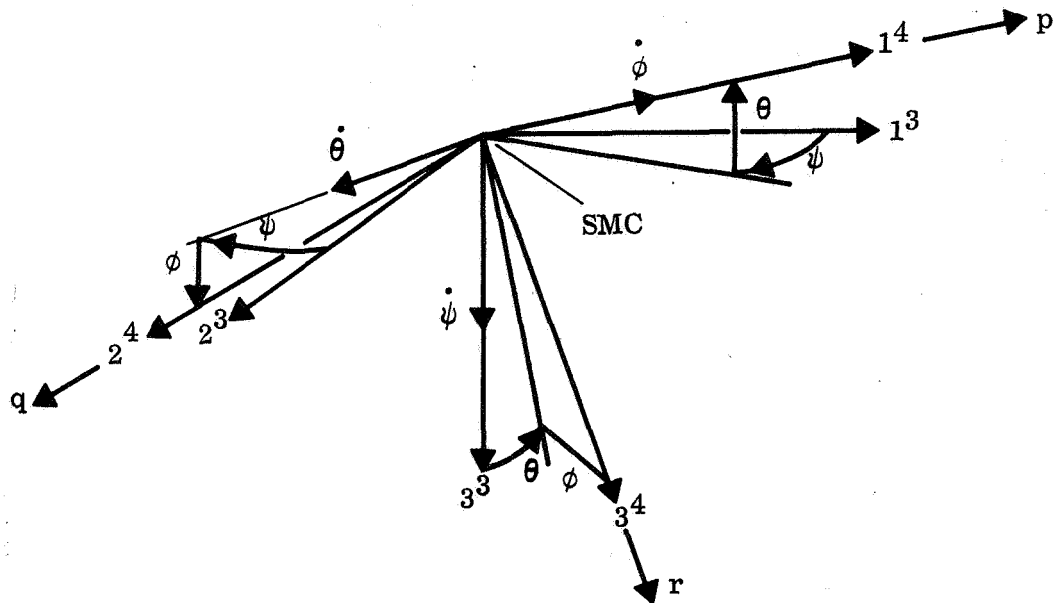


Figure A2. Vehicle angular perturbation model coordinate definition.

Axes 1, 2 and 3 (super 3) are defined to be the desired orientation of the Apollo body fixed reference axes (super 4 system). The deviation from the desired reference is expressed in terms of the Euler Angles $\psi$ (yaw), $\theta$ (pitch), and $\phi$ (roll). The angular rate of the Apollo body relative to the super 3 frame is given by either the Euler angle rates $\dot{\psi}$, $\dot{\theta}$, and $\dot{\phi}$ or the same total rate in terms of Apollo body fixed angular rate components p (roll), q (pitch) and r (yaw) rates. These angles deviate a small amount from zero as controlled by the Apollo autopilot.

Figure A3 defines an inert frame (super 1) centered at the earth center. The negative $3^1$ axis is placed at the orbit perigee and the $2^1$ opposite to the orbit angular rate vector as shown.
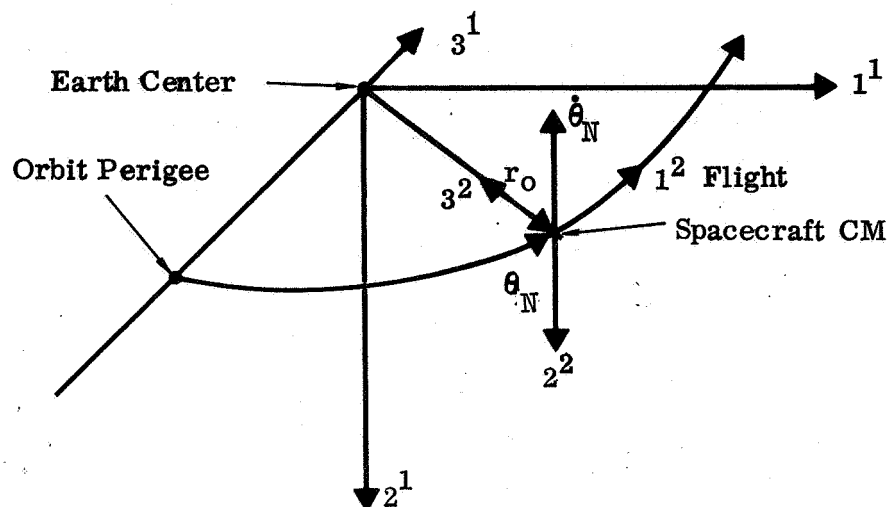
Figure A3. Orbit definition.

Figure A3 also illustrates an "orbit" reference frame (super 2) centered at the space-craft SMC (a distance $r_0$ from the center of the earth). As shown the $3^2$ direction is down along local vertical and the $2^2$ is opposite to the orbit normal. If the super 2 frame was the desired attitude of the Apollo vehicle then the Apollo desired roll axis would be directed along the flight vector (for a circular orbit).

It is assumed that an attitude referenced to the earth is desired for the Centrifuge experiment. The desired attitude is specified by two angles E and H referenced to the "orbit" or super 2 frame. Figure A4 defines these angles.
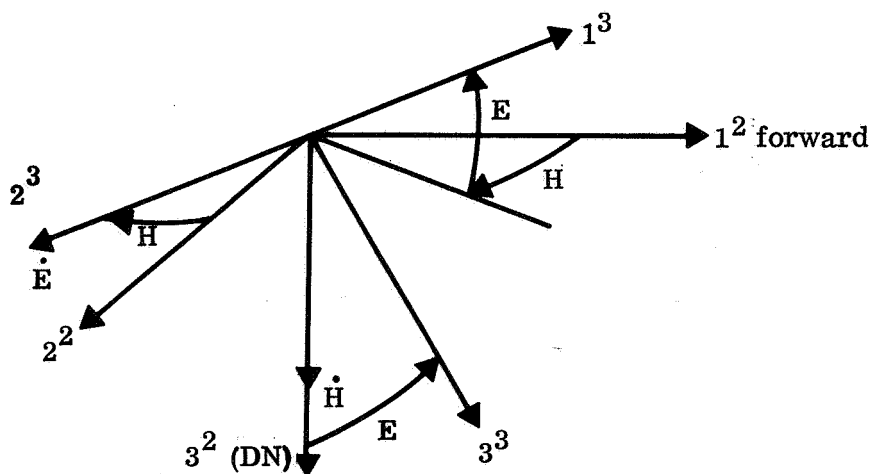


Figure A4. Earth referenced attitude selection

The super 3 frame is the desired frame of reference first introduced in Figure A2.

Under the assumptions that the desired attitude is earth oriented and also that a low altitude (say about 200 to 500 n.mi.) nearly circular orbit is acceptable, the desired attitude frame is rotating with respect to inertia in a manner directly related to the orbit angular rate. Use $\omega_{13}$ for this rate. It is evaluated later.

Coordinates are now sufficiently defined to allow calculation of the system angular momentum and its time derivative relative to the SMC. When equated to the sum of the torque from the Apollo autopilot and the orbit environment, angular motion equations result.

### Derivation of System Momentum

$$\vec{H}_T = \vec{H}_A + \vec{H}_B + \vec{H}_C \tag{1}$$

where $\vec{H}_T$ is the system angular momentum calculated relative to the SMC.

$\vec{H}_A$, $\vec{H}_B$, $\vec{H}_C$ are the Apollo, Balancer and Centrifuge angular momenta calculated relative to the SMC.

With torques and momentum calculated relative to the SMC

$$\vec{T} = \vec{T}_C + \vec{T}_E = \dot{\vec{H}}_T \tag{2}$$

where $\vec{T}$ is the total external torque acting on the system calculated relative to the SMC.

$\vec{T}_C$ is the Apollo attitude control thrusters torque calculated relative to the SMC.

$\vec{T}_E$ is the environmental torque (e.g., gravity torque) acting on the system calculated relative to the SMC.

The analysis, as constructed to this point does not consider body bending, fuel slosh or centrifuge dynamic or static unbalance. These effects are important but can be considered separately. In this derivation the bodies are considered rigid.

The torques acting on the system, identified in Eq. 2, are developed later. For now consider the calculation of the angular momentum and its total time derivative. For a body with CM offset from the SMC, the momentum relative to the SMC is,

$$\vec{H} = \vec{S} \times M\dot{\vec{S}} + \vec{H}_G \tag{3}$$

A4

where $\vec{H}$ is the angular momentum vector calculated relative to the SMC

$\vec{S}$ is the vector distance from the SMC to the body MC

M is the body mass

$\vec{H}_G$ is the body angular momentum vector calculated with respect to the body MC.

For the three bodies, the momentums

$$\vec{H}_A = \vec{S}_A \times M_A \, \dot{\vec{S}}_A + \vec{H}_{AG}$$

$$\vec{H}_B = \vec{S}_B \times M_B \, \dot{\vec{S}}_B + \vec{H}_{BG} \qquad (4)$$

$$\vec{H}_C = \vec{S}_C \times M_C \, \dot{\vec{S}}_C + H_{CG}$$

where the subscript A refers to the Apollo body, the subscript B refers to the balancer, the subscript C refers to the centrifuge.

The $\vec{S} \times M \, \dot{\vec{S}}_A$ is the additional amount due to non-coincident body MC and SMC. Consider the calculation of that term.

$$\Delta \vec{H} \equiv \vec{S}_A \times M_A \, \dot{\vec{S}}_A + \vec{S}_B \times M_B \, \dot{\vec{S}}_B + \vec{S}_C \times M_C \, \dot{\vec{S}}_C \qquad (5)$$

Note that the vectors $\vec{S}_A$, $\vec{S}_B$ and $\vec{S}_C$ are fixed to the Apollo body. Their derivatives are then,

$$\dot{\vec{S}}_A = \vec{W}_A \times \vec{S}_A, \quad \dot{\vec{S}}_B = \vec{W}_A \times \vec{S}_B, \quad \dot{\vec{S}}_C = \vec{W}_A \times \vec{S}_C \qquad (6)$$

where $\vec{W}_A$ is the angular rate of the Apollo body relative to the inert reference.

The total additional amount of momentum is then

$$\Delta \vec{H} = \vec{S}_A \times M_A \, (\vec{W}_A \times \vec{S}_A) = M_A \left[ S_A^2 \, \vec{W}_A - (\vec{W}_A \cdot \vec{S}_A) \vec{S}_A \right] +$$

$$+ \vec{S}_B \times M_B \, (\vec{W}_A \times \vec{S}_B) \quad M_B \left[ S_B^2 \, \vec{W}_A - (\vec{W}_A \cdot \vec{S}_B) \vec{S}_B \right] + \qquad (7)$$

$$+ \vec{S}_C \times M_C \, (\vec{W}_A \times \vec{S}_C) \cdot M_C \left[ S_C^2 \, \vec{W}_A - (\vec{W}_A \cdot \vec{S}_C) \vec{S}_B \right]$$

The vector identity

$$\vec{A} \times (\vec{B} \times \vec{C}) = (\vec{A} \cdot \vec{C})\,\vec{B} - (\vec{A} \cdot \vec{B})\,\vec{C}$$

was used to generate the rightmost term of Eq. 7. Expand one of the rightmost terms of Eq. 7 using the Apollo body fixed reference frame (frame 4). The result is

$$M\left[S^2\vec{W} - (\vec{W} \cdot \vec{S})\vec{S}\right] = M\,(S^2_A)\begin{bmatrix} W_1 \\ W_2 \\ W_3 \end{bmatrix} - (W_1 S_1 + W_2 S_2 + W_3 S_3)\begin{bmatrix} S_1 \\ S_2 \\ S_3 \end{bmatrix} \tag{8}$$

$$= M\begin{bmatrix} S_2^2 + S_3^2 & -S_1 S_2 & -S_1 S_3 \\ -S_1 S_2 & S_1^2 + S_3^2 & -S_2 S_3 \\ -S_1 S_3 & -S_2 S_3 & S_1^2 + S_2^2 \end{bmatrix}\begin{bmatrix} W_1 \\ W_2 \\ W_3 \end{bmatrix} \tag{9}$$

$$\equiv \left[\Delta I\right]\left[W\right] \tag{10}$$

Compare the result given in Eq. 9 with the inertia matrix of the Apollo vehicle with the inertias calculated relative to the Apollo MC.

$$\left[I_{AG}\right] \equiv \begin{bmatrix} I_{A11} & -I_{A12} & -I_{A13} \\ -I_{A12} & I_{A22} & -I_{A23} \\ -I_{A13} & -I_{A23} & I_{A33} \end{bmatrix} \tag{11}$$

where $\left[I_{AG}\right]$ is the inertia matrix of the Apollo body calculated about the Apollo body CM.

It is evident from comparisons of Eqs. 9 and 11 that

$$\left[H_A\right] + \left[\Delta H\right] = \left\{\left[I_{AG}\right] + \left[\Delta I_A\right] + \left[\Delta I_B\right] + \left[\Delta I_C\right]\right\}\left[W_A\right] \tag{12}$$

A6

where $\left[\Delta I_A\right]$, $\left[\Delta I_B\right]$, $\left[\Delta I_C\right]$ are the additional contributions to the basic Apollo vehicle inertia matrix due to offset of the body CM from the SMC.

$\left[W_A\right]$ is the Apollo body fixed angular rate components with respect to an inert reference.

To summarize, Eq. 12 says that the effective rotational inertias of the Apollo vehicle can be considered to be that calculated considering the centrifuge and balancer bodies as point masses located at the body CM. Define this inertia matrix as

$$\left[I_{AE}\right] = \left[I_{AG}\right] + \left[\Delta I_A\right] + \left[\Delta I_B\right] + \left[\Delta I_C\right] \tag{13}$$

The total momentum, given previously in Eq. 1 can be rewritten using the effective inertia of Eq. 13 as follows:

$$\left[H_T\right] = \left[I_{AE}\right]\left[W_A\right] + \left[I_B\right]\left[W_B\right] + \left[I_C\right]\left[W_C\right] \tag{14}$$

where $\left[I_B\right]$, $\left[I_C\right]$ are the moments of inertia matrices of the balancer and centrifuge respectively calculated about the body CM; $W_A$, $W_B$, $W_C$ are the angular rates of the Apollo, balancer, centrifuge in body axis components relative to the inert frame.

It is desired to calculate the matrix $(H_T)$ in Apollo fixed axes to generate the desired solutions for $(W_A)$ and the resultant deviation angles $\theta$, $\psi$, and $\phi$. Notation indicating reference frame and transformation matrices is needed at this point. The notation used is as follows:

$(W^k_{ij})_\ell$    is the $\ell$ component in frame k of the angular rate of frame j relative to frame i.

$\left[\alpha_{ij}\right]$    is the transformation matrix which when used to premultiply a vector in frame i gives the same vector in frame j.

$(H^j)_i$    is the i component of vector H in frame j.

Using the above notation

$$\left[(H^4_A)_i\right] = \left[I_{AE}\right]\left[(W^4_A)_i\right] = \begin{bmatrix} I_{AE11} & -I_{AE12} & -I_{AE13} \\ -I_{AE12} & I_{AE22} & -I_{AE23} \\ -I_{AE13} & -I_{AE23} & I_{AE33} \end{bmatrix} \begin{bmatrix} (W^4_A)_1 \\ (W^4_A)_2 \\ (W^4_A)_3 \end{bmatrix} \tag{15}$$

directly gives the contribution of the Apollo vehicle and centrifuge plus balancer body point masses to the system momentum with components calculated in the Apollo reference frame (frame 4).

To obtain the momentums of the balancer and centrifuge in the desired same frame the required steps are indicated below for the centrifuge body. The balancer body contribution is identical in form.

$$(H^5_{CG})_i = \begin{bmatrix} I_{C1} & 0 & 0 \\ 0 & I_{C2} & 0 \\ 0 & 0 & I_{C3} \end{bmatrix} \begin{bmatrix} (W^5_A)_1 + \dot{\gamma}_C \\ 0 \\ 0 \end{bmatrix} \tag{16}$$

$$= \begin{bmatrix} I_C \end{bmatrix} \begin{bmatrix} (W^5_C)_i \end{bmatrix} \tag{17}$$

$$\begin{bmatrix} (H^4_{CG})_i \end{bmatrix} = \begin{bmatrix} \alpha_{45} \end{bmatrix}^T \begin{bmatrix} I_C \end{bmatrix} \begin{bmatrix} (W^5_C)_i \end{bmatrix} \tag{18}$$

$$= \begin{bmatrix} \alpha_{45} \end{bmatrix}^T \begin{bmatrix} I_C \end{bmatrix} \begin{bmatrix} \alpha_{45} \end{bmatrix} \begin{bmatrix} (W^4_A)_i + (W^4_{45})_i \end{bmatrix} \tag{19}$$

The transform from the 4 to the 5 frame is indicated by $\alpha_{45}$ and the transpose (in this case also the inverse because $\alpha_{45}$ is an orthogonal matrix) is indicated by $\begin{bmatrix} \alpha_{45} \end{bmatrix}^T$.

This transform is

$$\begin{bmatrix} \alpha_{45} \end{bmatrix} = \begin{bmatrix} \gamma_C \end{bmatrix} \begin{bmatrix} \alpha \end{bmatrix} \equiv \begin{bmatrix} 1 & 0 & 0 \\ 0 & C\gamma_C & S\gamma_C \\ 0 & -S\gamma_C & C\gamma_C \end{bmatrix} \begin{bmatrix} C\alpha & 0 & -S\alpha \\ 0 & 1 & 0 \\ S\alpha & 0 & C\alpha \end{bmatrix} \tag{20}$$

The angle $\alpha$ is constant but $\gamma_C$ changes at centrifuge spin rate. Temporarily it is desired to keep the two matrices separate in rewriting Eq. 19 as given below.

$$\left[ (H_{CG}^4)_i \right] = \left[ \alpha \right]^T \left[ \gamma_C \right]^T \left[ I_C \right] \left[ \gamma_C \right] \left[ \alpha \right] \left[ (W_A^4)_i + (W_{45}^4)_i \right] \tag{21}$$

Note that $(W_A^4)_i$ is the body axis rotation rates of the Apollo vehicle and $(W_{45}^4)_i$ is the centrifuge spin rate in the Apollo vehicle frame. The first is what it is intended to calculate, the second is prescribed by centrifuge experiment requirements. The matrix combination $\left[ \gamma_C \right]^T \left[ I_C \right] \left[ \gamma_C \right]$ is time variable and it is desired to evaluate same to determine permissible simplifications.

$$\left[ \gamma_C \right]^T \left[ I_C \right] \left[ \gamma_C \right] = \begin{bmatrix} I_{C1} & 0 & 0 \\ 0 & \begin{array}{c}(I_{C3} + I_{C2})/2 \\ -(I_{C3} - I_{C2})\,C2\gamma_C/2\end{array} & -(I_{C3} - I_{C2})\,S2\gamma_C/2 \\ 0 & -(I_{C3} - I_{C2})\,S2\gamma_C/2 & \begin{array}{c}(I_{C3} + I_{C2})/2 + \\ (I_{C3} - I_{C2})\,S2\gamma_C/2\end{array} \end{bmatrix} \tag{22}$$

$I_{C1}$ is the spin moment of inertia of the centrifuge. $I_{C2}$ and $I_{C3}$ are the lateral unequal inertias. Note that if the lateral inertias were equal the matrix would be constant magnitude immediately introducing considerable simplification. As it is, a momentum change at twice centrifuge spin frequency is introduced but further work will show that the variable portion of the matrix may be neglected. Indeed if it were not negligible it would cause vibrations at twice spin frequency of the same nature as that due to centrifuge static and dynamic unbalance (except that these cause vibration at spin frequency) and would require that the centrifuge be built with lateral symmetry.

To show that the variable portion of the matrix may be neglected first separate the variable and constant portions of the matrix of Eq. 22 as follows.

$$\left[ \gamma_C \right]^T \left[ I_C \right] \left[ \gamma_C \right] \equiv \left[ I_C' \right] + \left[ I_C'' \right]$$

$$= \begin{bmatrix} I_{C1} & 0 & 0 \\ 0 & \dfrac{(I_{C3} + I_{C2})}{2} & 0 \\ 0 & & \dfrac{(I_{C3} + I_{C2})}{0} \end{bmatrix} + \dfrac{I_{C3} - I_{C2}}{2} \begin{bmatrix} 0 & 0 & 0 \\ 0 & -C2\gamma_C & -S2\gamma_C \\ 0 & -S2\gamma_C & +C2\gamma_C \end{bmatrix} \tag{23}$$

Now consider the contribution of the variable portion of the matrix of Eq. 23 to the momentum of the centrifuge given in Eq. 21.

$$\left[ (H^4_{CU})_i \right] \equiv \left[ \alpha \right]^T \left[ I''_C \right] \left[ \alpha \right] \left[ (W^4_A)_i + (W^4_{45})_i \right] \tag{24}$$

Multiplying out $\left[ \alpha \right]^T \left[ I''_C \right] \left[ \alpha \right] \left[ (W^4_{45})_i \right]$,

where from Figure 1,

$$\left[ (W^4_{45})_i \right] = \begin{bmatrix} \dot{\gamma}_C \, C\alpha \\ 0 \\ -\dot{\gamma}_C \, S\alpha \end{bmatrix} \tag{25}$$

yields 0. Eq. 24 reduces to

$$\left[ (H^4_{CU})_i \right] = \left[ \alpha \right]^T \left[ I''_C \right] \left[ \alpha \right] \left[ (W^4_A)_i \right] \tag{26}$$

The variable momentum of Eq. 26 is not zero but turns out to be a small quantity because the angular rate (small) of the Apollo vehicle is involved rather than the angular rate of the centrifuge (large). A good estimate of the magnitude of this torque is obtained by expanding Eq. 26 and using reasonable numerical values of unbalance inertia and Apollo angular rate. The below matrix multiplication accomplishes the expansion of the coefficient of the Apollo angular rate term.

$$\left[ \alpha \right]^T \left[ I''_C \right] \left[ \alpha \right] = \frac{I_{C3} - I_{C2}}{2} \begin{bmatrix} S^2\alpha \, C2\gamma_C & -S\alpha S2\gamma_C & \dfrac{S2\alpha}{2} C2\gamma_C \\ -S2\gamma_C \, S\alpha & -C2\gamma_C & -S2\gamma_C \, C\alpha \\ \dfrac{S2\alpha}{2} C2\gamma_C & -C\alpha S2\gamma_C & C2\gamma_C \, C^2\alpha \end{bmatrix} \tag{27}$$

Realizing that the momentum time derivative gives the torque exchange between the centrifuge and the Apollo body and that this torque is at twice spin frequency a maximum value of variable momentum from Eq. 27 is

$$H_U = \frac{I_U}{2} W_A \sin 2\gamma_C \tag{28}$$

A10

where $H_U$ is the unbalance momentum

$W_A$ is the Appollo angular rate

$I_U$ is the unbalance in centrifuge transverse inertia
(equal to $I_{C3} - I_{C2}$)

The maximum value of the unbalance torque is obtained by differentiating Eq. 28.

$$T_U = \dot{H}_U = I_U \dot{\gamma}_C W_A \qquad (29)$$

where $T_U$ is the unbalance torque.

Reasonable values for the pertinent parameters are

$$I_U = 700 \text{ lb-ft-sec}^2$$

$$\dot{\gamma}_C = 60 \text{ RPM or } 6.28 \text{ rad/sec}$$

$$W_A = .2 \text{ deg/sec (Apollo DAP max rate line)}$$
$$= 0.0035 \text{ rad/sec}$$

$$T_U = (700)(6.28)(.0035) = 15.4 \text{ ft-lbs.}$$

So a good current estimate of unbalance torque under conservative assumptions is $\pm 15$ ft-lbs of torque oscillating about zero at twice spin frequency. Assuming that the torque appears in Apollo pitch the resultant peak acceleration, rate and displacement is

$$\dot{W}_U = \frac{T_U}{I_P} = (15 \times 57.3)/220,000 = .39 \times 10^{-2} \text{ deg/sec}^2$$

$$W_U = \frac{\dot{W}_U}{2\dot{\gamma}_C} = \frac{.39 \times 10^{-2}}{2 \times 6.28} = .312 \times 10^{-3} \text{ deg/sec}$$

$$\theta_U = \frac{W_U}{2\dot{\gamma}_C} = \frac{.39 \times 10^{-3}}{2 \times 6.28} = .25 \times 10^{-4} \text{ deg}$$

At these low levels of motion, even if twice spin frequency corresponded to a body mode with 2 order of magnification resulting, the motion and g-loads would still be negligible. It is concluded that the variable portion of the momentum matrix of Eq. 23 is negligible and $\left[ (H_{CG}^{\ 4})_i \right]$ of Eq. 21 rewritten as follows:

$$\left[ (H_{CG}^{4})_i \right] = \left[\alpha\right]^T \left[I_C'\right] \left[\alpha\right] \left[(W_A^4)_i + (W_{45}^4)_i\right]$$

$$= \left[\alpha\right]^T \left[I_C'\right] \left[\alpha\right] \left[(W_A^4)_i\right] + \left[\alpha\right]^T \left[I_C'\right] \begin{bmatrix} \dot{\gamma}_C \\ 0 \\ 0 \end{bmatrix} \qquad (30)$$

The corresponding term for the balancer is

$$(H_{BG}^4)_i = \left[\alpha\right]^T \left[I_B'\right] \left[\alpha\right] \left[(W_A^4)_i\right] + \left[\alpha\right]^T \left[I_B'\right] \begin{bmatrix} -K_B\dot{\gamma}_C \\ 0 \\ 0 \end{bmatrix} \qquad (31)$$

$$\text{where} \quad \left[I_B'\right] = \begin{bmatrix} I_{B1} & 0 & 0 \\ 0 & (I_{B2} + I_{B3})/2 & 0 \\ 0 & 0 & (I_{B2} + I_{B3})/2 \end{bmatrix} \qquad (32)$$

are the balancer principal moments of inertia and $K_B$ is the ratio of balancer counter rotational speed to centrifuge speed.

The intent of the development between Eq. 21 to this point was to show that the unequal lateral inertias is not a design constraint for the centrifuge and also to exclude it from the equations because of the resultant simplification. Now returning to the calculation of momentum, Eqs. 15, 30 and 31 are used in the total momentum Eq. 14 to yield.

$$\left[(H_T^4)_i\right] = \left[ \left[I_{AE}\right] + \left[\alpha\right]^T \left\{ \left[I_C'\right] + \left[I_B'\right]\right\} \left[\alpha\right] \right] \left[(W_A^4)_i\right]$$

$$+ \left[\alpha\right]^T \begin{bmatrix} (I_{C1} - K_B I_{B1})\,\dot{\gamma}_C \\ 0 \\ 0 \end{bmatrix} \qquad (33)$$

The matrix addition multiplying the Apollo body fixed angular rates is constant. Define

$$\left[ J_A \right] \equiv \left[ \left[ I_{AE} \right] + \left[ \alpha \right]^T \left\{ \left[ I_C' \right] + \left[ I_B' \right] \right\} \left[ \alpha \right] \right] \tag{34}$$

$$J_N \equiv I_{C1} - K_B I_{B1}$$

Now rewrite Eq. 33 using these definitions

$$\left[ (H_{Ti}^4) \right] = \left[ J_A \right] \left[ (W_A^4)_i \right] + \begin{bmatrix} J_N \dot{\gamma}_C C\alpha \\ 0 \\ -J_N \dot{\gamma}_C S\alpha \end{bmatrix} \tag{35}$$

The momentum is considered to be reduced to its simplest form in Eq. 35 so we can proceed to take the total derivative to equate to the total torque. We no longer need the cumbersome but explicit notation in regard to coordinate frame because from now on, all computations are in the Apollo fixed frame. The subscript T is dropped from the momentum and the subscript A from the Apollo angular rate and the total effective inertia $\left[ J_A \right]$,

$$T_i = \left[ J \right] \dot{W}_i + \begin{bmatrix} J_N \ddot{\gamma}_C C\alpha \\ 0 \\ -J_N \ddot{\gamma}_C S\alpha \end{bmatrix} + W_i \times H_i \tag{36}$$

To solve for $\dot{W}_i$ multiply by $\left[ J \right]^{-1}$,

$$\dot{W}_i = \left[ J \right]^{-1} \left[ T_i - W_i \times H_i - \begin{bmatrix} J_N \ddot{\gamma}_C C\alpha \\ 0 \\ -J_N \ddot{\gamma}_C S\alpha \end{bmatrix} \right] \tag{37}$$

In the discussion of coordinates the angular rate of the desired attitude reference frame (frame 3) with respect to inertia was identified as $\vec{W}_{13}$. The value of $\vec{W}_{13}$ components in the Apollo reference axes is needed. This is simply the orbit angular rate projected in the Apollo reference frame. For low eccentricity orbits

$$\theta_N = \frac{2\pi t}{T_o} + 2\epsilon S\left(2\pi \frac{t}{T_o}\right) \tag{38}$$

where   $\theta_N$ is the orbit anomaly angle counted from perigee

   $t$   is the time

   $T_o$ is the orbit period

   $\epsilon$   is orbit eccentricity

For reference

$$T_o = 2\pi \bigg/ \left[ g_E R_E^2 / R_{AV}^3 \right]^{1/2}$$

$$R_{AV} = 1/2\,(R_P + R_A) + R_E \tag{39}$$

$$\epsilon \cong (R_A - R_P) / (R_A + R_P + 2\,R_E)$$

where   $g_E$ is the earth surface gravitational constant (32.17 ft/sec$^2$)

   $R_E$ is earth radius (3443 n.mi.)

   $R_P$ is orbit perigee altitude

   $R_A$ is orbit apogee altitude

Then the orbit angle rate and acceleration is

$$\dot{\theta}_N = \frac{2\pi}{T_o} \left[ 1 + 2\epsilon C\left(\frac{2\pi t}{T_o}\right) \right]$$

$$\ddot{\theta}_N = \frac{-8\pi^2}{T_o^2}\,\epsilon S\left(2\pi \frac{t}{T_o}\right) \tag{40}$$

This angular rate and acceleration is directed along the negative $2^2$ direction (See Figure A3).  In frame 4, the Apollo frame

$$(W_{13})_i = \left[\alpha_{34}\right]\left[\alpha_{23}\right] \begin{bmatrix} 0 \\ -\dot{\theta}_N \\ 0 \end{bmatrix} = \left[\alpha_{24}\right] \begin{bmatrix} 0 \\ -\dot{\theta}_N \\ 0 \end{bmatrix} \tag{41}$$

where $\left[ \alpha_{23} \right] = \begin{bmatrix} CE \cdot CH & CE \cdot SH & -SE \\ -SH & CH & 0 \\ SE \cdot CH & SE \cdot SH & CE \end{bmatrix}$

and (for the assumed small angles of $\theta$, $\psi$, and $\phi$)

$$\left[ \alpha_{34} \right] = \begin{bmatrix} 1 & \psi & -\theta \\ -\psi & 1 & \phi \\ \theta & -\phi & 1 \end{bmatrix}$$

This requires that the time derivative of the matrix $\alpha_{34}$ be calculated because,

$$(\dot{W}_{13})_i = \left[ \dot{\alpha}_{24} \right] \begin{bmatrix} 0 \\ -\dot{\theta}_N \\ 0 \end{bmatrix} + \left[ \alpha_{24} \right] \begin{bmatrix} 0 \\ -\ddot{\theta}_N \\ 0 \end{bmatrix} \tag{42}$$

This matrix time derivative depends upon $\dot{\theta}$, $\dot{\psi}$, and $\dot{\phi}$ or p, q, and r which are two ways of expressing the angular rate of the Apollo vehicle relative to the selected attitude reference. It is elected to calculate $\left[ \dot{\alpha}_{24} \right]$ from knowledge of p, q and r.

The relationships giving the time derivative are

$$\dot{\alpha}_{24} (1, J)^* = q \, \alpha_{24} (J, 3) - r \, \alpha_{24} (J, 2)$$

$$\dot{\alpha}_{24} (2, J) = r \, \alpha_{24} (J, 1) - p \, \alpha_{24} (J, 3) \, , \, J = 1, 2, 3 \tag{43}$$

$$\dot{\alpha}_{24} (3, J) = p \, \alpha_{24} (J, 2) - q \, \alpha_{24} (J, 1)$$

so the angular rate (and time derivative of its components) of the selected attitude reference frame with components given in the Apollo body fixed frame is calculated from Eqs. 41, 42 and 43.

Returning to Eq. 37, it is rewritten below to directly calculate the time derivatives of p, q and r.

---

* In $\alpha$ (I, J), I is row, J is column location.

$$
\begin{bmatrix} \dot{p} \\ \dot{q} \\ \dot{r} \end{bmatrix} = \begin{bmatrix} J \end{bmatrix}^{-1} \left\{ T_i - W_i \times H_i - \begin{bmatrix} J_N \ddot{\gamma}_C C\alpha \\ 0 \\ -J_N \ddot{\gamma}_C S\alpha \end{bmatrix} \right\} - (\dot{W}_{13})_i \tag{44}
$$

Eq. 44, when integrated, gives the value of p, q and r respectively, the body fixed roll, pitch and yaw rate components of the Apollo vehicle. These rates give the value of the time derivative of the Euler angles $\dot{\psi}$, $\dot{\phi}$, and $\dot{\theta}$ as follows

$$
\begin{bmatrix} p \\ q \\ r \end{bmatrix} = \begin{bmatrix} \phi \end{bmatrix} \left[ \begin{bmatrix} \dot{\phi} \\ 0 \\ 0 \end{bmatrix} + \begin{bmatrix} \theta \end{bmatrix} \begin{bmatrix} 0 \\ \dot{\theta} \\ 0 \end{bmatrix} + \begin{bmatrix} \psi \end{bmatrix} \begin{bmatrix} 0 \\ 0 \\ \dot{\psi} \end{bmatrix} \right] \tag{45}
$$

where $\quad \begin{bmatrix} \psi \end{bmatrix} = \begin{bmatrix} C\psi & S\psi & 0 \\ -S\psi & C\psi & 0 \\ 0 & 0 & 1 \end{bmatrix}$

$$
\begin{bmatrix} \theta \end{bmatrix} = \begin{bmatrix} C\theta & 0 & -S\theta \\ 0 & 1 & 0 \\ S\theta & 0 & C\theta \end{bmatrix}
$$

$$
\begin{bmatrix} \phi \end{bmatrix} = \begin{bmatrix} 1 & 0 & 0 \\ 0 & C\phi & S\phi \\ 0 & -S\phi & C\phi \end{bmatrix}
$$

Eq. 42 expanded and then simplified to small angles of $\phi$, $\psi$ and $\theta$ yields the familiar relations,

$$
\begin{bmatrix} p \\ q \\ r \end{bmatrix} = \begin{bmatrix} \dot{\phi} - \theta\dot{\psi} \\ \dot{\phi}\psi + \dot{\theta} \\ \dot{\psi} - \phi\dot{\theta} \end{bmatrix}, \quad \begin{bmatrix} \dot{\psi} \\ \dot{\theta} \\ \dot{\phi} \end{bmatrix} = \begin{bmatrix} q\phi + r \\ q - r\phi \\ p + \theta\dot{\psi} \end{bmatrix} \tag{46}
$$

The rightmost expressions of Eq. 46 are integrated to yield the values of the roll, pitch and yaw deviation angles from the selected attitude reference.

To complete the derivation of equations, there remains the calculation of the external torques on the Apollo, centrifuge, balancer bodies system. These torques as mentioned previously in Eq. 2 were subdivided into those from the environment (air drag, gravity, magnetic, etc.) and those from the Apollo service module autopilot.

It is assumed that the experiment will be conducted at orbital altitudes of 200 n.mi. and above where air drag will be negligible. It is then believed that gravity and magnetic torques will dominate, both typically in the same order of magnitude. The torque due to gravity was evaluated and considered to be the total external torque. The expression for gravity torque used below ignores the small additional contribution due to cross products of inertia.

$$(T_g)_i = \frac{3 g_E R_E^2}{r_o^3} \begin{bmatrix} \alpha_{24}(2,3) \ \alpha_{24}(3,3) \left[ J(3,3) - J(2,2) \right] \\ \alpha_{24}(3,3) \ \alpha_{24}(1,3) \left[ J(1,1) - J(3,3) \right] \\ \alpha_{24}(1,3) \ \alpha_{24}(2,3) \left[ J(2,2) - J(1,1) \right] \end{bmatrix} \tag{47}$$

The remaining torque is due to the Apollo Service Module reaction jets which comprise four clusters of three 100 lb. engines firing in pairs to generate pure couples on the Apollo vehicle. Their separation distance being about 15 ft. yields a roll, pitch or yaw torque of ±1500 ft-lbs. of torque in response to on or off signals from the autopilot.

A mathematical model of the autopilot, sufficiently accurate to represent an attitude hold function is required for the centrifuge experiment. This is the subject of the next and last section of this appendix. References 1 and 2, identified in the below footnote, and a meeting with cognizant personnel of the Systems Analysis Branch, Guidance and Control Division of MSC (Manned Space Center), Houston, Texas were used in arriving at the model.

---

1. MIT Instrumentation Laboratory Report E-1964, "Apollo Command & Service Module Reaction Control by the Digital Autopilot," R. Crisp, D. Keene, May 1966.

2. MIT Instrumentation Laboratory Report R-547, "Guidance & Navigation System Operations Plan, Mission AS-278," October 1966, Vol. 1, Section 3.

# Apollo Autopilot Math Model Formulation

Figures A5 and A6 are directly taken from References 1 and 2. They illustrate the essential qualities of a single axis of control afforded by the DAP in the control mode of interest. That is, the attitude hold mode. All three control axes are identical so the single axis illustrations apply for all three axes of control. Figure A5 illustrates how the angular rate is derived from the attitude angle. In essence the attitude information as derived from a sensor is differentiated with appropriate filtering to prevent passage of noise signals due to body bending.* The filter transfer function exhibits a natural frequency of 0.4 rad/sec at a damping factor of 0.8. This filter has a serious time delay in responding to the change in rate accompanying attitude engine firing. To recover this information, the vehicle angular acceleration during engine firing is calculated based upon the known control torque and estimated current value of moment of inertia. This estimated angular acceleration is integrated with respect to engine firing time to yield the estimated change in angular rate. In addition the estimate is fed back in a manner allowing the filter to correct the magnitude of the estimate.

Herein it is assumed that the filter, augmented by the engine torque signal yields a sufficiently high dynamic bandpass such that no lag need be incorporated in the autopilot math model.

That is, the filter receives the quantity $\theta$, $\psi$, or $\phi$ and yields $\dot{\theta}$, $\dot{\psi}$ and $\dot{\phi}$. No significant inaccuracy of the results, as applied to the centrifuge, should result.

The attitude and rate deviation signals from the desired reference are utilized in a manner illustrated by Figure A6. Ideally whenever the rate displacement combination is outside the "WAIT" area of the phase plane, an engine firing of appropriate polarity is commanded. This engine firing is terminated when the rate-displacement combination crosses the desired line. In addition, once commanding the engines to fire, they are maintained on for a minimum period of 0.014 seconds (minimum impulse). Figure A6 includes numerical values defining the allowable rate and attitude deviations from the desired reference attitude. As indicated the rate limit is ±0.2 deg/sec and the attitude limit is 0.5 or 5 degrees depending on pilot selection.

Figure A7 is the actual phase plane used in this centrifuge study. It is the same as Figure A6 except that the desired rate-displacement line is slightly altered at the sloping portions. The reason for this is to incorporate the minimum impulse

---

* According to Reference 1, shaped to attenuate the maximum expected bending to less than $10^{-5}$ rad/sec.

Figure A5. Filter Block Diagram.
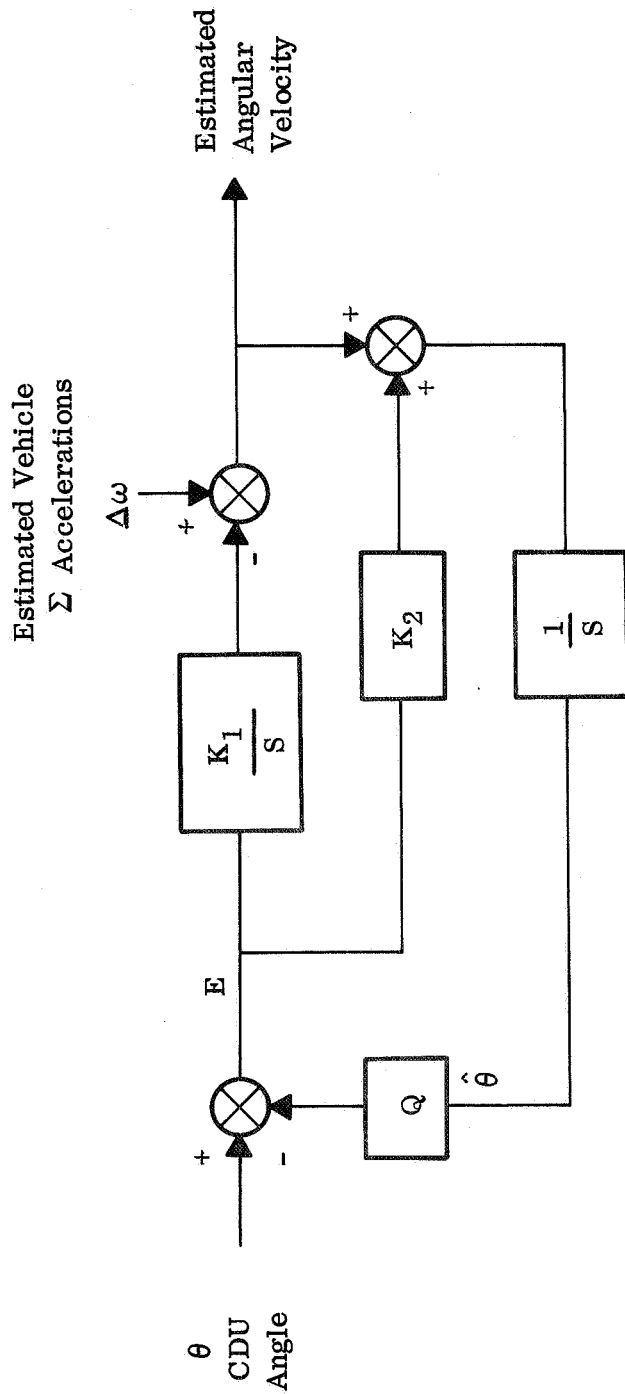
$$K_1 = \omega_n^2 = .16$$

$$K_2 = 2\xi\,\omega_n = .64$$

EQUIVALENT TRANSFER FUNCTION:

$$\frac{\hat{\omega}(S)}{\hat{\theta}(S)} = \frac{S}{S^2/K_1 + K_2/K_1\ S + 1}$$

DIFFERENCE EQUATIONS:

$$\hat{\omega} = \hat{\omega}_{-1} + K_1\ TE_{-1} + \Delta\omega$$

$$\hat{\theta} = \hat{\theta}_{-1} + K_2\ TE_{-1} + T\hat{\omega}_{-1}$$
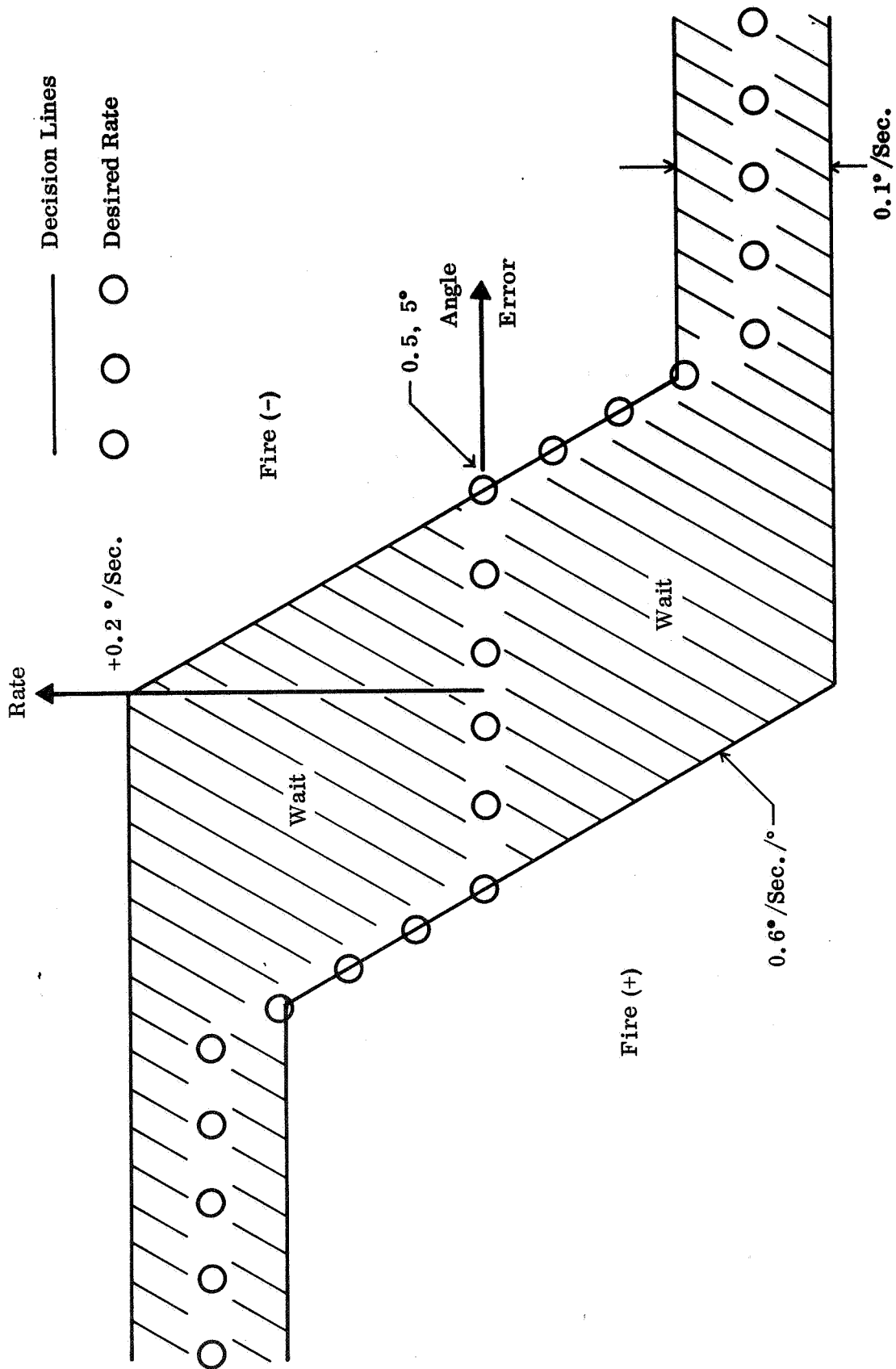
Figure A6.  Phase plane showing switching logic.
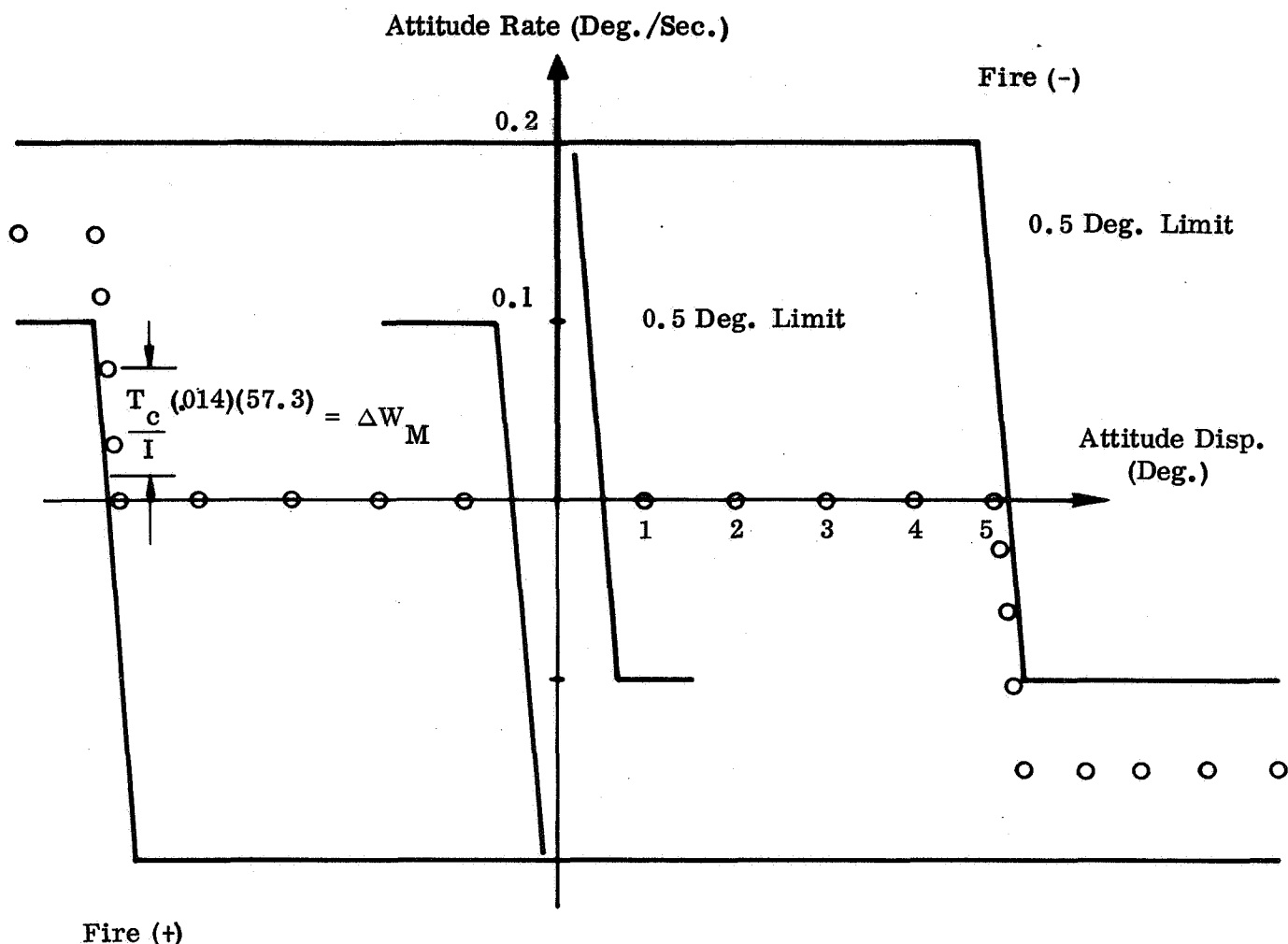
Figure A7. DAP Phase plane used in simulation study.

corresponding to a 0.014 minimum engine on-time. The rate deviation at the altered portion of the desired line is

$$\Delta W_M = \frac{T_C (0.014) (57.3)}{I} \tag{48}$$

where $\Delta W_M$ is the rate deviation (deg/sec)

$T_C$ is the particular axis control torque (ft-lbs)

$I$ is the particular axis moment of inertia (lb-ft-sec$^2$)

Inspection of Figure A7 will show that it is not possible to traverse the distance between the decision and desired lines with less than 0.014 second engine on time.

Figure A8 is a good summary of single engine parameters as related to control system performance. It was taken from Reference 1. While the variation in specific impulse and impulse magnitude/engine was not simulated to the extent indicated on Figure A8, this data was used to estimate fuel consumption and minimum impulse. The value of specific impulse used was 280 seconds for long time engine firings. We note further that using the 0.014 second firing corresponds to about 1 lb-sec.

In the digital simulation, the full amount of torque was assumed generated instantaneously with engine on command and vice versa with engine off command. With 100 lb. engines, the minimum impulse is 1.4 lb. seconds, a value considered sufficiently close for present purposes.

In addition, instead of computing fuel usage accounting for specific impulse change with engine firing time, the total torque impulse was obtained by integrating the torque output with time. The curve of Figure A8 is used to estimate the appropriate value of specific impulse to be applied in fuel weight calculation.

The autopilot, of course, feeds engine on or off electrical signals to the service module reaction control system (RCS).

Figure A9 summarizes pertinent information as regards the RCS in connection with the attitude control problem. As indicated, the RCS system comprises four clusters of 100 lb. jets spaced equally about the service module periphery. They are operated in pairs to yield pure couples as follows:

| | Pitch | Yaw | Roll | |
|---|---|---|---|---|
| (+) | 1 & 3 | 5 & 7 | 9 & 11 or 13 & 15 | |
| | | | | Pilot select for roll |
| (−) | 2 & 4 | 6 & 8 | 10 & 12 or 14 & 16 | |

The spacing is about 15 feet but the control moment for each axis is 1400 lb–ft rather than the 1500 which the diagram implies due to geometrical factors not shown.

Each cluster is supplied from adjacent fuel and oxidizer tanks. Pitch expends equally out of the 2 and 4 tanks, yaw out of the 1 and 3 tanks and roll from either the 1 and 3 or the 2 and 4 tanks, depending upon pilot selection.
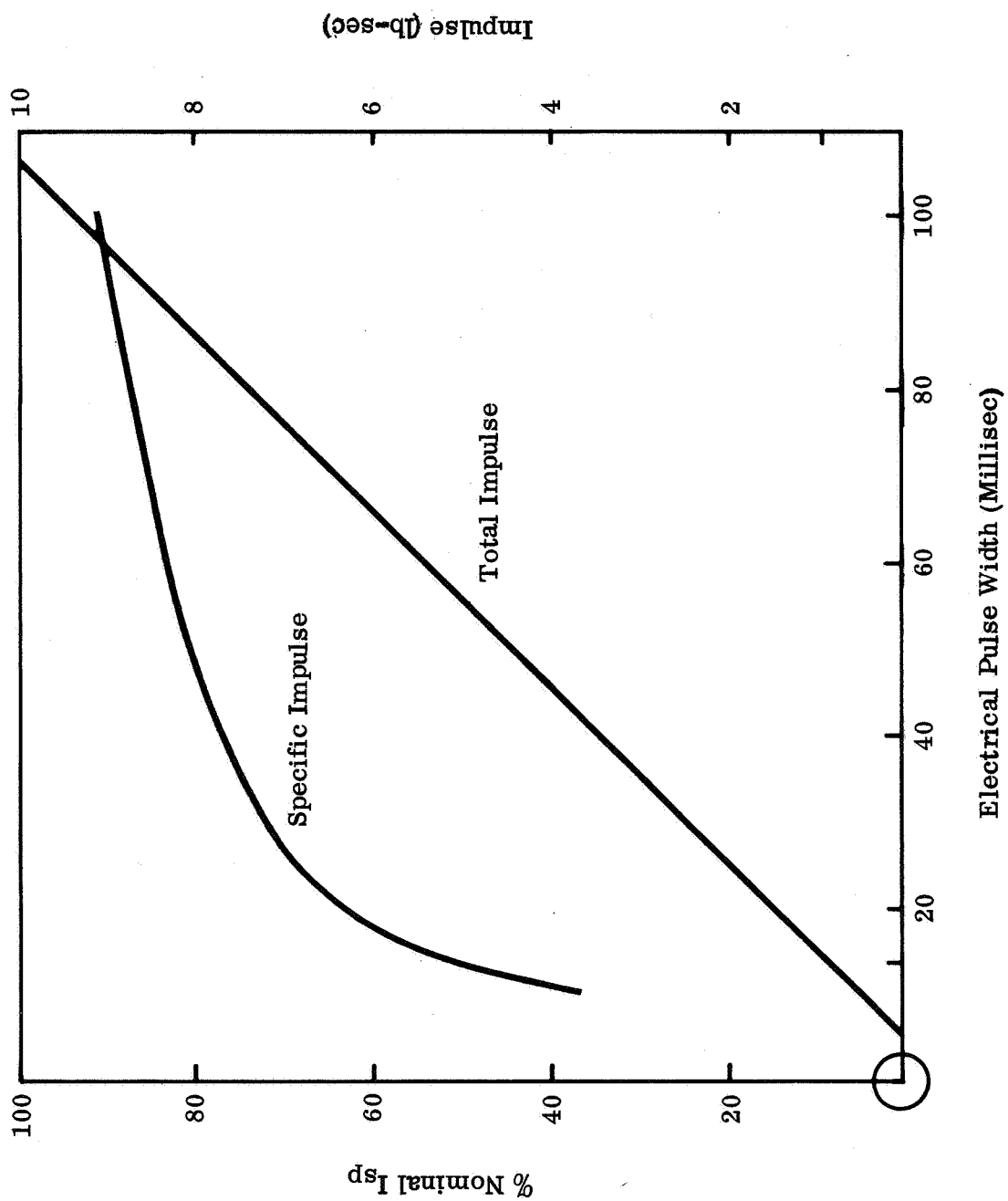
Figure A8. Typical reaction jet performance.

Service Module

Pitch Axis

Quad A

6 9 12 — Quad B

Command Module

Roll Axis

16

2 3

13

15

1 4

14 X

Z

SPS

Service Module

5

10 11 8

Quad D

Quad C

Yaw Axis
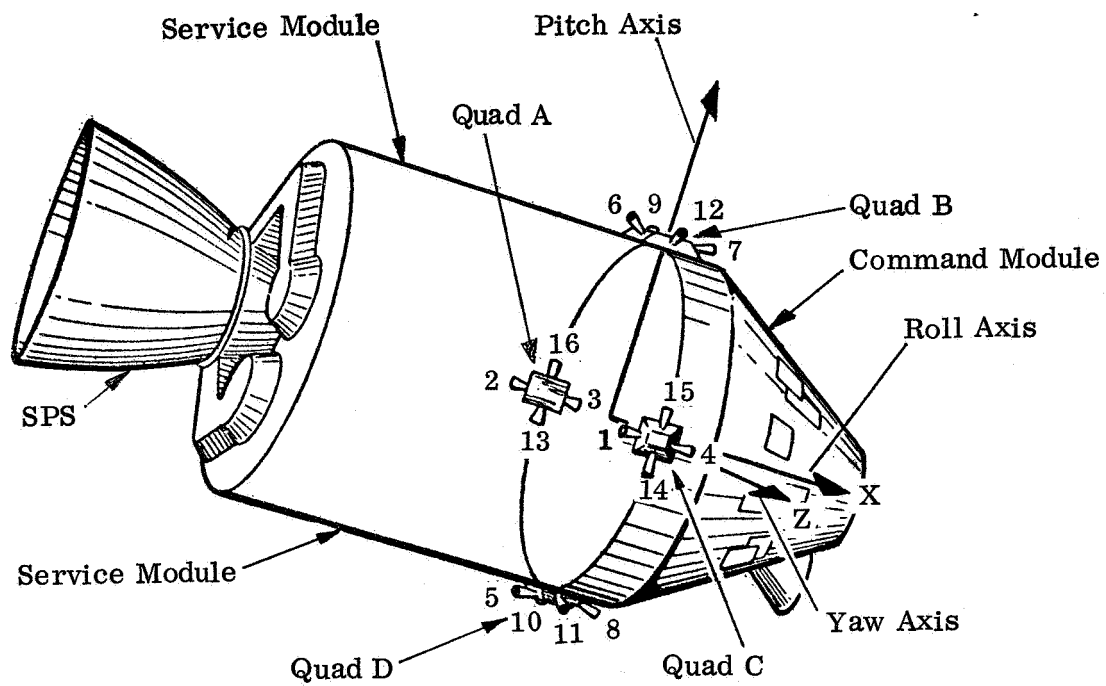
Figure A9. Apollo spacecraft.

# APPENDIX B
## CONING MOTION DUE TO CENTRIFUGE INSTALLATION ON APOLLO CSM
## (EQUATION DERIVATION)

Appendix A derived in detail the differential equations of motion for installation of the centrifuge and balancer (if needed) aboard the Apollo CSM. In addition, Apollo Service Module DAP Autopilot and Reaction Control System models were generated. The results of Appendix A were programmed in a digital simulation to determine present DAP capability to control the centrifuge spin axis motion.

Herein we are concerned with simplifying the resultant differential equations to the extent that they can be integrated to obtain an estimate of the motion. This estimate is to be used to check the digital program output and provide a fundamental understanding of the effect of centrifuge installation. The simplifications consist of the assumption that vehicle is within the firing decision lines of the DAP auotpilot and, as such, that the autopilot will not fire plus certain kinetic simplifications identified below.

## Coordinate Definitions

Figure B1 defines pertinent coordinates.
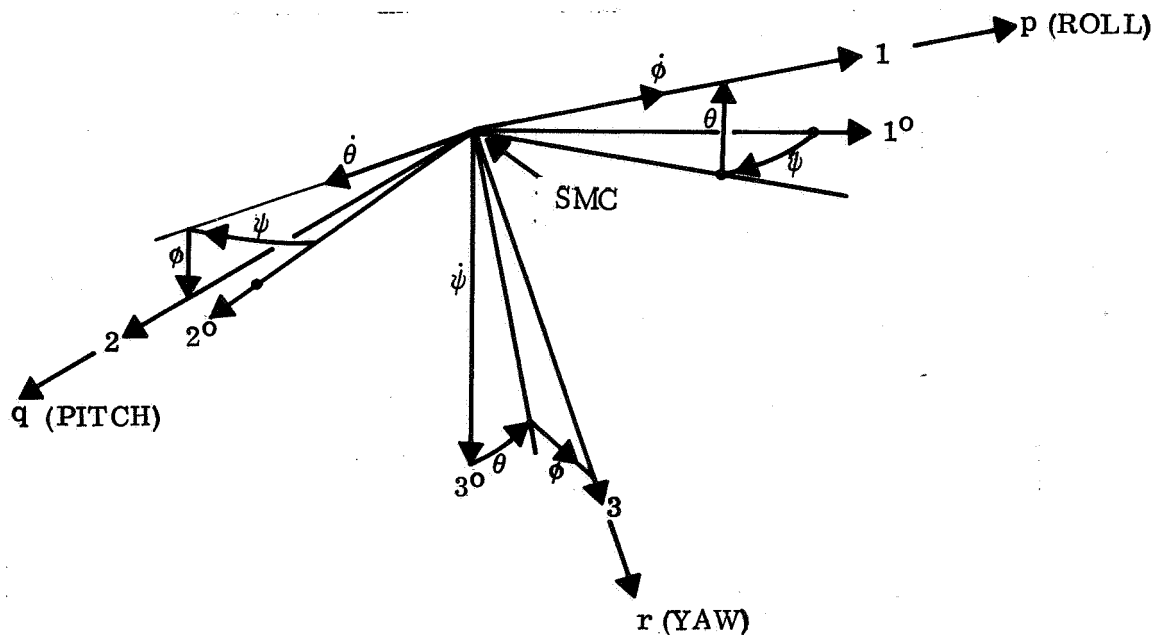


Figure B1. Vehicle angular perturbation model coordinate definition.

The super "o" frame is considered inert. The 1, 2 and 3 (no superscript) axes are fixed to the Apollo vehicle principal axes. Both frames of reference are centered at the system center of mass (SMC). The angular deviation of the Apollo vehicle is defined by the Angles $\phi$ (roll), $\theta$ (pitch) and $\psi$ (yaw). These angles are considered small. The total angular rate of the Apollo with respect to the inert frame is given by either $\dot{\theta}$, $\dot{\psi}$, and $\dot{\phi}$ or the body fixed components, p, q and r.

Figure B2 defines the centrifuge, balancer rotating bodies installation on the Apollo. The angle $\alpha$ defining the centrifuge spin axis direction is shown in general but herein the values 0 and 90 degrees are the two values of interest.
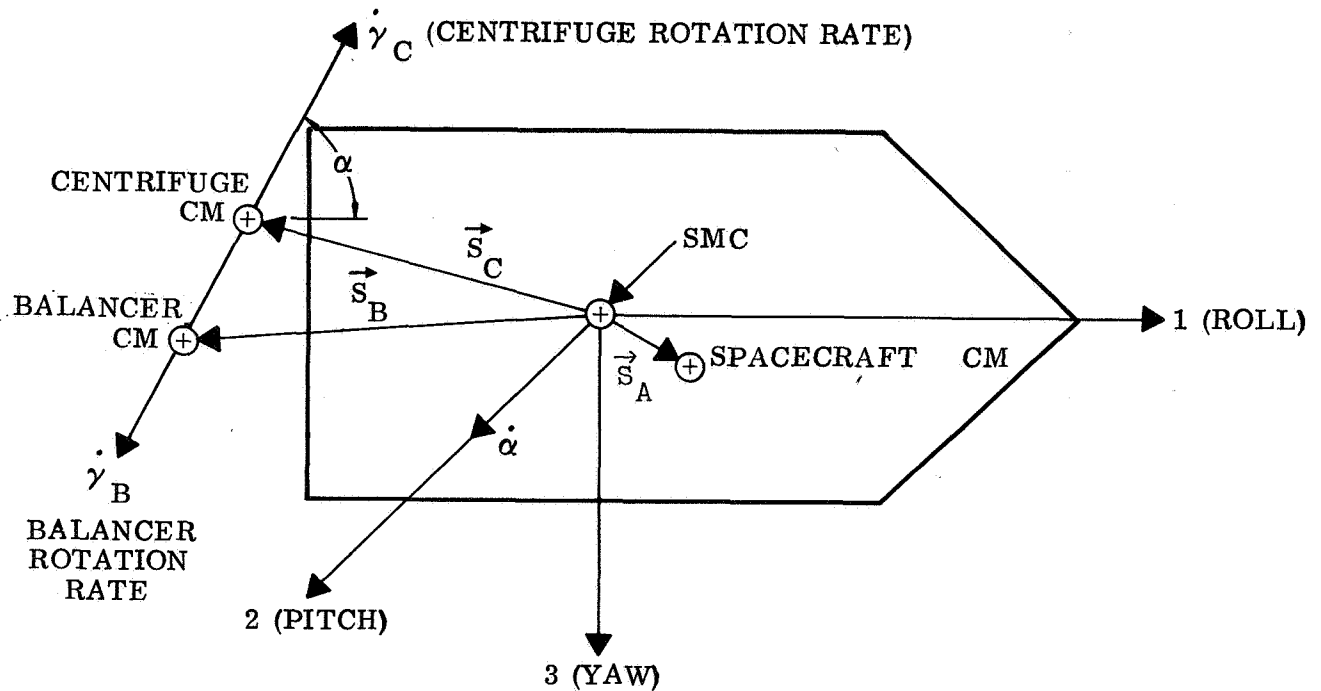


Figure B2. Centrifuge, balancer installation coordinates.

The angular rate of the centrifuge and balancer are $\dot{\gamma}_C$ and $\dot{\gamma}_B$ respectively.

Derivation of Simplified Equations

Appendix A gives the following relations for system momentum (Eq. 35).

$$\left[ H_i \right] = \left[ J \right] \left[ \omega_i \right] + \begin{bmatrix} J_N \dot{\gamma}_C C\alpha \\ 0 \\ -J_N \dot{\gamma}_C S\alpha \end{bmatrix} \tag{1}$$

where $\omega_i$ is the body fixed angular rate components

$[J]$ is the effective moment of inertia matrix of the Apollo vehicle

$J_N$ is the net unbalanced moment of inertia of the centrifuge, balancer combination

$H_i$ is the system momentum calculated with respect to the SMC

$\dot{\gamma}_C$, $\dot{\gamma}_B$ are the angular rates of the centrifuge and balancer respectively, relative to the Apollo vehicle.

The $[J]$ matrix depends upon the basic Apollo matrix and the centrifuge, balancer matrices, weight and location. They are all fixed numbers yielding constant values of the elements of the $[J]$ matrix. This is evaluated in Appendix A. For present purposes it should be noted that the moments of inertia of the centrifuge and balancer about their CM are negligible in comparison to the Apollo moments of inertia (including mass and location of the centrifuge and balancer). Furthermore, for this analysis, $[J]$ contains only the principal inertias. The quantity $J_N$ depends upon the balancer and centrifuge spin moment of inertia and their rotational speeds,

$$J_N = I_C - K I_B \tag{2}$$

where $I_C$ is the centrifuge spin moment of inertia

$I_B$ is the balancer spin moment of inertia

$K$ is the ratio of balancer to centrifuge spin rate

$J_N$ is the effective moment of inertia of the centrifuge plus balancer

The components of angular rate $\omega_i$ of Eq. 1 are exactly p, q and r but p, q and r, for small values of $\psi$, $\phi$ and $\theta$, is (from Eq. 46 of Appendix A).

$$\begin{bmatrix} p \\ q \\ r \end{bmatrix} = \begin{bmatrix} \dot{\phi} - \theta\dot{\psi} \\ \phi\dot{\psi} + \dot{\theta} \\ \dot{\psi} - \phi\dot{\theta} \end{bmatrix} \cong \begin{bmatrix} \dot{\phi} \\ \dot{\theta} \\ \dot{\psi} \end{bmatrix} \tag{3}$$

Incorporating these simplifications in the momentum Eq. 1 yields,

$$H_i = \begin{bmatrix} J_1 \dot{\phi} \\ J_2 \dot{\theta} \\ J_3 \dot{\psi} \end{bmatrix} + \begin{bmatrix} J_N \dot{\gamma}_C C\alpha \\ 0 \\ -J_N \dot{\gamma}_C S\alpha \end{bmatrix} = \begin{bmatrix} J_1 \dot{\phi} + MC\alpha \\ J_2 \dot{\theta} \\ J_3 \dot{\psi} - MS\alpha \end{bmatrix} \tag{4}$$

Where M is the constant net momentum of the centrifuge and balancer. Now taking the total time derivative of the system momentum and equating to external torque yields the desired result.

$$
T_i = \begin{bmatrix} J_1 \ddot{\phi} \\ J_2 \ddot{\theta} \\ J_3 \ddot{\psi} \end{bmatrix} + \begin{bmatrix} \dot{\phi} \\ \dot{\theta} \\ \dot{\psi} \end{bmatrix} \quad X \quad \begin{bmatrix} J_1 \dot{\phi} + MC\alpha \\ J_2 \dot{\theta} \\ J_3 \dot{\psi} - MS\alpha \end{bmatrix} \tag{5}
$$

$$
T_i = \begin{bmatrix} J_1 \ddot{\phi} \\ J_2 \ddot{\theta} \\ J_3 \ddot{\psi} \end{bmatrix} + \begin{bmatrix} J_3 \dot{\theta}\dot{\psi} - MS\alpha\dot{\theta} - J_2 \dot{\theta}\dot{\psi} \\ J_1 \dot{\psi}\dot{\phi} + MC\alpha\dot{\psi} - J_3 \dot{\phi}\dot{\psi} + MS\alpha\dot{\phi} \\ J_2 \dot{\phi}\dot{\theta} - J_1 \dot{\phi}\dot{\theta} - MC\alpha\dot{\theta} \end{bmatrix} \tag{6}
$$

which, when products of small angular rates are neglected, yields

$$
T_i = \begin{bmatrix} J_1 \ddot{\phi} - MS\alpha\dot{\theta} \\ J_2 \ddot{\theta} + MC\alpha\dot{\psi} + MS\alpha\dot{\phi} \\ J_3 \ddot{\psi} - MC\alpha\dot{\theta} \end{bmatrix} \tag{7}
$$

As mentioned previously, the installation angle $\alpha$ equal to zero and 90 are of interest. For each case a set of simpler equations result.

$$
\underline{\alpha = 0 \text{ deg.}} \qquad\qquad \underline{\alpha = 90 \text{ deg.}}
$$

$$
T_i = \begin{bmatrix} J_1 \ddot{\phi} \\ J_2 \ddot{\theta} + M\dot{\psi} \\ J_3 \ddot{\psi} - M\dot{\theta} \end{bmatrix} \qquad T_i = \begin{bmatrix} J_1 \ddot{\phi} - M\dot{\theta} \\ J_2 \ddot{\theta} + M\dot{\phi} \\ J_3 \ddot{\psi} \end{bmatrix} \tag{8}
$$

Solution of Eq. 8 subject to initial conditions in rate and displacement yields the intended fundamental understanding of the influence of the centrifuge. It is specified that the torques applied are zero, but an initial angular displacement and rate exists in pitch (this is sufficient excitation to see the results for $\alpha$ equal zero or 90 degrees). Taking $\alpha$ equal to zero first, the solution to Eq. 8 as a function of the pitch initial condition are

$$\underline{\alpha = 0 \text{ deg.}}$$

$$\ddot{\phi} = \dot{\phi} = \phi = 0$$

$$\dot{\theta} = \dot{\theta}_o \cos(Mt/\sqrt{J_2 J_3})$$

$$\theta = \theta_o + (\dot{\theta}_o \sqrt{J_2 J_3}/M) \sin (Mt/\sqrt{J_2 J_3}) \qquad (9)$$

$$\dot{\psi} = \dot{\theta}_o \sqrt{J_2/J_3} \sin (Mt/\sqrt{J_2 J_3})$$

$$\psi = (\dot{\theta}_o J_2/M) \left[ 1 - \cos (Mt/\sqrt{J_2 J_3}) \right]$$

For the $\alpha$ equal zero case the inertias $J_2$ (pitch) and $J_3$ (yaw) are essentially equal. The resultant motion is a circular rotation of the roll axis about the point defined by $\theta_o$ and

$$\psi_I = \frac{\dot{\theta}_o J}{M} , \quad J_2 = J_3 = J \qquad (10)$$

This is the precession angle common in spinning bodies. The coning motion has a half angle magnitude equal to $\psi_I$ and of period (full revolution)

$$P = \frac{2 \pi J}{M} \qquad (11)$$

A preliminary set of parameters enables evaluation of the motion.

$$J_1 = 25,000 \text{ slug ft}^2$$

$$J_2 = 220,000 \text{ slug ft}^2$$

$$J_3 = 220,000 \text{ slug ft}^2$$

$$M = 4,900 \text{ lb. ft. sec. (60 RPM, no balancer)}$$

$$\dot{\theta}_o = .1 \text{ deg/sec (typical)}$$

From the above set of parameters

$$P = \frac{2\pi (220,000)}{4,900} = 282 \text{ sec. or } 4.7 \text{ minutes}$$

$$\psi_I = \frac{.1 \times 220,000}{4,900} = 4.5 \text{ deg.}$$

So in response to an angular rate of 0.1 deg/sec., the roll axis cones with a half angle equal to 4.5 degrees and one complete revolution occurs in 4.7 minutes for the case where the centrifuge spin axis is aligned with the Apollo roll axis.

Now consider the case where $\alpha$ equals 90 degrees and integrate the corresponding Eq. 8. The result is

$$\underline{\alpha = 90 \text{ degrees}}$$

$$\ddot{\psi} = \dot{\psi} = \psi = 0$$

$$\dot{\theta} = \dot{\theta}_0 \, \text{Cos} \, (Mt/\sqrt{J_1 \, J_2})$$

$$\theta = \theta_0 + (\dot{\theta}_0\sqrt{J_1 \, J_2}/M) \, \text{Sin}(Mt/\sqrt{J_1 J_2}) \tag{12}$$

$$\dot{\phi} = \dot{\theta}_0\sqrt{J_2/J_1} \, \text{Sin} \, (Mt/\sqrt{J_1 J_2})$$

$$\phi = (\dot{\theta}_0 \, J_2/M) \left[ 1 - \text{Cos} \, (Mt/\sqrt{J_1 \, J_2}) \right]$$

The roll axis inertia, $J_1$ is about an order of magnitude less than the pitch axis inertia, $J_2$. The coupling is from pitch to roll, the period is different and the magnitudes of the angular couplings is different, all relative to the $\alpha$ equal zero case. The period is

$$P = \frac{2\pi\sqrt{J_1 \, J_2}}{M} \tag{13}$$

The coning is about the Apollo yaw axis (or about the centrifuge axis) and is elliptical in shape. The maximum pitch and roll angle ignoring the initial condition in pitch and the precession angle in $\phi$ is,

$$\theta_M = \dot{\theta}_0\sqrt{J_1 \, J_2}/M$$

$$\phi_M = \dot{\theta}_0 \, J_2/M$$

$$\dot{\phi}_M = \dot{\theta}_0\sqrt{J_2/J_1}$$

Again using $\dot{\theta}_0$ equal to 0.1 deg/sec and the values of parameters given above,

P = 95 sec

$\theta_M$ = 1.5 degrees

$\phi_M$ = 4.5 degrees

$\dot{\phi}_M$ = 0.297 degrees/sec

# APPENDIX C

## CENTRIFUGE COUNTERBALANCE SENSOR SYSTEM

### Influencing Factors

The sensing system has the primary task of resolving the presence of three dynamic disturbances affecting the centrifuge performance or affecting other experiments on the total spacecraft. These disturbances are:

a.  Static unbalance – defined as the offset of the centrifuge center of mass (CM) from the spin axis. The resultant is a force normal to the spin axis and through the offset CM.

b.  Dynamic unbalance - defined as an angular misalignment of the centrifuge axis with the spin axis. The resultant is a pure couple acting along a normal to the spin axis and fixed to the centrifuge rotating body.

c.  Acceleration torque - defined as an angular acceleration of the centrifuge mass about the spin axis whereby a reactive torque is transmitted to the spacecraft.

The most difficult task in devising a sensor system lies in providing the ability to discriminate. The factors involved in the discrimination are those of geometric direction of the forces to be sensed, their possible coincidence, structural deflections, fabrication tolerances, friction, and practical features such as ability to install and adjust. Force transducers suitable for this application have full range travels on the order of ±.001 in. to ±.012 in. When it is realized that multiple sensors are required in order to distinguish the source of the disturbing force, it becomes apparent that a keen effort must be applied to prevent the sensor from being influenced by other factors. During the period of acceleration a large force couple exists in a plane parallel to the spin plane (exception: use of CMGs to balance acceleration torques of the centrifuge, in which case a minor force couple exists due to bearing drag) and has a very significant influence on any sensors lying in the same or parallel planes. It has been established that the sensor system must be operational during acceleration, hence an unbalanced static condition must be filtered from the acceleration couple for those systems not using CMGs.

The design of the centrifuge requires that the sensor system must be located geometrically in the hub area. This particular geometric arrangement in a cantilevered centrifuge causes a CM offset to produce a lateral force (relative to spin axis) and a moment acting normal to the spin plane. Since the dynamic unbalance couple also acts normal to the spin axis, a problem of discrimination exists if these moments and couples are to be used to energize sensors.

## Ground Rules and Assumptions

Some of these ground rules were established as the course of investigation proceeded. They were arbitrarily changed as other affecting information became available, such as changes in mass distribution, mass moments of inertia and validation of limits imposed by definition of experiments.

As a result of the spacecraft dynamics investigations it was determined that the worst case couple produced by a dynamic unbalance was of a low enough magnitude that trim weight compensation would not be necessary. This offered considerable relief in both the sensing and the trim weight system. Although it is not necessary to generate a sensor response to dynamic unbalance, it is still necessary to prevent the dynamic unbalance (force couple) from registering on the static unbalance sensors or, alternately, a means must be devised to discriminate between the inputs.

It was also determined that the counter-momentum system (CMGs) need not necessarily be dependent upon sensing the acceleration torques. Again, a sensor response is not required but the influence from acceleration torques must be isolated from static unbalance sensing.

The primary ground rules are tabulated below:

a. Only static unblance is required to be sensed by the force transducer system.

b. Structurally, the hub components must be capable of developing the full stall torque of the drive motor without impairing the subsequent operation of the sensor system. Pending better definition of the drive motor, this is set at 1000 ft - lb torque at the output pinion of the drive motor gear box.

c. The threshold of active balancing is set at 10 lbs of force resulting from an offset CM (static unbalance). The sensors objectively shall be capable of detecting unbalances at force equivalent to 5 lbs or below to allow for anomalies in the remainder of the system.

d. The maximum acceleration/decelration of the centrifuge while under drive motor control will be held to .171 rad/sec$^2$.

## Selected System

Several factors were considered in the decision process to select a system from three prime candidates. All systems were similar but generally were considered single-plane or 2-plane systems; these planes being parallel to the spin plane. The chosen system is a single-plane type with this plane just below the primary structural frame and just above the hub rotation bearings. The primary factor in the choice of this system stems from ground rule No. 1.

Important features of the selected system are:

a. A near minimum of sensors. This factor is important because of the micrometer accuracy needed to adjust each sensor. Additionally, since malfunction within the acceleration control and/or counterweight positioning can result in loads far in excess of the force transducer limits, an overtravel, bottom-out structural point is provided. The overtravel allowance must be in the region of .001 in. and again micrometer type accuracy is needed. In short, each sensor sets a requirement for two micrometer type adjustments.

b. Accessibility to sensors and the aforementioned adjustment devices. Some of the alternate configurations required extension devices on the adjustor. Sensor replacement would also be difficult because of submergence within the hub.

## Description of System

The location of the sensor plane is 39.6 in. from the centerline of rotation of the couch (spin plane). This plane is also 1.75 in. from the primary structure frame. See Fig. C1 Convair Drawing SRC-SD-407. Each of the six sensors is suspended by tie-rod and acts in tension only, having a range of 0 to 200 lb. Each is preloaded to 100 lb. Positive stops are provided at each of four pick-up lugs to react overloads. In normal operation the sensors react all pertinent loads and it is only the abnormal conditions which will cause structural bottoming.

A circular ring of approximate "C" cross section, connects the hub and its equipment to the centrifuge primary structural frame. This ring contains the pick-up reaction lugs for the sensor system and is connected at the reaction lugs to a cross-bridge structural frame via four jaw type fittings. The reaction lugs are essentially free floating within the jaw fittings, being suspended laterally by the sensors and having lateral movement within the range permitted by the positive stops. Vertical movement is dimensionally controlled to .002-.004 in. by the machined reaction lugs and jaw fitting. The upper and lower faces of the jaw fitting are teflon lined to reduce lateral friction drag so as to inhibit this influence upon the forces transmitted to the sensors.

The cross-bridge frame attaches to a circular flange of the main spin bearing inner race cylinder structure.

The cross-bridge frame and the circular "C" ring contain all of the elements of the sensor system. Overall dimensions are 34.6 x 49 x 6.75 thick. The complete sensor system can be set up, adjusted and tested separate from the centrifuge. In the event the sensor system is not required, it could be replaced by a simple structural conical adapter. If it is desired to operate the centrifuge with the sensors inactive there are no detrimental effects.

SENSOR ASSEMBLY SUPPORTS
- Z-Z SENSOR BEAM (2)
- JAW FITTING (4)
- VERTICAL RESTRAINT WEBS (4 PLACES)
- Y-Y SENSOR FRAME (4)

SENSOR CROSS BRIDGE STRUCTURE
- SENSOR SUPPORT RING
- CENTRIFUGE ATTACH RING
- PRIMARY CROSS BEAM (2)
- DRIVE HUB ATTACH FITTING (12)
- CROSS BEAM SPLICE FITTINGS
- SECONDARY RADIAL BEAMS (4)

14.40 TYP

- SHROUD
- CENTRIFUGE ATTACHMENTS (12)
- CENTRIFUGE MAIN STRUCTURAL FRAME

- SENSOR ASSEMBLY (6)
- TORQUE STOP ADJUSTMENT
- Z-Z LATERAL STOP ADJUSTMENT
- Y-Y LATERAL STOP ADJUSTMENT

PLAN VIEW
SCALE: 1/2

Figure C1a.  Drive Hub and Sensor System
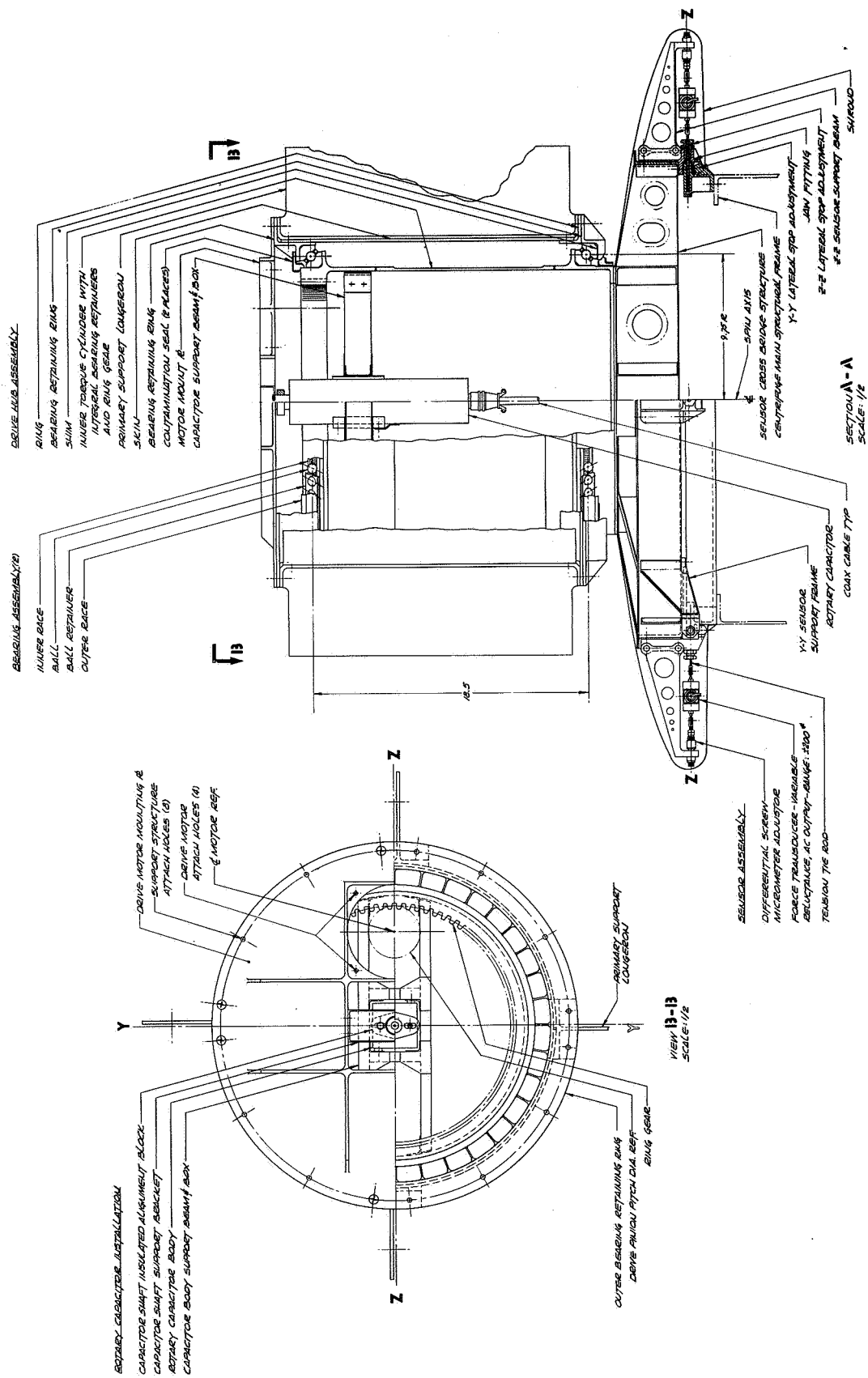
Figure C1b. Drive Hub and Sensor System

Two ball bearings of special construction comprise the hub rotation and retention system. These bearings are spaced 18.50 in. apart, have a race diameter of 19.50 in., and are identical. They react radial and thrust loads. The bearings are mounted to an inner race cylinder structure which picks up the sensor cross-bridge frame at one end and has a cross beam at the other. A rotary capacitor is mounted on the cross beam coincidental with the centrifuge spin axis. The outer races of the bearings are contained in a barrel assembly which is the primary load carrying stationary structure.

## Analysis of Sensor System

As noted previously, three dynamic disturbances affect the sensors. These are static unbalance, dynamic unbalance and acceleration torques. The selected system need only distinguish the static unbalance and the problem lies in filtering out the other two. The following paragraphs describe the characteristics of these forces relative to performance of the system.

The tolerable CM offset equivalent force is 10 lb. The goal for sensor capability is set at 5 lb. or below.

The forces at selected offsets of 2", 4" and 6" are shown in Table C1, and plotted on Figures C2 and C3. The 6" offset approximates the condition of maximum subject and couch displacement (re-entry) without a corresponding displacement of the counterweights.

$$F = ma, \text{ where } a = R\omega^2$$

$$F = mR\omega^2 = 61.2 \, R\omega^2 = 10.20 \, \omega^2 \text{ for 2" offset}$$

$$20.40 \, \omega^2 \text{ for 4" offset}$$

$$30.60 \, \omega^2 \text{ for 6" offset}$$

$a$ = radial acceleration, $\text{ft/sec}^2$

$\omega$ = angular velocity, rad/sec

$m$ = mass of centrifuge = 61.2 $\dfrac{\text{lb. sec.}^2}{\text{ft}}$ ; $W$ = 1973 lb.

$F$ = force

$R$ = radius or offset, ft.

Dynamic unbalance produces a pure couple acting about a normal to the spin axis and fixed to the centrifuge rotating body. The geometry of the sensor system, whereby a single plane of sensors is utilized, was purposely conceived to reduce to zero the forces reacting the dynamic unbalance in the sensor plane. Although the forces do not act in the sensor plane, there is a retarding friction force produced when the dynamic

Table C1. "Static" Unbalance Force Vs. RPM for Selected C.M. Offsets.

| | | $\omega^2$ | F | | |
|---|---|---|---|---|---|
| | | | 2"<br>OFFSET | 4"<br>OFFSET | 6"<br>OFFSET |
| 1 | RPM | .01093 | .1118 | .223 | .335 |
| 2.5 | " | .0684 | .70 | 1.398 | 2.096 |
| 3 | " | .0986 | 1.006 | 2.010 | 3.020 |
| 4 | " | .1750 | 1.788 | 3.570 | 5.350 |
| 5 | " | .2740 | 2.790 | 5.570 | 8.360 |
| 6 | " | .3935 | 4.020 | 8.010 | 12.050 |
| 7 | " | .5350 | 5.460 | 10.90 | 16.390 |
| 8 | " | .6990 | 7.140 | 14.24 | 21.40 |
| 9 | " | .8890 | 9.120 | 18.20 | 27.30 |
| 10 | " | 1.093 | 11.18 | 22.30 | 33.50 |
| 20 | " | 4.370 | 44.60 | 89.10 | 133.80 |
| 30 | " | 9.830 | 100.60 | 200.20 | 300.50 |
| 40 | " | 17.50 | 178.80 | 356.5 | 535.0 |
| 50 | " | 27.35 | 279.0 | 556.0 | 835.0 |
| 60 | " | 39.35 | 402.0 | 802.0 | 1203.0 |
| 70 | " | 53.60 | 548.0 | 1092.0 | 1640.0 |
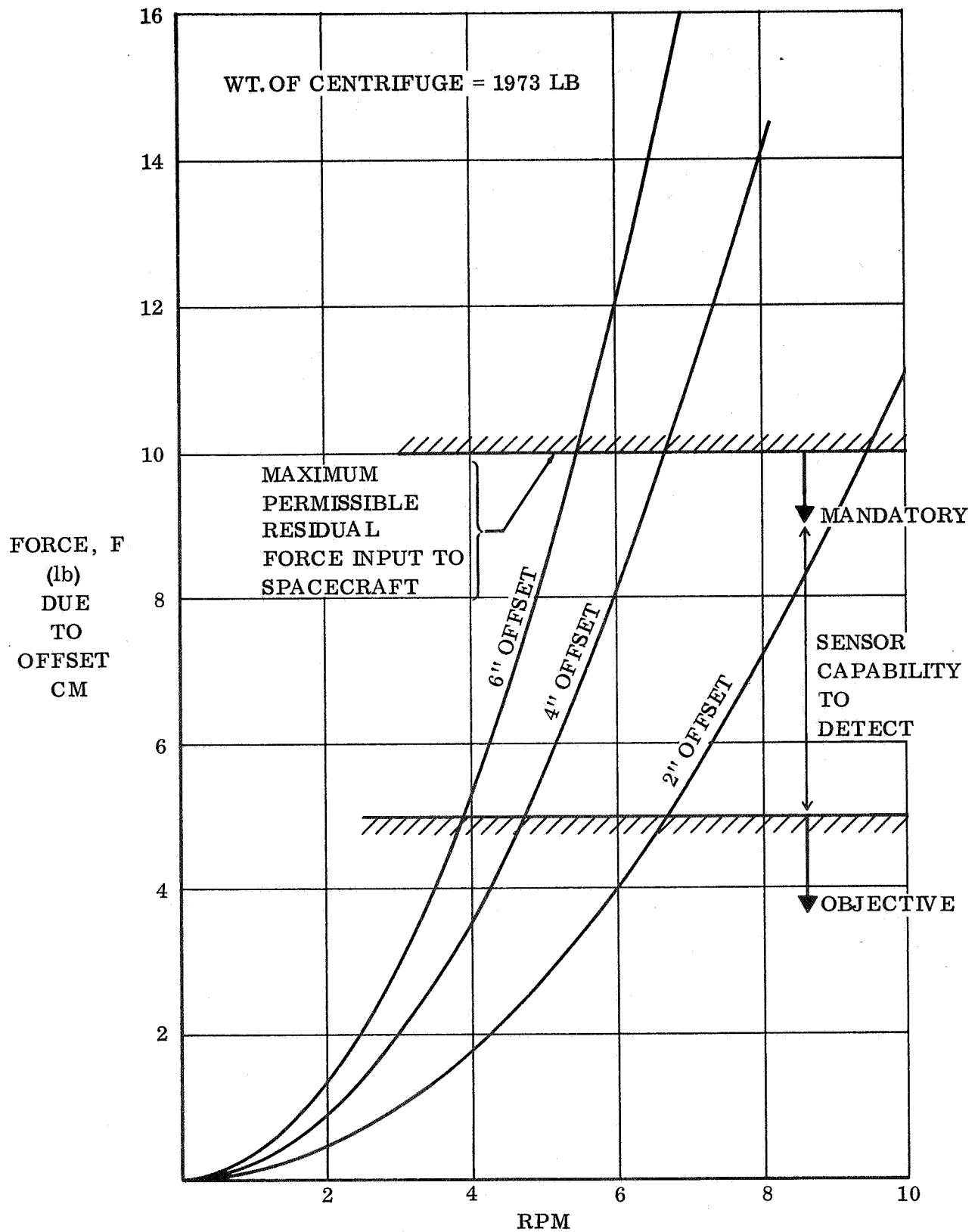
Figure C2. "Static" Unbalance Force Vs. RPM for
Selected C.M. Offsets
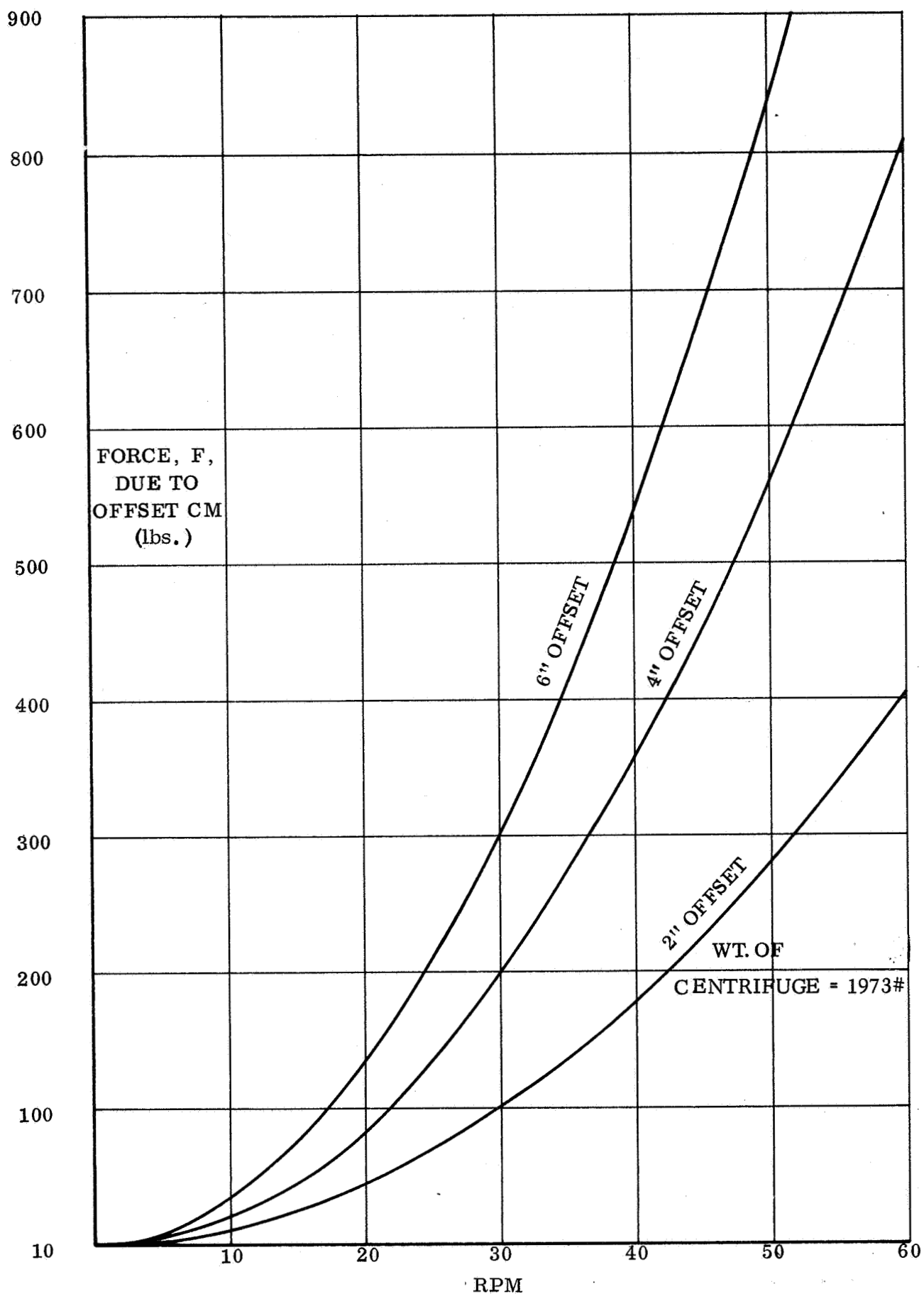
Figure C3. "Static" Unbalance Force Vs. RPM for Selected C.M. Offsets.

The figure shows Force, F, due to offset CM (lbs.) on the vertical axis from 10 to 900, plotted against RPM on the horizontal axis from 0 to 60. Three curves are shown labeled 6" OFFSET, 4" OFFSET, and 2" OFFSET. A note reads "WT. OF CENTRIFUGE = 1973#".

unbalance occurs simultaneously with a static unbalance condition. This friction force is important, as will be noted later. The maximum dynamic unbalance couple is 150 ft-lb. (see Dynamic Analysis) and occurs during the re-entry test.

Acceleration torques produce a couple in the sensor plane and thus cannot be denied direct registration on any non-radial sensors. The resulting force values for the tangential sensors of SRC-SD-407 are high relative to threshold forces resulting from CM offset, and hence present a problem in sensitivity and discrimination. The maximum acceleration is $.171 \text{ rad/sec}^2$ (ground rule No. d), producing a maximum torque for the re-entry profile of 250 ft. -lb. Torques slightly above this will cause bottoming of stops at the reaction lugs of the attaching ring and will overwhelm CM offset resultant forces on the sensors. Since most cases of CM offset will occur along the Z-Z axis, the four sensors which must combine the torque loads with offset-CM loads are aligned along the Y-Y axis. The 250 ft-lb. torque is the forcing factor requiring sensor preloads on the order of 100 lb. This will be more evident in the example cases to be discussed later.

Figure C4 shows the sensors arrangement and pertinent force systems in orthogonal views. The sensors are labeled A, B, C, D, E and F. The symbols within the boxes represent the actual forces felt by that sensor. $F_F$ and $F_f$ represent friction forces in opposition to lateral motion by the direct forces in the Z and Y directions respectively. The subscript $p$, denotes preload in the appropriate sensor.

In Plan View

$$\overset{\overset{+}{\rightarrow}}{\sum} F_z = 0 = -F \sin\theta - (A_p - F_z) + (D_p + F_z) + 2F_F$$

where

$$A_p = D_p \text{ (preloads cancel)}$$

$$F_z = \frac{F \sin\theta - 2F_F}{2} \tag{1}$$

$$+\uparrow \sum F_y = 0 = -F\cos\theta + (B_p + F_y - F_T) + F_f + (C_p + F_y + F_T) + F_f$$

$$- (F_p - F_y + F_T) - (E_p - F_T - F_y)$$

where

$$B_p = F_p \text{ and } C_p = E_p \text{ (preloads cancel)}$$

$$F_y = \frac{F\cos\theta - 2F_f}{4} \tag{2}$$

| SENSOR | FORCES |
|--------|--------|
| A | $A_p - F_z$ |
| B | $B_p + F_y - F_t$ |
| C | $C_p + F_y + F_t$ |
| D | $D_p + F_z$ |
| E | $E_p - E_y - F_t$ |
| F | $F_p - F_y + F_t$ |

$A_p = B_p = C_p = D_p = E_p = F_p$ (PRELOAD)
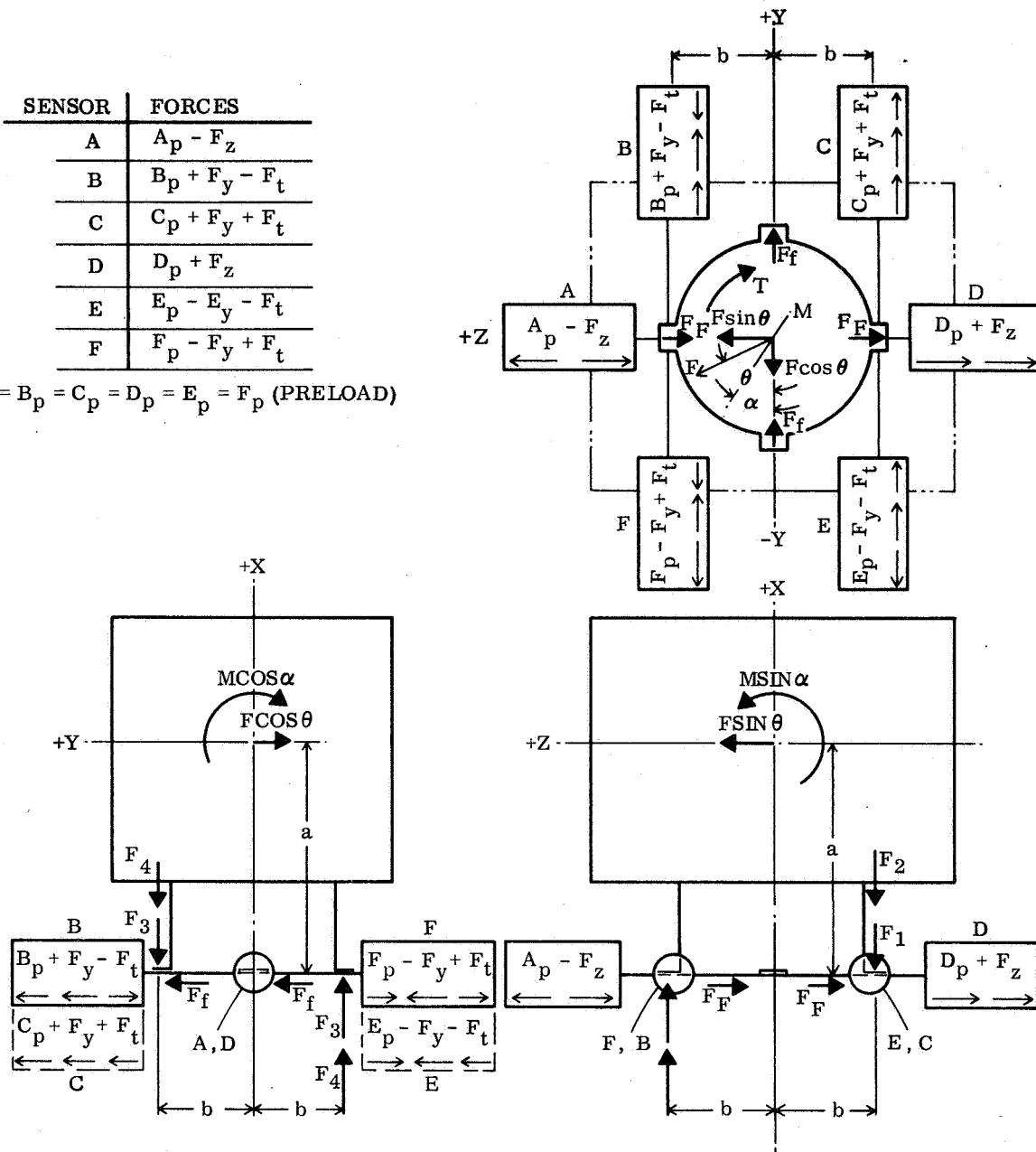


$$F_z = \frac{FSIN\theta - 2F_F}{2}$$

$$F_y = \frac{FCOS\theta - 2F_f}{4}$$

$$F_t = \frac{T}{4b}$$

$$F_F = (F_1 + F_2)\,\mu$$

$$F_f = (F_3 + F_4)\,\mu$$

$$F_1 = \frac{FSIN\theta a}{2b}$$

$$F_2 = \frac{MSIN\alpha}{2b}$$

$$F_3 = \frac{FCOS\theta a}{2b}$$

$$F_4 = \frac{MCOS\alpha}{2b}$$

$$\mu = .04 \text{ (TEFLON)}$$

$a = 38.75$

$b = 14.40$

Figure C4. Sensor force diagram.

$$\widehat{\sum M_o^+} = 0 = T + (B_p + F_y - F_T)b + (E_p - F_T - F_y)b - (C_p + F_y + F_T)b$$

$$- (F_p - F_y + F_T)b$$

where

$$B_p = F_p \text{ and } C_p = E_p \text{ (preloads cancel)}$$

$$F_T = \frac{T}{4b} \tag{3}$$

In RH View

$$\overset{+}{\vec{\sum}} F_z = 0 = -F_{\sin} \theta + (D_p + F_z) + F_F - (A_p - F_z) + F_F$$

where

$$D_p = A_p \text{ (preloads cancel)}$$

$$F_z = \frac{F\sin \theta - 2F_F}{2}$$

$$+ \uparrow \sum F_y = 0 = F_1 + F_2 - F_1 - F_2$$

$$\widehat{\sum M_o^+} = 0 = -M_{\sin} \alpha - F \sin \theta a + F_1 b + F_2 b + F_1 b + F_2 b \text{ (no vertical sensors)}$$

$$F_1 = \frac{F\sin \theta a}{2_b} \tag{4}$$

$$F_2 = \frac{M_{\sin\alpha}}{2_b} \tag{5}$$

$$F_F = (F_1 + F_2)\mu \tag{6}$$

$\mu =$ coefficienct of friction

In LH View

$$\overrightarrow{\sum F_x} = 0 = F\cos\theta + (F_p - F_y + F_T) + (E_p - F_T - F_y) - F_f - (B_p + F_y - F_T)$$

$$- (C_p + F_y + F_T) - F_f$$

where

$$F_p = B_p \text{ and } E_p = C_p$$

$$F_y = \frac{F\cos\theta - 2 F_f}{4}$$

$$+\uparrow \sum F_y = 0 = F_3 + F_4 - F_3 - F_4$$

$$\overset{\frown}{\sum} M_o = 0 = F \cos\theta a + M \cos\alpha - 2F_3 b - 2F b$$

(but there are no sensors aligned vertically)

$$F_3 = \frac{F\cos\theta a}{2b} \tag{7}$$

$$F_4 = \frac{M\cos\alpha}{2b} \tag{8}$$

$$F_f = (F_3 + F_4)\mu \tag{9}$$

## Sensor Thresholds and Limits

From the convention of directions established in Figure C4, the desired force
sensing along the Z-Z axis is obtained by algebraic subtraction of sensor D from A.
Force sensing along the Y-Y axis is obtained by algebraic subtraction of sensors
E + F from B + C. This latter task is a bit more nebulous due to the unavoidable
presence of spin-up (or down) torques also registering on sensors B, C, E, and F.

The sensors selected to perform this task would be equivalent to PACE Engineering Co. force transducer LC1 except that a range of $\pm 200$ lb. is required (largest current model is $\pm 100$ lb.). The claimed sensitivity is 1 part in 10,000 and a hysteresis excursion of $\pm.25\%$. A useable output then is assumed to be at any change of force on the sensor greater than .5 lb. The point at which the counterbalance drive system is to be activated is when the paired sensors acting along the Z-Z or Y-Y axes have a force difference, $\Delta F_S$, of 3 lb.

Working to the $\Delta F_S$ noted above, the threshold limits will be established at the instant of centrifuge start-up.

Case I - The CM offset is along the Z-Z axis (most probable case).

$\theta = 90,^\circ \sin \theta = 1.00$; $\alpha = 90^\circ$, $\sin \alpha = 1.00$

$$F_Z = \frac{F \sin \theta - 2F_F}{2}$$

then :

$$2F_Z = F \sin \theta - 2F_F$$

or :

$$F = \frac{2F_Z + 2F_F}{\sin \theta}$$

but :

$$2F_Z = \Delta F_S$$

or :

$$F_Z = \Delta F_S/2$$

then :

$$F = \frac{2(\Delta F_S/2) + 2 F_F}{\sin \theta} = \frac{\Delta F_S + 2F_F}{\sin \theta}$$

$$F_F = (F_1 + F_2)\mu$$

$$F_1 = Fa \sin \theta/2b$$

$$F_2 = \frac{M \sin \alpha}{2b}$$

then :

$$F_F = \left[ \frac{F\, a \sin \theta}{2b} + \frac{M \sin \alpha}{2b} \right] \mu$$

and :

$$F = \frac{\Delta F_S + 2\mu \left[ \dfrac{F\, a \sin \theta + M \sin \alpha}{2} \right]}{\sin \theta}$$

or :

$$F \sin \theta \left( 1 - \frac{\mu\, a}{b} \right) = \Delta F_S + \frac{M\, \mu\, \sin \alpha}{b}$$

or :

$$F = \frac{\Delta F_S + (M \mu\, \sin \alpha)/b}{\sin \theta \left( 1 - \dfrac{\mu\, a}{b} \right)}$$

but :

$$\sin \alpha = \sin \theta = 1.00; \quad \frac{\mu\, a}{b} = \frac{(.04)\,(38.75)}{(14.40)} = .1076$$

then :

$$F = \frac{\Delta F_S + M\mu/b}{1 - .1076} = \frac{\Delta F_S + (.04M/14.40)}{.8924}$$

$$= \frac{\Delta F_S}{.8924} + .00311\, M$$

for :

$$\Delta F_S = 3.0 \text{ lb.}$$

$$F = \frac{3.0}{.8924} + .00311\, M = 3.36 + .00311 M$$

also :

$$F_T = T/4b = \frac{(250)(12)}{(4)(14.40)} = 52.08 \text{ lb.}$$

Note that in the region of start-up the influence of the dynamic moment, M, can be considered negligible. Thus counterbalance corrections will begin essentially when F = 3.36 lb.

Referring to curve of Figure C2, and plotting rpm against CM offset, at 3.36 lb. equivalent force, the curve of Figure C5 is obtained. This represents the thresh-holds at which counterbalancing will begin for CM offsets along the Z-Z axis. Since sensors A and D are aligned along the Z-Z axis, and since they are so arranged that spin-up torque has no effect upon their output, they will be most effective in the most probable initial condition of static unbalance.
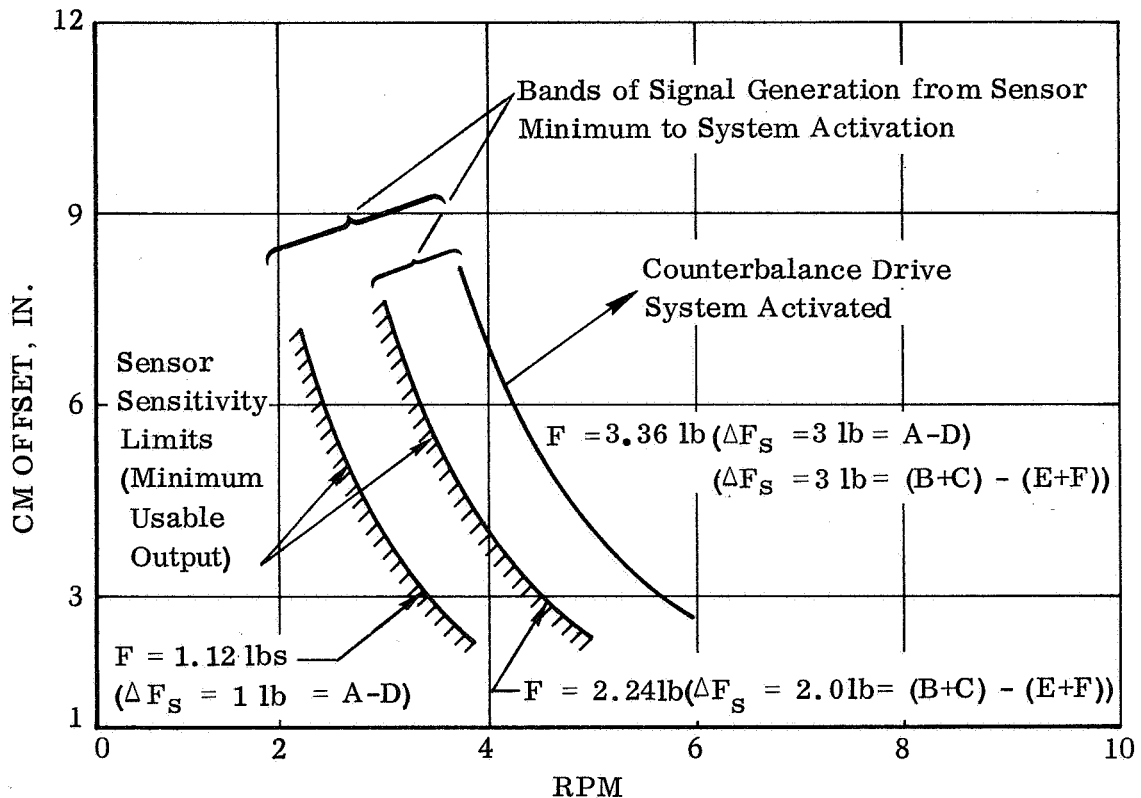


Figure C5. Counterbalance Drive Actuation - Margins from Sensor Sensitivity Limits.

Case II - This considers the less prevalent case of CM offset along the Y-Y axis. In this case the $\Delta F_s$ of 3 lb. is the difference in register between sets (B + C) and (E + F)

$$\theta = 0^{\circ}, \ \cos \theta = 1.00; \ \alpha = 0^{\circ}, \ \cos \alpha = 1.00$$

$$Fy = \frac{F \cos \theta - 2F_f}{4}$$

then :

$$4 \ Fy = F \cos \theta - 2F_f$$

or :

$$F = \frac{4 \ Fy + 2F_f}{\cos \theta}$$

but :

$$4Fy = \Delta F_s$$

or :

$$Fy = \Delta F_s/4$$

then :

$$F = \frac{4 \ (\Delta F_s/4) + 2F_f}{\cos \theta} = \frac{\Delta F_s + 2F_f}{\cos \theta}$$

$$F_f = (F_3 + F_4)\mu$$

$$F_3 = \frac{F \ a \cos \theta}{2b}$$

$$F_4 = \frac{M \cos \alpha}{2b}$$

then :

$$F_f = \left[ \frac{F \ a \cos \theta}{2b} + \frac{M \cos \alpha}{2b} \right] \mu$$

and

$$F = \dfrac{\Delta F_s + 2\mu \left[ \dfrac{F\, a \cos\theta}{2b} + \dfrac{M \cos\alpha}{2b} \right]}{\cos\theta}$$

or

$$F\, (\cos\theta)(1 - \dfrac{\mu a}{b}) = \Delta F_s + \dfrac{M\mu \cos\alpha}{b}$$

or

$$F = \dfrac{\Delta F_s + M\mu \cos\alpha/b}{\cos\theta\,(1 - \dfrac{\mu a}{b})}$$

but

$$\cos\alpha = \cos\theta = 1.00; \quad \dfrac{\mu a}{b} = .1076$$

then

$$F = \dfrac{\Delta F_s + M\mu/b}{1 - .1076} = \dfrac{\Delta F_s}{.8924} + .00311\, M$$

for

$$\Delta F_s = 3.0\ \text{lb}$$

$$F = 3.36 + .00311\, M \cong 3.36\ \text{lb}$$
$$\text{(since M is negligible at start-up)}$$

also

$$F_T = 52.08\ \text{lb.}$$

The Y-Y axis counterbalance drive system is activated per Figure C5 at the same offset force level as for the Z-Z axis. Note, however, that sensors B, C, and F are required to possess a usable output in the region of .75 lb. which approaches the probable sensor sensitivity limit of .5 lb. This is noted on Figure C5 by the decreased band of signal generation between the sensitivity limit and the point of drive system activation.

Case III - The offset CM is at an angle of $\theta = 45^{\circ}$. If the effects of moment at start-up are ignored, the threshold of counterbalance activation will be:

$$\theta = 45^{\circ}; \quad \sin\theta = \cos\theta = .707$$

Table C2. Force Sensor Inputs

| Sensor | Force Sources | $\Delta F$ | Sensor Resultant | $\Delta F_s$ |
|---|---|---|---|---|
| **CASE I** | | | | |
| A | $A_p - F_z = 100 - 1.5$ | -1.5 | 98.50 | |
| B | $B_p + F_y - F_T = 100 + 0 - 52.08$ | -52.08 | 47.92 | |
| C | $C_p + F_y + F_T = 100 + 0 + 52.08$ | 52.08 | 152.08 | (A-D) = -3.0 lb. |
| D | $D_p + F_z = 100 + 1.5$ | 1.50 | 101.50 | |
| E | $E_p - F_y - F_T = 100 - 0 - 52.08$ | -52.08 | 47.92 | (B + C) - (E + F) = 0.0 |
| F | $F_p - F_y + F_T = 100 - 0 + 52.08$ | 52.08 | 152.08 | |

The negative value for $\Delta F_s$ indicates the direction for correction along the Z-Z axis. The 3.0 lb. indicates the force level at which the equivalent voltage output commands correction from the Z-Z axis drivers.

The 0.0 $\Delta F_s$ for (B+C) - (E+F) indicates no signal for Y-Y correction.

| Sensor | Force Sources | $\Delta F$ | Sensor Resultant | $\Delta F_s$ |
|---|---|---|---|---|
| **CASE II** | | | | |
| A | $A_p - F_z = 100-0$ | 0.0 | 100.0 | |
| B | $B_p + F_y - F_T = 100 + .75 - 52.08$ | -51.33 | 48.67 | |
| C | $C_p + F_y + F_T = 100 + .75 + 52.08$ | 52.83 | 152.83 | (A-D) = 0.0 |
| D | $D_p + F_z = 100 + .0$ | 0.0 | 100.0 | |
| E | $E_p - F_y - F_T = 100 - .75 - 52.08$ | -52.83 | 47.17 | (B + C) -(E + F) = 3.0 |
| F | $F_p - F_y + F_T = 100 - .75 + 52.08$ | 51.33 | 151.33 | |

The plus value for $\Delta F_s$ indicates direction. The 3.0 lb. indicates the force level at which the equivalent voltage output commands correction from the Y-Y drivers.

| Sensor | Force Sources | $\Delta F$ | Sensor Resultant | $\Delta F_s$ |
|---|---|---|---|---|
| **CASE III** | | | | |
| A | $A_p - F_z = 100 -1.5$ | -1.5 | 98.50 | |
| B | $B_p + F_y - F_T = 100 + .75 - 52.08$ | -51.33 | 48.67 | |
| C | $C_p + F_y + F_T = 100 + .75 + 52.08$ | 52.83 | 152.83 | (A-D) = -3.0 |
| D | $D_p + F_z = 100 + 1.5$ | 1.5 | 101.50 | |
| E | $E_p - F_y - F_T = 100 - .75 - 52.08$ | -52.83 | 47.17 | (B + C) -(E + F) = 3.0 |
| F | $F_p - F_y + F_T = 100 - .75 + 52.08$ | 51.33 | 151.33 | |

The 3.0 lb. in both axis indicates the force level at which the equivalent voltage output commands correction in both axes with direction determined by the sign.

in Z - direction

$$F = \frac{\Delta F_s}{\sin \theta \, (1 - \frac{\mu a}{b})}$$

$$F = \frac{3.0}{.707 \, (.8924)} = 4.75 \text{ lb.}$$

in Y - direction

$$F = \frac{\Delta F_s}{\cos \theta \, (1 - \frac{\mu a}{b})}$$

$$F = \frac{3.0}{(.707) \, (.8924)} = 4.75 \text{ lb.}$$

The 4.75 lb. represents the maximum condition of force from a CM offset before correction is initiated. In cases of offset CM between angles of $0^o$ to $45^o$ and $45^o$ to $90^o$, the drive system for the nearest axis will be initiated ahead of the other. This effectively drives the angle $\theta$ toward $45^o$, and when combined with an increase in rpm (F increases) the other axis drive system will be energized at that time when the generated level of voltage is equivalent to a $\Delta F_s$ of 3.0 lb. or greater. The time interval is dependent upon centrifuge acceleration but would likely be a fraction of a second or perhaps as long as a few seconds.

Table C2 summarizes the force conditions as felt by the sensors for the foregoing cases. Figure C6 shows the threshold response as related to the offset CM force at angles $\theta$. Note that the objective of initiating corrections from the sensor system at equivalent offset forces below 5 lb. is met. (See also Figure C2)

Figure C6 shows the threshold response as related to the offset CM force at angles $\theta$. Note that the objective of initiating corrections from the sensor system at equivalent offset forces below 5 lb. is met. (See also Figure C1)

The foregoing paragraphs established that the system is functionally capable at the regime of start-up and corrections will be initiated at rpms generally below 7. (See Figure C6.) This assumes that the drive motor is controlled such that angular acceleration does not exceed .171 rad/sec$^2$. At the low rpms it was shown that dynamic unbalance has negligible effects.

The next consideration is the high rpm case where the dynamic unbalance has significant inputs.
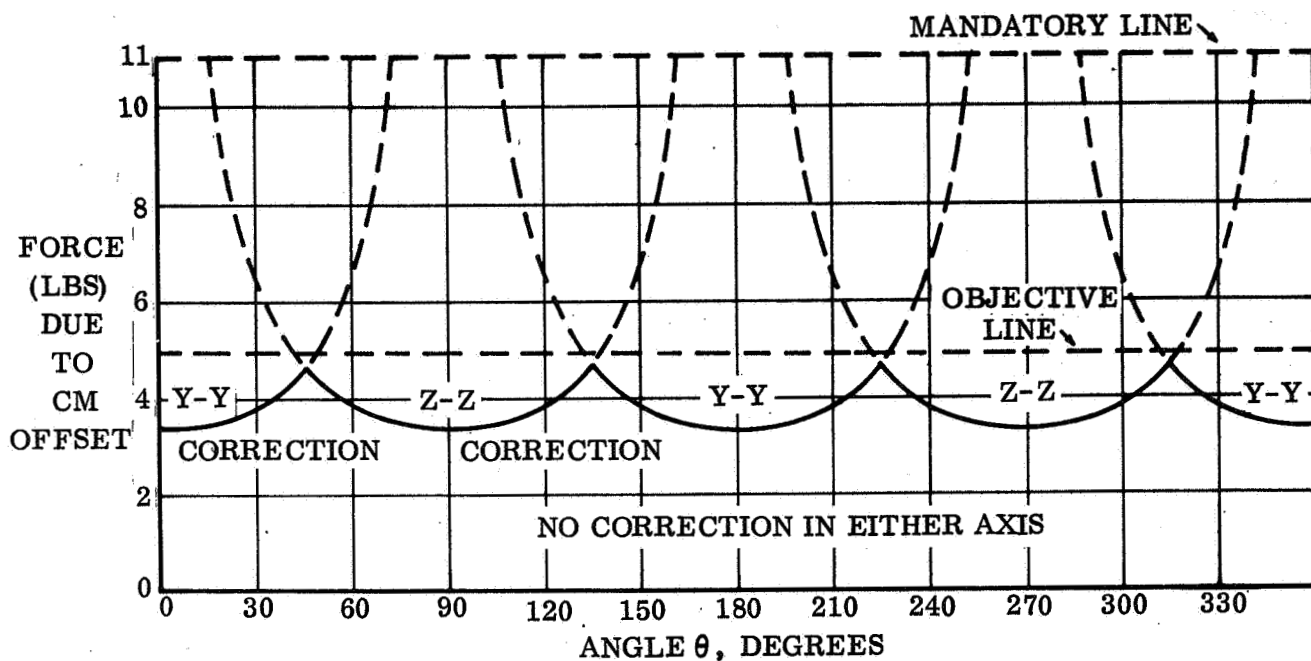
Figure C6.  Imbalance Force at Counterbalance Drive Actuation
Vs. Coordinate Direction - Start-up Regime.

The sensor geometry intentionally precludes the direct imposition of forces onto the sensors from dynamic unbalance.  The reacting forces are taken by the structure directly in a direction normal to the plane of sensor activity.  There is, however, an indirect effect upon the ability of the sensors to pick up static unbalance forces through the mechanism of friction.  It is conceivable that for some circumstances of combined static and dynamic unbalance the dynamic couple will alleviate the unwanted friction opposition contributed by the moment of the unbalanced static force $F_1$ and $F_3$ resulting from sensor plane displacement of 38.75 in. from the CM along X-X axis .

The condition posing the worst circumstances for the sensors occurs during the re-entry experiment at maximum angular velocity (65.3 rpm, 9 g's).

Three cases will be assumed:

Case I:      $\theta = 90°$, $\sin \theta = 1.00$; $T = 250$ ft.-lb.;  rpm $= 65.3$

$\alpha = 90°$, $\sin \alpha = 1.00$; $M = 150$ ft.-lb. (same direction as F in Z-X plane)

The torque, T, is actually something less than 250 ft.-lb. since the desired speed has just been attained and the motor no longer must produce an acceleration. Proper programming in fact would probably consist of easing the acceleration perhaps

several seconds before the intended rpm was reached. Nevertheless the 250 ft.-lb. will be used in this illustration.

$$F = 3.36 + .00311 \, M$$

$$= 3.36 + (.00311)(150)(12)$$

$$= 3.36 + 5.60 = 8.96 \, lb.$$

$$F_T = 52.08 \, lb.$$

Case II:  $\theta = 45°$, $\sin \theta = .707$; $T = 250$ ft.-lb. ; rpm $= 65.3$

$\alpha = 90°$, $\sin \alpha = 1.00$, $\cos \alpha = 0$; $M = 150$ ft.-lb (in Z-X plane)

in the Z - direction:

$$F = \frac{\Delta F_s + M \frac{\mu}{b} \sin \alpha}{\sin \theta \left(1 - \frac{\mu a}{b}\right)}$$

$$= \frac{3.0 + (150)(12) \frac{.04}{14.40}(1.00)}{.707 \, (.8924)} = \frac{3.0 + 5.00}{(.707)(.8924)}$$

$$= \frac{8.00}{(.707)(.8924)} = 12.67 \, lb.$$

in the Y- direction

$$F = \frac{\Delta F_s + \frac{M \mu \cos \alpha}{b}}{\cos \theta \left(1 - \frac{\mu a}{b}\right)}$$

$$= \frac{3.0 + 0}{(.707)(.8924)} = 4.75 \, lb.$$

This indicates that movement will initially occur along the Y-Y axis as soon as $F = 4.75$ lb. and F will not reach 12.67 lb. as $\theta$ will be driven toward $90°$. A plot of the four quadrants of action produces the intersecting curves shown on Figure C2 in which $\theta =$ variable and $\alpha = 90°$.
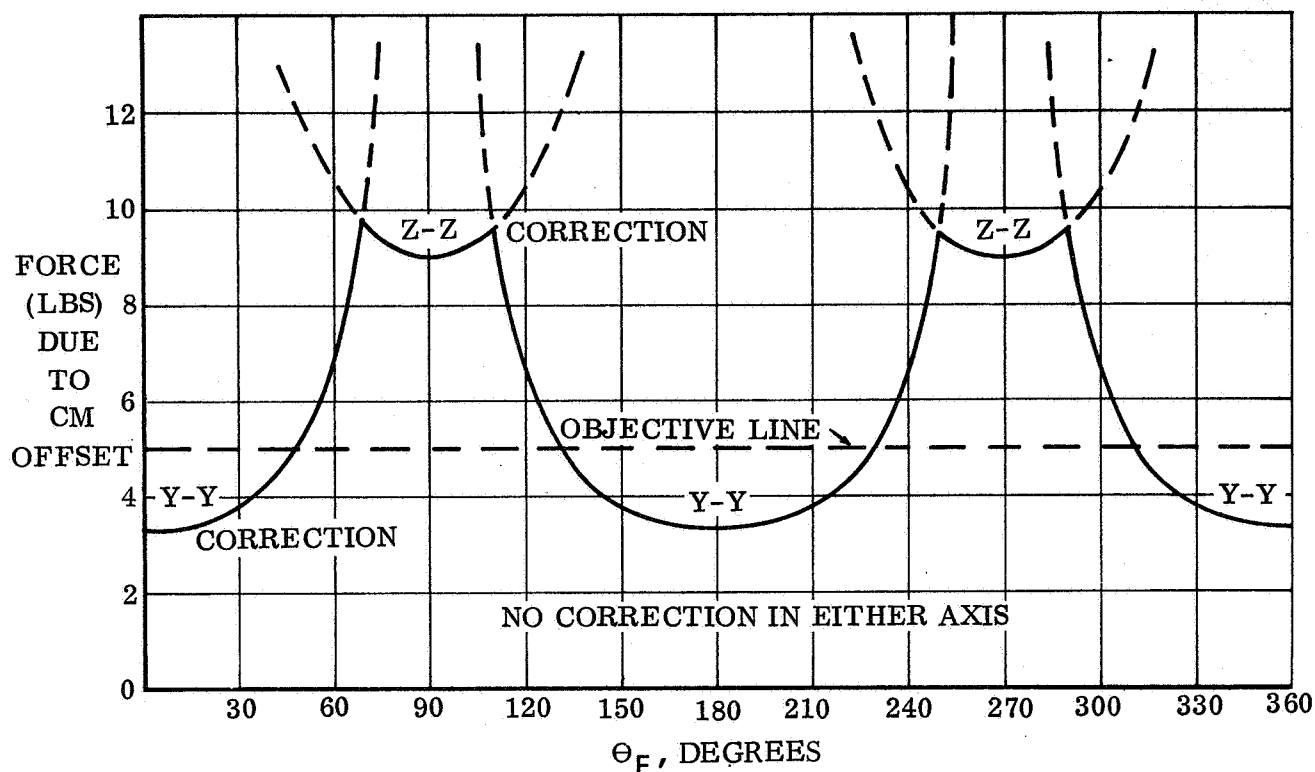
C22

Figure C7. Force Vector Relations.

Case III:  $\theta = 45^\circ$, $\sin \theta = \cos \theta = .707$; T = 250 ft. -lb.; rpm = 65.3

$\alpha = 45^\circ$, $\sin \alpha = \cos \alpha = .707$, M = 150 ft. -lb.

(same direction as F)

in the Z direction

$$F = \frac{\Delta F_s + \dfrac{M \mu \cos\alpha}{b}}{\cos\theta \left(1 - \dfrac{\mu a}{b}\right)}$$

$$= \frac{3.00 + \dfrac{(150)(12)(.04)(.707)}{14.40}}{(.707)(.8924)} = \frac{3.00 + 3.535}{(.707)(.8924)}$$

$$= \frac{6.535}{(.707)(.8924)} = 10.35 \text{ lb.}$$

in the Y - direction

by similarity, F = 10.35 lb.

The curve of Figure C8 represents this condition. Theta is varied and $\alpha = 45°$. Note from Figure C7 and C8 that the objective of initiating corrections from the sensor system at forces below 5 lb. is not met and that the peak response also slightly exceeds the mandatory 10 lb. line. It is considered that in actual operation the curve will approach a lower value, however. The rationale for this belief stems from the near proximity of the sensor assembly to the bearing area since at the high rpms stated, the slight dynamic jitter will have the effect of lowering the coefficient of friction - and about half of the total threshold force equivlant is due to friction contribution.
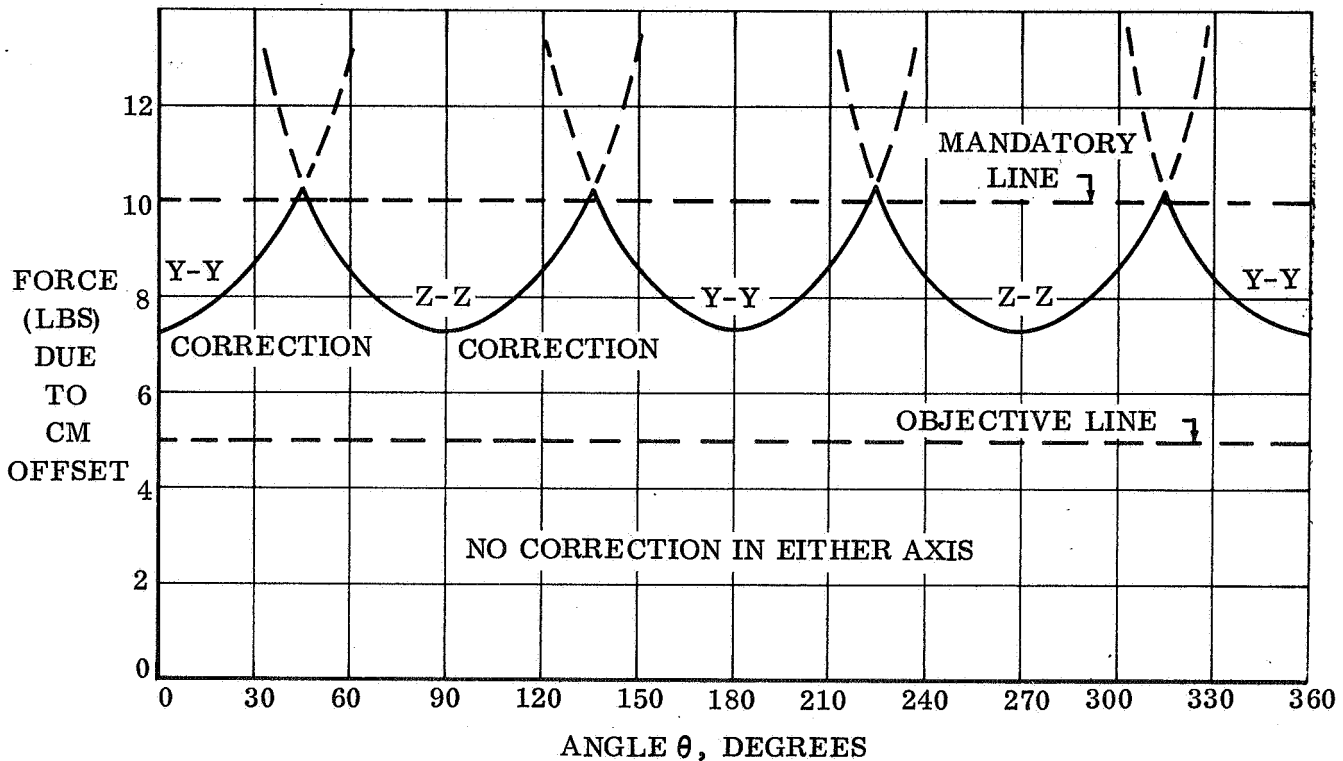


Figure C8. Force Vector Relations.

To determine that region at which the moment, M, causes the sensors to exceed the objective of a 5 lb. threshold, the curve of Figure C8 will be considered a maximum condition (at which $\theta = 45°$ when $\alpha = 45°$)

$$F = \frac{\Delta F_s + \dfrac{M\mu\sin\alpha}{b}}{\sin\theta\left(1 - \dfrac{\mu a}{b}\right)} = \frac{3.00 + \dfrac{M(12)(.04)(.707)}{(14.40)}}{.707\,(.8924)}$$

$$= \frac{3.00 + .0236M}{(.707)(.8924)} = 4.75 + .0374\,M$$

The moment, M, can be expressed as a force couple with the force being $F_M$ and the moment arm S; then

$$M = F_M S$$

$F_M$ is the force due to reaction to centripetal force in which

$$F_M = ma_R$$

$a_R$ is the centripetal acceleration and is related to angular velocity by

$$a_R = R\omega^2.$$

Then $F_M = mR\omega^2$ and $M = SmR\omega^2$ in which m, R and S are constants, making M $= K\omega^2$. From this, values for M can be determined at various rpms which in turn are used to relate the threshold sensing to centrifuge rpm as shown in Table C3.

Evaluating K:

At maximum rpm (65.3), M = 150 ft. - lb.

then

$$\omega_{max} = 65.3 \text{ x } \frac{2\pi}{60} = 6.84 \text{ rad/sec.}$$

and

$$M = K\omega^2 = 150 = (6.84)^2 K$$

or

$$K = 150/(6.84)^2 = 3.205$$

Table C3.  Summary of Sensor Forces at Selected RPM for Maximum Speed Regime, Case III Conditions.

| RPM | $\omega$ | $M = 3.205\omega^2$ | $F = 4.75 + .0374\,M$ |
|---|---|---|---|
| 65.3 | 6.84 | 150 | 4.75 + 5.61 = 10.36 |
| 60 | 6.28 | 126.3 | 4.75 + 4.72 = 9.47 |
| 50 | 5.24 | 88.0 | 4.75 + 3.29 = 8.04 |
| 40 | 4.19 | 56.3 | 4.75 + 2.11 = 6.86 |
| 30 | 3.14 | 31.6 | 4.75 + 1.18 = 5.93 |
| 20 | 2.09 | 14.0 | 4.75 + .52 = 5.27 |
| 10 | 1.047 | 3.51 | 4.75 + .13 = 4.88 |
| 5 | .523 | .88 | 4.75 + .03 = 4.78 |
| 0 | 0 | 0 | 4.75 + .0 = 4.75 |

This of course is the extreme case. Assuming also the more probable case where $\theta = 90^{\circ}$ with $\alpha$ at $90^{\circ}$ the curves of Figure C9 are plotted. (See Table C3 for data for the "normal" curve of Figure C8). True operating characteristics will be within the shaded band and most probably near the lower limit. It is evident, then that the sensitivity of the sensor system can be enhanced by closely controlling those features of the centrifuge which contribute to dynamic unbalance. Figure C3 is rather significant in that the dynamic unbalance contribution is readily seen as a function of centrifuge speed. Without the friction contribution the curves would be horizontal straight lines with values as determined by the left side origin.

Table C4. Summary of Sensor Forces at Selected RPM for Maximum
Speed Regime Case I Conditions.

| RPM | $\omega$ | M | F = 3.36 + (.0374) M |
|-----|----------|---|----------------------|
| 65.3 | 6.84 | 150 | 3.36 + 5.61 = 8.97 |
| 60 | 6.28 | 126.3 | 3.36 + 4.72 = 8.08 |
| 50 | 5.24 | 88.0 | 3.36 + 3.29 = 6.65 |
| 40 | 4.19 | 56.3 | 3.36 + 2.11 = 5.47 |
| 30 | 3.14 | 31.6 | 3.36 + 1.18 = 4.54 |
| 20 | 2.09 | 14.0 | 3.36 + .52 = 3.88 |
| 10 | 1.047 | 3.51 | 3.36 + .13 = 3.49 |
| 5 | .523 | .88 | 3.36 + .03 = 3.39 |
| 0 | 0 | 0 | 3.36 + 0 = 3.36 |

Recalling Figure C3 it should be noted that sensors B, C, E and F include the forces due to drive motor torque. This torque is taken directly by the sensors and sets their full range (200 lb.) and preload values (100 lb.). The purpose of including this torque within the sensor reading has not been completely understood by others who are not directly associated with the problem. The primary reason is that unless the drive torque is taken through the sensor, it is of such a significantly larger value than the offset CM force that the force whose detection is required would be obliterated. Such a case exists in Alternate No. 1 in the next section. Although it is not intentionally so, the torques can be used to drive the countermomentum system.

The driving torques result in sensor loads near the extremes of the prescribed linearity curve where deviation is greatest, hence a spurious signal may be generated. This is an area of uncertainty. However, it is emphasized that control of torque by control

of drive motor acceleration is necessary within the aforementioned limits of 250 ft.-lb. to insure that undesirable outputs from the sensors are not created.
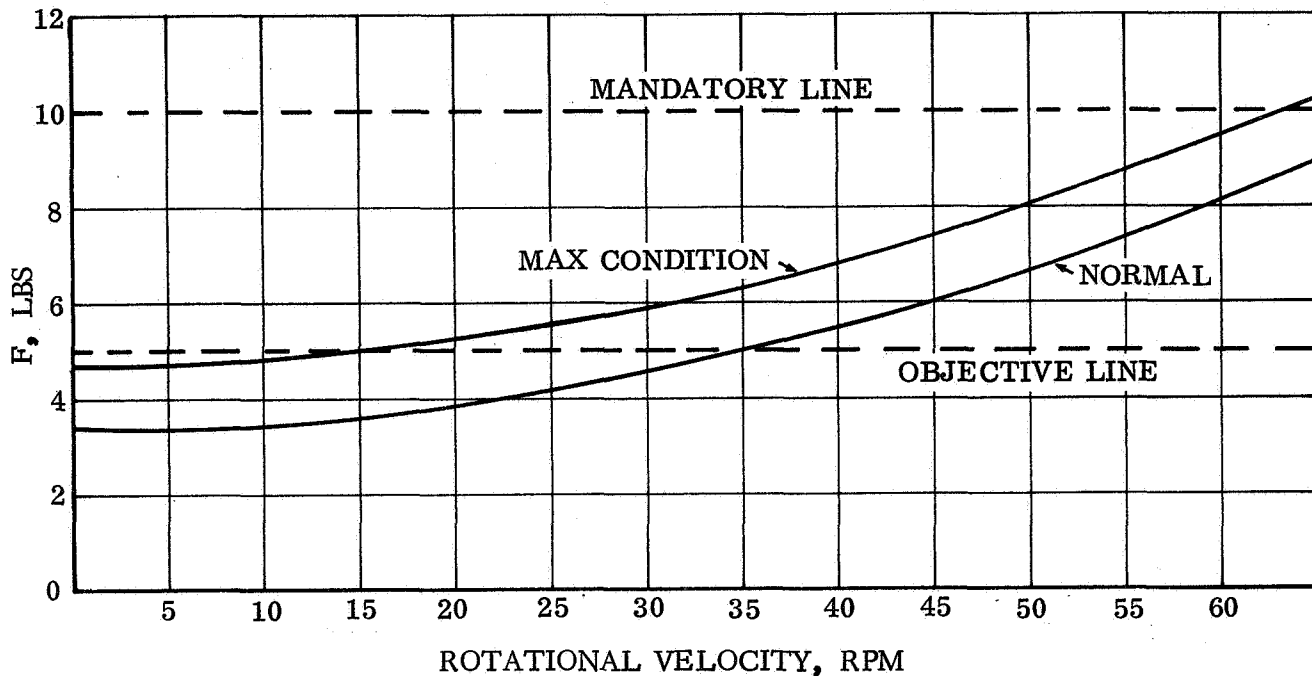


Figure C9. Unbalance Force Band-width Vs. RPM.

Alternate Systems

In the course of arriving at the selected system, several other concepts were investigated to certain depths and in most cases to different ground rules. Therefore, those concepts cannot be considered strictly as alternates to the selected system. Only two of these will be described here and are included for the purpose of perhaps showing to some degree the problem areas that are present, but not readily seen, in some concepts. These systems are designated Alternates 1, and 2. The assigned numbers bear no significance. Briefly, they are: (1) Similar to the selected system and conceived to the same ground rules. Four sensors are used instead of six. The main problem lay in torque and friction loads producing a system less sensitive than the selected system. (2) Consisted of ten sensors and was conceived to register all three modes of disturbing forces. It was not sensitive to friction forces. Minimum difference between ground and orbit configuration was inherent. Most complex with prime difficulty of manufacture and assembly and precision adjustment, difficult accessibility, and not easily omitted if desired.

## Alternate 1

The sensor force system is shown in Figure C10. Note that it is similar to the selected system; the primary difference being in the treatment of torque. This system attempts to remove torque from the sensor readings and route it directly through structure. However, it is the torque influence which defeats the system. The same convention is used here as for the selected system, and the appropriate forces are shown on Figure C10.

The driving torque is transmitted through a double universal joint. This also requires a longitudinal slip joint. Such a device is shown in Figure C11. In order for sensors A, B, C and D to register a change in force it is necessary that displacement should occur, even though it is on the order of .001/.002. For the universal joint to permit this, the pivot points must displace and a slight angular misalignment will occur. If one of the U-joints is analyzed at the pivot, an equivalent force, P, to cause this rotation can be obtained. This force, P, then also consists of the force prohibiting movement that is desired at the sensors.

The torque is 250 ft.-lb. or 3000 in.-lb. To be most favorable it is assumed roller needles are used and a coefficient of friction of .005 is assumed (dry lube only can be used).

$$F_N = \frac{3000}{1.5} = 2000 \text{ lb.} \qquad\qquad F_F = F_N \mu$$

$$F_F = 2000 (.005) = 10 \text{ lb.} \qquad\qquad Pa = F_F (.31)(2)$$

$$P = \frac{F_F (.31)(2)}{a} \qquad\qquad P = \frac{(10)(.31)(2)}{a} = \frac{6.2}{a}$$

But the same must occur at the other U joint; hence $P = \dfrac{12.4}{a}$.

For practical purposes, "a" will be in the neighborhood of 2 in. and therefore P will be 6.2 lbs. Now if one examines the equations on Figure C10 and compares to Figure C4 of the selected system it will be noted that they are the same

| SENSOR | FORCES |
|--------|--------|
| A | $A_p - F_Z$ |
| B | $B_p + F_y$ |
| C | $C_p + F_Z$ |
| D | $D_p - F_y$ |

$A_p = C_p = B_p = D_p = \text{PRELOAD}$



$$F_Z = \frac{F \sin \theta - 2F_F}{2}$$

$$F_y = \frac{F \cos \theta - 2F_f}{2}$$

$$F_F = (F_1 + F_2)\mu$$

$$F_f = (F_3 + F_4)\mu$$

$$F_1 = \frac{F \sin \theta \, a}{2b}$$

$$F_2 = \frac{M \sin \alpha}{2b}$$

$$F_3 = \frac{F \cos \theta \, a}{2b}$$

$$F_4 = \frac{M \cos \alpha}{2b}$$
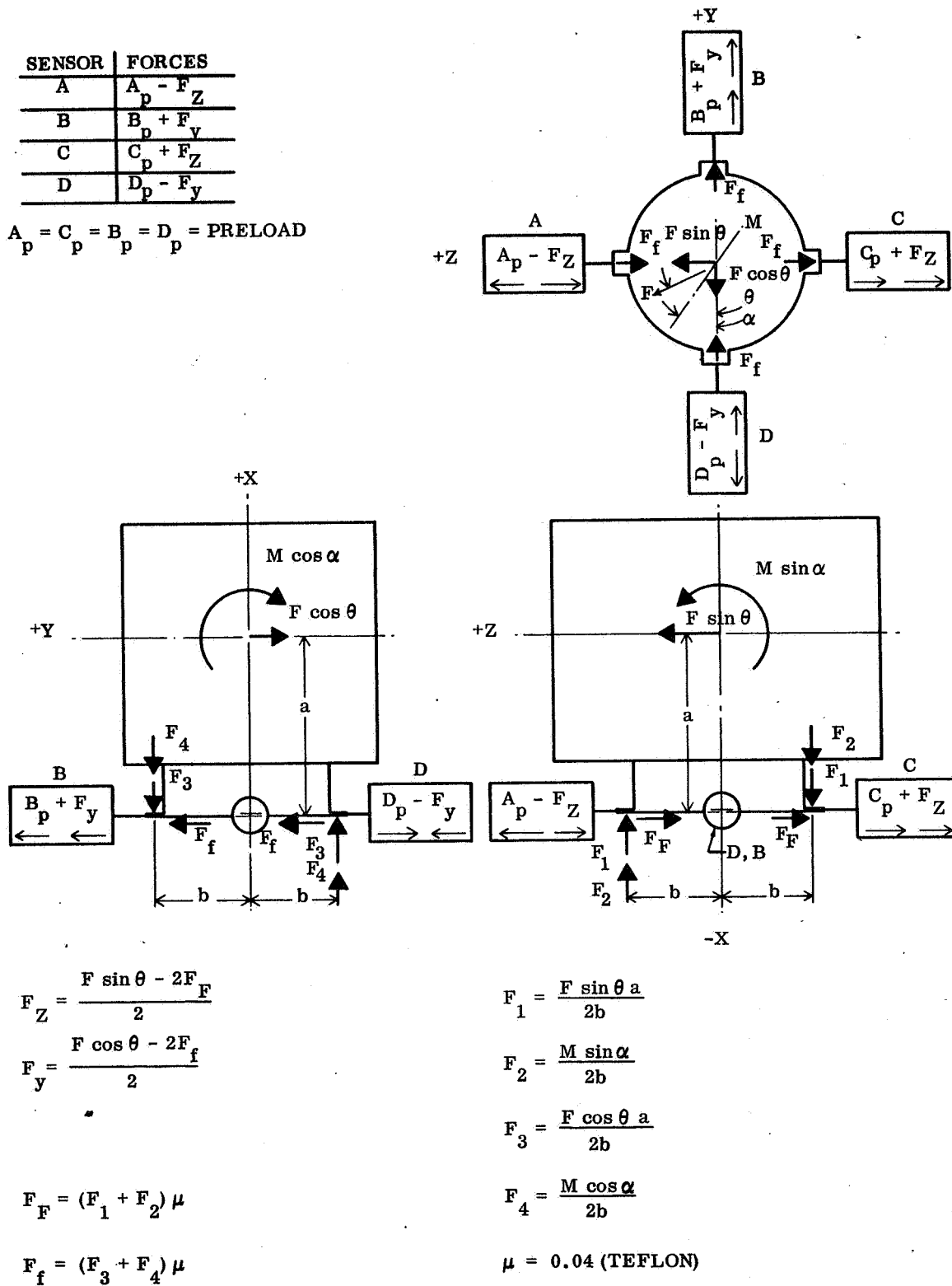
$$\mu = 0.04 \; (\text{TEFLON})$$
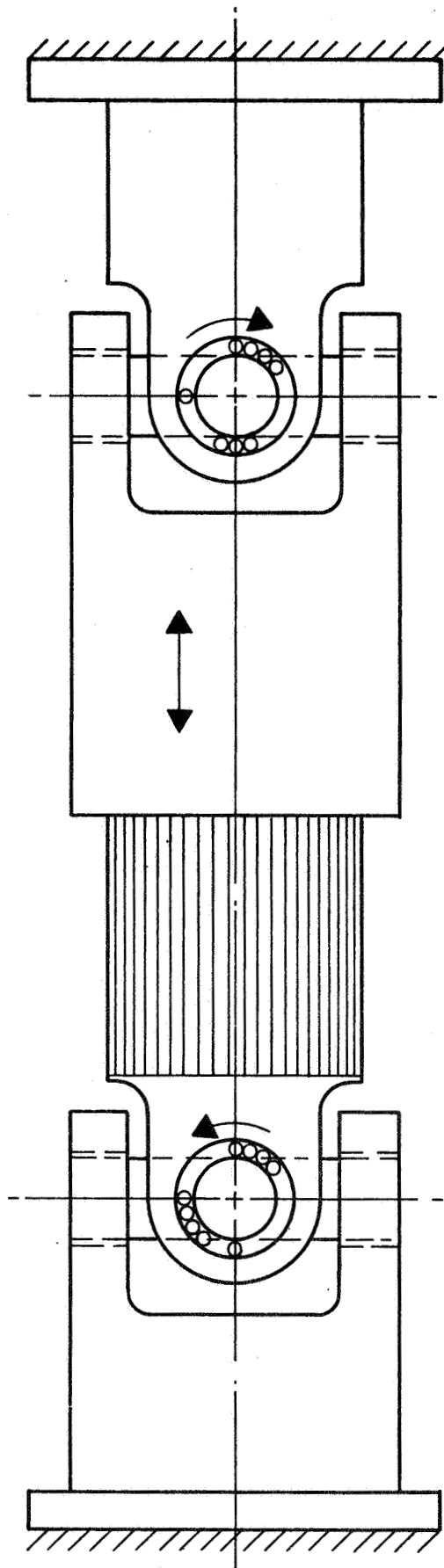
Figure C10.  Sensor Force Diagram – Alternate No. 1.

Figure C11. Universal Joint Torque Transmitter
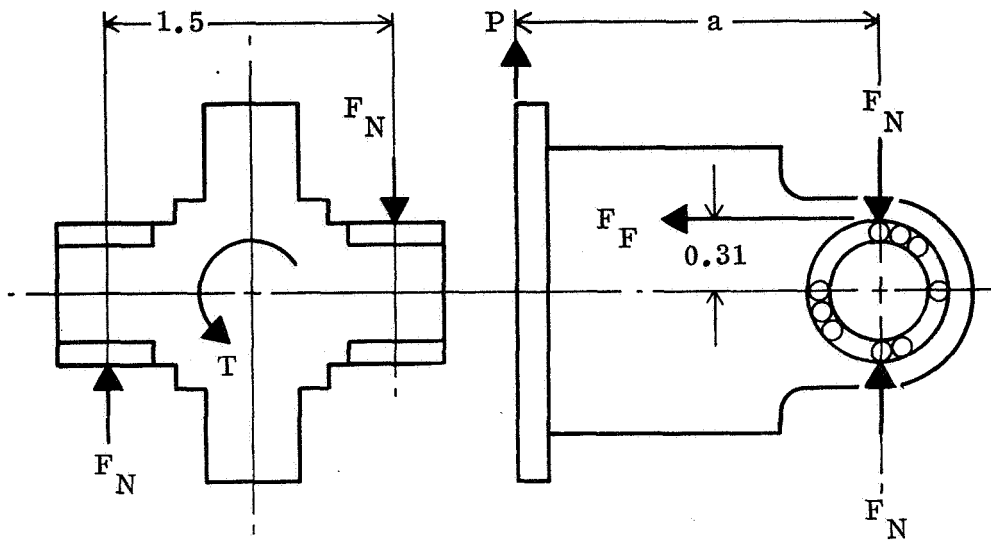
Figure C12. U-Joint Pivot.

and that forces $F_1$, $F_2$, $F_3$ and $F_4$ exist in both systems as a retarding friction force. Also working as a retarding force is the load P above. Its magnitude is actually greater than the friction resistance and must be additive to the friction resistance. Obviously considerable sensor sensitivity is lost and points up the basic reason for routing the torque through the sensors in the selected system.

Another very serious fault with Alternate 1 lies in the assumption that the U-joints would be in perfect initial alignment. This would likely be impossible. Now if some eccentricity did exist initially, and the 250 ft.-lb. of torque is applied, this eccentricity will not be removed since the joint is essentially locked up as compared to the "floating joint" desired. If displacement actually did occur and the trim weights were signalled to move, considerable overshoot might be required before a null signal would occur from the sensors. The system would have the inherent trait of stiction and poor sensitivity.

Alternate 2

This alternate would be the prime candidate in the event all three modes were to be sensed. It is comparatively complicated and would present some problems in the rigging and subsequent adjustments. In fact, in view of the lower tier of sensors being submerged within the hub, it was anticipated that adjustment settings would be accomplished by torque tubes extending from the micrometer screws to an area of accessibility.

The sensor force system is shown in Figure C13. Note that the sensors are grouped in two parallel planes. In this system friction is of no consequence in the orbit
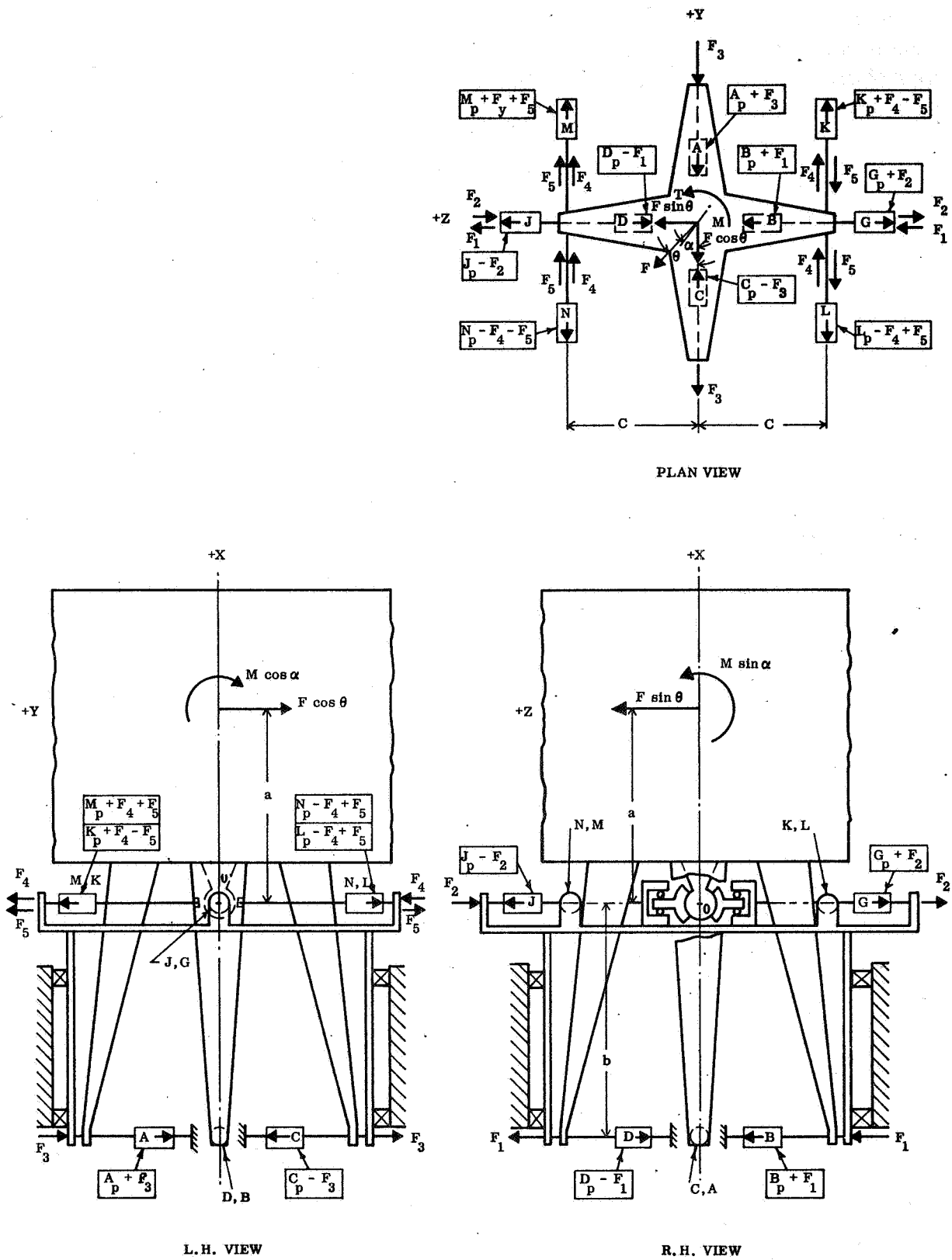
Figure C13. Sensor Force Diagram - Alternate No. 2

version since there are no vertical forces. Friction at the ball joint has a minimal effect due to moment arm ratios of 20:1 or greater. The torque sensors must lie in the upper plane or an interference couple will exist. Again a tie-rod suspension system is used to get away from the friction effects and lateral instability at the sensors.

# ABSTRACT

This document is a portion of the final report prepared under Contract NAS 1-7309, Feasibility Study of a Centrifuge Experiment for the Apollo Applications Program. The contract was performed for the Langley Research Center, National Aeronautics and Space Administration, Hampton, Virginia. The complete final report consists of the following documents:

| | | |
|---|---|---|
| NASA CR-66649<br>GDC-DCL-68-001<br>(SRC-AN-703) | Volume I | Space Research Centrifuge Configuration, Installation and Feasibility Studies |
| NASA CR-66650<br>GDC-DCL-68-002<br>(SRC-SD-604) | Volume II | Specification and Test Requirements - Space Research Centrifuge Engineering Development Prototype |
| NASA CR-66651<br>GDC-DCL-68-003<br>(SRC-MS-112) | Volume III | Experimental Requirements for the Space Research Centrifuge |
| GDC-DCL-68-004<br>(SRC-MS-302) | Volume IV | Manned Centrifuge Test Report |

This study examines the application of an on-board centrifuge as a versatile research tool for the measurement of human physiological responses in the space environment. A realistic orbital centrifuge is configured based on a specified series of experiments dealing primarily with vestibular and cardiovascular physiology. Experiment feasibility is established in terms of spacecraft stability, reliability, safety, economics, weight, power and other influential factors. A ground based prototype of the orbital machine is defined and the required test program outlined. The effects of cross-coupled angular accelerations induced by the interaction of the astronaut/machine/vehicle motions is examined by a series of ground centrifuge tests with human subjects.